

Mahendra Rai  
Nelson Duran  
*Editors*

# Metal Nanoparticles in Microbiology

 Springer

# Metal Nanoparticles in Microbiology



Mahendra Rai • Nelson Duran  
Editors

# Metal Nanoparticles in Microbiology

 Springer

*Editors*

Mahendra Rai, Ph.D.  
Professor and Head  
Biotechnology Department  
SGB Amravati University  
Amravati-444 602  
Maharashtra, India  
mkrai123@rediffmail.com

Professor Nelson Duran  
Biological Chemistry Laboratory  
Instituto de Química  
Universidade Estadual de Campinas  
CEP 13084862, Caixa Postal 6154  
Campinas, S.P., Brazil  
duran@iqm.unicamp.br

ISBN 978-3-642-18311-9                      e-ISBN 978-3-642-18312-6  
DOI 10.1007/978-3-642-18312-6  
Springer Heidelberg Dordrecht London New York

Library of Congress Control Number: 2011925677

© Springer-Verlag Berlin Heidelberg 2011

This work is subject to copyright. All rights are reserved, whether the whole or part of the material is concerned, specifically the rights of translation, reprinting, reuse of illustrations, recitation, broadcasting, reproduction on microfilm or in any other way, and storage in data banks. Duplication of this publication or parts thereof is permitted only under the provisions of the German Copyright Law of September 9, 1965, in its current version, and permission for use must always be obtained from Springer. Violations are liable to prosecution under the German Copyright Law.

The use of general descriptive names, registered names, trademarks, etc. in this publication does not imply, even in the absence of a specific statement, that such names are exempt from the relevant protective laws and regulations and therefore free for general use.

*Cover design:* deblik, Berlin

Printed on acid-free paper

Springer is part of Springer Science+Business Media ([www.springer.com](http://www.springer.com))

# Preface

Nanotechnology is a multidisciplinary and interdisciplinary science dealing with various aspects of research and technology at nanolevel. Nanoparticles range from 1 to 100 nm, which form building blocks of nanotechnology. Metal nanoparticles such as gold, silver, platinum and copper have gained considerable attention in recent times due to their fundamental and technological interest. These nanoparticles have unique catalytic, electronic and optical properties different from the metallic particles. Usually, the nanoparticles can be synthesized by physical, chemical and biological methods. The physical and chemical methods involve the use of strong chemical reducing agents such as sodium borohydride and weak reducing agents such as sodium citrate, alcohols, use of gamma- and UV rays, etc. Studies have reported that the biological methods depict an inexpensive and eco-friendly method for synthesis of nanoparticles. To date, biosynthesis of nanoparticles has been demonstrated by the use of biological agents such as bacteria, fungi, yeasts actinomycetes and plants.

Synthesis of nanoparticles using microbes or plants is a new and emerging eco-friendly science. Many investigators have been using biological methods for the synthesis of nanoparticles. So far, there is no book on biogenic nanoparticles. Therefore, this would be the first book of its kind all over the world.

The book covers synthesis of nanoparticles by different microbes (bacteria, cyanobacteria and fungi) and plants, the mechanism involved in biosynthesis and multiple applications of the nanoparticles.

The book would be immensely useful for diverse discipline of students and teachers of nanotechnology, biology, chemistry, physics, botany, zoology, chemical technology, earth sciences, medicine, pharmacology, mycology, microbiology, pathology and biotechnology.

The book incorporates the contributions of leading researchers in the field of biogenic metal nanoparticles. The editors highly appreciate the contribution by eminent scholars and their patience during the publication of the book.

We wish to express our sincere thanks to Dr. Jutta Lindenberg for her continued interest, critical suggestions and prompt response during the editing process. MKR

and ND thankfully acknowledge the help and support rendered by the students. MKR expresses thanks to his children Shivangi, Shivani and Aditya for their unconditional love, support and help.

Amravati, Maharashtra, India  
Campinas, SP, Brazil

Mahendra Rai  
Nelson Duran

# Contents

- 1 Biogenic Nanoparticles: An Introduction to What They Are, How They Are Synthesized and Their Applications** ..... 1  
Mahendra Rai, Aniket Gade, and Alka Yadav

## Part I Synthesis and Fundamentals

- 2 An Insight into the Bacterial Biogenesis of Silver Nanoparticles, Industrial Production and Scale-up** ..... 17  
Venkataraman Deepak, Kalimuthu Kalishwaralal, Sureshbabu Ram Kumar Pandian, and Sangiliyandi Gurunathan
- 3 Biosynthesis of Gold Nanoparticles: A Review** ..... 37  
Maggy F. Lengke, Charoen Sanpawanitchakit, and Gordon Southam
- 4 A Bacterial Backbone: Magnetosomes in Magnetotactic Bacteria** ... 75  
Christopher T. Lefèvre, Fernanda Abreu, Ulysses Lins, and Dennis A. Bazylinski
- 5 Enzymatic Synthesis of Platinum Nanoparticles: Prokaryote and Eukaryote Systems** ..... 103  
Chris Whiteley, Yageshni Govender, Tamsyn Riddin, and Mahendra Rai
- 6 Biomolecules–Nanoparticles: Interaction in Nanoscale** ..... 135  
N. Vigneshwaran and Prateek Jain

## Part II Synthesis and Process Development

- 7 Microbial Synthesis of Metal Nanoparticles** ..... 153  
Irena Maliszewska



<b>8 Basic and Practical Procedures for Microbial Synthesis of Nanoparticles</b> .....	177
Ahmad-Reza Shahverdi, Mojtaba Shakibaie, and Pardis Nazari	
<b>9 Development of a Process Chain for Nanoparticles Production by Yeasts</b> .....	197
Nikolay Krumov and Clemens Posten	
<b>Part III Applications</b>	
<b>10 Applications of Gold Nanoparticles: Current Trends and Future Prospects</b> .....	225
Zygmunt Sadowski and Irena H. Maliszewska	
<b>11 Biogenic Silver Nanoparticles: Application in Medicines and Textiles and Their Health Implications</b> .....	249
Priscyla D. Marcato and Nelson Durán	
<b>12 Nanobiosensors and Their Applications</b> .....	269
A. Reshetilov, P. Iliasov, T. Reshetilova, and Mahendra Rai	
<b>13 Metallic Nanoparticles: Biological Perspective</b> .....	285
Sunil K. Singh, Siddhartha Shrivastava, and Debabrata Dash	
<b>Index</b> .....	299

# Contributors

**Ahmad-Reza Shahverdi**, Department of Pharmaceutical Biotechnology and Biotechnology Research Center, Tehran University of Medical Sciences, Tehran, Iran, shahverd@sina.tums.ac.ir

**Alka Yadav**, Department of Biotechnology, Sant Gadge Baba Amravati University, Amravati 444 602, Maharashtra, India

**Aniket Gade**, Department of Biotechnology, Sant Gadge Baba Amravati University, Amravati 444 602, Maharashtra, India

**Charoen Sanpawanitchakit**, EnviroGroup Limited, 3561 Stagecoach Road, Suite 205, Longmont, CO 80504, USA

**Chris Whiteley**, Department of Biochemistry, Microbiology and Biotechnology, Rhodes University, P.O.Box 94, Grahamstown 6140, South Africa, C.Whiteley@ru.ac.za

**Christopher T. Lefèvre**, School of Life Sciences, University of Nevada at Las Vegas, 4505 Maryland Parkway, Las Vegas, NV 89154-4004, USA, christopher.lefevre@unlv.edu

**Clemens Posten**, Department of Bioprocess Engineering, Institute of Process Engineering in Life Sciences, Karlsruhe Institute of Technology, Fritz-Haber-Weg 2, build. 30.44, Karlsruhe, Germany, clemens.posten@kit.edu

**Debabrata Dash**, Department of Biochemistry, Institute of Medical Sciences, Banaras Hindu University, Varanasi, Uttar Pradesh 221005, India, ddass@sify.comddass@stayam.net.in

**Dennis A. Bazylnski**, School of Life Sciences, University of Nevada at Las Vegas, 4505 Maryland Parkway, Las Vegas, NV 89154-4004, USA, dennis.bazylnski@unlv.edu

**Fernanda Abreu**, Instituto de Microbiologia Professor Paulo de Góes, Universidade Federal do Rio de Janeiro, 21941-590 Rio de Janeiro, Brazil, abreufernandadeavila@hotmail.com

**Gurunathan Sangiliyandi**, Department of Biotechnology, Kalasalingam University, Anand Nagar, Krishnankoil 626190, Tamil Nadu, India, lvsangs@yahoo.com

**Irena H. Maliszewska**, Chemical Faculty Wybrzeze, Wrocław University of Technology, Wyspiańskiego 27, 50370 Wrocław, Poland; Division of Medicinal Chemistry and Microbiology, Faculty of Chemistry, Wrocław University of Technology, Wyspiańskiego 27, 50-370 Wrocław, Poland, irena.helena.maliszewska@pwr.wroc.pl

**Iliasov P.**, G. K. Skryabin Institute of Biochemistry and Physiology of Microorganisms, RAS, 142290, Pushchino, Nauki Av., 5, Russia

**Kalimuthu Kalishwaralal**, Department of Biotechnology, Kalasalingam University, Anand Nagar, Krishnankoil 626190, Tamil Nadu, India

**Maggy F. Lengke**, Geomega Inc., 2525 28th Street, Suite 200, Boulder, CO 80301, USA, maggylengke@yahoo.com

**Mahendra Rai**, Department of Biotechnology, Sant Gadge Baba Amravati University, Amravati-444 602, Maharashtra, India, mkrai123@rediffmail.com, pmkrai@hotmail.com

**Mojtaba Shakibaie**, Department of Pharmaceutical Biotechnology and Biotechnology Research Center, Tehran University of Medical Sciences, Tehran, Iran; Department of Pharmaceutical Biotechnology, Kerman University of Medical Sciences, P.O. Box 76175-493, Kerman, Iran, m\_shakibaie@razi.tums.ac.ir

**N. Vigneshwaran**, Chemical and Biochemical Processing Division, Central Institute for Research on Cotton Technology, Adenwala Road, Matunga, Mumbai, Maharashtra 400019, India, nvw75@yahoo.com

**Nelson Durán**, Chemistry Institute, Biological Chemistry Laboratory, Universidade Estadual de Campinas, C.P. 6154, CEP 13083-970 Campinas, São Paulo, Brazil; Natural Science and Humanity Center, Universidade Federal de ABC, Santo Andre CEP 09.210-170, São Paulo, Brazil, duran@iqm.unicamp.br

**Nikolay Krumov**, Department of Bioprocess Engineering, Institute of Process Engineering in Life Sciences, Karlsruhe Institute of Technology, Fritz-Haber-Weg 2, build. 30.44, Karlsruhe, Germany, nikolay.krumov@kit.edu

**Pardis Nazari**, Department of Pharmaceutical Biotechnology and Biotechnology Research Center, Tehran University of Medical Sciences, Tehran, Iran, pnazari@razi.tums.ac.ir

**Prateek Jain**, Chemical and Biochemical Processing Division, Central Institute for Research on Cotton Technology, Adenwala Road, Matunga, Mumbai, Maharashtra, 400019, India

**Priscyla D. Marcato**, Chemistry Institute, Biological Chemistry Laboratory, Universidade Estadual de Campinas, C.P. 6154, CEP 13083-970 Campinas, São Paulo, Brazil, pmarcato@gmail.com

**Reshetilov A.**, G. K. Skryabin Institute of Biochemistry and Physiology of Microorganisms, RAS, 142290, Pushchino, Nauki Av., 5, Russia, anatol@ibpm.pushchino.ru

**Reshetilova T.**, G. K. Skryabin Institute of Biochemistry and Physiology of Microorganisms, RAS, 142290, Pushchino, Nauki Av., 5, Russia

**Siddhartha Shrivastava**, Department of Biochemistry, Institute of Medical Sciences, Banaras Hindu University, Varanasi, Uttar Pradesh 221005, India

**Sunil K. Singh**, Department of Biochemistry, Institute of Medical Sciences, Banaras Hindu University, Varanasi, Uttar Pradesh 221005, India

**Sureshbabu Ram Kumar Pandian**, Department of Biotechnology, Kalasalingam University, Anand Nagar, Krishnankoil 626190, Tamil Nadu, India

**Tamsyn Riddin**, Department of Biochemistry, Microbiology and Biotechnology, Rhodes University, P.O.Box 94, Grahamstown 6140, South Africa

**Ulysses Lins**, Instituto de Microbiologia Professor Paulo de Góes, Universidade Federal do Rio de Janeiro, 21941-590 Rio de Janeiro, Brazil, ulins@micro.ufrj.br

**Venkataraman Deepak**, Department of Biotechnology, Kalasalingam University, Anand Nagar, Krishnankoil 626190, Tamil Nadu, India

**Yageshni Govender**, Department of Biochemistry, Microbiology and Biotechnology, Rhodes University, P.O.Box 94, Grahamstown 6140, South Africa

**Zygmunt Sadowski**, Chemical Faculty Wybrzeze, Wrocław University of Technology, Wyspińskiego 27, 50370 Wrocław, Poland, zygmunt.sadowski@pwr.wroc.pl

# Chapter 1

## Biogenic Nanoparticles: An Introduction to What They Are, How They Are Synthesized and Their Applications

Mahendra Rai, Aniket Gade, and Alka Yadav

### 1.1 Introduction

The field of nanotechnology is an immensely developing field as a result of its wide-ranging applications in different areas of science and technology. The term nanotechnology is defined as the creation, exploitation and synthesis of materials at a scale smaller than 1  $\mu\text{m}$ . The word “nano” is derived from a Greek word meaning dwarf or extremely small (Rai et al. 2008). The concept of nanotechnology was given by physicist Professor Richard Feynman in his historic talk “there’s plenty of room at the bottom” (Feynman 1959), though the term nanotechnology was introduced by Tokyo Science University Professor Norio Taniguchi (Taniguchi 1974). Nanobiotechnology is a multidisciplinary field and involves research and development of technology in different fields of science like biotechnology, nanotechnology, physics, chemistry, and material science (Huang et al. 2007; Rai et al. 2008). Nanoparticles are metal particles with size 1–100 nm and exhibit different shapes like spherical, triangular, rod, etc. Research on synthesis of nanoparticles is the current area of interest due to the unique visible properties (chemical, physical, optical, etc.) of nanoparticles compared with the bulk material (Rai et al. 2009a; Sau and Rogach 2010).

Progress in the field of nanotechnology has been rapid and with the development of innovative synthesis protocols and characterization techniques (Sharma et al. 2009). But most of the synthesis methods are limited to synthesis of nanoparticles in small quantities and poor morphology (Sau and Rogach 2010). Chemical and physical synthesis methods often result in synthesis of a mixture of nanoparticles with poor morphology, and these methods also prove to be toxic to the environment due to the use of toxic chemicals and also of elevated temperatures for synthesis process (Rai et al. 2008; Birla et al. 2009). Biogenic synthesis of nanoparticles with controlled morphology needs more attention, as the biogenic synthesis of

---

M. Rai (✉), A. Gade, and A. Yadav

Department of Biotechnology, Sant Gadge Baba Amravati University, Amravati 444 602, Maharashtra, India

e-mail: mkrai123@rediffmail.com; pmkrai@hotmail.com

nanoparticles is carried out by using biological means like bacteria (Husseiny et al. 2007; Shahverdi et al. 2007, 2009), fungi (Kumar et al. 2007a, b; Parikh et al. 2008; Gajbhiye et al. 2009; Govender et al. 2009), actinomycetes (Ahmad et al. 2003a, b), lichens (Shahi and Patra 2003), algae (Singaravelu et al. 2007; Chakraborty et al. 2009), etc. The biogenic entities are found to secrete large amount of proteins which are found to be responsible for metal-ion reduction and morphology control (Thakkar et al. 2010). The microbial cultures are easy to handle and also the downstream processing of biomass is simpler as compared to the synthetic methods (Ingle et al. 2008). Biogenic nanoparticles are toward a greener approach and environment friendly, as no toxic chemical is involved in synthesis, and also the synthesis process takes place at ambient temperature and pressure conditions (Gade et al. 2008; Mukherjee et al. 2008). Hence, a number of researchers are focusing toward the synthesis of biogenic nanoparticles compared with the chemically or physically synthesized nanoparticles (Sastry et al. 2003; Bhattacharya and Gupta 2005; Riddin et al. 2006; Duran et al. 2007; Ingle et al. 2008; Kumar and Yadav 2009; Thakkar et al. 2010).

## 1.2 Methods of Synthesis of Nanoparticles

Owing to the wide range of applications offered by nanoparticles in different fields of science and technology, different protocols have been designed for their synthesis (Reddy 2006). The nanoparticles can be synthesized using the top-down (physical) approach which deals with methods such as thermal decomposition, diffusion, irradiation, arc discharge, etc., and bottom-up (chemical and biological) approach which involves seeded growth method, polyol synthesis method, electrochemical synthesis, chemical reduction, and biological entities for fabrication of nanoparticles. Different synthesis methods involve the use of different types of chemical, physical, and biological agents to yield nanoparticles of different sizes and shapes.

The most often used method for the chemical synthesis of nanoparticles is the chemical reduction method, which deals with the reduction of metal particles to nanoparticles using chemical reducing agents like sodium borohydride or sodium citrate (Jana et al. 2000; Cao and Hu 2009). Other chemical agents utilized for the synthesis are *N,N*-dimethyl formamide (DMF) (Pastoriza-Santos and Liz-Marzan 2000), poly(*N*-vinyl pyrrolidone) (PVP), ethyl alcohol (Kim 2007), tetra-*n*-tetrafluoroborate (TFATFB), CTAB (Hanauer et al. 2007), etc. Seeded growth method is a colloid chemical method for the synthesis of nanoparticles which involve preparation of seeds by reducing metal ions with the suitable reducing agent. The fine particles so formed are called seed particles which are then added to growth solutions containing metal ions and additives like L-ascorbic acid and hexadecyltrimethylammonium bromide (CTAB) (Hanauer et al. 2007). Polyol is also used in the synthesis of nanoparticles. In the polyol method a metal precursor is dissolved in a liquid polyol in the presence of capping agent. The metal sol is prepared using methanol or ethyl alcohol as a solvent and reducing agent while PVP is used as a

protective and capping agent (Kim 2007). Electrochemical synthesis method induces chemical reactions in an electrolyte solution with the use of an applied voltage. A wide variety of nanomaterials could be synthesized using this method (Rodríguez-Sánchez et al. 2000; Sau and Rogach 2010).

Physical methods used for the synthesis of nanoparticles include thermal decomposition, laser irradiation, electrolysis, condensation, diffusion, etc. The thermal decomposition method is used for the synthesis of monodisperse nanoparticles. Fatty acids are dissolved in hot NaOH solution and mixed with metal salt solution which leads to formation of metal precipitate (Yang and Aoki 2005). In diffusion method, crystals and short wires of copper are enclosed in glass ampoules and sealed at low pressure; further, the ampoules are annealed at 500°C for 24 h. The crystals are removed from the ampoules and cooled on a metallic plate at room temperature. The so formed crystals are further characterized (Rodríguez-Perez et al. 2006). In the UV irradiation technique, polycarbonate films are cut and placed on glass microscope slide and exposed to UV radiation which results in the formation of hydroxyl groups on polycarbonate films. Further, these polycarbonate films are silanized with 3-(aminopropyl) triethoxysilane (APS) in denatured ethanol for 2 h and rinsed with deionised water which leads to the formation of silver film on the polycarbonate film (Aslan et al. 2006). The arc-discharge method involves use of two graphite electrodes which act as cathode and anode and are immersed in metal salt solution. The electrodes are brought in contact to strike an arc and separated immediately to sustain arc inside salt solution. The synthesis of nanoparticles is carried out at an open circuit and an optimized direct current (Fernandez-Pacheco et al. 2006; Ashkarran et al. 2009).

Biological agents used for the synthesis of nanoparticles include mainly microbes (Sastry et al. 2003; Konishi et al. 2004; Lengke and Southam 2006; Duran et al. 2007; Ingle et al. 2008; Birla et al. 2009; Gajbhiye et al. 2009) and plants (Gardea-Torresedey et al. 2003; Shankar et al. 2004; Chandran et al. 2006; Huang et al. 2007; Song and Kim 2009; Bar et al. 2009a, b; Jha et al. 2009). The biological methods used for the synthesis of nanoparticles include both extracellular and intracellular methods (Ahmad et al. 2003a, b; Rai et al. 2008; Mukherjee et al. 2008; Shaligram et al. 2009). The synthesis of nanoparticles using bacteria and actinomycetes usually involves the intracellular synthesis method. In which the bacterial cell filtrate is treated with metal salt solution and kept in a shaker in dark at ambient temperature and pressure conditions (Nair and Pradeep 2002; Ahmad et al. 2003a, b; Mouxing et al. 2006). For the extracellular synthesis of nanoparticles using bacteria, the bacterial culture is centrifuged at  $8,000 \times g$  and the supernatant is challenged with metal salt solution (Kalishwaralal et al. 2008; Das et al. 2009; Ogi et al. 2010). In case of fungi also nanoparticles are intracellularly synthesized by treating the fungal mycelium with metal salt solution and further incubation for 24 h (Mukherjee et al. 2001). Dried mycelium of fungi is also used for synthesis of nanoparticles. In this method the fungal mycelium is harvested by centrifugation and subsequently freeze dried, and this freeze-dried mycelium is immersed in metal salt solution and kept on a shaker (Chen et al. 2003). However, in the extracellular method the filtrate of the mycelium is treated with metal salt solution and incubated

for 24 h (Basavaraja et al. 2007; Fayaz et al. 2009; Shaligram et al. 2009). In algal synthesis of nanoparticles washed culture of algae without the presence of any medium is treated with metal salt solution and kept in dark with controlled pH and temperature conditions (Singaravelu et al. 2007; Govindraju et al. 2008; Thakkar et al. 2010). The synthesis of nanoparticles using yeast involves two steps which include firstly the synthesis of nanoparticles and next recovery of the synthesized nanoparticles (Kowshik et al. 2003). For the synthesis process, yeast culture is challenged with metal salt solution and incubated in dark for 24 h. Further, the cells are separated from the medium by centrifugation and the cell-free extract is used for recovery of nanoparticles. For recovery of nanoparticles, specifically designed apparatus (polycarbonate bottle with sampling cup) is used, which separates nanoparticles from the extract by differences in thawing temperature. The cell-free medium containing nanoparticles is filled in the bottle up to the brim and kept at  $-20^{\circ}\text{C}$  in upright position. During freezing, the nanoparticles get denser than medium and settle down. The bottle is then kept at  $0^{\circ}\text{C}$  and allowed to thaw. The concentrated colloidal solution obtained in the sampling cup is centrifuged at  $23,000 \times g$  for 24 h, the particles are suspended in distilled water, and further the particles are dried in vacuum.

### 1.3 Superiority of Biological Methods

Different types of physical and chemical methods are employed for the synthesis of nanoparticles. The use of these synthesis methods requires both strong and weak chemical reducing agents and protective agents (sodium borohydride, sodium citrate and alcohols) which are mostly toxic, flammable, cannot be easily disposed off due to environmental issues and also show a low production rate (Mohanpuria et al. 2008; Rai et al. 2008; Sharma et al. 2009; Bar et al. 2009b). For example, in the seeded growth method chemical reducing agents like sodium citrate and sodium borohydride (Jana et al. 2000) are used, whereas in the polyol synthesizing process methanol and ethanol are used (Kim 2007). Moreover, these are capital intensive and are inefficient in materials and energy use (Ingle et al. 2008). In addition, in many cases, synthesis is carried out at elevated temperatures, which generate a large amount of heat. For example, in thermal decomposition method, synthesizing process is carried out at very high temperature (Yang and Aoki 2005).

The biological method for the synthesis of nanoparticles employs use of biological agents like bacteria, fungi, actinomycetes, yeast and plants (Rai et al. 2008; Thakkar et al. 2010). Thus, the biological method provides a wide range of resources for the synthesis of nanoparticles. The rate of reduction of metal ions using biological agents is found to be much faster and also at ambient temperature and pressure conditions. For instance, in case of synthesis of nanoparticles using *Aspergillus niger* synthesis of silver nanoparticles was observed within 2 h of treatment of fungal filtrate with silver salt solution (Gade et al. 2008). Thus, the biological method requires minimum time for synthesis of nanoparticles.



Shape- and size-controlled nanoparticles could be synthesized by modulating the pH or the temperature of the reaction mixture. Gericke and Pinches (2006) obtained different shape morphologies (triangle, hexagons, spheres, and rods) by modulating the pH of reaction mixture to 3, 5, 7 and 9. Riddin et al. (2006) also demonstrated that at 65°C temperature less amount of nanoparticles were synthesized, whereas at 35°C temperature more amount of nanoparticles were synthesized.

The biological agents secrete a large amount of enzymes, which are capable of hydrolyzing metals and thus bring about enzymatic reduction of metals ions (Rai et al. 2009b). In case of fungi, the enzyme nitrate reductase is found to be responsible for the synthesis of nanoparticles (Kumar et al. 2007a, b).

The biomass used for the synthesis of nanoparticles is simpler to handle, gets easily disposed of in the environment and also the downstream processing of the biomass is much easier. Synthesis can be carried out at ambient temperature and pressure conditions that require less amounts of chemical (Ingle et al. 2008). The synthesizing process is less labor-intensive, low-cost technique, nontoxic and is more of a greener approach.

Thus, considering the above points the biological method employed for the synthesis of nanoparticles proves to be superior compared with the physical and chemical methods of synthesis due to its environment friendly approach and also as a low cost technique.

## 1.4 Mechanism of Synthesis

The exact mechanism for the synthesis of nanoparticles using biological agents has not been devised yet as different biological agents react differently with metal ions and also there are different biomolecules responsible for the synthesis of nanoparticles. In addition, the mechanism for intra- and extracellular synthesis of nanoparticles is different in various biological agents.

The cell wall of the microorganisms play a major role in the intracellular synthesis of nanoparticles. The cell wall being negatively charged interacts electrostatically with the positively charged metal ions. The enzymes present within the cell wall bioreduce the metal ions to nanoparticles, and finally the smaller sized nanoparticles get diffused of through the cell wall. Mukherjee et al. (2001) reported stepwise mechanism for intracellular synthesis of nanoparticles using *Verticillium* sp. The author divided the mechanism of synthesis of nanoparticles into trapping, bioreduction and synthesis. The fungal cell surface when comes in contact with metal ions interacts electrostatically and traps the ions. Next, the enzymes present in the cell wall bioreduce the metal ions. Finally, aggregation of particles and synthesis of nanoparticles take place. Moreover, Nair and Pradeep (2002), in the case of bacteria *Lactobacillus* sp., observed that during the initial step of synthesis of nanoparticles, nucleation of clusters of metal ions takes place, and hence there is an electrostatic interaction between the bacterial cell and metal clusters which leads to the formation of nanoclusters. Lastly, the smaller sized nanoclusters get diffused

through the bacterial cell wall. In actinomycetes also, the reduction of metal ions occur on the surface of mycelia along with cytoplasmic membrane leading to the formation of nanoparticles (Ahmad et al. 2003a, b). Sintubin et al. (2009) proposed the mechanism for the synthesis of silver nanoparticles by using lactic acid bacteria. According to them whenever pH increases, more competition occurs between protons and metal ions for negatively charged binding sites.

The mechanism of extracellular synthesis of nanoparticles using microbes is basically found to be nitrate reductase-mediated synthesis. The enzyme nitrate reductase secreted by the fungi helps in the bioreduction of metal ions and synthesis of nanoparticles. A number of researchers supported nitrate reductase for extracellular synthesis of nanoparticles (Duran et al. 2005; Kumar et al. 2007a, b; He et al. 2007; Gade et al. 2008; Ingle et al. 2008). Duran et al. (2005) conducted the nitrate reductase assay test through the reaction of nitrite with 2,3-diaminophthalene. The emission spectrum demonstrated two major peaks of fluorescence intensity at 405 and 490 nm relating to the maximum emission of nitrite and 2,3-diaminonaphthotriazole (DAN), respectively. The intensity of these two bands was found to be increased with the addition of a 0.1%  $\text{KNO}_3$  solution, confirming the presence of nitrate reductase. Thus, it was concluded that the enzyme reductase is responsible for the reduction of  $\text{Ag}^+$  ions and the subsequent formation of silver nanoparticles. The findings of Duran et al. (2005) were further confirmed by Ingle et al. (2008); in the study, commercially available nitrate reductase disks were used; the color of the disk turned reddish from white when challenged with fungal filtrate signifying the presence of nitrate reductase. Thus, it can be concluded that the enzyme a NADH-dependent reductase is associated with reduction of  $\text{Ag}^+$  to  $\text{Ag}^0$  in the case of fungi.

A similar mechanism was also reported in the case of extracellular synthesis of gold nanoparticles using *Rhodospseudomonas capsulata* (He et al. 2007). The bacterium *R. capsulata* is known to secrete cofactor NADH and NADH-dependent enzymes. The bioreduction of gold ions was found to be initiated by the electron transfer from the NADH by NADH-dependent reductase as electron carrier. Next, the gold ions obtain electrons and are reduced to Au (0) and hence result in the formation of gold nanoparticles. Nangia et al. (2009) proposed the synthesis of gold nanoparticles by bacterium *Stenotrophomonas maltophilia*. The authors suggested that the biosynthesis of gold nanoparticles and their stabilization via charge capping in *S. maltophilia* involved NADPH-dependent reductase enzyme which converts  $\text{Au}^{3+}$  to  $\text{Au}^0$  through electron shuttle enzymatic metal reduction process.

Synthesis of CdS nanoparticles using *Schizosaccharomyces pombe* has been considered to be dependent on a stress protein response (Kowshik et al. 2002). Enzyme phytochelatin gets activated on exposure of *S. pombe* to cadmium and synthesizes phytochelatins. These phytochelatins chelate the cytoplasmic cadmium to phytochelatin–Cd complex. Next, an ATP-binding cassette-type vacuolar protein transports phytochelatin–Cd complex across the vacuolar membrane. Inside the vacuole sulfide gets added to the complex to form a high-molecular-weight phytochelatin–CdS<sup>-2</sup> complex or CdS nanocrystal.

Mukherjee et al. (2008) reported a possible mechanism on encapsulation of nanoparticles using the Raman spectrum. The Raman spectra clearly indicated

that C=O bonds of carboxylate ions and Ag–N bonds from the free amine groups lie perpendicular to the nano silver surface and get directly associated with the capping of silver nanoparticles. Broadened symmetric and asymmetric bands of  $\text{CO}_2^-$  were observed, which resulted due to distortion of respective bonds and encapsulation of silver nanoparticles. The absence of peak at Ag–S vibration clearly indicated that disulfide linkages do not play any role in stabilization. Thus, the authors conclude that some of the peptide linkages from amino acids undergo hydrolysis to synthesize free carboxylate ions and free amino groups which possibly act in the encapsulation of silver nanoparticles.

## 1.5 Multiple Functionalities of Nanoparticles

Nanotechnology is an integration of different fields of science which holds promise in the pharmaceutical industry, medicine and agriculture (Mohanpuria et al. 2008). The unique properties of nanoparticles different from the bulk material have attracted the attention of several workers to harness the multiple functionalities of nanoparticles.

- Silver nanoparticles are utilized in the area of electronics, silica-coated Ag nanowires, and electric circuits (Kvistek and Pucek 2005).
- Colloidal gold nanoparticles can be used in the treatment of cancer therapy and arthritis.
- Detection of viruses is generally performed by either antigens (immunoassays) or genome sequences (polymerase chain reaction-based methods). However, sensitivity of such detection techniques is a problematic issue. Valanne et al. (2005) reported a novel sandwich-enzyme linked immunosorbent method for direct detection of adenoviruses with the help of covalently coated monoclonal anti-hexon antibodies onto highly fluorescent europium (III)-chelate doped nanoparticles (~107 nm) (Saini et al. 2006).
- The technique of nanofiltration is a novel method to remove both enveloped and non-enveloped viruses (Hennebel et al. 2009). Omar and Kempf (2002) reported removal of IgG-coated non-enveloped viruses including bovine parvovirus and bovine enterovirus with the help of 20- and 50-nm-sized nanofilters (Saini et al. 2006).
- Gold nanoparticles due to its biocompatibility and strong interaction with soft bases like thiols play a major role in the treatment of cancer (Bhattacharya and Mukherjee 2008). Epithelial ovarian cancer a common malignancy of female genital tract could be cured with the use of gold nanoparticles. Vascular endothelial growth factor (VEGF) performs a vital role in the progression of ovarian cancer and also tumor growth and gold nanoparticles possess the capability to inhibit the progression of ovarian growth and metastasis (Bamberger and Perrett 2002; Bhattacharya and Mukherjee 2008). Also, in case of multiple myeloma (MM), a cancer of plasma cells, gold nanoparticles are observed to inhibit the

function of VEGF which induces cell proliferation. This inhibition of VEGF further leads to upregulation of cell cycle inhibitor proteins like p21 and p27 which inhibit proliferation (Bhattacharya et al. 2007; Bhattacharya and Mukherjee 2008).

- Chronic lymphocytic leukemia (CLL), a cancer caused due to the overproduction of lymphocytes. Chronic leukemia starts in the bone marrow but could spread to other organs also. It was reported that as gold nanoparticles possess the ability to inhibit the function of heparin-based growth factor, gold nanoparticles alone can inhibit the function of factors secreted by CLL cells and induce apoptosis (Zent et al. 2006; Bhattacharya et al. 2007; Bhattacharya and Mukherjee 2008).
- Rheumatoid arthritis which is considered as an incurable disease, bare gold nanoparticles are found to serve as a possible cure. Tsai et al. (2007) reported that naked gold nanoparticles possess the capacity to inhibit VEGF-induced proliferation. It also significantly reduces macrophage infiltration into synovium (Bhattacharya and Mukherjee 2008).
- Nanoparticles can be used in the construction of miniaturized devices, which can be helpful in drug delivery (Nair and Laurencin 2007).
- Thiol-stabilized nanoparticles are used as “bio-catalyst” (Brust and Kiely 2002). Nanoparticles can be used as fluorescence labeling system in microbial detection (Liu 2006). Nanoparticles can be widely used as signal reporters to detect biomolecules in DNA assay, immunoassay and cell bioimaging (Liu 2006).
- Catheters coated with nanocrystalline silver serve as a tool to prevent infections. Silver nanoparticles are found to be active against most of the noscomial infections related to catheters and also predominantly accumulate at the site of insertion. Thus, silver nanoparticles function as a protective agent against infection with no risk of systemic toxicity (Roe et al. 2008).
- Nanosilver dressings are found to induce major improvements in the healing of wounds with respect to antimicrobial efficiency, ease in using and faster re-epithelialization (Marazzi et al. 2007). It was reported that re-epithelialization in a patient with a third-degree burn was observed as a result of the treatment of nanosilver dressing as it provided a protection against infections and also promoted early formation of neodermis and uncomplicated wound closure (Marazzi et al. 2007; Rai et al. 2009a).
- Zirconium is a particularly hard metal and used as a hard abrasive surface for micro-cutting tools or for high-temperature coatings in engine components (Bansal et al. 2004).
- Titanium nanoparticles have practical applications in many forms of transport such as automobiles, aircraft, ships, etc. Titanium nanoparticles are also particularly useful for the production of pigments, paints and cosmetics (Bansal et al. 2005; Prasad et al. 2007).
- The bone cells are accustomed to interact with nanostructured materials as the collagen fibrils, hydroxyapatite and proteoglycans found in bone tissues are in the nanometer scale. Hence, nanomaterials like alumina and titania are efficiently used for the regeneration and repair of bone tissues (Sato and Webster

2004). It is observed that the bone cells could recognize and elicit desired cellular functions like adhesion, migration and proliferation as nanomaterials possess the capability to mimic the dimensions of constituent components of bone (Balasundaram and Webster 2006). Some examples of bone implants include nanoceramics, nanopolymers, nanometals and composites (Laurencin et al. 2008).

## 1.6 Key Areas of Research

The synthesis of nanoparticles using the biosynthetic route is an environmental-friendly method compared with the chemical and physical methods, but there are certain key areas of research which need to be pointed out. The synthesis of biogenic nanoparticles using the biological agents involve both intracellular and extracellular methods, and the mechanism for both the methods is yet unknown. In the intracellular method of synthesis, the exact role of microbial and plant cell wall should be to be elucidated, whereas, in case of extracellular synthesis using microbes the role of other fungal enzymes in the synthesis of nanoparticles needs to be studied. In extracellular synthesis of nanoparticles a number of reducing and capping agents are found to be involved. The effect of these reducing agents on the shape and size of nanoparticles also need to be clarified. The effect of different factors on the dispersity of nanoparticles deserves further research. The size of nanoparticles also plays a key role in the determination of its activity. For example, in case of HIV-1 infections, silver nanoparticles interact in a size-dependent manner; hence, the size of the nanoparticles should also be considered as a determining factor during the synthesis of nanoparticles. The yield of nanoparticles obtained using a particular system modulates the efficiency of the system for the synthesis of nanoparticles; thus, the yield is a major concern.

## 1.7 Conclusion

Different tools of nanotechnology show the capability of synthesizing nanoscale materials with specific physical, chemical, and optoelectronic properties. Various physical and chemical methods have been designed for the synthesis of nanoparticles, but the different problems related to these methods have made the researchers to search for alternative methods. The biological agents in the form of microbes have emerged up as an efficient candidate for the synthesis of nanoparticles. These biogenic nanoparticles are cost efficient, simpler to synthesize, and focus toward a greener approach. But the exact mechanism of synthesis of biogenic nanoparticles needs to be worked out. Hence, a detailed study to elucidate the exact mechanism for the synthesis of nanoparticles needs to be carried out, as different microbial agents react differently during the synthesis of nanoparticles. Thus, drafting the

different issues and the reducing agents related to the synthesis of biogenic nanoparticles would help in developing the biosynthetic route as the most efficient method for the synthesis of nanoparticles.

**Acknowledgments** We thank Rajiv Gandhi Science and Technology Commission Mumbai, Govt. of Maharashtra for the financial support.

## References

- Ahmad A, Mukherjee P, Senapati S, Mandal D, Khan MI, Kumar R, Sastry M (2003a) Extracellular biosynthesis of silver nanoparticles using the fungus *Fusarium oxysporum*. *Colloids Surf B* 28:313–318
- Ahmad A, Senapati S, Khan MI, Kumar R, Ramani R, Shrinivas V, Sastry M (2003b) Intracellular synthesis of gold nanoparticles by a novel alkalotolerant actinomycete, *Rhodococcus* species. *Nanotechnology* 14:824–828
- Ashkarran AA, Zad AI, Mahdavi SM, Ahadian MM, Nezhad MRH (2009) Rapid and efficient synthesis of colloidal gold nanoparticles by arc discharge method. *Appl Phys A: Mater Sci Process* 96(2):423–428
- Aslan K, Holley P, Geddes CD (2006) Metal-enhanced fluorescence from silver nanoparticle-deposited polycarbonate substrates. *J Mater Chem* 16:2846–2852
- Balasundaram G, Webster TJ (2006) Nanotechnology and biomaterials for orthopedic medical applications. *Nanomedicine* 1(2):169–176
- Bamberger ES, Perrett CW (2002) Angiogenesis in epithelial ovarian cancer. *Mol Pathol* 55:348–359
- Bansal V, Rautray D, Ahamd A, Sastry M (2004) Biosynthesis of zirconia nanoparticles using the fungus *Fusarium oxysporum*. *J Mater Chem* 14:3303–3305
- Bansal V, Rautray D, Bharde A, Ahire K, Sanyal A, Ahmad A, Sastry M (2005) Fungus-mediated biosynthesis of silica and titania particles. *J Mater Chem* 15:2583–2589
- Bar H, Bhui DK, Sahoo GP, Sarkar P, De SP, Misra A (2009a) Green synthesis of silver nanoparticles using latex of *Jatropha curcas*. *Colloids Surf A: Physicochem Eng Asp* 339:134–139
- Bar H, Bhui DK, Sahoo GP, Sarkar P, Pyne S, Misra A (2009b) Green synthesis of silver nanoparticles using seed extract of *Jatropha curcas*. *Colloids Surf A: Physicochem Eng Asp* 348:212–216
- Basavaraja S, Balaji SD, Lagashetty A, Rajasab AH, Venkataraman A (2007) Extracellular biosynthesis of silver nanoparticles using the fungus *Fusarium semitectum*. *Mater Res Bull* 43(5):1164–1170
- Bhattacharya D, Gupta RK (2005) Nanotechnology and potential of microorganisms. *Crit Rev Biotechnol* 24(4):199–204
- Bhattacharya R, Mukherjee P (2008) Biological properties of naked nanoparticles. *Adv Drug Deliv Rev* 60:1289–1306
- Bhattacharya R, Patra CR, Verma R, Griep PR, Mukherjee P (2007) Gold nanoparticles inhibit the proliferation of multiple myeloma cells. *Adv Mater* 19:711–716
- Birla SS, Tiwari VV, Gade AK, Ingle AP, Yadav AP, Rai MK (2009) Fabrication of silver nanoparticles by *Phoma glomerata* and its combined effect against *Escherichia coli Pseudomonas aeruginosa* and *Staphylococcus aureus*. *Lett Appl Microbiol* 48:173–179
- Brust M, Kiely CJ (2002) Some recent advances in nanostructure preparation from gold and silver particles: a short topical review. *Colloids Surf A: Physicochem Eng Asp* 202:175–186
- Cao J, Hu X (2009) Synthesis of gold nanoparticles using halloysites. *e-J Surf Sci Nanotechnol* 7:813–815

- Chakraborty N, Banerjee A, Lahiri S, Panda A, Ghosh AN, Pal R (2009) Biorecovery of gold using cyanobacteria and eukaryotic alga with special reference to nanogold formation – a novel phenomenon. *J Appl Phycol* 21(1):145–152
- Chandran SP, Ahmad A, Chaudhary M, Pasricha R, Sastry M (2006) Synthesis of gold nanoparticles and silver nanoparticles using *Aloe vera* plant extract. *Biotechnol Prog* 22(2):577–583
- Chen JC, Lin ZH, Ma XX (2003) Evidence of the production of silver nanoparticles via pretreatment of *Phoma* sp 32883 with silver nitrate. *Lett Appl Microbiol* 37:105–108
- Das SK, Das AR, Guha AK (2009) Gold nanoparticles: microbial synthesis and applications in water hygiene management. *Langmuir* 25(14):8192–8199
- Duran N, Marcato PD, Alves OL, DeSouza G, Esposito E (2005) Mechanistic aspects of biosynthesis of silver nanoparticles by several *Fusarium oxysporum* strains. *J Nanobiotechnol* 3:1–8
- Duran N, Alves OL, De Souza GIH, Esposito E, Marcato PD (2007) Antibacterial effect of silver nanoparticles by fungal process on textile fabrics and their effluent treatment. *J Biomed Nanotechnol* 3:203–208
- Fayaz AM, Balaji K, Girilal M, Kalaichelvan PT, Venkatesan R (2009) Mycobased synthesis of silver nanoparticles and their incorporation into sodium alginate films for vegetable and fruit preservation. *J Agric Food Chem* 57:6246–6252
- Fernandez-Pacheco R, Arruebo M, Marquina C, Ibarra R, Arbiol J, Santamaria J (2006) Highly magnetic silica-coated iron nanoparticles prepared by the arc-discharge method. *Nanotechnology* 17:1188–1192
- Feynman R (1959) Lecture at the California Institute of Technology, December 29
- Gade AK, Bonde P, Ingle AP, Marcato PD, Duran N, Rai MK (2008) Exploitation of *Aspergillus niger* for synthesis of silver nanoparticles. *J Biobased Mater Bioenergy* 2:243–247
- Gajbhiye M, Kesharwani J, Ingle A, Gade A, Rai M (2009) Fungus-mediated synthesis of silver nanoparticles and their activity against pathogenic fungi in combination with fluconazole. *Nanomed Nanotechnol Biol Med* 5:382–386
- Gardea-Torresedey JL, Gomez E, Jose-Yacamán M, Parsons JG, Peralta-Videa JR, Tioani H (2003) Alfalfa sprouts: a natural source for the synthesis of silver nanoparticles. *Langmuir* 19:1357–1361
- Gericke M, Pinches A (2006) Microbial production of gold nanoparticles. *Gold Bull* 39(1):22–28
- Govender Y, Riddin T, Gericke M, Whiteley CG (2009) Bioreduction of platinum salts into nanoparticles: a mechanistic perspective. *Biotechnol Lett* 31:95–100
- Govindraju K, Basha SK, Kumar VG, Singaravelu G (2008) Silver, gold and bimetallic nanoparticles production using single-cell protein (*Spirulina platensis*) Geitler. *J Mater Sci* 43:5115–5122
- Hanauer M, Lotz A, Pierrat S, Sonnichsen C, Zins I (2007) Separation of nanoparticles by gel electrophoresis according to size and shape. *Nano Lett* 7(9):2881–2885
- He S, Guo Z, Zhang Y, Zhang S, Wang J, Gu N (2007) Biosynthesis of gold nanoparticles using the bacteria *Rhodospseudomonas capsulata*. *Mater Lett* 61:3984–3987
- Hennebel T, Gussemé BT, Boon N, Verstraete W (2009) Biogenic metals in water treatment. *Trends Biotechnol* 27(2):90–98
- Huang J, Chen C, He N, Hong J, Lu Y, Qingbiao L, Shao W, Sun D, Wang XH, Wang Y, Yiang X (2007) Biosynthesis of silver and gold nanoparticles by novel sundried *Cinnamomum camphora* leaf. *Nanotechnology* 18:105–106
- Husseyin MI, El-Aziz MA, Badr Y, Mahmoud MA (2007) Biosynthesis of gold nanoparticles using *Pseudomonas aeruginosa*. *Spectrochim Acta A: Mol Biomol Spectrosc* 67:1003–1006
- Ingle A, Gade A, Pierrat S, Sonnichsen C, Rai MK (2008) Mycosynthesis of silver nanoparticles using the fungus *Fusarium acuminatum* and its activity against some human pathogenic bacteria. *Curr Nanosci* 4:141–144
- Jana NR, Pal T, Sau TK, Wang ZL (2000) Seed-mediated growth method to prepare cubic copper nanoparticles. *Curr Sci* 79(9):1367–1370
- Jha AK, Prasad K, Prasad K, Kulkarni AR (2009) Plant system: nature's nanofactory. *Colloids Surf B: Biointerfaces* 73:219–223

- Kalishwaralal K, Deepak V, Ramkumarpandian S, Nellaiah H, Sangiliyandi G (2008) Extracellular biosynthesis of silver nanoparticles by the culture supernatant of *Bacillus licheniformis*. *Mater lett* 62:4411–4413
- Kim JS (2007) Antibacterial activity of Ag<sup>+</sup> ion-containing silver nanoparticles prepared using the alcohol reduction method. *J Ind Eng Chem* 13(4):718–722
- Konishi Y, Nomura T, Tsukiyama T, Saioto N (2004) Microbial preparation of gold nanoparticles by anaerobic bacterium. *Trans Mater Res Soc Japan* 29:2341–2343
- Kowshik M, Deshmukh N, Kulkarni SK, Paknikar KM, Vogel W, Urban J (2002) Microbial synthesis of Semiconductor CdS nanoparticles, their characterization, and their use in fabrication of an ideal diode. *Biotechnol Bioeng* 78(5):583–588
- Kowshik M, Ashatapatre S, Kharrazi S, Kulkarni SK, Paknikari KM, Vogel W, Urban J (2003) Extracellular synthesis of silver nanoparticles by a silver-tolerant yeast strain MKY3. *Nanotechnology* 14:95–100
- Kumar V, Yadav SK (2009) Plant-mediated synthesis of silver and gold nanoparticles and their applications. *J Chem Technol Biotechnol* 84:151–157
- Kumar AS, Ansary AA, Ahmad A, Khan MI (2007a) Extracellular biosynthesis of CdSe quantum dots by the fungus, *Fusarium Oxysporum*. *J Biomed Nanotechnol* 3:190–194
- Kumar SA, Abyaneh MK, Gosavi SW, Kulkarni SK, Pasricha R, Ahmad A, Khan MI (2007b) Nitrate reductase-mediated synthesis of silver nanoparticles from AgNO<sub>3</sub>. *Biotechnol Lett* 29:439–445
- Kvistek L, Prucek R (2005) The preparation and application of silver nanoparticles. *J Mater Sci* 22:2461–2473
- Laurencin CT, Kumbar SG, Nukavarapu SP (2008) Nanotechnology and orthopedics: a personal perspective. *Nanotechnol Nanomed* 1(1):6–10
- Lengke M, Southam G (2006) Bioaccumulation of gold by sulfate-reducing bacteria cultured in the presence of gold (I)-thiosulfate complex. *Geochim Cosmochim Acta* 70:3646–3661
- Liu WT (2006) Nanoparticles and their biological and environmental applications. *J Biosci Bioeng* 102(1):1–7
- Marazzi M, Angelis AD, Ravizza A, Ordanini MN, Falcone L, Chiaratti A, Crovato F, Calo D, Veronese S, Rapisarda V (2007) Successful management of deep facial burns in a patient with extensive third degree burns: the role of a nanocrystalline dressing in facilitating resurfacing. *Int Wound J* 4:8–14
- Mohanpuria P, Rana NK, Yadav SK (2008) Biosynthesis of nanoparticles: technological concepts and future applications. *J Nanopart Res* 7:9275–9280
- Mouxing F, Qingbiao L, Daohua S, Yinghua L, Ning H, Xu D, Huixuan W, Jiale H (2006) Rapid Preparation Process of Silver Nanoparticles by Bioreduction and Their Characterizations. *Chin J Chem Eng* 14(1):114–117
- Mukherjee P, Ahmad A, Mandal D, Senapati S, Sainkar SR, Khan MI, Ramani R, Parischa R, Ajayakumar PV, Alam M, Sastry M, Kumar R (2001) Bioreduction of AuCl<sub>4</sub><sup>-</sup> ions by the fungus *Verticillium* sp and surface trapping of the gold nanoparticles formed. *Angew Chem Int Ed* 40(19):3585–3588
- Mukherjee P, Roy M, Mandal BP, Dey GK, Mukherjee PK, Ghatak J, Tyagi AK, Kale SP (2008) Green synthesis of highly stabilized nanocrystalline silver particles by a non-pathogenic and agriculturally important fungus *T. asperellum*. *Nanotechnology* 19:103–110
- Nair LS, Laurencin CT (2007) Silver nanoparticles: synthesis and therapeutic applications. *J Biomed Nanotechnol* 3:301–316
- Nair B, Pradeep T (2002) Coalescence of nanoclusters and formation of submicron crystallites assisted by *Lactobacillus* strains. *Cryst Growth Design* 2:293–298
- Nangia Y, Wangoo N, Goyal N, Shekhawat G, Suri CR (2009) A novel bacterial isolate *Stenotrophomonas maltophilia* as living factory for synthesis of gold nanoparticles. *Microb Cell Fact*. doi:10.1186/1475-2859-8-39
- Ogi T, Saitoh N, Nomura T and Konishi Y (2010) Room-temperature synthesis of gold nanoparticles and nanoplates using *Shewanella algae* cell extract. *J Nanopart Res*. doi:10.1007/s11051-009-9822-8



- Omar A, Kempf C (2002) Removal of neutralized model parvoviruses and enteroviruses in human IgG solutions by nanofiltration. *Transfusion* 42(8):1005–1010
- Parikh RY, Singh S, Prasad BLV, Patole MS, Sastry M, Shouche YS (2008) Extracellular synthesis of crystalline silver nanoparticles and molecular evidence of silver resistance from *Morganella* sp: towards understanding biochemical synthesis mechanism. *ChemBioChem* 9:1415–1422
- Pastoriza-Santos I, Liz-Marzan LM (2000) Reduction of silver nanoparticles in DMF Formation of monolayers and stable colloids. *Pure Appl Chem* 72(1–2):83–90
- Prasad K, Jha AK, Kulkarni AR (2007) *Lactobacillus* assisted synthesis of titanium nanoparticles. *Nano Res Lett* 2:248–250
- Rai M, Yadav A, Gade A (2008) Current trends in phytosynthesis of metal nanoparticles. *Crit Rev Biotechnol* 28(4):277–284
- Rai M, Yadav A, Gade A (2009a) Silver nanoparticles: as a new generation of antimicrobials. *Biotechnol Adv* 27:76–83
- Rai M, Yadav A, Bridge P, Gade A (2009b) Myconanotechnology: a new and emerging science. In: Rai MK, Bridge PD (eds) *Applied mycology*, vol 14. CAB International, New York, pp 258–267
- Reddy VR (2006) Gold nanoparticles: synthesis and applications. *Synlett* 11:1791–1792
- Riddin TL, Gericke M, Whiteley CG (2006) Analysis of the inter- and extracellular formation of platinum nanoparticles by *Fusarium oxysporum* f sp *lycopersici* using response surface methodology. *Nanotechnology* 17:3482–3489
- Rodriguez-Perez A, Flores-Acosta M, Peirez-Salas R, Rodriguez-Mijangos R (2006) Cu halide nanoparticle formation by diffusion of copper in alkali halide crystals. *Rev Mexi de Fisica* 52 (2):151–154
- Rodríguez-Sánchez L, Blanco MC, López-Quintela MA (2000) Electrochemical Synthesis of Silver Nanoparticles. *J Phys Chem. B* 104(41):9683–9688
- Roe D, Karandikar B, Bonn-Savage N, Gibbins B, Rouillet JB (2008) Antimicrobial surface functionalization of plastic catheters by silver nanoparticles. *J Antimicrob Chemother* 61 (4):869–876
- Saini V, Zharov VP, Brazel CS, Nikles DE, Johnson DT, Everts M (2006) Combination of viral biology and nanotechnology: new applications in nanomedicine. *Nanomed: Nanotechnol Biol Med* 2:200–206
- Sastry M, Ahmad A, Khan MI, Kumar R (2003) Biosynthesis of metal nanoparticles using fungi and actinomycetes. *Curr Sci* 85(2):162–170
- Sato M, Webster TJ (2004) Nanobiotechnology: implications for the future of nanotechnology in orthopedic applications. *Expert Rev Med Devices* 1(1):105–114
- Sau TK, Rogach AL (2010) Nonspherical noble metal nanoparticles: colloid-chemical synthesis and morphology control. *Adv Mater* 22(16):1781–1804
- Shahi SK, Patra M (2003) Microbially synthesized bioactive nanoparticles and their formulation active against human pathogenic fungi. *Rev Adv Mater Sci* 5:501–509
- Shahverdi AR, Minaeian S, Shahverdi HR, Jamalifar H, Nohi AA (2007) Rapid synthesis of silver nanoparticles using culture supernatants of *Enterobacteria*: a novel biological approach. *Process Biochem* 42:919–923
- Shahverdi N, Wong CW, Nur Yasumira AA (2009) Rapid biosynthesis of silver nanoparticles using culture supernatant of bacteria with microwave irradiation. *Eur J Chem* 6(1):61–70
- Shaligram NS, Bule M, Bhambure RM, Singhal RS, Singh SK, Szakacs G, Pandey A (2009) Biosynthesis of silver nanoparticles using aqueous extract from the compactin producing fungal strain. *Process Biochem* 44:939–948
- Shankar SS, Ahmad A, Rai A, Sastry M (2004) Rapid synthesis of Au, Ag and bimetallic Au core-Ag shell nanoparticles by using neem (*Azadirachta indica*) leaf broth. *J Colloid Interface Sci* 275(5):496–502
- Sharma VK, Yngard RA, Lin Y (2009) Silver nanoparticles: green synthesis and their antimicrobial activities. *Adv Colloid Interface Sci* 145:83–96

- Singaravelu G, Arockiamary JS, Ganesh Kumar V, Govindraju K (2007) A novel extracellular synthesis of monodisperse gold nanoparticles using marine alga, *Sargassum wightii* Greville. *Colloid Surf B: Biointerface* 57:97–101
- Sintubin L, Windt WE, Dick J, Mast J, Ha DV, Verstarete W, Boon N (2009) Lactic acid bacteria as reducing and capping agent for the fast and efficient production of silver nanoparticles. *Appl Microbiol Biotechnol* 87:741–749
- Song JY, Kim BS (2009) Rapid biological synthesis of silver nanoparticles using plant leaf extracts. *Bioproc Biosyst Eng* 44:1133–1138
- Taniguchi N (1974) On the basic concept of nano-technology Proceedings of the International Conference on Production Engineering Tokyo Part II Japan Society of Precision Engineering
- Thakkar KN, Mhatre SS, Parikh RY (2010) Biological synthesis of metallic nanoparticles. *Nanomedicine* 6(2):257–262
- Tsai CY, Shiau AL, Chen SY, Chen YH, Cheng PC, Chang DH, Chen CH, Chou CR, Wang CL, Wu CL (2007) Amelioration of collagen-induced arthritis in rats by nanogold. *Arthritis Rheumatoid* 56:544–554
- Valanne A, Huopalahti S, Soukka T, Vainionpää R, Lovgren T, Harma H (2005) A sensitive adenovirus immunoassay as a model for using nanoparticle label technology in virus diagnostics. *Clin J Virol* 33:217–223
- Yang N, Aoki K (2005) Voltammetry of the silver alkylcarboxylate nanoparticles in suspension. *Electrochim Acta* 50:4868–4872
- Zent CS, Call TG, Hogan WJ, Shanafelt TD, Kay NE (2006) Uptake on risk-stratified management for chronic lymphocytic leukemia. *Leuk Lymphoma* 47:1738–1746

**Part I**  
**Synthesis and Fundamentals**

# Chapter 2

## An Insight into the Bacterial Biogenesis of Silver Nanoparticles, Industrial Production and Scale-up

Venkataraman Deepak, Kalimuthu Kalishwaralal, Sureshbabu Ram Kumar Pandian, and Sangiliyandi Gurunathan

### 2.1 Introduction

“Nano” refers to any parameter when it is expressed as a measure of  $10^{-9}$  times of SI units. Until recent past, the very existence of nanoparticles and their applications remained undetected. Nanotechnology was first proposed to have applications in the field of electronics for the miniaturization of the electronic devices. In fact, the term “Nanotechnology” has been coined by Norino Taniguchi, a researcher at the University of Tokyo, Japan (Taniguchi 1974). This slowly expanded to various fields. Even when various scientists reported the remediation of various heavy metals by microorganisms, the remediated nanosized zero valent metal crystal remained unnoticed (Mullen et al. 1989). But, when the significances of the nanoparticles were discovered, their applications also increased. When it comes to silver nanoparticles, they are used as antimicrobial agents in most of the public places such as elevators and railway stations in China. Besides, they are used as antimicrobial agents in surgically implanted catheters in order to reduce the infections caused during surgery and are proposed to possess antifungal, antiinflammatory, antiangiogenic and antipermeability activities (Kalishwaralal et al. 2009; Gurunathan et al. 2009a, b; Sheikpranbabu et al. 2009). Primarily, silver nanoparticles are considered as an alternative to silver ions (obtained from silver nitrate), which were used as antimicrobial agents. Silver was used as storage devices during historical periods and silver nitrate solution was directly used for wound healing during Second World War (Chu et al. 1988; Deitch et al. 1987; Margraff and Covey 1977; Silver 2003; Atiyeh et al. 2007; Law et al. 2008). Before the advent of silver nanoparticles, silver was the main component in the various creams for wounds. However, silver ions have the disadvantage of forming complexes and the effect of the ions remained only for a short time. This disadvantage has been overcome by the use of the silver nanoparticles which are in inert form and also exhibit

---

V. Deepak, K. Kalishwaralal, S. Ram Kumar Pandian, and S. Gurunathan (✉)  
Department of Biotechnology, Kalasalingam University, Anand Nagar, Krishnankoil 626190,  
Tamil Nadu, India  
e-mail: lvsangs@yahoo.com

antimicrobial function by inducing the production of reactive oxygen species such as hydrogen peroxide. Both the top-down and bottom-up approaches have been followed to synthesize nanoparticles. Here, chemical and biological methods have been successfully applied to synthesize silver nanoparticles.

## 2.2 Brief History

Silver was known only as a metal till recently and it is only when the nano era came into existence that people started to believe that silver could even be produced at the nanoscale. As previously mentioned, nanoparticles remained unnoticed even when many organisms were used for remediation of various metals. The competent organisms have been used to remove various reactive metal salts from the environment. Both the Gram positive and Gram negative metals have been used for the biosorption of metals such as silver, cadmium and copper. Various organisms have been tested for their efficiency to adsorb these metal ions and these metal ions remained as a colloidal aggregate mostly on the cell surface, occasionally on the cytoplasm. The size of the nanoparticles played no significant role during those times. These capable organisms were in turn termed as the “competent organisms” which could bind large amounts of metal ions (Beveridge and Murray 1976; Mullen et al. 1989; Doyle et al. 1980; Beveridge and Fyfe 1985). Cell walls of Gram positive bacteria such as *Bacillus subtilis* were found to bind with large quantities of metals than the Gram negative bacteria such as *Escherichia coli* (Beveridge and Fyfe 1985). The synthesis methods in the early 1980s described the reduction of metal ion as a two-step procedure; in first step very small particles were synthesized, which were then enlarged to several nanometers. The difference remained in the use of the reducing agent for the synthesis where in the former step a stronger reducing agent was used, and in latter step a weaker reducing agent was used (Sintubin et al. 2009). Chemical methods were used for the size-dependent synthesis of silver nanoparticles, a controlled process mediated by the addition of specific reducing agents at raised temperatures and various pH values. Silver nanoparticles were also synthesized through an array of methods such as spark discharging, electrochemical reduction, solution irradiation and cryochemical synthesis.

The biosynthesis of nanoparticles as an emerging highlight of the intersection of nanotechnology and biotechnology has received increasing attention due to a growing need to develop environmentally benign technologies in material synthesis (Kalishwaralal et al. 2008). The biological synthesis of nanoparticles germinated from the experiments on biosorption of metals with Gram negative and Gram positive bacteria. The synthesized molecules were not identified as nanoparticles but as aggregates (Mullen et al. 1989).

The role of microbial cells in the fate of metals in the environment was not thoroughly examined; however, it was conceived that they represent an important component of metal dynamics. The first evidence of synthesizing silver nanoparticles was established in 1984 using the microorganism *Pseudomonas stutzeri* AG259, a bacterial strain that was originally isolated from silver mine (Haefeli et al. 1984;

Zhang et al. 2005; Nair and Pradeep 2002). Thin sections of bacteria under the transmission electron microscope showed the deposition of the silver on the cell membrane. This opened new avenues towards the preparation of nanostructured materials that incorporate silver-based crystalline particles with defined structural, compositional and morphological properties. Biological methods are gaining impetus because of the use of normal conditions for the synthesis that enable control over the size of the nanoparticles. The formation of nanoparticles has been well elucidated in *Morganella* sp. The organism was grown at different concentrations of  $\text{AgNO}_3$ , but the bacterium was able to grow at 0.5 mM  $\text{AgNO}_3$ . The growth rate decreased with increase in  $\text{AgNO}_3$  concentration. The bacterium was allowed to grow up to the late exponential phase, and different concentrations of  $\text{AgNO}_3$  were then added. As a consequence, similar experiments have been performed in the closely related bacterium *E. coli* to understand the role of silver resistance in AgNPs production from *Morganella* sp. (Parikh et al. 2008).

### 2.3 An Account of Organisms Synthesizing Silver Nanoparticles

Biological methods of silver nanoparticle synthesis require a special ability: “Resistance of the organism to silver ions” (the resistance mechanism will be explained later in this chapter). It is to be noted that those organisms which synthesize silver nanoparticles are also vulnerable to higher concentrations of silver ions. For example, *Bacillus licheniformis* is one such organism used to synthesize silver nanoparticle at 1 mM concentration, i.e., when the concentration of the silver ion in the environment is 1 mM, the organism can synthesize silver nanoparticles without undergoing cell death. But, when the concentration of the silver ions is raised, say 10 mM, the organism undergoes cell death within minutes, i.e., when the concentration crosses the threshold level (Kalimuthu et al. 2008; Pandian et al. 2010). Even though the organism has the resistance to silver ions, it becomes useless at the higher concentration. That is why silver can be rightly called “moiety with two functions” – one is inducing the organism to synthesize nanoparticles at lower concentration, another is the induction of cell death at higher concentration. The following are some of the organisms which had been reported to synthesize silver nanoparticles.

#### 2.3.1 Various Species of Microorganisms Synthesizing Silver Nanoparticles

Bacteria:

S. No	Organism	Size (nm)	Author (year)
1	<i>Pseudomonas stutzeri</i> AG259	200	Tanja et al. (1999)
2	<i>Lactobacillus</i> Strains	500	Nair and Pradeep (2002)
3	<i>Bacillus megaterium</i>	46.9	Fu et al. (1999)
4	<i>Klebsiella pneumonia</i> (culture supernatant)	50	Ahmad et al. (2007)

(continued)

S. No	Organism	Size (nm)	Author (year)
5	<i>Bacillus licheniformis</i>	50	Kalimuthu et al. (2008)
6	<i>Bacillus licheniformis</i> (culture supernatant)	50	Kalishwaralal et al. (2008)
7	<i>Corynebacterium</i> sp.	10–15	Zhang et al. (2005)
8	<i>Bacillus subtilis</i> (culture supernatant)	5–60	Saifuddin et al. (2009)
9	<i>Geobacter sulfurreducens</i>	200	Law et al. (2008)
10	<i>Morganella</i> sp.	20 ± 5	Parikh et al. (2008)
11	<i>Bacillus subtilis</i>	5–60	Saifuddin et al. (2009)
12	<i>Escherichia coli</i>	1–100	Gurunathan et al. (2009a, b)
13	<i>Proteus mirabilis</i>	10–20	Samadi et al. (2009)
14	<i>Bacillus</i> sp.	5–15	Pugazhenthiran et al. (2009)
15	<i>Bacillus cereus</i>	4 and 5	Ganesh Babu and Gunasekaran (2009)
16	<i>Staphylococcus aureus</i>	1–100	Nanda and Saravanan (2009)
17	Lactic acid bacteria	11.2	Sintubin et al. (2009)
18	<i>Brevibacterium casei</i>	50	Kalishwaralal et al. (2010)

### Fungi:

S. No	Organism	Size (nm)	Author (year)
1	<i>Fusarium oxysporum</i>	5–50	Ahmad et al. (2003)
2	<i>Aspergillus fumigatus</i>	5–25	Bhainsa and D'Souza (2006)
3	<i>Aspergillus niger</i>	20	Gade et al. (2008)
4	<i>Phanerochaete chrysosporium</i>	100	Vigneshwaran et al. (2006)
5	<i>Aspergillus flavus</i>	8.92 ± 1.61	Vigneshwaran et al. (2007)
6	<i>Cladosporium cladosporioides</i>	10–100	Balaji et al. (2009)
7	<i>Fusarium semitectum</i>	10–60	Basavaraja et al. (2008)
8	<i>Trichoderma asperellum</i>	13–18	Mukherjee et al. (2008a, b)
9	<i>Cladosporium cladosporioides</i>	10–100	Balaji et al. (2009)
10	<i>Trichoderma viride</i>	5–40	Fayaz et al. (2010)
11	<i>Penicillium fellutanum</i>	1–100	Kathiresan et al. (2009)
12	<i>Penicillium brevicompactum</i> WA 2315	23–105	Shaligram et al. (2009)
13	<i>Verticillium</i> sp.	25 ± 12	Mukherjee et al. (2001)
14	<i>Fusarium solani</i>	5–35	Gade et al. (2009)
15	<i>Fusarium acuminatum</i>	5–40	Ingle et al. (2008)
16	<i>Aspergillus clavatus</i>	10–25	Verma et al. (2010)

### Plants:

S. No	Organism	Size	Author (year)
1	<i>Azadirachta indica</i>	50	Shankar et al. (2004)
2	<i>Cinnamomum camphora</i> leaf	55–80	Huang et al. (2007)
3	<i>Glycine max</i> (soybean) leaf extract	25–100	Vivekanandhan et al. (2009)
4	<i>Jatropha curcas</i>	10–20	Bar et al. (2009)
5	<i>Cinnamomum camphora</i> Leaf	5–40	Huang et al. (2008)
6	<i>Phyllanthus amarus</i>	18–38	Kasthuri et al. (2009)
7	<i>Carica papaya</i>	60–80	Mude et al. (2009)
8	<i>Gliricidia sepium</i>	10–50	Raut et al. (2009)
9	<i>Coriandrum sativum</i> leaf extract	26	Sathyavathi et al. (2010)

When genomic analysis of these organisms has been performed, it may show that one thing which confers resistance to silver ions will be common in most of the above-mentioned organisms.

## 2.4 Mechanism Involved in Silver Nanoparticle Synthesis

Not all the organisms are found to be competent for the synthesis of silver nanoparticles. As previously mentioned, those organisms which contain the “Silver resistance machinery” can synthesize silver nanoparticles provided that the concentration of the silver ions does not cross the “threshold limit”. The resistance mechanism differs with organisms. Extracts from bio-organisms may act both as reducing and capping agents in Ag NPs synthesis. The reduction of  $\text{Ag}^+$  ions by combinations of biomolecules found in these extracts such as enzymes/proteins, amino acids, polysaccharides and vitamins is environmentally benign, yet chemically complex. But, the mechanism which is widely accepted for the synthesis of silver nanoparticles is the presence of enzyme “Nitrate reductase” (Anil Kumar et al. 2007; Kalimuthu et al. 2008). Nitrate reductase is an enzyme in the nitrogen cycle responsible for the conversion of nitrate to nitrite (Duran et al. 2005). The reduction mediated by the presence of the enzyme in the organism has been found to be responsible for the synthesis. The use of a specific enzyme  $\alpha$ -NADPH-dependent nitrate reductase in the in vitro synthesis of nanoparticles is important because this would do away with the downstream processing required for the use of these nanoparticles in homogeneous catalysis and other applications such as non-linear optics. During the catalysis, nitrate is converted to nitrite, and an electron will be shuttled to the incoming silver ions. This has been excellently described in the organism *B. licheniformis*. *B. licheniformis* is known to secrete the cofactor NADH and NADH-dependent enzymes, especially nitrate reductase, that might be responsible for the bioreduction of  $\text{Ag}^+$  to  $\text{Ag}^0$  and the subsequent formation of silver nanoparticles. Figure 2.1 shows that the nitrate reductase present in the bacteria may aid the synthesis of silver nanoparticles (Kalimuthu et al. 2008).

Although all these are speculation, direct evidence was provided by Anil Kumar et al. (2007) who directly used the purified nitrate reductase from the organism *Fusarium oxysporum* for the synthesis of silver nanoparticle in test tube. Their reaction mixture contained only the enzyme nitrate reductase, silver nitrate and NADPH. Slowly, the reaction mixture turned brown with all the characteristics of silver nanoparticles. This is the first direct evidence for the involvement of nitrate reductase in the synthesis of silver nanoparticles.

Although silver nanoparticles synthesis is considered as a “capability” of the organism, it is primarily considered as a defense mechanism by the organisms to the incoming very reactive silver ions. Interesting facts about silver nanoparticle synthesis can be understood when the real mechanism involved in the antimicrobial activity of silver ions is known (Silver et al. 2006). Silver ions are very reactive and are known to bind with various vital components of the cells inducing cell death.



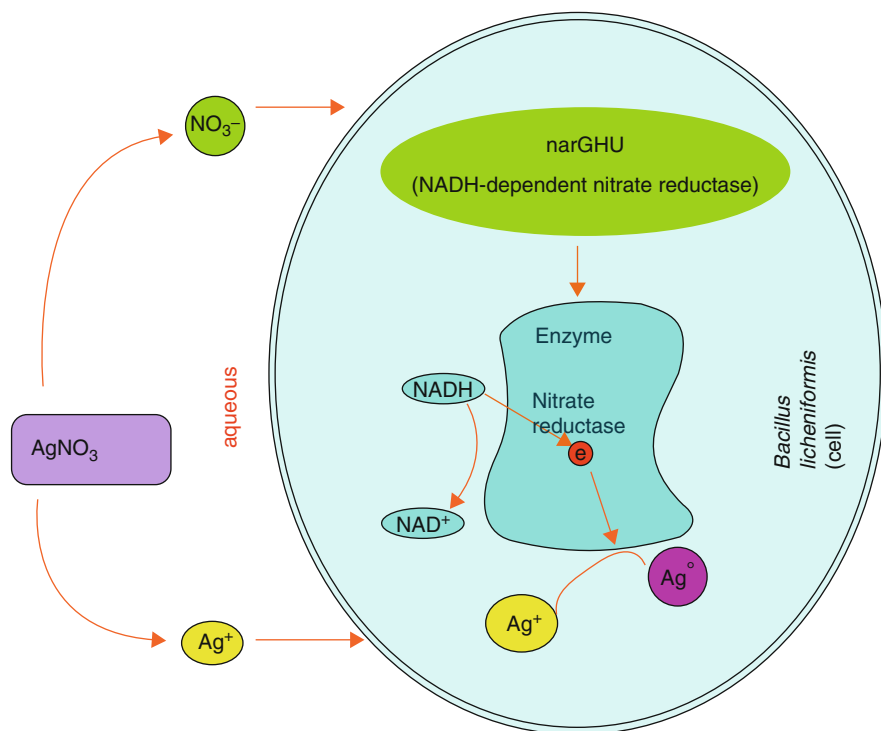


**Fig. 2.1** A hypothetical diagram of how silver ions are reduced to silver atom by the enzyme nitrate reductase [figure adopted from Kalimuthu et al. (2008)]

Interestingly, “apoptosis” is a mechanism which is considered to be applicable not only to multicellular organisms but also to unicellular microorganisms. (Engelberg-Kulka et al. 2006). The following are the effects by which silver ions exhibit their antimicrobial functions. (1) Binding of silver ions to the negatively charged DNA (prokaryotes do not contain histones) thereby making the DNA to lose its structure and also inhibiting the replication of DNA. (2) Binding of silver ions with the thiol-containing proteins, thereby inhibiting the function of proteins. (3) Induction of reactive oxygen species synthesis leading to the formation of highly reactive radicals that destroy the cells. Silver ions are known to particularly inhibit enzymes such as NADH dehydrogenase II in the respiratory system, which is implicated as a candidate for the site of production of reactive oxygen species in vivo. The free radicals resulting from  $\text{H}_2\text{O}_2$  are mainly hydroxyl ( $\text{OH}^-$ ) groups that result from the Fenton reaction (Matsumura et al. 2003; Gautam and Sharma 2002; Cabiscol et al. 2000). This mechanism can also be indirectly studied, i.e., catalase is considered as a scavenger of reactive oxygen species in microbes. During experiments with *B. licheniformis* the increase in the silver ions concentration was accompanied by an increase in the catalase synthesis, which is upto the minimal inhibitory concentration, beyond which even catalase did not help the cell to

“survive”. This was also evidenced by Matsumura et al. (2003) where the mutated strain of *E. coli* UM1 (katE katG), deficient in catalase, was found to be more sensitive to both silver zeolite and silver nitrate than its parent. This shows that silver ions induce apoptosis in bacteria. Therefore, the bacterial cell tries to protect itself from the incoming silver ions, by converting them to inactive  $\text{Ag}^0$  form. Further incoming silver ions were also shuttled with electrons and this leads to the growth of the crystals (Fig. 2.2).

This defense mechanism is applicable to various metals, where the difference occurs only in the respective enzyme. Here, in *B. licheniformis*, the nitrate reductase is found at the cell membrane as respiratory nitrate reductase. A picture of cells treated with silver nitrate shows the particles to be present on the circumference of the cell, i.e., at the cell membrane (Fig. 2.3) (Pandian et al. 2010). Therefore, it can be regarded as that in most of the organisms identified to synthesize silver nanoparticles, nitrate reductase will be a part and parcel of the organism.

Moreover, when the condition of the silver nanoparticle synthesis is alkaline, the synthesis will be faster than in acidic conditions. In other words, synthesis enhances as the pH increases towards alkaline region and reaches the maximum at pH 10 after

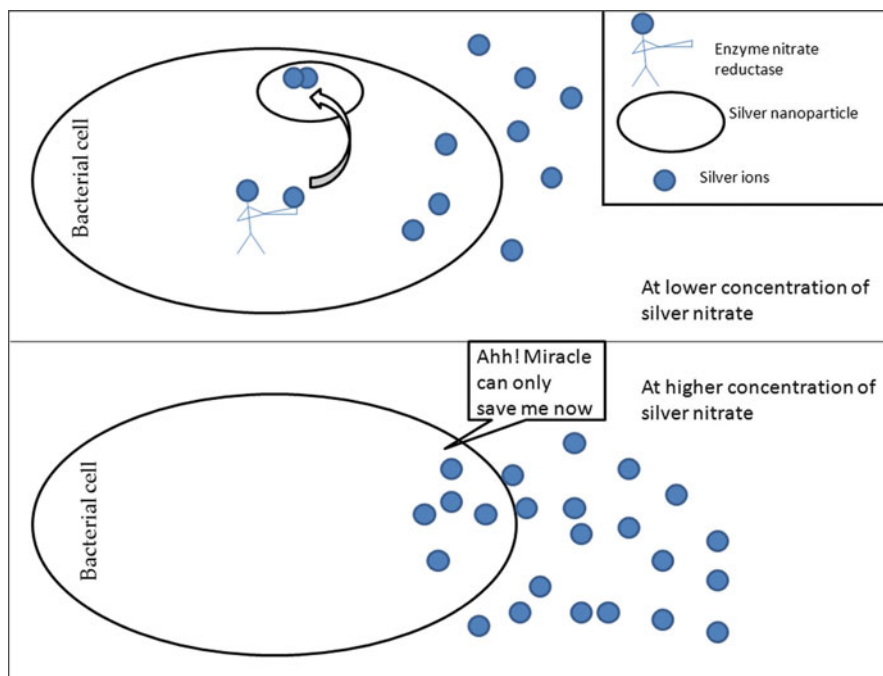


**Fig. 2.2** Silver is a bifunctional molecule. At lower concentration the enzyme responsible for nanoparticle synthesis (nitrate reductase) may convert the incoming  $\text{Ag}^+$  to  $\text{Ag}^0$  and favor the deposition of them as crystals. Whereas at higher concentrations (beyond the threshold limit), the conversion may occur, but more reactive silver ions induces “apoptosis” in bacterial cells by various mechanisms

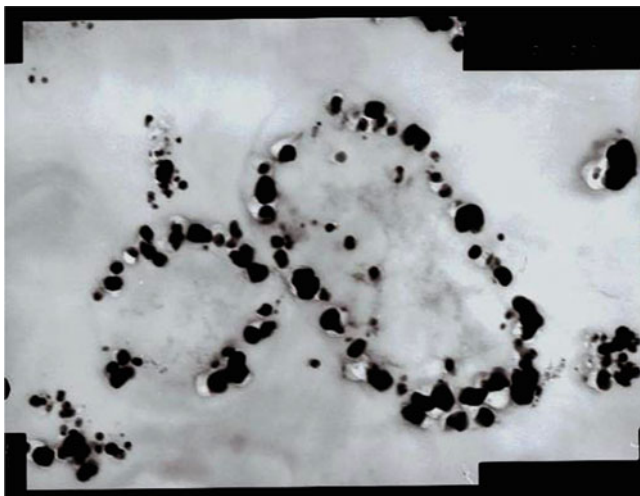


**Fig. 2.3** TEM image of thin section of the bacteria challenged with 1 mM silver nitrate, showing the synthesis of silver nanoparticles along the circumference of the bacteria. Image adopted from Pandian et al. (2010)

which the speed of the nanoparticle synthesis decreases. This shows that the synthesis of silver nanoparticles will be favored by the alkaline environment. At alkaline conditions there is no need of agitating the mixture for the formation of silver nanoparticles and all the silver ions supplied will be converted to silver nanoparticles even within 30 min. The proteins involved in the synthesis may bind with silver at thiol regions ( $-SH$ ) forming a  $-S-Ag$  bond, a clear indication of which aids the conversion of  $Ag^+$  to  $Ag^0$ . In addition, the alkaline ion ( $-OH$ ) is very much required for the reduction of metal ions. It takes 4 days for the production of silver ions in normal conditions whereas it is very much less than an hour when the pH is made alkaline. Moreover, under alkaline conditions the ability of the enzyme responsible (not only nitrate reductase) for the synthesis of silver nanoparticles increases (Sanghi and Verma 2009).

#### **2.4.1 Size Control Over the Biological Synthesis of the Nanoparticles**

Although chemical synthesis aids the size control over the synthesis of nanoparticles, size control can also be achieved in biological methods. A report by Gurunathan et al. (2009a, b) showed that by controlling the environment of nanoparticle synthesis, silver nanoparticles of various sizes and shapes could be synthesized. At room temperature, silver nanoparticles of 50 nm are synthesized whereas at  $60^\circ C$  nanoparticles of 15 nm are synthesized. Similarly at acidic pH the size of the nanoparticle ranged 45 nm whereas at pH 10 the size is just 15 nm. Even the size of 2–20 nm silver nanoparticles could be synthesized by organisms such as *Verticillium* sp.

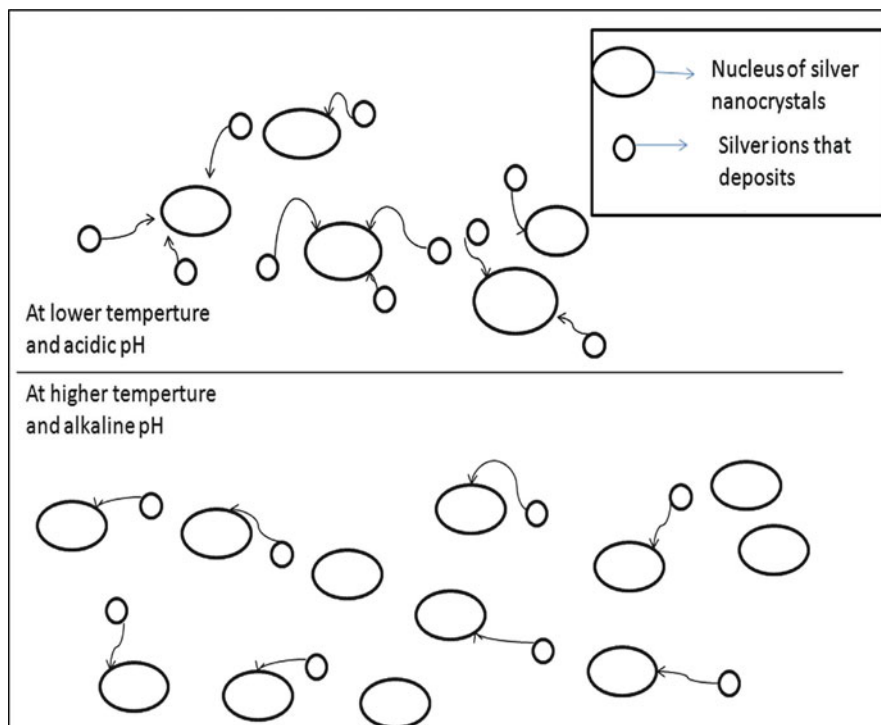


**Fig. 2.4** A schematic imaginary diagram that depicts the reason for size control over the synthesis of silver nanoparticles. At lower temperature and pH, less nucleation occurs thereby forming larger particles whereas at higher pH and temperature more nucleation may occur thus forming smaller particles

(Mukherjee et al. 2001) intracellularly. The size-controlled synthesis of silver nanoparticles by controlling the environment is due to the formation of many seed crystals. At acidic pH and lower temperatures there will be less nucleation for silver crystal formation on which new incoming silver atoms deposit to form larger sized particles. But as the pH and temperature increase, the dynamics of the ions increase and more nucleation regions are formed due to the availability of  $\text{-OH}$  ions and increased temperature. The conversion of  $\text{Ag}^+$  to  $\text{Ag}^0$  increases followed by increase in the kinetics of the deposition of the silver atoms (Fig. 2.4).

## 2.5 Process Design for Silver Nanoparticulate Synthesis in the Industry and Identification of the Chief Components Involved in Synthesis

The above-mentioned fact is limited only to the biomass, i.e., only to the cells. The problems which may occur during nanoparticle synthesis by the biomass are:

- (a) Primarily silver nanoparticles are attached to the cell membrane. So the first step will be to break the cells and to isolate the silver nanoparticles.
- (b) To purify the nanoparticles from the other components present in the supernatant.

This may sound tedious for some applications and large-scale production. To overcome the first problem, the particles can be synthesized using a culture supernatant. But when it comes to the supernatant, there are various components which may aid the synthesis of silver nanoparticles. There are also reports of synthesis of silver nanoparticles by the culture supernatant. Although supernatant can contain the enzyme nitrate reductase, it is less likely that NADPH is present in the supernatant. It is here where the question arises, what is the real factor that aids the synthesis of silver nanoparticles by the cell-free culture supernatant? Culture supernatant is found to be the easiest way for the size-controlled synthesis of silver nanoparticles. The environment of the culture supernatant can be easily modified and maintained than the biomass, where the components in the cytoplasm would try to maintain constant environment such as heat shock proteins. Therefore, culture supernatant can be used for the synthesis of silver nanoparticles rather than cells itself. But, synthesis of nanoparticles by culture supernatant as a whole is not specific. Moreover, the culture supernatant possesses the second problem of downstream processing. When synthesis of silver nanoparticles is closely analyzed some components are vital for the synthesis. The components required for the synthesis of silver nanoparticles are:

- (a) Silver nitrate
- (b)  $\text{NADH}_2$
- (c) Stabilizer
- (d) Catalyst that converts silver ion to nanoparticles

Therefore a mixture similar to culture supernatant can be prepared which can be successfully applied for the nanoparticle synthesis. This could overcome the afore-said problems in the nanoparticle synthesis.

The reasons for using a mixture similar to culture supernatant for the synthesis of silver nanoparticles are given below.

### ***2.5.1 Large Quantity of Synthesis***

Since silver ion is toxic to cells, the concentration of silver ions for the synthesis should be lesser than what we say as the “threshold level”, i.e., the conditions beyond which the cells die. So for the synthesis of silver nanoparticles by biomass the optimum concentration that has been patented is 1 mM (Ahamd et al. 2003; Kalimuthu et al. 2008). But higher concentrations of silver ions had been reported for the synthesis of silver nanoparticles by the crude culture supernatant (Gurunathan et al. 2009a, b). When a specific mixture is used, the concentrations can be increased as the amount of enzyme is increased.

### ***2.5.2 Specific Reaction Can be Induced by Adding Various Inducers***

Silver nanoparticle synthesis can be made specific, because only the enzyme nitrate reductase will be present in the supernatant (Kalishwaralal et al. 2008). Moreover, the activity of the enzyme can be induced by various inducers of the enzyme. Because ionic silver has the ability to bind with the various components present in the cells, 100% yield of silver nanoparticle synthesis will be attained after a specific period of time which may be due to the impedance created by the cell wall and plasma membrane because of osmotic pressure. These could be overcome by using the enzyme alone.

### ***2.5.3 Easy Control of Size (and shape) by Controlling the Environment***

Previously Gurunathan et al. (2009a, b) have reported the size-controlled synthesis of silver nanoparticles by controlling the temperature and pH of the supernatant of *E. coli*. The supernatant was added with 1 mM AgNO<sub>3</sub> and incubated at various temperatures and pH. The average size distribution varied according to the environment. When the temperature was increased the size of the nanoparticles reduced up to 60°C, which increased thereafter. This can be explained on the basis of thermal kinetics, i.e., as temperature increases and favors more nucleation the particle size is reduced. But, after a certain temperature deposition of silver was rather more than the nucleation and aggregation may also have been a part of it. In case of pH the average size went on decreasing up to pH 10 after which it also increased.

### ***2.5.4 Immobilization of Enzymes***

Biomass once used for the synthesis of nanoparticles cannot be reused, which applies for the enzymes in free form also. But when the enzymes are immobilized using a support the enzymes can be used for a large number of reactions. Essentially the enzymes should be immobilized upon the surface of particle of immobilization to rule out the diffusion limitation (Clark 1994).

### ***2.5.5 Easy Downstream Steps for the Purification of Nanoparticles***

Think of a small comparison. Will it be easy to purify the compound with large number of impurities or with very less impurities. Obviously the latter is the

better. Using purified enzymes will make the downstream steps much simpler as the enzyme will mostly be the impurity, but when immobilized enzymes are used this can also be ruled out where the downstream steps can be very much reduced.

### ***2.5.6 Easy for Scaling-up of the Reactions***

Use of biomass for the large-scale synthesis requires various power-consuming processes such as agitation and harvesting the biomass. In addition, the purification of the nanoparticles is a tedious process. Here using immobilized nitrate reductase will also reduce most of the power consumption processes and downstream processing steps.

### ***2.5.7 Separation of Nanoparticles by Gel Electrophoresis According to Size and Shape***

The synthesis of nanoparticles results in a wide distribution in the size of the nanoparticles. An easy method for separation of the nanoparticles using gel has been reported (Hanauer et al. 2007). To use size- and/or shape-dependent material properties, such as quantum confinement or plasmon resonances, it is critical to have nanoparticles with the lowest size and shape dispersion possible. An alternative to the high-yield synthesis of nanoparticles with ultranarrow size distribution is the postsynthetic separation of particles similar to cleaning procedures in organic synthesis. Gel electrophoresis is commonly used to separate biomolecules, but this technique is also used in the separation of nanoparticles based on size. The separation is mediated by the number of polymer chains attached and these are characterized by the strong colors induced by plasmon resonance. The strong influence of size and shape on the frequency or wavelength of the plasmon resonance would make it desirable to obtain monodisperse samples for various applications. Compared to the other separation techniques, gel electrophoresis has the advantage of allowing multiple runs in parallel on the same gel, which is a considerable advantage at the stage of understanding mechanisms and optimizing conditions. To stabilize the nanoparticles, we coat them with a layer of polyethylene glycol (PEG, MW 5,000), which is covalently attached at one end to the metal surface via a thiol group ("PEGylation"). The other end of the polymer chain may carry different functional groups, which we exploit for controlling the overall particle charge and mobility. The size and shape of the nanoparticles obtained are used to synthesize particles of different shapes and these have been analyzed using gel electrophoresis.

## 2.6 Scaling-up of Silver Nanoparticle Synthesis

One of the important challenges in nanomaterials production is scaling up laboratory processes to the industrial scale. Mathematical modeling is an integral component of our research strategy, both for process scale-up and design and for process optimization and control. Large-scale biological synthesis of nanoparticles has always been a big challenge. Here also the synthesis of silver nanoparticles by biomass is a tedious process. Therefore, the second option of nanoparticle synthesis by nitrate reductase will be a better option. Scaling up of silver nanoparticle synthesis biologically should start from the first step of production of nitrate reductase. In a report by Vaidyanathan et al. (2010) this step has been reported where they have optimized the synthesis of nitrate reductase by the organism *B. licheniformis*. The optimization of nitrate reductase led to the enhanced synthesis of silver nanoparticles. The synthesis was found to be dependent on the enzyme activity. Since all the culture supernatants were supplied with same concentration of silver ions, there is no chance of extra silver ions coming into picture. This has revealed that increase in the amount of enzyme increases the rate of reaction.

Although, currently there are no reports on very large quantity of synthesis of silver nanoparticles, some prototypes have been designed in continuous flow reactors similar to chemical methods. The use of plant product from *Cinnamomum camphora* leaf has been used to synthesize silver nanoparticles in a continuous flow tubular microreactor (Huang et al. 2008). Scaled-up production of monodisperse colloidal nanoparticles has become an important research subject in recent years. In this regard, continuous flow reactors are generally favored over batch reactors. Decomposition of organometallic precursors in organic solvents is one of the most commonly used approaches to nanoparticles because the narrow size distribution can be achieved in such reaction systems. Rapid injection of precursors into a heated mixture of solvent, coordinating ligands, and other precursors is often required. A batch process is suitable for those reactions, but often limited to small-scale synthesis due to the low production yield of nanoparticles and the time-consuming nature of the process. A flow reactor, on the other hand, can generate products on a continuous basis once the reaction reaches steady state and is more appropriate for a large-scale production than the batch reactor. Furthermore, targeted reaction temperatures can be achieved in second or even millisecond time scales in a microreactor. The advantage of tubular reactor is that it can be easily scaled up by increasing the length of the reactor (Synthesis of Silver Nanoparticles in a Continuous Flow Tubular Microreactor). Based on the above methods, two kinds of process design can be made for the synthesis of silver nanoparticles by the biomass and the enzyme.

Using the former design the biomass synthesized can be harvested and used for the synthesis of silver nanoparticles (Fig. 2.5). But it may require some more additional downstream steps such as purification of the nanoparticle from the other proteins. But when the immobilized enzymes are used, the downstream



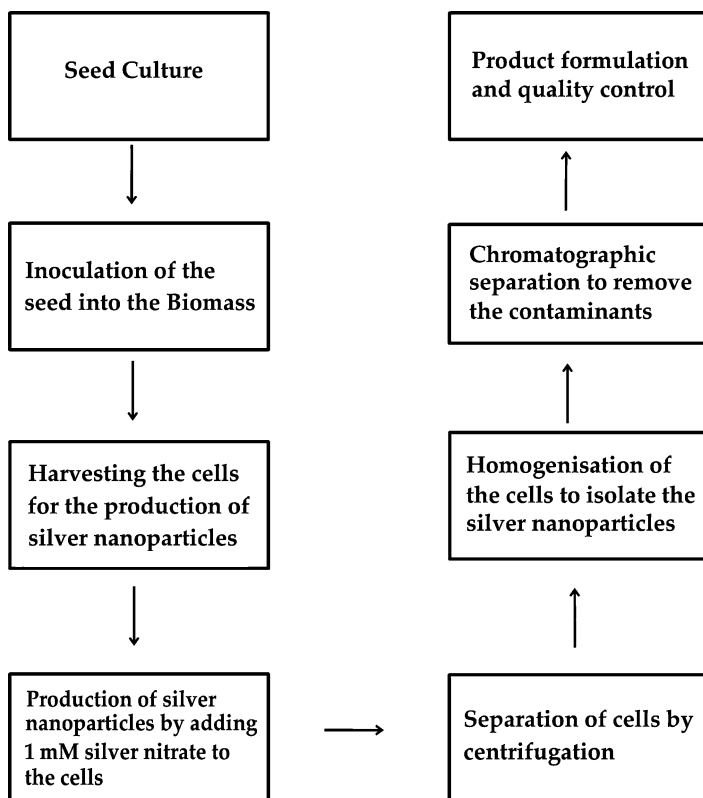


**Fig. 2.5** Process design for the industrial scale synthesis of silver nanoparticle synthesis by biomass

steps will be very less and will be advantageous as the nitrate reductase can be reused for the synthesis of silver nanoparticles (Fig. 2.6).

## 2.7 Conclusion

Reducing the size of a particle has a greater impact on the property of the molecule and the properties also completely differ from the bulk material. But the synthesis of nanomaterials at nanoscale involves tedious phenomena (reducing agents) when synthesized chemically. Moreover, the chemically synthesized nanoparticles require another step for the prevention of aggregation of the particles. But, biological synthesis of silver nanoparticles uses harmless, eco-friendly reducing agents and the nanoparticle structure is stabilized by the proteins present in the environment eliminating the extra step in preventing the aggregation of

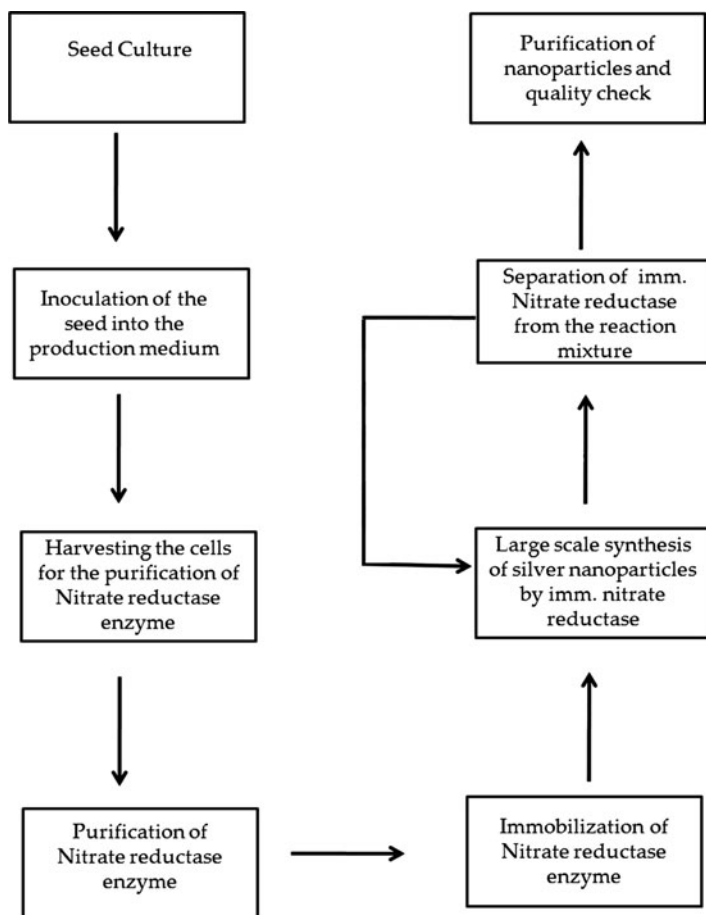


**Fig. 2.6** Process design for the industrial scale synthesis of silver nanoparticle by immobilized nitrate reductase

chemically synthesized nanoparticles by stabilizers. Since the biological molecules are eco-friendly, the pollution due to chemicals and byproducts can be prevented from reaching the environment. The size and shape of the particle can also be completely regulated by controlling the environment where the nanocrystal growth occurs (pH and temperature). Moreover, biological methods have the greater advantage of easy bulk synthesis which can be exploited for industrial scale production too.

**Acknowledgments** The Authors are thankful to Council of Scientific and Industrial Research (CSIR), New Delhi for the award of Senior Research Fellowship (Reference No. 9/10/2(0001)/2k10-EMR-I (DV); 9/10/2(0003)/2k10-EMR-I (KK); 9/10/2(0002)/2k10-EMR-I(SRKP)). Prof. G. Sangiliyandi is thankful to CSIR project grant (no 37/0347) which helped him in the basic research of silver nanoparticles synthesis.

## References

- Ahmad A, Mukherjee P, Senapati S, Mandal D, Khan MI, Kumar R (2003) Extracellular biosynthesis of silver nanoparticles using the fungus *Fusarium oxysporum*. *Colloids Surf B* 28:313–318
- Ahmad RS, Sara M, Hamid RS, Hossein J, Ashraf-Asadat N (2007) Rapid synthesis of silver nanoparticles using culture supernatants of *Enterobacteria*: a novel biological approach. *Process Biochem* 42:919–923
- Anil Kumar S, Abyaneh MK, Gosavi Sulabha SW, Ahmad A, Khan MI (2007) Nitrate reductase-mediated synthesis of silver nanoparticles from  $\text{AgNO}_3$ . *Biotechnol Lett* 29:439–445
- Atiyeh BS, Costagliola M, Hayek SN, Dibo SA (2007) Effect of silver on burn wound infection control and healing: review of the literature. *Burns* 33:139–148
- Balaji DS, Basavaraja S, Bedre Mahesh D, Prabhakar BK, Venkataraman A (2009) Extracellular biosynthesis of functionalized silver nanoparticles by strains of *Cladosporium cladosporioides*. *Colloids Surf B* 68:88–92
- Bar H, Bhui DK, Gobinda PS, Priyanka S, Santanu P, Ajay M (2009) Green synthesis of silver nanoparticles using seed extract of *Jatropha curcas*. *Colloids Surf A Physico Chem Eng Asp* 348:212–216
- Basavaraja S, Balaji SD, Lagashetty A, Rajasab AH, Venkataraman A (2008) Extracellular biosynthesis of silver nanoparticles using the fungus *Fusarium semitectum*. *Mater Res Bull* 43(5):1164–1170
- Beveridge TJ, Fyfe WS (1985) Metal fixation by bacterial cell walls. *Can J Earth Sci* 22:1893–1898
- Beveridge TJ, Murray RGE (1976) Uptake and retention of metals by cell walls of *Bacillus subtilis*. *J Bacteriol* 127:1502–1518
- Bhainsa KC, D'Souza SF (2006) Extracellular biosynthesis of silver nanoparticles using the fungus *Aspergillus fumigatus*. *Colloids Surf B* 47:160–164
- Cabiscol E, Tamarit J, Ros J (2000) Oxidative stress in bacteria and protein damage by reactive oxygen species. *Internal Microbiol* 3:3–8
- Chu CS, McManus AT, Pruitt BA, Mason AD (1988) Therapeutic effects of silver nylon dressing with weak direct current on *Pseudomonas aeruginosa* infected burn wounds. *J Trauma* 28:1488–1492
- Clark DS (1994) Can immobilization be exploited to modify enzyme activity? *Trends Biotechnol* 12(11):439–443
- Deitch EA, Marin A, Malakanov V, Albright JA (1987) Silver nylon cloth: *in vivo* and *in vitro* evaluation of antimicrobial activity. *J Trauma* 27:301–304
- Doyle RJ, Matthews TH, Streips UN (1980) Chemical basis for selectivity of metal ions by the *Bacillus subtilis* cell wall. *J Bacteriol* 143:471–480
- Duran N, Marcato PD, Alves O, Souza G (2005) Mechanistic aspects of biosynthesis of silver nanoparticles by several *Fusarium oxysporum* strains. *J Nanotechnol* 3:8
- Engelberg-Kulka H, Amitai S, Kolodkin-Gal I, Hazan R (2006) Bacterial programmed cell death and multicellular behavior in bacteria. *PLoS Genet* 10:135
- Fayaz M, Tiwary CS, Kalaichelvan PT, Venkatesan R (2010) Blue orange light emission from biogenic synthesized silver nanoparticles using *Trichoderma viride*. *Colloids Surf B* 75(1):175–178
- Fu JK, Zhang WD, Liu YY, Lin ZY, Yao BX, Weng SZ (1999) Characterization of adsorption and reduction of noble metal ions by bacteria. *Chin J Chem Univ* 20:1452–1454
- Gade AK, Bonde P, Ingle AP, Marcato PD, Durán N, Rai MK (2008) Exploitation of *Aspergillus niger* for synthesis of silver nanoparticles. *J Biobased Mater Bioenergy* 3:123–129
- Gade A, Ingle A, Bawaskar M, Rai M (2009) *Fusarium solani*: a novel biological agent for the extracellular synthesis of silver nanoparticles. *J Nanopart Res* 11:2079–2085
- Ganesh Babu MM, Gunasekaran P (2009) Production and structural characterization of crystalline silver nanoparticles from *Bacillus cereus* isolate. *Colloids Surf B* 74(1):191–195
- Gautam AS, Sharma A (2002) Involvement of caspase-3 like protein in rapid cell death of *Xanthomonas*. *Mol Microbiol* 44:393–401

- Gurunathan S, Lee KJ, Kalishwaralal K, Sheikpranbabu S, Vaidyanathan R, Eom SH (2009a) Antiangiogenic properties of silver nanoparticles. *Biomaterials* 30:6341–6350
- Gurunathan S, Kalishwaralal K, Vaidyanathan R, Venkataraman D, Pandian SRK, Muniyandi J, Hariharan N, Eom SH (2009b) Biosynthesis, purification and characterization of silver nanoparticles using *Escherichia coli*. *Colloids Surf B* 74(1):328–335
- Haefeli C, Franklin C, Hardy K (1984) Plasmid-determined silver resistance in *Pseudomonas stutzeri* isolated from silver mine. *J Bacteriol* 158:389–392
- Hanauer M, Pierrat S, Zins I, Lotz A, Solmnichsen C (2007) Separation of nanoparticles by gel electrophoresis according to size and shape. *Nano Lett* 7(9):2881–2885
- Huang J, Li Q, Sun D, Lu Y, Su Y, Yang X (2007) Biosynthesis of silver and gold nanoparticles by novel sundried *Cinnamomum camphora* leaf. *Nanotechnology* 18:105104.1–105104.11
- Huang J, Lin L, Li Q, Sun D, Wang Y, Lu Y, He N, Yang K, Yang X, Wang H, Wang W, Lin W (2008) Continuous-flow biosynthesis of silver nanoparticles by lixivium of Sundried *Cinnamomum camphora* leaf in tubular microreactors. *Ind Eng Chem Res* 47(16):6081–6090
- Ingle AP, Gade AK, Pierrat S, Sönnichsen C, Rai MK (2008) Mycosynthesis of silver nanoparticles using the fungus *Fusarium acuminatum* and its activity against some human pathogenic bacteria. *Curr Nanosci* 4:141–144
- Kalimuthu K, Babu RS, Venkataraman D, Mohd B, Gurunathan S (2008) Biosynthesis of silver nanocrystals by *Bacillus licheniformis*. *Colloids Surf B* 65:150–153
- Kalishwaralal K, Deepak V, RamkumarPandian S, Nellaiah H, Sangiliyandi G (2008) Extracellular biosynthesis of silver nanoparticles by the culture supernatant of *Bacillus licheniformis*. *Mater Lett* 62:4411–3
- Kalishwaralal K, Banumathi E, Pandian SBRK, Deepak V, Muniyandi J, Eom SH (2009) Silver nanoparticles inhibit VEGF induced cell proliferation and migration in bovine retinal endothelial cells. *Colloids Surf B* 73:51–7
- Kalishwaralal K, Deepak V, Pandian SRK, Kottaisamy M, BarathManiKanth S, Kartikeyan B, Gurunathan S (2010) Biosynthesis of silver and gold nanoparticles using *Brevibacterium casei*. *Colloids Surf B* 77(2):257–262
- Kasthuri J, Kathiravan K, Rajendiran N (2009) Phyllanthin-assisted biosynthesis of silver and gold nanoparticles: a novel biological approach. *J Nanopart Res* 11(5):1075–1085
- Kathiresan K, Manivannan S, Nabeel MA, Dhivya B (2009) Studies on silver nanoparticles synthesized by a marine fungus, *Penicillium fellutanum* isolated from coastal mangrove sediment. *Colloids Surf B* 71(1):133–137
- Law N, Ansari S, Livens FR, Renshaw JC, Lloyd JR (2008) The formation of nano-scale elemental silver particles via enzymatic reduction by *Geobacter sulfurreducens*. *Appl Environ Microbiol* 74:7090–7093
- Margraff HW, Covey TH (1977) A trial of silver–zinc–allantoine in the treatment of leg ulcers. *Arch Surg* 112:699–704
- Matsumura Y, Yoshikata K, Kunisak S, Tsuchido T (2003) Mode of bactericidal action of silver zeolite and its comparison with that of silver nitrate. *Appl Environ Microbiol* 69:4278–4281
- Mude N, Ingle A, Gade A, Rai M (2009) Synthesis of silver nanoparticles using callus extract of *Carica papaya* – a first report. *J Plant Biochem Biotechnol* 18(1):83–86
- Mukherjee P, Ahmad A, Mandal D, Senapati S, Sainkar SR, Khan MI, Parishcha R, Ajaykumar PV, Alam M, Kumar R, Sastry M (2001) Fungus-mediated synthesis of silver nanoparticles and their immobilization in the mycelial matrix: a novel biological approach to nanoparticle synthesis. *Nano Lett* 1:515–519
- Mukherjee P, Roy M, Mandal BP, Dey GK, Mukherjee PK, Ghatak J, Tyagi AK, Kale SP (2008a) Green synthesis of highly stabilized nanocrystalline silver particles by a non-pathogenic and agriculturally important fungus *T. asperellum*. *Nanotechnology* 19:075103.1–075103.7
- Mukherjee P, Roy M, Mandal BP, Dey GK, Mukherjee PK, Ghatak J (2008b) Green synthesis of highly stabilized nanocrystalline silver particles by a non-pathogenic and agriculturally important fungus *T. asperellum*. *Nanotechnology* 19:7

- Mullen MD, Wolf DC, Ferris FG, Beveridge TJ, Flemming CA, Bailey GW (1989) Bacterial sorption of heavy metals. *Appl Environ Microbiol* 55:3143–3149
- Nair B, Pradeep T (2002) Coalescence of nanoclusters and formation of submicron crystallites assisted by *Lactobacillus* strains. *Cryst Growth Des* 2:293–298
- Nanda A, Saravanan M (2009) Biosynthesis of silver nanoparticles from *Staphylococcus aureus* and its antimicrobial activity against MRSA and MRSE. *Nanomedicine* 5(4):452–456
- Pandian SRK, Deepak V, Kalishwaralal K, Viswanathan P, Gurunathan S (2010) Mechanism of bactericidal activity of silver nitrate – a concentration dependent bi-functional molecule. *Braz J Microbiol* 41:805–809
- Parikh RY, Singh S, Prasad BL, Patole MS, Sastry M, Shouche YS (2008) Extracellular synthesis of crystalline silver nanoparticles and molecular evidence of silver resistance from *Morganella* sp.: towards understanding biochemical synthesis mechanism. *ChemBiochem* 9:1415–1422
- Pugazhenthiran N, Anandan S, Kathiravan G, Prakash NKU, Crawford S, Ashokkumar M (2009) Microbial synthesis of silver nanoparticles by *Bacillus* sp. *J Nanopart Res* 11(7):1811–1815
- Raut R, Jaya SL, Niranjana DK, Vijay BM, Kashid S (2009) Photosynthesis of silver nanoparticle using *Gliricidia sepium* (Jacq.). *Curr Nanosci* 5(1):117–122
- Saifuddin N, Wong CW, AA Nur yasumira (2009) Rapid biosynthesis of silver nanoparticles using culture supernatant of bacteria with microwave irradiation. *Eur J Chem* 6:61–70
- Samadi N, Golkaran D, Eslamifard A, Jamalifar H, Fazeli MR, Mohseni FA (2009) Intra/extracellular biosynthesis of silver nanoparticles by an autochthonous strain of *Proteus mirabilis* isolated from photographic waste. *J Biomed Nanotechnol* 5(3):247–253
- Sanghi R, Verma P (2009) Biomimetic synthesis and characterisation of protein capped silver nanoparticles. *Bioresour Technol* 100(1):501–504
- Sathyavathi R, Krishna MB, Rao SV, Saritha R, Rao DN (2010) Biosynthesis of silver nanoparticles using *Coriandrum sativum* leaf extract and their application in nonlinear optics. *Adv Sci Lett* 3(2):138–143
- Shaligram NS, Bule M, Bhambure R, Singhal RS, Singh SK, Szakacs G, Pandey A (2009) Biosynthesis of silver nanoparticles using aqueous extract from the compactin producing fungal strain. *Process Biochem* 44(8):939–943
- Shankar SS, Rai A, Ahmad A, Sastry M (2004) Rapid synthesis of Au, Ag and bimetallic Au core–Ag shell nanoparticles using Neem (*Azadirachta indica*) leaf broth. *J Colloid Interface Sci* 275:496–502
- Sheikpranbabu S, Kalishwaralal K, Venkataraman D, Eom SH, Park J, Gurunathan S (2009) Silver nanoparticles inhibit VEGF- and IL-1 $\beta$ -induced vascular permeability via Src dependent pathway in porcine retinal endothelial cells. *J Nanobiotechnol* 7:8
- Silver S (2003) Bacterial silver resistance: molecular biology and uses and misuses of silver compounds. *FEMS Microbiol Rev* 27:341–353
- Silver S, Phung LT, Silver G (2006) Silver as biocides in burn and wound dressings and bacterial resistance to silver compounds. *J Ind Microbiol Biotechnol* 33:627–34
- Sintubin L, De Windt W, Dick J, Mast J, Ha DV, Verstraete W, Boon N (2009) Lactic acid bacteria as reducing and capping agent for the fast and efficient production of silver nanoparticles. *Appl Microbiol Biotechnol* 84(4):741–749
- Taniguchi N (1974) Proceedings of International Conference on Precision Engineering (ICPE), Tokyo, Japan
- Tanja K, Ralph J, Eva O, Claes-Göran G (1999) Silver-based crystalline nanoparticles, microbially fabricated. *Proc Natl Acad Sci* 96:13611–13614
- Vaidyanathan R, Gopalram S, Kalishwaralal K, Deepak V, Pandian SRK, Gurunathan S (2010) Enhanced silver nanoparticle synthesis by optimization of nitrate reductase activity. *Colloids Surf B* 75(1): 335–341
- Verma VC, Kharwar RN, Gange AC (2010) Biosynthesis of antimicrobial silver nanoparticles by the endophytic fungus *Aspergillus clavatus*. *Nanomedicine* 5(1):33–40
- Vigneshwaran N, Kathe AA, Varadarajan PV, Nachane PR, Balasubramanya RH (2006) Biomimetics of silver nanoparticles by white rot fungus, *Phanerochaete chrysosporium*. *Colloids Surf B* 53:55–59

- Vigneshwaran N, Ashtaputre NM, Varadarajan PV, Nachane RP, Paralikar KM, Balasubramanya RH (2007) Biological synthesis of silver nanoparticles using the fungus *Aspergillus flavus*. *Mater Lett* 66:1413–1418
- Vivekanandhan S, Misra M, Mohanty AK (2009) Biological synthesis of silver nanoparticles using Glycine max (soybean) leaf extract: an investigation on different soybean varieties. *J Nanosci Nanotechnol* 9(12):6828–6833
- Zhang H, Li Q, Lu Y, Sun D, Lin X, Deng X (2005) Biosorption and bioreduction of diamine silver complex by *Corynebacterium*. *J Chem Technol Biotechnol* 80:285–290

# Chapter 3

## Biosynthesis of Gold Nanoparticles: A Review

Maggy F. Lengke, Charoen Sanpawanitchakit, and Gordon Southam

### 3.1 Introduction

Gold is one of the rarest metals on earth, and its importance has been acknowledged since antiquity. Gold is not only used in jewelry industry but also in a diverse range of industrial applications covering the field of biology and medicine, environment, and technology (e.g., Oldenburg et al. 1998; Vieira and Volesky 2000; Salata 2004; Sperling et al. 2008; Cai et al. 2008; Chen et al. 2008; Mohanpuria et al. 2008). Because of the increased demand of gold in many industrial applications, there is a growing need for cost effectiveness as well as to implement green chemistry in the development of new nanoparticles. Although various chemical and physical synthesis methods successfully produce pure and well-defined nanoparticles, these methods remain expensive and involve the use of hazardous chemicals. In consequence, biological processes that lead to the formation of nanoscale inorganic materials are appealing as possible environmentally friendly nanofactories.

The synthesis of gold nanoparticles of different sizes, ranging from <1 to several hundred nanometers, and shapes has been conducted in both aqueous and nonpolar organic solutions (Brust et al. 1994; Handley 1989; Selvakannan et al. 2003; Daniel and Astruc 2004). The usual synthetic route to prepare gold nanoparticles involves the reduction of a gold salt (usually a halide) in solution by various reducing agents in the presence of a stabilizer (Brust et al. 1994; Handley 1989; Selvakannan et al. 2003; Daniel and Astruc 2004; Masala and Seshadri 2004). The use of rapid reductants (e.g., white phosphorus, tannic acid, formamide, *o*-anisidine) results in bigger and generally spherical nanoparticles, while weak reducing agents (e.g., citrate, tartarate)

---

M.F. Lengke (✉)

Geomega Inc, 2525 28th Street, Suite 200, Boulder, CO 80301, USA

e-mail: maggylengke@yahoo.com

C. Sanpawanitchakit

EnviroGroup Limited, 3561 Stagecoach Road, Suite 205, Longmont, CO 80504, USA

G. Southam

Department of Earth Sciences, University of Western Ontario, London, ON, N6A 5B7, Canada

results in a slow reaction generating small nanoparticles (Handley 1989; Daniel and Astruc 2004). Sulfur-containing ligands (e.g., xanthates, disulfides, dithiols or trithiols), phosphanes, phosphines, amines, chalcogenides, carboxylates, and polymers have all been used to stabilize gold nanoparticles (Brust et al. 1994; Daniel and Astruc 2004).

Biological methods using organisms, such as bacteria and fungi (e.g., Southam and Beveridge 1994, 1996; Canizal et al. 2001; Kashefi et al. 2001; Mukherjee et al. 2001, 2002; Shankar et al. 2003; Keim and Farina 2005; Nair and Pradeep 2002; Ahmad et al. 2005; Lengke and Southam 2005, 2006, 2007; Lengke et al. 2006a, b, c, 2007), plants (e.g., Gardea-Torresdey et al. 2002), plant extracts (e.g., Shankar et al. 2003, 2004), and dead plant biomass (e.g., Gardea-Torresdey et al. 1999, 2000), for the synthesis of gold nanoparticles are relatively new areas, and are currently being explored. Although the biosynthesis of gold nanoparticles is relatively new, the interactions between bacteria and metals have been well documented (e.g., Heath 1981; Nash et al. 1981; Ehrlich 2002) and the ability of bacteria to accumulate metals has been recognized in the bioremediation field (e.g., Lloyd 2002; Dermont et al. 2008). Previous studies of the biosynthesis of gold nanoparticles have been focused on the use of gold (III)–chloride  $[\text{AuCl}_4^-]$  and gold(I)–thiosulfate  $[\text{Au}(\text{S}_2\text{O}_3)_2^{3-}]$  complexes. Therefore, the objective of this chapter is to review the current state of knowledge concerning the biosynthesis of gold nanoparticles by bacteria, cyanobacteria, and algae using these two gold complexes, based on the existing literature.

## 3.2 Gold Chemistry

Gold can occur in one of the six oxidation states, from  $-1$  to  $+5$  (Puddephatt and Vittal 1994), which can be related to its relatively high electronegativity. The most common form of gold complexes is in aurous  $[\text{Au(I)}]$  and auric  $[\text{Au(III)}]$  oxidation states (Emery and Leddicotte 1961). The dissolution of gold in aqueous solution is a combination process of oxidation and complexation. In the presence of a complexing ligand, Au(I) and Au(III) can form stable complexes, otherwise they can be reduced in solution to metallic gold (Nicol et al. 1987). The stability of gold complexes is related not only to the properties of the complexing ligand, but also more specifically to the donor atom of the ligand that is bonded directly to the gold atom. According to Nicol et al. (1987), the first rule is that the stability of gold complexes tends to decrease when the electronegativity of the donor atom increases. For example, the stability of gold halide complexes in solution follows the order  $\text{I}^- > \text{Br}^- > \text{Cl}^- > \text{F}^-$ . The second rule is that Au(III) is generally favored over Au(I) with hard ligands and Au(I) over Au(III) with soft ligands. The soft ligands containing less electronegative donor atoms such as S, C, P, and I form more stable complexes with Au(I), whereas the hard electron-donor ligands such as F, Cl, O, and N prefer Au(III). The preferred co-ordination number of Au(I)



is 2, tending to form linear complexes, and that of Au(III) is 4, tending to form square planar complexes.

The review of gold complexes below is limited for the gold(III)–chloride and gold(I)–thiosulfate because the published biosynthesis of gold nanoparticles by bacteria, cyanobacteria, and algae mainly utilized these two gold complexes.

### ***3.2.1 Gold(I)–Thiosulfate Complex***

Gold(I)–thiosulfate complex is a predominant species at a wide range of pH (acidic to alkaline) and moderate oxidizing to reducing conditions (Senanayake et al. 2003). Sodium thiosulfate is one component of an alternative lixiviant to cyanide for extraction of gold (Aylmore and Muir 2001), and it forms a strong complex with Au(I). The advantage of this approach is that thiosulfate is essentially non-toxic, and ore types that are refractory to gold cyanidation (e.g., carbonaceous or Carlin type ores) can be leached by thiosulfate. Some problems with this alternative process include the high consumption of thiosulfate, and the lack of a suitable recovery technique, because gold(I)–thiosulfate does not adsorb to activated carbon, a standard technique used in gold cyanidation to separate the gold complex from the ore slurry.

### ***3.2.2 Gold(III)–Chloride Complex***

Gold (III)–chloride complex is stable under oxidizing and acidic conditions (Ran et al. 2002). It decomposes above 160°C or in light. Many studies of biosynthesis gold nanoparticles had utilized the gold(III)–chloride acid solid as a starting material to form gold(III)–chloride complex (e.g., Nair and Pradeep 2002; Lengke et al. 2006a, b, c, 2007). Gold(III)–chloride acid solid ( $\text{HAuCl}_4 \cdot x\text{H}_2\text{O}$ ) can be produced by dissolving gold in aqua regia and then evaporating nitric acid ( $\text{HNO}_3$ ) with hydrochloric acid (HCl). This solid is also referred to as acid gold trichloride or gold(III)–chloride trihydrate (Emery and Leddicotte 1961; [http://en.wikipedia.org/wiki/Gold\(III\)\\_chloride](http://en.wikipedia.org/wiki/Gold(III)_chloride)). Gold(III)–chloride acid – appearing as long, bright yellow, needle-like crystals – is very hygroscopic and highly soluble in water and ethanol.

## **3.3 Biosynthesis of Gold Nanoparticles**

The interactions between bacteria/cyanobacteria/algae and gold have been well documented since 1986 for biosorption and biorecovery of gold. Our review includes 46 published papers, utilizing bacteria (24), cyanobacteria (8), and algae

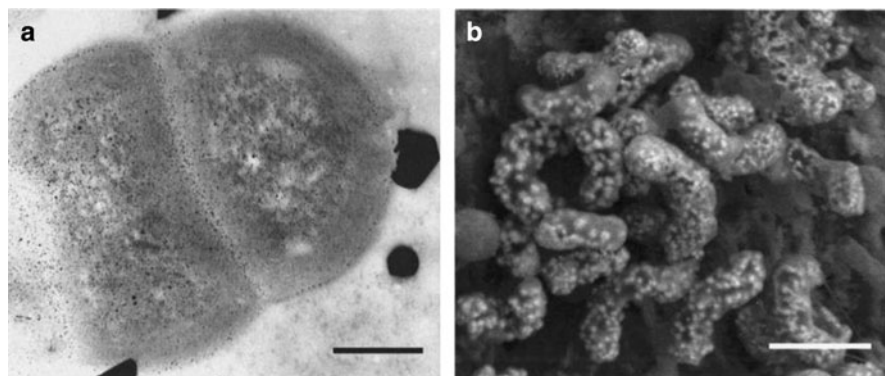


**Fig. 3.1** (a) A TEM micrograph of a thin section of cyanobacteria cell with the gold nanoparticles inside the cell, (b) a SEM micrograph of gold nanoparticles on the surface of sulfate-reducing bacteria (*Desulfovibrio* sp). Scale bars in (a) and (b) are 0.5 and 1.5  $\mu\text{m}$ , respectively

(14) to determine whether gold can be accumulated from gold(I)–thiosulfate and gold(III)–chloride solutions. Because of purposes other than the biosynthesis of gold particles, some studies of biosorption and biorecovery neither included details of the shape and size of gold particles (e.g., Kashefi et al. 2001; Nakajima 2003) nor described the experimental conditions such as pH, temperature, duration, initial gold concentrations, or bacterial population (e.g., Ting et al. 1995; Kashefi et al. 2001). In general, gold nanoparticles were precipitated intracellularly and/or extracellularly depending on the species (Fig. 3.1). The shape of gold particles precipitated by bacteria/cyanobacteria/algae includes spherical, oval, spongy clots, mushroom, irregular, triangular, tetragonal, hexagonal, octahedral, rod, cubic, dodecahedral, icosahedral, coil or wire, plate, and thin foil, with size ranging from 1 nm to several  $\mu\text{m}$  (Fig. 3.2), as discussed below.

### 3.3.1 Gold(I)–Thiosulfate Complex

The interactions between bacteria and cyanobacteria with a gold–thiosulfate complex have been studied by Lengke and Southam (2005, 2006, 2007) and Lengke et al. (2006a), and are summarized in Table 3.1. *Acidithiobacillus thiooxidans* isolated from the Driefontein Consolidated gold mine in Witwatersrand Basin, Republic of South Africa was able to produce gold particles in the presence of up to 0.26 mmol/L gold at pH  $\sim$  1.9–2.2 and 25°C within a period of 35–75 days (Lengke and Southam 2005). In the presence of dead bacterial cells and in the chemical abiotic experiments, gold was not precipitated under similar experimental conditions and duration. The bacterial system was able to precipitate 87–100% of the gold under diurnal light exposure, while only 11–69% of the gold was precipitated in the dark. The gold nanoparticles were precipitated inside the bacterial cells with the size  $<$ 10 nm,

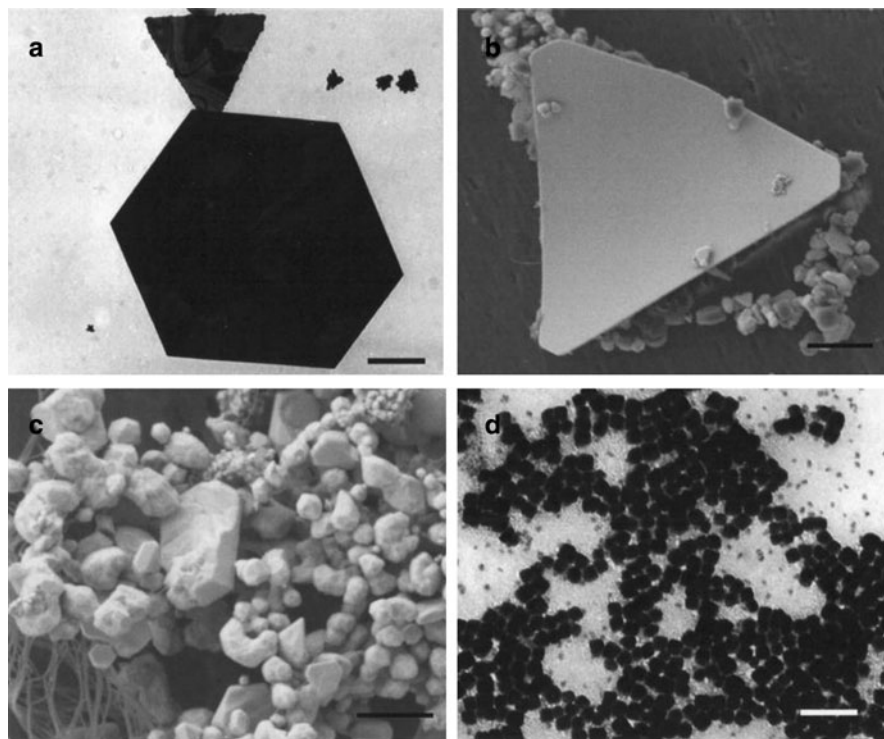


**Fig. 3.2** TEM and SEM micrographs of selected gold nanoparticles formed by cyanobacterial interactions with gold(III)-chloride and gold(I)-thiosulfate complexes. *Scale bars* in (a), (b), (c), and (d) are 0.5, 2, 1, and 0.1  $\mu\text{m}$ , respectively

forming a spherical shape. Outside the bacterial cells, the gold had formed coiled or wire, irregular, and rounded structures with an approximate size of 0.5–5  $\mu\text{m}$ , and a crystalline octahedral shape.

Heterotrophic sulfate-reducing bacteria (SRB) isolated from the Driefontein Consolidated gold mine in Witwatersrand Basin, Republic of South Africa was able to produce gold particles in the presence of up to 2.6 mmol/L gold at pH  $\sim$  7.4–7.9 and 23–25°C within a period of 6–53 days, in the presence or absence of iron (Lengke and Southam 2006). Only in the presence of live bacterial cells, gold was precipitated from solution. The gold nanoparticles were precipitated inside and at the bacterial cells with the size  $<10$  nm, forming a spherical shape. In bulk solution, the gold had formed spherical, sub-octahedral to octahedral shape with size ranging from 0.5 to 6  $\mu\text{m}$  (Lengke and Southam 2006). The role of SRB in the precipitation of gold was also investigated through column experiments in the presence of up to 2.6 mmol/L gold at pH  $\sim$  7.4–8.5 and 23–25°C within a period of 148 days, in the presence or absence of iron (Lengke and Southam 2007). In the bacterial systems, SRB precipitated gold inside and at the cells, forming spherical nanoparticles ( $<10$  nm). In bulk solution, the formation of octahedral gold crystals,

**Table 3.1** A summary of bacterial and cyanobacterial interactions with a gold(I)-thiosulfate complex

No	Bacteria Name	Shape	Extracellular/ Intracellular	Size	pH	Temperature (°C)	Period	Initial gold concentrations (mol/L)	Bacterial population (cells/mL)	Experimental condition	References
<b>Bacteria</b>											
1	<i>Acidithiobacillus thiooxidans</i>	Spherical, irregular, coil or wire, octahedral	Extracellular and intracellular	<10 nm (intracellular); 0.5–5 µm (extracellular)	1.9 and 2.2	19 and 25	35 days	(0–0.26) × 10 <sup>-3</sup>	10 <sup>7</sup> –10 <sup>8</sup>	Bacteria stationary growth phase	Lengke and Southam (2005)
		Spherical, irregular, coil or wire, octahedral	Extracellular and intracellular	<10 nm (intracellular); 0.5–5 µm (extracellular)	5.4–1.9	25	75 days	(0–0.26) × 10 <sup>-3</sup>	10 <sup>6</sup> –10 <sup>8</sup>	Inoculate with bacteria	
		No precipitation	No		1.9	25	75 days	(0–0.26) × 10 <sup>-3</sup>		Dead cells (autoclaved)	
		No precipitation	No		1.9 and 5.4	25	75 days	(0–0.26) × 10 <sup>-3</sup>		Abiotic	
2	Heterotrophic sulfate-reducing bacteria (SRB)	Octahedral, spherical	Extracellular and intracellular	<10 nm (intracellular); 0.5–6 µm (extracellular)	7.4–7.9	23–25	53 days	(0–2.55) × 10 <sup>-3</sup>	7 × 10 <sup>6</sup> to 3.5 × 10 <sup>7</sup>	Bacteria stationary growth phase	Lengke and Southam (2006)
		Octahedral, spherical	Extracellular and intracellular	<10 nm (intracellular); 0.5–6 µm (extracellular)	7.4–7.9	23–25	6 days	(0–1.14) × 10 <sup>-3</sup>	5 × 10 <sup>3</sup> to 10 <sup>6</sup>	Inoculate with bacteria	
		No precipitation	No precipitation		7.7	23–25	53 days	(0–1.14) × 10 <sup>-3</sup>		Dead cells (autoclaved)	
		No precipitation	No precipitation		7.4–7.7	23–25	53 days	(0–2.55) × 10 <sup>-3</sup>		Abiotic	

3	Heterotrophic sulfate-reducing bacteria (SRB)	Spherical, octahedral, foil	Extracellular and intracellular	<10 nm (intracellular); 1 µm to several mm (extracellular)	7.4–8.5 23–25	148 days	(0–2.55) × 10 <sup>-3</sup>	4.5 × 10 <sup>8</sup> to 1.4 × 10 <sup>9</sup>	Bacteria	Lengke and Southam (2007)
		Spherical		1 µm	7.4–9.1 23–25	148 days	(0–2.55) × 10 <sup>-3</sup>		Abiotic	
	Cyanobacteria									
1	<i>Plectonema boryanum</i> UTEX 485	Irregular-thin	Extracellular	Extracellular	5.3 25	28 days	(2–2.8) × 10 <sup>-3</sup>	3.8 × 10 <sup>8</sup>	Cyanobacteria stationary growth phase	Lengke et al. (2006a)
		Irregular, cubic	Extracellular and intracellular	<10 nm (intracellular); 10–25 nm (extracellular)	5.3 60	28 days	(2–2.8) × 10 <sup>-3</sup>	3.8 × 10 <sup>8</sup>	Cyanobacteria stationary growth phase	
		Cubic	Extracellular and intracellular	<10 nm (intracellular); 10–25 nm (extracellular)	5.3–3.9 100	28 days	(2–2.8) × 10 <sup>-3</sup>	3.8 × 10 <sup>8</sup>	Cyanobacteria stationary growth phase	
		Irregular	Extracellular and intracellular	<10 nm (intracellular); 10–25 nm (extracellular)	5.3–3.0 200	1 day	(2–2.8) × 10 <sup>-3</sup>	3.8 × 10 <sup>8</sup>	Cyanobacteria stationary growth phase	
			No precipitation		5 25	28 days	(2–2.8) × 10 <sup>-3</sup>		Abiotic	
		Cuboctahedral	Precipitation	25 nm	5–3.9 60	28 days	(2–2.8) × 10 <sup>-3</sup>		Abiotic	
		Cuboctahedral	Precipitation	25 nm	5–2.2 100	28 days	(2–2.8) × 10 <sup>-3</sup>		Abiotic	
		Cuboctahedral	Precipitation	25 nm	5–1.9 200	1 day	(2–2.8) × 10 <sup>-3</sup>		Abiotic	

framboid-like structures ( $\sim 1.5 \mu\text{m}$ ), and gold foil (mm-scale) was observed in the bacterial systems, while only a spherical shape with a size  $\sim 1 \mu\text{m}$  was observed in the chemical abiotic systems.

*Plectonema boryanum* UTEX 485, a filamentous cyanobacterium, had been reacted with a gold–thiosulfate complex (up to 2.8 mmol/L gold) at 25–100°C for up to 1 month and at 200°C for 1 day (Lengke et al. 2006a). The interaction of cyanobacteria with a gold–thiosulfate complex caused the separation of filaments into their constituent cells and released membrane vesicles after 14 days at 25°C. The precipitation of irregular gold particles on the surface of membrane vesicles was observed. At 60–200°C, nanoparticles of gold and gold sulfide were deposited inside the cells ( $< 10 \text{ nm}$ ) and on the outer surface of the sheaths ( $\sim 10\text{--}25 \text{ nm}$ ). The larger nanoparticles of gold ( $\sim 20\text{--}25 \text{ nm}$ ) were distinctly cubic in shape. In the chemical abiotic systems, the gold–thiosulfate were stable for 1 month at 25°C, whereas gold nanoparticles ( $\sim 25 \text{ nm}$ ) with a cubohedral habit were precipitated at 60–200°C.

### 3.3.2 Gold(III)–Chloride Complex

The interactions between bacteria, cyanobacteria, and algae with a gold(III)–chloride complex have been studied using different species, and the results of these studies are summarized in Tables 3.2, 3.3, and 3.4. The first published laboratory study to understand the interaction of a mixed bacteria (*Bacillus mesentericus niger*, *Bacillus oligonitrophilus*, and *Bacterium nitrificans*) with initial elemental gold was conducted by Korobushkina and Korobushkin (1986). The objective of their study was to determine whether gold can be biologically re-deposited. The elemental gold was dissolved into solution, presumably as gold(III)–chloride or gold–organic complexes, and a reduction process occurred simultaneously, forming spherical/oval ( $1\text{--}2 \mu\text{m}$ ), spongy clots/clusters/nodules ( $0.1\text{--}20 \mu\text{m}$ ), and mushroom ( $0.1\text{--}0.5 \mu\text{m}$ ) shapes. Southam and Beveridge (1994, 1996) employed *Bacillus subtilis* 168 in their experiments at 4, 23–25, 60, and 90°C within 1 week to 8 months. Gold nanoparticles were initially precipitated inside the bacterial cells ( $5\text{--}50 \text{ nm}$ ) and were released into solution, forming spherical ( $20 \text{ nm}$ ) and hexagonal–octahedral ( $4\text{--}20 \mu\text{m}$ ) gold. The formation of crystalline octahedral gold was enhanced by an increase in the experimental duration and temperature. The potential of 14 hyperthermophilic and mesophilic dissimilatory iron(III) reducing bacteria to precipitate elemental gold from solutions was investigated by Kashefi et al. (2001) using hydrogen ( $\text{H}_2$ ), lactate, or acetate electron donor at neutral pH. Of 14 species, 6 were able to precipitate elemental gold only in the presence of  $\text{H}_2$  electron donor at 100°C. Most of the six bacteria precipitated gold at the cell surfaces (nm scale), except for *Geovibrio ferrireducens* (ATCC 51996). However, a closer inspection of the thin sections of several species [e.g., *Geobacter sulfurreducens* (ATCC 51573), *Pyrobaculum islandicum* (DSM 4184), *Thermotoga maritima* (DSM 3109)] indicated that gold was also precipitated intracellularly.

Table 3.2 A summary of bacterial interactions with a gold(III)–chloride complex

No	Bacteria name	Shape	Extracellular/ intracellular	Size	pH	Temperature (°C)	Period	Initial gold concentrations (mol/L)	Bacterial population (cells/mL)	Experimental condition	References
1	<i>Bacillus mesentericus niger</i>	Spherical, oval	Extracellular	1–2 µm (Extracellular)	7.5	25	360 days	$2.5 \times 10^{-3}$		Nutrient medium	Korobushkina and Korobushkin (1986)
	<i>Bacillus oligotrophilus</i>	Spongy clots/ clusters/ nodules	Extracellular	0.1–20 µm (Extracellular)							
	<i>Bacterium nitrificans</i>	Mushroom	Extracellular	0.1–0.5 µm (extracellular)							
2	<i>Bacillus subtilis</i> 168	Irregular, spherical	Extracellular and intracellular	5–50 nm (Intracellular)	2.69	60	7–224 days	$2.5 \times 10^{-3}$	20 mg/mL dry cell weight	Bacteria late stationary phase	Southam and Beveridge (1994)
		Hexagonal, octahedral	No precipitation	20 µm (Extracellular)		60	7–224 days	$5 \times 10^{-3}$		Abiotic	
3	<i>Bacillus subtilis</i> 168	Spherical, irregular, octahedral	Extracellular and intracellular	<20 nm (intracellular)	2.6	4	7–28 days	$2.5 \times 10^{-3}$	20 mg/mL dry cell weight	Bacteria late stationary phase	Southam and Beveridge (1996)
			Extracellular and intracellular	20 nm(1 h), 4–10 µm (4 weeks) – extracellular	2.6	21–23		$2.5 \times 10^{-3}$		Bacteria late stationary phase	
			Extracellular and intracellular		2.6	60		$2.5 \times 10^{-3}$		Bacteria late stationary phase	
			Extracellular and intracellular		2.6	90		$2.5 \times 10^{-3}$		Bacteria late stationary phase	
			No precipitation		2.6	4		$5 \times 10^{-3}$		Abiotic	
			No precipitation		2.6	21–23		$5 \times 10^{-3}$		Abiotic	
			No precipitation		2.6	60		$5 \times 10^{-3}$		Abiotic	
			No precipitation		2.6	90		$5 \times 10^{-3}$		Abiotic	
4	<i>Pyrobaculum islandicum</i> (DSM 4184)		Extracellular	few nm	6–6.2	100	0.5–3 h		0.025 mg/mL	H <sub>2</sub> -CO <sub>2</sub> (80:20 vol/vol) or N <sub>2</sub> - CO <sub>2</sub> (80:20 vol/vol) with lactate or acetate	Kashefi et al. (2001)

(continued)

Table 3.2 (continued)

No	Bacteria name	Shape	Extracellular/ intracellular	Size	pH	Temperature (°C)	Period	Initial gold concentrations (mol/L)	Bacterial population (cells/mL)	Experimental condition	References
	<i>Pyrobaculum aerophilum</i> (DSM 7523)			No precipitation	6–6.2	100	0.5–3 h		0.025 mg/mL	No electron donor	
	<i>Pyrococcus furiosus</i> (DSM 3638)			No precipitation	6–6.2	30	0.5–3 h		0.025 mg/mL	H <sub>2</sub> -CO <sub>2</sub> (80:20 vol/vol) or N <sub>2</sub> -CO <sub>2</sub> (80:20 vol/ vol) with lactate or acetate	
	<i>Archaeoglobus fulgidus</i> (DSM 4304)			No precipitation	7	100	0.5–3 h		0.025 mg/mL		
	<i>Ferroplasma placidus</i> (DSM 10642)			No precipitation	7	100	0.5–3 h		0.025 mg/mL		
	<i>Shewanella algae</i> strain BR7 (ATCC 51181)		Extracellular (also intracellular)	No precipitation	7	100	0.5–3 h		0.025 mg/mL	H <sub>2</sub> -CO <sub>2</sub> (80:20 vol/vol)	
	<i>Desulfuromonas vulgaris</i> (ATCC 35115)		Extracellular	No precipitation	7	100	0.5–3 h		0.025 mg/mL	N <sub>2</sub> -CO <sub>2</sub> (80:20 vol/vol) with lactate	
	<i>Desulfuromonas palmitatis</i> (ATCC 51701)			No precipitation	7	100	0.5–3 h		0.025 mg/mL	N <sub>2</sub> -CO <sub>2</sub> (80:20 vol/vol) with lactate	
	<i>Geothrix fermentans</i> (ATCC 700665)			No precipitation	7	100	0.5–3 h		0.025 mg/mL	N <sub>2</sub> -CO <sub>2</sub> (80:20 vol/vol) with lactate or acetate	



<i>Geobacter metallireducens</i> (ATCC 53774)	No precipitation	7	100	0.5–3 h	0.025 mg/mL	H <sub>2</sub> -CO <sub>2</sub> (80:20 vol/vol) or N <sub>2</sub> -CO <sub>2</sub> (80:20 vol/vol) with acetate	Karthikeyan and Beveridge (2002)
<i>Thermotoga maritima</i> (DSM 3109)	Extracellular (also intracellular)	7	100	0.5–3 h	0.025 mg/mL	H <sub>2</sub> -CO <sub>2</sub> (80:20 vol/vol)	Nair and Pradeep (2002)
<i>Geovibrio ferritducens</i> (ATCC 51996)	No precipitation	7	30	0.5–3 h	0.025 mg/mL	H <sub>2</sub> -CO <sub>2</sub> (80:20 vol/vol)	Nakajima (2003)
<i>Desulfotobacterium metallireducens</i>	Intracellular	7	100	0.5–3 h	0.025 mg/mL	H <sub>2</sub> -CO <sub>2</sub> (80:20 vol/vol)	
<i>Geobacter sulfurreducens</i> (ATCC 51573)	No precipitation	7	100	0.5–3 h	0.025 mg/mL	H <sub>2</sub> -CO <sub>2</sub> (80:20 vol/vol) or N <sub>2</sub> -CO <sub>2</sub> (80:20 vol/vol) with lactate	Karthikeyan and Beveridge (2002)
<i>Pseudomonas aeruginosa</i> PAO1 biofilm	Extracellular and intracellular	acid	20	0.5 h	1 × 10 <sup>-5</sup> to 5 × 10 <sup>-3</sup>	H <sub>2</sub> -CO <sub>2</sub> (80:20 vol/vol) or N <sub>2</sub> -CO <sub>2</sub> (80:20 vol/vol) with acetate	
<i>Lactobacillus</i> sp.	Spherical, triangular, hexagonal	4.4	25	3 days	1 × 10 <sup>-3</sup>		Nair and Pradeep (2002)
	Spherical	4.4	25	3 days	Au + Ag (equimolar)		
<i>Arthrobacter tumescens</i> IAM 1447	Extracellular and intracellular	3	30	1 h	15 mg/100 mL cell weight		Nakajima (2003)
<i>Bacillus subtilis</i> IAM 1026	Spherical	3	30	1 h	5 × 10 <sup>-5</sup>		

(continued)



*Brevibacterium*  
*helvolum* IAM  
1637

*Corynebacterium*  
*equi* IAM 1038

*Enterobacter*  
*aerogenes* IAM  
1183

*Erwinia herbicola*  
IAM 1562

*Escherichia coli*  
IAM 1264

*Micrococcus luteus*  
IAM 1056

*Nocardia coralina*  
IAM 12121

*Nocardia*  
*erythropolis*  
IAM 1399

*Nocardia rugosa*  
kcc-A0193

*Pseudomonas*  
*aeruginosa*  
IAM 1054

*Pseudomonas*  
*aeruginosa*  
IAM 1095

*Pseudomonas*  
*fluorescens*  
IAM 12022

*Pseudomonas*  
*maltophilia*  
IAM 1554

*Pseudomonas*  
*putida* IAM  
1506

*Serratia marcescens*  
IAM 1022

*Thiobacillus*  
*novellus* IFO  
12443

---

(continued)

Table 3.2 (continued)

No	Bacteria name	Shape	Extracellular/ intracellular	Size	pH	Temperature (°C)	Period	Initial gold concentrations (mol/L)	Bacterial population (cells/mL)	Experimental condition	References
9	Magnetotactic bacteria (cocci, bacilli and multicellular)	Irregular	Extracellular and intracellular	few nm		25	1 day	$0.1 \times 10^{-3}$		Uncultured bacteria	Keim and Farnia (2005)
10	<i>Ralstonia metalliarans</i>		Extracellular and intracellular	few nm (intracellular)		30	3 days	$0.4 \times 10^{-3}$ (Au) + $12.8 \times 10^{-3}$ (Ag) $5 \times 10^{-2}$	$10^3$ to $1.8 \times 10^7$	Inoculate with bacteria in a gold containing growth medium	Reith et al. (2006)
11	<i>Pseudomonas stutzeri</i> NCIMB 13420 <i>Bacillus subtilis</i> DSM 10 <i>Pseudomonas putida</i> DSM 291	Spherical, irregular	Extracellular and intracellular	<10 nm and above	5–6	30 28	5 days 1–3 days	$5 \times 10^{-2}$ $1.3–10^{-3}$	$4.2 \times 10^4$ to $1.5 \times 10^8$	Inoculate with bacteria in a growth medium without gold	Gericke and Pinches (2006a) Gericke and Pinches (2006b)
		Spherical	Intracellular	<10 nm	3	28	1–3 days	$1.3 \times 10^{-3}$		Dead cells (lysed) (1) Seening process	
		Spherical Spherical, irregular spherical, irregular Spherical, irregular	Intracellular Extracellular and intracellular Extracellular and intracellular Extracellular and intracellular	<10 nm <10 nm and above <10 nm and above <10 nm and above <10 nm and above	5 7 9 5		1 day	$1.3 \times 10^{-3}$	10 mg cells/mL	(2) Determine the effect of pH  (3) Determine the effect of temperature	



Table 3.2 (continued)

No	Bacteria name	Shape	Extracellular/ intracellular	Size	pH	Temperature (°C)	Period	Initial gold concentrations (mol/L)	Bacterial population (cells/mL)	Experimental condition	References
16	<i>Pseudomonas aeruginosa</i> with fluorescent pigment pyoverdinin <i>Pseudomonas aeruginosa</i> with blue pigment pyocyanin <i>Pseudomonas aeruginosa</i> ATCC 90271	Spherical	Extracellular	15 ± 5 nm  25 ± 15 nm  40 ± 10 nm	37	37	1 day	1 × 10 <sup>-3</sup>		Live bacteria	Hussey et al. (2007)
17	<i>Rhodobacter capsulatus</i> (purple non-sulfur bacteria)	Spherical, irregular	Extracellular and intracellular	No precipitation		37 25	1 day 20 h	1 × 10 <sup>-3</sup> 2 × 10 <sup>-4</sup>	1 × 10 <sup>9</sup>	Abiotic Live bacteria with N <sub>2</sub> gas and lactate	Feng et al. (2008)
18	<i>Bacillus licheniformis</i>	Cubes	Extracellular	10 nm 20–48 nm 10–100 nm		25	2 days	4 × 10 <sup>-4</sup> 8 × 10 <sup>-4</sup> 1 × 10 <sup>-3</sup>	1 g wet weight/ 100 mL 100 mg dry weight/ 100 mL	Live bacteria	Kalishwaralal et al. (2009)
19	<i>Bacillus megatherium</i> D01	Spherical, irregular, hexagonal, triangular, anisotropic Spherical	Extracellular Extracellular	<2.5 nm (10–30 min); 1–8 nm (1 h); 1–30 nm (>6 h)	3.2	26	9 h	0.5 × 10 <sup>-6</sup>	100 mg dry weight/ 100 mL	Live bacteria	Wen et al. (2009)
20	<i>Stenotrophomonas maltophilia</i>	Spherical, irregular	Extracellular Intracellular	1.5–2.5 nm; average 1.9 ± 0.8 nm 40 nm	3.2	26	4 h 8 h	0.5 × 10 <sup>-6</sup> 1 × 10 <sup>-3</sup>	1 g dry weight/L	Live bacteria and dodecamethiol as the capping ligand Dried biomass and dodecamethiol as the capping ligand	Nangia et al. (2009)

**Table 3.3** A summary of cyanobacterial interactions with a gold(III)-chloride complex

No	Bacteria name	Shape	Extracellular/ intracellular	Size	pH	Temperature (°C)	Period	Initial gold concentrations (mol/L)	Bacterial population (cells/mL)	Experimental condition	References
1	<i>Nostoc punctiforme</i>					25	0.5 h	$3 \times 10^{-5}$	0.1–0.12 mg/ mL dry cell weight	Live cyanobacteria	Karamushka et al. (1991a, b)
	<i>Microcystis aeruginosa</i>										
	<i>Spirulina platensis</i>										
	<i>Phormidium inundatum</i>										
	<i>Anabaena cylindrica</i>										
	<i>Anacystis nidulans</i>										
	<i>Synechococcus elongatus</i>										
	<i>Synechococcus parvulus</i>										
	<i>Phormidium borjanum</i>										
2	<i>Plectonema terebrans</i>		Extracellular and intracellular			25	14 days	$1 \times 10^{-2}$		Live cyanobacteria	Dyer et al. (1994)
			Extracellular and intracellular			25	14 days	$1 \times 10^{-2}$		Dead cells (autoclaved)	
3	<i>Plectonema borjanum</i> UTEX 485	Irregular, spherical, octahedral	Extracellular and intracellular	<10 nm (intracellular); 1 $\mu$ m (extracellular)	1.6–2.2	25	28 days	(2–2.8) $\times 10^{-3}$	8 mg/10 mL dry weight	Cyanobacteria stationary growth phase	Lengke et al. (2006a)
			Extracellular and intracellular	<10 nm (intracellular);	1.6–2.2	60	28 days	(2–2.8) $\times 10^{-3}$			

(continued)

Table 3.3 (continued)

No	Bacteria name	Shape	Extracellular/ intracellular	Size	pH	Temperature (°C)	Period	Initial gold concentrations (mol/L)	Bacterial population (cells/mL)	Experimental condition	References
		Irregular, spherical, octahedral		1 µm (extracellular)					8 mg/10 mL dry weight	Cyanobacteria stationary growth phase	
		Irregular, spherical, octahedral	Extracellular and intracellular	<10 nm (intracellular); 1–10 µm (extracellular)	1.6–2.2	100	28 days	(2–2.8) × 10 <sup>-3</sup>	8 mg/10 mL dry weight	Cyanobacteria stationary growth phase	
		Irregular, spherical, octahedral	Extracellular and intracellular	<10 nm (intracellular); 1–10 µm (extracellular)	1.6–2.2	200	1 day	(2–2.8) × 10 <sup>-3</sup>	8 mg/10 mL dry weight	Cyanobacteria stationary growth phase	
		Irregular, spherical, octahedral		No precipitation		25	28 days	(2–2.8) × 10 <sup>-3</sup>		Abiotic	
		Irregular, spherical, octahedral		No precipitation		60	28 days	(2–2.8) × 10 <sup>-3</sup>		Abiotic	
		Irregular, spherical, octahedral		25 nm		100	28 days	(2–2.8) × 10 <sup>-3</sup>		Abiotic	
		Irregular, spherical, octahedral		25 nm		200	1 day	(2–2.8) × 10 <sup>-3</sup>		Abiotic	
4	<i>Plectonema boryanum</i> UTEX 485	Irregular, spherical, octahedral	Extracellular and intracellular	<10 nm (intracellular); 1.5 µm (extracellular)	1.6–2.2	25	28 days	2 × 10 <sup>-3</sup>	8 mg/10 mL dry weight	Cyanobacteria stationary growth phase	Lengke et al. (2006b)
		Irregular, spherical, octahedral		<10 nm (intracellular); 1.5 µm (extracellular)	1.6–1.9	60	28 days	2 × 10 <sup>-3</sup>	8 mg/10 mL dry weight	Cyanobacteria stationary growth phase	
		Irregular, spherical, octahedral		<10 nm (intracellular); 1–10 µm (extracellular)	1.6–1.9	100	28 days	2 × 10 <sup>-3</sup>	8 mg/10 mL dry weight	Cyanobacteria stationary growth phase	
		Irregular, spherical, octahedral		<10 nm (intracellular); 1–10 µm (extracellular)	1.9–2.2	200	1 day	2 × 10 <sup>-3</sup>	8 mg/10 mL dry weight	Cyanobacteria stationary growth phase	



	Irregular, spherical, octahedral	Extracellular and intracellular	2.2	25	28 days	$2 \times 10^{-3}$	Dead cells (autoclaved)
		No precipitation	2.2	25	28 days	$2 \times 10^{-3}$	Abiotic
	Cubic	No precipitation	2.2	60	28 days	$2 \times 10^{-3}$	Abiotic
	Cubic	Precipitation	2.2-1.9	100	28 days	$2 \times 10^{-3}$	Abiotic
	Irregular, spherical, octahedral	Precipitation	2.2-1.6	200	1 day	$2 \times 10^{-3}$	Abiotic
5	<i>Plectonema boryanum</i> UTEX 485	Extracellular and intracellular	1.9-2.2	25	1 day	$(0.8-7.6) \times 10^{-3}$	Cyanobacteria stationary Lengke et al. (2006c)
	Irregular, octahedral	Extracellular and intracellular	1.9	25	2 days	$7.6 \times 10^{-3}$	weight mg/mL dry Cyanobacteria stationary Lengke et al. (2007)
6	<i>Plectonema boryanum</i> UTEX 485	Extracellular and intracellular	1.9	60	2 days	$7.6 \times 10^{-3}$	weight mg/mL dry Cyanobacteria stationary Lengke et al. (2007)
	Irregular, octahedral	Extracellular and intracellular	1.9	80	1 day	$7.6 \times 10^{-3}$	weight mg/mL dry Cyanobacteria stationary Lengke et al. (2007)
	Irregular, octahedral	Extracellular and intracellular	1.9	25	2 days	$7.6 \times 10^{-3}$	weight mg/mL dry Cyanobacteria stationary Lengke et al. (2007)
	Irregular, octahedral	No precipitation	1.9	60	2 days	$7.6 \times 10^{-3}$	weight mg/mL dry Cyanobacteria stationary Lengke et al. (2007)
	Irregular, octahedral	No precipitation	1.9	80	1 day	$7.6 \times 10^{-3}$	weight mg/mL dry Cyanobacteria stationary Lengke et al. (2007)

**Table 3.4** A summary of algae interactions with a gold(III)-chloride complex

No	Algae	Shape	Extraceellular/ intracellular	Size	pH	Temperature (°C)	Period	Initial gold concentrations (mol/L)	Algae concentration	Experimental condition	References
1	<i>Chlorella vulgaris</i> biomass				2-7	25	2 h	$1 \times 10^{-4}$ (equimolar of $\text{Au}^+$ , $\text{Hg}^{2+}$ , $\text{Pb}^{2+}$ , $\text{Al}^{3+}$ , $\text{Zn}^{2+}$ , and $\text{Cu}^{2+}$ )		Batch experiment with dead cells (lyophilized)	Damall et al. (1986)
					2-6	25		$1 \times 10^{-4}$ (equimolar of $\text{Au}^+$ , $\text{Hg}^{2+}$ , $\text{Pb}^{2+}$ , $\text{Al}^{3+}$ , $\text{Zn}^{2+}$ , and $\text{Cu}^{2+}$ )		Column experiment with dead cells (lyophilized) and polyacrylamide matrix	
2	<i>Chlorella vulgaris</i> biomass	Tetrahedral crystals, dcahedral, icosahedral structures	Extraceellular and intracellular	few nm		25	0.25 h	$(0.1-0.8) \times 10^{-3}$	2 mg/mL	Dead cells (lyophilized)	Hosea et al. (1986)
3	<i>Chlorella vulgaris</i> biomass				2-3	25	1 h	$1 \times 10^{-4}$	5 mg/mL	Dead cells	Greene et al. (1986)
4	<i>Chlorella vulgaris</i> biomass				1-8 3	25 25	1 h 0.5 h	$1 \times 10^{-4}$	5 mg/mL	Dead cells Dead cells (lyophilized)	Watkins et al. (1987)
5	<i>Sargassum natans</i> biomass <i>Sargassum fluitans</i> biomass <i>Macrocystis pyrifera</i> biomass	Spherical, irregular	Extraceellular		1-6.3	4-60	0.5-4 h	$0.05-5 \times 10^{-3}$		Dead cells	Kuyucak and Volesky (1989a, b)



Table 3.4 (continued)

No	Algae	Shape	Extraceellular/ intracellular	Size	pH	Temperature (°C)	Period	Initial gold concentrations (mol/L)	Algae concentration	Experimental condition	References
7	<i>Chlorella vulgaris</i> YA-1-1				4–10	25	up to 1 h	$3 \times 10^{-5}$	0.02–0.08 mg/ mL dry weight	Live algae	Karamushka et al. (1991a)
8	<i>Chlorella vulgaris</i> LARG-1				4–10	25	up to 1 h	$3 \times 10^{-5}$	0.02–0.08 mg/ mL dry weight	Live algae	Karamushka et al. (1991b)
	<i>Chlorella vulgaris</i> LARG-3										
	<i>Chlorella vulgaris</i> N 875										
	<i>Chlorella vulgaris</i> YA-1-1										
	<i>Scenedesmus obliquus</i>										
	<i>Porphyridium sordidum</i>										
	<i>Porphyridium cruentum</i>										
	<i>Porphyridium purpureum</i>										
9	<i>Chlorella vulgaris</i>							0.05 or $0.1 \times 10^{-3}$		Live algae, and different treatment applied	Ting et al. (1995)
10	Dealuminated seaweed waste	Hexagonal, tetrahedral, rod, irregular, dodecahedral	Extraceellular	20 nm to 5 $\mu$ m	2–10	25	1 day	$5 \times 10^{-6}$ to $3.8 \times 10^{-3}$	3 g/L dry weight	Dead cells	Romero- González et al. (2003)

11	<i>Saccharomyces cerevisiae</i> biomass	Extracellular	3	20–60	1 h	$5 \times 10^{-4}$	2.5 mg/mL dry weight	Dead cells	Lin et al. (2005)
12	<i>Sargassum wightii</i> biomass	Spherical Extracellular	8–12 nm		15 h	$1 \times 10^{-3}$	0.1 g/L dry weight	Dead cells	Singaravelu et al. (2007)
13	<i>Fucus vesiculosus</i> biomass	Irregular, spherical Extracellular	2–11	23	up to 24 h	$5 \times 10^{-4}$	1 g/L dry weight	Dead cells	Mata et al. (2009)

The interaction of *Pseudomonas aeruginosa* PAO1 biofilm and a gold(III)–chloride complex resulted in the formation of both extracellular and intracellular gold (Karthikeyan and Beveridge 2002). Most gold particles were precipitated at the cell surfaces with lesser amounts inside the cells and little throughout the exopolymeric substances (EPS). Nair and Pradeep (2002) used *Lactobacillus* sp. to assist the precipitation of gold, silver, and gold–silver alloy. Gold particles were precipitated both within and outside the cells in the range of 20–50 nm and >100 nm forming spherical, triangular, and hexagonal shapes. In the system containing both silver and gold, gold–silver alloy precipitated inside the bacterial cells, forming 100–300 nm crystals within 3 days. Nakajima (2003) and Tsuruta (2004) conducted gold biosorption to determine maximum gold accumulation using 8 and 25 bacterial species, respectively. However, the size and shape of gold accumulation were not described in their studies. *Escherichia coli* and *Pseudomonas maltophilia* have extremely high ability to accumulate gold from a gold(III)–chloride solution at pH 3 and 30°C (Nakajima 2003). Tsuruta (2004) found that some gram-negative bacterial species (e.g., *Acinetobacter calcoaceticus*, *Erwinia herbicola*, *Pseudomonas aeruginosa*, and *Pseudomonas maltophilia*) have high ability to sorb gold at pH 3 and 25°C. Uncultured magnetotactic cocci bacteria, collected from Itaipu lagoon, Rio de Janeiro, Brazil were able to precipitate gold in the capsule and granules (Keim and Farina 2005). 16S ribosomal DNA clones from bacterial biofilms of the secondary gold grains from two sites in Australia (Tomakin Park Gold Mine, New South Wales and the Hit and Miss Gold Mine, Queensland) displayed 99% similarity to *Ralstonia metallidurans* (Reith et al. 2006). The laboratory experiments using the same bacteria confirmed that elemental gold was precipitated during the interaction with a gold(III)–chloride solution with both viable and dead cells. Gericke and Pinches (2006a, b) conducted laboratory experiments using three bacterial species (*Pseudomonas stutzeri* NCIMB 13420, *Bacillus subtilis* DSM 10, and *Pseudomonas putida* DSM 291) to determine the effect of pH (3–9), temperature (25–50°C), and gold concentrations (1.3–13 mol/L) on the size and shape of gold particles. In all cases, gold was precipitated uniformly inside the cells as spherical shapes (<10 nm) at all pH values, but larger particles with irregular, undefined shapes formed at pH 7 and 9. The size and rate of gold precipitation increased with increasing temperature and gold concentrations. Konishi et al. (2006) investigated the reduction and precipitation of gold using *Shewanella algae* ATCC 51181. The results showed that elemental gold was only formed in the presence of bacteria with H<sub>2</sub> electron donor, forming 10–20 nm irregular shape. The biosynthesis of gold nanoparticles was investigated using *Escherichia coli* DH5 $\alpha$  by Du et al. (2007). The gold nanoparticles formed on the bacterial surfaces, mostly as spherical with triangular and quasi-hexagonal shapes. Deplanche and Macaskie (2007) achieved gold precipitation intracellularly (<10 nm) and extracellularly (20–50 nm) using both *Escherichia coli* and *Desulfovibrio desulfuricans* with H<sub>2</sub> as the electron donor. Gold particles were not precipitated in the abiotic conditions or the presence of heat-killed cells, and the presence of copper in solution inhibited gold precipitation. At pH 2, red suspension was observed, indicating the formation of smaller gold particles, and at pH 9, dark blue suspension was formed, presumably

containing larger gold particles. *Rhodopseudomonas capsulata* was able to precipitate gold from a gold(III)–chloride solution at pH 4–7, forming spherical, plate, triangular, and hexagonal gold with size ranging from 10 to 400 nm (He et al. 2007). Biosynthesis of gold nanoparticles using *Pseudomonas aeruginosa* was achieved and formed extracellular spherical gold with size ranging from 15 to 40 nm (Husseiny et al. 2007). Feng et al. (2008) discovered that *Rhodobacter capsulatus* were able to precipitate gold nanoparticles within and outside the bacterial cells, forming spherical and irregular gold with average size ranging from 10 to 48 nm. *Bacillus licheniformis* precipitated gold nanocubes (10–100 nm) within 2 days at 25°C (Kalishwaralal et al. 2009). Monodispersed gold nanoparticles capped with dodecanethiol were biosynthesized extracellularly by *Bacillus megatherium* D01 at 26°C (Wen et al. 2009). The presence of thiol capping ligand induced the formation of spherical gold nanoparticles with size <2.5 nm. Nangia et al. (2009) reported the biosynthesis of gold nanoparticles by *Stenotrophomonas maltophilia* forming ~40 nm spherical and irregular shapes at 25°C for 8 h.

In the cyanobacterial system, Karamushka et al. (1991a, b) investigated gold biosorption using nine different species, and all of them were able to accumulate gold. Dyer et al. (1994) found that live and dead cells of *Plectonema terebrans* were able to precipitate and accumulate elemental gold. The studies by Karamushka et al. (1991a, b) and Dyer et al. (1994) did not describe the size and shape of the gold formed. *Plectonema boryanum* UTEX 485, a filamentous cyanobacterium, had been reacted with a gold(III)–chloride complex (up to 2.8 mmol/L gold) at 25–100°C for up to ~1 month and at 200°C for 1 day (Lengke et al. 2006a, b, c, 2007). On the addition of a gold(III)–chloride solution to the cyanobacteria, all cyanobacteria were killed within several minutes at all temperatures investigated. A significant increase in the precipitation of gold occurred with increasing temperature from 25 to 60–200°C. Gold nanoparticles were precipitated inside the cells (<10 nm) and also formed octahedral shape in the bulk solution from 1 µm at 25°C to 10 µm at 100°C. For abiotic experiments using a gold(III)–chloride solution, total soluble gold was stable in solution at 25–80°C, but it decreased with time at 100 and 200°C, forming irregular or cubic gold (~25 nm).

In the algae system, most of the published literature focused on the biosorption and biorecovery of gold from solution (e.g., Darnall et al. 1986; Hosea et al. 1986; Watkins et al. 1987); therefore, the size and shape of gold particles were not described in their published papers. Darnall et al. (1986) conducted the biosorption and biorecovery experiments of Au, Hg, Pb, Al, Zn, and Cu on *Chlorella vulgaris* biomass at pH 2–7. Between pH 5 and 7, these metals bound strongly to the cell surfaces, but most of these algae-bound metals were desorbed back into solution by lowering the pH to 2, except for Au, Hg, and Ag. Hosea et al. (1986) also conducted the biosorption and biorecovery experiments of gold using *Chlorella vulgaris* biomass. Elemental gold was precipitated inside and outside the cells forming nanometer-scale of irregular and spherical gold. Biosorption of gold by *Chlorella vulgaris* biomass reached maximum binding at pH 3 (Greene et al. 1986). Inhibition and reversal of gold binding by strong ligands were pH dependent, with the order of effectiveness: thiourea > cyanide > mercaptoethanol > bromide. Watkins et al. (1987)

confirmed that *Chlorella vulgaris* biomass has high affinity for a gold(III)–chloride solution. Eleven species of brown, green, and red algae were tested for their ability to sorb gold from a gold(III)–chloride solution, and the maximum gold sorption was shown by *Sargassum natans* at pH 2.5 (Kuyucak and Volesky 1989a, b). The rates of gold biosorption increased at higher temperature from 4 to 60°C. The presence of other cations such as U, Fe, Zn, Ni, Ca, Ag, and Co did not affect the gold biosorption of *Sargassum natans* biomass at pH 2.5; however, anions such as sulfate, nitrate, and phosphate affected the biosorption ability. Gardea-Torresdey et al. (1990) showed that the gold binding capacity of five alga biomass increased as the algal carboxyl groups were esterified. Karamushka et al. (1991a, b) investigated gold biosorption using nine different species of algae and all of them were able to accumulate gold. The uptake of gold (III)–chloride solution was enhanced by several treatments such as acid, alkali, heat, and formaldehyde over the live/pristine cells (Ting et al. 1995). Gold precipitation by dealginated seaweed waste has been studied to elucidate the mechanisms of gold uptake from solution at pH 2–9 by Romero-González et al. (2003). In this study, gold was precipitated as hexagonal, tetrahedral, rod, irregular, and decahedral shapes with size ranging from ~20 nm to 5 µm. Lin et al. (2005) conducted a study of gold biosorption by *Saccharomyces cerevisiae* and determined that the gold bound on the cell wall had been reduced to elemental gold. Biosynthesis of gold nanoparticles was performed using *Sargassum wightii* biomass, collected from Mandapam Camp, Tamil Nadu, India (Singaravelu et al. 2007). The gold particles were precipitated as monodisperse spherical gold with size ranging from 8 to 12 nm. Mata et al. (2009) investigated gold biosorption and bioreduction using *Fucus vesiculosus* and reported that the maximum gold uptake occurred between pH 4 and 9, with optimum uptake at pH 7. The precipitated gold formed irregular or spherical shapes.

### 3.4 Mechanisms of Biosynthesis of Gold Nanoparticles

The mechanisms for the biosynthesis of gold particles by bacteria, cyanobacteria, and algae from two gold complexes have been tested using several methods including laboratory-based experiments, microscopy technique [transmission electron microscopy (TEM) or scanning electron microscopy (SEM)], Fourier transform infrared spectroscopy (FT-IR), and/or X-ray absorption spectroscopy (XAS), as discussed below.

#### 3.4.1 Gold(I)–Thiosulfate Complex

The mechanisms of gold precipitation from a gold(I)–thiosulfate complex by *Acidithiobacillus thiooxidans*, SRB, and *Plectonema boryanum* UTEX 485 are summarized here. Gold(I)–thiosulfate was entered into the cell of *Acidithiobacillus*



*thiooxidans* as part of a metabolic process (Lengke and Southam 2005). This gold complex was initially decomplexed to Au(I) and thiosulfate ( $S_2O_3^{2-}$ ) ions. Thiosulfate was used as energy source and Au(I) was presumably reduced to elemental gold within the bacterial cells. During the late stationary growth phase, the gold nanoparticles that were initially precipitated inside the cells were released from the cells, resulting in the formation of gold particles at the cell surface. Finally, the gold particles in the bulk solution were grown into micrometer-scale wire and octahedral gold.

The precipitation of gold(I)–thiosulfate complex by SRB was caused by three possible mechanisms: (1) iron sulfide formation, (2) localized reducing conditions, and (3) a metabolic process (Lengke and Southam 2006, 2007). In the iron system, the formation of iron sulfide generated by SRB could have adsorbed a gold(I)–thiosulfate complex onto freshly forming surfaces, leading to the precipitation of elemental gold. The localized reducing conditions generated by SRB were associated with metabolism. Thiosulfate ion from a gold(I)–thiosulfate complex was initially reduced to hydrogen sulfide ( $HS^-$ ), as the end product of metabolism. The release of hydrogen sulfide through the outer membrane pores decreased redox conditions around the cells and caused the precipitation of elemental gold. The precipitation of elemental gold by SRB through metabolic process was initiated when a gold(I)–thiosulfate entered the bacterial cells and was decomplexed to Au(I) and thiosulfate ( $S_2O_3^{2-}$ ) ions. Thiosulfate was used as energy source and Au(I) was presumably reduced to elemental gold within the bacterial cells. During the late stationary growth phase or death phase, the gold nanoparticles that were initially precipitated inside the cells were released into the bulk solution and formed sub-octahedral to octahedral, sub-spherical to spherical aggregates resembling framboids, and ultimately millimeter-thick gold foil at longer experimental duration.

In the cyanobacterial system (*Plectonema boryanum* UTEX 485) with the addition of gold(I)–thiosulfate complex, gold was precipitated as thin nanoparticles associated with the surfaces of membrane vesicles at 25°C (Lengke et al. 2006a). *Plectonema boryanum* UTEX 485 exhibits the characteristics of gram-negative bacteria which can produce membrane vesicles. When the cyanobacteria interacted with relatively high concentrations of gold(I)–thiosulfate complex, the cells released membrane vesicle as a protective shield to prevent the uptake of gold (I)–thiosulfate from solutions and to keep gold(I)–thiosulfate away from sensitive cellular components. The interaction of gold(I)–thiosulfate complex with membrane vesicle caused the precipitation of elemental gold, possibly through the reaction with phosphorus, sulfur, or nitrogen ligands of outer membrane proteins, lipopolysaccharide, periplasmic proteins, phospholipids, DNA, and RNA. In the experiments at 60–200°C, gold nanoparticles were precipitated both intracellularly (<10 nm) and extracellularly (~10–25 nm), the latter with a distinct cubic shape and admixed with gold sulfide from 60 to 100°C. The stress on cyanobacteria caused by increasing temperature presumably decreased the cell sensitivity to receiving gold(I)–thiosulfate, and this gold complex was then reduced to gold sulfide and gold inside the cells. During the death of cyanobacteria, nanoparticles of gold sulfide and

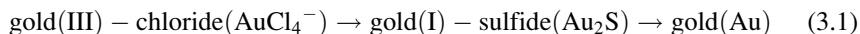
gold produced inside the cells were released through the cell membrane into solutions, as indicated by the precipitation of gold nanoparticles around the cells.

### 3.4.2 Gold(III)–Chloride Complex

In the bacterial system using a gold(III)–chloride solution, gold was precipitated intracellularly (<10 nm) and extracellularly (~1 to 10 μm) (e.g., Southam and Beveridge 1994, 1996; Karthikeyan and Beveridge 2002; Nair and Pradeep 2002; Reith et al. 2006; Gericke and Pinches 2006a, b; Deplanche and Macaskie 2007; Feng et al. 2008). The presence of intracellular gold nanoparticles suggests that gold entered the cells as a gold(III)–chloride complex and was then reduced to elemental gold. These bacteria were killed and the resulting release of organics caused further precipitation of gold (Southam and Beveridge 1996). A role of sulfur and phosphorus has been linked to the precipitation of octahedral gold at acidic pH by *Bacillus subtilis* 168 (Southam and Beveridge 1996). The precipitation of gold by magnetotactic cocci bacteria occurred in the Phosphorus–Sulfur–Iron (PSFe) granules which suggests the association of gold with these elements (Keim and Farina 2005). The reduction and precipitation of gold by dissimilatory iron(III) reducing bacteria were catalyzed by H<sub>2</sub> electron donor and not by lactate, indicating the involvement of hydrogenase (Kashefi et al. 2001). Deplanche and Macaskie (2007) further investigated the hydrogenase enzyme on the role of gold precipitation by *Escherichia coli* and *Desulfovibrio desulfuricans* ATCC 29577. They suggested that the periplasmic hydrogenases were involved in the gold precipitation but were not essential; however, the cytoplasmic hydrogenases and/or cytochrome c3 could be a complementary mechanism of gold reduction.

In the cyanobacterial system, the mechanisms of gold reduction by *Plectonema boryanum* UTEX 485 from gold(III)–chloride solutions have been studied at several gold concentrations (0.8–7.6 mmol/L) and at 25–80°C, using both fixed-time laboratory and real-time synchrotron radiation XAS experiments (Lengke et al. 2006c, 2007). The XAS results showed that Au(III) was reduced to Au(I) in a very fast reaction (within minutes), and Au(I) was immediately coordinated with sulfur atoms from cyanobacteria forming gold(I)–sulfide for all gold concentrations and temperatures. Within the cyanobacteria, sulfur presumably was present as cysteine or methionine groups of the outer membrane or periplasmic proteins. Sulfur from the cysteine or methionine groups was released into the bulk solutions through the outer membrane and immediately bound with the reduced gold forming gold(I)–sulfide on the cells or at the cell walls. The fast reduction of Au(III) to Au(I) and the fast release of organic sulfur from the dying and dead cyanobacteria at the higher temperatures investigated (60 and 80°C) resulted in the presence of gold (I)–sulfide as a major phase at the initial stage in the reaction. The reduction of gold (I)–sulfide to elemental gold was slower at 25°C than at 60 and 80°C. The cysteine or methionine within the outer membrane or periplasmic proteins also contained carbon and nitrogen, and this may explain indirect relationship between nitrogen

and gold. The steps of mechanism of gold reduction and precipitation by cyanobacteria are deduced:



In the algae system, the mechanisms of gold reduction by *Chlorella vulgaris* biomass from gold(III)–chloride solutions have been studied using XAS (Watkins et al. 1987). The XAS results showed that Au(III) was partly reduced to Au(I) and Au(I) was coordinated with sulfur atoms from free sulfhydryl residues and also to a light-atom element, probably nitrogen. Kuyucak and Volesky (1989b) showed that elemental gold was mostly precipitated on the cell wall of *Sargassum natans* biomass and suggested that the carbonyl (C ≡ O) groups of the cellulosic materials were the main functional group in the gold binding with N-containing groups involved in a lesser degree. Lin et al. (2005) suggested that the hydroxyl group of saccharides, the carboxylate anion of amino-acid residues, from the peptidoglycan layer on the cell wall appeared to be the sites for gold binding. However, the gold uptake by algal biomass increased after esterification, suggesting that carboxyl groups played a minor role in gold binding (Gardea-Torresdey et al. 1990). Romero-González et al. (2003) studied the mechanisms of gold biosorption by dealginated seaweed biomass using FT-IR and XAS. Although FT-IR showed the presence of carboxylate groups on the surface of the biomass, XAS showed that the reduction of gold species occurred on the biomass surfaces to form gold nanoparticles and was followed by retention of Au(I) at the sulfur containing sites. Therefore, the steps of mechanism of gold reduction and precipitation by algae are similar to cyanobacteria (Reaction 3.1).

### 3.5 Application of Gold Nanoparticles

The properties of gold nanoparticles remarkably differ from the bulk gold because of quantum size confinement imposed by nano-size regimen (Link et al. 1999; Reddy 2006). The electronic, magnetic, and catalytic properties of gold nanoparticles depend mainly on their size and shape (Link et al. 1999). For example, spherical gold nanoparticles show a strong absorption band in the visible region of electromagnetic field (~520 nm) but is absent for very small particles ( $\leq 2$  nm) as well as in the bulk gold. With a variety of unique properties, when gold nanoparticles are manipulated effectively, it can be applied to many different applications across the field of biology and medicine, environment, and technology (e.g., Oldenburg et al. 1998; Vieira and Volesky 2000; Salata 2004; Sperling et al. 2008; Chen et al. 2008; Cai et al. 2008).

Ancient cultures in Egypt, India, and China have used gold to treat diseases such as smallpox, skin ulcers, syphilis, and measles (Huaizhi and Yuantao 2001; Richards et al. 2002; Gielen and Tiekink 2005; Kumar 2007; Chen et al. 2008). Gold is currently used for medical devices including pacemakers

and gold plated stents (Edelman et al. 2001; Svedman et al. 2005), for the management of heart disease, middle ear gold implants, and gold alloys in dental restoration (Svedman et al. 2006). Organogold compounds are widely used for the treatment of rheumatoid arthritis but at high doses, side effects such as proteinuria and skin reactions have been observed (Sun et al. 2007; Chen et al. 2008).

### ***3.5.1 Biology and Medicine***

Gold nanoparticles have been primarily used for labeling and bioimaging applications (Sperling et al. 2008; Chen et al. 2008). The gold nanoparticles are directed and enriched at the region of interest, providing contrast for observation and visualization. With the characteristic of strongly absorption and scattering visible light, the light energy excites the free electrons in the gold nanoparticles to a collective oscillation, known as surface plasmon. The excited electron gas relaxes thermally by transferring the energy to the gold lattice, and finally the light absorption leads to heating of the gold nanoparticles. The interaction of gold nanoparticles with light can be used for the visualization of particles using optical microscopy, fluorescence microscopy, photothermal, and photoacoustic imaging. In addition, the interaction of gold nanoparticles with both electron waves and X-rays can also be used for visualization, e.g., using TEM. Other noninvasive diagnostic tools such as magnetic resonance imaging (MRI) and X-ray computed tomography (X-ray CT) have also utilized gold nanoparticles as contrasting agent due to the ease of surface modification and higher X-ray absorption coefficient, respectively (Debouttière et al. 2006; Kim et al. 2007).

Gold nanoparticles have been used for a long time for delivery of molecules into cells (Sperling et al. 2008; Chen et al. 2008). The molecules are adsorbed on the surface of gold nanoparticles and then are introduced into the cells using gene guns or particle ingestion. Inside the cells, these molecules will eventually detach themselves from the gold nanoparticles. Gene guns have been used for the introduction of plasmic DNA into plant cells and animal cells, which result in expression of the corresponding proteins inside the cells.

Gold nanoparticles can also be used as a heat source (Sperling et al. 2008; Cai et al. 2008). When gold particles absorb light, the free electrons in the gold particles are excited. Excitation at the plasmon resonance frequency causes a collective oscillation of the free electrons. During the interaction between the electrons and the crystal lattice of the gold nanoparticles, the electrons relax and the thermal energy is transferred to the lattice. The heat from the gold particles can be used for manipulating the surrounding tissues, e.g., hyperthermia, optically triggered opening of bonds, and opening of containers. Cells are sensitive to small increases in temperature and an increase of a few degrees can lead to cell death. If gold nanoparticles can be directed to the localized cancer tissue and is then heated

by external stimuli, the cells in the vicinity of the gold particles can be selectively killed. Photo-induced heating of gold nanoparticles can also be used for the opening of chemical bonds (e.g., melting double stranded DNA and disassembling protein aggregates). Finally, photo-induced heating of gold nanoparticles can also be used for remotely controlled release of cargo molecules from capsules inside living cells. A newly functionalized gold nanoparticle (dendrimers) has been designed for not only targeting and killing tumors but also to fight cancer (Nam et al. 2009; Escosura-Muñiz et al. 2009). Gold nanoparticle is engineered not only to identify, target, and kill tumors but also to carry the additional drug to slow down the growth of cancer cells or kill the cancer cells. Dendrimers acts as an arm to the gold nanoparticles so that different molecules are attached to the arms. Once the cancer cells are surrounded by gold nanoparticles, lasers or infrared light heats the gold particles and the dendrimers release the various molecules to kill the tumors.

Gold nanoparticles can also be used for active sensor applications (Sperling et al. 2008). The objectives for sensor applications are to determine the presence of analyte and to provide its concentration. The plasmon resonance frequency is a reliable feature of gold nanoparticles that can be used for sensing. The binding of molecules to the particle surface can change the plasmon frequency directly. On the other hand, the plasmon resonance frequency is changed when the average distance among gold nanoparticles is reduced by forming small aggregates. The effect of plasmon coupling can be used for colorimetric detection of the analyte, known as a gold-based sensor. In the presence of target sequence, the gold nanoparticles bind to the target by hybridization of complementary strands of DNA which lead to a change in the plasmon resonance and the solution appears to be a violet/blue color. When the sample is heated, single sequence mismatches result in a different melting temperature of the aggregates and cause color change. The same concept applied for DNA assays can also be used for RNA- and peptide-based sequences and enzyme. The color changes can also be used to measure lengths, known as “rulers on the nanometer scale”. The fluorescence quenching occurs when many fluorophores are in close proximity to gold surfaces and this effect can be used for several sensor strategies. Raman scattering is enhanced if the analyte is close to a gold surface, called as surface-enhanced Raman scattering. Gold nanoparticles modified with Raman-active reporter molecules have been used for the detection of DNA (Krug et al. 1999), protein (Ni et al. 1999), and two-photon excitation (Kneipp et al. 2006). Gold nanoparticles can also be used for the transfer of electrons in redox reactions (Willner et al. 2006). The enzyme is conjugated to the surface of the gold particles and is immobilized on the surface of an electrode (Xiao et al. 2003). An electrode covered with a layer of gold nanoparticles has a much higher surface roughness and larger surface area which lead to higher currents. In addition, due to the presence of small gold particles, the contact of the gold nanoparticles with the enzyme can be more intimate, i.e., located in a close proximity to the reactive center, which can facilitate the electron transport.

### 3.5.2 *Environment*

Gold nanoparticle based technologies are currently being developed for the environmental applications to pollution control and water purification (Das et al. 2009). Bimetallic gold–palladium nanoparticles provide an active catalyst to degrade trichloroethene (TCE), one of the major pollutants in groundwater to a non-toxic form (Wong et al. 2009). Palladium catalyst has been shown to degrade TCE in water but the cost is significant to be widely adopted. Although gold is more expensive than palladium, a combination of gold–palladium nanoparticles is much more reactive to remove TCE, resulting in more cost-effective application. Gold nanoparticles incorporated in a water purification device can effectively capture and remove halocarbon-based pesticides from drinking water (Das et al. 2009) and can also enhance the oxidation of mercury generated from coal power plants (Pradeep and Anshup 2009). A mixture of gold nanoparticles as well as the traditional platinum and palladium has been developed for automotive catalysts in diesel engines to increase hydrocarbon oxidation activity by U.S. Nanostellar (<http://www.nanostellar.com>). The use of gold nanoparticles as a catalyst has a major role to play in green chemistry (Dahl et al. 2007; Herzing et al. 2008). Most industrial oxidation processes tend to use chlorine or organic peroxides which result in large amounts of chloride salts and chlorinated organic byproducts. Gold nanoparticles supported on carbon active molecular oxygen in air are able to convert alkenes to partial oxidation products such as epoxides at atmospheric pressure and at 60–80°C (Hughes et al. 2005). Gold nanoparticles have been developed for selective oxidation of the biomass-derived chemicals, furfural and hydroxymethylfurfural, to form methyl esters. These chemicals are used for flavor and fragrance applications, in plastics and industrial solvents (Taarning et al. 2008).

### 3.5.3 *Technology*

Gold nanoparticles have been designed to improve computer memory (Lee et al. 2007). A three-dimensional computer memory device composed of layers of gold nanoparticles has been developed to increase the memory capacity of a single chip. The device is built on a base of silicon that is coated with hafnium oxide. Then, alternating layers of 16-nm sized gold nanoparticles and insulating polymers are formed on top. Another development of computer memory using gold nanoparticles is an organic nonvolatile bistable memory, which is a mixture of plastic and gold (Lin et al. 2007). Organic nonvolatile memories have been developed using plastic and other carbon-based chemicals but the organic memory devices tend to break down in air and under the stress of many read–write cycles. Therefore, a new memory consisting of gold nanoparticles mixed into a polymer and sandwiched between two aluminum electrodes is considered essential to be implemented in flexible electronics, such as radio-frequency identification, smart cards, e-paper, and flexible displays.

### 3.6 Future Directions

During the past two decades, the interaction of a variety of bacteria and two gold solutions [gold(I)–thiosulfate and gold(III)–chloride] have been well investigated, although the focus of these studies is not necessarily on the biosynthesis of gold nanoparticles. Living and dead bacteria/cyanobacteria/algae have huge potential for the production of gold nanoparticles; however, the previous studies are still largely in the discovery phase. Given the anticipated wide application of gold nanoparticles for commercial applications, consideration of the material design, processes, and applications using bacteria/cyanobacteria/algae that minimize hazard and waste will be essential for the transition of nanoscience discoveries to commercial products of nanotechnology. Future work should implement systematic experiments which include development of gold nanoparticles of well-defined size and shape. Better understanding of the mechanisms of gold biosynthesis will enable us to achieve better control over size, shape, and monodispersivity which will lead to the development of high precision in the production level and the application of nanoparticles for commercial scale applications.

### 3.7 Conclusions

We provide a comprehensive review of research conducted on the biosynthesis of gold nanoparticles by bacteria, cyanobacteria, and algae using gold(I)–thiosulfate [ $\text{Au}(\text{S}_2\text{O}_3)_2^{3-}$ ] and gold(III)–chloride [ $\text{AuCl}_4^-$ ] complexes. In general, many bacteria, cyanobacteria, and algae have the ability to produce gold nanoparticles with properties similar to chemically synthesised materials. Intracellular synthesis of gold nanoparticles, as well as extracellular formation of nanoparticles in the presence of these microorganisms has been successfully demonstrated. The shape of gold particles precipitated by bacteria/cyanobacteria/algae includes spherical, oval, spongy clots, mushroom, irregular, triangular, tetragonal, hexagonal, octahedral, rod, cubic, dodecahedral, icosahedral, coil or wire, plate, and thin foil, with size ranging from 1 nm to several millimeters. The mechanisms of gold precipitation from a gold(I)–thiosulfate complex by *Acidithiobacillus thiooxidans* and SRB are directly or indirectly associated with metabolism. For the dissimilatory iron(III) reducing bacteria using gold(III)–chloride complex, the involvement of cytoplasmic hydrogenases and/or cytochrome c3 could be a complementary mechanism of gold reduction. For the cyanobacteria and algae using gold(III)–chloride complex, Au(III) was reduced to Au(I), and Au(I) was immediately coordinated with sulfur atoms from the cysteine or methionine groups, forming gold(I)–sulfide. The reduction of gold(I)–sulfide to elemental gold was a slower step mechanism than the formation of gold(I)–sulfide.

Previous work on the biosynthesis of gold nanoparticles is still largely in the discovery phase. Given the anticipated wide application of gold nanoparticles for

commercial applications, continuing work is recommended to focus on the mechanisms of the biosynthesis of gold nanoparticles and the development of gold nanoparticles of well-defined size and shape.

## References

- Ahmad A, Senapati S, Khan MI, Kumar R, Sastry M (2005) Extra-/intracellular biosynthesis of gold nanoparticles by alkalotolerant fungus, *Trichothecium* sp. *J Biomed Nanotechnol* 1 (1):47–53
- Aylmore MG, Muir DM (2001) Thiosulfate leaching of gold – a review. *Miner Eng* 14(2):135–174
- Brust M, Walker M, Bethell D, Schiffrin DJ and Whyman R (1994) Synthesis of thiol derivatised gold nanoparticles in a two-phase liquid/liquid system. *Chem Commun*: 801–802
- Cai W, Gao T, Hong H, Sun J (2008) Applications of gold nanoparticles in cancer nanotechnology. *Nanotechnol Sci Appl* 1:17–32
- Canizal G, Ascencio JA, Gardea-Torresday J, Jose-Yacaman M (2001) Multiple twinned gold nanorods grown by bio-reduction techniques. *J Nanopart Res* 3:475–481
- Chen PC, Mwakwari SC, Oyelere AK (2008) Gold nanoparticles: from nanomedicine to nanosensing. *Nanotechnol Sci Appl* 1:45–66
- Dahl JA, Maddux BLS, Hutchison JE (2007) Toward greener nanosynthesis. *Chem Rev* 107:2228–2269
- Daniel M-C, Astruc D (2004) Gold nanoparticles: assembly, supramolecular chemistry, quantum size-related properties, and applications toward biology, catalysis and nanotechnology. *Chem Rev* 104:293–346
- Darnall DW, Greene B, Henzl MT, Hosea JM, McPherson RA, Sneddon J, Alexander MD (1986) Selective recovery of gold and other metal ions from an algal biomass. *Environ Sci Technol* 20 (2):206–208
- Das SK, Das AR, Guha AK (2009) Gold nanoparticles: microbial synthesis and application in water hygiene management. *Langmuir* 25(14):8192–8199
- Debouttière P-J, Roux S, Vocanson F, Billotey C, Beuf O, Favre-Réguillon A, Lin Y, Pellet-Rostaing S, Lamartine R, Perriat P, Tillement O (2006) Design of gold nanoparticles for magnetic resonance imaging. *Adv Funct Mater* 16(18):2330–2339
- Deplanche K, Macaskie LE (2007) Biorecovery of gold by *Escherichia coli* and *Desulfovibrio desulfuricans*. *Biotechnol Bioeng* 99(5):1055–1064
- Dermont G, Bergeron M, Mercier G, Richer-Lafleche M (2008) Metal-contaminated soils: remediation practices and treatment technologies. *Pract Periodical Hazard Toxic Radioactive Waste Manage* 12(3):188–209
- Du L, Jiang H, Liu X, Wang E (2007) Biosynthesis of gold nanoparticles assisted by *Escherichia coli* DH5 $\alpha$  and its application on direct electrochemistry of hemoglobin. *Electrochem Commun* 9:1165–1170
- Dyer BD, Krumbein WE, Mossman DJ (1994) Accumulation of gold in the sheath of *Plectonema terebrans* (filamentous marine cyanobacteria). *Geomicrobiol J* 12:91–98
- Edelman ER, Seifert P, Groothuis A, Morss A, Bornstein D, Rogers C (2001) Gold-coated NIR stents in porcine coronary arteries. *Circulation* 103:429–34
- Ehrlich HL (2002) *Geomicrobiology*, 4th edn. New York, Marcel Dekker, p 800
- Emery JF, Leddicotte GW (1961) The radiochemistry of gold. National Academy of Sciences - National Research Council, Washington DC, p 34
- Escosura-Muñiz ADL, Sánchez-Espinell C, Díaz-Freitas B, González-Fernández A, Costa MM, Merkoci A (2009) Rapid identification and quantification of tumor cells using an electrocatalytic method based on gold nanoparticles. *Anal Chem* 81:10268–10274
- Feng Y, Lin X, Wang Y, Wang Y, Hua J (2008) Diversity of aurum bioreduction by *Rhodobacter capsulatus*. *Mater Lett* 62:4299–4302



- Gardea-Torresdey JL, Becker-Hapak MK, Hosea JM, Darnall DW (1990) Effect of chemical modification of algal carboxyl groups on metal ion binding. *Environ Sci Technol* 24(9):1372–1378
- Gardea-Torresdey JL, Tiemann KJ, Gamez G, Dokken K, Tehuacanero S, Jose-Yacamán M (1999) Gold nanoparticles obtained by bio-precipitation from gold(III) solutions. *J Nanoparticles Res* 1:397–404
- Gardea-Torresdey JL, Tiemann KJ, Gamez G, Dokken K, Cano-Aguilera I, Furenlid LR, Renner MW (2000) Reduction and accumulation of gold(III) by *Medicago sativa* alfalfa biomass: X-ray absorption spectroscopy, pH, and temperature dependence. *Environ Sci Technol* 34:4392–4396
- Gardea-Torresdey JL, Parsons JG, Gomez E, Peralta-Videa J, Troini HE, Santiago P, Jose-Yacamán M (2002) Formation and growth of Au nanoparticles inside live alfalfa plants. *Nano Lett* 2(4):397–401
- Gericke M, Pinches A (2006a) Microbial production of gold nanoparticles. *Gold Bull* 39(1):22–28
- Gericke M, Pinches A (2006b) Biological synthesis of metal nanoparticles. *Hydrometallurgy* 83:132–140
- Gielen M, Tiekink ERT (2005) *Metallotherapeutic drugs and metal-based diagnostic agents. The use of metals in medicine.* Wiley, Hoboken, New York
- Greene B, Hosea M, McPherson R, Henzl M, Alexander MD, Darnall DW (1986) Interaction of gold(I) and gold(III) complexes with algal biomass. *Environ Sci Technol* 20(6):627–632
- Handley DA (1989) Methods for synthesis of colloidal gold. Chap. 2. In: Hayat MA (ed) *Colloidal gold: principles, methods and application*, vol 1. Academic, San Diego, pp 13–33
- He S, Guo Z, Zhang Y, Zhang S, Wang J, Gu N (2007) Biosynthesis of gold nanoparticles using the bacteria *Rhodospseudomonas capsulata*. *Mater Lett* 61:3984–3987
- Heath GR (1981) Ferromanganese nodules of the deep sea. *Economic Geology 75th Anniversary Volume*, 735–765.
- Herzing AA, Kiely CJ, Carley AF, Landon P, Hutchings GJ (2008) Identification of active gold nanoclusters on iron oxide supports for CO oxidation. *Science* 321:1331–1335
- Hosea M, Greene B, McPherson R, Henzl M, Alexander MD, Darnall DW (1986) Accumulation of elemental gold on the alga *Chlorella vulgaris*. *Inorg Chim Acta* 123:161–165
- Huaizhi Z, Yuantao N (2001) China's ancient gold drugs. *Gold Bull* 34:24–9
- Hughes MD, Xu YJ, Jenkins P, McMorn P, Landon P, Enache DI, Carley AF, Attard GA, Hutchings GJ, King F, Stitt EH, Johnston P, Griffin K, Kiely CJ (2005) Tunable gold catalysts for selective hydrocarbon oxidation under mild conditions. *Nature* 437:1132–1135
- Hussey MI, El-Aziz MA, Badr Y, Mahmood MA (2007) Biosynthesis of gold nanoparticles using *Pseudomonas aeruginosa*. *Spectrochim Acta A* 67:1003–1006
- Kalishwaralal K, Deepak V, Pandian SRK, Gurunathan S (2009) Biological synthesis of gold nanocubes from *Bacillus licheniformis*. *Biosource Technol* 100:5356–5358
- Karamushka VI, Ul'berg ZR, Gruzina TG, Sukhovii NV, Tsarenko PM (1991a) Characteristics of the concentration of trivalent gold by microalgal cells in an energized state. *Biotechnologiya* 2:65–68
- Karamushka VI, Ulberg ZR, Gruzina TG, Dukhin AS (1991b) ATP-dependent gold accumulation by living chlorella cells. *Acta Biotechnol* 11(3):197–203
- Karthikeyan S, Beveridge TJ (2002) *Pseudomonas aeruginosa* biofilms react with and precipitate toxic soluble gold. *Environ Microbiol* 4(11):667–675
- Kashefi K, Tor JM, Nevin KP, Lovley DR (2001) Reductive precipitation of gold by dissimilatory Fe(III)-reducing bacteria and archaea. *Appl Environ Microbiol* 67(7):3275–3279
- Keim CN, Farina M (2005) Gold and silver trapping by uncultured magnetotactic cocci. *Geomicrobiol J* 22:55–63
- Kim D, Park S, Lee JH, Jeong YY, Jon S (2007) Antibiofouling polymer-coated gold nanoparticles as a contrast agent for in vivo X-ray computed tomography imaging. *J Am Chem Soc* 129(24):7661–7665
- Kneipp J, Kneipp H, Kneipp K (2006) Two-photon vibrational spectroscopy for biosciences based on surface-enhanced hyper-Raman scattering. *Proc Natl Acad Sci USA* 103(46):17149–17153

- Konishi Y, Tsukiyama T, Ohno K, Saitoh N, Nomura T, Nagamine S (2006) Intracellular recovery of gold by microbial reduction of  $\text{AuCl}_4^-$  ions using the anaerobic bacterium *Shewanella alga*. *Hydrometallurgy* 81:24–29
- Korobushkina YeD, Korobushkin IM (1986) Interaction of gold with bacteria and the generation of new gold. *Dokl Akad Nauk SSSR* 287(4):978–980
- Krug JT, Wang GD, Emory SR, Nie S (1999) Efficient Raman enhancement and intermittent light emission observed in single gold nanocrystals. *J Am Chem Soc* 121(39):9208–9214
- Kumar CSSR (2007) *Nanomaterials for cancer diagnosis*. Wiley, Weinheim, Germany
- Kuyucak N, Volesky B (1989a) Accumulation of gold by algal biosorbent. *Biorecovery* 1:189–204
- Kuyucak N, Volesky B (1989b) The mechanism of gold biosorption. *Biorecovery* 1:219–235
- Lee JS, Cho J, Lee C, Kim I, Park J, Kim YM, Shin H, Lee J, Caruso F (2007) Layer-by-layer assembled charge-trap memory devices with adjustable electronic properties. *Nat Nanotechnol* 2:790–795
- Lengke MF, Southam G (2005) The effect of thiosulfate-oxidizing bacteria on the stability of the gold-thiosulfate complex. *Geochim Cosmochim Acta* 69(15):3759–3772
- Lengke MF, Southam G (2006) Bioaccumulation of gold by sulfate-reducing bacteria cultured in the presence of gold(I)-thiosulfate complex. *Geochim Cosmochim Acta* 70:3646–3661
- Lengke MF, Southam G (2007) The deposition of elemental gold from gold(I)-thiosulfate complex mediated by sulfate-reducing bacterial conditions. *Econ Geol* 102(1):109–126
- Lengke MF, Fleet ME, Southam G (2006a) Morphology of gold nanoparticles synthesized by filamentous cyanobacteria from gold(I)-thiosulfate and gold(III)-chloride complexes. *Langmuir* 22(6):2780–2787
- Lengke MF, Fleet ME, Southam G (2006b) Bioaccumulation of gold by filamentous cyanobacteria between 25 and 200°C. *Geomicrobiol J* 23:591–597
- Lengke MF, Ravel B, Fleet ME, Wanger G, Gordon RA, Southam G (2006c) Mechanisms of gold bioaccumulation by filamentous cyanobacteria from gold(III)-chloride complex. *Environ Sci Technol* 40(20):6304–6309
- Lengke MF, Ravel B, Fleet ME, Wanger G, Gordon RA, Southam G (2007) Precipitation of gold by the reaction of aqueous gold(III) chloride with cyanobacteria at 25–80°C – studied by x-ray absorption spectroscopy. *Can J Chem* 85(10):651–659
- Lin Z, Wu J, Xue R, Yang Y (2005) Spectroscopic characterization of  $\text{Au}^{3+}$  biosorption by waste biomass of *Saccharomyces cerevisiae*. *Spectrochim Acta A* 61:761–765
- Lin HT, Pei Z, Chen JR, Hwang GW, Fan JF, Chan YJ (2007) A new nonvolatile bistable polymer-nanoparticle memory device. *IEEE Electron Device Lett* 28(11):951–953
- Link S, Mohamed MB, El-Sayed MA (1999) Simulation of the optical absorption spectra of gold nanorods as a function of their aspect ratio and the effect of the medium dielectric constant. *J Phys Chem B* 103:3073–3077
- Lloyd JR (2002) Bioremediation of metals; the application of micro-organisms that make and break minerals. *Microbiol Today* 29:67–69
- Masala O, Seshadri R (2004) Synthesis routes for large volumes of nanoparticles. *Annu Rev Mater Res* 34:41–81
- Mata YN, Torres E, Blázquez ML, Ballester A, González F, Muñoz JA (2009) Gold(III) biosorption and bioreduction with the brown alga *Fucus vesiculosus*. *J Hazard Mater* 166:612–618
- Mohanpuria P, Rana NK, Yadav SK (2008) Biosynthesis of nanoparticles: technological concepts and future applications. *J Nanopart Res* 10:507–517
- Mukherjee P, Ahmad D, Mandal D, Senapati S, Saikar SR, Khan MI, Ramani R, Parischa R, Ajaykumar PV, Alam M, Sastry M, Kumar R (2001) Bioreduction of  $\text{AuCl}_4^-$  ions by the fungus, *Verticillium* sp. surface trapping gold nanoparticles formed. *Angew Chem Int Ed* 40(19):3585–3588
- Mukherjee P, Senapati S, Mandal D, Ahmad A, Khan MI, Kumar R, Sastry M (2002) Extracellular synthesis of gold nanoparticles by the fungus *Fusarium oxysporum*. *Chembiochem* 5:461–463
- Nair B, Pradeep T (2002) Coalescence of nanoclusters and formation of submicron crystallites assisted by *Lactobacillus* strains. *Cryst Growth Des* 2(4):293–298

- Nakajima A (2003) Accumulation of gold by microorganisms. *World J Microbiol Biotechnol* 19:369–374
- Nam J, Won N, Jin H, Chung H, Kim S (2009) pH-induced aggregation of gold nanoparticles for photothermal cancer therapy. *J Am Chem Soc* 131:13639–13645
- Nangia Y, Wangoo N, Sharma S, Wu J, Dravid V, Shekhawat GS, Suri CR (2009) Facile biosynthesis of phosphate capped gold nanoparticles by a bacterial isolate *Stenotrophomonas maltophilia*. *Appl Phys Lett* 94(23):1–3
- Nash JT, Granger HC, and Adams SS (1981) Geology and concepts of genesis of important types of uranium deposits. *Economic Geology 75th Anniversary Volume*, 63–116.
- Ni J, Lipert RJ, Dawson GB, Porter MD (1999) Immunoassay readout method using extrinsic Raman labels adsorbed on immunogold colloids. *Anal Chem* 71:4903–4908
- Nicol MJ, Fleming CA, Paul RL (1987) The chemistry of the extraction of gold. In: Stanley GG (ed) *The extractive metallurgy of gold in South Africa*, vol 2. South Africa Institute of Mining and Metallurgy, Johannesburg, South Africa, pp 831–905
- Oldenburg SJ, Averitt RD, Westcott SL, Halas NJ (1998) Nanoengineering of optical resonances. *Chem Phys Lett* 288:243–247
- Pradeep T, Anshup (2009) Noble metal nanoparticles for water purification: a critical review. *Thin Solid Films* 517(24):6441–6478
- Puddephatt RJ, Vittal JJ (1994) Gold: inorganic and coordination chemistry. In: King RB (ed) *Encyclopedia of inorganic chemistry*. Wiley, Chichester, UK, pp 1320–1331
- Ran Y, Fu J, Rate AW, Gikes RJ (2002) Adsorption of Au(I, III) complexes on Fe, Mn oxides and humic acid. *Chem Geol* 185:33–49
- Reddy VR (2006) Gold nanoparticles: synthesis and applications. *Synlett* 11:1791–1792
- Reith F, Rogers SL, McPhail DC, Webb D (2006) Biomineralization of gold: biofilms on bacterioform gold. *Science* 313:233–236
- Richards DG, McMillin DL, Mein EA, Nelson CD (2002) Gold and its relationship to neurological/glandular conditions. *Int J Neurosci* 112(1):31–53
- Romero-González ME, Williams CJ, Gardiner PHE, Gurman SJ, Habesh S (2003) Spectroscopic studies of the biosorption of gold(III) by dealginated seaweed waste. *Environ Sci Technol* 37(18):4163–4169
- Salata OV (2004) Application of nanoparticles in biology and medicine. *J Nanobiotechnol* 2:3–9
- Selvakannan PR, Mandal S, Phadtare R, Pasricha R, Sastry M (2003) Capping of gold nanoparticles by the amino acid lysine renders them water-dispersible. *Langmuir* 19:3545–3549
- Senanayake G, Perera WN, Nicol MJ (2003) Thermodynamic studies of the gold(III)/(I)/(0) redox system in ammonia-thiosulfate solutions at 25°C. In: Yong CA, Alfantazi AM, Anderson CG, Dreisinger DB, Harris B, James A (eds) *Hydrometallurgy 2003 - Fifth International Conference in Honor of Professo Ian Ritchie*, Vancouver, vol 1. TMS, Warrendale, Pennsylvania, pp 155–168
- Shankar SS, Ahmad A, Pasricha R, Sastry MJ (2003) Bioreduction of chloroaurate ions by geranium leaves and its endophytic fungus yields gold nanoparticles of different shapes. *J Mater Chem* 13:1822–1826
- Shankar SS, Rai A, Ankamwar B, Singh A, Ahmad A, Sastry M (2004) Biological synthesis of triangular gold nanoprisms. *Nature* 3:482–488
- Singaravelu G, Arockiamary JS, Ganesh Kumar V, Govindaraju K (2007) A novel extracellular synthesis of monodisperse gold nanoparticles using marine alga, *Sargassum wightii* Greville. *Colloids Surf, B* 57:97–101
- Southam G, Beveridge TJ (1994) The in vitro formation of placer gold by bacteria. *Geochim Cosmochim Acta* 58(20):4527–4530
- Southam G, Beveridge TJ (1996) The occurrence of sulfur and phosphorus within bacterially derived crystalline and pseudocrystalline octahedral gold formed in vitro. *Geochim Cosmochim Acta* 60(22):4369–4376
- Sperling RA, Gil PR, Zhang F, Zanella M, Parak WJ (2008) Biological application of gold nanoparticles. *Chem Soc Rev* 37:1896–1908

- Sun RW-Y, Ma D-L, Wong EL-M, Che C-M (2007) Some uses of transition metal complexes as anti-cancer and anti-HIV agents. *Dalton Trans* 43:4884–4892
- Svedman C, Tillman C, Gustavsson CG, Moller H, Frennby B, Bruze M (2005) Contact allergy to gold in patients with gold-plated intracoronary stents. *Contact Dermat* 52(4):192–196
- Svedman C, Dunér K, Kehler M, Moller H, Gruvberger B, Bruze M (2006) Lichenoid reactions to gold from dental restorations and exposure to gold through intracoronary implant of a gold-plated stent. *Clin Res Cardiol* 95:689–91
- Taarning E, Nielsen IS, Egeblad K, Madsen R, Christensen CH (2008) Chemicals from renewables: aerobic oxidation of furfural and hydroxymethylfurfural over gold catalysts. *ChemSusChem* 1:75–78
- Ting YP, Teo WK, Soh CY (1995) Gold uptake by *Chlorella vulgaris*. *J Appl Phycol* 7:97–100
- Tsuruta T (2004) Biosorption and recycling of gold using various microorganisms. *J Gen Appl Microbiol* 50:221–228
- Vieira RHSF, Volesky B (2000) Biosorption: a solution to pollution. *Int Microbiol* 3:17–24
- Watkins JW II, Elder RC, Greene B, Darnall D (1987) Determination of gold binding in an algal biomass using EXAFS and XANES spectroscopies. *Inorg Chem* 26(7):1147–1151
- Wen L, Lin Z, Gu P, Zhou J, Yao B, Chen G, Fu J (2009) Extracellular biosynthesis of mono-dispersed gold nanoparticles by a SAM capping route. *J Nanopart Res* 11:279–288
- Willner B, Katz E, Willner I (2006) Electrical contacting of redox proteins by nanotechnological means. *Curr Opin Biotechnol* 17:589–596
- Wong MS, Alvarez PJJ, Fang YL, Akcin N, Nutt MO, Miller JT, Heck KN (2009) Cleaner water using bimetallic nanoparticle catalysts. *J Chem Technol Biotechnol* 84:158–166
- Xiao Y, Patolsky F, Katz E, Hainfeld JF, Willner I (2003) Plugging into enzymes: nanowiring of redox enzymes by a gold nanoparticle. *Science* 299(5614):1877–1881

# Chapter 4

## A Bacterial Backbone: Magnetosomes in Magnetotactic Bacteria

Christopher T. Lefèvre, Fernanda Abreu, Ulysses Lins,  
and Dennis A. Bazylinski

### 4.1 Introduction

One of the most intriguing discoveries in the realm of microbiology was that of the phenomenon known as magnetotaxis and the magnetotactic bacteria. Magnetotactic bacteria are prokaryotes that passively align and actively swim along magnetic field lines (Bazylinski and Frankel 2004). They were apparently first described by Salvatore Bellini in 1963 in an obscure publication of the Instituto di Microbiologia of the University of Pavia, Italy (Bellini 2009a, b). He microscopically observed bacteria that swam towards the North Pole and hence called them “batteri magnetosensibili” (magnetosensitive bacteria) and believed that cells had an internal magnetic compass that was responsible for his observations although he never proved this point. Blakemore (1975), independently, rediscovered these organisms in 1974 and coined the terms magnetotaxis for the phenomena and magnetotactic bacteria for the microorganisms. Moreover, he uncovered and described the internal compass of Bellini: the magnetosome, the subject of this chapter. The magnetosome is defined as internal, membrane-bounded single-magnetic domain crystals of a magnetic mineral that is either an iron oxide or iron sulfide (Balkwill et al. 1980; Gorby et al. 1988).

The goal of this chapter is to review what is known regarding the bacterial magnetosome as to its function and how it is biomineralized by magnetotactic bacteria. In addition, we also describe the significance of magnetosomes and magnetosome mineral crystals in biotechnological applications.

---

C.T. Lefèvre and D.A. Bazylinski (✉)

School of Life Sciences, University of Nevada at Las Vegas, 4505 Maryland Parkway, Las Vegas, NV 89154-4004, USA

e-mail: christopher.lefevre@unlv.edu; dennis.bazylinski@unlv.edu

F. Abreu and U. Lins

Instituto de Microbiologia Professor Paulo de Góes, Universidade Federal do Rio de Janeiro, 21941-590 Rio de Janeiro, Brazil

e-mail: abreufernandadeavila@hotmail.com; ulins@micro.ufrj.br

## 4.2 The Magnetotactic Bacteria

The term “magnetoactive bacteria” has been found to have no taxonomic meaning and represents a morphologically, metabolically and phylogenetically diverse group of mainly aquatic prokaryotes that passively align parallel to the Earth’s geomagnetic field while they swim (Bazylinski and Frankel 2004).

### 4.2.1 Diversity of Magnetotactic Bacteria

The great diversity of the magnetotactic bacteria is exemplified by the many different cell morphologies observed in the group. These include coccoid, rod-shaped, vibrioid, spirilloid and multicellular forms (Fig. 4.1). All thus far described possess a Gram-negative cell wall and are motile by means of flagella whose arrangements are diverse and include monotrichous (polar), bipolar or lophotrichous with either one or two bundles of flagella.

Phylogenetically, all known cultured and uncultured magnetotactic bacteria collected from natural environments are members of the Domain Bacteria (Bazylinski and Frankel 2004). There is no known reason why there cannot be magnetotactic members of the Archaea but none have been discovered thus far.

Magnetotactic bacteria biomineralize iron oxide (magnetite) and/or iron sulfide (greigite) minerals in their magnetosomes (discussed in detail in a later section). The cultured and uncultured magnetite-producing magnetotactic bacteria, which include numerous cocci, rods and spirilla, occupy phylogenetic positions in the *Alpha*-, *Gamma*- and *Deltaproteobacteria* classes within the phylum *Proteobacteria* and the *Nitrospirae* phylum (Kawaguchi et al. 1995; Amann et al. 2007; Lefèvre et al. 2011).

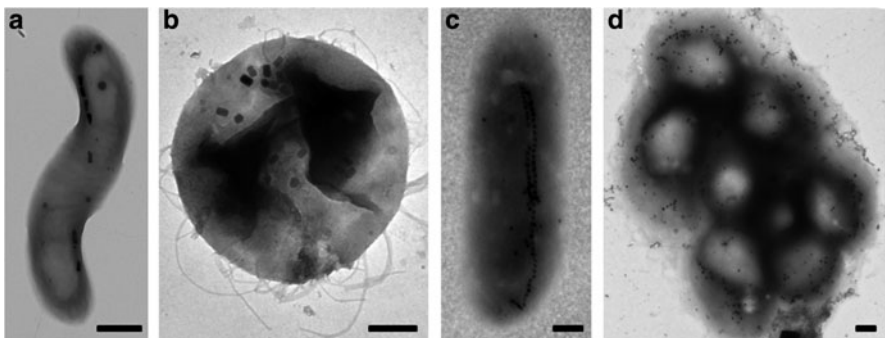


**Fig. 4.1** Transmission electron micrographic (TEM) images of various morphological forms of magnetotactic bacteria including: spirilla (a), cocci (b), rod-shaped (c) and multicellular (the MMP) (d). Magnetosomes are the dark electron-dense structures within each cell. Cells in a and b contain magnetite and those in c and d, greigite. Scale bar represents 200 nm

What is known about the phylogeny of the iron sulfide-producing magnetotactic bacteria is based on culture-independent environmental studies. Only two morphological types of greigite-producing bacteria have been found and partially described thus far: the many-celled (or multicellular) magnetotactic prokaryote (MMP) and series of large, thick, rod-shaped organisms. The MMP is an unusual, large, multicellular bacterium that consists of about 10–40 cells arranged in a roughly spherical or ovoid manner, and is motile as an intact unit but not as separate cells (Rodgers et al. 1990a, b; Keim et al. 2004a, b; Abreu et al. 2007; Wenter et al. 2009). Each cell is multiflagellated on one side. The MMP appears to have no single-cell stage in its life cycle: a single MMP divides into two separate MMPs (Keim et al. 2004b). Phylogenetically, the MMP is affiliated with the sulfate-reducing bacteria in the *Deltaproteobacteria* class suggesting that it is also a sulfate-reducing bacterium (DeLong et al. 1993; Simmons and Edwards 2007). The MMP has been found in brackish-to-marine habitats all over the world and, based on its unique morphology, it was generally assumed that it represented a single species. However, Simmons and Edwards (2007) reported 16S rRNA gene sequences from a natural population of MMPs and found the sequences representing five lineages separated by at least a 5% sequence divergence. Thus, the MMP should be considered a separate genus that contains several species in the *Deltaproteobacteria* class rather than a single species as previously thought (Simmons and Edwards 2007). The MMP morphological form appears not to be restricted to marine habitats as we recently discovered nonmagnetotactic forms of the MMP in nonmarine environments (Lefèvre et al. 2010a). The large rod-shaped greigite producers have only been observed in marine environments so far and one of these was found to be a member of the *Gammaproteobacteria* class (Simmons et al. 2004), although there is some doubt as to the true phylogeny of this organism (Amann et al. 2007).

#### 4.2.2 Ecology of Magnetotactic Bacteria

Magnetotactic bacteria are ubiquitous in water columns or sediments with vertical chemical stratification and a pH around neutral although recently we and others have found magnetotactic bacteria in some habitats with pH values of >9.0. They locally occur in relatively high cell numbers at the oxic–anoxic interface (OAI) and the anoxic regions of the habitat or both (Bazylinski et al. 1995; Bazylinski and Moskowitz 1997; Simmons et al. 2004; Moskowitz et al. 2008). In most freshwater systems where the sulfate concentration is very low or zero, the OAI is usually located at the sediment–water interface or several millimeters below it. The situation in many deep sea sites can be similar, although it can be markedly different in many, mostly undisturbed, marine coastal habitats. Natural seawater contains approximately 28 mM sulfate and in these situations, hydrogen sulfide generated by the action of anaerobic sulfate-reducing bacteria in the sediment diffuses upwards into the water column removing free O<sub>2</sub> causing the OAI to occur in the water column. This results in an inverse, oxygen:sulfide concentration double gradient where O<sub>2</sub> diffuses downward from air at the surface and S<sub>2</sub><sup>−</sup> diffuses

upwards from the anaerobic zone (Simmons et al. 2004; Frankel et al. 2007; Moskowitz et al. 2008). Only magnetite-producing magnetotactic bacteria have been found in freshwater systems while both magnetite and greigite producers have been found in marine environments. In marine systems, the magnetite producers are found mainly at the OAI and the greigite producers just below the OAI where  $S_2^-$  is present (Simmons et al. 2004; Moskowitz et al. 2008). The greigite producers have thus far only been found in marine habitats and none have been cultivated in pure culture to date.

### 4.2.3 *Physiology of Magnetotactic Bacteria*

Although the physiology and metabolic pathways of magnetotactic bacteria appear to be very diverse, there are some common features (Bazylinski and Williams 2007). All cultured magnetotactic bacteria are either anaerobes or microaerophiles or both (Bazylinski and Frankel 2004). Those that tolerate relatively high concentrations of  $O_2$  do not biomineralize magnetite under these conditions. Magnetotactic bacteria biomineralize two magnetic minerals: magnetite ( $Fe_3O_4$ ) or greigite ( $Fe_3S_4$ ), the sulfur isomorph of magnetite (Bazylinski and Frankel 2004). In *Magnetospirillum* species, magnetite synthesis appears to only occur at very low levels of  $O_2$  or under anaerobic conditions when nitrate is the alternate terminal electron acceptor to  $O_2$  (Bazylinski and Blakemore 1983a; Blakemore et al. 1985; Schüller and Baeuerlein 1998; Heyen and Schüller 2003). Greigite-producing magnetotactic bacteria have not yet been grown in pure culture, so little is known about them. However, ecological studies and phylogenetic analyses suggest that some of these organisms are anaerobic sulfate-reducing bacteria and thus it is thought that greigite biomineralization occurs solely under anaerobic conditions (DeLong et al. 1993; Simmons and Edwards 2007).

All cultured magnetotactic bacteria possess a respiratory form of metabolism using  $O_2$ , nitrate, sulfate or fumarate as terminal electron acceptors (Bazylinski and Blakemore 1983a; Sakaguchi et al. 1993, 2002) and in general, only organic acids and some amino acids are used as carbon sources. No cultured magnetotactic bacterium is known to utilize sugars as a carbon source. Only one magnetotactic bacterium is capable of fermentation: *Desulfovibrio magneticus* strain RS-1. In this case, pyruvate is fermented to acetate and  $H_2$  (Sakaguchi et al. 2002).

Many of the cultured magnetite-producing magnetotactic bacteria have been shown to be at least facultatively autotrophic utilizing either the Calvin–Benson–Bassham or the reverse tricarboxylic acid cycle for  $CO_2$  fixation (Bazylinski et al. 2004; Williams et al. 2006; Geelhoed et al. 2010) and reduced sulfur compounds as electron donors (Frankel et al. 1997; Bazylinski et al. 2004; Williams et al. 2006; Geelhoed et al. 2010). Most exhibit nitrogenase activity and thus fix atmospheric  $N_2$  (Bazylinski and Blakemore 1983b; Bazylinski et al. 2000). It is not known if any connection exists between these metabolic features and magnetosome synthesis although it seems doubtful as many nonmagnetotactic organisms also possess these features.



All cultured magnetotactic bacteria are mesophilic with regard to temperature and growth and do not grow much above 30°C. Most collected from natural environments also appear to be mesophilic based on the temperatures at which they were found although some moderately thermophilic uncultured magnetotactic bacteria belonging to the *Nitrospirae* phylum have been found to live in hot springs up to about 63°C (Lefèvre et al. 2010b).

#### 4.2.4 The Bacterial Magnetosome

The bacterial magnetosome is defined as an intracellular, membrane-bounded magnetic mineral crystal within a prokaryotic cell. The composition, size and morphology of the magnetic mineral crystal have great significance and all of these features indicate that the biomineralization of the bacterial magnetosome is under strict chemical, biochemical and genetic control. Hence, the biomineralization of magnetosomes is considered a biologically controlled process versus a biologically induced mineralization process (Lowenstam 1981; Bazylinski and Frankel 2003). The mineral products, which include magnetite, of the latter process are generally deposited extracellularly and resemble those produced inorganically and are thus very different from those synthesized by a biologically controlled mineralization process (Frankel and Bazylinski 2003; Jimenez-Lopez et al. 2010).

##### 4.2.4.1 Composition of Magnetosome Minerals

As previously stated, magnetotactic bacteria biomineralize crystals of iron-oxide and iron-sulfide minerals in their magnetosomes. The iron-oxide minerals include magnetite (Fe<sub>3</sub>O<sub>4</sub>) (e.g., Frankel et al. 1979) whereas the iron-sulfides include greigite (Fe<sub>3</sub>S<sub>4</sub>) (Mann et al. 1990; Heywood et al. 1990). Several other nonmagnetic iron-sulfide minerals have been identified in iron-sulfide magnetosomes, including mackinawite (tetragonal FeS) and a cubic FeS, which appear to be precursors to greigite (Pósfai et al. 1998a, b). Magnetic, monoclinic, pyrrhotite (Fe<sub>7</sub>S<sub>8</sub>) (Farina et al. 1990) and nonmagnetic iron pyrite (FeS<sub>2</sub>) (Mann et al. 1990) were also identified in a many-celled MMP that produces iron-sulfide magnetosomes but likely represent misinterpretations of electron diffraction patterns. No convincing precursors to magnetite have been recognized although ferrihydrite was at one point considered (Frankel et al. 1983). The mineral composition of the magnetosome appears to be under strict chemical control since cells of several cultured magnetotactic bacteria continue to synthesize magnetite, not greigite, even when hydrogen sulfide is present in the growth medium (Meldrum et al. 1993a, b).

Generally, magnetotactic bacteria biomineralize either magnetite or greigite but not both. However, some exceptions have been found. The greigite-producing, large rod-shaped bacteria and some forms of the MMP have been found to biomineralize both minerals in the same chains (Bazylinski et al. 1993b, 1995; Lins et al. 2007).

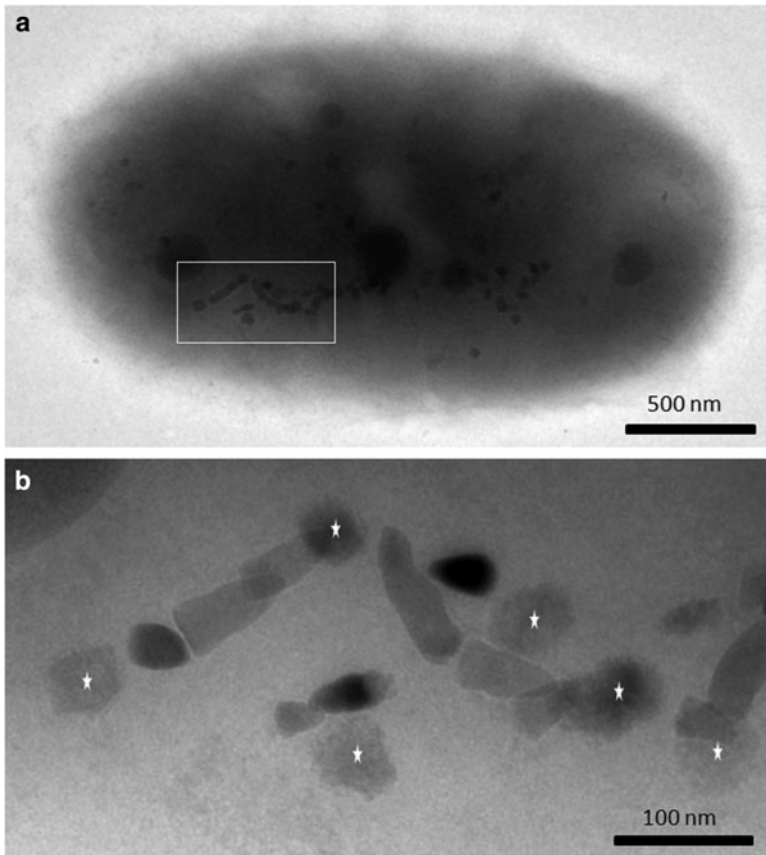


**Fig. 4.2** TEM image of an unstained cell of a rod-shaped bacterium containing magnetite and greigite (a) magnetosomes aligned in the same chain. (b) High magnification TEM image of magnetite and greigite (starred) crystals in the cell shown in a. Note that the magnetite crystals are *tooth- or bullet-shaped* which is typical for these microorganisms and that the greigite crystals are irregular in morphology with rough edges

Figure 4.2 shows magnetite and greigite crystals co-aligned in a double chain within a cell of this organism.

Magnetite crystals in magnetosomes are of high chemical purity (Bazylinski 1995; Bazylinski and Frankel 2000b). Early studies such as that of Gorby (1989) showed that iron was not be replaced by other transition metal ions, including titanium, chromium, cobalt, copper, nickel, mercury and lead, in the magnetite crystals of *Magnetospirillum magnetotacticum* when cells were grown in the presence of these ions. Towe and Moench (1981) reported trace amounts of titanium in the magnetite particles of an uncultured freshwater magnetotactic coccus collected from a wastewater treatment pond. Recently several studies indicate that iron can be replaced by certain metal ions in magnetosomes of some magnetotactic bacteria. Why early studies did not show this is probably due to the

much more sensitive detection techniques used presently. In addition, some uncultured magnetotactic bacteria appear to incorporate manganese in their magnetosomes when  $\text{MnCl}_2$  was added to the microcosms containing the cells (Keim et al. 2009) while the cells of the three species of *Magnetospirillum* in culture have been shown to incorporate cobalt present in the growth medium in magnetosome magnetite, most probably in the surface layers of the crystals (Staniland et al. 2008).

Contaminating metal ions have also been found in greigite magnetosomes. Variable but significant amounts of copper (0.1–10 atomic % relative to iron) have been found in the greigite particles of the MMP and the large rod-shaped bacteria collected from certain environments (Bazylinski et al. 1993a; Pósfai et al. 1998b). Copper appeared to be mostly concentrated on the surface of the particles.

#### 4.2.4.2 The Size of Magnetosome Crystals Has Physical Significance

The size of the magnetosome mineral crystals has great physical significance which is reflected in their magnetic properties. Almost all mature magnetosome magnetite and greigite crystals occur in a very narrow size range, the single domain (SD) size range which is approximately 35–120 nm (Bazylinski et al. 1994; Frankel and Bazylinski 1994; Moskowitz 1995; Bazylinski and Moskowitz 1997; Frankel et al. 1998). There is one notable exception: very large magnetite crystals with lengths up to 250 nm have been observed in an uncultured coccus (Spring et al. 1998; McCartney et al. 2001; Lins et al. 2005). Crystals of magnetite and greigite in the SD size range are stable single-magnetic domains and are permanently magnetic at ambient temperature (Butler and Banerjee 1975; Diaz-Ricci and Kirschvink 1992). These crystals are uniformly magnetized and have the maximum magnetic dipole moment per unit volume. Magnetic crystals larger than the SD size range are not uniformly magnetized because of the formation of domain walls or the so-called vortex or flower configurations (McCartney et al. 2001). In the case of the very large magnetosome magnetite crystals, these behave as single-magnetic domains when in close proximity to other crystals such as in a chain (McCartney et al. 2001). Non-uniform magnetization has the effect of significantly reducing the magnetic moments of the crystals. Crystals with lengths below about 35 nm are superparamagnetic (SPM). Although SPM particles are SD, thermally induced reversals of their magnetic moments result in a time-averaged moment of zero and thus are not permanently magnetic at ambient temperature and would be useless to the cell for magnetotaxis. Therefore, by controlling crystal size, magnetotactic bacteria have optimized the magnetic dipole moment per magnetosome.

#### 4.2.4.3 Crystal Morphologies in Magnetosomes

Several different morphologies of magnetosome magnetite and greigite crystals occur in magnetotactic bacteria (Fig. 4.3). However, in general, magnetite crystal shape is consistent within the cells of a single bacterial species or strain

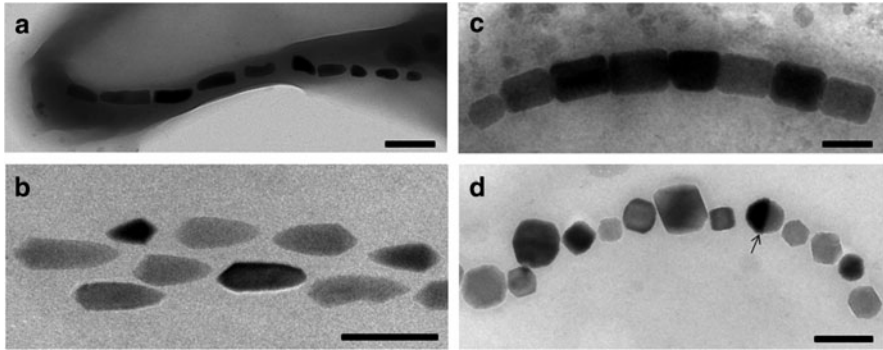


**Fig. 4.3** High-magnification TEM images of the different morphologies of magnetite magnetosome crystals. *Tooth- or bullet-shaped crystals* with one pointed and one flat end (**a**); *tooth-shaped crystals* that are pointed at each end (**b**); *Elongated pseudo-prismatic crystals* (**c**); and *cubo-octahedral crystals* (a twinned crystal is shown at the arrow) (**d**). Bar represents 200 nm

(Bazylinski et al. 1994) although minor variations have been observed in crystals of some species grown under different conditions (Meldrum et al. 1993a). High-resolution transmission electron microscopy, selected area electron diffraction and electron tomography have shown magnetite particles from magnetotactic bacteria to be well-ordered crystals of high structural integrity. Newly formed, immature SPM magnetite crystals of some organisms in culture tend to rounded edges and smoother crystal faces which become more defined as the particles mature and increase in size to the single-magnetic domain size range (Bazylinski and Frankel 2000a). It is not clear whether these observations apply to greigite crystals since there are no greigite-producing strains in pure culture. Nonetheless, much more morphological variations occur in greigite crystals within cells collected from natural environments. For example, several greigite particle morphologies have been observed within a single cell (Pósfai et al. 1998b) (Fig. 4.2).

Three general projected shapes of mature magnetite and greigite crystals have been observed in magnetotactic bacteria using various forms of electron microscopy (Bazylinski and Frankel 2000a, b). They include: (1) cuboidal (cubo-octahedral) (e.g., Balkwill et al. 1980; Mann et al. 1984a); (2) elongated pseudo-prismatic (quasi-rectangular in the horizontal plane of projection) (Towe and Moench 1981; Mann et al. 1984b; Meldrum et al. 1993a, b); and (3) tooth-, bullet- or arrowhead-shaped (anisotropic) (Mann et al. 1987a, b; Spring et al. 1993; Thornhill et al. 1994; Lefèvre et al. 2010b).

A number of different idealized morphologies of magnetite crystals have been determined using high-resolution transmission electron microscopy. Magnetite and greigite are in the  $Fd\bar{3}m$  space group and have the face-centered spinel crystal structure (Palache et al. 1944). Macroscopic crystals of magnetite display habits of the octahedral  $\{111\}$  form, and rarely dodecahedral  $\{110\}$ , or cubic  $\{100\}$  forms. The idealized habit of magnetite crystals in freshwater *Magnetospirillum* species, the most studied of the cultured magnetotactic bacteria, are cubo-octahedra composed

of  $\{100\} + \{111\}$  forms (Mann et al. 1984a), with equidimensional development of the six symmetry-related faces of the  $\{100\}$  form and of the eight symmetry-related faces of the  $\{111\}$  form. The habits of the non-equidimensional elongated crystals, like those in the marine vibrio strain MV-1 and the marine coccus strain MC-1, have been described as combinations of  $\{100\}$ ,  $\{111\}$  and  $\{110\}$  forms (Meldrum et al. 1993a, b). In these crystals, the 6, 8 and 12 symmetry-related faces of the respective forms constituting the habits do not develop equally. For example, crystals of strains MV-1 (Meldrum et al. 1993a) and MC-1 (Meldrum et al. 1993b) have pseudo prismatic habits elongated along a  $\langle 111 \rangle$  axis, with six well-developed (110) faces parallel to the elongation axis, and capped by (111) planes perpendicular to the elongation axis. In crystals of strain MV-1, the remaining six (111) faces form truncations of the end caps, and the remaining six (110) faces are very small or missing (Thomas-Keperta et al. 2001). In crystals of strain MC-1, truncations at each end consist of three (100) faces alternating with three (110) faces. Thus, six (110) faces are larger and six are smaller, and six (111) faces are virtually absent in this habit. Only the six (100) faces are equidimensional (Meldrum et al. 1993a). The pseudo-prismatic pattern of six elongated (110) faces capped by (111) faces with differing truncation planes is very common in magnetotactic bacteria that biomineralize nonequidimensional magnetite crystals.

The tooth-, bullet- and arrowhead-shaped crystals are the most anisotropic of the magnetotactic bacterial magnetite particles (Fig. 4.3a–b). In one uncultured coccoid magnetotactic bacterium, small and large crystals have different habits, suggesting that crystal growth occurs in two stages in which the nascent particles are cubo-octahedra which eventually elongate along a  $[111]$  axis to form a pseudo-octahedral prism with alternating (110) and (100) faces capped by (111) faces (Mann et al. 1987a, b). There are likely several ways that these anisotropic crystals form as some have a flattened end opposite the pointed end while others have a point at each end with one being longer than the other (Fig. 4.3a–b).

Although defects such as screw dislocations are rare in magnetosome magnetite crystals, crystal twinning is relatively common (ca. 10% of the crystals in some organisms) with individuals related by rotations of  $180^\circ$  around the  $[111]$  direction parallel to the chain direction and with a common (111) contact plane (Devouard et al. 1998). Multiple twins have also been observed but are less common.

Greigite crystals in magnetotactic bacteria have the same three general morphologies as magnetite (Pósfai et al. 1998b) that are composed primarily of  $\{111\}$  and  $\{100\}$  forms (Heywood et al. 1991). Greigite crystal morphologies in most uncultured rod-shaped bacteria may be species- and/or strain-specific although this remains to be proven with pure cultures. However, the MMP contains a combination of greigite crystal morphologies, including pleiomorphic, pseudo-rectangular prismatic, tooth-shaped and cubo-octahedral (Pósfai et al. 1998b).

Unlike magnetite crystals in magnetotactic bacteria, individual greigite crystals in these bacteria often exhibit patchy contrast or appear wrinkled when viewed with the electron microscope (Pósfai et al. 1998b) and instead of having well-defined, distinct facets, greigite crystal surfaces are often rounded and irregular (Fig. 4.2).

These defects have been interpreted as resulting from the mackinawite to greigite solid-state conversion process (Pósfai et al. 1998b). Thickness variations and other factors likely also contribute to the uneven contrast of these particles.

There may be a link between phylogeny and relatedness of magnetotactic bacteria and the composition and shape of the mineral crystals they biomineralize. For example, all *Magnetospirillum* species produce cubo-octahedral crystals of magnetite and all known magnetotactic bacteria of the *Nitrospirae* phylum synthesize bullet-shaped magnetosomes (Spring et al. 1993; Lefèvre et al. 2010a). This might indicate that closely related bacteria might have similar genes for magnetosome biomineralization (discussed in a later section).

#### 4.2.4.4 Arrangement of Magnetosomes Within the Cell

In most magnetotactic bacteria, magnetosomes are arranged in one or more chains that are anchored within the cell (Bazylinski and Frankel 2004). Magnetic interactions between magnetosome crystals in a chain cause their magnetic dipole moments to spontaneously orientate parallel to each other along the length of the chain by minimizing the magnetostatic energy (Frankel 1984). In this chain motif, the total magnetic dipole moment of the cell is the sum of the permanent magnetic dipole moments of the individual SD magnetosome particles. Magnetic measurements (Penninga et al. 1995), magnetic force microscopy (Proksch et al. 1995) and electron holography (Dunin-Borkowski et al. 1998, 2001) studies confirm this as they unequivocally show that the chain of magnetosomes in a magnetotactic bacterium functions as a single magnetic dipole and not as a collection of individual dipoles. By arranging the magnetosomes in chains, the cell has thus maximized its magnetic dipole moment. The magnetic dipole moment of the cell is generally large enough such that its interaction with the Earth's geomagnetic field overcomes the thermal forces tending to randomize the orientation of the cell in its aqueous surroundings (Frankel 1984). Cells experience a torque due to the rigid, anchored magnetosome chain that acts like a bacterial backbone in a magnetic field, causing the cell to align along magnetic field lines. Magnetotaxis results from the passive alignment of the cell along geomagnetic field lines while it swims. Living cells are not attracted or pulled toward either geomagnetic pole and dead cells, like living cells, align along geomagnetic field lines but do not swim.

Some uncultured magnetite- and greigite-producing magnetotactic bacteria do not arrange magnetosomes in chains but instead produce a clump of them at one end of the cell or clumps within partial chains (Moench 1988; Heywood et al. 1990; Mann et al. 1990; Pósfai et al. 1998a, b; Cox et al. 2002) (Fig. 4.1b). In these cases, the cellular magnetic dipole moment has not been maximized. However, despite this, based on the behavior of the cells in a magnetic field, even these organisms clearly possess a net magnetic dipole moment and thus they also behave like magnetotactic bacteria that have chains of magnetosomes.

### 4.2.5 *The Function of Magnetosomes: Magnetotaxis*

Initially, magnetotactic bacteria were thought to have one of two magnetic polarities, north or south seeking, depending on the magnetic orientation of the cell's magnetic dipole with respect to their direction of motion (Blakemore et al. 1980). The vertical component of the inclined geomagnetic field (except at the equator where the geomagnetic field lines are horizontal) appeared to select for a dominant polarity in each hemisphere by favoring cells whose polarity caused them to swim downward away from potentially high, toxic concentrations of oxygen near the surface and toward microaerobic/anaerobic sediments. This hypothesis appeared to be true in that some studies showed that north-seeking magnetotactic bacteria predominated in the Northern Hemisphere while south-seeking cells predominated in the Southern Hemisphere (Blakemore et al. 1980). However, this idea has not been found to be generally true and the major numbers of some species of magnetotactic bacteria in the Northern Hemisphere appear to be south seeking (Simmons et al. 2006). In addition, the behavior of a cultured polarly magneto-aerotactic bacterium, the coccus strain MC-1, was not consistent with this hypothesis. Cells of MC-1 did not grow at the bottom of O<sub>2</sub>-gradient culture tubes in the Northern Hemisphere but formed microaerophilic bands of cells at the OAI that contained albeit mostly north- but south-seeking cells as well (Frankel et al. 1997). This means that even those organisms with a polar preference can swim in both up and down directions even if they have a polar swimming preference under toxic conditions (the current definition of polarity with regard to the magnetotactic bacteria).

Magnetotaxis appears to function in conjunction with aerotaxis (magneto-aerotaxis) in the marine, microaerophilic coccus strain MC-1, and *M. magnetotacticum* (Frankel et al. 1997, 2007; Frankel and Bazylinski 2009) (Fig. 4.4). Although these bacteria appear to differ in their mechanism of aerotactic response and in the way they utilize the magnetic field with strain MC-1 using the field as a sense of direction (polar magneto-aerotaxis) and *M. magnetotacticum* using the field as an axis (axial magneto-aerotaxis), they both prefer the microaerobic conditions at the OAI and in this way magneto-aerotaxis works similarly for both organisms (Frankel et al. 1997, 2007). According to the magneto-aerotaxis hypothesis, the direction of migration along the magnetic field is determined by the direction of flagellar rotation (clockwise or counterclockwise), which in turn is determined by the aerotactic response of the cell (Frankel et al. 1997, 2007; Frankel and Bazylinski 2009) (Fig. 4.4). The presumed function of magneto-aerotaxis for strain MC-1 and *M. magnetotacticum* is increased efficiency in locating and maintaining position at a preferred oxygen concentration (and perhaps oxidation–reduction (redox) potential) at the OAI in vertical oxygen concentration and redox gradients in aquatic habitats (Frankel et al. 1997, 2007). While non-magnetotactic microaerophilic cells have a three-dimensional search problem using aerotaxis in locating and maintaining position at the OAI, magnetotactic cells, once passively aligned and swimming up and down along the inclined geomagnetic field lines, would have a single dimensional search problem (Frankel et al. 1997, 2007; Frankel and Bazylinski 2009). Magnetotactic bacteria that are not aerobic

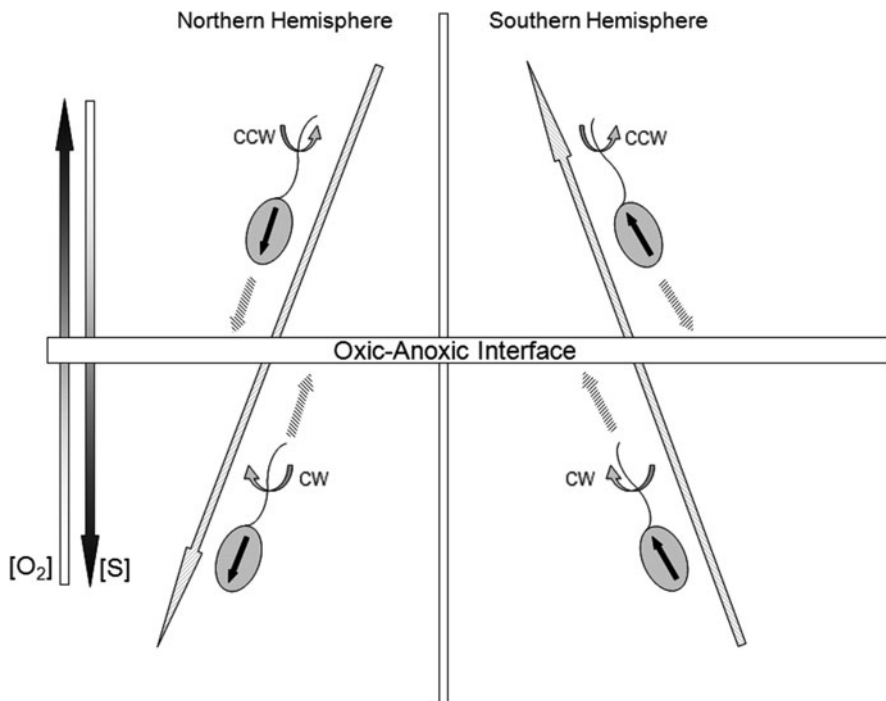


**Fig. 4.4** Schematic depicting model of how polar magneto-aerotaxis allows magnetotactic cells to locate and maintain position at their preferred oxygen concentration at the OAI in chemically stratified water columns and sediments. In this case, a double inverse concentration gradient of  $O_2$  and  $S^{2-}$  is present:  $O_2$  diffuses from the surface downward and  $S^{2-}$ , from the action of anaerobic sulfate-reducing in the anaerobic zone diffuses upwards. Cells passively align and swim along the inclined geomagnetic field lines (*large arrows*) relying on chemotaxis (aerotaxis). In both hemispheres, cells at higher than optimal oxygen concentration in the “oxidized state” swim forward by rotating their flagella counterclockwise (ccw), whereas cells at lower than optimal oxygen concentration in the “reduced state” rotate their flagella clockwise (cw) and swim backwards without turning around. Note that the geomagnetic field selects for cells with polarity such that ccw flagellar rotation causes cells to swim downward along the magnetic field lines in both hemispheres. Axial magnetospirilla behave differently as they possess a flagellum at each end of the cell and swim bidirectionally up and down along the magnetic field lines but again relying on aerotaxis to find and locate their optimal position on the gradient

(e.g., the greigite-producers) might utilize chemotaxis towards another compound (e.g., hydrogen sulfide) or redox rather than oxygen.

#### 4.2.6 *Biominingalization of Magnetosomes and Construction of the Magnetosome Chain*

Synthesis of the bacterial magnetosome chain involves several discrete steps including magnetosome vesicle formation, assembly of the vesicles in chains, iron



uptake by the cell, iron transport into the magnetosome vesicle and controlled magnetite (or greigite) biomineralization within the magnetosome vesicle (Bazylinski and Frankel 2004; Frankel and Bazylinski 2006). It is important to recognize that some of these steps must overlap temporally to ensure continued magnetosome synthesis during the life of the cell. In *Magnetospirillum magneticum*, it is unclear whether the magnetosome membrane actually represents a true, free-standing vesicle cutoff from the periplasm or a permanent invagination (Komeili et al. 2006; Komeili 2007) (discussed in a later section). If the magnetosome membrane is a permanent invagination of the cytoplasmic membrane that is not sealed off from the periplasm, then an intricate system for the transport of iron into a vesicle may not be required and iron may need only to be transported across the outer membrane into the periplasm.

#### 4.2.6.1 The Magnetosome Membrane

The magnetosome membrane which encloses magnetite crystals (Gorby et al. 1988; Schüler and Baeuerlein 1997) in magnetosomes appears to be the locus of control and regulation of magnetite biomineralization in magnetotactic bacteria (Schüler 2008). The magnetosome membrane of *M. magnetotacticum* and *Magnetospirillum gryphiswaldense* is a lipid bilayer consisting of proteins, fatty acids, glycolipids, sulfolipids, and phospholipids; components typical of a lipid bilayer type membrane (Gorby et al. 1988; Grünberg et al. 2004). This is in striking contrast to other inclusions in prokaryotes which are generally surrounded by a single layer of protein. Phospholipids make up 58–65% of the total lipids of the magnetosome membrane of *M. magneticum* (Nakamura and Matsunaga 1993) and the predominant phospholipids in all *Magnetospirillum* species are phosphatidylserine, phosphatidylglycerol, and phosphatidylethanolamine (Gorby et al. 1988; Nakamura and Matsunaga 1993; Grünberg et al. 2004). A comparison of the fatty acids of the magnetosome membrane, the cytoplasmic membrane (CM) and the outer membrane (OM) showed that the composition of the magnetosome membrane is similar to the CM but distinct from the OM (Tanaka et al. 2006) suggesting that the magnetosome membrane is derived from the CM. In addition, magnetite magnetosomes are almost always located adjacent to the CM in *Magnetospirillum* species (Bazylinski and Schübbe 2007). Using electron cryotomography, the magnetosome membrane in *M. magneticum* has been shown to originate as an invagination of the CM (Komeili et al. 2006). Another important question was whether these invaginations actually become magnetosome vesicles and are synthesized prior to magnetite biomineralization and exist as empty vesicles in the cell or if the magnetosome membrane envelopes the particle afterward. Komeili et al. (2006) showed that magnetite precipitation occurs after vesicle formation. Different stages of magnetite precipitation can be observed within magnetosome membrane invaginations/vesicles. Cells grown under iron limitation contained empty magnetosome invaginations/vesicles arranged in a chain engaged to the CM (Komeili et al. 2006). Only 35% of the magnetosomes examined showed the magnetosome membrane to be an

invagination of the CM suggesting that the invaginations pinch off and become true vesicles. Alternatively this may be a result of a technical problem involving the technique (Komeili 2007). It is also not known if this is a common characteristic of magnetosomes in all magnetotactic bacteria. In parallel experiments with *M. gryphiswaldense*, Scheffel et al. (2006) found empty magnetosome membrane vesicles in cells grown under iron limitation and also that magnetic cells contain, in addition to filled magnetosome vesicles, many empty vesicles inside the cell.

#### 4.2.6.2 Magnetosome Membrane Proteins

Numerous studies have shown that the magnetosome membrane contains proteins unique to it that are not present in the CM or the OM (Bazyliński and Frankel 2004; Schüler 2008). These proteins have been designated the Mam (for magnetosome membrane) or Mms (for magnetic particle membrane specific) proteins and the respective genes as the *mam* or *mms* genes. It is these proteins that are thought to be responsible for the biomineralization processes involved in magnetosome biomineralization and construction of the magnetosome chain. Although numerous magnetosome membrane proteins have been discovered, the roles of only a relatively few have been partially elucidated. Two main approaches have been used to determine the roles of these proteins: (1) there are *in vitro* studies where purified magnetosome membrane proteins are present in reactions where magnetite is inorganically precipitated; and (2) there are *in vivo* studies where genes that encode for specific magnetosome proteins are inactivated through site-directed mutation (knock-out mutants). A complete list of magnetosome-associated proteins and their presence in specific magnetotactic bacteria can be found in Bazyliński and Schübbe (2007).

Arakaki et al. (2003) found that when magnetite was inorganically precipitated in the presence of the magnetosome membrane protein Mms6 from *M. magneticum* strain AMB-1, the morphology of the crystals was affected and slightly approached that of mature magnetosome crystals in intact cells. Others have now confirmed these results (Amemiya et al. 2007; Prozorov et al. 2007). Mms6 is an amphiphilic protein consisting of an N-terminal LG-rich hydrophobic region and a C-terminal hydrophilic region containing repeats of acidic amino acids that suggests that cations such as Fe might bind to this latter part of the protein. Amemiya et al. (2007) concluded that the Mms6 protein: (1) acts as a template/scaffold for magnetite precipitation; (2) regulates the size of the magnetite crystals to approximately 20 nm; and (3) restricts the shape of the magnetite crystals to the cubo-octahedral habit by association with specific crystal faces.

There are several *in vivo* studies involving the role of specific magnetosome proteins in magnetite biomineralization in magnetotactic bacteria. The MamGFDC proteins, highly conserved among magnetotactic bacteria, make up about 35% of the proteins associated with the magnetosome membrane in *M. gryphiswaldense* (Scheffel et al. 2008). These proteins have been found to regulate the size of magnetosome magnetite crystals as mutants that lack these genes produced magnetite crystals

that were only about 75% of the size of the crystals produced by cells of the wild-type. The MamGFDC proteins appear to be at least partially functionally redundant and act synergistically in controlling the size of magnetite crystals in *M. gryphiswaldense* (Scheffel et al. 2008).

The MamK and MamJ proteins have been shown to be required for magnetosome chain assembly in *Magnetospirillum* species (Komeili et al. 2006; Pradel et al. 2006; Scheffel et al. 2006). Magnetosomes are attached by the acidic magnetosome membrane protein MamJ to a series of cytoskeletal filaments that traverse the cell along its long axis and are composed of MamK (Komeili et al. 2006; Pradel et al. 2006; Scheffel et al. 2006). Mutants in either of the genes responsible for coding for either protein biomineralize magnetosomes but they are not aligned in chains. Some magnetotactic bacteria, however, do not synthesize MamJ (they do not possess the gene) (Jögler et al. 2009a; Schübbe et al. 2009) and thus there may be other proteins that attach magnetosomes to MamK in these organisms. A simplified model for the role of some of the Mam proteins is shown in Fig. 4.5.

Many other magnetosome membrane proteins have been identified and based on their similarity to other known proteins, some have speculated on their roles in magnetosome biomineralization. Some of these are discussed below.

The protein MamA and its homologues (mam22 and mms24) are found in almost all cultured magnetotactic bacteria (Grünberg et al. 2001; Komeili et al. 2004; Matsunaga et al. 2005) and are members of the tetratricopeptide repeat (TPR) protein family (Okuda et al. 1996). These proteins are thought to be important in protein–protein interactions that might occur in the synthesis of magnetosomes and the magnetosome chain (Okuda et al. 1996; Okuda and Fukumori 2001) since

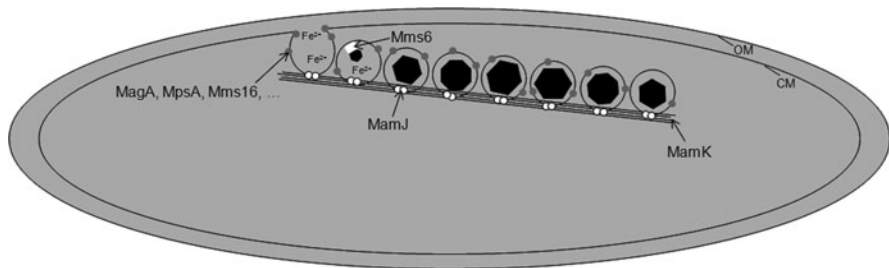


**Fig. 4.5** Cartoon depiction of a simplified model of how magnetosomes are formed in *Magnetospirillum* species showing the roles of several magnetosome proteins. The magnetosome vesicle forms as an invagination of the cell membrane (CM). At some point specific magnetosome membrane proteins are synthesized and are present on or in the magnetosome membrane (e.g., MagA, MpsA, Mms16, Mms6, MamJ here). Iron is transported from outside the cell across the outer membrane (OM) to the periplasm where some may enter the invagination becoming the magnetosome vesicle. If the vesicle pinches off from the CM then iron must be transported across the CM through the cytoplasm and then into the magnetosome vesicle. Magnetite precipitates inside the vesicle. The MamJ protein is a magnetosome membrane protein that anchors the magnetosome to the actin-like protein MamK that comprises a series of cytoskeletal filaments that traverse the cell along its long axis (Komeili et al. 2004, 2006; Scheffel et al. 2006; Komeili 2007)

multiple copies of TPR proteins are known to form scaffolds within proteins to mediate protein–protein interactions and to coordinate the assembly of proteins into multi-subunit complexes (Ponting and Phillips 1996). A deletion of the gene *mamA* in *M. magneticum* resulted in shorter magnetosome chains and it was concluded that MamA activates magnetosome vesicles (Komeili et al. 2004).

The proteins MamB and MamM appear to be present in all cultured magnetotactic bacteria and show strong similarity to heavy metal transporting proteins of the cation diffusion facilitator family. MamV also appears to be in this protein family but is only present in *M. magnetotacticum* and *M. magneticum*. Proteins in this family show an unusual degree of size variation, sequence divergence, and polarity, and catalyze the influx or efflux of metal ions (Paulsen et al. 1997). Thus, it is thought by some that these proteins might be involved in the transport of iron into magnetosome vesicles (Grünberg et al. 2001).

MamE and MamO show sequence similarity to HtrA-like serine proteases. The protein product of the *mamP* gene also shows similarity to this group of serine proteases and is present in the same operon as *mamE* and *mamO* but was not identified in the magnetosome membrane. HtrA is a heat-shock-induced, envelope-associated serine protease in *Escherichia coli* (Lipinska et al. 1989). The activity of HtrA is in the periplasm, where its main role appears to be in the degradation of misfolded proteins (Pallen and Wren 1997). These proteases are also known to be involved in nondestructive protein processing and modulation of signaling pathways by degrading important regulatory proteins. These proteins are characterized by one or two PDZ-domains (Fanning and Anderson 1996) and a trypsin-like protease domain. For these reasons, it is thought that MamE and MamO might function as chaperones in magnetosome formation (Grünberg et al. 2001).

MamN shows some similarity to certain transport proteins, some of which transport protons leading to an idea that this protein might function as a proton pump transporting protons accumulating during magnetite precipitation (Jogler and Schüler 2007). MamT contains two possible binding sites for the heme group present in cytochrome *c* and therefore could be involved in redox reactions within the magnetosome vesicle (Grünberg et al. 2004).

#### 4.2.6.3 Organization and Regulation of Magnetosome Genes

The genes that encode for magnetosome membrane protein are in close proximity to one another within the genome of every magnetotactic bacterium that has been sequenced (Schüler 2008). Within this genomic area, these genes are present as clusters. For example, *mamA* and *mamB* in *M. gryphiswaldense* are in a collinear order with six other genes that make up the *mamAB* cluster (Grünberg et al. 2001). Another group of magnetosome membrane protein genes, the *mamCD* cluster, simply consists of *mamC* and *mamD*. Similar localizations and arrangements of these genes exist in *M. magnetotacticum* and strain MC-1 (Grünberg et al. 2001) and *D. magneticus* (Nakazawa et al. 2009). Additional genes not linked directly to magnetosome membrane proteins present in these gene clusters have now been

identified and are thought to also be important in magnetosome biomineralization. For example, in *M. gryphiswaldense*, the *mamAB* cluster consists of 17 collinear genes on a segment of DNA about 16.4 kb in length. The *mamGFDC* cluster is about 2.1 kb in length and is located about 15-kb upstream of the *mamAB* operon and is composed of four genes. The 3.6-kb *mms6* cluster is located 368-bp upstream of the *mamGFDC* cluster and contains five genes (Schübbe et al. 2003). Not all magnetosome genes exist in clusters; *mamW*, which encodes for a magnetosome membrane protein, is not present in the three clusters discussed above, but is located about 10-kb upstream of the *mms6* cluster (Ullrich et al. 2005). In *M. gryphiswaldense*, all the *mam* and *mms* genes are located on a segment of DNA about 45 kb in length.

The operon-like, collinear organization of the *mamAB*, *mamGFDC*, and *mms6* clusters suggested that they might be transcribed as single long mRNAs and recent studies involving gene transcriptional analysis confirmed this idea and demonstrated the presence of one long transcript extending over more than 16 kb. The transcription starting points of the *mamAB*, *mamGFDC*, and *mms6*-operons were mapped closely upstream of the first genes in the operons, respectively (Schübbe et al. 2006). The organization of the magnetosome genes is well conserved in the different, but closely related, *Magnetospirillum* strains. The organization and sequence of the magnetosome genes is less conserved in other unrelated magnetotactic strains such as the coccus strain MC-1 and the vibrio strain MV-1 (Schübbe et al. 2003; Ullrich et al. 2005; Jogler et al. 2009a, b; Schübbe et al. 2009).

#### 4.2.6.4 The Magnetosome Gene Island and Its Significance

The genomic region that encompasses the clusters of magnetosomes genes in *M. gryphiswaldense* also contains 42 mobile elements as transposases of the insertion sequence type and integrases (Ullrich et al. 2005). These mobile elements as well as tRNA genes that can serve as attachment sites for integrases are common and important features in genomic islands (Reiter and Palm 1990; Blum et al. 1994; Mahillon and Chandler 1998; Mahillon et al. 1999). The magnetosome gene region in *M. gryphiswaldense* is about 130 kb in size and contains three tRNA genes upstream of the *mms* operon. Because this region shares other characteristics of a genomic island including a slightly different guanine and cytosine (G + C) content compared to the rest of the genome as well as containing many hypothetical genes and pseudogenes (Schübbe et al. 2003; Ullrich et al. 2005), it is now currently believed to represent a large magnetosome gene island. Similar genomic regions have been found in the genomes of other magnetotactic bacteria (Fukuda et al. 2006; Richter et al. 2007). Genomic islands are reported to be acquired by a horizontal gene transfer and most have a different G + C content than the core genome (Dobrindt et al. 2004).

The similar organization of the magnetosome operons in different magnetotactic bacterial strains suggests that the magnetosome gene island might have been transferred via horizontal gene transfer to many different types of bacteria thereby

explaining the great diversity of the group. Gene islands undergo frequent rearrangements and deletions resulting in a high rate of spontaneous mutations. Spontaneous mutations that lead to a loss of the magnetic phenotype with a frequency of  $10^{-2}$  were observed under starvation conditions in *M. gryphiswaldense* (Ullrich et al. 2005). High frequency of spontaneous mutants that had lost the ability to synthesize magnetosomes was also observed for other magnetotactic bacteria including strain MV-1 (Dubbels et al. 2004) and *M. magneticum* (Fukuda et al. 2006; Komeili et al. 2006). Possible additional evidence of horizontal gene transfer is the fact that nonmagnetotactic species of magnetotactic genera and forms have been found and some have been isolated in pure culture (Geelhoed et al. 2009, 2010; Lefèvre et al. 2010a).

Additional copies of magnetosome genes may exist outside the magnetosome genomic island and recently a second copy of the *mamK* gene located possibly in an islet was found outside the magnetosome genomic island in the genome of *Magnetospirillum magneticum* (Rioux et al. 2010).

#### 4.2.7 Applications of Magnetosomes and Magnetosome Crystals

The number of reported and published applications of magnetotactic bacterial cells and derivatives is enormous and thus we only discuss those regarding magnetosomes and magnetosome crystals. Several excellent reviews are available on the subject (Matsunaga 1991; Lang and Schüler 2006; Lang et al. 2007; Matsunaga and Arakaki 2007).

Magnetosomes contain single-magnetic domain crystals that have useful magnetic, physical and perhaps electrical properties. Moreover, the organic, phospholipid membrane that envelopes the crystals allows for the immobilization of biological molecules such as other proteins or nucleic acids on their surfaces and allows for many other potential applications.

Magnetite crystals from magnetosomes have been used in the immobilization of enzymes (e.g., glucose oxidase, uricase) which can result in a much higher specific activity of the enzyme than when immobilized on crystals of synthetic magnetite (Matsunaga and Kamiya 1987). Specific antibodies have been rendered magnetic using bacterial magnetite particles that have proven useful in various fluoroimmunoassays (Matsunaga et al. 1990) involving the detection of allergens (Nakamura and Matsunaga 1993) and squamous cell carcinoma cells (Matsunaga 1991) and the quantification of immunoglobulin G (Nakamura et al. 1991). Bacterial magnetite crystals have been used in the detection and removal of cells of *E. coli* with a fluorescein isothiocyanate-conjugated monoclonal antibody immobilized on bacterial magnetite (Nakamura et al. 1993).

Magnetite magnetosomes can also be used to immobilize nucleic acids. One interesting application is in the detection of single nucleotide polymorphism based on the fluorescence resonance energy transfer (FRET) technique. Double-stranded labeled DNA synthesized by PCR immobilized to magnetosomes hybridizes to

a target DNA and a fluorescence signal is detected (Nakayama et al. 2003; Ota et al. 2003; Tanaka et al. 2003; Yoshino et al. 2003; Maruyama et al. 2004).

Protein displays have been designed using specific magnetosome membrane proteins as anchor molecules for the assembly of foreign proteins on the surface of magnetite magnetosomes. Several magnetosome membrane proteins have been used as anchor proteins, including MagA, MpsA, Mms16 and Mms13 (MamC, Mam12) (Nakamura et al. 1995a, b; Matsunaga and Takeyama 1998; Matsunaga et al. 1999, 2000b, 2002; Okamura et al. 2001; Arakaki et al. 2003; Yoshino and Matsunaga 2005, 2006). The stability of these anchor proteins was tested by fusing them to the chemiluminescent protein luciferase (Matsunaga et al. 2000a, 2002; Yoshino and Matsunaga 2006) and the most stable protein was Mms13 (MamC, Mam12) (Yoshino and Matsunaga 2006).

Magnetosomes have been shown to be useful in the isolation of nucleic acids. Magnetosomes have been modified using compounds such as hyperbranched poly-amidoamine dendrimers or amino silanes for the extraction of DNA (Yoza et al. 2002, 2003a, b). An efficient means of isolating mRNA using oligo(dT)-modified magnetosomes has also been described (Sode et al. 1993).

Biotin and other molecules attached to a monolayer-modified substrate were detected by streptavidin immobilized to magnetosomes using a magnetic force microscope demonstrating that magnetosomes can be useful in detecting biomolecular interactions in medical and diagnostic analyses (Arakaki et al. 2004). For example, streptavidin-modified magnetosomes have been used for the immobilization of biotin-modified antibodies (Amemiya et al. 2005). Other biomedical applications include the use of magnetosomes in drug delivery (Matsunaga et al. 1997). As with cells of magnetotactic bacteria, magnetosomes have also been used in highly efficient magnetic cell separation (Kuhara et al. 2004).

#### **4.2.8 Magnetosomes and Magnetofossils**

Magnetite magnetosomes have had an enormous impact in geology, paleontology and astrobiology. Magnetite crystals resembling those present in some magnetosomes, specifically the elongated and anisotropic forms, of magnetotactic bacteria living in the present have been found in ancient and modern sediments (Chang and Kirschvink 1989; Chang et al. 1989) and in the Martian meteorite ALH84001 (Thomas-Keprta et al. 2000, 2001, 2002; Clemett et al. 2002). These structures have been referred to as “magnetofossils” and have been used to indicate the past presence of magnetotactic bacteria in sediments and in meteorite ALH84001. The presence and interpretation of these crystals in Martian meteorite ALH84001 in particular have sparked great controversy and debate since the implication was that the bacterial life had existed on ancient Mars (McKay et al. 1996; Thomas-Keprta et al. 2000, 2001, 2002; Buseck et al. 2001; Clemett et al. 2002; Weiss et al. 2004). In turn, this debate has led to a number of criteria to be used to distinguish biogenic magnetite from inorganically produced magnetite (Thomas-Keprta et al. 2000;

Arató et al. 2005; Kopp and Kirschvink 2008; Jimenez-Lopez et al. 2010). Nano-sized greigite crystals might also be used as a biomarker but again, like magnetite, biogenically produced greigite must be able to be distinguished from that produced inorganically (Pósfai et al. 2001). This debate, together with that regarding other putative microbial fossils, illustrates the need for and the ability to recognize and interpret reliable prokaryotic fossils (Bazyliński and Frankel 2003; Jimenez-Lopez et al. 2010).

### 4.2.9 Conclusions and Future Directions for Research

The bacterial magnetosome and its magnetic properties have been refined and optimized in the course of evolution by the organisms that synthesize them by controlling the chemical composition, size, and morphology of the magnetosome mineral crystal as well as their position within the cell. Control over these features is likely mediated by the protein products of the *mam* and *mms* genes, particularly those located in and near the magnetosome membrane. Because of recent progress in the development of genetic systems for several fastidious magnetotactic species and the annotation and publication of several genomes of magnetotactic organism (Matsunaga et al. 2005; Nakazawa et al. 2009; Schübbe et al. 2009), we predict that the next significant discoveries in the biomineralization of magnetosomes by magnetotactic bacteria will deal with the elucidation of specific functions of these proteins. In turn, once functions of specific magnetosome proteins have been determined, we also expect that genetic modifications will result in much higher yields of magnetosomes and bacterial magnetite that should facilitate the development of many new commercial and scientific applications for them.

**Acknowledgments** We thank R.B. Frankel for continued collaboration and encouragement. D.A.B. and C.T.L. are supported by U.S. National Science Foundation grant EAR-0920718. U.L. and F.A. acknowledge partial financial support from The National Council for Scientific and Technological Development (CNPq) of Brazil.

## References

- Abreu F, Martins JL, Silveira TS, Keim CN, Lins de Barros HGP, Filho FJG, Lins U (2007) '*Candidatus Magnetoglobus multicellularis*', a multicellular, magnetotactic prokaryote from a hypersaline environment. *Int J Syst Evol Microbiol* 57:1318–1322
- Amann R, Peplies J, Schüler D (2007) Diversity and taxonomy of magnetotactic bacteria. In: Schüler D (ed) *Magnetoreception and magnetosomes in bacteria*. Springer, Heidelberg, pp 25–36
- Amemiya Y, Tanaka T, Yoza B, Matsunaga T (2005) Novel detection system for biomolecules using nano-sized bacterial magnetic particles and magnetic force microscopy. *J Biotechnol* 120:308–314



- Amemiya Y, Arakaki A, Staniland SS, Tanaka T, Matsunaga T (2007) Controlled formation of magnetite crystal by partial oxidation of ferrous hydroxide in the presence of recombinant magnetotactic bacterial protein Mms6. *Biomaterials* 28:5381–5389
- Arakaki A, Webb J, Matsunaga T (2003) A novel protein tightly bound to bacterial magnetic particles in *Magnetospirillum magneticum* strain AMB-1. *J Biol Chem* 278:8745–8750
- Arakaki A, Hideshima S, Nakagawa T, Niwa D, Tanaka T, Matsunaga T, Osaka T (2004) Detection of biomolecular interaction between biotin and streptavidin on a self-assembled monolayer using magnetic nanoparticles. *Biotechnol Bioeng* 88:543–546
- Arató B, Szányi Z, Flies C, Schüller D, Frankel RB, Buseck PR, Pósfai M (2005) Crystal-size and shape distributions of magnetite from uncultured magnetotactic bacteria as a potential biomarker. *Am Mineral* 90:1233–1240
- Balkwill DL, Maratea D, Blakemore RP (1980) Ultrastructure of a magnetic spirillum. *J Bacteriol* 141:1399–1408
- Bazylinski DA (1995) Structure and function of the bacterial magnetosome. *ASM News* 61:337–343
- Bazylinski DA, Blakemore RP (1983a) Denitrification and assimilatory nitrate reduction in *Aquaspirillum magnetotacticum*. *Appl Environ Microbiol* 46:1118–1124
- Bazylinski DA, Blakemore RP (1983b) Nitrogen fixation (acetylene reduction) in *Aquaspirillum magnetotacticum*. *Curr Microbiol* 9:305–308
- Bazylinski DA, Frankel RB (2000a) Magnetic iron oxide and iron sulfide minerals within organisms. In: Baeuerlein E (ed) *Biomineralization: from biology to biotechnology and medical application*. Wiley-VCH, Weinheim, pp 25–46
- Bazylinski DA, Frankel RB (2000b) Biologically controlled mineralization of magnetic iron minerals by magnetotactic bacteria. In: Lovley D (ed) *Environmental microbe-mineral interactions*. ASM, Washington, DC, pp 109–144
- Bazylinski DA, Frankel RB (2003) Biologically controlled mineralization in prokaryotes. *Rev Mineral Geochem* 54:217–247
- Bazylinski DA, Frankel RB (2004) Magnetosome formation in prokaryotes. *Nat Rev Microbiol* 2:217–30
- Bazylinski DA, Moskowitz BM (1997) Microbial biomineralization of magnetic iron minerals: microbiology, magnetism and environmental significance. *Rev Mineral* 35:181–223
- Bazylinski DA, Schübbe S (2007) Controlled biomineralization by and applications of magnetotactic bacteria. *Adv Appl Microbiol* 62:21–62
- Bazylinski DA, Williams TJ (2007) Ecophysiology of magnetotactic bacteria. In: Schüller D (ed) *Magnetoreception and magnetosomes in bacteria*. Springer, Heidelberg, pp 37–75
- Bazylinski DA, Garratt-Reed AJ, Abedi A, Frankel RB (1993a) Copper association with iron sulfide magnetosomes in a magnetotactic bacterium. *Arch Microbiol* 160:35–42
- Bazylinski DA, Heywood BR, Mann S, Frankel RB (1993b)  $\text{Fe}_3\text{O}_4$  and  $\text{Fe}_3\text{S}_4$  in a bacterium. *Nature* 366:218
- Bazylinski DA, Garratt-Reed AJ, Frankel RB (1994) Electron microscopic studies of magnetosomes in magnetotactic bacteria. *Microsc Res Tech* 27:389–401
- Bazylinski DA, Frankel RB, Heywood BR, Mann S, King JW, Donaghay PL, Hanson AK (1995) Controlled biomineralization of magnetite ( $\text{Fe}_3\text{O}_4$ ) and greigite ( $\text{Fe}_3\text{S}_4$ ) in a magnetotactic bacterium. *Appl Environ Microbiol* 61:3232–3239
- Bazylinski DA, Dean AJ, Schüller D, Phillips EJP, Lovley DR (2000)  $\text{N}_2$ -dependent growth and nitrogenase activity in the metal-metabolizing bacteria, *Geobacter* and *Magnetospirillum* species. *Environ Microbiol* 2:266–273
- Bazylinski DA, Dean AJ, Williams TJ, Kimble-Long L, Middleton SL, Dubbels BL (2004) Chemolithoautotrophy in the marine, magnetotactic bacterial strains MV-1 and MV-2. *Arch Microbiol* 182:373–387
- Bellini S (2009a) On a unique behavior of freshwater bacteria. *Chin J Oceanol Limn* 27:3–5
- Bellini S (2009b) Further studies on “magnetosensitive bacteria”. *Chin J Oceanol Limn* 27:6–12
- Blakemore RP (1975) Magnetotactic bacteria. *Science* 190:377–379

- Blakemore RP, Frankel RB, Kalmijn AJ (1980) South-seeking magnetotactic bacteria in the southern-hemisphere. *Nature* 286:384–385
- Blakemore RP, Short KA, Bazylinski DA, Rosenblatt C, Frankel RB (1985) Microaerobic conditions are required for magnetite synthesis within *Aquaspirillum magnetotacticum*. *Geomicrobiol J* 4:53–71
- Blum G, Ott M, Lischewski A, Ritter A, Imrich H, Tschäpe H, Hacker J (1994) Excision of large DNA regions termed pathogenicity islands from tRNA-specific loci in the chromosome of an *Escherichia coli* wild-type pathogen. *Infect Immun* 62:606–614
- Buseck PR, Dunin-Borkowski RE, Devouard B, Frankel RB, McCartney MR, Midgley PA, Pósfai M, Weyland M (2001) Magnetite morphology and life on mars. *Proc Natl Acad Sci USA* 98:13490–13495
- Butler RF, Banerjee SK (1975) Theoretical single-domain grain size range in magnetite and titanomagnetite. *J Geophys Res* 80:4049–4058
- Chang SBR, Kirschvink JL (1989) Magnetofossils, the magnetization of sediments, and the evolution of magnetite biomineralization. *Annu Rev Earth Planet Sci* 17:169–195
- Chang SBR, Stolz JF, Kirschvink JL, Awramik SM (1989) Biogenic magnetite in stromatolites 2. Occurrence in ancient sedimentary environments. *Precamb Res* 43:305–315
- Clemett SJ, Thomas-Keptra KL, Shimmin J, Morphew M, McIntosh JR, Bazylinski DA, Kirschvink JL, McKay DS, Wentworth SJ, Vali H, Gibson EK Jr, Romanek CS (2002) Crystal morphology of MV-1 magnetite. *Am Mineral* 87:1727–1730
- Cox BL, Popa R, Bazylinski DA, Lanoil B, Douglas S, Belz A, Engler DL, Neelson KH (2002) Organization and elemental analysis of P-, S-, and Fe-rich inclusions in a population of freshwater magnetococci. *Geomicrobiol J* 19:387–406
- DeLong EF, Frankel RB, Bazylinski DA (1993) Multiple evolutionary origins of magnetotaxis in bacteria. *Science* 259:803–806
- Devouard B, Pósfai M, Hua X, Bazylinski DA, Frankel RB, Buseck PR (1998) Magnetite from magnetotactic bacteria: size distribution and twinning. *Am Mineral* 83:1387–1398
- Diaz-Ricci JC, Kirschvink JL (1992) Magnetic domain state and coercivity predictions for biogenic greigite (Fe<sub>3</sub>S<sub>4</sub>): a comparison of theory with magnetosome observations. *J Geophys Res* 97:17309–17315
- Dobrindt U, Hochhut B, Hentschel U, Hacker J (2004) Genomic islands in pathogenic and environmental microorganisms. *Nat Rev Microbiol* 2:414–424
- Dubbels BL, DiSpirito AA, Morton JD, Semrau JD, Neto JN, Bazylinski DA (2004) Evidence for a copper-dependent iron transport system in the marine, magnetotactic bacterium strain MV-1. *Microbiology* 150:2931–2945
- Dunin-Borkowski RE, McCartney MR, Frankel RB, Bazylinski DA, Pósfai M, Buseck PR (1998) Magnetic microstructure of magnetotactic bacteria by electron holography. *Science* 282:1868–1870
- Dunin-Borkowski RE, McCartney MR, Pósfai M, Frankel RB, Bazylinski DA, Buseck PR (2001) Off axis electron holography of magnetotactic bacteria: magnetic microstructure of strains MV-1 and MS-1. *Eur J Mineral* 13:671–684
- Fanning AS, Anderson JM (1996) Protein-protein interactions: PDZ domain networks. *Curr Biol* 6:1385–1388
- Farina M, Motta de Esquivel D, Lins de Barros HGP (1990) Magnetic iron-sulphur crystals from a magnetotactic microorganism. *Nature* 343:256–258
- Frankel RB (1984) Magnetic guidance of organisms. *Annu Rev Biophys Bioeng* 13:85–103
- Frankel RB, Bazylinski DA (1994) Magnetotaxis and magnetic particles in bacteria. *Hyperfine Interact* 90:135–142
- Frankel RB, Bazylinski DA (2003) Biologically induced mineralization by bacteria. *Rev Mineral* 54:217–247
- Frankel RB, Bazylinski DA (2006) How magnetotactic bacteria make magnetosomes queue up. *Trends Microbiol* 14:329–331

- Frankel RB, Bazylinski DA (2009) Magnetosomes and magneto-aerotaxis. *Contrib Microbiol* 16:182–193
- Frankel RB, Blakemore RP, Wolfe RS (1979) Magnetite in freshwater magnetic bacteria. *Science* 203:1355–1357
- Frankel RB, Papaefthymiou GC, Blakemore RP, O'Brien W (1983) Fe<sub>3</sub>O<sub>4</sub> precipitation in magnetotactic bacteria. *Biochim Biophys Acta* 763:147–159
- Frankel RB, Bazylinski DA, Johnson MS, Taylor BL (1997) Magneto-aerotaxis in marine coccoid bacteria. *Biophys J* 73:994–1000
- Frankel RB, Zhang JP, Bazylinski DA (1998) Single magnetic domains in magnetotactic bacteria. *J Geophys Res Solid Earth* 103:30601–30604
- Frankel RB, Williams TJ, Bazylinski DA (2007) Magneto-aerotaxis. In: Schüler D (ed) *Magneto-reception and magnetosomes in bacteria*. Springer, Heidelberg, pp 1–24
- Fukuda Y, Okamura Y, Takeyama H, Matsunaga T (2006) Dynamic analysis of a genomic island in *Magnetospirillum* sp. strain AMB-1 reveals how magnetosome synthesis developed. *FEBS Lett* 580:801–812
- Geelhoed JS, Sorokin DY, Epping E, Tourova TP, Banciu HL, Muyzer G, Stams AJM, van Loosdrecht MCM (2009) Microbial sulfide oxidation in the oxic-anoxic transition zone of freshwater sediment: involvement of lithoautotrophic *Magnetospirillum* strain J10. *FEMS Microbiol Ecol* 70:54–65
- Geelhoed JS, Kleerebezem R, Sorokin DY, Stams AJM, van Loosdrecht MCM (2010) Reduced inorganic sulfur oxidation supports autotrophic and mixotrophic growth of *Magnetospirillum* strain J10 and *Magnetospirillum gryphiswaldense*. *Environ Microbiol* 12:1031–1040
- Gorby YA (1989) Regulation of magnetosome biogenesis by oxygen and nitrogen. PhD Dissertation, University of New Hampshire, Durham, New Hampshire
- Gorby YA, Beveridge TJ, Blakemore RP (1988) Characterization of the bacterial magnetosome membrane. *J Bacteriol* 170:834–841
- Grünberg K, Wawer C, Tebo BM, Schüler D (2001) A large gene cluster encoding several magnetosome proteins is conserved in different species of magnetotactic bacteria. *Appl Environ Microbiol* 67:4573–4582
- Grünberg K, Müller EC, Otto A, Reszka R, Linder D, Kube M, Reinhardt R, Schüler D (2004) Biochemical and proteomic analysis of the magnetosome membrane in *Magnetospirillum gryphiswaldense*. *Appl Environ Microbiol* 70:1040–1050
- Heyen U, Schüler D (2003) Growth and magnetosome formation by microaerophilic *Magnetospirillum* strains in an oxygen-controlled fermentor. *Appl Microbiol Biotechnol* 61:536–544
- Heywood BR, Bazylinski DA, Garratt-Reed AJ, Mann S, Frankel RB (1990) Controlled biosynthesis of greigite (Fe<sub>3</sub>S<sub>4</sub>) in magnetotactic bacteria. *Naturwissenschaften* 77:536–538
- Heywood BR, Mann S, Frankel RB (1991) Structure, morphology and growth of biogenic greigite (Fe<sub>3</sub>S<sub>4</sub>). In: Alpert M, Calvert P, Frankel RB, Rieke P, Tirrell D (eds) *Materials synthesis based on biological processes*. Materials Research Society, Pittsburgh, pp 93–108
- Jimenez-Lopez C, Romanek CS, Bazylinski DA (2010) Magnetite as a prokaryotic biomarker: a review. *J Geophys Res-Biogeosci* 115:G00G03
- Jogler C, Schüler D (2007) Genetic analysis of magnetosome biomineralization. In: Schüler D (ed) *Magneto-reception and magnetosomes in bacteria*. Springer, Heidelberg, pp 133–161
- Jogler C, Kube M, Schübbe S, Ullrich S, Teeling H, Bazylinski DA, Reinhardt R, Schüler D (2009a) Comparative analysis of magnetosome gene clusters in magnetotactic bacteria provides further evidence for horizontal gene transfer. *Environ Microbiol* 15:1267–1277
- Jogler C, Lin W, Meyerdieks A, Kube M, Katzmann E, Flies C, Pan Y, Amann R, Reinhardt R, Schüler D (2009b) Toward cloning of the magnetotactic metagenome: identification of magnetosome island gene clusters in uncultivated magnetotactic bacteria from different aquatic sediments. *Appl Environ Microbiol* 75:3972–3979
- Kawaguchi R, Burgess JG, Sakaguchi T, Takeyama H, Thornhill RH, Matsunaga T (1995) Phylogenetic analysis of a novel sulfate-reducing magnetic bacterium, RS-1, demonstrates its membership of the δ-Proteobacteria. *FEMS Microbiol Lett* 126:277–282

- Keim CN, Abreu F, Lins U, Lins de Barros HGP, Farina M (2004a) Cell organization and ultrastructure of a magnetotactic multicellular organism. *J Struct Biol* 145:254–262
- Keim CN, Martins JL, Abreu F, Rosado AS, Lins de Barros HGP, Borojevic R, Lins U, Farina M (2004b) Multicellular life cycle of magnetotactic multicellular prokaryotes. *FEMS Microbiol Lett* 240:203–208
- Keim CM, Lins U, Farina M (2009) Manganese in biogenic magnetite crystals from magnetotactic bacteria. *FEMS Microbiol Lett* 292:250–253
- Komeili A (2007) Cell biology of magnetosome formation. In: Schüler D (ed) *Magnetoreception and magnetosomes in bacteria*. Springer, Heidelberg, pp 163–174
- Komeili A, Vali H, Beveridge TJ, Newman DK (2004) Magnetosome vesicles are present before magnetite formation, and MamA is required for their activation. *Proc Natl Acad Sci USA* 101:3839–3844
- Komeili A, Li Z, Newman DK, Jensen GJ (2006) Magnetosomes are cell membrane invaginations organized by the actin-like protein MamK. *Science* 311:242–245
- Kopp RE, Kirschvink JL (2008) The identification and biogeochemical interpretation of fossil magnetotactic bacteria. *Earth Sci Rev* 86:42–61
- Kuhara M, Takeyama H, Tanaka T, Matsunaga T (2004) Magnetic cell separation using antibody binding with protein A expressed on bacterial magnetic particles. *Anal Chem* 76:6207–6213
- Lang C, Schüler D (2006) Biogenic nanoparticles: production, characterization, and application of bacterial magnetosomes. *J Phys Condens Mater* 18:S2815–S2828
- Lang C, Schüler D, Faivre D (2007) Synthesis of magnetite nanoparticles for bio- and nanotechnology: genetic engineering and biomimetics of bacterial magnetosomes. *Macromol Biosci* 7:144–151
- Lefèvre CT, Abreu F, Lins U, Bazylinski DA (2010a) Non-magnetotactic multicellular prokaryotes from low saline, nonmarine aquatic environments and their unusual negative phototactic behavior. *Appl Environ Microbiol* 76:3220–3227
- Lefèvre CT, Abreu F, Schmidt ML, Lins U, Frankel RB, Hedlund BP, Bazylinski DA (2010b) Moderately thermophilic magnetotactic bacteria from hot springs in Nevada USA. *Appl Environ Microbiol* 76:3740–3743
- Lefèvre CT, Vioria N, Pósfai M, Frankel RB, Bazylinski DA (2011) Novel magnetite-producing magnetotactic bacteria phylogenetically affiliated with the *Gammaproteobacteria* class. ISME J Submitted for publication
- Lins U, McCartney MR, Farina M, Buseck PR, Frankel RB (2005) Crystal habits and magnetic microstructures of magnetosomes in coccoid magnetotactic bacteria. *Appl Environ Microbiol* 71:4902–4905
- Lins U, Keim CN, Evans FF, Buseck PR, Farina M (2007) Magnetite (Fe<sub>3</sub>O<sub>4</sub>) and greigite (Fe<sub>3</sub>S<sub>4</sub>) crystals in multicellular magnetotactic prokaryotes. *Geomicrobiol J* 24:43–50
- Lipinska B, Fayet O, Baird L, Georgopoulos C (1989) Identification, characterization, and mapping of the *Escherichia coli* htrA gene, whose product is essential for bacterial growth only at elevated temperatures. *J Bacteriol* 171:1574–1584
- Lowenstam HA (1981) Minerals formed by organisms. *Science* 211:1126–1131
- Mahillon J, Chandler M (1998) Insertion sequences. *Microbiol Mol Biol Rev* 62:725–774
- Mahillon J, Leonard C, Chandler M (1999) IS elements as constituents of bacterial genomes. *Res Microbiol* 150:675–687
- Mann S, Frankel RB, Blakemore RP (1984a) Structure, morphology and crystal growth of bacterial magnetite. *Nature* 310:405–407
- Mann S, Moench TT, Williams RJP (1984b) A high resolution electron microscopic investigation of bacterial magnetite. Implications for crystal growth. *Proc R Soc Lond Ser B* 221:385–393
- Mann S, Sparks NHC, Blakemore RP (1987a) Ultrastructure and characterization of anisotropic inclusions in magnetotactic bacteria. *Proc R Soc Lond Ser B* 231:469–476
- Mann S, Sparks NHC, Blakemore RP (1987b) Structure, morphology and crystal growth of anisotropic magnetite crystals in magnetotactic bacteria. *Proc R Soc Lond Ser B* 231:477–487

- Mann S, Sparks NHC, Frankel RB, Bazylinski DA, Jannasch HW (1990) Biomineralization of ferrimagnetic greigite ( $\text{Fe}_3\text{S}_4$ ) and iron pyrite ( $\text{FeS}_2$ ) in a magnetotactic bacterium. *Nature* 343:258–260
- Maruyama K, Takeyama H, Nemoto E, Tanaka T, Yoda K, Matsunaga T (2004) Single nucleotide polymorphism detection in aldehyde dehydrogenase 2 (ALDH2) gene using bacterial magnetic particles based on dissociation curve analysis. *Biotechnol Bioeng* 87:687–694
- Matsunaga T (1991) Applications of bacterial magnets. *Trends Biotechnol* 9:91–95
- Matsunaga T, Arakaki A (2007) Molecular bioengineering of bacterial magnetic particles for biotechnological applications. In: Schüler D (ed) *Magnetoreception and magnetosomes in bacteria*. Springer, Heidelberg, pp 227–254
- Matsunaga T, Kamiya S (1987) Use of magnetic particles isolated from magnetotactic bacteria for enzyme immobilization. *Appl Microbiol Biotechnol* 26:328–332
- Matsunaga T, Takeyama H (1998) Biomagnetic nanoparticle formation and application. *Supramol Sci* 5:391–394
- Matsunaga T, Tadokoro F, Nakamura N (1990) Mass culture of magnetic bacteria and their application to flow type immunoassays. *IEEE Trans Magn* 26:1557–1559
- Matsunaga T, Higashi Y, Tsujimura N (1997) Drug delivery by magnetoliposomes containing bacterial magnetic particles. *Cell Eng* 2:7–11
- Matsunaga T, Sato R, Kamiya S, Tanaka T, Takeyama H (1999) Chemiluminescence enzyme immunoassay using protein A-bacterial magnetite complex. *J Magn Magn Mater* 194:126–131
- Matsunaga T, Togo H, Kikuchi T, Tanaka T (2000a) Production of luciferase-magnetic particle complex by recombinant *Magnetospirillum* sp. AMB-1. *Biotechnol Bioeng* 70:704–709
- Matsunaga T, Tsujimura N, Okamura Y, Takeyama H (2000b) Cloning and characterization of a gene, *mgsA*, encoding a protein associated with intracellular magnetic particles from *Magnetospirillum* sp. strain AMB-1. *Biochem Biophys Res Commun* 268:932–937
- Matsunaga T, Arakaki A, Takahoko M (2002) Preparation of luciferase-bacterial magnetic particle complex by artificial integration of MagA-luciferase fusion protein into the bacterial magnetic particle membrane. *Biotechnol Bioeng* 77:614–618
- Matsunaga T, Okamura Y, Fukuda Y, Wahyudi AT, Murase Y, Takeyama H (2005) Complete genome sequence of the facultative anaerobic magnetotactic bacterium *Magnetospirillum* sp. strain AMB-1. *DNA Res* 12:157–166
- McCartney MR, Lins U, Farina M, Buseck PR, Frankel RB (2001) Magnetic microstructure of bacterial magnetite by electron holography. *Eur J Mineral* 13:685–689
- McKay DS, Gibson EK Jr, Thomas-Keptra KL, Vali H, Romanek CS, Clemett SJ, Chillier XD, Maechling CR, Zare RN (1996) Search for past life on mars: possible relic biogenic activity in martian meteorite ALH84001. *Science* 273:924–930
- Meldrum FC, Heywood BR, Mann S, Frankel RB, Bazylinski DA (1993a) Electron microscopy study of magnetosomes in a cultured coccoid magnetotactic bacterium. *Proc R Soc Lond Ser B* 251:231–236
- Meldrum FC, Heywood BR, Mann S, Frankel RB, Bazylinski DA (1993b) Electron microscopy study of magnetosomes in two cultured vibrioid magnetotactic bacteria. *Proc R Soc Lond Ser B* 251:237–242
- Moench TT (1988) *Biliphococcus magnetotacticus* gen. nov. sp. nov., a motile, magnetic coccus. *Antonie van Leeuwenhoek* 54:483–496
- Moskowitz BM (1995) Biomineralization of magnetic minerals. *Rev Geophys Suppl* 33:123–128
- Moskowitz BM, Bazylinski DA, Egli R, Frankel RB, Edwards KJ (2008) Magnetic properties of marine magnetotactic bacteria in a seasonally stratified coastal pond (Salt Pond, MA, USA). *Geophys J Int* 174:75–92
- Nakamura N, Matsunaga T (1993) Highly sensitive detection of allergen using bacterial magnetic particles. *Anal Chim Acta* 281:585–589
- Nakamura N, Hashimoto K, Matsunaga T (1991) Immunoassay method for the determination of immunoglobulin G using bacterial magnetic particles. *Anal Chem* 63:268–272

- Nakamura N, Burgess JG, Yagiuda K, Kudo S, Sakaguchi T, Matsunaga T (1993) Detection and removal of *Escherichia coli* using fluorescein isothiocyanate conjugated monoclonal antibody immobilized on bacterial magnetic particles. *Anal Chem* 65:2036–2039
- Nakamura C, Burgess JG, Sode K, Matsunaga T (1995a) An iron-regulated gene, *magA*, encoding an iron transport protein of *Magnetospirillum* sp. strain AMB-1. *J Biol Chem* 270:28392–28396
- Nakamura C, Kikuchi T, Burgess JG, Matsunaga T (1995b) Iron-regulated expression and membrane localization of the MagA protein in *Magnetospirillum* sp. strain AMB-1. *J Biochem (Tokyo)* 118:23–27
- Nakayama H, Arakaki A, Maruyama K, Takeyama H, Matsunaga T (2003) Single-nucleotide polymorphism analysis using fluorescence resonance energy transfer between DNA-labeling fluorophore, fluorescein isothiocyanate, and DNA intercalator, POPO-3, on bacterial magnetic particles. *Biotechnol Bioeng* 84:96–102
- Nakazawa H, Arakaki A, Narita-Yamada S, Yashiro I, Jinno K, Aoki N, Tsuruyama A, Okamura Y, Tanikawa S, Fujita N, Takeyama H, Matsunaga T (2009) Whole genome sequence of *Desulfovibrio magneticus* strain RS-1 revealed common gene clusters in magnetotactic bacteria. *Genome Res* 19:1801–1808
- Okamura Y, Takeyama H, Matsunaga T (2001) A magnetosome-specific GTPase from the magnetic bacterium *Magnetospirillum magneticum* AMB-1. *J Biol Chem* 276:48183–48188
- Okuda Y, Fukumori Y (2001) Expression and characterization of a magnetosome-associated protein, TPR-containing Mam22, in *Escherichia coli*. *FEBS Lett* 491:169–173
- Okuda Y, Denda K, Fukumori Y (1996) Cloning and sequencing of a gene encoding a new member of the tetratricopeptide protein family from magnetosomes of *Magnetospirillum magnetotacticum*. *Gene* 171:99–102
- Ota H, Takeyama H, Nakayama H, Katoh T, Matsunaga T (2003) SNP detection in transforming growth factor-beta1 gene using bacterial magnetic particles. *Biosens Bioelectron* 18:683–687
- Palache C, Berman H, Frondel C (1944) Dana's system of mineralogy. Wiley, New York
- Pallen MJ, Wren BW (1997) The HtrA family of serine proteases. *Mol Microbiol* 26:209–221
- Paulsen IT, Park JH, Choi PS, Saier MH Jr (1997) A family of Gram-negative bacterial outer membrane factors that function in the export of proteins, carbohydrates, drugs and heavy metals from Gram-negative bacteria. *FEMS Microbiol Lett* 156:1–8
- Penninga I, deWaard H, Moskowicz BM, Bazylinski DA, Frankel RB (1995) Remanence curves for individual magnetotactic bacteria using a pulsed magnetic field. *J Magn Magn Mater* 149:279–286
- Ponting CC, Phillips C (1996) Rapsyn's knobs and holes: eight tetratricopeptide repeats. *Biochem J* 314:1053–1054
- Pósfai M, Buseck PR, Bazylinski DA, Frankel RB (1998a) Reaction sequence of iron sulfide minerals in bacteria and their use as biomarkers. *Science* 280:880–883
- Pósfai M, Buseck PR, Bazylinski DA, Frankel RB (1998b) Iron sulfides from magnetotactic bacteria: structure, composition, and phase transitions. *Am Mineral* 83:1469–1481
- Pósfai M, Cziner K, Márton E, Márton P, Buseck PR, Frankel RB, Bazylinski DA (2001) Crystal-size distributions and possible biogenic origin of Fe sulfides. *Eur J Mineral* 13:691–703
- Pradel N, Santini CL, Bernadac A, Fukumori Y, Wu LF (2006) Biogenesis of actin-like bacterial cytoskeletal filaments destined for positioning prokaryotic magnetic organelles. *Proc Natl Acad Sci U S A* 103:17485–17489
- Proksch RB, Moskowicz BM, Dahlberg ED, Schaeffer T, Bazylinski DA, Frankel RB (1995) Magnetic force microscopy of the submicron magnetic assembly in a magnetotactic bacterium. *Appl Phys Lett* 66:2582–2584
- Prozorov T, Mallapragada SK, Narasimhan B, Wang L, Palo P, Nilsen-Hamilton M, Williams TJ, Bazylinski DA, Prozorov R, Canfield PC (2007) Protein-mediated synthesis of uniform superparamagnetic magnetite nanocrystals. *Adv Funct Mater* 17:951–957
- Reiter WD, Palm P (1990) Identification and characterization of a defective SSV1 genome integrated into a tRNA gene in the archaeobacterium *Sulfolobus* sp. B12. *Mol Gen Genet* 221:65–71

- Richter M, Kube M, Bazylinski DA, Lombardot T, Reinhardt R, Glockner FO, Schüler D (2007) Comparative genome analysis of four magnetotactic bacteria reveals a complex set of group specific genes with putative functions in magnetosome biomineralization and magnetotaxis. *J Bacteriol* 189:4899–4910
- Rioux J-B, Philippe N, Pereira S, Pignol D, Wu L-F, Ginet N (2010) A second actin-like MamK protein in *Magnetospirillum magneticum* AMB-1 encoded outside the genomic magnetosome island. *PLoS One* 5:e9151
- Rodgers FG, Blakemore RP, Blakemore NA, Frankel RB, Bazylinski DA, Maratea D, Rodgers C (1990a) Intercellular structure in a many-celled magnetotactic prokaryote. *Arch Microbiol* 145:18–22
- Rodgers FG, Blakemore RP, Blakemore NA, Frankel RB, Bazylinski DA, Maratea D, Rodgers C (1990b) Intercellular junctions, motility and magnetosome structure in a multicellular magnetotactic prokaryote. In: Frankel RB, Blakemore RP (eds) *Iron biominerals*. Plenum, New York, pp 231–237
- Sakaguchi T, Burgess JG, Matsunaga T (1993) Magnetite formation by a sulphate-reducing bacterium. *Nature* 365:47–49
- Sakaguchi T, Arakaki A, Matsunaga T (2002) *Desulfovibrio magneticus* sp. nov., a novel sulfate-reducing bacterium that produces intracellular single-domain-sized magnetite particles. *Int J Syst Evol Microbiol* 52:215–221
- Scheffel A, Gruska M, Faivre D, Linaroudis A, Pitzko JM, Schüler D (2006) An acidic protein aligns magnetosomes along a filamentous structure in magnetotactic bacteria. *Nature* 440:110–114
- Scheffel A, Gärdes A, Grünberg K, Wanner G, Schüler D (2008) The major magnetosome proteins MamGFDC are not essential for magnetite biomineralization in *Magnetospirillum gryphiswaldense* but regulate the size of magnetosome crystals. *J Bacteriol* 190:377–386
- Schübbe S, Kube M, Scheffel A, Wawer C, Heyen U, Meyerdieks A, Madkour MH, Mayer F, Reinhardt R, Schüler D (2003) Characterization of a spontaneous nonmagnetic mutant of *Magnetospirillum gryphiswaldense* reveals a large deletion comprising a putative magnetosome island. *J Bacteriol* 185:5779–5790
- Schübbe S, Würdemann C, Peplies J, Heyen U, Wawer C, Glöckner FO, Schüler D (2006) Transcriptional organization and regulation of magnetosome operons in *Magnetospirillum gryphiswaldense*. *Appl Environ Microbiol* 72:5757–5765
- Schübbe S, Williams TJ, Xie G, Kiss HE, Brettin TS, Martinez D, Ross CA, Schüler D, Cox BL, Nealson KH, Bazylinski DA (2009) Complete genome sequence of the chemolithoautotrophic marine magnetotactic coccus strain MC-1. *Appl Environ Microbiol* 75:4835–4852
- Schüler D (2008) Genetics and cell biology of magnetosome formation in magnetotactic bacteria. *FEMS Microbiol Rev* 32:654–672
- Schüler D, Baeuerlein E (1997) Iron transport and magnetite crystal formation of the magnetic bacterium *Magnetospirillum gryphiswaldense*. *J Phys IV* 7:647–650
- Schüler D, Baeuerlein E (1998) Dynamics of iron uptake and Fe<sub>3</sub>O<sub>4</sub> mineralization during aerobic and microaerobic growth of *Magnetospirillum gryphiswaldense*. *J Bacteriol* 180:159–162
- Simmons SL, Edwards KJ (2007) Unexpected diversity in populations of the many-celled magnetotactic prokaryote. *Environ Microbiol* 9:206–215
- Simmons SL, Sievert SM, Frankel RB, Bazylinski DA, Edwards KJ (2004) Spatiotemporal distribution of marine magnetotactic bacteria in a seasonally stratified coastal salt pond. *Appl Environ Microbiol* 70:6230–6239
- Simmons SL, Bazylinski DA, Edwards KJ (2006) South seeking magnetotactic bacteria in the Northern Hemisphere. *Science* 311:371–374
- Sode K, Kudo S, Sakaguchi T, Nakamura N, Matsunaga T (1993) Application of bacterial magnetic particles for highly selective messenger-RNA recovery system. *Biotechnol Tech* 7:688–694
- Spring S, Amann R, Ludwig W, Schleifer KH, Vangemeren H, Petersen N (1993) Dominating role of an unusual magnetotactic bacterium in the microaerobic zone of a fresh-water sediment. *Appl Environ Microbiol* 59:2397–2403

- Spring S, Lins U, Amann R, Schleifer K-H, Ferreira LCS, Esquivel DMS, Farina M (1998) Phylogenetic affiliation and ultrastructure of uncultured magnetic bacteria with unusually large magnetosomes. *Arch Microbiol* 169:136–147
- Staniland S, Williams W, Telling N, Van Der Laan G, Harrison A, Ward B (2008) Controlled cobalt doping of magnetosomes *in vivo*. *Nat Nanotechnol* 3:158–162
- Tanaka T, Maruyama K, Yoda K, Nemoto E, Udagawa Y, Nakayama H, Takeyama H, Matsunaga T (2003) Development and evaluation of an automated workstation for single nucleotide polymorphism discrimination using bacterial magnetic particles. *Biosens Bioelectron* 19:325–330
- Tanaka M, Okamura Y, Arakaki A, Tanaka T, Takeyama H, Matsunaga T (2006) Origin of magnetosome membrane: proteomic analysis of magnetosome membrane and comparison with cytoplasmic membrane. *Proteomics* 6:5234–5247
- Thomas-Keptra KL, Bazylinski DA, Kirschvink JL, Clemett SJ, McKay DS, Wentworth SJ, Vali H, Gibson EK Jr, Romanek CS (2000) Elongated prismatic magnetite (Fe<sub>3</sub>O<sub>4</sub>) crystals in ALH84001 carbonate globules: potential Martian magnetofossils. *Geochim Cosmochim Acta* 64:4049–4081
- Thomas-Keptra KL, Clemett SJ, Bazylinski DA, Kirschvink JL, McKay DS, Wentworth SJ, Vali H, Gibson EK Jr, McKay MF, Romanek CS (2001) Truncated hexa-octahedral magnetite crystals in ALH84001: presumptive biosignatures. *Proc Natl Acad Sci USA* 98:2164–2169
- Thomas-Keptra KL, Clemett SJ, Bazylinski DA, Kirschvink JL, McKay DS, Wentworth SJ, Vali H, Gibson EK Jr, McKay MF, Romanek CS (2002) Magnetofossils from ancient Mars: a robust biosignature in the Martian meteorite ALH84001. *Appl Environ Microbiol* 68:3663–3672
- Thornhill RH, Burgess JG, Sakaguchi T, Matsunaga T (1994) A morphological classification of bacteria containing bullet-shaped magnetic particles. *FEMS Microbiol Lett* 115:169–176
- Towe KM, Moench TT (1981) Electron-optical characterization of bacterial magnetite. *Earth Planet Sci Lett* 52:213–220
- Ullrich S, Kube M, Schübbe M, Reinhardt R, Schüler D (2005) A hypervariable 130-kilobase genomic region of *Magnetospirillum gryphiswaldense* comprises a magnetosome island which undergoes frequent rearrangements during stationary growth. *J Bacteriol* 187:7176–7184
- Weiss BP, Kim SS, Kirschvink JL, Kopp RE, Sankaran M, Kobayashi A, Komeili A (2004) Magnetic tests magnetosome chains in Martian meteorite ALH84001. *Proc Natl Acad Sci USA* 101:8281–8284
- Wenter R, Wanner G, Schüler D, Overmann J (2009) Ultrastructure, tactic behaviour and potential for sulfate reduction of a novel multicellular magnetotactic prokaryote from North Sea sediments. *Environ Microbiol* 11:1493–1505
- Williams TJ, Zhang CL, Scott JH, Bazylinski DA (2006) Evidence for autotrophy via the reverse tricarboxylic acid cycle in the marine magnetotactic coccus strain MC-1. *Appl Environ Microbiol* 72:1322–1329
- Yoshino T, Matsunaga T (2005) Development of efficient expression system for protein display on bacterial magnetic particles. *Biochem Biophys Res Commun* 338:1678–1681
- Yoshino T, Matsunaga T (2006) Efficient and stable display of functional proteins on bacterial magnetic particles using Mms13 as a novel anchor molecule. *Appl Environ Microbiol* 72:465–471
- Yoshino T, Tanaka T, Takeyama H, Matsunaga T (2003) Single nucleotide polymorphism genotyping of aldehyde dehydrogenase 2 gene using a single bacterial magnetic particle. *Biosens Bioelectron* 18:661–666
- Yoza B, Matsumoto M, Matsunaga T (2002) DNA extraction using modified bacterial magnetic particles in the presence of amino silane compound. *J Biotechnol* 94:217–224
- Yoza B, Arakaki A, Maruyama K, Takeyama H, Matsunaga T (2003a) Fully automated DNA extraction from blood using magnetic particles modified with a hyperbranched polyamidoamine dendrimer. *J Biosci Bioeng* 95:21–26
- Yoza B, Arakaki A, Matsunaga T (2003b) DNA extraction using bacterial magnetic particles modified with hyperbranched polyamidoamine dendrimer. *J Biotechnol* 101:219–228



# Chapter 5

## Enzymatic Synthesis of Platinum Nanoparticles: Prokaryote and Eukaryote Systems

Chris Whiteley, Yageshni Govender, Tamsyn Riddin, and Mahendra Rai

### 5.1 Introduction

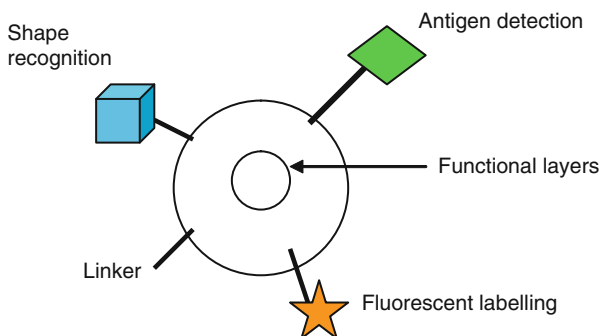
Nanobiotechnology is a multi-disciplinary field derived from the experimental use of nanoparticles (NPs) in biological systems (Penn et al. 2003; Salata 2004), including the sciences of biology, biochemistry, engineering, chemistry, physics and metallurgy. The unit nanometre derives its prefix *nano-* from the Greek word meaning “dwarf”, and since NPs, in the range of one to a few hundred nanometres, are found to have novel magnetic, electronic and optical properties dependent on their shape, size and composition (Mukherjee et al. 2002) they are set to demystify and revolutionise many biological processes and provide diagnostic and treatment options for previously untreatable diseases or ailments. NPs exist in a variety of forms, from nanowires to magnetic, noble and transition metals and non-metal water-soluble nanocrystals or quantum dots (QD’s), all of which are exceptionally versatile and highly stable. Their small size allows them to interact with proteins and pass through most of the cellular machinery unnoticed by the immune system as the larger protein acts as a shield from any immune response. NPs have the desirable ability to act as a “scaffold”, as they allow for the attachment of biomolecules (antibodies, peptides, DNA) through a number of methods including covalent and hydrogen bonding thereby extending their already exceptional versatility (Vinogradov et al. 2002) (Fig. 5.1). These interactions are surprisingly robust due to the increase in reactivity provided by the large surface-area-to-mass ratio of NPs (Aitken et al. 2004).

---

C. Whiteley (✉), Y. Govender, and T. Riddin  
Department of Biochemistry, Microbiology and Biotechnology, Rhodes University, P.O. Box 94,  
Grahamstown 6140, South Africa  
e-mail: C.Whiteley@ru.ac.za

M. Rai  
Department of Biotechnology, Sant Gadge Baba University, Amravati, Maharashtra, India

**Fig. 5.1** Typical conformations of NPs acting as a scaffold upon which other biomolecules, such as fluorescent signalling probes and peptides, can be attached (Adapted from Salata 2004)



Nanotechnology was thus referred to as the term for designing, characterisation, production and application of structures, devices and systems by controlling shape and size at the nanometre scale (Cao 2004). Rao et al. (2004) described nanoscience and nanotechnology as a field which focuses on (1) the development of synthetic methods and surface analytical tools for building structures and materials, (2) understanding the change in chemical and physical properties due to miniaturisation and (3) the use of such properties in the development of novel and functional materials and devices. Nanotechnology therefore offers exciting possibilities to study a state of matter, which is an intermediary between bulk and isolated atoms or molecules, and the effect of spatial confinement on electron behaviour, providing an opportunity to explore the problems related to surface or interface because of their interfacial nature (Zhang et al. 1994).

The “first” scientific study of nanoparticles took place in 1831, when Michael Faraday investigated the red ruby colloids of gold and made public that the colour was due to the small size of metal particles. For over 2,000 years, gold and silver have been used in glassware usually as nanocrystals, where they have been frequently used as colourants for church windows (Erhardt 2003). It was only in 1959 that Nobel laureate and physicist Richard Feynman used atoms and molecules for fabricating devices, though it was only later in 1974 that the term nanotechnology was derived. Norio Taniguchi, a researcher at the University of Tokyo, used this term while engineering materials at the nanometre level (Bhat 2003).

It is living cells that are the best examples of machinery that operate on the nanoscale, and currently there is no engineered mechanical, biological or chemical technology that matches the ability to perform at perfection levels seen in living cells. Living organisms are built of cells ( $\sim 10 \mu\text{m}$  in diameter) but the cell components are much smaller (usually in the sub-micron size domain). Proteins present in these cells have a typical size of 5 nm (Salata 2004), which can be compared to the smallest man made nanoparticle. This size comparison has led to the possible use of nanoparticles as probes, which would afford scientists the ability to identify and understand cellular machinery (Taton 2002).

## 5.2 Applications

A multitude of possible applications of metallic NPs exist, including single-electron transistors (SET's) (Bolotin et al. 2004), fuel cells (Waszczuk et al. 2001), fluorescent labelling of biological components (Ravnic et al. 2007), DNA/RNA detection via binding of DNA/RNA specific probes (Thaxton et al. 2005), as well as potential uses in biomedical diagnostic devices (Jain 2005), biosensors (Guo et al. 2007), nanocomputers (Mandal et al. 2005) and drug and gene transport systems (Panyam and Labhasetwar 2003).

Commercially, there has been major advancement in the use of nanomaterials for pharmaceutical applications, mainly for drug delivery (Salata 2004). Numerous companies have exploited the quantum size effects in semiconductor nanocrystals, which are used for various industrial applications such as tagging of biomolecules for the use of bio-conjugated gold nanoparticles for cellular labelling (Bhat 2003). Colloidal silver nanoparticles are currently being used in anti-microbial formulations and dressings (Mazzola 2003), whilst titanium nanoparticles have been used in filters for bactericidal purposes (Salata 2004). Nanomaterials have various applications and not surprisingly there are various techniques currently used to produce nanoparticles.

Platinum nanoparticles possess an unusual property which may be useful for manufacturing new substances and for the development of new materials. Researchers at the Japan Fine Ceramics Centre, Nagoya, Japan, discovered that platinum nanoparticles when heated to high temperatures fuse together with the material they coat, and using microscopy discovered that the platinum molecules actually “burrow” into the surface of zeolite they cover (Kato et al. 2004). These scientists suggested that this phenomenon could be used to produce tailored porous materials, thereby providing a number of applications in the ceramics industry. Other practical applications of platinum nanoparticles include their use in semiconductor chips, hydrogen storage in fuel cells and particle chemotherapy targeted against cancer cells (Salata 2004). The latest application of platinum nanoparticles is the advent of a new digital memory device, created by the incorporation of platinum nanoparticles into the tobacco mosaic virus to make a novel electronic memory element (Knez and Gösele 2006).

## 5.3 Properties

The unique properties of metal NPs are determined by their size and shape (Ahmad et al. 2003a, b). The optical properties of NPs are highly desirable due to the fact that they have “tunable” emission spectra, and can therefore be made to order for a number of applications such as fluorescent labelling, which require labels with narrow absorption wavelengths for multi-labelling experiments (Wu et al. 2005) (Fig. 5.2)

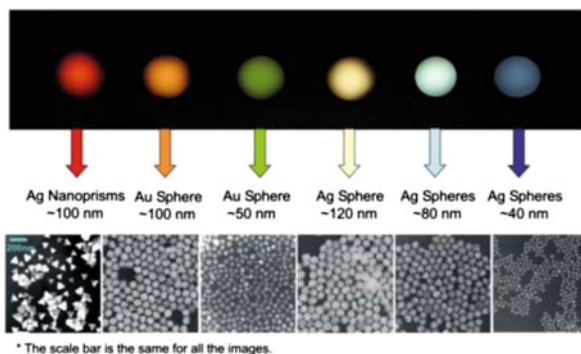


**Fig. 5.2** Rayleigh light scattering of nanocrystals: shape, size and composition matter. <http://www.chem.northwestern.edu/%7Emknggrp/BioNanomaterials2003rev1.htm>

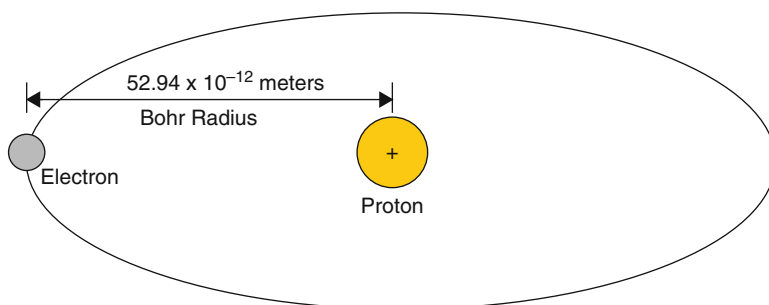


**Fig. 5.3** Bohr radius of hydrogen atom as described by Bohr (Adapted from Mills 2000)

The properties of NPs become most pronounced when the particles are physically smaller than the “exciton Bohr radius” of the compound which they are composed of (Beard et al. 2002). The “Bohr radius”, as explained by Niels Bohr, is the smallest and lowest energy level orbital for the single electron within a hydrogen atom. An “exciton” is an electron/hole pair in a hydrogen atom-like state with an electron (negative charge) and the hole (positive charge), which undergoes a Coulombic interaction and results in a bound entity. The “spatial distance” between the electron/hole pair is defined as the “exciton Bohr radius” of a particular compound (usually 1–5 nm). This nanoscale size results in “the quantum confinement effect”, where the exciton of the particle is confined to an area which is physically smaller than the exciton Bohr radius resulting in the unique properties possessed by these particles (Sun et al. 2001; Beard et al. 2002) (Fig. 5.3).

Every substance, irrespective of composition, exhibits different properties when their size is reduced to less than 100 nm. The electron structure of a nanocrystal critically depends on its size, since for small particles the electronic energy levels are discrete and non-continuous as in bulk materials. Laws relating to physical, chemical, biological, electrical, magnetic and other properties at the nanoscale are different from those applicable to macro matter. It is the laws of quantum

mechanics that apply at this scale (Bhat 2003) and result in one or more of the following changes:

1. Miniaturisation which is accompanied by a change in the physical properties
2. The bulk material behaviour is dominated by surface behaviour
3. Metals become harder, whilst ceramics become softer
4. Thin polymers become less permeable
5. The production of stronger, more heat resistant, transparent materials
6. An increased chemical resistance corresponding with reduced weight
7. The development of new electrical properties
8. Emergence of new biological properties

The optical, mechanical, electrical, magnetic and chemical properties can therefore be systematically manipulated by adjusting the size, shape and composition of nanoscale materials. Therefore, analytical tools and synthetic methods allow for the control, composition and design of this nanometre range, yielding important advances in almost all fields of science. A process through which the properties of these NPs can be controlled and manipulated may therefore prove to be revolutionary to many sciences (Sastry et al. 2003).

## 5.4 Safety Aspects of Nanoparticles

It is common knowledge that the properties of many common materials are significantly changed when reduced to a nanoscale size, as the overall increase in the particle surface area results in increased reactivity with their environment. The small size of NPs endows them with the ability to overcome the mammalian immune system and easily enter any biological system via inhalation and digestion and pass through the blood–brain barrier. Despite these unique properties, it is unsettling to note that very little research is being done on the possible implications that NPs may have on the environment and human health (Gwinn and Vallyathan 2006). The advantages of NPs in medicine, biochemistry and nanotechnology are widely documented (Bruchez et al. 1998; Akerman et al. 2002; Cao et al. 2002; Georganopoulou et al. 2005). As the current knowledge surrounding NP toxicity is highly limited, however, a wise course of action would be to minimise the exposure of biological systems to NPs until data supporting their safety is determined (Oberdörster et al. 2000; Kubik et al. 2005).

## 5.5 Synthetic Methods for Metal Nanoparticles

Tremendous growth in the nanotechnology field is due to the availability of new methods for the synthesis of nanomaterials, including various organic, inorganic and biological systems (Bhattacharya and Gupta 2005), as well as improved tools

for characterisation and manipulation. Innovative applications of nanoparticles and nanomaterials are rapidly emerging, and hence the synthesis of nanoparticles and their self-assembly may be regarded as the cornerstone of this type of nanotechnology (Gardea-Torresdey et al. 2002). Although solution-based chemical methods have been the building blocks for nanoparticle synthesis, there has been an increase in focus to develop green chemistry or eco-friendly methods for nanomaterials synthesis (Sastry et al. 2004; Bhattacharya and Gupta 2005). Since nanomaterials are abundant in nature as living organisms operate basically at a nanoscale level, the nanoparticles are viewed as fundamental building blocks of nanotechnology and are the starting point for the preparation of various nanostructured materials and devices (Senapati et al. 2005).

Nanoparticles can be produced using two techniques, (1) the top-down approach or (2) the bottom-up approach. The top-down approach refers to the breakdown of larger structures by use of ultra fine grinders, lasers and vaporisation followed by cooling (Senapati et al. 2005). The bottom-up approach allows for the rearrangement of these molecules to form complex structures with new and useful properties. For the top-down approach, the main challenge is the creation of increasingly small structures with sufficient accuracy, as compared to the bottom-up approach, where the main challenge lies in making the structure large enough and of adequate quality to be useful as a nanomaterial (Fendler 1998). The bottom-up approach supports a better opportunity to obtain nanostructures with fewer defects and with more homogeneous chemical composition. An initial hurdle in NP synthesis, however, was in the fact that the top-down approach could not be used due to the laws of quantum mechanics and the effects of quantum confinement on the particle's electrons. Hence, a new "bottom-up" developmental approach was referred in which the NPs are "built up", atom by atom by self-organisation or self-assembly (Seeman and Belcher 2002; La Van et al. 2003; Senapati et al. 2005).

### **5.5.1 Chemical**

Chemical methods are complicated, outdated, costly, inefficient and produce hazardous waste which pose a sizeable risk to the environment and human health (Gamez et al. 2003). A further disadvantage of these methods is due to the fact that the shape of the NPs produced is generally limited to spheres, which in turn greatly limits their potential properties.

#### **5.5.1.1 Ion Exchange**

Ion exchange resins are currently employed in the production of nickel NPs varying from 3 to 5 nm (Gamez et al. 2003). The nickel ions are initially adsorbed onto a polyimide surface and then become reduced to nickel NPs via hydrogen reduction (Akamatsu et al. 2003).

### 5.5.1.2 The Sol Process

In this approach, the reagents (metal ion solutions) are rapidly added into a reaction vessel containing a hot co-ordinating solvent such as alkyl phosphate, pyridine and alkylamine furan (Qu et al. 2001). This quick addition of reagents to the reaction vessel increases the precursor concentration, with the solution becoming supersaturated due to the high chemical reaction temperatures. As a result, a short nucleation burst occurs and the concentration of the metal species in solution drops below the critical point of nucleation (Peng and Peng 2001). This method produces a nanocluster growth of metal species, and if this period of growth during the nucleation time is short enough, nanoclusters maybe uniform and mono-dispersed (Qu et al. 2001). There are a number of reports in the literature on nanoparticle synthesis utilizing this method, with a wide range of nanoparticles been successfully synthesised such as CdSe (Qu et al. 2001), CdS (Qu et al. 2004), ZnO (Shim and Guyot-Sionnest 2001), bimetallic clusters such as CdSe/ZnS (Talapin et al. 2001), CdSe/CdS (Chen et al. 2003) and CdSe nanorods (Peng et al. 2002).

### 5.5.1.3 Precipitation

During this process, organic molecules are utilised to control the release of the reagents and metal ions in solution during the precipitation process (Senapati et al. 2005). By engineering the factors, such as reactant concentration, pH and temperature, successful syntheses of CdTe (Gao et al. 1998), HgTe (Rogach et al. 1999), CdS/HgS/CdS (Braun et al. 2001) and CdS/(HgS)<sub>2</sub>/CdS (Harrison et al. 2000) nanoparticles have been produced.

### 5.5.1.4 Pyrolysis

Pyrolysis has been used to prepare various kinds of nanoparticles including metals, metal oxides, semiconductors and composite materials. Generally, the pyrolytic synthesis of compounds leads to powder with a size distribution in the micrometer range, though to get uniform nanosized material, revisions of the procedure need to be changed such as slowing of the reaction or decomposition in an inert solution (Senapati et al. 2005).

### 5.5.1.5 Micelles

A variety of nanoparticles such as Pt, Rh, Pd and Ir have been synthesised using this process of reversed micelles (Sangregorio et al. 1996) with reducing agents such as NaBH<sub>4</sub>, N<sub>2</sub>H<sub>4</sub> and H<sub>2</sub> being used (Ingelsten et al. 2001). The water content of the micelles seems to greatly affect the shape of nanoparticles and nanowires of BaCO<sub>3</sub> and BaSO<sub>4</sub> have been synthesised (Qi et al. 1997).

## 5.5.2 *Biological*

Biological routes involving prokaryote/eukaryote systems provide great advantages over traditional methods, as they have the potential to be a cost efficient, simple, environmentally friendly and an efficient form of metal NP synthesis, which could produce NPs that are superior in quality and value. The primary advantage of a biological route is the ability to manipulate the properties of the NPs by gaining control over the mechanism that determines their size and shape (Mukherjee et al. 2002; Ahmad et al. 2003a, b).

Both prokaryotic and eukaryotic organisms including bacteria, fungi, actinomycetes and yeasts synthesise biogenic geometric metal particles, in the nanometre range via a bioreductive process, when exposed to metal chloride solutions (Ahmad et al. 2003a, b; Sastry et al. 2003; Mukherjee et al. 2003; Riddin et al. 2006, 2009; Ingle et al. 2008, 2009; Govender et al. 2009, 2010; Rai et al. 2008, 2009a, b; Gade et al. 2008; Birla et al. 2009). This bioreduction of metal particles occurred via an active and/or passive process. In either case, the process is part of an organism's enzymatic survival mechanism, as a build up of metal ions within a biological system is regarded as being toxic (Ibrahim et al. 2001; Duran et al. 2005).

### 5.5.2.1 **Metallothioneins (Metal Binding Peptides)**

Synthesis of nanoparticles by this process maybe regarded as a passive one and involves the interaction of the positively charged metal ions with the negative sulfhydryl groups on the cysteine residues or imidazole rings on histidine residues of metallothioneins (metal binding peptides) (Fig. 5.4). The location of the cysteine/histidine residues may potentially be involved in a template-like aggregation of the metal particles resulting in the geometric shapes observed (i.e., Fig. 5.2). Mercury is toxic as it binds to, and inactivates, essential thiols which are a part of enzymes and proteins. Bacteria contain a set of genes which forms an Hg (II) resistance operon which detoxifies and removes Hg (II) (Ji and Silver 1995; Ehrlich 1997). This set of genes also encodes the production of a periplasmic binding protein and membrane associated transport system, which collects Hg (II) from the surrounding environment and transports it to the cytoplasm for detoxification (Misra 1992).

### 5.5.2.2 **Hydrogenase/Reductase Enzymes**

Hydrogen plays an important role in the metabolism of microorganisms, where the reaction is catalysed by metalloenzymes known as hydrogenases (Armstrong 2004). These hydrogenase enzymes are found in a variety of organisms ranging from aerobes to anaerobes, autotrophs to heterotrophs, prokaryotes to eukaryotes, fermentative organisms and sulfate reducers and differ in molecular weight,



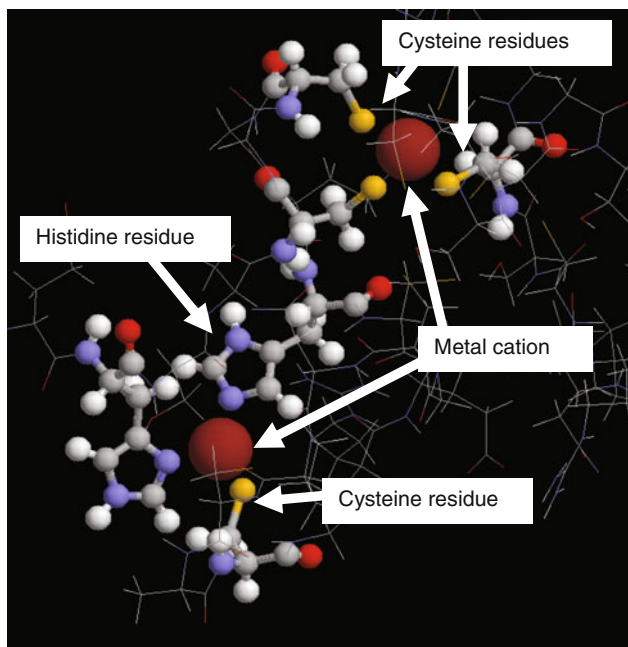


**Fig. 5.4** Passive Process. Metal cations interact with anionic sulfhydryl groups on cysteine residues and/or imidazole rings of histidine residues of metallothioneins

quaternary structure, active site orientation and specificity with respect to the type of electron carriers (Zadvorny et al. 2004). The first hydrogenase was described in 1931 as a bacterial enzyme that catalysed the reversible oxidation of hydrogen to protons and electrons according to reaction 1 (Stephenson and Stickland 1931).

The catalytic processes of hydrogenases involve the following steps:

1. Activation or production of hydrogen at the active centre
2. Transfer of two electrons between the active site and the redox partner of the hydrogenase
3. Transfer of two hydrogen atoms between the active centre and the medium solvent (De Lacy et al. 2000)

Most, if not all, hydrogenases can catalyse the reaction in either direction *in vitro*, though *in vivo* they are usually committed to catalyse either hydrogen uptake or evolution depending on the demands of the host organism (Vignais et al. 2001).

### The NiFe Hydrogenase

The Ni–Fe hydrogenases are heterodimeric proteins that are found in the periplasm and cytoplasm (Nicolet et al. 2000) and consist of small (S) [28 kDa] and large (L)

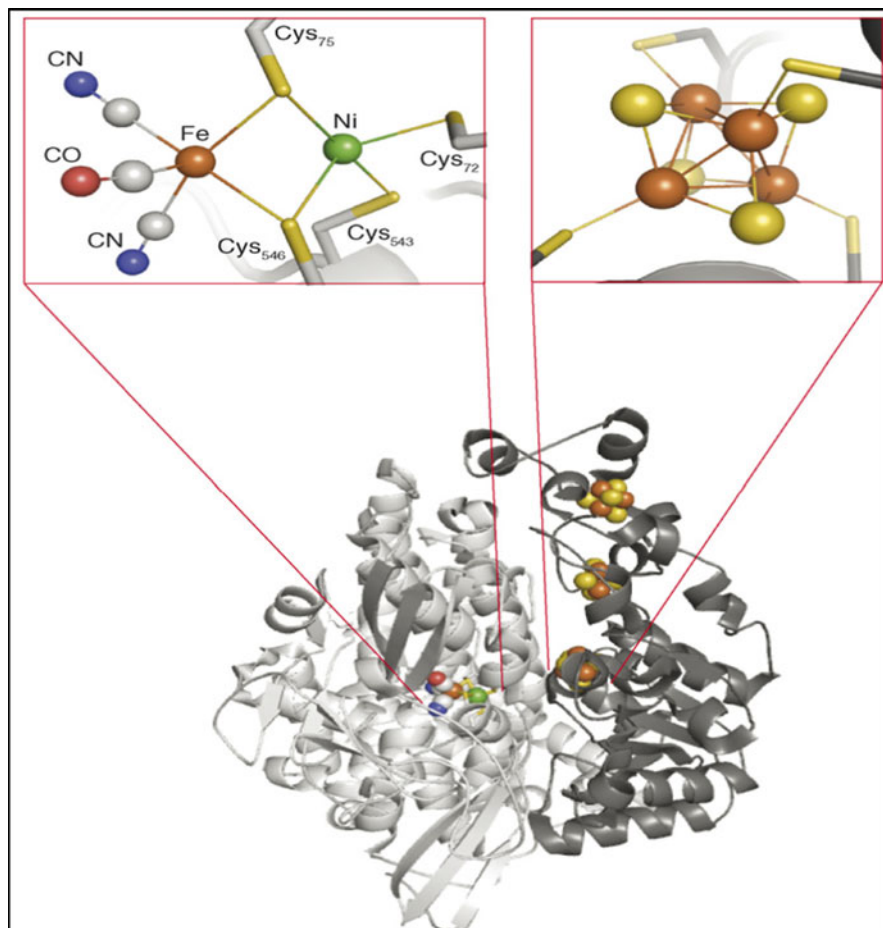


**Fig. 5.5** The structures of the readily oxidised form of the [NiFe] hydrogenase from *Desulfovibrio fructosovorans*, the dinuclear cluster of the active site in the large subunit, and one of the Fe–S clusters in the small subunit are shown. The large subunits are depicted as *light grey ribbons* and the small subunits are *dark grey ribbons*. The colour scheme is as follows: iron, orange; nickel, green; sulphur, yellow; oxygen, red; and nitrogen, blue. Figure adapted from Leach and Zamble (2007)

[60 kDa] subunits with the small subunit containing three iron–sulfur clusters while the large subunit contained a nickel–iron centre (Fig. 5.5). These enzymes, when isolated, are found to catalyse both  $H_2$  evolution and uptake, with low-potential multiheme cytochromes such as cytochrome  $c_3$  acting as either electron donors or acceptors, depending on their oxidation state. Ni–Fe hydrogenases have low specific activities and have been shown to function in the oxidation of hydrogen. This class of hydrogenases is found predominantly in all *Desulfovibrio* sp. thus much research has been done on this type of enzyme from *D. gigas* (Albracht 1994). X-ray structure studies revealed that the active site, located in the large subunit near

the interface with the small subunit, consisted of a binuclear NiFe centre along with the existence of hydrophobic channels that connect the molecular surface of the enzyme with the active site (Fig. 5.5). There is still some great controversy on whether the splitting of the hydrogen occurs on the nickel or iron atom (De Lacy et al. 2000).

The ability of NiFe hydrogenase from *Desulfovibrio fructosovorans* to reduce technetium (VII) (De Luca et al. 2001) has been demonstrated previously and the mechanisms of enzymatic reduction of metal ions by chemotrophic bacteria have been proposed (Lovely et al. 1993; Lloyd et al. 2000; Lloyd 2003).

### Fe-hydrogenases [Fe-hases]

There are currently two recognized families:

1. The cytoplasmic, soluble, monomeric Fe-hases found in strict anaerobes such as *Clostridium pasteurianum* and *Megaspaera elsdenii* that are extremely sensitive to inactivation by O<sub>2</sub> and catalyses both H<sub>2</sub> evolution and uptake. They are also found in the chloroplast of green alga *Scenedesmus obliquus*, and they catalyse H<sub>2</sub> evolution.
2. The periplasmic, heterodimeric Fe-hases from *Desulfovibrio sp.* These Fe-hases can be purified aerobically and catalyse mainly H<sub>2</sub> oxidation.

Fe-hases generally contain two [4Fe–4S] clusters in a ferredoxin-like domain and have high specific activities and function to evolve hydrogen. Studies on the *Desulfovibrio desulfuricans* Fe-hases have shown that it is a periplasmic protein made of two different subunits of molecular masses 43 and 10 kDa (Fig. 5.6)

The involvement of reductase/hydrogenase enzymes, possibly in conjunction with an electron shuttling compound such as quinones or cytochrome c<sub>3</sub>, where the metal ions function as electron acceptors thereby becoming reduced to neutral metal species can be regarded, generally, as an active process (Lloyd et al. 2001; Payne et al. 2002; Rashamuse and Whiteley 2007; Govender et al. 2009, 2010) (Fig. 5.7) and is thought to be due to its low redox potentials (Michel et al. 2001; Chardin et al. 2003), although the complete enzymatic mechanism has not yet been fully elucidated. The neutral particles precipitate out of solution and accumulate by nucleation and/or bioaccumulation either on the cell wall/membrane or extracellularly (Carpentier et al. 2003).

As previously mentioned, the enzymatic conversion of toxic metal ions to less toxic metal species via redox reactions is expected to be part of a microbial survival mechanism. It is only in relatively recent years that scientists have turned towards bacteria as possible eco-friendly nanofactories. Gold nanoparticles of nanoscale dimensions can be readily precipitated within bacterial cells during incubation with Au<sup>3+</sup> (Southam and Beveridge 1996; Bhattacharya and Gupta 2005). It has also been demonstrated that the metal-resistant bacterium *Pseudomonas stutzeri* AG259 (isolated from a silver mine) formed silver nanoparticles with well-defined size (ranging from a 3 to 200 nm) and distinct morphology when challenged

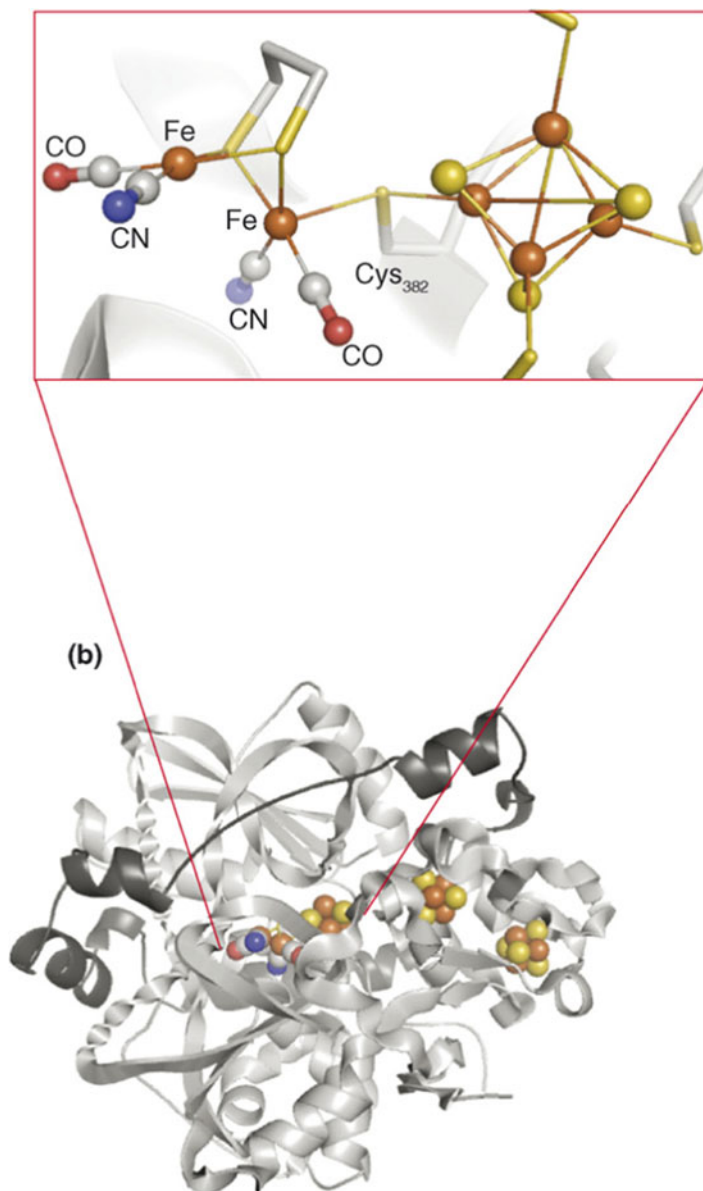


**Fig. 5.6** The structure of the [Fe-only] hydrogenase from *Desulfovibrio desulfuricans* is shown as well as the H cluster. The large subunits are depicted as *light grey ribbons* and the small subunits are *dark grey ribbons*. The colour scheme is as follows: iron, orange; nickel, green; sulphur, yellow; oxygen, red; and nitrogen, blue. Figure adapted from Leach and Zamble (2007)

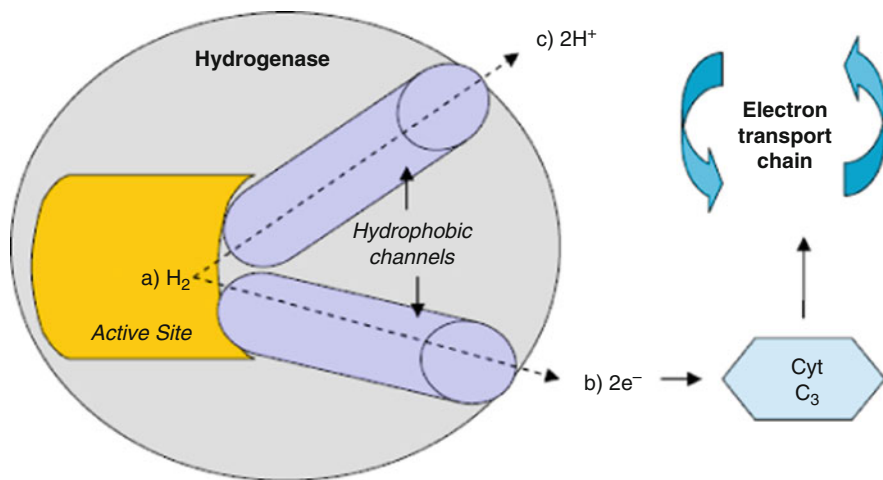


**Fig. 5.7** Diagrammatic representation of hydrogen activation by hydrogenase (Adapted from De Lacy et al. 2000)

with concentrated  $\text{AgNO}_3$  (Klaus-Joerger et al. 2001). Nair and Pradeep (2002) demonstrated that *Lactobacillus*, present in buttermilk, produced nanoparticles when exposed to gold and silver ions, resulting in the production of nanoparticles within the bacterial cell. They also concluded that the nucleation of these nanoparticles occurred on the cell surface through sugars and enzymes in the cell wall, following which the metal nuclei are transported into the cell where they aggregate and grow to larger-sized particles. Holmes and co-workers (1995) demonstrated that exposure of *Klebsiella aerogenes* to  $\text{Cd}^{2+}$  ions resulted in the formation of CdS nanoparticles in the nanometre range 20–200 nm. In an extension of the bacteria-based methodology for the growth of nanoparticles, the thermophilic iron-reducing *Thermo-anaerobacter ethanolicus* was shown to convert metals (Co, Cr, Ni) into magnetic octahedral-shaped nanoparticles (Roh et al. 2001).

A copper reducing enzyme, copper reductase catalyses Cu (II) reduction to Cu (I) with NADH or NADPH as the electron donor (Wakatsuki et al. 1991; Gadd 1993). That study showed the location of Cu reductase to be in the cell wall and the process to have a role in the regulation of Cu uptake (Wakatsuki et al. 1991). Examples of hydrogenase metal reduction include a number of chemotrophic bacteria, which are capable of reducing a variety of heavy metal ions, such as U(VI) (Payne et al. 2002), Cr(VI) (Michel et al. 2001), Fe(III) (Loujou et al. 1998) and Tc(VII) (Lloyd and Macaskie 1996) while some phototrophic bacteria have been shown to be able to reduce Ni(II), Pt(IV) and Pd(II) (Zadvorny et al. 2004, 2006), all via hydrogenase action with an electron donor.

In addition to the prokaryotic system there are a number of eukaryotes that are capable of metal reduction, often via hydrogenase action. Riddin and colleagues (2006) demonstrated that an extracellular protein solution from a *Fusarium*

*oxysporum* fungal strain was effective in producing biogenic Pt(0) NPs from the bioreduction of Pt(IV). They proposed that a hydrogenase enzyme was responsible and that the reduction mechanism occurred via a two-cycle process involving Pt(II) as the intermediate. Later work (Govender et al. 2009) confirmed the presence of a periplasmic hydrogenase enzyme in this *F. oxysporum* strain that possessed Pt(IV) reductase activity. Fungal species, when exposed to metal salts, produced nanoparticles extracellularly. *Thermospora* sp. (Ahmad et al. 2003a, b), and *Tricothecium* sp. (Ahmad et al. 2005) reduced AuCl<sub>4</sub> producing Au nanoparticles extracellularly, and *Aspergillus fumigatus* reduced AgNO<sub>3</sub> to Ag nanoparticles (Bhainsa and D'Souza 2006). Dameron and co-workers (1989) were the first to demonstrate that the yeasts such as *Schizosaccharomyces pombe* and *Candida glabrata* were capable of intracellular production of CdS nanoparticles when challenged with cadmium salt in solution. The use of fungi in the synthesis of nanoparticles is a relatively recent addition to the list of microbes. One of the novel works defining the use of fungi for nanoparticle synthesis was carried out by Mukherjee and colleagues for production of silver nanoparticles using *Verticillium* (Mukherjee et al. 2001) and gold (Mukherjee et al. 2002). Other fungal reductions of metals include the reduction of tellurite to elemental tellurium (Smith 1974; Gadd 1993), selenate to selenium, with site of deposition on the fungal cell walls and membranes (Konetzka 1977).

Whilst various studies have been initiated on identification of microorganisms as possible nanofactories, very little work has been conducted on the actual mechanisms of nanoparticle formation. Enzymatic transformation of metal salts to produce nanoparticles appears to be more superior over other processes, although it has its limitations. The fact that enzymes work best at specific optimum conditions is one major problem associated with the use of this technique since metal salts at different pH and temperature tend to inhibit the activity of the redox enzyme. Another controlling factor for these enzymes, including the hydrogenases, is the electrochemical potential that reflects the ability of reducing or oxidising equivalents (Elliot et al. 2002). One of the initial findings was that exposure of *F. oxysporum* to aqueous CdSO<sub>4</sub> solution yielded quantum CdS dots (Ahmad et al. 2002), with results indicating that a NADH-dependant enzyme was responsible. Hydrogen peroxide (H<sub>2</sub>O<sub>2</sub>) generated during the biocatalytic oxidation of substrates in the presence of molecular oxygen by oxidase enzymes has been shown to reduce AuCl<sub>4</sub> producing Au nanoparticles (Willner et al. 2006). Various redox reactions utilise the different oxidised and reduced nicotinamide adenine dinucleotide (phosphate) (NAD(P)<sup>+</sup>/NAD(P)H) cofactor systems to synthesise Au nanoparticles by the reduction of AuCl<sub>4</sub> (Xiao et al. 2004). Currently, only a nitrate reductase has been identified to be directly responsible for the biosynthesis of silver nanoparticles (Mukherjee et al. 2002) but no mechanism has been elucidated for platinum nanoparticle formation in *F. oxysporum*.

A number of possible options exist which may explain the process of metal reduction in these organisms. Durán and colleagues (2005) described a hypothesis with supporting experimental data of the mechanistic action of extracellular silver and gold NP formation by the fungus *F. oxysporum*. They suggested that

a nitrate-dependant reductase in conjunction with an extracellular electron shuttle process involving quinones was responsible for the extracellular formation of noble metal NPs. These workers supported earlier findings by Mukherjee et al. (2002) by performing screening experiments on three *F. oxysporum* fungi and a single *F. moniliforme* strain for both gold and silver NP formation. They found that all *F. oxysporum* strains screened resulted in the formation of Ag and Au NPs at an extracellular level, while the *F. moniliforme* strain did not result in any NP formation either intracellularly or extracellularly. Duran and co-workers went on to explain that both *Fusarium* fungi contained similar reductase enzymes, thought to be significant in ferric iron ( $\text{Fe}^{3+}$ ) reduction. One specific reductase, unique to *F. oxysporum*, was involved in the reduction of Ag(I) and/or Au(I) to Ag(0) and/or Au(0), respectively. Furthermore, they stated that naphthaquinones, anthraquinones and their derivatives were acting as potential electron shuttle systems since naphthaquinones were present in both *Fusarium* fungi, while anthraquinones were only found in *F. oxysporum* strains. From this they hypothesised that noble metal ion reduction occurs by the joint action of anthraquinones and the reductase enzyme found to be unique to *F. oxysporum* strains (Fig. 5.8).

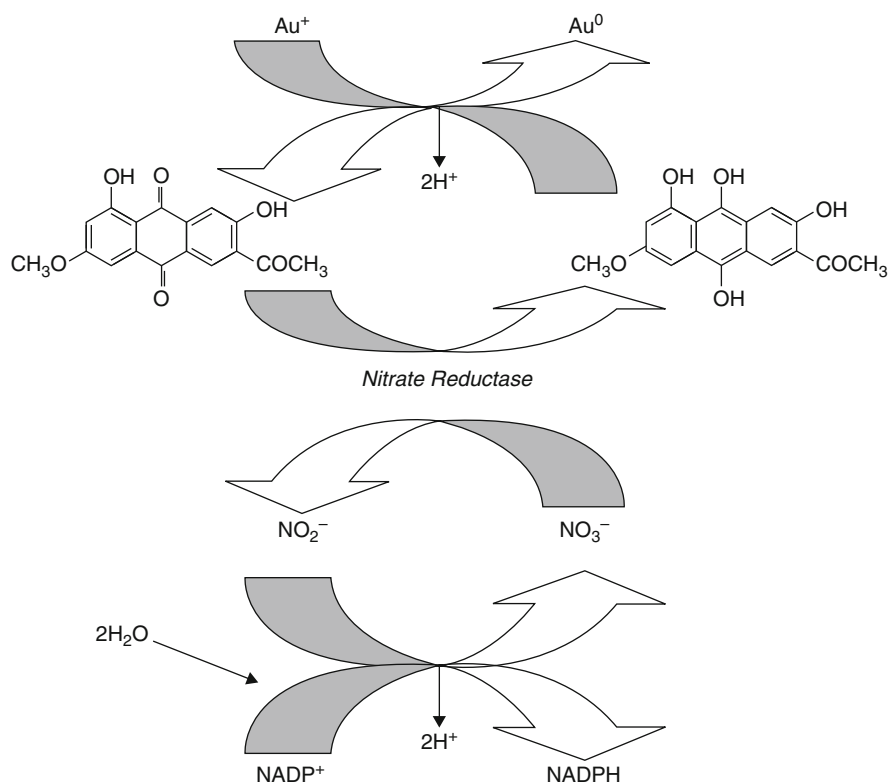


**Fig. 5.8** Hypothesised mechanism adapted from Duran et al. 2005 for the extracellular formation of silver and gold NPs by three *F. oxysporum* fungi

Literature illustrates that enzymes are known to play a role in metal transformations; however, the role of enzymes in nanoparticle formation is a relatively new and developing field of study.

## 5.6 Analysis of Platinum Nanoparticles

### 5.6.1 Quantitative

The reduction of platinum can be routinely monitored by visual inspection and UV spectroscopy at 230 nm [Pt(II)] and 261 nm [Pt(IV)] and measuring their concentration by means of respective standard curve. These absorbance values correlated well to values found in literature for Pt(II) (225 nm) (Heinglein and Giersig 2000) and Pt(IV) (261 nm) (Liu et al. 2004).

### 5.6.2 Qualitative

#### 5.6.2.1 Transmission Electron Microscopy

The deposits of platinum nanoparticles can be observed as described (Ngwenya and Whiteley 2006). Typically, a sample was fixed overnight in a 2.5% glutaraldehyde solution in sodium phosphate buffer (0.1 M, pH 7.0). The glutaraldehyde solution was decanted and the pellet washed ( $2 \times 10$  min) with cold sodium phosphate buffer (0.1 M, pH 7.0). The secondary staining step with 1% OsO<sub>4</sub> was not included due to possible interference by this heavy metal. The samples were then dehydrated by a series of successive ethanol concentrations (30, 50, 70, 80, 90%) with two changes of absolute ethanol (100%) at 15 min per ethanol concentration. Infiltration of the cells was performed by washing twice in propylene oxide for 15 min. The cells were then subjected to a series of increasing resin (Araldite):propylene oxide concentrations (25:75%, 50:50% and 75:25%; 60 min per step). The final infiltration step occurred in pure resin (100%) and was left overnight. After infiltration in pure resin, the pellet samples were transferred to capsule mats containing pure resin in individual moulds for each sample. The capsule mat was allowed to polymerise (36 h, 60°C) in an oven. Sections (100 nm) were cut using an ultramicrotome and placed on a carbon-coated copper grid and analysed with a JEOL JEM-1210 electron microscope at an operating electron voltage of between 80 and 90 kV.

Digital pictures of the samples were collected using the MegaView (Soft Imaging System) with analySIS Image Processing Software.



### 5.6.2.2 Energy Dispersive X-Ray (EDAX)

The presence of platinum can be confirmed from the EDAX spectra obtained from the EDAX-DX-4 energy dispersive X-ray system [Ngwenya and Whiteley 2006] using a TESCAN VEGA (LMU) SEM with INCAPentaFETX3 (Oxford Instruments) EDAX attachment operating at 20 kV. Samples should be collected in 1.5-ml micro-centrifuge tubes, pelleted by centrifugation ( $13,000 \times g$ , 2 min, 20°C), the supernatant discarded and the cell pellet removed and spread thinly onto a carbon strip attached to a brass SEM support and air-dried in a Heraeus laboratory oven at 60°C overnight. The SEM-EDAX can be calibrated by quantoptimisation with a copper (Cu) standard under standard operating conditions.

### 5.6.2.3 Visual Inspection

Formation of platinum nanoparticles can be monitored by visual inspection of the samples when the colour changes from yellow to brown to black (Liu et al. 2004; Huang et al. 2004).

## 5.7 Synthesis of Platinum Nanoparticles

### 5.7.1 Prokaryotes: Sulfate-Reducing Bacteria

Though many studies have synthesised platinum nanoparticles using chemical methods (Peng and Peng 2001; Qu et al. 2001; Liu et al. 2007; Shukla et al. 2007), the formation of these nanoparticles by biological methods has not been fully investigated. In 2006, Lengke and colleagues synthesised spherical platinum nanoparticles within bacterial cells of the filamentous cyanobacterium *Plectonema boryanum* UTEX 485 (Lengke et al. 2006) and Konishi et al. (2007) synthesised biogenic platinum nanoparticles using the bacterium *Shewanella algae*.

Sulfate-reducing bacteria (SRB) have been cited in the literature as excellent models for metal bioremediation. Metals maybe removed from a salt solution by metal-hydrogenase activity, where the metal ion becomes reduced to a lower, often less toxic oxidation state, due to the catalytic action of the redox, hydrogenase enzymes (Lloyd et al. 1998; Rashamuse and Whiteley 2007; Govender et al. 2009, 2010). It is well documented that SRB contain a variety of hydrogenase enzymes both cytoplasmic and periplasmic, either free or membrane bound capable of hydrogen uptake or hydrogen evolution (Postgate 1965; De Lacy et al. 2000). Despite their prior classification as strict anaerobes, extensive research has shown that a number of species, particularly that of *Desulfovibrio*, are highly tolerant to oxygen. Fournier and coworkers (Fournier et al. 2004) demonstrated that, in SRB cells, the activity of the periplasmic hydrogenase was increased significantly in the

presence of oxygen and suggested the involvement of superoxide dismutase (SOD) and/or superoxide reductase (SOR) as a protective mechanism against oxidative stress of this typically oxygen-sensitive enzyme. The cytoplasmic hydrogenase, on the other hand, was responsible for the evolution of hydrogen under anaerobic environments (Das et al. 2006). Furthermore, the reduction of a number of metals by a periplasmic hydrogenase was completely inhibited in SRB cells pre-treated with Cu(II) (Lloyd et al. 1999; De Luca et al. 2001). Cytoplasmic hydrogenases, on the other hand, are unaffected by Cu(II) (Lloyd et al. 1999) and so Whiteley's group (Riddin et al. 2009) proposed, with experimental evidence, a two-step enzymatic process for the bioreduction of Pt(IV) to Pt(0). First, Pt(IV) ion was reduced in the cytoplasm, by a cytoplasmic hydrogenase redox system to Pt(II) whence it diffused to the periplasm to become reduced to Pt(0) by one or more of the periplasmic hydrogenases. Furthermore, Whiteley's group (Riddin et al. 2009) examined the bioreduction of the Pt(II) ions by SRB cells and established that it was much slower than that of Pt(IV) implying that the mechanism of their reduction was different supporting an argument that the reduction of Pt(II) occurred due to the action of a different enzyme than the reduction of Pt(IV). Qualitatively, the samples containing cells pre-treated with Cu(II) exhibited a fairly insignificant colour change from light yellow to brown indicating, once again, that the Pt(0) formation had been affected. Furthermore, their results suggested that the Pt(IV) ion was completely reduced before reduction of the Pt(II) ion will begin. An active enzymatic process, involving a periplasmic hydrogenase, was responsible for step 2 of this mechanism [i.e., Pt(II)  $\rightarrow$  Pt(0)] (Fig. 5.9) and since this step of the overall reduction mechanism remained active in the absence of an added electron donor, this periplasmic hydrogenase was capable of using endogenous stores of electrons for metal reduction and consequently was oxygen sensitive. These results further demonstrated that

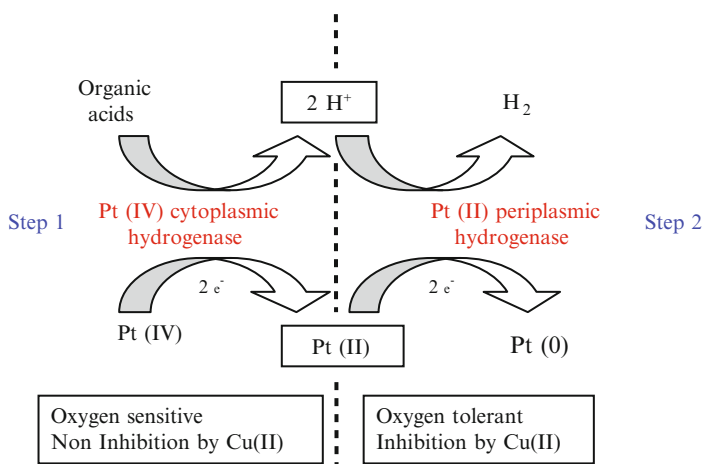


**Fig. 5.9** Suggested mechanism for the double two-electron bioreduction of Pt(IV) into nanoparticles via an intermediary Pt(II)

two separate mechanisms were involved in the reduction of Pt(IV) – an oxygen-tolerant reductase/hydrogenase [step 1] and a “novel” oxygen sensitive periplasmic hydrogenase [step 2].

Further analysis by this same research group (Riddin et al. 2009) indicated the TEM images and EDAX spectral graphs of SRB cells, which had been incubated with the Pt(IV) salt in the presence of an exogenous supply of hydrogen as the electron donor, to show a number of cells with electron dense platinum deposits located mainly in the periplasm (Fig. 5.10a<sub>1</sub>, b<sub>1</sub>). Though this finding did not indicate which platinum ion was present in the periplasm it did imply that a bioreduction, by means of the periplasmic hydrogenase, was taking place along with the formation of Pt(0) nanoparticles. The EDAX spectral graphs and TEM images of SRB cells incubated with Pt(IV) salt under an aerobic atmosphere gave similar results to those in an anaerobic environment when a hydrogen electron donor was present (Fig. 5.10a<sub>2</sub> and b<sub>2</sub>). The electron dense platinum nanoparticles were deposited, predominantly, in the periplasm with only trace amounts identified on the cell surface once again supporting the findings that an oxygen-sensitive periplasmic hydrogenase was involved in the bioreduction. It is very interesting to

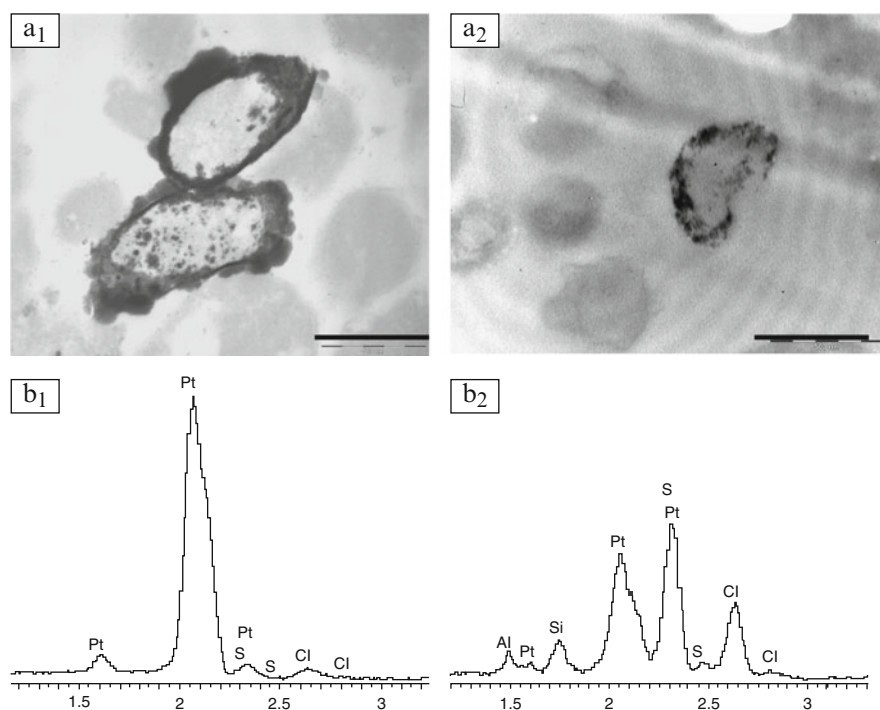


**Fig. 5.10** (a) TEM images of cells incubated with Pt(IV). (1) With hydrogen as exogenous electron donor. *Scale bar* = 500 nm. (2) With no exogenous electron donor. *Scale bar* = 1,000 nm (b) EDAX spectral graph of samples indicating presence of platinum: (1) with hydrogen as exogenous electron donor. (2) With no exogenous electron donor

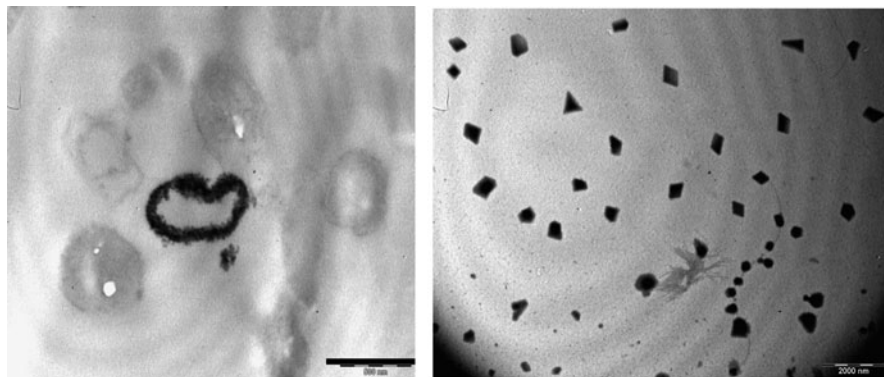


**Fig. 5.11** TEM images of electron dense platinum nanoparticles. Scale bar = 2,000 nm

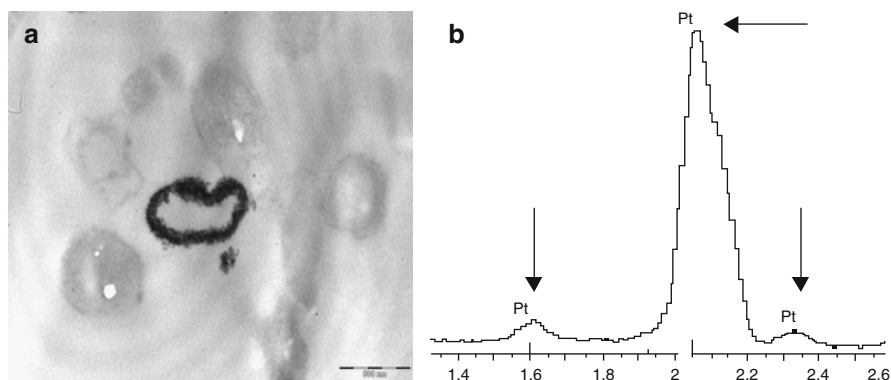


**Fig. 5.12** (a) TEM images of cells incubated with Pt(II) with electron dense metal deposits within the periplasmic regions. Scale bar = 1,000 nm. (b) EDAX spectral graph of samples indicating presence of platinum

note that, in the absence of the spatial restrictions of the cell wall, Pt(IV) was reduced to Pt(0) by the cell-free crude extract to form geometric Pt(0) nanoparticles (Fig. 5.11), presumably by the same reduction mechanism identified as before.

The EDAX spectral graphs and TEM images of SRB cells incubated with Pt(II) salt under an aerobic atmosphere showed the presence of platinum and the deposit of black platinum nanoparticles within the periplasm (Fig. 5.12). Qualitative analysis of the solution after SRB cells had been exposed to Pt(II) under the same conditions showed a colour change from light yellow to dark brown indicating Pt(0) nanoparticle formation while the SRB cells that had been incubated in the presence of 5 mM Cu(II) gave a barely perceptible colour change. The TEM images of the cells indicated black electron dense regions mainly restricted to the cell surface and only a small amount (5%) found within the periplasm (Fig. 5.13). EDAX spectral

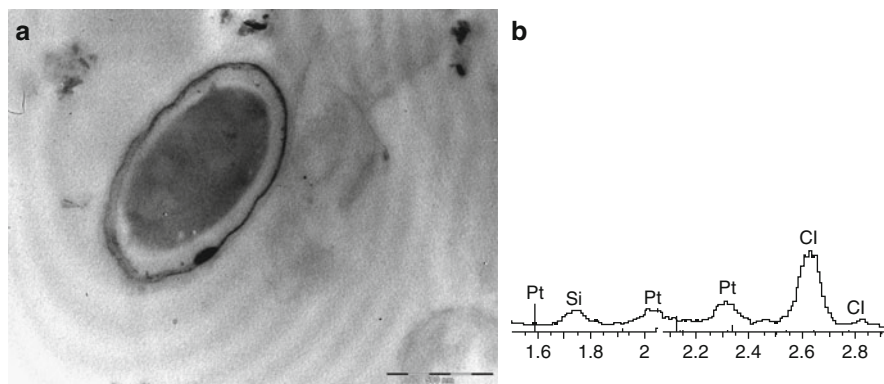


**Fig. 5.13** Screening for platinum ion reduction by SRB cells pre-treated with 5 mM Cu(II). (a) TEM images of cells with particularly low concentrations of electron dense metal deposits within the periplasmic regions. Majority of the metal is located on the cell surfaces. *Scale bars* = 500 nm. (b) EDAX spectral graph of sample showing low levels of Pt(0)

graphs showed an insignificant amount of Pt(0) deposited implying that the enzymatic bioreduction had been inhibited.

Previous work, involving hydrogenase enzymes from sulphate-reducing bacteria, (Ngwenya and Whiteley 2006; Rashamuse and Whiteley 2007) along with other workers (Konishi et al. 2007), had identified that platinum salts were bioreduced and platinum metal deposited in the periplasm of the cell under anaerobic conditions. Since the hydrogenase enzyme concentration was located within this periplasm it suggested that this enzyme was responsible for the bioreduction of  $\text{H}_2\text{PtCl}_6$  with the platinum salt substituted for sulfate as the final electron acceptor. In this case, the periplasmic hydrogenase used evolved hydrogen as an electron donor resulting in the higher than normal initial hydrogenase activity for the Pt(II) ion (step 2) in samples containing viable cells. Since a competitive nature existed between the Pt(IV) and Pt(II) ions and the cytoplasmic hydrogenase had a high affinity for Pt(IV), Pt(II) reduction would only proceed, at a slower rate, once Pt(IV) has been completely reduced. The endogenous production of hydrogen/electrons via the oxidation of organic compounds, evolved by the cytoplasmic hydrogenase, would, initially, be rapid, slowing down as the finite store of organic compounds/substrate became limiting. Since the bioreduction of the Pt(IV) ion is unaffected in the presence of Cu(II), the rate-limiting step in this case was that of Pt(II) to Pt(0) further supporting the hypothesis that a periplasmic hydrogenase was involved that most likely utilised limited, endogenously produced hydrogen during the reduction of Pt(II). It is still unclear which enzyme(s) is/are responsible for the initial reduction of Pt(IV) to Pt(II) (step 1) (Fig. 5.9). Furthermore, these findings confirmed earlier studies and hypothesis (Riddin et al. 2006; Govender et al. 2009, 2010) that such a bioreductive mechanism was a two-step reduction process with Pt(IV) becoming reduced to Pt(0) via the intermediate ion Pt(II). In SRB, it has been shown (Voordouw 2002) that a cytoplasmic

hydrogenase was involved in the endogenous production of hydrogen, along with excess electrons, by pyruvate oxidation. Furthermore, it was proposed (Odom and Peck 1981) that the *Desulfovibrio spp.* produced molecular H<sub>2</sub> via a cytoplasmic hydrogenase that scavenges these excess electrons and consequently, according to Whiteley's group, this endogenously produced hydrogen, dispersed through the cell to the periplasm where it became available for use by the periplasmic hydrogenase. The endogenous electrons were used, in the absence of sulfate, for the reduction of the platinum metal ions by the periplasmic hydrogenase that was protected from oxidative stress by the SOD. The Pt(IV) ion was reduced via a two-cycle, biologically dependant process to elemental platinum [Pt(0)] via the intermediate cation, Pt(II), in the presence or absence of an exogenous electron donor (Fig. 5.9).

If different enzymes were responsible for each of the two steps described, with one being inhibited by Cu (II), then each enzyme had to operate via a separate, yet concerted mechanism. Other cases of metal bioreduction involving a two-step enzymatic mechanism have been reported. It had been demonstrated (Opperman and van Heerden 2007) that two separate mechanisms for Cr(IV) reduction were observed under anaerobic versus aerobic conditions in the thermophilic bacterium *Thermus scotoductus*. The anaerobic mechanism required lactate as the electron donor while the aerobic mechanism occurred via the Cr(IV) reductase action of a soluble, constitutively expressed cytoplasmic, NADH-dependant enzyme, either in the presence or absence of an exogenous electron donor. The rate of reduction, however, was increased significantly in the presence of exogenous electron donor. These authors explained that it was not uncommon for bacteria to maintain their metal hydrogenase activity in the absence of an exogenous electron donor. Bacteria produced and stored high-energy carbohydrate polymers that became metabolised in times of metabolic starvation, releasing the stored energy for general cell maintenance while simultaneously producing an endogenous store of electrons for use in metal reductase activity. It was reasonable to suppose that such a mechanism involving an anaerobic step (oxygen sensitive) and an aerobic step (oxygen tolerant) could exist for the total bioreduction of Pt(IV) to Pt(0).

Since oxygen did not inhibit the overall reduction of platinum even with hydrogen as the electron donor, the role of the oxygen-tolerant cytoplasmic hydrogenase could be excluded. An active mechanism of Pt(II) → Pt(0) reduction was further supported by the apparent lack of this step in heat-killed cells and those cells that had been incubated with Cu(II) indicating that an active, enzymatic/protein-based process – most likely the periplasmic hydrogenase enzyme (Rashmuse and Whiteley 2007) was involved. As neither step 1 [Pt(IV) → Pt(II)] nor step 2 of the overall reduction mechanism was inhibited by the presence of low levels of oxygen or absence of an electron donor, this hydrogenase was capable of using endogenous stores of electron donors for metal reduction. Certain species of SRB, like *D. desulfuricans* were capable of producing endogenous electron donors, such as hydrogen, from the oxidation of organic compounds (i.e., lactate) during stationary phase metabolism in the absence of sulphate.

### 5.7.2 Eukaryotes: *Fusarium oxysporum*

Whiteley's group (Govender et al. 2009, 2010) compared the ability of the hydrogenase isolated and purified from *F. oxysporum* (Govender et al. 2010) to reduce  $\text{H}_2\text{PtCl}_6$  or  $\text{PtCl}_2$  to produce nanoparticles (Fig. 5.14). They found that at pH 7.5 and 38°C, which were optimum conditions for hydrogenase activity, there was a rapid bioreduction of  $\text{PtCl}_2$  with a 90% reduction after 8 h. For  $\text{H}_2\text{PtCl}_6$ , however, there was little or no evidence for any bioreduction since 96% platinum salt remained after 8 h under the same conditions (Fig. 5.14). From a previous study (Govender, et al. 2009), it was found that the enzyme had <10% activity at pH 9 and 65°C yet at this pH and temperature there was over 90% reduction after 8 h. On the other hand, with  $\text{PtCl}_2$  at pH 9 and 65°C the bioreduction was virtually nil with over 90% of the platinum salt remaining (Fig. 5.14). These findings implied that the bioreduction of  $\text{H}_2\text{PtCl}_6$  occurred on the enzyme at a site that was remote to the active site while the reduction of  $\text{PtCl}_2$  occurred through an active enzymatic process on the same enzyme. The  $\text{H}_2\text{PtCl}_6$  was in a 4<sup>+</sup> oxidation state, and the metal (Pt) centres adopted an octahedral geometry, thus forming a complex wherein half of the chloride ligands bridge between the platinum atoms. Such a structure was too large to enter the active region of the hydrogenase active site and the consequence of this platinum salt acting as a final electron acceptor is remote. An increase in pH and temperature to 9 and 65°C, respectively, would support the conditions for the collapse of this octahedral symmetry and allow the bioreduction to occur via a passive route.  $\text{PtCl}_2$ , on the other hand was in a 2<sup>+</sup> oxidation state and adopted a smaller trigonal planar structure that, quite readily, can enter the active region of the hydrogenase. Studies have suggested that the active sites of proteins maybe responsible for nanoparticle formation (Yoshimura 2006; Riddin et al. 2006).

TEM images showed that nanoparticles produced by the bioreduction of  $\text{PtCl}_2$  were distinctly large rectangular and triangular to those produced from  $\text{H}_2\text{PtCl}_6$

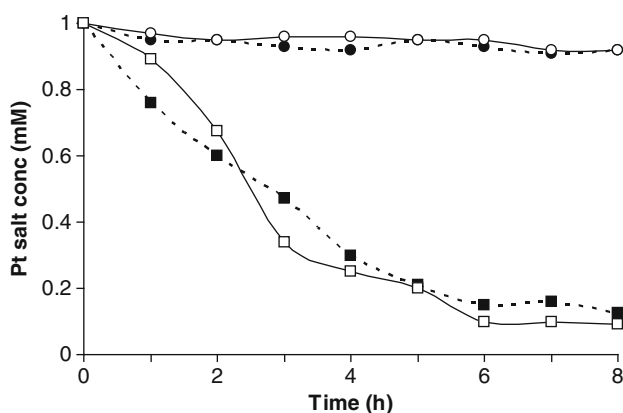


**Fig. 5.14** Reduction of hexachloroplatinic acid ( $\text{H}_2\text{PtCl}_6$ ) Filled square pH 9.0, 65°C, Bullet pH 7.5, 38°C; and platinum (II) chloride ( $\text{PtCl}_2$ ) open square pH 7.5, 38°C, circle pH 9.0, 65°C with purified hydrogenase. Data points are the mean of duplicate values with standard deviation

(Fig. 5.15a) (Govender et al. 2009). Spherical nanoparticles were produced by the bioreduction of  $\text{H}_2\text{PtCl}_6$  and these appeared to be monodispersed and varying in size (Fig. 5.15b). Nanoparticles produced by the hydrogenase at pH 9,  $65^\circ\text{C}$  were circular, triangular, pentagonal and hexagonal, often appearing as nanoplates, (Fig. 5.16) over a wide size distribution with the majority of them being between

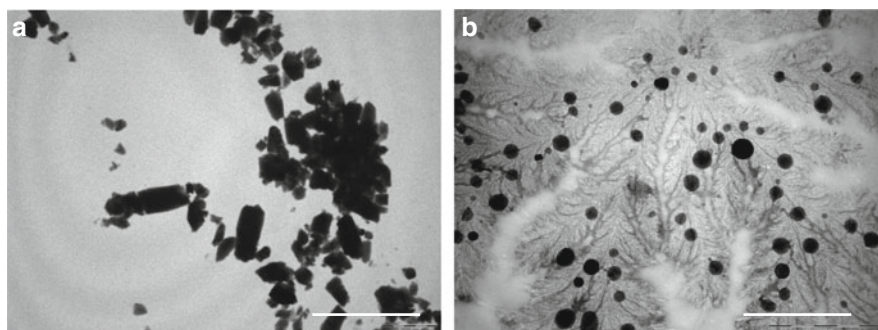


**Fig. 5.15** (a) Platinum nanoparticles produced during the reduction of  $\text{PtCl}_2$  at pH 7.5,  $38^\circ\text{C}$  Scale bar represents 1,000 nm. (b) Spherical platinum nanoparticles produced during the reduction of  $\text{H}_2\text{PtCl}_6$  at pH 9,  $65^\circ\text{C}$ . Scale bars = 1,000 nm

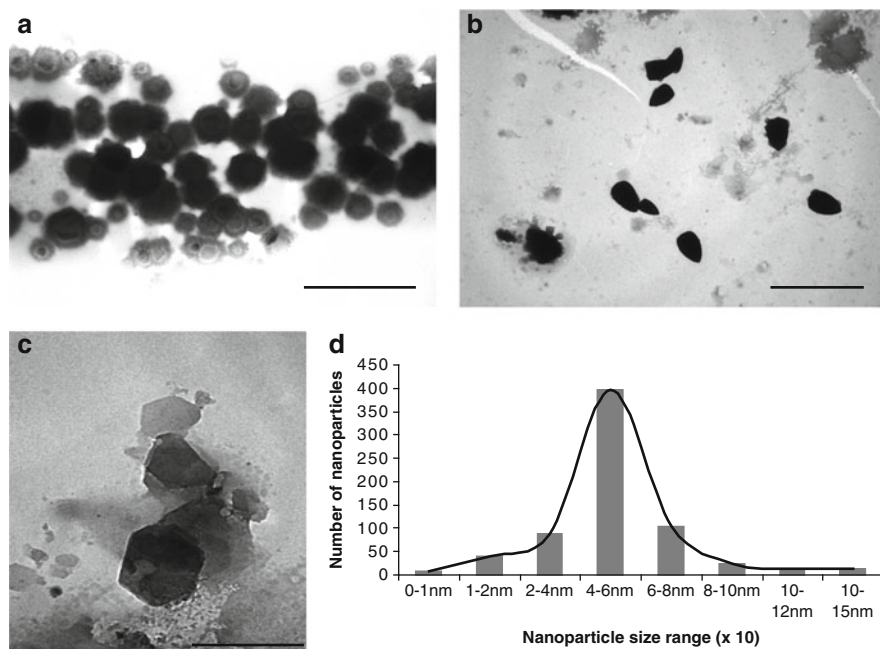


**Fig. 5.16** Platinum nanoparticles produced during the reduction of  $\text{H}_2\text{PtCl}_6$  at pH 9,  $65^\circ\text{C}$ . (a) Circular and hexagonal; (b) Pentagonal; (c) Triangular and hexagonal nanoplates. All scale bars represent 200 nm. (d) The size histogram of nanoparticles



20 and 80 nm, with the mean size range was 40–60 nm. These nanoplates appeared to be stacked close to, or on top of, each other and it was thought that this could occur as a result of an overlap in nucleation times and subsequent attachment of the nanoparticles resulting in aggregation. These results indicated that in addition to pH and temperature, the oxidation state of the platinum salt played an important role in the mechanism and formation of the nanoparticles though the size and shape of the particles were uncontrollable.

In order to confirm the formation of the platinum nanoparticles, they were randomly spot scanned with X-ray energy dispersive spectroscopy (Fig. 5.17a) confirming the presence of elemental platinum [Pt(0)] in the sample and supporting our initial hypothesis that  $\text{H}_2\text{PtCl}_6$  is bioreduced by a hydrogenase to produce platinum nanoparticles. The observed nickel peaks may be indicative of the Ni–Fe hydrogenase used for this platinum nanoparticle synthesis. The bright yellow colour of  $\text{H}_2\text{PtCl}_6$  ions before exposure to the fungal cell free extract and the distinct colour change to dark brown or black on completion of the bioreduction from *F. oxysporum* isolate can be clearly seen (Fig 5.17b) suggesting that the fungus reduced  $\text{H}_2\text{PtCl}_6$  resulting in the production of platinum nanoparticles.

The platinum salt binds to the enzyme at a peripheral site, remote from the active region, thereby inhibiting the enzyme non-competitively. Under an atmosphere of hydrogen and at pH 9 and  $65^\circ\text{C}$ , a four-electron transfer takes place reducing Pt(IV) to Pt metal via a Pt(II) intermediate (Fig. 5.9). If the initial two-electron reduction of Pt(IV) to Pt(II) occurred on the molecular surface of the enzyme and that ideal conditions for biological synthesis of platinum nanoparticles *in vitro* were pH 9 and

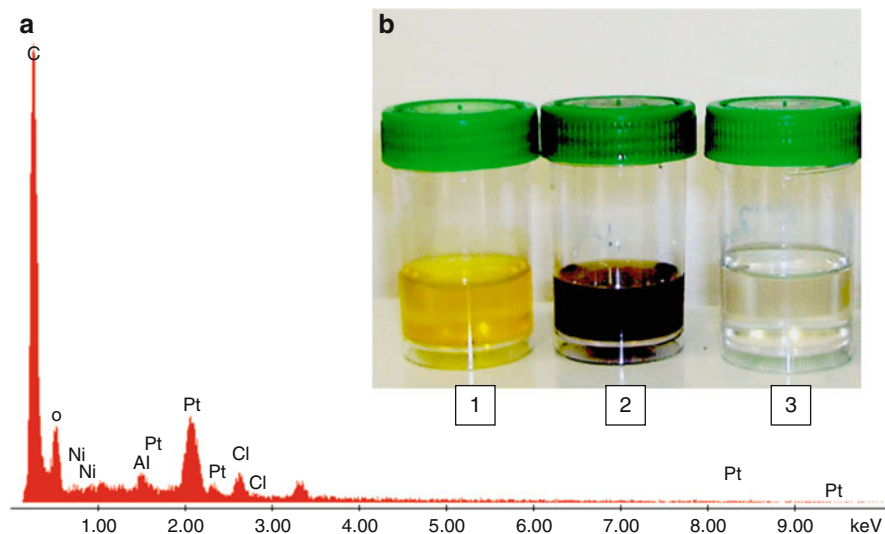


**Fig. 5.17** (a) X-ray energy dispersive spectroscopic spot scan of the platinum nanoparticles visualised on the holey grid. (b) Visual indication of platinum hexachloroplatinic acid reduction. (1) Control containing only  $\text{H}_2\text{PtCl}_6$ , (2) fungal cell-free extracts exposed to  $\text{H}_2\text{PtCl}_6$ , (3) control containing only fungal extracts of isolate in  $\text{ddH}_2\text{O}$

65°C though the conditions optimal for the activity of the periplasmic hydrogenase were pH 7.5 and 38°C then it would not be feasible for this periplasmic hydrogenase to be involved in the bioreduction of the Pt(IV) during its passage from the external surroundings through the periplasm to the cytoplasm.

## 5.8 Concluding Comments

The prokaryotic SRB and the eukaryotic fungus *F. oxysporum* reduced Pt(IV) to Pt(0) via the intermediate cation Pt(II) by different two-step two-electron reduction mechanisms.

In the SRB case, two different hydrogenase enzymes were involved in each step. First, a cytoplasmic hydrogenase/reductase that was oxygen tolerant, that was not inhibited by Cu (II), that required no exogenous electron donors and that produced hydrogen (and excess electrons) from metabolite oxidation and/or Pt(IV) reduction was responsible for converting Pt(IV) into Pt(II). Second, a periplasmic hydrogenase that was oxygen sensitive, that was inhibited by Cu (II) and that used the endogenously formed hydrogen donors [and Pt(II) ions] to form Pt(0) nanoparticles.

In the eukaryotic (*F. oxysporum*), only one periplasmic hydrogenase was involved. Though it was initially suggested that  $\text{H}_2\text{PtCl}_6$  acted as an electron acceptor during the redox mechanism of a hydrogenase (Rashamuse and Whiteley 2007) it was subsequently established that this was not the case (Govender et al. 2009). A network of hydrophobic channels existed between the active site and the molecular surface in hydrogenase enzymes (Yoshimura 2006) which served as a passage for metal ions. Even though the diameter of these channels (0.45–0.60 nm) was too small for  $\text{H}_2\text{PtCl}_6$ , it was not too small for  $\text{PtCl}_2$ . At pH 9 and 65°C, the  $\text{H}_2\text{PtCl}_6$  was rapidly reduced by a passive two-electron transfer process into a Pt(II) species at a remote site on the molecular surface of the enzyme. This Pt(II) migrated to the active region through the network of channels and was reduced, at pH 7.5 and 38°C, by a second, slower two-electron reduction into Pt(0). During this process, positively charged platinum particles act as electron acceptors, whereby they become reduced to a neutral metal species after two cycles, leading to the reduction of the platinum salt and subsequent nanoparticle formation.

## References

- Ahmad A, Mukherjee P, Mandal D, Senapati S, Khan MI, Kumar R, Sastry M (2002) Enzyme mediated extracellular synthesis of CdS nanoparticles by the fungus *Fusarium oxysporum*. *J Am Chem Soc* 124:12108–12109
- Ahmad A, Senapati S, Khan MI, Kumar R, Ramani R, Srinivas V, Sastry M (2003a) Intracellular synthesis of gold nanoparticles by a novel alkalotolerant actinomycete, *Rhodococcus* species. *Nanotechnology* 14:824–828

- Ahmad A, Senapati S, Khan MI, Kumar R, Sastry M (2003b) Extracellular biosynthesis of monodisperse gold nanoparticles by a novel extremophilic actinomycete, *Thermomonospora* sp. *Langmuir* 19:3550–3553
- Ahmad A, Senapati S, Khan MI, Kumar R, Sastry M (2005) Extra-/Intracellular biosynthesis of gold nanoparticles by an alkalotolerant fungus, *Tricothecium* sp. *J Biomed Nanotechnol* 1:47–53
- Aitken RJ, Kreeley KS, Tran CL (2004) Physical characteristics and properties of nanoparticles. In: *Nanoparticles: an occupational hygiene review*. Edinburgh: Crown copyright, pp 7–18.
- Akamatsu K, Nakahashi K, Ikeda S, Nawafune H (2003) Fabrication and structural characterisation of nanocomposites consisting of Ni nanoparticles dispersion in polyimide films. *Eur Phys J D* 24:377–380
- Akerman ME, Chan WC, Laakkonen P, Bhatia SN, Ruoslahti E (2002) Nanocrystal targeting in vivo. *Proc Nat Acad Sci USA* 99:12617–12621
- Albracht SPJ (1994) Nickel hydrogenases: in search of the active site. *Biochim Biophys Acta* 1188:167–204
- Armstrong FA (2004) Hydrogenases: active site puzzles and progress. *Curr Opin Chem Biol* 8:133–140
- Beard MC, Turner GM, Schmuttenmaer CA (2002) Size-dependent photoconductivity in CdSe nanoparticles as measured by time-resolved tetrahertz spectroscopy. *Nano Lett* 2:983–987
- Bhainsa KC, D'Souza SF (2006) Extracellular biosynthesis of silver nanoparticles using the fungus *Aspergillus fumigatus*. *Colloids Surf B Biointerfaces* 47:160–164
- Bhat JSA (2003) Heralding a new future – nanotechnology. *Curr Sci* 85:147–154
- Bhattacharya D, Gupta RK (2005) Nanotechnology and potential of microorganisms. *Crit Rev Biotechnol* 25:199–204
- Birla SS, Tiwari VV, Gade AK, Ingle AP, Yadav AP, Rai MK (2009) Fabrication of silver nanoparticles by *Phoma glomerata* and its combined effect against *Escherichia coli*, *Pseudomonas aeruginosa* and *Staphylococcus aureus*. *Lett Appl Microbiol* 48:173–179
- Bolotin KI, Keummeth F, Pasupathy AN, Ralph DC (2004) Metal-nanoparticle single electron transistors fabricating using electromigration. *Appl Phys Lett* 84:3154–3157
- Braun M, Burda C, El-Sayed MA (2001) Variation of the thickness and number of wells in the CdS/HgS/CdS quantum dot quantum well system. *J Phys Chem A* 105:5548–5551
- Bruchez J, Moronne MM, Gin P, Weiss S, Alivisatos AP (1998) Semiconductor nanocrystals as fluorescent biological labels. *Science* 281:2013–2016
- Cao G (2004) *Nanostructures and nanomaterials: synthesis, properties and applications*. Imperial College Press, London
- Cao YC, Jin R, Mirkin CA (2002) Nanoparticles with Raman spectroscopic fingerprints for DNA and RNA detection. *Science* 297:1536–1540
- Carpentier W, Sandra K, De Smet I, Brige A, De Smet L, Van Beeumen J (2003) Microbial reduction and precipitation of vanadium by *Shewanella oneidensis*. *Appl Environ Microbiol* 69:3636–3639
- Chardin B, Giudii-Ortoni MT, De Luca G, Guigliarelli B, Bruschi M (2003) Hydrogenases in sulphate-reducing bacteria function as chromium reductase. *Appl Microbiol Biotechnol* 63:315–321
- Chen X, Lou Y, Samia AC, Burda C (2003) Coherency strain effects on the optical response of core/shell heteronanostructures. *Nanotechnol Lett* 3:799–803
- Dameron CT, Reese RN, Mehra RK, Kortan AR, Carroll PJ, Steigerwald ML, Winge BLE, Winge DR (1989) Biosynthesis of cadmium sulphide quantum semiconductor crystallites. *Nature* 338:596–597
- Das D, Dutta T, Nath K, Kotayi SM, Das KAK, Veziroglu TN (2006) Role of [Fe] hydrogenase in biological hydrogen production. *Curr Sci* 90:1627–1637
- De Lacy AL, Santamaria E, Hatchikian EC, Fernandez VM (2000) Kinetic characterisation of *Desulfovibrio gigas* hydrogenase upon selective chemical modification of amino acid groups as a tool for structure-function relationships. *Biochim Biophys Acta* 1481:371–380

- De Luca G, de Philip P, Dermoun Z, Rousset M, Vermeglio A (2001) Reduction of technetium (VII) by *Desulfovibrio fructosovorans* is mediated by the nickel-iron hydrogenase. *Appl Environ Microbiol* 67:4583–4587
- Duran N, Marcato PD, Alves OL, de Souza GIH, Esposito E (2005) Mechanistic aspects of biosynthesis of silver nanoparticles by several *Fusarium oxysporum* strains. *J Nanobiotechnol* 3:8–14
- Ehrlich HL (1997) Microbes and metals. *Appl Microbiol Biotechnol* 48:687–692
- Elliot SJ, Leger C, Pershad HR, Hirst J, Heffron K, Ginot N, Blasco F, Rothery RA, Weiner JH, Armstrong FA (2002) Detection and interpretation of redox potential optima in the catalytic activity of enzymes. *Biochim Biophys Acta* 1555:54–59
- Erhardt D (2003) Materials conservation: not-so-new technology. *Nat Mater* 2:509–510
- Fendler JH (1998) Nanoparticles and nanostructured films: preparation, characterisation and applications. Wiley, NY
- Fournier M, Dermoun Z, Durand MC, Dolla A (2004) A new function of the *Desulfovibrio vulgaris* Hildenborough [Fe] hydrogenase in the protection against oxidative stress. *J Biochem* 279:1787–1793
- Gadd GM (1993) Tansley review no. 47 interactions of fungi with toxic metals. *New Phytol* 124:25–60
- Gade AK, Bonde P, Ingle AP, Marcato PD, Duran N, Rai MK (2008) Exploitation of *Aspergillus niger* for synthesis of silver nanoparticles. *J Biobased Mater Bioenergy* 2:243–247
- Gamez G, Gardea-Torresdey JL, Tiemann KJ, Parsons J, Dokken K, Yacaman J (2003) Recovery of gold (III) from multi-elemental solutions by alfalfa biomass. *Adv Environ Res* 7:563–571
- Gao M, Rogach AL, Kornowski A, Kirstein S, Eychmuller A, Mohwald P, Weller H (1998) Strongly photoluminescent CdTe nanocrystals by proper surface modification. *J Phys Chem B* 102:8360–8363
- Gardea-Torresdey JL, Parsons JG, Gomez E, Peralta-Videa J, Troianl HE, Santiago P, Yacaman MJ (2002) Formation and growth of Au nanoparticles inside alfalfa plants. *Nanotechnol Lett* 2:397–401
- Georganopoulou DG, Chang L, Nam J, Thaxton CS, Mufson EJ, Klein WL, Mirkin CA (2005) From the cover: nanoparticle based detection in cerebral spinal fluid of a soluble pathogenic biomarker for Alzheimers disease. *Proc Natl Acad Sci* 102:2273–2276
- Govender Y, Riddin TL, Gericke M, Whiteley CG (2009) Bioreduction of platinum salts into nanoparticles: a mechanistic perspective. *Biotechnol Lett* 31:95–100
- Govender Y, Riddin TL, Gericke M, Whiteley CG (2010) On the enzymatic formation of platinum nanoparticles. *J Nanopart Res* 12:261–271. doi:10.1007/s11051-009-9604-3
- Guo C, Boullanger P, Jiang L, Liu T (2007) Highly sensitive gold nanoparticles biosensor chips modified with a self-assembled bilayer for detection of Con A. *Biosens Bioelectron* 22:1830–1834
- Gwinn MR, Vallyathan V (2006) Nanoparticles: health effects: pros and cons. *Environ Health Persp* 114:1818–1825
- Harrison MT, Kershaw SV, Rogach AL, Kornowski A, Eychmuller A, Weller H (2000) Wet chemical synthesis of highly luminescent HgTe/CdS core/shell nanocrystals. *Adv Mater* 12:123–130
- Heinglein A, Giersig M (2000) Reduction of Pt(II) by H<sub>2</sub>: effects of citrate and NaOH and reaction mechanism. *J Phys Chem B* 104:6767–6772
- Holmes JD, Smith PR, Evans-Gowing R, Richardson DJ, Russell DA, Sodeau DJ (1995) Energy-dispersive X-ray analysis of the extracellular cadmium sulphide crystallites of *Klebsiella aerogenes*. *Arch Microbiol* 163:143–147
- Huang J, He C, Liu X, Xiao Y, Mya KY, Chai J (2004) Formation and characterization of water soluble platinum nanoparticles using a unique approach based on a hydrosilylation reaction. *Langmuir* 20:5145–5148
- Ibrahim Z, Ahmad A, Baba B (2001) Bioaccumulation of silver and the isolation of metal-binding protein from *Pseudomonas diminuta*. *Brazil Arch Biol Tech* 44:223–225

- Ingelsten HH, Bagwe R, Palmqvist A, Skoglundh M, Svanberg C, Holmberg K, Shah D (2001) Kinetics of the formation of nano-sized platinum particles in water-in-oil microemulsions. *J Coll Int Sci* 241:104–111
- Ingle A, Gade A, Pierrat S, Sonnichsen C, Rai M (2008) Mycosynthesis of silver nanoparticles using the fungus *Fusarium acuminatum* and its activity against some human pathogenic bacteria. *Curr Nanosci* 4:141–144
- Ingle A, Gade A, Bawaskar M, Rai M (2009) *Fusarium solani*: A novel biological agent for the extracellular synthesis of silver nanoparticles. *J Nanopart Res* 11:2079–2085
- Jain KK (2005) Nanotechnology in clinical laboratory diagnostics. *Clin Chim Acta* 358:37–54
- Ji G, Silver S (1995) Bacterial resistance mechanism for heavy metals of environmental concern. *J Ind Microbiol* 14:61–75
- Kato H, Minami T, Kanazawa T, Sasaki Y (2004) Mesopores created by platinum nanoparticles in zeolite crystals. *Angew Chem Int Edit* 43:1251–1254
- Klaus-Joergert T, Joergert R, Olsson E, Granqvist CG (2001) Bacteria as workers in the living factory: metal accumulating bacteria and their potential for materials science. *Trends Biotechnol* 19:15–20
- Knez M, Gösele U (2006) Bionanoelectronics: viruses show their good side. *Nat Nanotechnol* 1:22–23
- Konetzka WA (1977) Microbiology of metal transformations. In: Weinberg ED (ed) *Microorganisms and minerals*. New York, Marcel Dekker Inc, pp 317–342
- Konishi Y, Ohno K, Saitoh N, Nomura T, Nagamine S, Hishida H, Takahashi Y, Uruga T (2007) Bioreductive deposition of platinum nanoparticles on the bacterium *Shewanella algae*. *J Biotechnol* 128:648–653
- Kubik T, Bogunia-Kubik K, Sugisaka M (2005) Nanotechnology on duty in medical applications. *Curr Pharm Biotechnol* 6:17–33
- LaVan DA, McGuire T, Langer R (2003) Small scale systems for *in vivo* drug delivery. *Nat Biotechnol* 21:1184–1191
- Leach MR, Zamble DB (2007) Metallocentre assembly of the hydrogenase enzymes. *Curr Opin Chem Biol* 11:159–165
- Lengke MF, Fleet ME, Southam G (2006) Synthesis of platinum nanoparticles by reaction of filamentous cyanobacteria with platinum (IV) chloride complex. *Langmuir* 22:7318–7323
- Liu Z, Ling XY, Su X, Lee JM (2004) Carbon-supported Pt and Pt Ru nanoparticles as catalysts for a direct methanol fuel cell. *J Phys Chem B* 108:8234–8240
- Liu Z, Shamsuzzoha M, Ada ET, Reichat M, Nikles DE (2007) Synthesis and activation of platinum nanoparticles with controlled size for fuel cell electrocatalysts. *J Power Sources* 164:472–480
- Lloyd JR (2003) Microbial reduction of metals and radionuclides. *FEMS Microbiol Revs* 27:411–425
- Lloyd JR, Macaskie LE (1996) A novel phosphorimager- based technique for monitoring the microbial reduction of technetium. *Appl Environ Microbiol* 65:578–582
- Lloyd JR, Nolthing HF, Sole VA, Bosecker K, Macaskie LE (1998) Technetium reduction and precipitation by sulphate reducing bacteria. *Geomicrobiol J* 15:43–56
- Lloyd JR, Ridley J, Khizniak T, Lyalikova NN, Macaskie LE (1999) Reduction of technetium by *Desulfovibrio desulfuricans*: Biocatalyst characterization and use in a flow through bioreactor. *Appl Environ Microbiol* 65:2691–2696
- Lloyd JR, Sole VA, Van Praagh CV, Lovely DR (2000) Direct and Fe(II)-mediated reduction of technetium by Fe(III)-reducing bacteria. *Appl Environ Microbiol* 66:3743–3749
- Lloyd JR, Mabbett AN, Williams DR, Macaskie LE (2001) Metal reduction by sulphate-reducing bacteria: physiology, diversity and metal specificity. *Hydrometall* 59:327–337
- Loujou E, Bianco P, Bruschi M (1998) Kinetic studies on the electron transfer between bacterial c-type cytochromes and metal oxides. *J Electroanal Chem* 452:167–177
- Lovely DR, Widman PK, Woodward JC, Phillips EJP (1993) Reduction of uranium by cytochrome c3 of *Desulfovibrio vulgaris*. *Appl Environ Microbiol* 59:3572–3576

- Mandal S, Phadtare S, Sastry M (2005) Interfacing biology with nanoparticles. *Curr Appl Phys* 5:118–127
- Mazzola L (2003) Commercialising nanotechnology. *Nat Biotechnol* 21:1137–1143
- Michel C, Brugna M, Aubert C, Bernadac A, Bruschi M (2001) Enzymatic reduction of chromate: comparative studies using sulphate-reducing bacteria. Key role polyheme cytochrome c hydrogenases. *Appl Microbiol Biotechnol* 55:95–100
- Mills RL (2000) The hydrogen atom revisited. *Int J Hydrogen Energy* 25:1171–1183
- Misra TK (1992) Bacterial resistance to inorganic mercury salts and organomercurials. *Plasmid* 27:4–16
- Mukherjee P, Ahmad A, Mandal D, Senapati S, Sainkar SR, Khan MI, Pasricha R, Ajayakumar PV, Alam M, Kumar R, Sastry S (2001) Fungus mediated synthesis of silver nanoparticles and their immobilisation in the mycelial matrix: a novel biological approach to nanoparticle synthesis. *Nano Lett* 1:515–519
- Mukherjee P, Ahmad A, Mandal D, Senapati S, Sainkar SR, Khan MI, Ramani R, Parischa R, Ajayakumar PV, Alam M, Sastry M, Kumar R (2002) Bioreduction of AuCl<sub>4</sub> ions by the fungus, *Verticillium* sp. surface trapping gold nanoparticles formed. *Angew Chem Int Ed* 40:3585–3588
- Mukherjee P, Senapati S, Mandal D, Ahmad A, Islam Khan M, Kumar R, Sastry M (2003) Extracellular synthesis of gold nanoparticles by the fungus *Fusarium oxysporum*. *Chem Bio Chem* 5:461–463
- Nair B, Pradeep T (2002) Coalescence of nanoclusters and formation of submicron crystallites assisted by *Lactobacillus* strains. *J Cryst Gr Des* 2:293–298
- Ngwenya N, Whiteley CG (2006) Recovery of rhodium (III) from solution and industrial wastewaters by a sulphate reducing consortium. *Biotechnol Prog* 22:1604–1611
- Nicolet Y, Lemon BJ, Fontecilla-Camps JC, Peters JW (2000) A novel FeS cluster in Fe-only hydrogenases. *Trends Biochem Sci* 25:138–143
- Oberdörster G, Finkelstein JN, Johnston C, Gelein R, Cox C, Baggs R, Elder AC (2000) Acute pulmonary effects of ultrafine particles in rats and mice. *Res Rep Health Eff Inst* 96:65–74
- Odom JM, Peck HD Jr (1981) Hydrogen cycling as a general mechanism for energy coupling in the sulfate-reducing bacteria *Desulfovibrio* sp. *FEMS Microbiol Lett* 12:47–50
- Opperman DJ, van Heerden E (2007) Aerobic Cr(VI) reduction by *Thermus scotoductus* strain SA-01. *J Appl Microbiol* 103:1907–1913
- Panyam J, Labhasetwar V (2003) Biodegradable nanoparticles for drug and gene delivery to cells and tissue. *Adv Drug Deliv Rev* 55:329–347
- Payne RB, Gentry DM, Rapp-Giles BJ, Casalot L, Wall JD (2002) Uranium reduction by *Desulfovibrio desulfuricans* strain G20 and a cytochrome c3 mutant. *Appl Environ Microbiol* 68:3129–3132
- Peng ZA, Peng X (2001) Formation of high-quality CdTe, CdSe, and CdS nanocrystals using CdO as a precursor. *J Am Chem Soc* 123:183–184
- Peng Q, Dong Y, Deng Z, Li Y (2002) Selective synthesis and characterization of CdSe nanorods and fractal nanocrystals. *J Inorg Chem* 41:5249–5254
- Penn SG, He L, Natan MJ (2003) Nanoparticles for bioanalysis. *Curr Opin Chem Biol* 7:609–615
- Postgate JR (1965) Recent advances in the study of the sulphate-reducing bacteria. *Bacteriol Rev* 29:425–441
- Qi L, Ma J, Cheng H, Zhao Z (1997) Reverse micelle based formation of BaCO<sub>3</sub> nanowires. *J Phys Chem* 101:3460–3463
- Qu L, Peng ZA, Peng X (2001) Alternative routes toward high quality CdSe nanocrystals. *Nanotech Lett* 1:333–337
- Qu L, Yu WW, Peng X (2004) In Situ observation of the nucleation and growth of CdSe nanocrystals. *Nanotechnol Lett* 4:465–469
- Rai M, Yadav A, Gade A (2008) CRC 675 – Current trends in photosynthesis of metal nanoparticles. *Crit Rev Biotechnol* 28:277–284

- Rai M, Yadav P, Bridge P, Gade A (2009a) Myconanotechnology: a new and emerging science. In: Rai M, Bridge PD (eds) Applied mycology. CABI publication, UK, pp 258–267
- Rai M, Yadav A, Gade A (2009b) Silver nanoparticles as a new generation of antimicrobials. *Biotechnol Adv* 27:76–83
- Rao CNR, Muller A, Cheetham AK (2004) The chemistry of nanomaterials: synthesis, properties and applications, vol 1. Wiley-VCH, Weinheim
- Rashmuse KJ, Whiteley CG (2007) Bioreduction of Pt(IV) from aqueous solution using sulphate reducing bacteria. *Appl Microbiol Biotechnol* 75:1429–1435
- Ravnic DJ, Zhang Y, Turhan A, Tsuda A, Pratt JP, Huss HT, Mentzer SJ (2007) Biological and optical properties of fluorescent nanoparticles developed for intravascular imaging. *Microsci Res Tech* 70:776–781
- Riddin TL, Gericke M, Whiteley CG (2006) Analysis of the inter- and extracellular formation of platinum nanoparticles by *Fusarium oxysporum* f. sp. lycopersici using response surface methodology. *Nanotechnol* 17:3482–3489
- Riddin TL, Govender Y, Gericke M, Whiteley CG (2009) Two different hydrogenase enzymes from sulphate reducing bacteria are responsible for the bioreductive mechanism of platinum into nanoparticles. *Enzyme Microb Technol* 45:267–273
- Rogach AL, Kornowski A, Gao M, Eychmuller A, Weller H (1999) Synthesis and characterization of a size series of extremely small thiol-stabilized CdSe nanocrystals. *J Phys Chem B* 103:3065–3069
- Roh Y, Lauf RJ, McMillan AD, Zhang C, Rawn CJ, Bai J, Phelps TJ (2001) Microbial synthesis and the characterization of metal-substituted magnetites. *Solid State Commun* 110:529–534
- Salata O (2004) Application of nanoparticles in biology and medicine. *J Nanobiotechnol* 2:3–8
- Sangregorio C, Galeotti M, Bardi U, Baglioni P (1996) Synthesis of Cu<sub>3</sub>Au nanocluster alloy in reverse micelles. *Langmuir* 12:5800–5802
- Sastry M, Ahmad A, Islam Khan M, Kumar R (2003) Biosynthesis of metal nanoparticles using fungi and actinomycete. *Curr Sci* 85:162–163
- Sastry M, Ahmad A, Khan MI, Kumar R (2004) Microbial nanoparticle production. In: Niemeyer CM, Mirkin CA (eds) Nanobiotechnology. Wiley-VCH, Weinheim, Germany, pp 126–135
- Seeman NC, Belcher AM (2002) Emulating biology: building nanostructures from the bottom up. *Proc Natl Acad Sci USA* 99:6451–6455
- Senapati S, Ahmad A, Khan MI, Sastry M, Kumar R (2005) Extracellular biosynthesis of bimetallic Au–Ag alloy nanoparticles. *Small* 1:517–520
- Shim M, Guyot-Sionnest P (2001) Organic-capped ZnO nanocrystals: synthesis and n-type character. *J Am Chem Soc* 123:11651–11654
- Shukla N, Svedberg EB, Eil J (2007) Surfactant isomerization and dehydrogenation of FePt nanoparticles. *Coll Surf Physiochem Eng Asp* 301:113–11
- Smith DG (1974) Tellurite reduction in *Schizosaccharomyces pombe*. *J Gen Microbiol* 83:389–392
- Southam G, Beveridge TJ (1996) The occurrence of bacterially derived sulphur and phosphorus within pseudocrystalline and crystalline octahedral gold formed in vitro. *Geochim Cosmochim Acta* 60:4369–4376
- Stephenson M, Stickland LH (1931) Hydrogenase: a bacterial enzyme activating hydrogen. *Biochem J* 25:205–214
- Sun CQ, Chen TP, Tai BK, Huang SLH, Zhanga YB, Pan LK, Lau SP, Sun XW (2001) An extended “quantum confinement” theory: surface-coordination imperfection modifies the entire band structure of a nanosolid. *J Phys Appl Phys* 34:3470–3479
- Talapin DV, Rogach AL, Kornowski A, Haase M, Weller H (2001) Highly luminescent monodisperse CdSe and CdSe/ZnS nanocrystals synthesized in a hexadecylamine-trioctylphosphine oxide-trioctylphosphine mixture. *Nanotechnol Letts* 1:207–211
- Taton TA (2002) Nanostructures as tailored biological probes. *Trends Biotechnol* 20:277–279
- Thaxton CS, Georanopoulou DG, Mirkin CA (2005) Gold nanoparticle probes for the detection of nucleic acid targets. *Clin Chim Acta* 363:120–126

- Vignais PM, Billoud B, Meyer J (2001) Classification and phylogeny of hydrogenases. *FEMS Microbiol Rev* 25:455–501
- Vinogradov S, Bronich T, Kabanov A (2002) Nanosized cationic hydrogels for drug delivery: preparation, properties and interactions with cells. *Adv Drug Delivery* 54:135–147
- Voordouw G (2002) Carbon monoxide cycling by *Desulfovibrio vulgaris* Hildenborough. *J Bacteriol* 184:5903–5911
- Wakatsuki T, Hayakawa S, Hatayama T, Kitamura T, Imahara H (1991) Purification and some properties of copper reductase from cell surface of *Debaryomyces hansenii*. *J Ferm Bioeng* 72:158–161
- Waszczuk P, Wieckowski A, Zeleny P, Gottesfeld S, Coutanceau C, Léger JM, Lamy C (2001) Adsorption of CO poison on fuel cell nanoparticle electrodes from methanol solutions: a radioactive labeling study. *J Electroanal Chem* 511:55–64
- Willner I, Baron R, Willner B (2006) Growing metal nanoparticles by enzymes. *Adv Mater* 18:1109–112
- Wu Y, Yang W, Wang C, Hu J, Fu S (2005) Chitosan nanoparticles as a novel delivery system for ammonium glycyrrhizinate. *Int J Pharm* 295:235–245
- Xiao Y, Pavlov V, Levine S, Niazov T, Markovitch G, Willner I (2004) Catalytic growth of Au nanoparticles by NAD (P) H cofactors: optical sensors for NAD (P)<sup>+</sup>-dependent biocatalyzed transformations. *Angew Chem Int Ed* 43:4519–4522
- Yoshimura H (2006) Protein assisted nanoparticle synthesis. *Coll Surf A Physiochem Eng Asp* 283:464–470
- Zadvornyy OA, Zorin NA, Gogotov IN, Gorlenko VM (2004) Properties of stable hydrogenase from the purple sulphur bacterium *Lamprobacter modestohalophilus*. *J Biochem Moscow* 69:164–169
- Zadvornyy OA, Zorin NA, Gogotov IN (2006) Transformation of metals and metal ions by hydrogenases from phototrophic bacteria. *Arch Microbiol* 184(5):279–285
- Zhang JZ, O’Neil RH, Roberti WT (1994) Femtosecond studies of photoinduced electron dynamics at the liquid–solid interface of aqueous CdS colloids. *J Phys Chem* 98:3859–3864



# Chapter 6

## Biomolecules–Nanoparticles: Interaction in Nanoscale

N. Vigneshwaran and Prateek Jain

### 6.1 Introduction

Nanomaterials that measure 1–1,000 nm allow unique interaction with biological systems at the molecular level (Yezhelyev et al. 2006). As nanoparticles and biomolecules are of similar length scale, it seems logical that the combination of biomacromolecules to nanomaterials can provide interesting tool for mimicking the biomolecules which are present at cellular systems, probing the mechanisms of biological processes, as well as developing chemical means by handling and manipulating biological components (Katz and Willner 2004). The interactions of biomolecules and metal nanoparticles arise that determine the size of nanoparticles, modify the surface of nanoparticles to enhance solubility/biocompatibility/bio-recognition, and detoxification of toxic metals.

Nanoparticles can be synthesized in sizes ranging from a few nanometers to few hundreds of nanometers, which is comparable to those of a cell (5–100  $\mu\text{m}$ ), a virus (10–500 nm), a protein (1–50 nm), or a nucleic acid (2 nm wide and 5–100 nm long). This allows close interaction between the nanoparticles and the biological entity of interest thus leading to better integration of nanotechnology and biotechnology. In addition to the advantage in their size, the physicochemical properties of nanoparticles that are very different from those of bulk materials enhance their proposed applications.

With sophistication and advances in various fields, the macromolecule and nanoparticles interaction helped in ultra-trace detection, imaging, biomolecules detection, drug and DNA/RNA delivery, cancer therapy, and photodynamic therapy. The different groups of macromolecules that interact with nanoparticles are given in Fig. 6.1. The interaction of nanoparticles with nucleic acids and proteins are very high due to the presence of active functional groups on the surface; while that of carbohydrates and lipids is comparatively lower.

---

N. Vigneshwaran (✉) and P. Jain

Chemical and Biochemical Processing Division, Central Institute for Research on Cotton Technology, Adenwala Road, Matunga, Mumbai 400019, India  
e-mail: nvw75@yahoo.com

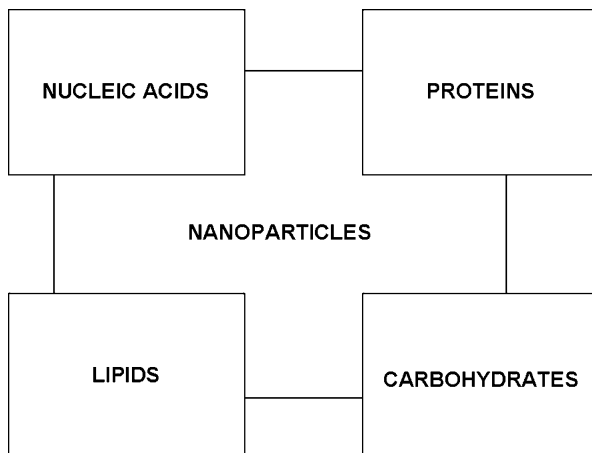


**Fig. 6.1** Interaction of nanoparticles with various biomolecules

## 6.2 Nucleic Acid–Nanoparticles Interaction

Among the various nanoparticles, gold followed by silver and platinum are highly explored for use in various molecular level applications due to their high affinity with nucleic acids. A major breakthrough happened in 1996 when Mirkin, Alivisatos and co-workers coupled nanoparticles to DNA (Mirkin et al. 1996; Alivisatos et al. 1996) and proved that nanoparticles were highly sensitive spectroscopic reporters for the base-pairing of DNA. Mirkin showed that high-packing density of siRNA on the surface of gold nanoparticles inhibits its degradation by various enzymes and facilitates its uptake by HeLa cells (Giljohann et al. 2009). A new colorimetric sensor for mercuric ions was developed by Lie (Xue et al. 2008) by exploiting the highly cooperative base-pairing of DNA bound gold nanoparticles that result in sharp melting transitions. The binding of mercuric ions between mismatched thymine base tips the balance in favor of hybridization and particle aggregation at room temperature. The folding state of DNA aptamers on gold nanoparticles surfaces modulates their electrostatic interaction and thus also affects the aggregation of particles. The oligonucleotides are usually coupled on the surface of gold nanoparticles by means of thiol adsorption.

As electrochemical intercalators, gold (Au) nanoparticles show high catalysis activity and compatibility for detection of biological molecules. An electrochemical approach for sequence-specific DNA-binding transcription factor detection by Au nanoparticle-catalyzed silver (Ag) enhancement at interface between electrodes and electrolyte solutions was reported by Pan et al. 2008 (Fig. 6.2). Here unimolecular hairpin oligonucleotides were self-assembled onto Au electrode surface and their elongation on Au electrode surface was carried out to form double-stranded oligonucleotides with transcription factor NF- $\kappa$ B (nuclear factor-kappa B) binding sites. Au nanoparticle-catalyzed Ag deposition was detected by anodic

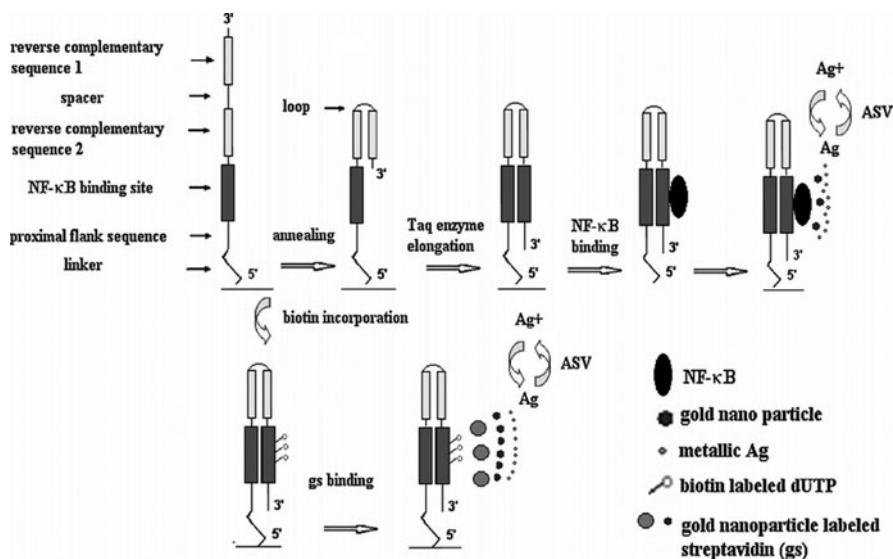


**Fig. 6.2** Principle of Au nanoparticle-based electrochemical detection of NF- $\kappa$ B and DNA interaction. Unimolecular hairpin oligonucleotides were immobilized on Au electrodes with 5' modified with thiol group. Then elongation of the unimolecular hairpin oligonucleotides to double-stranded oligonucleotides was carried out. Electrochemical approaches were applied to verify the elongation on Au electrodes. One was detection of the intrinsic guanine signals of double-stranded DNA without any indicators. The other was incorporation of biotin-labeled dUTP during the elongation followed by the addition of Au nanoparticle-labeled streptavidin and detection of ASV signals of Au nanoparticle-catalyzed Ag deposition. After the verification steps, NF- $\kappa$ B was bound to elongated double-stranded DNA and Au nanoparticles were reacted with the bound NF- $\kappa$ B. Subsequently, the ASV signals of Au nanoparticle-catalyzed Ag deposition were analyzed [with permission from Pan et al. (2008)]

stripping voltammetry (ASV) for NF- $\kappa$ B binding. It was found that this method for the detection of sequence-specific DNA-binding protein showed pronounced specificity and that the detection limit was as low as 0.1 pM.

### 6.3 Protein–Nanoparticles Interaction

Calvo exploits both the scattering and electrochemical properties of gold–glucose oxidase (core–shell) nanoparticles to develop a surface-enhanced Raman-based sensor for detection of glucose in the millimolar concentration (Scodeller et al. 2008). The optical spectroscopic study (Delfino and Cannistraro 2009) on the hybrid system obtained by conjugating the electron transfer blue copper protein Az to 20-nm sized gold nanoparticles provided interesting information on the interactions occurring at the interface between the protein and the metal surface

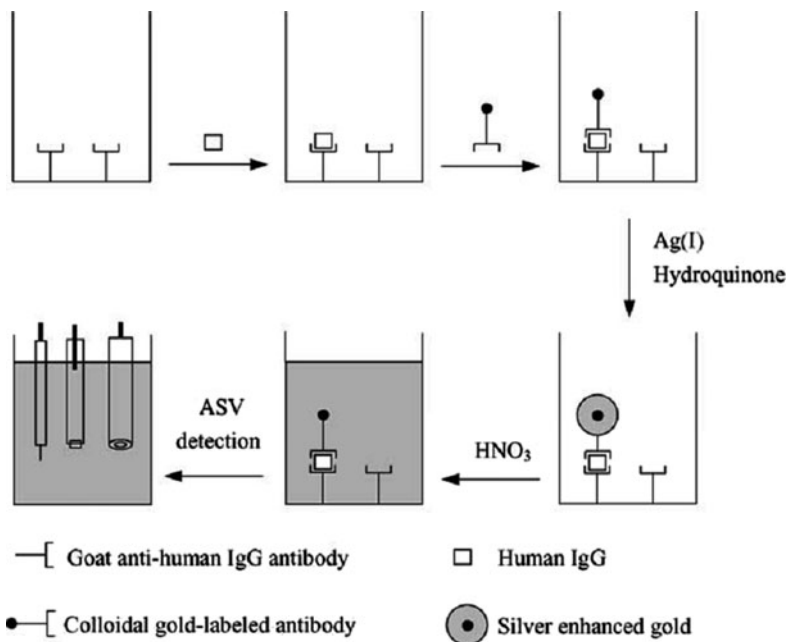


**Fig. 6.3** Schematic representation of the analytical procedure of the heterogeneous electrochemical immunoassay based on silver-enhanced gold nanoparticle label [with permission from Chu et al. (2005)]

and on the resulting photophysical properties of the system. The analysis of the plasmon resonance band of the composite along with DLS results confirmed the interaction of Az with gold surface, probably involving a monolayer of protein molecules grafted on AuNPs. Each nanoparticle was estimated to bind at maximum 140 Az molecules which were thought to preserve their natural folding. The binding constant of proteins is proved to vary depending on the shape of nanoparticles; it was higher for BSA with spherical shaped gold nanoparticles than to that of rod shaped (Iosin et al. 2009). The principle of the heterogeneous electrochemical immunoassay (Chu et al. 2005) based on silver-enhanced colloidal gold is depicted in Fig. 6.3 and it was applied to human IgG analyte. Primary antibodies specific for human IgG are adsorbed passively on the walls of a polystyrene microwell. The human IgG analyte is first captured by the primary antibody and then sandwiched by a secondary colloidal gold-labeled antibody. After removal of the unbound labeled antibody, the silver-enhancer solution is added and incubated in the dark. As the silver ions in the silver-enhancer solution can only be catalytically reduced exclusively on the gold colloids, a large amount of specific silver deposition is produced at the walls of the polystyrene microwell through the catalytic reduction of the silver ions on the antibody–colloidal gold conjugate. The silver metal thus deposited is then dissolved in an acidic solution and the silver ions ( $\text{AgI}$ ) released in solution are quantitatively determined at a glassy-carbon electrode by ASV.

The electrochemical signal is directly proportional to the amount of analyte (human IgG) in the standard solution or sample.

The paracrystalline proteinaceous surface layers (S-layers) are one of the most common surface structures present in all major phylogenetic groups of bacteria and in almost all archaea. They are composed of protein or glycoprotein monomers of a molecular weight between 40 and 200 kDa with the ability to self-assemble into two-dimensional paracrystalline arrays exhibiting oblique (p1, p2), square (p4), or hexagonal (p3, p6) symmetries or other structures. Due to the crystalline arrangement of the S-layer, functional groups such as carboxyl-, amino- or hydroxyl groups, are found in well-defined position and orientation on the protein meshwork. S-layers have been used as templates for the fabrication of different inorganic nanocrystal arrays (Pollmann et al. 2006).

## 6.4 Lipids–Nanoparticles Interaction

Pulmonary surfactant adsorption to form a surface film normally occurs through unique vesicular structures known as tubular myelin (Bakshi et al. 2008). Gold nanoparticles inhaled into the alveolar space during the breathing process could impact with such surface films, become wetted, and lined with phospholipids bilayers (Fig. 6.4).

## 6.5 Carbohydrates–Nanoparticles Interaction

Although several researchers worked on nanomaterials functionalized with proteins, peptides, DNA and RNA during the last decade, very few of them reported on nanoparticles covered with carbohydrates. The accurate detection of carbohydrates is of interest for improving long-term health care. Numerous efforts have been made using spectroscopic methods such as absorbance and luminescence to investigate carbohydrate binding to labeled organic compounds or superstructures. Tiopronin-coated silver nanoparticles [Fig. 6.5 (Zhang et al. 2004)] were prepared using a modified Brust reaction with a 1:1 mole ratio of tiopronin and silver nitrate in methanol. The boronic acid capped on the silver nanoparticle had a higher detective sensitivity for the polysaccharide. This method may help to facilitate the study of complex macromolecular structures such as glycoproteins, which have a substantial polysaccharide component.

Though at its nascent stage, a variety of applications (Fig. 6.6) of glyco-quantum dots, gold glyconanoparticles and magnetic glyconanoparticles will be developed in the near future (Fuente and Penades 2006). The interesting physical, chemical, and biological properties of the glyconanoclusters will allow them to extend their utility in Biomedicine, Biotechnology, and Material Science.

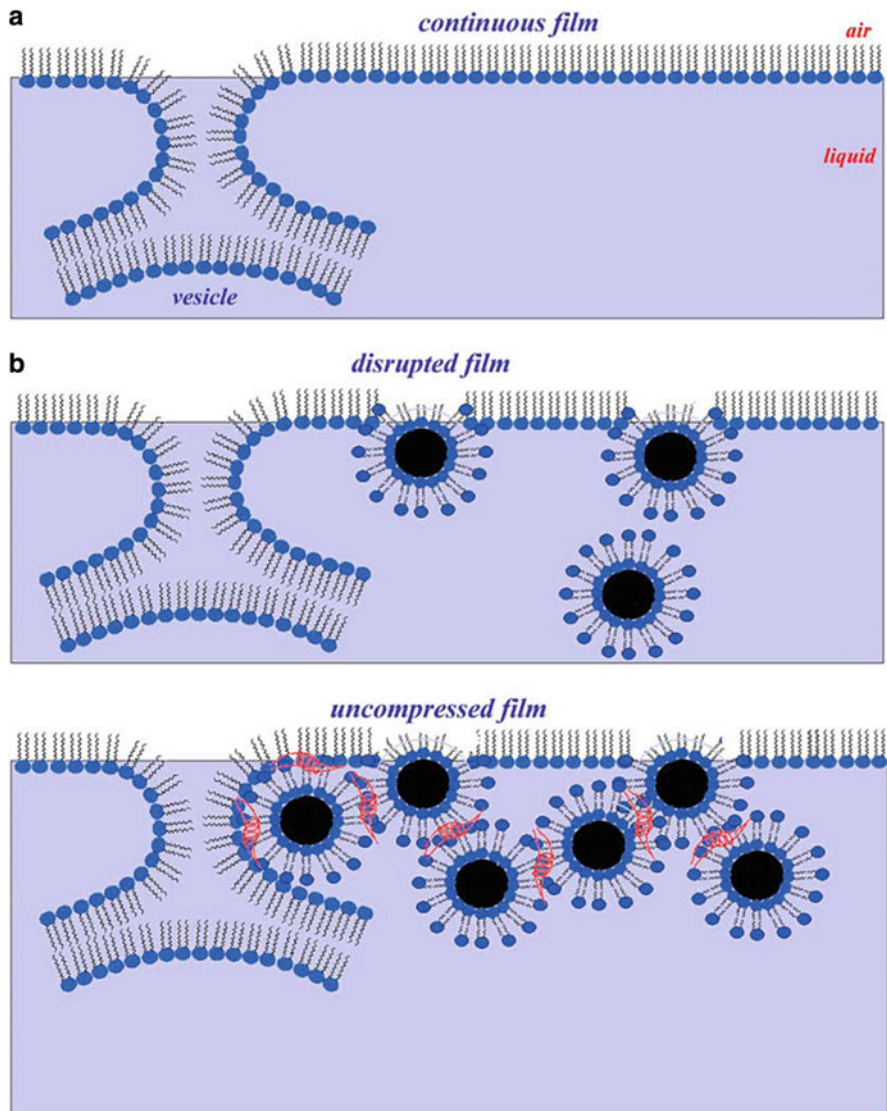


**Fig. 6.4** Schematic representation of potential inhibitory effects of Au NP on pulmonary surfactant in the alveolar space (not to scale). (a) A continuous surfactant film (monolayer and underlying multilayer) formed by the rupture of pulmonary surfactant vesicles at the air–liquid interface as the hypothetical rate-limiting intermediate structure between bilayer vesicles and the interfacial monolayer (see the literature (3, 7, 67) for further details). (b) The disrupted interfacial surfactant film due to the entrapping of Au NP (from the air phase as pollutants) by pulmonary surfactant. (c) The self-aggregation of lipid capped Au NP in the presence of SP-B shown in ladder like lines. [with permission from Bakshi et al. (2008)]

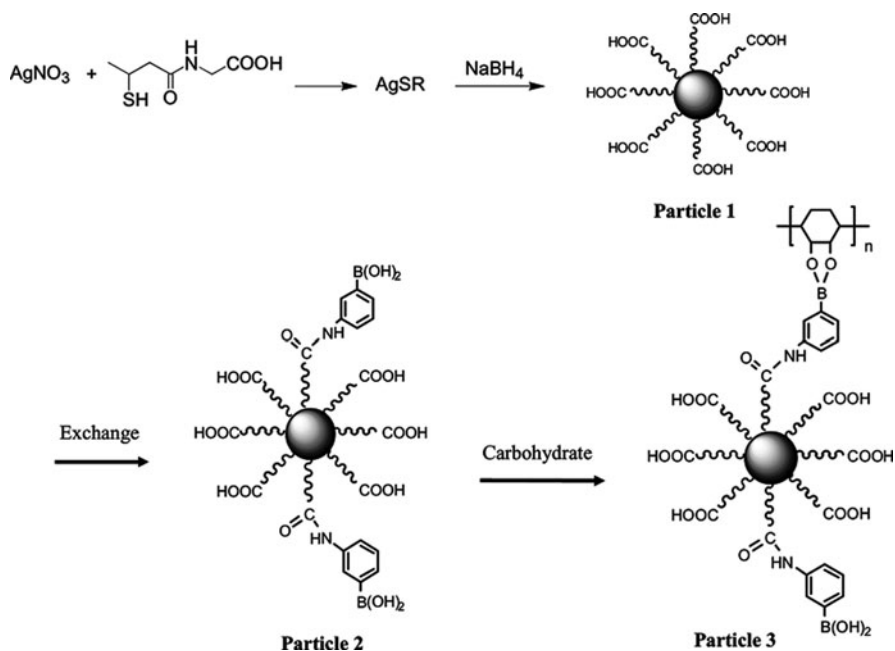


**Fig. 6.5** Preparation of tiopronin-monolayer-protected silver nanoparticle, ligand exchange by compound 1, and coupling with saccharide [with permission from Zhang et al. (2004)]

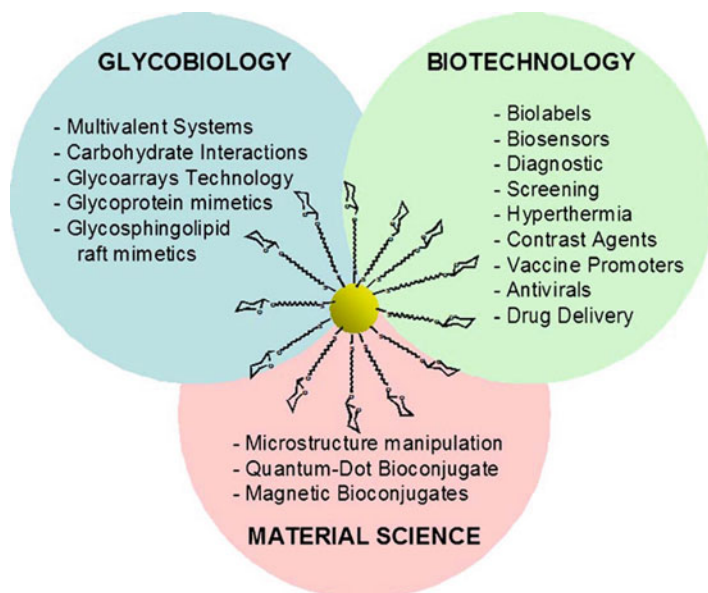


**Fig. 6.6** The glyconanoparticle concept and its potential applications [with permission from Fuente and Penades (2006)]

Although the use of colloidal particles of metals and semiconductors as pigments dates back many centuries, and although the recipe for stable 6 nm diameter particles of gold (“Ruby gold”) was famously devised by Faraday in 1857 (Zhu et al. 2008) the unique properties of nanomaterials and their promise for applications in biochemistry, cell biology, and medicine have only recently been appreciated.

Research in the current decade has led to a much more sophisticated set of tools for controlling the size, shape, dispersity, and surface chemistry of nanoparticles. The complexity of nanoparticle structures as nanoshells, prisms, Janus particles, derivatized nanotubes, core–shell particles, and striped nanowires, to name a few, offers new tools to tailor particles to specific problems in ultra-trace detection, imaging, drug delivery, DNA/RNA delivery, and therapy. Sophisticated schemes for signal amplification, enhanced bioaffinity through multivalency, and cooperative binding highlight the synergy of nanoparticles as platforms for biological molecular recognition. The deliberate design of nanoparticles for biological applications, for example for drug delivery or for dual functions (such as imaging and magnetic manipulation of cells), has been enabled by these new advances in nanoparticle synthesis. Nanoparticles can have several functionalities that enhance their effectiveness for drug delivery, including transport and targeting within cells and controlled release.

Both biotechnology and materials science meet at the same length scale (nanometer). To exploit and to utilize the concepts administered in natural nanometer-scale systems, the development of nanochemistry is crucial (Philp and Stoddart 1996). On the other hand, commercial requirements to produce increasingly miniaturized microelectronic devices strongly motivate the elaboration of nanoscale systems. The structural dimensions of computer microprocessors are currently in the range of about 200 nm. They are only just available by conventional top down processes (miniaturization processes) such as photolithography, but for the foreseeable future, such technologies hardly allow the large-scale production of parts that are significantly smaller than 100 nm. “There is plenty of room at the bottom”, as Nobel physicist Richard Feynman pointed out more than 50 years ago (Feynman 1961).

## 6.6 Interactions of Macromolecules and Nanoparticles in Various Applications

### 6.6.1 Biotemplates and Biomimetics

The study of biosynthesis of nanomaterials offers a valuable contribution into materials chemistry. Yan et al. (2003) have reported DNA templated synthesis of highly conductive, uniform-width, silver nanowires. The ability of some microorganisms such as bacteria and fungi to control the synthesis of metallic nanoparticles offers a viable approach as an alternative to chemical and physical ones. Recently, Sadowski et al. (2008) have reported the biosynthesis of silver nanoparticles using *Penicillium*



fungi. Various organic molecules and polymers such as amino acids, citric acid, vitamins, cyclodextrin, chitosan, starch, etc. can be employed as biotemplates for the synthesis of metal nanoparticles. Recently Xia et al. reported a facile synthetic approach for preparing water-soluble  $\text{Fe}_3\text{O}_4$  NPs using cyclodextrin in aqueous medium.

Biomimetic processes have attracted huge attention in recent years due to their significant applications in biomedical areas such as bone tissue engineering. Titanium is a well-known bone repairing material widely used in orthopedics and dentistry. It has a high fracture resistance, ductility, and weight to strength ratio. Unfortunately, it suffers from the lack of bioactivity, as it does not support cell adhesion and growth well. Apatite coatings are known to be bioactive and to bond to the bone. Ma et al. (2003) have employed a biomimetic process, to form a nanocrystallite apatite coating on metal. A thin bone-like apatite layer was coated onto titanium (Ti) metals via an alkali pretreatment. Their work has shown that the apatite layer grown in this way exhibits nanostructure and has similar stoichiometry to that of natural bone. It was also observed that the thickness of the apatite layer increases as the immersion period increases. Their studies have shown that a uniform coating of carbonate-containing apatite (hydroxyapatite) is firmly adhered on the Ti metal. The adhesion of the apatite layer on the Ti substrate was confirmed by a shear test, which showed an average value of 9.5 MPa indicating good mechanical properties. The bioactivity of the coating was examined by cell culturing experiments and was found to be satisfactory.

### 6.6.2 Drug Delivery

Nanoparticle-based drug delivery systems are increasingly being used for treatment of certain types of cancer, as opposed to chemotherapy or radiation therapy. The conventional treatments are administered resulting in deleterious side-effects as the drug/therapy attacks normal, healthy cells in addition to the target tumor cells. The application of magnetic nanoparticles (MNPs) as carriers for drug delivery overcomes this major disadvantage of nonspecificity. The objectives are twofold: (1) to reduce the amount of systemic distribution of the cytotoxic drug, thus reducing the associated side-effects; and (2) to reduce the dosage required by more efficient, localized targeting of the drug. In magnetically targeted therapy, a cytotoxic drug is attached to a biocompatible magnetic nanoparticle carrier such as superparamagnetic iron oxide nanoparticles (SPIONs) of  $\gamma\text{-Fe}_2\text{O}_3$  or  $\text{Fe}_3\text{O}_4$ . These particles are well dispersed in water, or form composites with organic or inorganic matrices in the form of beads. Superparamagnetic magnetization can reach nearly the magnetization saturation of ferromagnetic iron oxide by application of an external magnetic field. This behavior allows the tracking of such particles in a magnetic field gradient without losing the advantage of a stable colloidal suspension. These drug/carrier complexes are injected into the patient via the circulatory system usually in the form of a biocompatible ferrofluid. When the particles have entered the

bloodstream, external, high-gradient magnetic fields are used to concentrate the complex at a specific target site within the body. Once the drug/carrier is concentrated at the target, the drug can be released either via enzymatic activity or changes in physiological conditions such as pH, osmolality, or temperature, and be taken up by the tumor cells.

Depending on the synthesis procedure, nanocapsules are obtained where the MNPs are coated with a biocompatible molecule attached through a linker. Coating with a neutral and hydrophilic compound (i.e., polyethylene glycol, polysaccharides, dysopsonins (HSA), biotin, etc.) increases the circulatory half-life from minutes to hours or days. The key parameters in the behavior of MNPs are related to surface chemistry, size (magnetic core, hydrodynamic volume, and size distribution), and magnetic properties (magnetic moment, remanence, coercivity).

In 1996, the first Phase I clinical trial was carried out by Lubbe et al. (1996) in patients with advanced and unsuccessfully pretreated cancers using MNPs loaded with epirubicin. FeRx, Inc. (founded in 1997) produced doxorubicin-loaded MNPs (Goodwin et al. 1999) consisting of metallic Fe ground together with activated carbon. A Phase II clinical study in patients with primary liver cancer was conducted using these MNPs, although the trial was not successful. Chemicell GmbH has commercialized TargetMAG-doxorubicin NPs (Steinfeld and Pauli 2006) involving a multidomain magnetite core and a cross-linked starch matrix with terminal cations that can be reversibly exchanged by the positively charged doxorubicin. The particles have a hydrodynamic diameter of 50 nm and are coated with 3 mg/ml doxorubicin. These NPs loaded with mitoxantrone (Wiekhorst et al. 2006) have already been used in animal models with successful results. Chemicell has also commercialized FluidMAG® for drug delivery applications. MNP hydro-gel (MagNaGel®) from Alnis Biosciences, Inc. is a material comprising chemotherapeutic agents, Fe oxide colloids, and targeting ligands.

A wide variety of molecules has been loaded onto organic and inorganic shells, e.g., by chemical functionalization or physical absorption. The list includes tumor-recognition moieties such as antibodies in “smart” contrast agents, and enzymes, toxins, genes(transfection) (Schillinger et al. 2005), growth factors, radionucleotides, folic acid, and drugs (mitoxantrone, tamoxifen, cefradine, doxorubicin, ammonium glycyrrhizinate, fludarabine, danorubicin, cisplatin and gemcitabine, pingyangmycin, nonsteroidal anti-inflammatory drugs (Taepaiboon et al. 2006), amethopterin, mitomycin, paclitaxel, diclofenac sodium, and adriamycin) for drug delivery applications.

Another approach to cancer treatment is hyperthermia where the tumor region is heated locally to the intended temperature without damaging normal tissue. The procedure involves dispersing magnetic particles throughout the target tissue and applying an AC magnetic field with sufficient strength and frequency to cause the particles to heat. The generated heat conducts into the immediately surrounding diseased tissue, and the cancer is destroyed. Magnetic liposomes composed of Mn-ferrite have been prepared through thin film hydration (Pradhan et al. 2007), loaded with 2:1 ratio of egg-phosphatidyl choline (egg-PC) and cholesterol, which have been found suitable for treating hyperthermia.

In addition to cancer treatment, MNPs can also be used in anemic chronic kidney disease and disorders associated with the musculoskeletal system (i.e., local inflammatory processes, side effects). For those disorders, superparamagnetic Fe oxide NPs (SPION), in conjunction with external magnetic fields, seem a suitable alternative for drug delivery to inflammatory sites (Neuberger et al. 2005).

### 6.6.3 *Bioimaging and Magnetic Resonance Imaging*

The rapid development of bio-medical sciences demands new advanced techniques and instruments to investigate cells and cellular processes. In the last years, luminescent nanoparticles (NPs) have attracted growing attention as a versatile and promising tool for bio-imaging. Bio-imaging involves developing multifunctional nanoparticles with tailored optical and/or magnetic properties for visualizing complex cellular structures (in tissues and organs), receptors, tumor cells, and masses.

The II–VI semiconductor nanocrystals were prepared for use as fluorescent probes in biological staining and diagnostics. The advantages of the broad, continuous excitation spectrum were demonstrated in a dual-emission, single-excitation labeling experiment on mouse fibroblasts (Bruchez et al. 1998).

The II–VI quantum dots (QDs) have demonstrated usefulness for several applications ranging from cell labeling to tracking cell migration, from flow cytometry to genomic and proteomic detection, high throughput screening of biology, etc., however, their application in biology and medicine is hampered by their inherent chemical toxicity. Unlike bulk Si that is not a good light emitter, nanostructured Si can emit photons in the visible- near IR range with a reasonable efficiency. It follows that silicon nanoparticles (Si-NPs) have the potential to overcome the inherent limitations in the biomedical use of QDs since silicon is inert, nontoxic, abundant, and economical. Moreover, the silicon surface is apt to chemical functionalization, thus allowing for numerous stabilization and bioconjugation steps. For *in vitro* and *in vivo* applications, NPs were coated with a biocompatible polymer such as functional silanes terminated with amine or epoxy groups, and then were conjugated with poly (ethyleneglycol) to prevent the formation of large aggregates in order to improve biodistribution. It was also found that the use of HF/HNO<sub>3</sub> mixture as etching agent can make the Si-NPs photoluminescent with various emission colors depending on the etching time. Preliminary *in vivo* experiments were performed by detection of the photoluminescence signal in continuous mode after intravenous injection of a colloidal solution of Si-NPs in tail vein of a mouse.

Another class of materials of great interest for bio-imaging is the metallic NPs of Ag and Au. When compared with organic chromophores, the absorption and scattering cross-section of Au and Ag NPs are several orders of magnitude higher. As a result, these NPs have recently been explored as contrast agents (CA) for optical imaging of tumors. In addition, it is possible to tailor the spectral dependence of absorption and scattering coefficients of Au and Ag spherical NPs by engineering their geometrical parameters. The optical resonant behavior is due to the collective

electronic or plasmonic resonance which depends not only from the metal but also from the particle shape. Tuning the plasmon resonance, combined with the easy bioconjugation of Au nanostructures, results in a combination of features which are ideal for biomedicine.

An interesting and novel application of nanoparticles in biology is their use as intracellular magnetic labels in nuclear magnetic resonance imaging (MRI). The presence of MNPs near a cell results in a much faster rate of magnetic relaxation of protons in the cell. Since NMR imaging is based on the rate of magnetic relaxation, there is distinct contrast introduced. Iron oxide nanoparticles are the most commonly used superparamagnetic contrast agents. Dextran-coated iron oxides are biocompatible and are excreted via the liver after the treatment. They are selectively taken up by the reticuloendothelial system, a network of cells lining blood vessels whose function is to remove foreign substances from the bloodstream. MRI contrast relies on the differential uptake of different tissues; thus by modifying the size and the nature of coating, it is possible to modify the organ distribution and the pharmacokinetics and consequently the clinical application. Magnetic iron oxide NPs can be used as negative MRI contrast agents (Laurent et al. 2008). They have marked T2 relaxivity due to their high magnetic moment, which generates microscopic field inhomogeneities. Consequently they produce a strong decrease in signal intensity in the organs in which they accumulate. There are currently two distinct classes in this family of products depending on the size of the particles: SuperParamagnetic Iron Oxide (SPIO), with mean particle diameter greater than 50 nm, and Ultra-small SPIO particles (USPIO) smaller than 50 nm.

Cengelli et al. (2006) have developed SPIONs coated with dextran or polyvinyl alcohol, to enhance detection of neurodegenerative diseases. They monitored the uptake by isolated brain-derived endothelial and microglial cells and found no cytotoxicity or inflammatory activation even at a much higher levels.

In another study concerning atherosclerosis by Hildebrandt et al. (2007), SPIONs were coated with dextran having negatively charged functionalities, in order to connect specific peptide labels by electrostatic interactions. Peptides containing a specific recognition sequence and amino acids that are positively charged under physiological conditions were bound to the negatively charged dextran. These peptides can then selectively bind to the receptors on the damaged artery walls and can be imaged. Similar work using PEG-gallol has been carried out (Amstad et al. 2007) but with Neutravidin, a peptide binding protein, as the linker between PEG and peptide.

#### **6.6.4 Sensors and Biosensors**

Localized surface plasmon resonance of metal nanoparticles has been exploited in several ways for sensing applications, because this optical characteristic is the basis of various new and highly promising set ups to transduce biorecognitive interactions into visible signals. Semiconductor nanoparticles are viable for sensors due to

three main reasons – (1) the sensitivity of surface plasmon band to its immediate environment offers an opportunity to detect attached molecules and environmental changes, (2) the reversible aggregation of plasmon resonant particles through specific linkers provides an excellent means for colorimetric assays, and (3) the ultra-bright light scattering from each plasmon resonant particle makes the optical detection of a single molecular target possible.

Nam et al. (2003) have developed an ultra-sensitive nanoparticle-based bar-coding method for detecting protein analytes. The system relies on magnetic microparticle probes with antibodies that specifically bind a target of interest [prostate-specific antigen (PSA) in this case] and nanoparticle probes that are encoded with DNA that is unique to the protein target of interest and antibodies that can sandwich the target captured by the microparticle probes. Magnetic separation of the complexed probes and target followed by dehybridization of the oligonucleotides on the nanoparticle probe surface allows the determination of the presence of the target protein by identifying the oligonucleotide sequence released from the nanoparticle probe. Because the nanoparticle probe carries with it a large number of oligonucleotides per protein binding event, there is substantial amplification and PSA can be detected at 30 aM concentration.

Edelstein et al. (2000) have developed the BARC sensor for the detection of biological warfare agents. The Bead ARray Counter (BARC) is a multi-analyte biosensor that uses DNA hybridization, magnetic microbeads, and giant magneto-resistive (GMR) sensors to detect and identify biological warfare agents. The current prototype is a table-top instrument consisting of a microfabricated chip (solid substrate) with an array of GMR sensors, a chip carrier board with electronics for lock-in detection, a fluidics cell and cartridge, and an electromagnet. DNA probes are patterned onto the solid substrate chip directly above the GMR sensors, and sample analyte containing complementary DNA hybridizes with the probes on the surface. Labeled, micron-sized magnetic beads are then injected that specifically bind to the sample DNA. A magnetic field is applied, removing any beads that are not specifically bound to the surface. The beads remaining on the surface are detected by the GMR sensors, and the intensity and location of the signal indicate the concentration and identity of pathogens present in the sample. The current BARC chip contains a 64-element sensor array; however, with advancement in technology, chips with millions of these GMR sensors will soon be commercially available, allowing simultaneous detection of thousands of analytes. Because each GMR sensor is capable of detecting a single magnetic bead, in theory, the BARC biosensor should be able to detect the presence of a single analyte molecule.

Enzymes are also commonly used in biosensors because of their high specificity. Biosensor applications require a highly active immobilized enzyme system that allows the maintenance of an efficient connection between the sensing molecule and the transduction component of the biosensor. Immobilization strategies include covalent bonding, physical adsorption, cross-linking, encapsulation, or entrapment. Betancor et al. (2006) have reported a strategy for chemically associating silica nanospheres containing entrapped  $\beta$ -galactosidase to a silicon support for the detection of lactose. The immobilization strategy resulted in a three-dimensional

network of silica attached directly at the silicon surface, providing a significant increase in surface area and a corresponding 3.5-fold increase in enzyme loading compared to enzyme attached directly at the surface. The immobilized  $\beta$ -galactosidase prepared by silica deposition was stable and retained more than 80% of its initial activity after 10 days at 24°C.

A range of biosensors immobilized with specific enzymes are already available that include urease base (Pijanowska and Torbicz 1997) biosensors for urea, lipase-based biosensors for triglycerides, glucose oxidase-based glucose biosensor, acetylcholine esterase biosensors (Starodub et al. 1999) for pesticide detection and many more.

## 6.7 Future Perspectives

The future development in basic understanding of nanoparticles and their interaction with macromolecules depends heavily on joint ventures between materials science, chemistry, physics, and life sciences. In addition, the current advances in bioinformatics and biotechnology will also be beneficial in this field to understand the nature of interactions at the nanoscale. In spite of various efforts going on all over the World, still there is a tremendous need to explore the nanoscale interaction with a collaborative mode between experts in their respective areas. Although commercial applications are very rare as of now, this interdisciplinary work has a huge potential for designing and development of novel materials for use in sensors, transducers, and biomedical components.

## 6.8 Conclusions

Interaction of nanomaterials and macromolecules are exciting in the sense both are in the same scale range but difficult to visualize directly. This exploration is being driven by the current needs of applications in various fields like biomedical and material science. With a collaborative effort of experts from various fields, it might open the way for novel nanosensors, nano-scale solar devices/batteries, molecular switches, and interface between mechanical and living systems. Thus, it is certain to make more advanced and interesting developments in this area of research over the coming decade.

## References

- Alivisatos AP, Johnsson KP, Peng XG, Wilson TE, Loweth CG, Bruchez MP, Schultz PG (1996) Organization of 'nanocrystal molecules' using DNA. *Nature* 382:609–611
- Amstad E, Zurcher S, Wong JY, Textor M, Reimhult E (2007) Surface functionalization of single superparamagnetic iron oxide nanoparticles for targeted magnetic resonance imaging (MRI). *Eur Cell Mater* 14(3):43

- Bakshi MS, Zhao L, Smith R, Possmayer F, Peterson NO (2008) Metal nanoparticle pollutants interfere with pulmonary surfactant function in vitro. *Biophys J* 94:855–868
- Betancor L, Luckarift HR, Spain JC (2006) Three dimensional immobilization of  $\beta$ -galactosidase on a silicon surface. *Biotechnol Bioeng* 99(2):261–267
- Bruchez M Jr, Moronne M, Gin P, Weiss S, Alivisatos AP (1998) Semiconductor nanocrystals as fluorescent biological labels. *Science* 281(5385):2013
- Cengelli F, Maysinger D, Tschudi-Monnet F, Montet X, Corot C, Fink AP, Hofmann H, Juillerat-Jeanneret L (2006) Interaction of functionalized superparamagnetic iron oxide nanoparticles with brain structure. *J Pharmacol Exp Ther* 318(1):108–116
- Chu X, Fu X, Chen K, Shen GL, Yu RQ (2005) An electrochemical stripping metalloimmunoassay based on silver-enhanced gold nanoparticle label. *Biosens Bioelectron* 20:1805–1812
- de la Fuente JM, Penades S (2006) Glyconanoparticles: types, synthesis and applications in glycoscience, biomedicine and material science. *Biochim Biophys Acta* 1760(4): 631–651
- Delfino I, Cannistraro S (2009) Optical investigation of the electron transfer protein azurin-gold nanoparticle system. *Biophys Chem* 139:1–7
- Edelstein RL, Tamanaha CR, Sheehan PE, Miller MM, Baselt DR, Whitman LJ (2000) The BARC biosensor applied to the detection of biological warfare agents. *Biosens Bioelectron* 14: 805–813
- Feynman RP (1961) There's plenty of room at the bottom: An invitation to enter a new field of physics. In: Miniaturization. Gilbert HD (ed), Reinhold, New York, pp 282–296
- Giljohann DA, Seferos DS, Prigodich AE, Patel PC, Mirkin CA (2009) Gene regulation with polyvalent siRNA–nanoparticle conjugates. *J Am Chem Soc* 131(6):2072–2073
- Goodwin S, Peterson C, Hoh C, Bittner C (1999) Targeting and retention of magnetic targeted carriers (MTCs) enhancing intra-arterial chemotherapy. *J Magn Magn Mater* 194(1–3): 132–139
- Hildebrandt N, Hermsdorf D, Signorell R, Schmitz SA, Diederichsen U (2007) Superparamagnetic iron oxide nanoparticles functionalized with peptides by electrostatic interaction. *ARKIVOC* 5:79–90
- Iosin M, Toderas F, Baldeck PL, Astilean S (2009) Study of protein-gold nanoparticle conjugates by fluorescence and surface enhanced Raman scattering. *J Mol Struct* 924–926:196–200
- Katz E, Willner I (2004) Integrated nanoparticles-biomolecule hybrid systems: synthesis, properties and applications. *Angew Chem Int Ed* 33:6042–6108
- Laurent S, Forge D, Port M, Roch A, Robic C, Vander Elst L, Muller RN (2008) Magnetic iron oxide nanoparticles: synthesis, stabilization, vectorization, physicochemical characterizations, and biological applications. *Chem Rev* 108:2064
- Lubbe AS, Bergemann C, Huhnt W, Fricke T, Riess H, Brock JW, Huhn D (1996) Preclinical experiences with magnetic drug targeting: tolerance and efficacy. *Cancer Res* 56:4694–4701
- Ma J, Wong H, Kong LB, Peng KW (2003) Biomimetic processing of nanocrystallite bioactive apatite coating on titanium. *Nanotechnology* 14:619
- Mirkin CA, Letsinger RL, Mucic RC, Storhoff JJ (1996) A DNA-based method for rationally assembling nanoparticles into macroscopic materials. *Nature* 382:607–609
- Nam JM, Thaxton CS, Mirkin CA (2003) Nanoparticle-based bio-bar codes for the ultrasensitive detection of proteins. *Science* 301(5641):1884
- Neuberger T, Schopf B, Hofmann H, Hofmann M, von Rechenberg B (2005) Superparamagnetic nanoparticles for biomedical applications: possibilities and limitations of a new drug delivery system. *J Magn Magn Mater* 293(1):483–496
- Pan Q, Zhang R, Bai Y, He N, Lu Z (2008) An electrochemical approach for detection of specific DNA-binding protein by gold nanoparticle – catalyzed silver enhancement. *Anal Biochem* 375:179–186
- Philp D, Stoddart JF (1996) Self-assembly in natural and unnatural systems. *Angew Chem Int Ed Eng* 35:1154–1196
- Pijanowska DG, Torbicz W (1997) pH-ISFET based urea biosensor. *Sens Actuators B* 44:370–376

- Pollmann K, Raff J, Merroun M, Fahmy K, Selenska-Pobell S (2006) Metal binding by bacteria from uranium mining waste piles and its technological applications. *Biotechnol Adv* 24:58–68
- Pradhan P, Giri J, Banerjee R, Bellare J, Bahadur D (2007) Preparation and characterization of manganese ferrite-based magnetic liposomes for hyperthermia treatment of cancer. *J Magn Magn Mater* 311(1):208–215
- Sadowski Z, Maliszewska IH, Grochowalska B, Polowczyk I, Koźlecki T (2008) Synthesis of silver nanoparticles using microorganisms. *Mater Sci Poland* 26(2):419
- Schillinger U, Brill T, Rudolph C, Huth S, Gersting S, Krotz F, Hirschberger J, Bergemann C, Plank C (2005) Advances in magnetofection – magnetically guided nucleic acid delivery. *J Magn Magn Mater* 293(1):501–508
- Scodeller P, Flexer V, Szamocki R, Calvo EJ, Tognalli N, Troiani H, Fainstein A (2008) Wired-Enzyme Core-Shell Au Nanoparticle Biosensor. *J Am Chem Soc* 130:12690–12697
- Starodub NF, Torbicz W, Pijanowska D, Starodub VM, Kanjuk MI, Dawgul M (1999) Optimisation methods of enzyme integration with transducers for analysis of irreversible inhibitors. *Sens Actuators B* 58:420–426
- Steinfeld U, Pauli N (2006) T. Lymphocytes as potential therapeutic drug carrier for cancer treatment. *Int J Pharm* 311:229–236
- Taepaiboon P, Rungsardthong U, Supaphol P (2006) Drug-loaded electrospun mats of poly(vinyl) alcohol fibers and their release characteristics of four model drugs. *Nanotechnology* 17(9):2317–2329
- Wiekhorst F, Lyer S, Tietze R, Jurgons R, Richter H, Schwarz K, Trahms L, Alexion C (2006) Distribution of magnetic nanoparticles after magnetic drug targeting in an *ex vivo* Bovine Artery Model. *J Nanosci Nanotechnol* 6:3222
- Xue X, Wang F, Liu X (2008) One-step, room temperature, colorimetric detection of mercury ( $Hg^{2+}$ ) Using DNA/nanoparticle conjugates. *J Am Chem Soc* 130:3244–3245
- Yan H, Park SH, Finkelstein G, Reif JH, LaBean TH (2003) DNA-templated self-assembly of protein arrays and highly conductive nanowires. *Science* 301(5641):1882
- Yezhelyev MY, Gao X, Xing Y, Al-Hajj A, Nie S, Regan RMO (2006) Emerging use of nanoparticles in diagnosis and treatment of breast cancer. *Lancet Oncol* 7:657–667
- Zhang J, Geddes CD, Lakowicz JR (2004) Complexation of polysaccharide and monosaccharide with thiolate boronic acid capped on silver nanoparticle. *Anal Biochem* 332:253–260
- Zhu Z, Tang Z, Phillips JA, Yang R, Wang H, Tan W (2008) Regulation of singlet oxygen generation using single-walled carbon nanotubes. *J Am Chem Soc* 130:10856–10857



**Part II**  
**Synthesis and Process Development**

# Chapter 7

## Microbial Synthesis of Metal Nanoparticles

Irena Maliszewska

### 7.1 Introduction

One of the most important aspects in researching nanotechnology is the synthesis of metal nanoparticles of well-defined sizes, shapes and controlled monodispersity. The most common methods of preparation are based on harsh chemicals, such as strong reducing agents, surfactants, polymer capping agents and, occasionally, organic solvent systems, to achieve better results. Therefore, there is a necessity to develop an environmental friendly nanoparticle formation processes which do not use toxic chemicals in their synthesis protocols. Thus, researchers in the field of nanoparticle synthesis have turned to biological systems for inspiration.

Many organisms, both unicellular and multicellular, are known to produce inorganic materials, either intracellularly or extracellularly with properties similar to chemically synthesized materials (Bäuerlein 2003). The synthesis of nanomaterials such as silica, metals and metal alloys by biological molecules is known as biomineralization. Over millions of years of evolution nature has evolved various mechanisms to produce such nanomaterials for a wide variety of purposes. Remarkably, all of this synthesis occurs under ambient conditions. This is in sharp contrast to the caustic reagents, high temperatures and pressures that are modernly utilized for industrial synthesis of the same kinds of materials. Moreover, in many cases the nanomaterials are produced under genetic control resulting in specific morphologies, sizes and crystallinities of the structures.

Biological systems provide many examples of specifically modified nanostructured molecules. Perhaps, the best known is the magnetotactic bacteria (Lang et al. 2007). This heterogenous group of prokaryotes could be found in the sediments of a variety of aqueous environments. All of the above bacteria intracellularly

---

I. Maliszewska

Division of Medicinal Chemistry and Microbiology, Faculty of Chemistry, Wrocław University of Technology, Wyspiańskiego 27, 50-370 Wrocław, Poland  
e-mail: irena.helena.maliszewska@pwr.wroc.pl

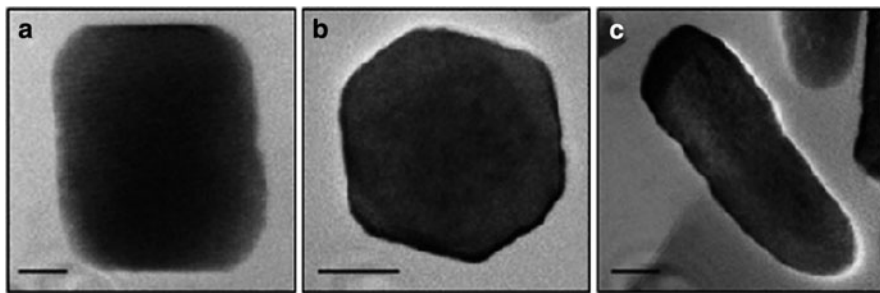


**Fig. 7.1** TEM images of magnetosomes from different bacterial strains: (a) *parallelepipedal projection* of a possibly *pseudo-hexagonal prism*, (b) *hexagonal projection* of a possibly *cuboctahedral crystal*, and (c) *tooth-shaped (anisotropic) magnetosomes* (scale bar 20 nm) [Reproduced from Macromol Biosci (2007) 7:144–151, Wiley-VCH Verlag GmbH & Co. KGaA, Weinheim]

synthesize magnetic nanocrystals in magnetosomes (Fig. 7.1). These particles, composed of greigite ( $\text{Fe}_3\text{S}_4$ ) or magnetite ( $\text{Fe}_3\text{O}_4$ ), have a size range of 40–140 nm and are enveloped by a membrane. The ability of magnetotactic bacteria to navigate along the Earth's magnetic lines helps them to migrate towards the micro- and anaerobic environments in soil or water.

Further examples of nanostructures in biology include diatoms, a group of unicellular eukaryotic organisms (algae) (Bäuerlein 2003). These are found in seas and oceans, brackish water and in fresh water. One of the advantages of using diatoms is that they can be readily recognized by their characteristic ornamented cell walls, which are mostly made of amorphous polysilicic acid. Like diatoms, sponges (phylum *Porifera*), the oldest known metazoan organisms, produce a variety of intricate skeletal elements. Sponges have an especially important ability to build robust structures of amorphous silica ( $\text{SiO}_2 \times n\text{H}_2\text{O}$ ), and/or to utilize calcium carbonate instead.

The production of many other metal and metal alloy nanoparticles by organisms is a consequence of detoxification pathways. More specifically, metals such as gold, silver, copper, cadmium and manganese are present in the environment and play an important part in the biochemical reaction processes, including water cleavage during the oxygenic photosynthesis, respiration with oxygen or nitrate, nitrogen fixation, hydrogen assimilation and the cleavage of urea among other reactions. These are all based on the formation of heavy metal complex compounds. However, at higher concentrations, these heavy metal ions form nonspecific complex compounds in the cell, which can lead to toxic effects (even trace elements such as  $\text{Zn}^{+2}$ ,  $\text{Ni}^+$  and  $\text{Cu}^{+2}$  are toxic at higher concentrations). Other heavy metal cations, for instance  $\text{Hg}^+$ ,  $\text{Cd}^{+2}$  and  $\text{Ag}^+$  are extremely toxic and are highly dangerous for biological functions. For example, they may bind to enzymes in the electron transport chain, which normally coordinate with ions such as magnesium, manganese, zinc or iron, thus preventing the enzyme from shuttling the electrons appropriately, and poisoning the respiratory chain. They might also interfere with the membrane permeability or with the DNA. Thus, the intracellular concentration of

heavy metal ions has to be controlled. The toxic metal ions are incorporated nonspecifically through the cationic membrane system, which normally transports metabolically important cations. Bacteria have evolved specific mechanisms to counteract this kind of uptake, thereby preventing excessive accumulation of toxic metals. These mechanisms include enzymatic detoxification/reduction of the metal ions to less toxic metal salts or zero-valent metals, metal–ion efflux system, and decreases in the membrane permeability. Many studies have confirmed that the enzymatic catalysis and nonenzymatic reduction are the two most important mechanisms involved in bioreduction.

In different microorganisms, various enzymes are believed to take part in the bioreduction process involving the transport of electrons from certain electron donors to metal electron acceptors. Some studies of nonenzymatic reduction mechanism suggested that some organic functional groups of microbial cell walls could be responsible for the bioreduction process (Crookes–Goodson et al. 2008).

All the above mechanisms could result in the intracellular or extracellular complexation and the deposition of metal nanoparticles.

Scientists have identified many species of bacteria, yeast, molds, algae and plants that can synthesize metal nanoparticles. The use of microorganisms in the synthesis of nanoparticles is a relatively new and exciting area of nanotechnology.

In most cases, microorganisms were identified through the addition of metal salts to the growth media or the cell extract followed by monitoring cells or the medium for the presence of nanoparticles. The formation of metal nanoparticles could easily be monitored by visual observation of the solution, as well as by recording of the UV–Vis spectra of the reaction mixture. Highly dispersed metal solutions are, as a rule, intensely colored and these colors depend on the particle's size, shape and composition and the presence of adsorption layers and their structure (Krutyakov et al. 2008). The absorption spectra of many metallic nanoparticles are characterized by a strong broad absorption band that is absent in the bulk spectra. This band is called the surface plasmon resonance (SPR) (Mulvaney 1996).

## 7.2 Bacteria in Metal Nanoparticle Synthesis

Among the many microorganisms, bacteria have received the most publicity in the area of biosynthesis of metal nanoparticles.

Klaus et al. (1999) and Joerger et al. (2000) have shown that bacterium *Pseudomonas stutzeri* AG259, which has been isolated from a silver mine, is capable of reducing aqueous silver nitrate solutions to allow for metal nanoparticles with the diameter of 3–200 nm. The particle size and morphology are dependent on several physical and chemical parameters, e.g., pH, incubation time, growth in the light or dark, and composition of the culture medium (Joerger et al. 2000).

Additionally, a small number of silver sulfide crystals were also observed in the middle of whole cells. The results obtained from the EDX spectrum

(energy-dispersive X-ray analysis) showed that these crystals had a molecular formula of  $\text{Ag}_2\text{S}$  (acanthile). These authors also emphasized that the synthesis of acanthile crystals may be caused by facile reactions of silver ions with  $\text{H}_2\text{S}$  gas produced by *P. stutzeri* AG259 (Slawson et al. 1992).

The *Corynebacterium* strain SH09, also isolated from a silver mine was used for biosorption and bioreduction of diamine silver complex (Zhang et al. 2005). This strain had a strong biosorption ability for  $[\text{Ag}(\text{NH}_3)_2]^+$  and, under certain conditions (temperature  $60^\circ\text{C}$ ), also reduced  $\text{Ag}^+$  to  $\text{Ag}^0$ . The resulting  $\text{Ag}^0$  crystals had an average size in the range of 10–15 nm. Their study demonstrated that the biosorption and bioreduction of silver ions could have occurred on the cell wall. Most likely, the ionized carboxyl of amino acid residues and an amide of the peptide chains were the main groups trapping  $[\text{Ag}(\text{NH}_3)_2]^+$  onto the *Corynebacterium* strain's SH09 cell wall. Afterwards some of the reducing groups, such as aldehyde or ketone, reduced  $[\text{Ag}(\text{NH}_3)_2]^+$  and formed  $\text{Ag}^0$  nuclei which further grew into  $\text{Ag}^0$  crystals.

In an elegant study by a group working in Teheran (Shahverdi et al. 2007), the rapid formation of silver nanoparticles by the culture supernatants of different *Enterobacteria* strains has been shown. The authors have demonstrated that piperitone could partially inhibit the reduction of silver ions by supernatants of *Klebsiella pneumoniae* and other different strains of *Enterobacteriaceae* screened. It was earlier reported that natural products such as piperitone (3-methyl-6-(1-methylethyl)-2-cyclohexen-1-one) inhibited the nitroreductase of *Enterobacteriaceae*. This enzyme is an oxygen-insensitive flavoprotein which is able to reduce the nitro group in many different compounds under aerobic conditions (Rafii et al. 2005). The results obtained from these studies suggested that the nitroreductase enzymes may be involved in the reduction process of silver ions (Shahverdi et al. 2007).

Further study (Mokhari et al. 2009) showed that no formation of metallic silver nanoparticles by the supernatant was observed when the procedure took place in the dark. The visible-light emission can significantly cause the synthesis of nanoparticles. Finally, it could be concluded that in this case, the silver ions reduction was mainly due to conjugation shuttles with the participation of the reductase. The hypothetical mechanisms of light-assisted synthesis of silver nanoparticles using the culture supernatant of *K. pneumoniae* are shown in Fig. 7.2. Therefore, it appears that the cell-associated nitroreductase enzymes may be involved in the photoreduction of silver ions.

It is well known that the electronic and optical properties of metal nanoparticles are totally dependent on their shape and size. Gurunathan et al. (2009) recently demonstrated that the size of silver nanoparticles synthesized by the culture supernatant of *Escherichia coli* could be controlled by various parameters, e.g.,  $\text{AgNO}_3$  concentration, reaction temperature and pH.

In another study by Parikh et al. (2008), the bacterium isolated from an insect gut *Morganella* sp. (family *Enterobacteriaceae*) was also able to synthesize crystalline silver nanoparticles. This strain was found to be highly resistant to silver cations. The authors postulated that the molecular mechanisms of silver

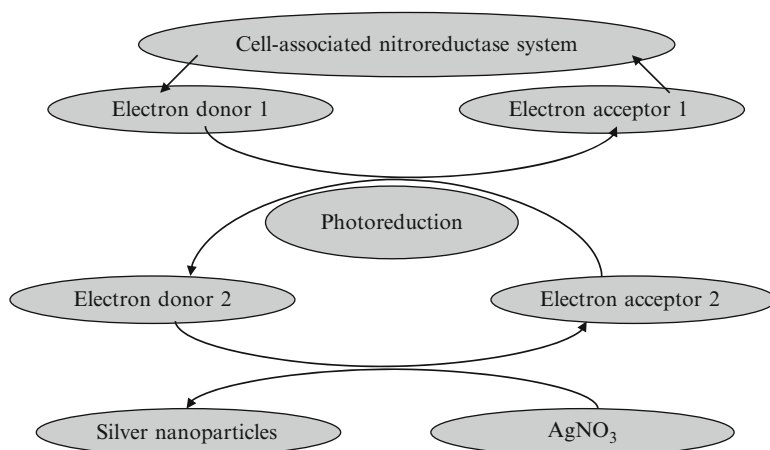


**Fig. 7.2** Hypothetical mechanism of light-assisted synthesis of silver nanoparticles by culture supernatants of *Klebsiella pneumoniae* (Mokhari et al. 2009)

resistance and its gene products might play a key role in the process of synthesis of silver nanoparticles.

*Bacillus licheniformis* (Kalimuthu et al. 2008) was isolated from municipal waste and later used for the biosynthesis of silver nanoparticles. The average particle size was 50 nm. The authors concluded that the enzyme involved in the bioreduction of  $\text{Ag}^+$  ions and the formation of silver nanoparticles may be nitrate reductase. *B. licheniformis* is known to secrete the cofactor NADH and NADH-dependent enzymes, especially nitrate reductase. These observations are in line with the findings of Duran et al. (2005) who speculated that the reduction of silver ions by *Fusarium oxysporum* strains occurs by a nitrate-dependent reductase and a quinone that could act as electron shuttle in metal reduction (see Fig. 7.7).

Bacteria not normally exposed to large concentrations of metal ions might also be used in the growth of metal nanoparticles. Nair and Pradeep (2002) have synthesized nanoparticles of silver, gold and their alloys using the *Lactobacillus* sp., lactic acid producing bacteria and the active bacterial component of buttermilk. When chloroauric acid ( $\text{HAuCl}_4$ ) was added to the biomass, two distinct size ranges were observed for the gold nanocrystals: one in the range of 20–50 nm (called clusters) and the second above 100 nm (called crystals). Clusters were present within and outside the bacterial contour, while the crystals were only detected within the bacterial contour. Various crystal morphologies, including triangular and other shapes, were found.

Silver-based clusters were formed with  $\text{AgNO}_3$  and, as above, two kinds of particles were found. The smallest particles were in the range of 15 nm while the largest were around 500 nm. Their study demonstrated that crystal growth appeared via intracellular reduction of the metal ions, while most of the smaller metal clusters, which nucleate the growth, are diffused into the cell through the reduction

of the outside medium. In addition, they also formed within the cell (Nair and Pradeep 2002).

In the past two decades, research has shown that gold nanoparticles have several potential applications, such as in catalysts, chemical sensing, biosensing, biological labeling and optical devices, owing to their unique chemical, optical and physical properties (Corma and Garcia 2008; Boisselier and Astruc 2009).

Over thirty years ago, Beveridge and Murray (1980) demonstrated the *Bacillus subtilis* 168 was able to reduce  $\text{Au}^{+3}$  ions to gold nanoparticles with a range of 5–25 nm.

Since then, several types of bacteria have been used to synthesize gold nanoparticles from aqueous  $\text{HAuCl}_4$  solution either intra or extracellularly.

For example, Nakajima (2003) screened 30 species of various microorganisms for gold accumulation. An extremely high ability to accumulate gold from a solution containing  $\text{Au}^{+3}$  was found in bacterial strains such as *E. coli* and *Pseudomonas maltophilia*. The accumulation was very rapid and was affected by the pH of the solution.

Another example of gold deposition in prokaryotes is the demonstration by Kashefi et al. (2001). These authors screened a range of anaerobic Fe(III)-reducing bacteria (mesophiles and thermophiles) for their ability to reduce  $\text{Au}^{+3}$  and observed a complete reduction of  $\text{Au}^{+3}$  after 25 min using the *Pyrobaculum islandicum*.

The use of various strains of *Pseudomonas aeruginosa* for extracellular biosynthesis of gold nanoparticles was described in the study by Husseiny et al. (2007). Gold nanoparticles were formed due to the reduction of gold ions by bacterial supernatants, but the mechanism for this biosynthesis is not yet understood.

Microbial precipitation of gold was also achieved using *E. coli* and *Desulfovibrio desulfuricans* (Deplanche and Macaskie 2008). The bioreductive recovery of gold from an aqueous solution was achieved within 2 h, showing crystalline  $\text{Au}^0$  particles in the cell, in the periplasm and on the cell surface. The size of the nanoparticles was smaller at the acidic pH of 2.0 as compared to that at the pH of 6.0–7.0. The partial inhibition by  $\text{Cu}^{+2}$  combined with the mixture of nanoparticle morphologies suggests two distinct biochemical routes to reduce  $\text{Au}^{+3}$ . The authors concluded that the periplasmic hydrogenase of the bacteria studied is involved in this process although it is not essential.

Konishi et al. (2006, 2007a, b) observed the microbial reduction and the precipitation of gold and platinum using mesophilic anaerobic bacterium *Shewanella algae*. Consequently it could be concluded that the pH of the solution is an important factor in controlling the morphology of gold nanoparticles and in the location of gold deposition.

In a solution of pH 7.0, gold nanoparticles of the size of 10–20 nm were deposited in the periplasm of *S. algae* cells. At pH 2.8, nanoparticles in the size of 15–200 nm were deposited directly on the bacterial cells, and the nanoparticles exhibited a wide variety of shapes. In a solution of pH 2.0, gold nanoparticles about 20 nm in size were deposited intracellularly (Fig. 7.3).

The microbial reduction of  $\text{Au}^{+3}$  by the *S. algae* was dependent on the presence of a specific electron donor, the molecular  $\text{H}_2$ . It was concluded that the *S. algae*

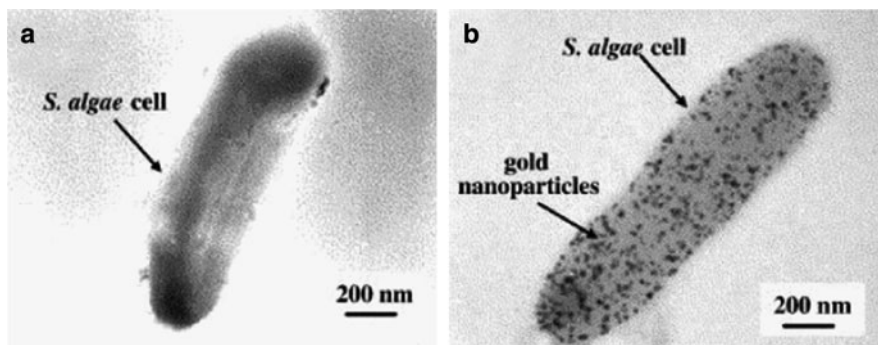
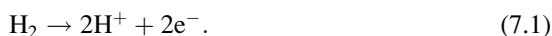
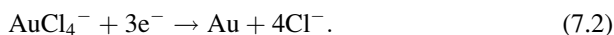


**Fig. 7.3** (a) TEM image of the *S. algae* cell before exposure to  $\text{HAuCl}_4$  solution. (b) TEM image of the *S. algae* cell after exposure to  $\text{HAuCl}_4$  solution for 90 min [Reproduced from Hydrometallurgy (2006) 81:24–29, Elsevier]

hydrogenase catalyzes the activation of molecular  $\text{H}_2$  using the molecule as the electron donor according to the following reaction:

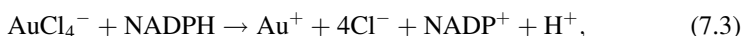


As a result, the *S. algae* cells are likely to transfer electrons to  $\text{AuCl}_4^-$  ions, reducing them to a gold metal:



It has been known for a long time that hydrogenase is involved in  $\text{U}^{+6}$  reduction by *Micrococcus lactyliticus* (Woolfolk and Whiteley 1962), in addition to  $\text{Se}^{+6}$  reduction by *Clostridium pasteurianum* (Yanke et al. 1995). Moreover, hydrogenases from the sulfate-reducing bacteria have been shown to be capable of reducing  $\text{Tc}^{+7}$  and  $\text{Cr}^{+6}$  (Michel et al. 2001). In another study, Zadvorny et al. (2006) demonstrated that the hydrogenases isolated from phototrophic bacteria were able to reduce  $\text{Ni}^{+2}$  to  $\text{Ni}^0$  under an  $\text{H}_2$  atmosphere.

More recently, Shiyong et al. (2007, 2008) and Nangia et al. (2009a, b) have reported the intracellular biosynthesis of gold nanoparticles by the strains *Rhodospseudomonas capsulata* and *Stenotrophomonas maltophilia*. The authors believe that the specific NADPH-dependent enzyme present in the isolated strains reduced  $\text{Au}^{+3}$  to  $\text{Au}^0$  through an electron shuttling mechanism, leading to the synthesis of mono-dispersed nanoparticles. A two-step process is needed to reduce gold ions. During the first step, the  $\text{AuCl}_4^-$  ions are reduced to the  $\text{Au}^+$  species (7.3). Then, the latter product is reduced by NADHP to a metallic gold (7.4).





The morphological control over the size and shape of gold nanoparticles has been achieved through the use of filamentous cyanobacterium *Plectonema boryanum* UTEX 485. When the biomass of this strain was reacted with aqueous  $\text{Au}(\text{S}_2\text{O}_3)_2^{-3}$  and  $\text{AuCl}_4^-$  in the solution of 25–100°C for 1 month and at 200°C for 1 day, the reaction resulted in the precipitation of cubic gold nanoparticles (<10–25 nm) and octahedral gold particles (1–10  $\mu\text{m}$ ), respectively (Lengke et al. 2006a, b). The mechanisms of gold accumulation by the cyanobacteria studied from gold chloride initially promoted the precipitation of amorphous gold sulfide at the cell walls and finally deposited metallic gold in octahedral form near the cell surfaces and in solutions (Lengke et al. 2006c). Moreover, the authors concluded that the formation of gold nanoparticles by *P. boryanum* UTEX 485 occurs by three possible mechanisms involving iron sulfide, localized reducing conditions and metabolism (Lengke and Southam 2006).

An alkalothermophilic (extremophilic) actinomycetate, *Thermomonospora* sp., having the optimum growth at pH 9.0 and 50°C was isolated from compost and used for gold nanoparticle synthesis (Ahmad et al. 2003a, b, c). The bioreduction of the  $\text{AuCl}_4^-$  ions in solution occurs after nearly 120 h of reaction, indicating an extremely slow process. Polyacrylamide gel electrophoresis indicates the presence of four protein bands with the molecular masses between 80 and 10 kDa. The authors believed that one or more of these proteins may be enzymes that are responsible for the reduction of gold ions.

In contrast, intracellular synthesis of gold nanoparticles occurs in alkalotolerant *Rhodococcus* sp. (Ahmad et al. 2003a).

In addition to silver and gold nanoparticles, there is a great interest in exploiting microorganisms for the synthesis of semiconductors (so-called quantum dots), such as CdS, ZnS and PbS. These kinds of new types of materials are very important for their applications in optical devices, electronics and biotechnologies (Murray et al. 2000).

Cunningham et al. (1993) demonstrated that *Clostridium thermoaceticum* could precipitate CdS at the cell surface, as well as in the medium from  $\text{CdCl}_2$  in the presence of cysteine hydrochloride. It is most likely that cysteine acts as the source of the sulfide.

When *K. pneumoniae* was exposed to  $\text{Cd}^{+2}$  ions in the growth medium, authors observed the formation of 20–200 nm CdS on the cell surface (Holmes et al. 1997).

It was found that the buffer composition of the growth medium plays an integral part in forming these cadmium sulfide nanoparticles.

Labrenz et al. (2000) has demonstrated that spherical sphalerite nanoparticles (ZnS) are formed within natural biofilms, which are dominated by the sulfate-reducing bacteria belonging to the *Desulfobacteriaceae* family.

Sweeney et al. (2004) observed microbial reduction and intracellular formation of CdS nanoparticles using the bacterium *E. coli*. It could be concluded that the growth of the nanoparticles was growth-phase dependent and cellular thiol levels might contribute to the ability of *E. coli* to form the quantum dots.

More recently, a simple route for the synthesis of cadmium sulfide nanoparticles by photosynthetic bacteria *Rhodospseudomonas palustris* was demonstrated by

Bai et al. (2009). TEM analysis showed the uniform distribution of nanoparticles, having an average size of  $8.01 \pm 0.25$  nm. The above authors also emphasized that cysteine desulphydrase, an intracellular enzyme, was responsible for the formation of CdS nanocrystals, while protein secreted by *R. palustris* stabilized the cadmium sulfide nanoparticles. In addition, *R. palustris* was able to transport CdS nanoparticles out of the cell.

Nanoparticles of platinum-group metals are widely used in industrial and automotive catalysts because they are highly resistant to corrosion and are able to achieve oxidation at high temperatures.

Lengke et al. (2006b) synthesized spherical platinum nanoparticles using cyanobacterium *P. boryanum* UTEX 485 (Fig. 7.4). The addition of  $\text{PtCl}_4^0$  to the bacterial culture initially promoted the precipitation of  $\text{Pt}^{+2}$ -organic metal as spherical nanoparticles ( $\leq 0.3 \mu\text{m}$ ) in the solution, which then dispersed within the bacterial cells. The cyanobacteria were immediately killed either by the  $\text{PtCl}_4^0$ , the acidic pH or elevated temperatures (60–180°C), the resulting release of organics caused

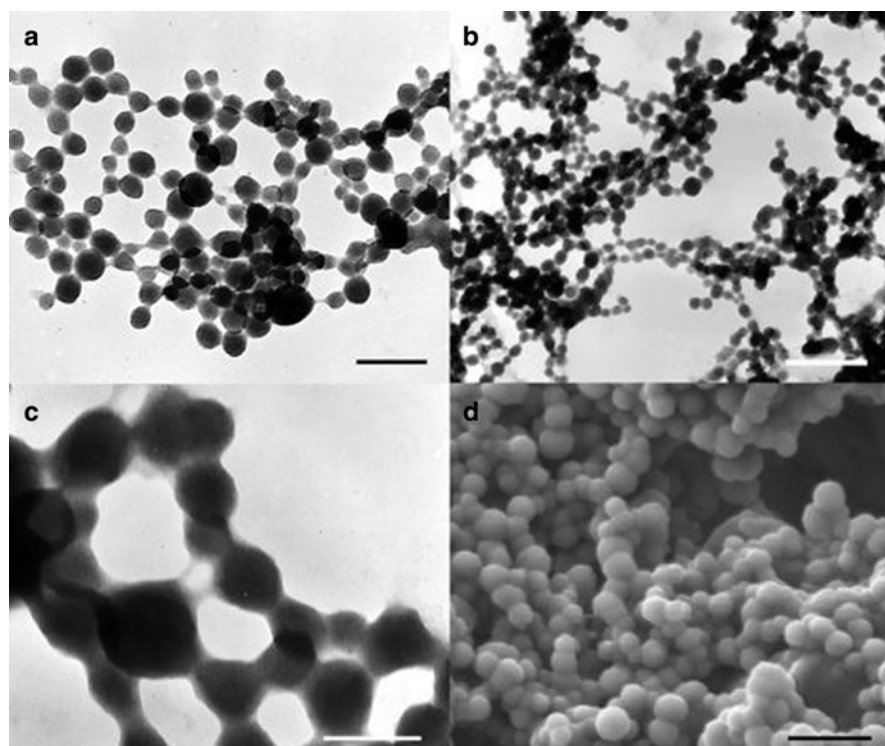


**Fig. 7.4** TEM micrographs of whole mounts of amorphous spherical nanoparticles of platinum, forming long bead-like chains in cyanobacterium *Plectonema boryanum* UTEX 485- $\text{PtCl}_4^0$  systems. (a) 60°C and 14 days; (b, c) 80°C and 21 days; (d) SEM micrographs of spherical platinum-bearing nanoparticles at 80°C and 28 days. [Reproduced from Langmuir (2006) 22:7318–7323. American Chemical Society]

further precipitation of platinum. With an increase in temperature, the Pt<sup>2</sup>-organic nanoparticles were recrystallized and formed nanoparticles consisting of a platinum metal.

The authors (Konishi et al. 2007a, b) also demonstrated that resting cells of bacterium *Shewanella algae* were able to transfer electrons to PtCl<sub>6</sub><sup>-2</sup> ions, reducing them to elemental platinum at room temperature and pH 7.0 in the presence of lactate as the electron donor. These biogenic nanoparticles were located in the periplasm, thus it is likely that an enzyme responsible for this process is localized in the periplasm. More efforts are required to fully elucidate the mechanism of bioreductive deposition of platinum by *Shewanella algae*.

Another example of bioreduction of Pt<sup>+4</sup> into the Pt<sup>0</sup> nanoparticles was demonstrated by Riddin et al. (2009). A mixed and uncharacterized consortium of sulphate-reducing bacteria was used to investigate the mechanism in the platinum nanoparticle formation. It was shown that two different hydrogenase enzymes were involved. First, the Pt<sup>+4</sup> ions were reduced to Pt<sup>+2</sup> by an oxygen-sensitive cytoplasmic hydrogenase. Then, the formed ions were reduced to Pt<sup>0</sup> nanoparticles by a periplasmic hydrogenase that was oxygen tolerant and was inhibited by Cu<sup>+2</sup> (Fig. 7.5).

The synthesis of extracellular and intracellular palladium nanoparticles of different sizes by bacteria belonging to the family *Desulfovibrio* (Lloyd et al. 1998; Yong et al. 2002a, b; Baxter-Plant et al. 2003), *Shewanella oneidensis* (de Windt et al. 2005, 2006) and *Bacillus sphaericus* JG-A12 (Pollmann et al. 2006) has been demonstrated. The checked and suggested mechanisms for bioreduction of palladium by *D. desulfuricans* were probably catalyzed by hydrogenlyase reactions (Yong et al. 2002a).

It is important to note that the dissimilatory metal-reducing bacteria such as *Shewanella* sp., *Geobacter* sp., and *D. desulfuricans* were used for the reduction of U<sup>+6</sup> and the formation of intra or extracellular UO<sub>2</sub> nanoparticles (Gorby and Lovley 1992; Lovley and Phillips 1992; Liu et al. (2002)). However, these investigations did not identify the mediators of the U<sup>+6</sup> reduction.

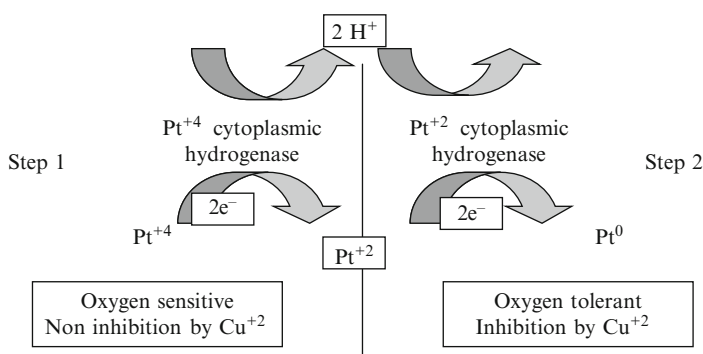


**Fig. 7.5** Postulated mechanism for the double two-electron reduction of Pt<sup>+4</sup> into Pt<sup>0</sup> nanoparticles (Riddin et al. 2009)

It was also reported (Fredrickson et al. 2002) that the extracellular formation of  $\text{UO}_2$  nanoparticles by *Shewanella putrefaciens* strain CN32 involved the outer membrane cytochromes. Finally, Marshall et al. (2006) showed that c-type cytochromes of a dissimilatory metal-reducing bacterium *S. oneidensis* MR-1 are essential for the reduction of  $\text{U}^{+6}$  and the extracellular deposition of  $\text{UO}_2$  nanoparticles. In this study, Marshall and co-workers established that MtrC, a decaheme c-type cytochrome, previously reported to be involved in the  $\text{Fe}^{+3}$  and  $\text{Mn}^{+4}$  reduction is responsible for the electrons transferred to  $\text{U}^{+6}$ .

Nanometer-sized magnetite ( $\text{Fe}_3\text{O}_4$ ) and maghemite ( $\gamma\text{-Fe}_2\text{O}_3$ ) are widely used in the medical and diagnostic applications, cell separation, biosensing, hypothermia and drug delivery, in addition to radionuclide therapy. It is well known that with a few exceptions, magnetotactic bacteria show the ability to form magnetic crystals under ambient conditions.

One final example of metal nanoparticles is their formation using bacteria through the use of metal-substituted magnetite crystals. This is a microbial process which exploits the ability of iron-reducing microorganisms to synthesize extracellular *M*-substituted magnetite nanoparticles using akagenite and dopants in a soluble form and it has been reported by Roh et al. (2001) and Moon et al. (2007). The thermophilic *Thermoanaerobacter* sp. TOR-39 and psychrotolerant iron-reducing bacterium *Shewanella* sp. were used to form *M*-substituted magnetite nano-crystals  $\text{MFe}_{3-y}\text{O}_4$ , where the *M* crystals were Mn, Zn, Ni, Co and Cr. Generally, microbial reduction can produce magnetite particles of well-defined sizes (typically tens of nanometers) and crystallographic morphology.

### 7.3 Fungi in Metal Nanoparticle Synthesis

It has long been considered that among the eukaryotes, yeasts are explored mostly in the formation of metal nanoparticles. It was shown that intracellular CdS nanoparticles can be formed when *Candida glabrata* and *Schizosaccharomyces pombe* were exposed to  $\text{Cd}^{+2}$  ions (Reese and Winge 1988; Dameron et al. 1989; Kowshik et al. 2002a, b). These nanoparticles are coated with short peptides known as phytochelatins, which have the general structure  $(\gamma\text{-Glu-Cys})_n\text{-Gly}$ , where *n* varies from 2 to 6 (Dameron et al. 1989).

Further work on the synthesis of quantum dots by yeast demonstrated that *Toluopsis* sp., which was found in the extensive screening program, is capable of synthesizing PbS nanocrystals intracellularly (Kowshik et al. 2002a).

Recently, Kowshik et al. (2003) described the extracellular synthesis of silver nanoparticles by silver-tolerant yeast strain MKY3. The exact mechanism leading to the reduction of silver ions is not yet understood and the authors postulated that biochemical reducing agents are secreted by the yeast cells in response to silver stress.

It is interesting to note that Ahmad et al. (2007) used alkalotolerant and thermophilic fungus *Humicola* sp. for  $\text{CuAlO}_2$  synthesis, which was difficult to realize in

chemical protocols, especially under technologically desirable low-temperature conditions. The CuAlO<sub>2</sub> nanoparticles were capped with natural protein making them water dispersible.

In other studies by Agnihotri et al. (2009) and Pimprikar et al. (2009) the tropical marine yeast *Yarrowia lipolytica* NCIM 3589 was able to synthesize gold nanoparticles. SEM and TEM microscopy showed that nanoparticles were associated with the cell wall, but might be released outside when nanoparticle-loaded cells were incubated at low temperature (20°C) for 48 h (Pimprikar et al. 2009).

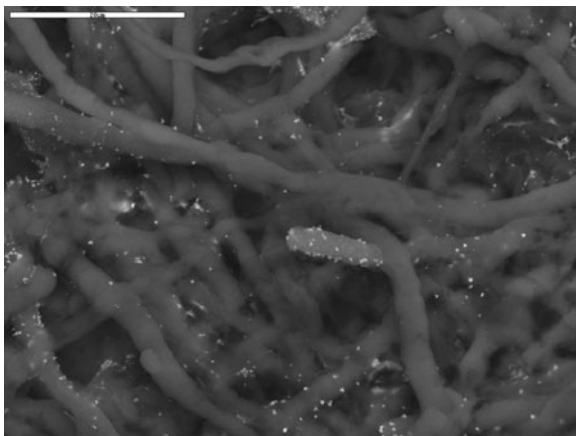
Zinc phosphate is a new type of nontoxic, ecological anticorrosive pigment with excellent properties, and has been synthesized by a chemical precipitation method with yeast as bio-templates (Yan et al. 2009). The mechanism of the formation of Zn<sub>3</sub>(PO<sub>4</sub>)<sub>2</sub> has been suggested. The authors believed that the nonionic hydroxyl groups, carboxyl groups and other negatively charged groups on the cell may bind the zinc ions through ionic–dipolar interaction when Zn<sup>+2</sup> was introduced. Phosphate radicals dropped in the mixture were enveloped in zinc cations which were bonded on yeasts. Electrostatic effect and steric hindrance played a multiple role to avoid agglomeration of the product in the synthesis.

During the last two decades, a number of different genera of fungi have been screened and it has been shown that these microorganisms are extremely good candidates in the synthesis of metal and metal sulphide nanoparticles. Sastry et al. (2003) concluded from their study that compared to bacteria, fungi secrete large amounts of enzymes, which are involved in metal nanoparticle synthesis and are simpler to deal with in the laboratory.

Pighi et al. (1989) and Chen et al. (2003) reported that fungus *Phoma* strains PT35 and 3.2883 were able to accumulate silver. More recent and detailed investigations into the use of *Phoma glomerata* in the synthesis of silver nanoparticles was demonstrated by Birla et al. (2009). The SEM micrograph study showed the presence of spherical nanoparticles in the range 60–80 nm. These synthesized nanoparticles showed bactericidal activity against *E. coli*, *P. aeruginosa* and *S. aureus* (Birla et al. 2009).

The appearance of a distinctive purple color in the biomass of *Verticillium* after exposure to HAuCl<sub>4</sub> solution indicates the formation of gold nanoparticles intracellularly (Mukerjee et al. 2001b). Additionally, the exposure of this fungal biomass to aqueous Ag<sup>+</sup> ions resulted in the intracellular reduction of the metal ions and the formation of silver nanoparticles of dimension 25 ± 12 nm (Mukerjee et al. 2001a). However, they could not find the exact mechanisms of formation of gold and silver nanoparticles by *Verticillium* sp. Since the nanoparticles are formed on the surface of the mycelia and not in the solution, they believed that the first step involves trapping of the Ag<sup>+</sup> ions on the surface of the fungal cells, possibly via electrostatic interaction between gold ions and negatively charged carboxylate groups in enzymes present in the cell wall of the mycelia. Thereafter, the silver ions are reduced by enzymes present in the cell wall leading to the formation of silver nuclei, which subsequently grow by further reduction of Ag ions and accumulation on these nuclei. The TEM results indicate the presence of some silver nanoparticles on the cytoplasmic membrane as well as within the cytoplasm. It is

**Fig. 7.6** SEM image of the *Penicillium* sp. fungal cells after immersion in aqueous solution of  $\text{AgNO}_3$  (Maliszewska et al. 2009)



possible that some Ag ions diffuse through the cell wall and are reduced by enzymes present on the cytoplasmic membrane and within the cytoplasm. It may also be possible that some of the smaller silver nanoparticles diffuse across the cell wall to be trapped within the cytoplasm.

In addition, in our laboratory we observed the presence of uniformly distributed silver nanoparticles on the surface of the *Penicillium* sp. cells (Fig. 7.6). This observation indicates that the nanoparticles formed by the reduction of silver ions are bound to the surface of the fungus cells (Maliszewska et al. 2009).

The results obtained from the Gericke and Pinches (2006) study demonstrated the possibility to manipulate the size and shape of gold nanoparticles synthesized by *Verticillium luteoalbum* and the isolate 6-3. It was shown that the age of the culture did not have an effect on the shape of the synthesized gold nanoparticles. However, it is to be noted that the number of particles decreased when older cells were used in the experiment. Moreover, the variety in the shapes of gold nanoparticles formed at different pH levels indicates that the changes in this parameter could play an important role during optimization of the process controlling nanoparticle morphology. For example, the gold particles formed at pH 3.0 and pH 5.0 by *V. luteoalbum* were mostly spherical in shape and relatively uniform in size, with an average diameter of less than 10 nm. In addition, a large number of bigger particles including triangles, hexagons and rods also occurred at these pH values. The shapes of the gold nanoparticles formed at pH 7 were similar to those synthesized at pH 9 and included small spherical nanoparticles, as well as bigger particles with irregular shapes (Gericke and Pinches 2006).

The rate of accumulation of the gold nanoparticles was also related to the incubation temperature. It is observed that increased temperature levels allowed particle growth at a faster rate.

From the practical point of view, it would be better if the metal ions could be reduced outside the fungal biomass, leading to the formation of nanoparticles in the

solution. Mukherjee et al. (2002) and Ahmad et al. (2003a, b, c) screened a number of species belonging to different genera of molds and observed the extracellular synthesis of silver and gold nanoparticles by the treatment of the biomass of *F. oxysporum* with silver or gold ions.

Moreover, the aqueous extract of the fungal biomass can reduce gold and silver ions to the corresponding nanoparticles. Apart from individual metal nanoparticles, the formation of highly stable Au–Ag alloy by *F. oxysporum* was observed (Senapati et al. 2005). Variation in the amount of biomass used in the experiment reveals that the secreted cofactor NADH plays an important role in determining the composition of Au–Ag alloy nanoparticles. The authors suggested that the reduction of  $\text{Au}^{+3}$  and  $\text{Ag}^{+1}$  ions occurs due to reductases released by the fungus into the solution.

It was later demonstrated that a nitrate-dependent reductase and shuttle quinone from several *F. oxysporum* strains were involved in the extracellular synthesis of silver nanoparticles. However, it was not true with all strains of *Fusarium* (Duran et al. 2005). For example, *Fusarium moniliforme* produced reductase enzyme but could not form silver nanoparticles during the incubation with silver ions. Thus, the probable mechanism of silver reduction includes the conjugated oxidation–reduction reactions of electron carriers in which NADP-dependent nitrate reductase takes part (Fig. 7.7). Finally, an *in vitro* synthesis of silver nanoparticles, which involved

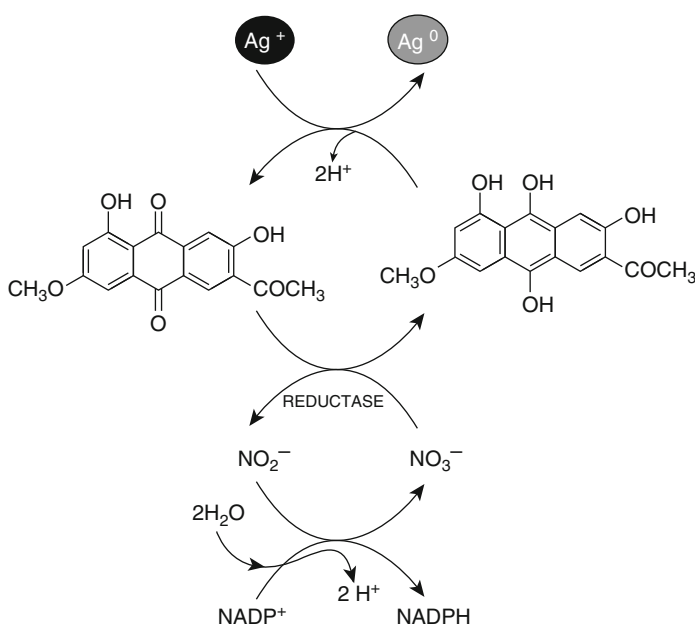


**Fig. 7.7** Hypothetical mechanisms of silver nanoparticle biosynthesis by *Fusarium oxysporum* [Reproduced with permission from J Nanobiotechnol (2005) doi:10.1186/1477-3155-3-8, BioMed Central Ltd.]

$\alpha$ -NADP-dependent nitrate reductase, was modeled (Kumar et al. 2007a, b). The reaction was conducted under anaerobic conditions in the presence of  $\alpha$ -NADPH as cofactor, a protein phytochelatin (acts as stabilizer of nanoparticles), 4-hydroxyquinoline (as electron carrier) and nitrate reductase from *F. oxysporum*.

It seems that filamentous fungi belonging to *Fusarium* genus are very good candidates for the development of extracellular synthesis of various metal nanoparticles.

For example, Karbasian et al. (2008) used the biomass of *F. oxysporum* PTCC 5115 for the production of silver nanoparticles. This process was optimized through response surface methodology-central composite design. The factors that affected the process were pH, temperature, agitation rate, time of reaction, weight of biomass and concentration of silver nitrate.

It was discovered that *F. oxysporum* may also be used to synthesize semiconductors CdS nanoparticles (Ahmad et al. 2002). These particles were monodisperse and range in size from 5 to 20 nm. They suggest that the mechanisms for the formation of CdS nanoparticles from  $\text{Cd}^{+2}$  and  $\text{SO}_4^{-2}$  ions by *F. oxysporum* were probably catalyzed by reductase enzymes released into solution.

Another significant application of this fungus is in the extracellular synthesis of highly luminescent CdSe quantum dots at room temperature reported by Kumar et al. (2007a, b).

Another study (Bharde et al. 2006) has shown the protein-mediated extracellular formation of magnetite. The authors discovered that exposure of fungi *F. oxysporum* and *Verticillium* sp. to an aqueous solution of  $\text{K}_3[\text{Fe}(\text{CN})_6]$  and  $\text{K}_4[\text{Fe}(\text{CN})_6]$  results in the production of magnetite. These nanoparticles are crystalline and exhibit magnetic single-domain characteristics.

It was also shown that *F. oxysporum* is able to synthesize zirconia (Bansal et al. 2004), silica and titanium (Bansal et al. 2005) and platinum (Riddin et al. 2006) nanoparticles.

More recently, Basavaraja et al. (2008) and Ingle et al. (2009) demonstrated extracellular biosynthesis of silver nanoparticles by *Fusarium semitectum* and *Fusarium solani* (USM-3799). The results obtained from these studies suggested that the protein might have played an important role in the reduction of  $\text{Ag}^+$  and in the stabilization of silver nanoparticles through coating of protein moiety on the silver nanoparticles.

Extensive work has been done using different species of fungi for extracellular biosynthesis of metal nanoparticles such as silver or gold.

For example, Bhainsa and D'Souza (2006) and Prabhu et al. (2009) investigated extracellular synthesis of silver nanoparticles by *Aspergillus fumigatus*.

Vigneshwaran et al. (2006, 2007) demonstrated the biosorption of silver in the form of nanoparticles by fungi *Phanerochaete chrysosporium* and *Aspergillus flavus*. The authors emphasized that the synthesis process was complete and that these silver nanoparticles were well separated and surrounded by a layer of organic matrix. The results of SEM and TEM suggested that the proteins, secreted by fungi, might have an important role in the stabilization of the silver nanoparticles.



Extracellular formation of silver nanoparticles by various fungi belonging to *Penicillium* genus has recently been described (Sadowski et al. 2008; Kathiresan et al. 2009; Maliszewska and Sadowski 2009; Maliszewska et al. 2009; Shaligram et al. 2009).

Kathiresan et al. (2009) observed that the fungus *Penicillium fellutanum*, isolated from coastal mangrove sediment, can reduce  $\text{Ag}^+$  within 10 min of the silver ions coming in contact with the culture filtrate. Polyacrylamide gel electrophoresis indicates the presence of one protein band in the filtrate of fungal biomass with a molecular weight of 70 kDa. The authors believed that the enzyme protein of nitrate reductase is responsible for the reduction of silver ions. It is interesting to note that this process might be controlled by pH, temperature, silver ions concentration and exposure time to silver nitrate.

Nikhil et al. (2009) presented an eco-friendly process for the synthesis of silver nanoparticles using a fungus *Penicillium brevicompactum* WA2315. The authors also postulated that NADH-dependent nitrate reductase is involved in the reduction of silver ions to metallic silver. The reduction may occur by means of the electrons from NADH where NADH-dependent reductase can act as a carrier. FTIR spectroscopic studies on these silver nanoparticles confirmed that the carbonyl groups from the amino acid residues and peptides of proteins have a strong ability to bind silver, and probably formed a coat covering the metal nanoparticles to prevent their agglomeration.

Further examples of bioreduction of  $\text{Ag}^+$  into  $\text{Ag}^0$  nanoparticles were demonstrated by Mukherjee et al. (2008) and Fayaz et al. (2009). These authors used fungi belonging to the genus *Trichoderma* – *Trichoderma asperellum* and *Trichoderma viride*, respectively, for the formation of silver nanoparticles. The exact mechanism of the synthesis of silver nanoparticles with these fungal extracts is not understood, but based on their results, the authors speculated that some of the peptide linkages from amino acids first undergo hydrolysis to produce free carboxylate ions and free amino groups, which then possibly act as the capping agents for the silver nanoparticles.

An endophytic fungus *Colletotrichum* sp. growing in geranium leaves (Shankar et al. 2003) and alkalotolerant fungus *Tricothecium* sp., when exposed to aqueous chloroaurate ions, synthesized gold nanoparticles (Ahmad et al. 2005).

Xie et al. (2007) and Bhambure et al. (2009) showed that *Aspergillus niger* may also be used for the synthesis of gold nanoparticles. The exposure of the mycelia-free spent medium or extract of *A. niger* to gold ions resulted in the growth of gold nanoparticles of various shapes and sizes (Xie et al. 2007). The experimental results implied that the formation of gold nanoplates in the spent medium was mediated by an enzymatic reaction (Fig. 7.8). The temperature and pH of the solution were found to strongly influence the shapes of these anisotropic gold nanoparticles.

The final example of metal biosynthesis is the extracellular formation of silver nanoparticles using mycelia-free spent medium of *Cladosporium cladosporioides* (Balaji et al. 2009) and *Corioliolus versicolor* (Sanghi and Verma 2009). In general, the reduction process of silver ions was sensitive to the solution's pH and reaction temperature.

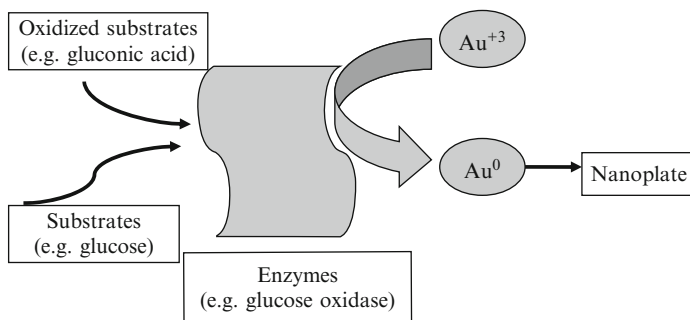


**Fig. 7.8** Schematic illustration of the enzymatic process to synthesize Au nanoplates in the spent medium of *A. niger* (Xie et al. 2007)

## 7.4 Conclusions

Metallic nanoparticles exhibit completely new or improved properties compared to larger particles of bulk materials. Consequently, these particles have several important applications: catalysts in chemical properties, optical receptors, coating materials for solar energy absorption, antimicrobial agents, transfection vectors and fluorescent labels.

The “green” synthesis strategy requires the related materials to be eco-friendly, nontoxic and renewable. Nanobiotechnology describes the application of biological systems for the production of these new functional nanomaterials.

In the past three decades, researchers have shown that several types of bacteria, yeast and fungi had an extremely high ability to synthesize various metal and metal alloy nanoparticles with different chemical composition, size and shapes, and controlled monodispersity.

It seems that microbes produce nanoparticles as a consequence of the detoxification pathway. But the mechanism of bioreduction of metal ions is still an open question. I believe that many more possible mechanisms are involved in this process.

In general, the first step involves trapping of the metal ions on the surface of the cell, possibly via electrostatic interaction between the ions and nonionic hydroxyl groups, carboxyl groups and other negatively charged groups on the cell. Thereafter, ions are reduced by enzymes (e.g., reductase) or/and carbonyl groups leading to formation of metal nuclei, which further grow to frame crystals.

Only in one example, nitrate reductase from the fungus *F. oxysporum* has been well documented to catalyze the reduction of silver nitrate to silver nanoparticles utilizing NADPH as reducing agent.

It is important to note that formed nanoparticles are very stable in solution because they are surrounded by a layer of organic matrix. The results of SEM and TEM suggest that the protein secreted by microorganisms might have an important role in the stabilization of metal nanoparticles.

Recently, it has been demonstrated that the size and shape of metal nanoparticles synthesized by microorganisms could be controlled by various parameters, e.g., metal ion concentration, reaction temperature, pH of solution, etc.

Use of microorganisms (particularly fungi) could be an alternative to chemical or physical methods for the production of metal nanoparticles.

**Acknowledgement** This work was supported by MN i SW Grant No. N N 507 5150 38.

## References

- Agnihotri M, Joshi S, Kumar AR, Zinjarde S, Kulkarni S (2009) Biosynthesis of gold nanoparticles by the tropical marine yeast *Yarrowia lipolytica* NCIM 3589. *Mater Lett* 63:1231–1234
- Ahmad A, Mukherjee P, Mandal D, Senapati S, Khan MI, Kumar R, Sastry M (2002) Enzyme mediated extracellular synthesis of CdS nanoparticles by the fungus *Fusarium oxysporum*. *J Am Chem Soc* 124:12108–12109
- Ahmad A, Mukherjee P, Senapati S, Mandal D, Khan MI, Kumar R, Sastry M (2003a) Extracellular synthesis of silver nanoparticles of silver nanoparticles using the fungus *Fusarium oxysporum*. *Colloids Surf B: Biointerfaces* 28:313–318
- Ahmad A, Senapati S, Khan MI, Kumar S, Sastry M (2003b) Extracellular biosynthesis of monodisperse gold nanoparticles by a novel extremophilic actinomycete, *Thermomonospora* sp. *Langmuir* 19:3550–3553
- Ahmad A, Senapati S, Khan MI, Ramani R, Srinivas V, Sastry M (2003c) Intracellular synthesis of gold nanoparticles by a novel alkalotolerant actinomycete *Rhodococcus* species. *Nanotechnology* 14:8240828
- Ahmad A, Senapati S, Khan MI, Kumar S, Sastry M (2005) Extra-/intracellular biosynthesis of gold nanoparticles by an alkalotolerant fungus *Tricothecium* sp. *J Biomed Nanotechnol* 1:47–53
- Ahmad A, Jagadale T, Dhas V, Khan S, Patil S, Paricha R, Ravi V, Ogale S (2007) Fungus-based synthesis of chemically difficult-to-synthesize multifunctional nanoparticles of  $\text{CuAlO}_2$ . *Adv Mater* 19:3295–3299
- Bai HJ, Zhang ZM, Guo Y, Yang GE (2009) Biosynthesis of cadmium sulfide nanoparticles by photosynthetic bacteria *Rhodospseudomonas palustris*. *Colloids Surf B: Biointerfaces* 70:142–146
- Balaji DS, Basavaraja S, Deshpande R, Mahesh DB, Prabhakar BK, Venkataraman A (2009) Extracellular biosynthesis of functionalized silver nanoparticles by strains of *Cladosporium cladosporioides*. *Colloids Surf B: Biointerfaces* 68:88–92
- Bansal V, Rautaray D, Ahmad A, Sastry M (2004) Biosynthesis of zirconia nanoparticles using the fungus *Fusarium oxysporum*. *J Mater Chem* 14:3303–3305
- Bansal V, Rautaray D, Bharde A, Ahire K, Sanyal A, Ahmad A, Sastry M (2005) Fungus-mediated biosynthesis of silica and titania particles. *J Mater Chem* 15:2583–2589
- Basavaraja S, Balaji SD, Lagashetty A, Rajasab AH, Venkataraman A (2008) Extracellular biosynthesis of silver nanoparticles using the fungus *Fusarium semitectum*. *Mater Res Bull* 43:1164–1170
- Bäuerlein E (2003) Biomineralization of unicellular organisms: an unusual membrane biochemistry for the production of inorganic nano- and microstructures. *Angew Chem Int Ed* 42:614–641
- Baxter-Plant VS, Mikhhereenko IP, Macaskie LE (2003) Sulphate-reducing bacteria, palladium and reductive dehalogenation of chlorinated aromatic compounds. *Biodegradation* 14:83–90
- Beveridge TJ, Murray RGE (1980) Site of metal deposition in the cell wall of *Bacillus subtilis*. *J Bacteriol* 141:876–887

- Bhainsa KC, D'Souza SF (2006) Extracellular biosynthesis of silver nanoparticles using the fungus *Aspergillus fumigatus*. *Colloids Surf B* 47:160–164
- Bhambure R, Bule M, Shaligram N, Kamat M, Singhal R (2009) Extracellular biosynthesis of gold nanoparticles using *Aspergillus niger* – its characterization and stability. *Chem Eng Technol* 32:1036–1041
- Bharde A, Rautaray D, Bansal V, Ahmad A, Sarkar I, Yusuf SM, Sanyal M, Sastry M (2006) Extracellular biosynthesis of magnetite using fungi. *Small* 2:135–141
- Birla SS, Tiwari VV, Gade AK, Ingle AP, Yadav AP, Rai MK (2009) Fabrication of silver nanoparticles by *Phoma glomerata* and its combined effect against *Escherichia coli*, *Pseudomonas aeruginosa* and *Staphylococcus aureus*. *Lett Appl Microbiol* 48:173–179
- Boisselier E, Astruc D (2009) Gold nanoparticles in nanomedicine: preparations, imaging, diagnostics, therapies and toxicity. *Chem Soc Rev* 38:1759–1782
- Chen JC, Lin ZH, Ma XX (2003) Evidence of the production of silver nanoparticles via pretreatment of *Phoma* sp. 3.2883 with silver nitrate. *Lett Appl Microbiol* 37:105–108
- Corma A, Garcia H (2008) Supported gold nanoparticles as catalysts for organic reactions. *Chem Soc Rev* 37:2096–2126
- Crookes-Goodson WJ, Slocik JM, Naik RR (2008) Bio-directed synthesis and assembly of nanomaterials. *Chem Soc Rev* 37:2403–2412
- Cunningham DP, Lundie LL, Leon L Jr (1993) Precipitation of cadmium by *Clostridium thermoaceticum*. *Appl Environ Microbiol* 59:7–14
- Dameron CT, Reese RN, Mehra RK, Kortan AR, Carroll PJ, Steigerwald ML, Brus LE, Winge DR (1989) Biosynthesis of cadmium sulfide quantum semiconductor crystallites. *Nature* 338:596–597
- de Windt W, Aelterman P, Verstraete W (2005) Bioreductive deposition of palladium (0) nanoparticles on *Shewanella oneidensis* with catalytic activity towards reductive dechlorination of polychlorinated biphenyls. *Environ Microbiol* 7:314–325
- de Windt W, Boon N, van den Bulcke J, Rubberecht L, Prata F, Mast J, Hennebel T, Verstraete W (2006) Biological control of the size and reactivity of catalytic Pd(0) produced by *Shewanella oneidensis*. *Antonie van Leeuwenhoek* 90:377–389
- Deplanche K, Macaskie LE (2008) Biorecovery of gold by *Escherichia coli* and *Desulfovibrio desulfuricans*. *Biotechnol Bioeng* 99:1055–1064
- Duran N, Marcato PD, Alves OL, De Souza GHI, Esposito E (2005) Mechanistic aspects of biosynthesis of silver nanoparticles by several *Fusarium oxysporum* strains. *J Nanobiotechnol*. doi:10.1186/1477-3155-3-8
- Fayaz AM, Balaji K, Kalaichelvan PT, Venkatesan R (2009) Fungal based synthesis of silver nanoparticles- an effect of temperature on the size of particles. *Colloids Surf B: Biointerfaces* 74:123–126
- Fredrickson JK, Zachara JM, Kennedy DW, Liu C, Duff MC, Hunter DB, Dohnalkova A (2002) Influence of Mn oxides on the reduction of uranium(VI) by the metal-reducing bacterium *Shewanella putrefaciens*. *Geochim Cosmochim Acta* 66:3247–3262
- Gericke M, Pinches A (2006) Microbial production of gold nanoparticles. *Gold Bull* 39:22–27
- Gorby YA, Lovley DR (1992) Enzymatic uranium precipitation. *Environ Sci Technol* 26:205–207
- Gurunathan S, Kalishwaralal K, Vaidyanathan R, Deepak V, Pandian SRK, Muniyandi J, Hariharan N, Eom SH (2009) Biosynthesis, purification and characterization of silver nanoparticles using *Escherichia coli*. *Colloids Surf B: Biointerfaces* 74:328–335
- Holmes JD, Richardson DJ, Saed S, Evans-Gowing R, Russell DA, Sodeau JR (1997) Cadmium-specific formation of metal sulfide 'Q-particle' by *Klebsiella pneumoniae*. *Microbiology* 143:2521–2530
- Husseiny MI, El-Aziz MA, Badr Y, Mahmoud MA (2007) Biosynthesis of gold nanoparticles using *Pseudomonas aeruginosa*. *Spectrochim Acta Part A* 67:1003–1006
- Ingle A, Rai M, Gate A, Bawaskar M (2009) *Fusarium solani*: a novel biological agent for the extracellular synthesis of silver nanoparticles. *J Nanopart Res* 11:2079–2085

- Joerger R, Klaus T, Granqvist CG (2000) Biologically produced silver carbon composite materials for optically functional thin-film coatings. *Adv Mater* 12:407–409
- Kalimuthu K, Babu RS, Venkataraman D, Bilal M, Gurunathan S (2008) Biosynthesis of silver nanoparticles by *Bacillus licheniformis*. *Colloids Surf B Biointerfaces* 65:150–153
- Karbasian M, Atyabi SM, Siadat SD, Momen SB, Norouziyan D (2008) Optimizing nano-silver formation by *Fusarium oxysporum* PTCC 5115 employing response surface methodology. *Am J Agric Biol Sci* 3:433–437
- Kashefi K, Tor JM, Nevin KP, Lovley DR (2001) Reductive precipitation of gold by dissimilatory Fe(III)-reducing Bacteria and Archaea. *Appl Environ Microbiol* 67:3275–3279
- Kathiresan K, Manivannan S, Nabeel MA, Dhivya B (2009) Studies on silver nanoparticles synthesized by a marine fungus, *Penicillium fellutanum* isolated from coastal mangrove sediment. *Colloids Surf B Biointerfaces* 71:133–137
- Klaus T, Joerger R, Olsson E, Granqvist CG (1999) Silver- based crystalline nanoparticles, microbially fabricated. *Proc Natl Acad Sci U S A* 96:13611–13614
- Konishi Y, Tsukiyama T, Ohno K, Saitoh N, Nomura T, Nagamine S (2006) Intracellular recovery of gold by microbial reduction of AuCl<sup>-</sup> ions using the anaerobic bacterium *Shewanella algae*. *Hydrometallurgy* 81:24–29
- Konishi Y, Ohno K, Saitoh N, Nomura T, Nagamine S, Takahashi Y, Uruga T (2007a) Bioreductive deposition of platinum nanoparticles on the bacterium *Shewanella algae*. *J Biotechnol* 128:648–653
- Konishi Y, Tsukiyama T, Tachimi T, Saitoh N, Nomura T, Nagamine S (2007b) Microbial deposition of gold nanoparticles by the metal-reducing bacterium *Shewanella algae*. *Electrochim Acta* 53:186–192
- Kowshik M, Dashmukh N, Vogel W, Urban J, Kulkarni SK, Paknikar KM (2002a) Microbial synthesis of semiconductor CdS nanoparticles, their characterization, and their use in the fabrication of an ideal diode. *Biotechnol Bioeng* 78:583–588
- Kowshik M, Vogel W, Urban J, Kulkarni SK, Paknikar KM (2002b) Microbial synthesis of semiconductor PbS nanocrystallites. *Adv Mater* 14:815–818
- Kowshik M, Ashtaputre S, Kharrazi S, Vogel W, Urban J, Kulkarni SK, Paknikar KM (2003) Extracellular synthesis of silver nanoparticles by a silver-tolerant yeast strain MKY3. *Nanotechnology* 14:95–100
- Krutyakov YA, Kudrinskiy AA, Olenin AY, Lisichkin GV (2008) Synthesis and properties of silver nanoparticles: advances and prospects. *Rus Chem Rev* 77:233–257
- Kumar SA, Abyaneh MK, Gosavi SW, Kulkarni SK, Paricha R, Ahmad A, Khan MI (2007a) Nitrate reductase-mediated synthesis of silver nanoparticles from AgNO<sub>3</sub>. *Biotechnol Lett* 29:439–445
- Kumar SA, Ansary AA, Ahmad A, Khan MI (2007b) Biosynthesis of extracellular CdSe quantum dots by the fungus *Fusarium oxysporum*. *J Biomed Nanotechnology* 3:190–194
- Labrenz M, Druschel GK, Thomsen-Ebert T, Gilbert B, Welch SA, Kemner KM, Logan GA, Summons RE, Stasio GD, Bond PL, Lai B, Kelly SD, Banfield JF (2000) Formation of sphalerite (ZnS) deposits in natural biofilms of sulfate-reducing bacteria. *Science* 290:1744–1747
- Lang C, Schüler D, Favier D (2007) Synthesis of magnetite nanoparticles for bio- and nanotechnology: genetic engineering and biomimetics of bacterial magnetosomes. *Macromol Biosci* 7:144–151
- Lengke MF, Southam G (2006) Bioaccumulation of gold by sulfate-reducing bacteria cultured in the presence of gold(I)-thiosulfate complex. *Geochim Cosmochim Acta* 70:3646–3661
- Lengke MF, Fleet ME, Southam G (2006a) Morphology of gold nanoparticles synthesized by filamentous cyanobacteria from gold(I)-thiosulfate and gold(III)-chloride complexes. *Langmuir* 22:2780–2787
- Lengke MF, Fleet ME, Southam G (2006b) Synthesis of platinum nanoparticles by reaction of filamentous cyanobacteria with platinum (IV)-chloride complex. *Langmuir* 22: 7318–7323

- Lengke MF, Ravel B, Fleet ME, Wanger G, Gordon RA, Southam G (2006c) Mechanisms of gold bioaccumulation by filamentous cyanobacteria from gold(III)-chloride complex. *Environ Sci Technol* 40:6304–6309
- Liu C, Gorby YA, Zachara JM, Fredrickson JK, Brown CF (2002) Reduction kinetics of Fe(III), Co(III), U(VI), Cr(VI) and Tc(VII) in cultures of dissimilatory metal-reducing bacteria. *Biotechnol Bioeng* 80:637–649
- Lloyd JR, Yong P, Macaskie LE (1998) Enzymatic recovery of elemental palladium by using sulfate-reducing bacteria. *Appl Environ Microbiol* 64:4607–4609
- Lovley DR, Phillips EJ (1992) Reduction of uranium by *Desulfovibrio desulfuricans*. *Appl Environ Microbiol* 58:850–856
- Maliszewska I, Sadowski Z (2009) Synthesis and antibacterial activity of silver nanoparticles. *J Phys: Conf Ser*. doi:10.1088/1742-6596/146/1/0112024
- Maliszewska I, Szewczyk K, Waszak K (2009) Biological synthesis of silver nanoparticles. *J Phys: Conf Ser*. doi:10.1088/1742-6596/146/1/012025
- Marshall MJ, Beliaev AS, Dohnalkova AC, Kennedy DW, Shi L, Wang Z, Boyanov MI, Lai B, Kemner KM, McLean JS, Reed SB, Culley DE, Bailey VL, Simonson CJ, Saffarini DA, Romine MF, Zachara JM, Fredrickson JK (2006) c-Type of cytochrome-dependent formation of U(IV) nanoparticles by *Shewanella oneidensis*. *PLoS Biol* 4:1–17
- Michel C, Brugna M, Aubert C, Bernadac A, Bruschi M (2001) Enzymatic reduction of chromate: comparative studies using sulfate-reducing bacteria: key role of polyheme cytochromes c and hydrogenases. *Appl Microbiol Biotechnol* 55:95–100
- Mokhari N, Daneshpajouh S, Seedbagheri S, Atashdehghan R, Abdi K, Sarkar S, Minaian S, Shahverdi HR, Shahverdi AR (2009) Biological synthesis of very small nanoparticles by culture supernatant of *Klebsiella pneumoniae*: the effects of visible-light irradiation and the liquid mixing process. *Mater Res Bull* 44:1415–1421
- Moon JW, Roh Y, Lauf RJ, Vali H, Yeary L, Phelps TJ (2007) Microbial preparation of metal-substituted magnetite nanoparticles. *J Microbiol Methods* 70:150–158
- Mukherjee P, Ahmad A, Mandal D, Senapati S, Sainkar SR, Khan MI, Parischa R, Ajayakumar PV, Alam M, Kumar R, Sastry M (2001a) Fungus mediated synthesis of silver nanoparticles and their immobilization in the mycelial matrix: a novel biological approach to nanoparticle synthesis. *Nano Lett* 1:515–519
- Mukherjee P, Ahmad A, Mandal D, Senapati S, Sainkar SR, Khan MI, Ramani R, Parischa R, Ajayakumar PV, Alam M, Sastry M, Kumar R (2001b) Bioreduction of AuCl<sub>4</sub><sup>-</sup> ions by the fungus *Verticillium* sp. and the surface trapping of the gold nanoparticles formed. *Angew Chem Int Ed* 40:3585–3588
- Mukherjee P, Senapati S, Mandal D, Ahmad A, Khan MI, Kumar R, Sastry M (2002) Extracellular synthesis of gold nanoparticles by the fungus *Fusarium oxysporum*. *ChemBioChem* 5:461–463
- Mukherjee P, Roy M, Dey GK, Mukherjee PK, Ghatak J, Tyagi AK, Kale SP (2008) Green synthesis of highly stabilized nanocrystalline silver particles by a non-pathogenic and agriculturally important fungus *T. asperellum*. *Nanotechnology*. doi:10.1088/0957-4484/19/7/075103
- Mulvaney P (1996) Surface plasmon spectroscopy of nanosized metal particles. *Langmuir* 12:788–800
- Murray CB, Kagan CR, Bawendi MG (2000) Synthesis and characterization of monodisperse nanocrystals and close-packed nanocrystal assemblies. *Annu Rev Mater Sci* 30:545–610
- Nair B, Pradeep T (2002) Coalescence of nanoclusters and formation of submicron crystallites assisted by *Lactobacillus* strains. *Cryst Growth Des* 2:293–298
- Nakajima A (2003) Accumulation of gold by microorganisms. *World J Microbiol Biotechnol* 19:369–374
- Nangia Y, Wangoo N, Goyal N, Shekhawat G, Suri CR (2009a) A novel bacterial isolate *Stenotrophomonas maltophilia* as living factory for synthesis of gold nanoparticles. *Microb Cell Fact* 8:1–7

- Nangia Y, Wangoo N, Sharma S, Wu JS, Dravid V, Shekhawat GS, Suri CR (2009b) Facile biosynthesis of phosphate capped gold nanoparticles by a bacterial isolate *Stenotrophomonas maltophilia*. *Appl Phys Lett* 94:233901-1–233901-3
- Nikhil SS, Bule M, Bhambure R, Singhal S, Singh SK, Szakacs PA (2009) Biosynthesis of silver nanoparticles using aqueous extract from the compactin producing fungal strain. *Process Biochem* 44:939–943
- Parikh RY, Singh S, Prasad BLV, Patde MS, Sastry M, Shouche YS (2008) Extracellular synthesis of crystalline silver nanoparticles and molecular evidence of silver resistance *Morganella sp*: towards understanding biochemical synthesis mechanisms. *Chem Bio Chem* 9:1415–1422
- Pighi L, Pumbel T, Schinner F (1989) Selective accumulation of silver by fungi. *Biotechnol Lett* 11:275–280
- Pimprikar PS, Joshi SS, Kumar AR, Zinjarde SS, Kulkarni SK (2009) Influence of biomass and gold salt concentration on nanoparticle synthesis by the tropical marine yeast *Yarrowia lipolytica* NCIM 3589. *Colloids Surf B: Biointerfaces* 74:309–316
- Pollmann K, Merroun M, Raff J, Hennig C, Selenska-Pobell S (2006) Manufacturing and characterization of Pd nanoparticles formed on immobilized bacterial cells. *Lett Appl Microbiol* 43:39–45
- Prabhu N, Revathi N, Darsana R, Sruthi M, Chinnaswamy P, Innocent DJP (2009) Antibacterial activities of silver nanoparticles synthesized by *Aspergillus fumigatus*. *Icfai Univ J Biotechnol* III(2):50–55
- Rafii F, Hehman GL, Shahveri AR (2005) Factors affecting nitroreductase activity in the biological reduction of nitrocompounds. *Curr Enz Inhibit* 1:223–230
- Reese RN, Winge DR (1988) Sulfide stabilization of the cadmium- $\gamma$ -glutamyl peptide complex of *Schizosaccharomyces pombe*. *J Biol Chem* 263:12832–12835
- Riddin TL, Gericke M, Whiteley CG (2006) Analysis of the inter- and extracellular formation of platinum nanoparticles by *Fusarium oxysporum* f. sp. *lycopersici* using response surface methodology. *Nanotechnology* 17:3482–3489
- Riddin TL, Govender Y, Gericke M, Whiteley CG (2009) Two different hydrogenase enzymes from sulphate-reducing bacteria are responsible for the bioreductive mechanism of platinum into nanoparticles. *Enzyme Microbiol Technol* 45:267–273
- Roh Y, Lauf RJ, McMillan AD, Zhang C, Rawn CJ, Bai J, Phelps TJ (2001) Microbial synthesis and characterization of metal-substituted magnetites. *Solid State Commun* 118:529–534
- Sadowski Z, Maliszewska I, Grochowalska B, Polowczyk I, Koźlecki T (2008) Synthesis of silver nanoparticles using microorganisms. *Mater Sci Poland* 26:419–424
- Sanghi R, Verma P (2009) Biomimetic synthesis and characterization of protein capped nanoparticles. *Biores Technol* 100:501–504
- Sastry M, Ahmad A, Khan MI, Kumar R (2003) Biosynthesis of metal nanoparticles using fungi and actinomycete. *Curr Sci* 85:162–170
- Senapati S, Ahmad A, Khan MI, Sastry M, Kumar R (2005) Extracellular biosynthesis of bimetallic Au-Ag alloy nanoparticles. *Small* 1:517–520
- Shahverdi AR, Minaeian S, Shahverdi HR, Jamalifar H, Nohi AA (2007) Rapid synthesis of silver nanoparticles using culture supernatants of *Enterobacteria*: a novel biological approach. *Process Biochem* 42:919–923
- Shaligram NS, Bule M, Bhambure R, Singhal RS, Singh SK, Szakacs G, Pandey A (2009) Biosynthesis of silver nanoparticles using aqueous extract from the compactin producing fungal strain. *Process Biochem* 44:939–943
- Shankar SS, Ahmad A, Parischa S, Sastry M (2003) Bioreduction of chloroaurate ions by geranium leaves and its endophytic fungus yields gold nanoparticles of different shapes. *J Mater Chem* 13:1822–1826
- Shiying H, Guo Z, Zhang Y, Zhang S, Wang J, Gu N (2007) Biosynthesis of gold nanoparticles using the bacteria *Rhodospseudomonas capsulata*. *Mater Lett* 61:3984–3987
- Shiying H, Zhang Y, Guo Z, Gu N (2008) Biological synthesis of gold nanowires using extract of *Rhodospseudomonas capsulata*. *Biotechnol Prog* 24:476–480

- Slawson RM, Trevors JT, Lee H (1992) Silver accumulation and resistance in *Pseudomonas stutzeri*. Arch Microbiol 158:398–404
- Sweeney RY, Mao C, Gao X, Burt JL, Belcher AM, Georgiou G, Iverson BL (2004) Bacterial biosynthesis of cadmium sulfide nanocrystals. Chem Biol 11:1553–1559
- Vigneshwaran N, Kathe AA, Varadajan PV, Nachane RP, Balasubramanya RH (2006) Biomimetics of silver nanoparticles by white rot fungus, *Phaenerochaete chrysosporium*. Colloids Surf B: Biointerfaces 53:55–59
- Vigneshwaran N, Ashtaputre NM, Varadarajan PV, Nachane RP, Paralikar KM, Balasubramanya RH (2007) Biological synthesis of silver nanoparticles using the fungus *Aspergillus flavus*. Mater Lett 61:1413–1418
- Woolfolk CA, Whiteley HR (1962) Reduction of inorganic compounds with molecular hydrogen by *Micrococcus lactilyticus*. I. Stoichiometry with compounds of arsenic, selenium, tellurium, transition and other elements. J Bacteriol 84:647–658
- Xie J, Lee JY, Wang DIC, Ting YP (2007) High-yield synthesis of complex gold nanostructures in a fungal system. J Phys Chem C 111:16858–16865
- Yan S, He W, Sun C, Zhang X, Zhao H, Li Z, Zhou W, Tian X, Sun X, Han X (2009) The biomimetic synthesis of zinc phosphate nanoparticles. Dyes Pigm 80:254–258
- Yanke LJ, Bryant RD, Laishley EJ (1995) Hydrogenase of *Clostridium pasteurianum* as a novel selenite reductase. Anaerobe 1:61–67
- Yong P, Rowson NA, Farr JPG, Harris IR, Macaskie LE (2002a) Bioaccumulation of palladium by *Desulfovibrio desulfuricans*. J Chem Technol Biotechnol 77:593–601
- Yong P, Rowson NA, Farr JPG, Harris IR, Macaskie LE (2002b) Bioreduction and biocrystallization of palladium by *Desulfovibrio desulfuricans* NCIMB 8307. Biotechnol Bioeng 20:369–379
- Zadvorny OA, Zorin NA, Gogotov IN (2006) Transformation of metals and metal ions by hydrogenases from phototrophic bacteria. Arch Microbiol 184:279–285
- Zhang H, Li Q, Lu Y, Sun D, Lin X, Deng X, He N, Zheng S (2005) Biosorption and bioreduction of diamine silver complex by *Corynebacterium*. J Chem Technol Biotechnol 80:285–290



# Chapter 8

## Basic and Practical Procedures for Microbial Synthesis of Nanoparticles

Ahmad-Reza Shahverdi, Mojtaba Shakibaie, and Pardis Nazari

### 8.1 Introduction

The reduction of particles to nanometric dimensions is one of the most important aspects in nanotechnology. On the nanoscale, physical and chemical properties of material are significantly different from macroscopic and even microscopic ones (Poole and Owens 2003). The large surface-to-volume ratio, an important property of nanoparticles, makes them distinct from larger particles. Furthermore, in comparison to the bulk material, the electronic, optical, catalytic, and magnetic characteristics of nanoparticles are very different (Schmid 2001; Panigrahi et al. 2004). Actually, particles at the nanoscale do not obey the laws of classical physics anymore because quantum effects become predominant (Panigrahi et al. 2004). Therefore, nanotechnology provides scientists the wonderful opportunity to investigate the laws of nature at the atomic scale. The prospect to control material on the molecular and atomic scale attracts many physicists, chemists, biologists, and engineers worldwide (Kohler and Fritzsche 2004). All their disciplines have met at the nanoscale in the effort to understand and control the nanoparticles with the final aim to find novel applications that could help in curing diseases or in making less pollution in the air or water (Kubik et al. 2005).

A variety of physical and chemical methods are being employed to synthesize the nanoparticles. Basically, these methods were divided into two types: bottom-up and top-down processes (Wong et al. 2009). In top-down methods, a bulk solid

---

A.-R. Shahverdi (✉) and P. Nazari

Department of Pharmaceutical Biotechnology and Biotechnology Research Center, Tehran University of Medical Sciences, Tehran, Iran  
e-mail: shahverd@sina.tums.ac.ir; pnazari@razi.tums.ac.ir

M. Shakibaie

Department of Pharmaceutical Biotechnology and Biotechnology Research Center, Tehran University of Medical Sciences, Tehran, Iran

and

Department of Pharmaceutical Biotechnology, Kerman University of Medical Sciences, P.O. Box 76175-493, Kerman, Iran  
e-mail: m\_shakibaie@razi.tums.ac.ir

material is broken into many nanoscale pieces with various techniques such as mechanical milling or laser degradation. Generally, with these methods, some properties of nanoparticles like particle size or shape could be controlled by time and temperature of the process. In bottom-up processes, nanoparticles are synthesized atom by atom. Consequently, a very small size of nanoparticles and uniformity in size distribution was achieved (Xu et al. 2006; Wong et al. 2009).

Currently, there is an impressive development in industrialization and urbanization that is damaging the environment by introducing a number of harmful and unwanted substances in natural ecosystems. To develop a simple and eco-friendly technology for synthesis of nanoparticles with novel properties, researchers in this field have turned to biological systems (Mohanpuria et al. 2008). Biosynthetic methods employing either microorganisms (Murray et al. 2000; Mandal et al. 2006) or plant extracts (Ramezani et al. 2008) have known a simple and novel alternative to chemical and physical methods. Biological production of nanoparticles by microorganisms could be defined as a new type of bottom-up technique by which atoms are assembled to grow from smaller to bigger particles (Shahverdi et al. 2007). Despite stability and a green method of preparation, the nanoparticle formation rate is not comparable to nonbiological synthesis methods. In fact, biological synthesis would have greater commercial acceptance if the nanoparticles could be synthesized more rapidly and economically on a large scale. However, in order to achieve better control of size, composition, shape, stability, and rate of nanoparticle production, biological procedures could be used with some optimization (Bhattacharya and Rajinder 2005; Mohanpuria et al. 2008).

There is a particular interest in the biosynthesis of nanoparticles that could find successful applications in fields like medicine, biophysics, environmental issues, and nanomaterial design. Based on this view, the main object of this chapter is to present a different practical approach and guidelines for microbial synthesis and characterization of nanoparticles.

## 8.2 Microbial Screening

Screening is one of the most important steps for finding a microorganism that can synthesize a specific metal nanoparticle. At screening process, microorganisms from different sources such as a local type culture collections or environment can be screened. Conversion of some inorganic ions such as  $\text{Ag}^+$  into their metallic forms can take place by way of microorganisms isolated from different metal-enriched environments such as seawater and metal-containing wastewater from some industries. Collection of samples from these places is a high priority for finding bacteria that can convert a specific metal ion into its nanoparticles. Isolation and enrichment of metal-reducing microorganisms should be carried out by using culture media supplemented with the desired metal ions at different concentrations. However, different microorganisms have different susceptibilities to metal ions, but generally metal-reducing microorganisms are resistant to higher concentrations.

In order to determine which bacterial colony could synthesize the metal nanoparticles, a detectable signal such as a change in culture media color due to nanoparticle production, appearance of a new peak in the UV–Vis spectrum related to surface plasmon resonance and other confirmatory ways are very critical and should be followed. Although the main objective of this chapter is bacterial synthesis of nanoparticle methods for undergraduate students, for a successful screening of nanoparticle producers, we need to apply and explain various important microbiological methods here. In the next paragraphs, the screening of selenium nanoparticle producers and the related methods for microbial identification and nanoparticle characterization will be discussed as an example for a practical work in laboratory scale (Jafari Fesharaki et al. 2010; Garg 2005). Selenium is a metalloid chemical element, a member of group XVI of the periodic table.

### **8.2.1 Sampling**

Fresh water samples from different regions such as seawater, lakes, rivers or wastewater, where the concentration of metal ions is probably high, should be collected in sterile bottles (Oremland et al. 2004).

### **8.2.2 Serial Dilution**

1. Label six sterile test tubes 1 through 6, and with a 10 mL pipette, dispense 9 mL normal saline solution (NaCl 0.9%w/v) into each tube.
2. Add 1 mL fresh water sample to the first tube in sterile condition.
3. Shake mixture in tube 1 until the sample becomes dispersed throughout the tube.
4. Make a tenfold dilution from tube 1 through tube 6 by transferring 1 mL of first tube to the next one. Use a fresh sterile pipette for each transfer, and be sure to thoroughly pipette the sample up and down before each transfer (Benson 2002).

### **8.2.3 Isolation**

1. Prepare 100 mL nutrient agar medium (meat extract 1 g/L, yeast extract 2 g/L, peptone 5 g/L, sodium chloride 5.0 g/L, final pH 7.4 and agar 15–20 g/L) and sterilize it using autoclave for 20 min at 121°C (15 psi).
2. Allow solution to cool to 50°C.
3. Weigh 140.5 mg of SeO<sub>2</sub> or 280 mg of selenium chloride and dissolve it in sterile water in a 10 mL volumetric balloon (Shakibaie et al. 2010). These selenium salts are categorized as toxic materials, and safety protocol should be studied and considered during sample handling. Many material safety data sheets of selenium have been published on the web and are freely available for all users.

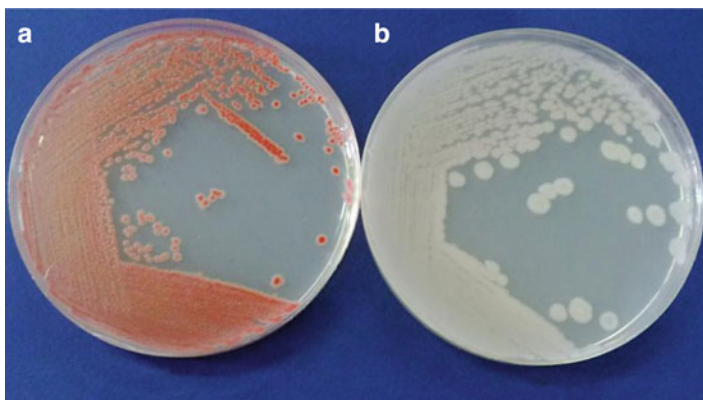


**Fig. 8.1** Visible growth of *Bacillus* sp. MSh-1 on nutrient agar plate with  $\text{SeO}_2$  (a) and without  $\text{SeO}_2$  (b)

4. For sterilization of  $\text{SeO}_2$  or  $\text{SeCl}_4$  solution, filter it through a  $0.22 \mu\text{m}$  filter in a sterile condition.
5. Culture media with different concentrations of selenium ion should be selected and used for this experiment to guarantee a positive response. As an example for preparation of selenium ions supplemented culture media (10, 50 and 100 mg/L), mix 0.1, 0.5 and 1 mL sterile  $\text{SeO}_2$  solution or  $\text{SeCl}_4$  solution with molten nutrient agar medium ( $50^\circ\text{C}$ ) to final volume of 100 mL in sterile flask (500 mL). Subsequently, transfer each prepared media to disposal Petri dishes, and mark each Petri dish appropriately.
6. Transfer 1 mL solution from sample dilutions of  $10^{-4}$  to  $10^{-6}$  (tubes 4, 5, and 6) onto the surface of selenium ions supplemented with nutrient agar media in triplicate (10, 50, and 100 mg/L), and spread the sample solutions over the surface of each agar plate.
7. Label inoculated Petri dishes with your initials and incubates at  $30^\circ\text{C}$  for 24–48 h.
8. After the incubation, reddish or nonred colonies may be observed on the surface of culture plates. The observation of red colonies could be a sign of selenium nanoparticle-producing bacteria (Fig. 8.1). To ensure that the red color is not contributing to other bacterial pigments such as prodigiosin, transfer these colonies onto plain nutrient agar plates without selenium ions (Oremland et al. 2004).

### 8.3 Pure Culture

The microbial mass isolated in the first screening described above may be contaminated. For identification, characterization, and further study of an individual species that produce nanoparticles, a pure culture should be provided by conventional

methods. Several methods for isolation and purification of an auxenic culture from a mixed culture are available in the literature (Benson 2002; Garg 2005). The routine streak plate technique is frequently used for this purpose in the laboratory and discussed in this chapter.

### **8.3.1 Streak Plate Method**

1. Sterilize an inoculating loop or transfer needle by placing it at an angle over a flame, and remove the lid from a culture plate containing the selenium-reducing isolates.
2. Cool the inoculating loop by stabbing it into the agar in a spot that does not contain a bacterial colony, and pick a colony and scrape off a little of the selenium-reducing bacteria using the loop.
3. Lift the lid of a new selenium ion-supplemented nutrient agar (100 mg/L) plate just enough to insert the loop, and streak the loop containing the bacteria at the top end of the selenium ion-supplemented nutrient agar (100 mg/L) plate, moving in a zig-zag horizontal pattern until 1/3 of the plate is covered.
4. Sterilize the loop again in the flame.
5. Cool it at the edge of the agar away from the bacteria in the plate that you just streaked, and rotate the plate about 60° and spread the bacteria from the first streak into a second area using the same motion in step 3.
6. Sterilize the loop again using the procedure in step 4.
7. Rotate the plate about 60°, and spread the bacteria from the second streak into a new area in the same pattern and sterilize the loop again.
8. Replace the lid and invert the plate.
9. Label Petri dishes and incubate at 30°C for 24–48 h (Benson 2002).
10. After this, you should see bacterial cells growing in streaks and in isolated areas as single colonies with red color.

## **8.4 Identification of the Isolate**

After isolating a selenium-reducing strain, the next step is to attempt to identify the unknown microorganism. Two approaches would lead us to this purpose; the first one is determining phenotypic characteristics, which involves investigating the organism's morphological, cultural, and biochemical properties. The second one is molecular biology techniques.

### **8.4.1 Determining Phenotypic Characteristics**

This strategy involves making different kinds of culture media and slides. Some key tests must be done for all kinds of bacteria that categorize the organisms into

primary groups. Each group includes different families and genera that could be determined using separation outline diagrams in microbiological textbooks (Forbes et al. 1998). Here, some of the most important ones are noted.

#### 8.4.1.1 Gram Stain

The starting point in the identification of an unknown microorganism is learning about its morphological characteristics, whether it is rod, coccus, or spiral shaped and what the reaction to Gram staining is. The following protocol will provide valuable information regarding these points and divide bacteria into two main groups: Gram-positive and Gram-negative bacteria (Benson 2002).

1. Transfer a loopful of the liquid culture to a clean glass slide and spread it over a small area. If using solid media, place a drop of water and transfer a small colony to the drop and spread it.
2. Allow the slide to air-dry.
3. Fix the dried slide by passing it several times over a flame. The slide shouldn't become too hot to touch.
4. Cover the slide with the crystal violet solution for 1 min. Wash with running tap water.
5. Flood the slide with Gram's iodine solution for about 1 min. Wash with tap water.
6. Flood the slide with 95% ethanol for 10 s for decolorization, and wash off with tap water. If the smear is too thick, it may require longer decolorization.
7. Flood the slide with safranin solution for 45 s to counterstain. Wash with tap water.
8. Examine the slide under oil immersion microscopy.

*Results:* Organisms that retain the dye complexes after washing in ethanol stain purple and are termed Gram-positive; those that decolorize with ethanol treatment stain red due to the safranin counterstain and are termed Gram-negative (Forbes et al. 1998).

#### 8.4.1.2 Oxygen Requirement

Semi-solid Fluid Thioglycollate Medium (FTM) is designed to test the aerotolerance of bacteria. Methylene blue is used as an indicator in this culture medium, which is colorless in an anaerobic environment and greenish-blue in the presence of oxygen. Rapid oxygen uptake and diffusion into the FTM is prevented by agar. Different obligate aerobic, microaerobic, facultative anaerobic, and obligate anaerobic bacteria can grow in different layers of this medium. Oxygen is excluded during the autoclaving process, but at room temperature, oxygen gradually diffuses back into the medium, which is evidenced by a thin blue-green layer at the top of the tube (Benson 2002).

1. Suspend 30 g/L FTM powder in distilled water, and dispense in tubes in a way such that each tube contains approximately 7–8 mL of this fresh medium.
2. Autoclave tubes for 15 min at 121°C. The prepared medium is clear and yellowish.
3. Inoculate the FTM with the unknown organism. The bacteriological loop should reach the bottom of the tubes.
4. Incubate for several days at 35–37°C.

*Results:* Obligate aerobes will only grow in oxygen-rich top layer. Obligate anaerobes will only grow in the lower areas of the tube. Microaerophiles will grow in a thin layer below the oxygenated layer. Facultative anaerobes can grow throughout the medium, but primarily in the middle of the tube.

### 8.4.1.3 Motility Test

Two approaches can be used for investigating organism motility. One involves making a wet mount slide, but it's not suitable for pathogens, and the second is using a semisolid medium (Benson 2002).

#### Wet Mount (Hanging Drop) Method

1. Place a drop of liquid bacterial culture onto the center of a clean glass slide.
2. Hold a coverslip at 45° allowing the drop to spread along the edge of the slide and then gently invert it to avoid trapping any air bubbles.
3. Observe the slide microscopically ( $\times 400$ ) for motile organisms.

*Results:* Motile bacteria will show a darting, zig-zag, tumbling or other movement. Nonmotiles show no movement.

#### Semisolid Medium

The following formula (g/L) can be used for testing an organism's motility: (Peptone 10 g, NaCl 5 g, Beef extract 3 g and Agar 4 g).

1. Add sufficient components to distilled water to make 100 mL semisolid medium. Mix completely and warm it on a heat plate stirrer to obtain a homogenized solution. Next, distribute molten agar media into tubes in 10 mL volumes.
2. Autoclave all tubes for 15 min at 121°C. Cool tubes in an upright position.
3. Inoculate tubes with a full sample needle of pure culture and stab the center of the medium straight down at more than half the depth of the medium.
4. Incubate tubes for 24–48 h at 35°C.

*Results:* Nonmotile organisms only grow along the line of inoculation, while motile organisms spread out along the line of inoculation and produce a cloudy appearance.

#### **8.4.1.4 Spore Stain**

If the unknown organism is Gram-positive, it should be checked for formation of endospores. Bacterial spores are the most resistant forms of life known. During Gram staining of bacterial isolates, endospores can be observed as transparent holes in some Gram-positive bacteria (Mahon and Manuselis 2000; Benson 2002). Below is a spore staining protocol:

1. Make a slide preferably of older cultures, and fix it with several passes through a flame.
2. Place the slide on a screen and hold it over a moderate flame.
3. Flood it with saturated aqueous malachite green and allow to steam off for 10 min. The liquid should not dry up, so dye must be added frequently.
4. After cooling the slide, rinse it with tap water to remove excess stain.
5. Counterstain the slide with aqueous safranin for a minute. Rinse the slide and observe with oil immersion microscopy.

*Results:* Spores stain a light green, while vegetative cells stain pink.

#### **8.4.1.5 Acid-Fast Staining**

If the isolated bacteria is a Gram-positive, nonspore-forming rod, it should be determined if the organism is acid-fast or not. Acid-fast bacteria have waxy cell walls that can resist decolorization treatment with acid alcohol (Mahon and Manuselis 2000).

1. Make a smear as noted previously in Sect. 8.4.1.1.
2. Flood the smear with carbol fuchsin stain.
3. Pass the slide through a flame to steam for 5 min. Add additional stain if it boils off.
4. Wash the slide with water to remove excess dye.
5. Add acid-alcohol gradually for 15–20 s.
6. Rinse with water.
7. Counterstain with methylene blue for 1 min.
8. Wash with water and examine under oil immersion microscopy.

*Results:* Acid-fast bacteria will appear red, but non-acid-fast will stain blue.

#### **8.4.1.6 Catalase Test**

This test is used to detect the presence of catalase enzyme, which is evident due to decomposition of hydrogen peroxide to release oxygen and water. Hydrogen peroxide as an oxidative end product of aerobic sugar breakdown is formed by



some bacteria. The enzyme catalase prevents accumulation of the toxic hydrogen peroxide (Forbes et al. 1998; Benson 2002).

1. Place one drop of hydrogen peroxide solution on a slide.
2. Place a bacterial colony onto the center of the slide.
3. Look for vigorous bubbling within 10 s.

*Results:* Bubbling indicates the presence of catalase.

#### 8.4.1.7 Oxidase Test

The oxidase production assay is one of the most important tests used to determine if an organism possesses the cytochrome oxidase enzyme. Using the test, we can differentiate certain groups of bacteria. The reagent that is used is 1% *N,N,N',N'*-tetramethyl-*p*-phenylenediamine dihydrochloride in distilled water. Also, commercially impregnated oxidase test strips are available (Benson 2002).

##### *Filter paper method*

1. Soak a piece of filter paper in the reagent solution.
2. Pick up a colony from a fresh growth plate and rub onto the filter paper.
3. Examine for blue color within 10 s.

##### *Oxidase test strips*

1. Rub a fresh colony onto the strips.
2. Examine for blue color within 10 s.

*Results:* Development of blue color is evidence of oxidase production.

### 8.4.2 Identification of Isolated Bacterium by 16s rDNA Method

All tests mentioned in above sections give some important information about phenotypic and physiologic characteristics of bacteria, but further identification methods outlined in determinative bacteriology books may be needed for full characterization. 16s rDNA-based polymerase chain reaction (PCR) detection method is one of the most widely used techniques and can be successfully performed for identifying the isolates in laboratories. Identification of the genus and species of selected isolates using the 16s rDNA method should be carried out on a pure culture of microorganisms. Briefly, the 16s rDNA gene is amplified by PCR using universal primers. After sequencing of the amplified segment, its sequence should be compared with other sequences in the gene bank using the Basic Local Alignment Search Tool (BLAST). The comparison of rDNA sequences is a powerful tool for study of phylogenetic and evolutionary relationships among bacteria, archaeobacteria, and eukaryotic organisms (Weisburg et al. 1991). Identification of prokaryotes by the 16s rDNA method is done in six steps: Primary PCR, electrophoresis, final PCR step, electrophoresis, sequencing, and BLAST.

### 8.4.2.1 Primary PCR

The selection of suitable primer pairs and optimization of PCR conditions are two main critical points of this step. The selection of conserved sequences should be performed by alignment of various 16s rDNA genes in different bacteria (Weisburg et al. 1991). Classification of primers is based on the ordinary method in which F is known as forward primer and R is known as reverse primer. Some of these primers are given in Table 8.1. Numbers indicated in the first column in Table 8.1 show the location of the primer's sequences in the 16s rDNA gene in *Escherichia coli*, and we could choose the sequence length of the 16s rDNA gene we want to amplify. It is clear that for identification of a bacterium, the more sequence length of the 16s rDNA gene that is amplified, the more accuracy in identification that is achieved.

#### (A) Preparation of template DNA

1. Prepare an overnight culture of bacteria in a liquid medium (Sambrook and Russell 2001).
2. Transfer 50  $\mu$ L of overnight culture to a 0.2 mL microtube. In all steps of PCR protocol, the microtubes, tips, and other materials must be sterilized. Use gloves after sterilization process and during handling of the reagents.
3. Centrifuge the microtube at 14,000 rpm for 5 min and discard the supernatant.
4. Add 50  $\mu$ L of sterile dH<sub>2</sub>O to sediment and resuspend it by pipetting.
5. Centrifuge the microtube at 14,000 rpm for 5 min and discard the supernatant.
6. For more washing of sediment, repeat steps 4 and 5.
7. Once again, add 50  $\mu$ L of sterile dH<sub>2</sub>O to sediment and incubate the microbial suspension in a thermocycler at 90°C for 10 min. Cells will disrupt during this stage.
8. Centrifuge the microtube at 14,000 rpm for 5 min.
9. Transfer the supernatant, which contains the genomic DNA, to a new microtube and use it as template DNA.
10. Preserve the template DNA at -20°C for the next step (Sambrook and Russell 2001).

#### (B) Preparation of PCR Mix

All of the values listed in Table 8.2 have been calculated for a final volume of 25  $\mu$ L. The total volume is dependent on the number of testing primers. For evaluation of PCR protocol, we need two microtubes: test tube and negative control. The negative control contains all the PCR ingredients, but does not have genomic DNA as a template. Also, in order to ensure that other DNA templates do

**Table 8.1** Some universal primers for amplification of bacterial 16s rDNA gene (Furushita et al. 2003)

Primer	Sequence
27F	5'-AGA GTT TGA TCC TGG CTC AG-3'
1492R	5'-TAC GGT TAC CTT GTTACG ACT T-3'
1525R	5'-AAG GAG GTG ATC CAG CC-3'
517R	5'-GTA TTA CCG CGG CTG CTG GC-3'

**Table 8.2** The values of different reagents for preparation of PCR mix

Reagent	Volume ( $\mu\text{l}$ )	$x \times 2$	+10%	Final concentration
PCR buffer (10 $\times$ )	2.5	5	5.5	1 $\times$
dNTP (10 mM)	0.5	1	1.1	200 $\mu\text{M}$
Forward primer (10 $\mu\text{M}$ )	2.5	5	5.5	1 $\mu\text{M}$
Reverse primer (10 $\mu\text{M}$ )	2.5	5	5.5	1 $\mu\text{M}$
Taq polymerase (5 U/ $\mu\text{L}$ )	0.25	0.5	0.55	5 U/100 $\mu\text{L}$
MgCl <sub>2</sub> solution(50 mM)	0.75	1.5	1.65	1.5 mM
Sterile dH <sub>2</sub> O	11	22	24.2	–
Total	20	40	44	–

**Table 8.3** The values of different reagents for test and control microtube

Reagent	Test ( $\mu\text{L}$ )	Negative control ( $\mu\text{L}$ )
PCR mix	20	20
Template DNA	5	–
Sterile dH <sub>2</sub> O	–	5
Total	25	25

not contaminate the PCR reagents, we should use a negative control. It should be noted here for preparation of the final PCR mix (Table 8.2) that all values must be multiplied by 2. For pipetting errors, added 10% to these values (Sambrook and Russell 2001).

For preparation of PCR mix, follow these steps:

1. Clean the surface of a table with 70% ethanol.
2. For preparation of PCR, mix all reagents and add them to a sterile 1.5 mL microtube based on the values in Table 8.2.
3. Label two 0.2 mL microtubes as *test* and *negative control* and add reagents step by step according to Table 8.3.

### (C) PCR

For doing the PCR with 27F and 1492R primers, the following program can be used by a thermocycler (Furushita et al. 2003):

1. Initial devaluation temperature: 94°C for 180 s
2. Follow with 30 cycles (Denaturation: 94°C, 60 s; Annealing: 60°C, 45 s; Extension: 72°C, 90 s)
3. Final extension: 72°C, 300 s

If no product was obtained during PCR amplification process, further optimization of PCR conditions should be done, or another pair of primers should be used.

### 8.4.2.2 Electrophoresis

Electrophoresis is a necessary tool for showing the PCR products and for determination of sequence length that is amplified. Ethidium bromide (highly carcinogenic dye) is used for visualization of double-stranded genomic amplified products. This

**Table 8.4** Tris–acetate EDTA (TAE) buffer for electrophoresis

Buffer	Working solution (1×) ingredients	Stock solution/liter (50×) ingredients
TAE	40 mM Tris–acetate 1 mM EDTA	1,242 g of Tris base 57.1 mL of glacial acetic acid 100 mL of 0.5 M EDTA (pH 8.0)

compound is categorized as carcinogenic material. Therefore, all electrophoresis steps must be performed in a specific place, and all people in this place must use gloves (Sambrook and Russell 2001).

(A) *Tris–acetate EDTA (TAE) buffer preparation*

This buffer was used for agarose gel electrophoresis, and usually was prepared as a 50× stock and stored at room temperature. For gel preparation, this stock was diluted to 1× buffer with appropriate distilled water (Sambrook and Russell 2001).

For preparation of 50× buffer stock solution, please look at Table 8.4. Also, the molarities of ingredients in working buffer solution have been listed in this table.

(B) *Gel preparation*

1. Weigh 0.5 g agarose and add it to 50 mL TAE buffer (Sambrook and Russell 2001).
2. Heat the flask in a microwave oven for 10 s intervals until all agarose crystals are melted and dissolved. Notice that the solution should not be boiled during heating process.
3. Wait until its temperature reaches 50°C, and then add 2.5 μL of ethidium bromide and mix gently.
4. Select an appropriate gel casting tray. The open ends of the trays are closed with tape while the gel is being cast and then removed prior to electrophoresis.
5. Insert a sample comb around which molten agarose is poured to form sample wells in the gel.
6. After the gel has solidified, the comb is removed, using care not to rip the bottom of the wells. The gel, still in its plastic tray, is inserted horizontally into the electrophoresis chamber and just barely covered with buffer (Sambrook and Russell 2001).

(C) *Electrophoresis Run*

1. Mix reagents containing DNA ladder (1 μL), 6× loading dye solution (1 μL), and deionized water (4 μL). DNA ladder that contains DNA with different lengths should be used as a reference for determination of PCR product length.
2. Mix 5 μL of PCR products (negative control and test) with 1 μL of 6× loading buffer separately, and transfer them into individual comb places.
3. Samples containing DNA mixed with loading buffer and negative control solution are then pipetted into the sample wells; the lid and power leads are attached to the apparatus. Turn on the power supply and based on the distance between the two electrodes, apply a voltage between 1 and 5 V/cm for 30–45 min. Observing bubbles coming out of the electrodes confirms that current is flowing. DNA will migrate towards the positive electrode (Sambrook and Russell 2001).

4. Turn off the power supply and transfer the electrophoresis sample cast tray onto the ultraviolet transilluminator.
5. Turn on the transilluminator and set it to wavelength 312 nm. Amplified DNA bands are visualized. For the negative control, we mustn't see amplified bands. Shortly after, take a photo of the gel and transfer the gel to a specific waste box.
6. Clean the surface of the transilluminator with 70% ethanol (Sambrook and Russell 2001).

### 8.4.2.3 Sequencing

In the first step, sufficient PCR product for DNA sequencing analysis should be prepared. The previously described method (Sect. 8.4.2.1) can be used for final PCR experiment. In this PCR step the higher amounts of PCR ingredients must be selected for amplification. The amplified DNA products contain some impurities such as nucleotides and PCR primers. It should be submitted to the DNA sequencing department or life sciences company for further purification of PCR product and sequencing.

### 8.4.2.4 BLAST Protocol

1. Enter this web site: <http://www.ncbi.nlm.nih.gov/BLAST> (Claverie and Noterdame 2007).
2. In section *Basic BLAST*, please select “nucleotide BLAST” item.
3. Copy the final sequence of the 16s rDNA gene to the “Enter Query Sequence” box.
4. In section “Choose Search Set at Database port”, click other option item.
5. Enter the BLAST option.

The results consist of different parts, including Accession number, Description, Max score, Total score, Query coverage, E value, and Max identity, which can be used for identification of an isolated bacterium with alignment of its amplified 16s rDNA sequence and other submitted gene sequences published in the gene bank (Claverie and Noterdame 2007).

## 8.5 Synthesis of Metal or Metalloid Nanoparticles Using the Isolated Bacteria

Metal or metalloid nanoparticles can be biologically prepared by the reduction of metal ions by microorganisms such as *Enterobacteria* (Shahverdi et al. 2007). Some metal ions have considerable antibacterial activity against bacteria, so the

minimum inhibitory concentration (MIC) of desired metal ions should be firstly investigated against metal ion-reducing isolates. The sub-MIC concentration of metal ions that guarantee the microorganisms' growth should be selected and added to culture medium for intracellular-producing metal nanoparticles. MICs can be determined by agar or broth dilution methods using conventional methods described in books and literature detailing microbiological methods.

1. Prepare 100 mL nutrient broth medium. Add the correct amount of metal salt, which is not to be more than MIC.
2. Inoculate the medium with a pure culture of screened bacterium. Incubate it on a rotary shaker (150 rpm) at 30°C.
3. After 48 h, nanoparticles will be deposited in bacterial cells and may change the color of culture (for example, selenium nanoparticles give a red color) (Jafari Fesharaki et al. 2010).
4. Centrifuge cell suspension containing nanoparticles at 5,000–8,000 rpm for 10 min.
5. Resuspend the cell pellets in 0.9% NaCl solution and centrifuge at 5,000–8,000 rpm for 10 min.
6. Repeat the washing process three times to ensure removal of any undesirable materials.
7. Transfer pellets to a mortar and disrupt cells by liquid nitrogen.
8. Resuspend and centrifuge (12,000 rpm) the pellets in NaCl (0.5 M), sucrose (0.5 M), and finally resuspend into a complete salt solution [NaCl (17.5 g/L), KCl (0.74 g/L), MgSO<sub>4</sub>·7H<sub>2</sub>O (12.3 g/L), Tris HCl (0.15 g/L), and pH = 7.5] (Oremland et al. 2004).
9. Lyse the remaining cells with 35 mL of the complete salt solution containing 20 mg of egg white lysozyme by incubation at 22°C for 18 h. The lysed mixture is rinsed away from the nanoparticles by washing and centrifuge (12,000 rpm) with the complete salt solution and deionized water (Oremland et al. 2004).
10. Finally, resuspend the cleaned nanoparticles in deionized water for further characterization.

## 8.6 Nanoparticle Characterization

An important stage in biosynthesis of nanoparticles is physico-chemical characterization of generated nanoparticles. Knowing about size, shape, surface area, homogeneity, and other features will provide valuable information of nanoscale systems and insight into synthesis control of nanoparticles for commercial applications. Some common techniques of characterization are UV–visible spectrometry, Fourier transform infrared spectroscopy (FTIR), electron microscopy (TEM, SEM), dynamic light scattering (DLS), powder X-ray diffraction (XRD), and energy dispersive spectroscopy (EDS). Here, a brief description of each technique is prepared. For more information, refer to nanomaterial science texts.

### **8.6.1 *UV–Visible Spectrometry***

UV–visible spectroscopy has proven to be very useful for analyzing of different nanoparticles such as gold and silver nanoparticles (Ramezani et al. 2008). Observation of strong broad surface plasmon peaks at visible regions (400–600 nm) has been well documented for various metal nanoparticles, with sizes ranging widely from 2 to 100 nm. A UV–visible spectrophotometer consists of two devices, namely a spectrometer for producing light with different wavelengths, and a photometer for measuring the intensity of light. The instruments are arranged so that liquid in a cuvette can be placed between the spectrometer beam and the photometer. Further information is available about the mentioned spectroscopic method and this technique has been well described by different authors (Anderson et al. 2004; Hesse et al. 2008).

### **8.6.2 *Fourier Transform Infrared Spectroscopy***

A FTIR can be useful for preliminary investigation of surface chemistry of biogenic nanoparticles (i.e., those chemicals that contain carbon). In FTIR, the wavelength of the light is in the infrared range. Infrared light lies in between the microwave portions of the electromagnetic spectrum and visible light. This technique is widely used for identification of chemical residues such as amine, carbonyl, and hydroxyl functional groups in a molecule (Anderson et al. 2004; Hesse et al. 2008).

### **8.6.3 *Transmission Electron Microscope***

Through this technique, a fine electron beam passes through a very thin specimen. The source of electrons is a heated filament on the top of an evacuated column and electric coils, called electric lenses, which produce magnetic fields to control beam features. Due to specimen density variation, the shadow of the beam falls on a fluorescent screen near the bottom of the column and makes the image. The resolution power of a TEM is thousand times better than a light microscope and can resolve objects of a few angstroms (Poole and Owens 2003). With the use of TEM, some data about nanoparticle dimensions and shape could be obtained (Fig. 8.2).

### **8.6.4 *Scanning Electron Microscope***

The electron beam comes from a filament, typically a tungsten filament, and is condensed by a condenser lens and then by an objective lens focused onto the sample as a very sharp point. This beam scans over the surface of the specimen,

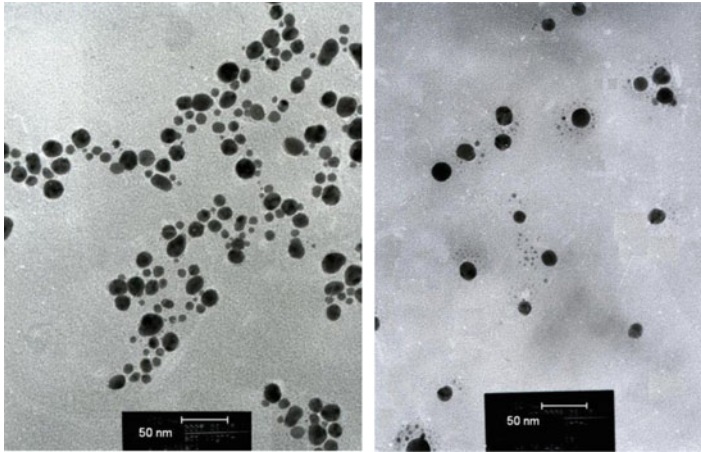


**Fig. 8.2** Transmission electron microscopy micrographs of metal nanoparticles with particle size of <math>< 50\text{ nm}</math>

and various signals including photons and electron signals are emitted from the sample surface. Different kinds of detectors are used to collect signals, and using secondary and backscattered electrons the image is formed. Secondary electrons have relatively low energy and are a surface-sensitive signal. This signal causes high-resolution topographic information and SEM imaging. Backscattered electrons possess higher energy than secondary electrons and come from deeper regions and therefore give good phase contrast information. Because all points were mentioned, the SEM image could provide us two main types of data, one is the topographic structure of the surface and the second one is the distinction of different phases in the sample (Poole and Owens 2003).

### **8.6.5 Dynamic Light Scattering**

DLS is a noninvasive technique to measure the size and size distribution of very fine particles dispersed or dissolved in a liquid. When a monochromatic light beam such as a laser hits the moving particles, those in Brownian motion in a liquid scatter in all directions. Since the distance between the scattered particles constantly differs with time, a change in scattered light intensity is observed. This change contains information about particle diameter and size and also size distribution, which could be computed using formulas. Available commercial particle sizing systems can perform this experiment in a short time, and they can almost completely automatically analyze the received data to give calculated results of particle size measurements (Poole and Owens 2003; Kohler and Fritzsche 2004).



### **8.6.6 Powder X-Ray Diffraction**

XRD is one of the primary analytical techniques used for phase identification and crystalline structure determinations in solid-state materials. Non-amorphous materials are composed of repeating regular planes of atoms that form a crystal lattice. In this method, a monochromatic X-ray directed onto a sample and the interaction between these planes of atoms and X-rays lead to diffracted rays being emitted. Depending on the atomic composition of the crystalline lattice and their arrangement, various minerals diffract X-ray beams differently. These diffracted X-rays are then collected and processed, and by comparison of the sample diffraction pattern with standard reference patterns and measurements, the material identification will be allowed (Kohler and Fritzsche 2004).

### **8.6.7 Energy Dispersive Spectroscopy**

It is an analytical technique used for chemical composition determination of a sample. The sample undergoes an electron beam bombardment and the surface comprising atoms eject their outer-shell electrons. Then, after the higher-state electrons filled the resulted vacancies, the energy difference between these two states of electrons was emitted as an X-ray beam. The emitted X-rays were detected and analyzed for their energy. Since the X-ray energy is a distinctive characteristic of each element; it could be used to componential analysis of samples (Poole and Owens 2003; Kohler and Fritzsche 2004).

## **8.7 Conclusion**

Today, nano metal particles have drawn the attention of scientists because of their extensive application to new technologies in chemistry, electronics, medicine, and biotechnology. Beside many physical and chemical methods which have been developed for preparing metal nanoparticles, nanobiotechnology also serves as an important method in the development of clean, nontoxic, and environmentally friendly procedures for the synthesis and assembly of metal nanoparticles. To be utilized in different scientific fields, biological synthesis still requires the optimization of reaction conditions, and an understanding of the biochemical and molecular mechanisms of the reaction for obtaining better chemical composition, shape, size, and monodispersity. In this chapter a brief overview for using bacteria in the biosynthesis of nanoparticles as an alternative to nonbiological methods has been described. By noticing the potential of the natural world to produce bio-nanomaterials under normal conditions, we are trying to explain simple practical methods that can be used for bacterial synthesis of metal or metalloid nanoparticles. For this purpose,

Chap. 8 began with screening procedures for isolating and purification of specific nanoparticle producer bacteria from the environment and continued with different simple methods for identification of the isolate. Then, preparation and recovery of the bio-nanoparticles were completely described and finally, different methods for characterization of the nanoparticles were briefly explained. The impetus for writing this chapter is to present simple guidelines for undergraduate students and other researchers who want to work in this field and we hope that it can be applicable.

## References

- Anderson RJ, DJ Ben dell, Groundwater PW (2004) Organic spectroscopic analysis. Royal Society of Chemistry, Cambridge
- Benson HJ (2002) Microbiological applications: laboratory manual in general microbiology, 8th edn. Mc Graw Hill Companies, New York
- Bhattacharya D, Rajinder G (2005) Nanotechnology and potential of microorganisms. Crit Rev Biotechnol 25:199–204
- Claverie JM, Noterdame C (2007) Bioinformatics for dummies, 2nd edn. Wiley, New York
- Forbes BA, Sahm DF, Weissfeld AS (1998) Bailey & Scott's diagnostic microbiology, 10th edn. Mosby, Missouri
- Furushita M, Shiba T, Maeda T, Yahata M, Kaneoka A, Takahashi Y, Torii K, Hasegawa T, Ohta M (2003) Similarity of tetracycline resistance genes isolated from fish farm bacteria to those from clinical isolates. Appl Environ Microbiol 69(9):5336–5342
- Garg FC (2005) Experimental microbiology. CBS, Delhi
- Hesse M, Meier H, Zeeh B (2008) Spectroscopic methods in organic chemistry, 2nd edn. Thieme, Stuttgart
- Jafari Fesharaki P, Nazari P, Shakibaie M, Rezaee S, Banoe M, Abdollahi M, Shahverdi AR (2010) Biosynthesis of selenium nanoparticles using *Klebsiella pneumoniae* and their recovery by a simple sterilization process. Braz J Microbiol 41:461–466
- Kohler M, Fritzsche W (2004) Nanotechnology, an introduction to nanostructuring techniques. Wiley-VCH, Germany
- Kubik T, Bogunia-Kubik K, Sugisaka M (2005) Nanotechnology on duty in medical applications. Curr Pharm Biotechnol 6(1):17–33
- Mahon CR, Manuselis G (2000) Text book of diagnostic microbiology, 2nd edn. Saunders, Pennsylvania
- Mandal D, Bolander ME, Mukhopadhyay D, Sarkar G, Mukherjee P (2006) The use of microorganisms for formation of metal nanoparticles and their application. Appl Environ Microbiol 69:485–492
- Mohanpuria P, Rana NK, Yadav SK (2008) Biosynthesis of nanoparticles: technological concepts and future applications. J Nanopart Res 10:510–517
- Murray CB, Kangan CR, Bawendi MG (2000) Synthesis and characterization of monodisperse nanocrystals and closed-packed nanocrystal assemblies. Annu Rev Mater Sci 30:545–610
- Oremland RS, Herbel MJ, Blum JS, Langley S, Beveridge TJ, Ajayan PM, SuttoT EAV, Curran S (2004) Structural and spectral features of selenium nanospheres produced by Se-respiring bacteria. Appl Environ Microbiol 70:52–60
- Panigrahi S, Kundu S, Ghosh SK, Nath S, Pal T (2004) General method of synthesis for metal nanoparticles. J Nanopart Res 4:411–414
- Poole CP Jr, Owens FJ (2003) Introduction to nanotechnology. Wiley, New York

- Ramezani N, Ehsanfar Z, Shamsa F, Amin G, Shahverdi HR, Monsef Esfahani HR, Shamsaie A, Dolatabadi Bazaz R, Shahverdi AR (2008) Screening of medicinal plant methanol extracts for the synthesis of gold nanoparticles by their reducing potential. *Z Naturforsch* 63b:903–908
- Sambrook J, Russell DW (2001) *Molecular cloning a laboratory manual*. Cold Spring Harbor, New York
- Schmid G (2001) *Nanoscale materials in chemistry*. Wiley, New York
- Shahverdi AR, Minaeian S, Shahverdi HR, Jamalifar H, Nohi AA (2007) Rapid synthesis of silver nanoparticles using culture supernatants of *Enterobacteria*: a novel biological approach. *Process Biochem* 42(5):919–923
- Shakibaie M, Khorramizadeh MR, Faramarzi MA, Sabzevari O, Shahverdi AR (2010) Biosynthesis and recovery of selenium nanoparticles and the effects on matrix metalloproteinase-2 expression. *Biotechnol Appl Biochem* 56:7–15
- Weisburg WG, Barns SM, Pelletier DA, Lane DJ (1991) 16S ribosomal DNA amplification for phylogenetic study. *J Bacteriol* 173(2):697–703
- Wong TS, Brough B, Ho CM (2009) Creation of functional micro/nano systems through top-down and bottom-up approaches. *Mol Cell Biomech* 6(1):1–55
- Xu C, van Zalinge H, Pearson JL, Glidle A, Cooper JM, Cumming DR, Haiss W, Yao J, Schiffrin DJ, Proupin-Pérez M, Cosstick R, Nichols RJ (2006) A combined top-down bottom-up approach for introducing nanoparticle networks into nanoelectrode gaps. *Nanotechnology* 17(14):3333–3339

# Chapter 9

## Development of a Process Chain for Nanoparticles Production by Yeasts

Nikolay Krumov and Clemens Posten

### 9.1 Introduction

Biological systems have always been interesting alternative source of ideas and solutions for technological challenges. Living cells provide unique conditions for building up highly organized, nano-sized complexes, involving prestructuring matrixes, autocatalysis and controlled self-assembly. The idea to use the potential of microorganisms to produce spatially structured materials for technical uses has historical backgrounds. The incorporation of nitroglycerine in diatomite mediated the invention of dynamite in 1867 by Alfred Nobel (Nobel 1868). Nowadays, microorganisms are objects of scientific interest for their ability to produce uniform nanoparticles, stabilized by natural, assembled polymer coating, revealing nontoxic and environmentally friendly synthetic pathways.

Living cells are highly organized systems with a sophisticated level of molecular control over the biosynthesis of inorganic materials (Fig. 9.1). The ability to produce spatially structured nanomaterials has evolutionary background. In order to populate different ecological niches, organisms have adopted special cell functions. The three main reasons for them to produce nanoparticles are (1) chemolithotrophy for energy production, (2) use of these particles for special functions and (3) detoxification for survival in toxic environments. All those well-known mechanisms are the basis for the new, nature-inspired approach for inorganic particles production, i.e., biosynthesis of nanomaterials by microorganisms.

In the present chapter, we focus on the perspectives arising from the biosynthetic potential of yeasts to produce nanoparticles. The choice of biological object–producer is based on centuries of knowledge, experience and tradition in cultivating and manipulating yeasts and the current significant share in food industry and industrial microbiology occupied by these microorganisms. We suggest an elaborated process chain for the production of nanoparticles by yeasts, including all

---

N. Krumov (✉) and C. Posten

Department of Bioprocess Engineering, Institute of Process Engineering in Life Sciences, Karlsruhe Institute of Technology, Fritz-Haber-Weg 2, Build. 30.44, Karlsruhe, Germany  
e-mail: nikolay.krumov@kit.edu; clemens.posten@kit.edu

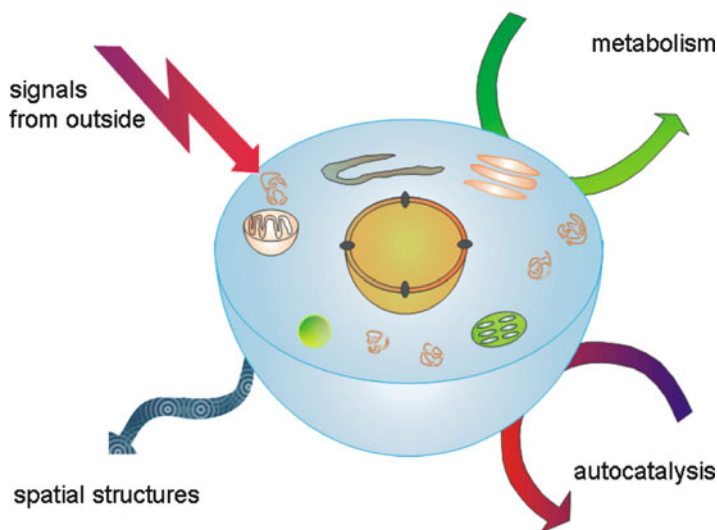


**Fig. 9.1** Living cell: interactions

significant operation steps of a technological process: isolation and screening of strains, cultivation, purification and product characterization.

## 9.2 Yeasts: Cell Factory for Production of Nanoparticles

### 9.2.1 *Strains: Producers of Nanoparticles*

To design a biotechnological process chain with industrial significance several important parameters require detailed consideration. These include precise selection of suitable strains with unique and desired properties, introduction of inexpensive alternative substrates, process optimization and yield enhancement, product characteristics and application requirements. The choice of yeast strains is of major significance for the production of nanoparticles, specifically regarding their properties.

Biotechnological processes such as bioleaching and bioremediation are known for decades to exploit the capacity of microorganisms to extract and/or accumulate metals (Gericke and Pinches 2006). Extensive studies and current scientific publications have revealed the potential of bacteria, actinomycetes, algae, yeasts and fungi in biosynthesis of nanoparticles (Slocik et al. 2004; Mandal et al. 2006; Krumov et al. 2009) and the number of promising microorganism–producers is already significant.

Of all the eukaryotes, yeast species are probably the most studied and applied in bioprocesses, which qualify them as an attractive object for nanoparticle synthesis.

Although recognized mainly for their ability to produce semiconductor nanoparticles, particularly cadmium sulfide (CdS), recent studies demonstrate the potential of yeasts to form other nanoparticle types.

*Saccharomyces cerevisiae*, also known as baker's yeast, is probably the best studied yeast species, regarding physiology and genetics, and definitely one with the biggest industrial significance, incorporating two million ton global yearly production, mainly for food applications (Hui 2006). Several publications discuss the potential of baker's yeast biomass for bioremediation by biosorption of heavy metals, e.g., cadmium and lead (Goksungur et al. 2005) or by binding cadmium to glutathione (GSH) with the resulting cadmium–bisglutathionate complex and consecutive transport into vacuoles (Breierova et al. 2002). The perception about the potential of *S. cerevisiae* to synthesize metal nanoparticles has changed and confirmation data are already present. Spherical amorphous iron phosphate nanoparticles with broad size distribution of 50–200 nm are formed within baker's yeast cells exposed to FeCl<sub>3</sub> solution (He et al. 2009). These nanoparticles are well dispersed in the cell and synthesized as a result of nucleation and growth control by proteins and other biomolecules as previously suggested (Mandal et al. 2006). In other studies the formation of almost spherical extracellular TiO<sub>2</sub> nanoparticles, synthesized by *S. cerevisiae*, is reported (Jha et al. 2009). A broad distribution of particle size ranging from 8 to 35 nm, with a mean particle size of 12 nm, was determined. The TiO<sub>2</sub> nanoparticles from baker's yeast are presumably a result of oxidation/oxygenation process triggered by a family of oxygenases harbored in the endoplasmic reticulum.

Most of the biological processes involving yeast species capable of nanomaterials synthesis result in intracellular nanoparticles formation but a few exceptions are present. A silver tolerant yeast strain MKY3 extracellularly reduces Ag<sup>+</sup> ions to metallic silver resulting in nanoparticles of size 2–5 nm (Kowshik et al. 2003). The mechanism of extracellular Ag nanoparticles synthesis suggests excretion of biochemical reducing agents by the yeast cells in response to silver stress. The size restriction of the particles is supposed to be related to small proteins, binding to the highly reactive silver cations.

The formation of noble metal nanoparticles is common for a number of bacteria and fungi such as *Pseudomonas stutzeri*, *Lactobacillus* sp., *Fusarium oxysporum* and *Verticillium* sp. (Slocik et al. 2004; Mandal et al. 2006; Krumov et al. 2009), and recently recognized in several yeast species. Promising results are obtained from experiments with the yeast species *Pichia jadinii* (formerly *Candida utilis*) (Gericke and Pinches 2006). Gold nanoparticles ranging from few to approximately 100 nm, with spherical shape for the smaller and hexagonal and triangular for the bigger ones, are intracellularly synthesized. The nanoparticle formation mechanism employed by *P. jadinii* presumably involves reduction of gold ions by enzymes and proteins present in yeasts' cell walls or cytoplasm. Morphology control by polypeptides was previously reported for the crystallization of gold to nanoparticles (Brown et al. 2000; Braun et al. 2002).

Gold nanoparticles both extracellularly (Agnihotri et al. 2009) and intracellularly (Pimprikar et al. 2009) are also produced by the marine yeast *Yarrowia lipolytica*

3589, earlier designated as *Candida lipolytica*. Numerous studies establish *Y. lipolytica* as an important microorganism with biological relevance and biotechnological applications (Bankar et al. 2009). This species is reported to be remarkably resistant to copper (Ito et al. 2007) with metal accumulation mechanisms, involving melanin, and leading to entrapment of heavy metal in the periplasm and other cell wall parts. Low concentrations of toxic metals such as Ni or Cd induce high cellular levels of metallothioneins (metal-binding proteins) in *Y. lipolytica* (Strouhal et al. 2003). This yeast has the ability to tolerate not only heavy metals but is also an efficient degrader of hydrocarbons, possessing the necessary enzymatic setup for their detoxification (Bankar et al. 2009). All these properties characterize *Y. lipolytica* as a promising object not only for remediation of environmental contaminants (including heavy metals) but also for production of metallic nanoparticles.

There is a significant amount of scientific information about the synthesis of semiconductor nanocrystals by yeast (Dameron et al. 1989a, b; Kowshik et al. 2002b; Krumov et al. 2007). Kowshik et al. (2002a) described the synthesis of intracellular 2–5 nm PbS crystallites, exhibiting semiconductor properties, by yeast strain of *Torulopsis* sp. challenged with lead. The authors suggested an analogous synthesis mechanism, first proposed for the formation of CdS nanoparticles in *Schizosaccharomyces pombe* and *Candida glabrata*, and presumably valid for a variety of metal sulfide nanoparticles in yeasts. Most profound analysis and knowledge, over the years, are collected namely for the synthesis of CdS nanoparticles from these two yeast species.

*S. pombe*, referred also as fission yeast, and first described by Lindner (1893), are easy to cultivate and suitable for genetic and molecular manipulations, which qualifies them as a desired object for scientific experiments (Barnett et al. 1990). Fission yeast researchers Paul Nurse, Lee Hartwell and Tim Hunt have received the Nobel Prize for medicine in 2001 for their work concerning cell cycle regulation, and in 2002 the genome of *S. pombe* was published (Wood et al. 2002). This made the fission yeast the sixth model eukaryotic organism with completely known genome.

The other acknowledged yeast strain producer of CdS nanoparticles, *C. glabrata*, also attracts a significant scientific interest. Previously designated as *Torulopsis glabrata* and *Cryptococcus glabratus*, this yeast species performs asexual budding and has no known filamentous form except for pseudohyphal growth as a result of nitrogen starvation (Csank and Hayens 2000). Dujon et al. (2004) disclosed completely the genome of *C. glabrata*. This broadened the understanding of the processes within the cells and enabled directed manipulations and control of their metabolism.

Yeast-derived CdS nanoparticles exhibit all the features required for biological applications. The three properties of great importance for the quality of colloidal nanoparticles are crystallinity, narrow size distribution and good water solubility. The peptide-coating prevents the particles from agglomeration and from Ostwald ripening, leading to a higher stability compared to that of chemically synthesized nanoparticles. Additionally, the peptide-coating provides the nanoparticles with

a hydrophilic surface without additional preparation steps. Semiconductor CdS nanoparticles derived from *S. pombe* and *C. glabrata* feature all electronic, photochemical and optical properties of synthetically produced CdS nanoparticles while lacking their disadvantages.

### 9.2.2 Mechanisms for Nanoparticles Formation

Microorganisms are regarded as potential bioremediators, extracting metals from the environment by active or passive mechanisms. Numerous studies have revealed that all yeast genera can accumulate different heavy metals but particularly interesting is the capability of accumulating significant amounts of highly toxic metals (Breierova et al. 2002). To avoid negative or lethal effects yeast cells require strict intracellular control of metal ions' level. Toxicity results from over storage of ions of essential metals or cell exposure to metals with no biological significance such as mercury, lead or cadmium. Cells, capable of growing in media with high metal ion concentration, are marked as resistant. Yeast cell capacity to transform absorbed metal ions into complex polymer compounds that are nontoxic for the cell is defined as resistance.

Yeast strains from different genera employ different mechanisms for nanoparticle formation resulting in substantial variations in size, particle location, monodispersity and properties. These species have developed different mechanisms for overcoming the toxic effects of heavy metals such as enzymatic oxidation or reduction, sorption at the cell wall and in some cases subsequent chelating with extracellular peptides or polysaccharides, controlled cell membrane transport of heavy metals towards or their active efflux from the cell (Breierova et al. 2002). While sorption is a passive defense mechanism and resistance by different transport strategies is a priority for the prokaryotic microorganisms, eukaryotes isolate metal ions into sub cellular organelles or attach them to polymers, forming nontoxic complexes. The major molecules that contribute to the detoxification mechanisms in yeast cells are GSH and two groups of metal-binding ligands: metallothioneins and phytochelatins (PC), both well characterized. These molecules determine the mechanism for the formation of nanoparticles by most of the yeast species studied and stabilize the complexes.

GSH with the structure  $\gamma$ -Glu-Cys-Gly is an important tripeptide involved in various metabolic processes in bacteria, yeasts, plants and animals. The unique redox and nucleophilic properties classify this compound as a detoxicator, actively taking part in the bioreduction and defense against free radicals and xenobiotics. GSH is also a structural unit in phytochelatin molecules, which is one of its major functions.

Metallothioneins are low-molecular, cysteine-rich metal-binding proteins, derived by mRNA translation (Kagi 1993). The great number of cysteine residues binds different metals by S–S bonds. Metallothioneins are classified according to the arrangement of these residues (Cherian and Chan 1993). Low molecular mass,



ability to bind metal ions and specific amino acid composition with high levels of cysteine and low level of aromatic amino acid residues are common among all metallothionein classes (Kagi and Schaffer 1988). The synthesis of these proteins is determined by a gene family. Although the model has been created on the basis of detoxification of  $\text{Cu}^{2+}$  ions it is also valid for other metals in yeast (Butt and Ecker 1987). According to this model, metallothioneins adopt the function of indirect autoregulator of their own gene expression by controlling the concentration of free intracellular  $\text{Cu}^{2+}$  ions (Butt and Ecker 1987). Metallothionein synthesis occurs within a couple of hours after the initial yeast cell contact with metal ions (Cobbett and Goldsbrough 2002). In animals, the function of metallothioneins is associated with the defense against cadmium toxicity and resistance towards  $\text{Cu}^{2+}$  and  $\text{Zn}^{2+}$ . Nevertheless there are evidences that metallothioneins play a similar role in some plants and yeast species, e.g., *S. cerevisiae* and *C. glabrata* (Mehra et al. 1988; Mehra and Winge 1991). Although metallothioneins were regarded as the only molecules involved in maintaining metal ion homeostasis in *S. cerevisiae*, by binding excess heavy metal ions by thiolate coordination, recent discoveries reveal the ability of baker's yeast to synthesize phytochelatin mediated by two vacuolar serine carboxypeptidases (Wünschmann et al. 2007).

Phytochelatin (PCs) were discovered in the yeast *S. pombe* (Murasugi et al. 1983), but are common for most plants (Grill et al. 1985), and some animal species (Cobbett 2000) and were recently found in some fungi and marine diatoms (Cobbett and Goldsbrough 2002). The name has Greek origin and consists of "phyto" representing their presence in plants and "chelatin" for the ability to form chelating complexes with metals. Although initially they were described as cadmium-binding peptides (Kondo et al. 1983; Grill et al. 1985), phytochelatin formation is induced by a large number of elements such as  $\text{Cd}^{2+}$ ,  $\text{Pb}^{2+}$ ,  $\text{Zn}^{2+}$ ,  $\text{Sb}^{3+}$ ,  $\text{Ag}^+$ ,  $\text{Ni}^{2+}$ ,  $\text{Hg}^{2+}$ ,  $\text{HAsO}_4^{2-}$ ,  $\text{Cu}^{2+}$ ,  $\text{Sn}^{2+}$ ,  $\text{SeO}_3^{2-}$ ,  $\text{Au}^+$ ,  $\text{Bi}^{3+}$ ,  $\text{Te}^{4+}$ ,  $\text{W}^{6+}$ , when supplemented to the medium (Grill et al. 1987).

Phytochelatin has the general structure  $(\gamma\text{-Glu-Cys})_n\text{-Gly}$ , where  $n = 2\text{--}11$ , and a multitude of structural variants has been described in the scientific literature (Rauser 1995, 1999; Zenk 1996; Cobbett 2000). Structurally, phytochelatin are related to GSH, serving as a substrate for their enzymatic biosynthesis, which has been confirmed by a number of physiological, biochemical and genetic studies (Rauser 1995, 1999; Zenk 1996; Cobbett 2000). Defined by some authors as functional analogs to metallothioneins, phytochelatin differ significantly from the latter especially regarding the synthesis mechanism, being a product of enzymatic biosynthesis (Cobbett and Goldsbrough 2002). The enzyme phytochelatin synthase or  $\gamma\text{-Glu-Cys}$  dipeptidyl transpeptidase (EC 2.3.2.15) catalyzes the reaction of transpeptidation of  $\gamma\text{-Glu-Cys}$  dipeptide from a GSH molecule to a second molecule of GSH resulting in phytochelatin PC2, or to molecule phytochelatin – resulting in  $n + 1$  oligomer (Grill et al. 1989). Phytochelatin synthesis begins within minutes after exposing the yeast cell to metal ions and is regulated by enzyme activation in the presence of these ions. The best activators are cadmium ions followed by ions of Ag, Bi, Pb, Zn, Cu, Hg and Au (Clemens et al. 1999; Ha et al. 1999; Vatamaniuk et al. 1999).

According to some authors, the substrate for the biosynthesis of phytochelatins is the “blocked” GSH molecule with attached metal (metal thiolates) (Vatamaniuk et al. 2000). The function of metal ions in the enzyme activation process is recognized rather as an important, integrated part of the substrate, than as a result of direct interaction with the enzyme. According to this model phytochelatin biosynthesis is terminated as a result of substrate exhaustion.

In plants and yeasts Cd–phytochelatin complexes are formed in the cytosol but accumulate in vacuoles (Salt and Wagner 1993). Detailed studies of the fission yeast *S. pombe* revealed that nearly the whole cadmium and phytochelatin amounts are located in vacuoles (Ortiz et al. 1995). Figure 9.2 presents the distribution of cadmium and sulfur in *S. pombe* cells detected by energy-filtering transmission electron microscope element specific imaging (EFTEM ESI). By sequestration of Cd–PC complexes inside vacuoles, yeast cells remove the toxic metal from important metabolic pathways and confine the biomineralization process to a limited space, effectively restricting the size of the resulting nanoparticles (Carney et al. 2007). *In vivo* experiments with the same yeast species demonstrate that phytochelatins play significant part in the detoxification of cadmium and arsenic ions. A hypothesis, to be proved, concerns their contribution for the essential metal ion homeostasis and both iron and sulfur metabolisms (Zenk 1996).

Compared to metallothioneins, phytochelatins feature many advantages, derived from their unique structure and especially the repeated  $\gamma$ -Glu-Cys units. For instance, they exhibit better metal-binding capacity (Mehra and Mulchandani 1995). In addition, phytochelatins can incorporate large amounts of inorganic sulfur resulting in increased capacity of these peptides to bind cadmium (Mehra et al. 1994) and the enzymatic biosynthesis guarantees quicker cell response (within

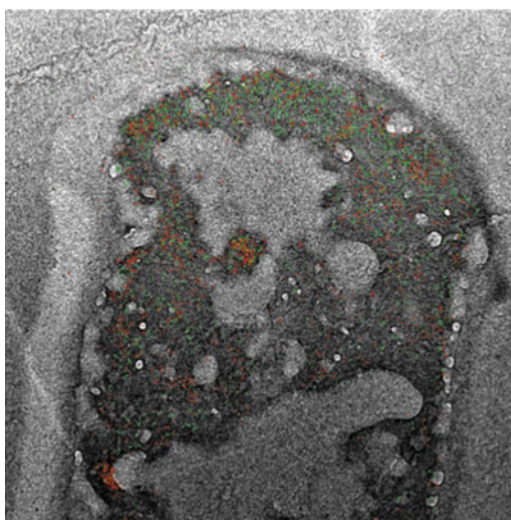


**Fig. 9.2** EFTEM ESI image of *S. pombe*: cadmium (red) and sulfur (green) (Krumov et al. 2007)

few minutes) towards the changed environmental conditions, e.g., presence of metal ions.

More profound studies explore the CdS nanoparticles formation mechanism in *S. pombe* and *C. glabrata*. Evidences lead to the conclusion that the synthesis model proposed for these two yeast species could be transferred as a generic strategy for other strains and metals (Kowshik et al. 2002a).

The biomineralization of cadmium by the yeasts *S. pombe* and *C. glabrata* is a metal-triggered biotransformation, in which metal ions are consequently chelated with small selective peptides and co-precipitated with inorganic sulfur, resulting in nontoxic CdS clusters (Perego and Howell 1997).

Dameron et al. (1989b) suggests that the CdS crystals isolated from *S. pombe* and *C. glabrata* are monodisperse, with an average diameter of 2 nm. The crystal lattice consists of 85 CdS pairs covered by approximately 30  $(\gamma\text{-Glu-Cys})_n\text{-Gly}$  peptides, with  $n = 3\text{--}5$ . Dameron and Winge (1990a) developed the model presented in Fig. 9.3.

Both yeast species synthesize phytochelatins from GSH in an enzyme reaction catalyzed by phytochelatin synthase. The mechanism of metal ion introduction into the phytochelatins is still under clarification, but the significant role of GSH in this process is undisputed (Hayashi et al. 1991). Experiments with cadmium-treated *C. glabrata* cells demonstrate predominant complexes Cd–GSH within the first 6 h of exposure, followed by a transformation to phytochelatins (Barbas et al. 1992). As a conclusion the metal–GSH complex appears to be the substrate for the phytochelatin synthesis reaction, contrary to the thesis that metal ions are directly transferred to newly synthesized phytochelatins.

In phytochelatins produced by *S. pombe* and *C. glabrata* the peptide bond between glutamate and cysteine residues include  $\gamma$ -carboxyl glutamate group instead

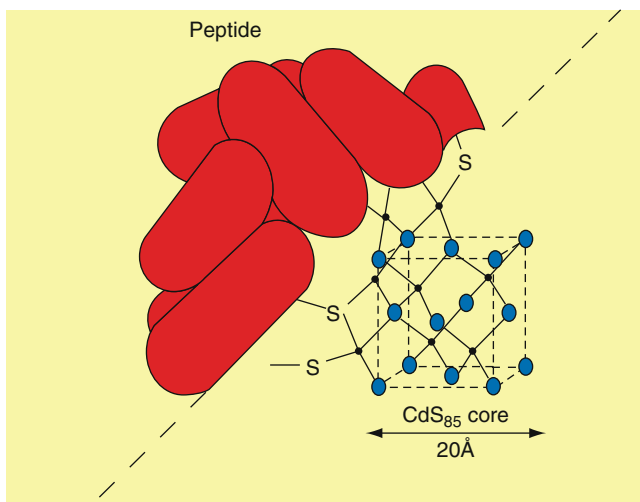


**Fig. 9.3** Graphic representation of the peptide-coated CdS nanoparticles (Dameron and Winge 1990a)

of  $\alpha$ -carboxyl. The  $\gamma$ -peptide bond is a confirmation for the enzymatic instead of ribosomal phytochelatin synthetic pathway. Natural  $\gamma$ -peptides exhibit bigger conformational freedom allowing higher number of possible bonds, thus influencing the difference in affinity of natural ( $\gamma$ -) and synthetic ( $\alpha$ -) phytochelatin towards metals (Bae et al. 2000).

In a comparative study involving the two yeast species described, peptide heterogeneity of the particle coatings has been found. The cells of *S. pombe* and *C. glabrata* synthesize heterogeneous mixtures of phytochelatin as stress response reaction to the presence of metals in the medium. Hayashi et al. (1988) report predominantly  $(\gamma\text{-Glu-Cys})_2\text{-Gly}$  and  $(\gamma\text{-Glu-Cys})_3\text{-Gly}$  phytochelatin in *S. pombe* cells, but in stationary phase cultures have also been synthesized peptides with  $n = 6$  (Grill et al. 1986; Reese et al. 1988; Mehra and Winge 1988). In contrast to *S. pombe* and most plant species, *C. glabrata* scarcely produces peptides longer than  $(\gamma\text{-Glu-Cys})_2\text{-Gly}$ . Furthermore, in both yeast species peptides with missing terminal Gly amino acid (desGly) occur in high concentrations (Mehra et al. 1988). Up to 20% of all related peptides in *S. pombe* and *C. glabrata* are desGly (Mehra and Winge 1988; Mehra et al. 1988).

*C. glabrata* is capable of synthesizing CdS nanoparticles covered with GSH or  $\gamma$ -glutamylcystein layer depending on the composition of the feeding medium (Dameron et al. 1989a). However, these peptides cannot stabilize the nanocrystals as good as the phytochelatin. GSH-covered particles are unstable in neutral pH and easily undergo aggregation. This instability is the reason for the size heterogeneity of CdS-GSH nanoparticles derived from *C. glabrata* in comparison to phytochelatin-covered crystals (Bae and Mehra 1998).

Phytochelatin-coated nanoparticles derived from both yeast species are analogous to the semiconductor quantum dots studied in solid state physics. Yeast synthesis mechanism overcomes one of the biggest disadvantages of physical and chemical synthetic pathways – the agglomeration into larger particles. Nanocrystals derived from yeasts are naturally stabilized by the phytochelatin layer, which also effectively controls particle size – 2 nm for *C. glabrata* and 1.8 nm for *S. pombe* (Dameron et al. 1989b). Strict control over size is a typical characteristic of all biomineralization processes (Mann 1993) and also demonstrates the importance of the capping template in controlling particle formation. PCs coatings with optimized composition avoid the formation of large CdS particles, capable of destroying the vacuoles, thus preventing the release of nanoparticles or free  $\text{Cd}^{2+}$  into the cytosol (Carney et al. 2007). The synthesis of nanoparticles with greater monodispersity and higher stability is essential for the survival of yeast species exposed to heavy metal stress conditions; it also opens vast new possibilities for the technical applications of those particles. Keeping the size of the crystals within the nano scale is critical for their properties. Clusters with diameter less than 10 nm do not exhibit the bulk material properties and have size-dependent optical properties (Rossetti et al. 1984; Nozik et al. 1985; Brus 1986). The industrial and commercial potential of this biotechnological mechanism is defined by the successful and relevant selection of the system biological object – nanoparticle precursor.

### 9.3 Upstream Processes: Isolation, Identification and Screening of Industrial Relevant Yeast Strains

Metal presence in soils is associated with two major sources – mineral rock weathering and anthropogenic activity. The latter could be subdivided into five different groups: metalliferous mining and smelting (arsenic, cadmium, lead and mercury); industry (arsenic, cadmium, chromium, cobalt, copper, mercury, nickel, zinc); atmospheric deposition (arsenic, cadmium, chromium, copper, lead, mercury, uranium); agriculture (arsenic, cadmium, copper, lead, selenium, uranium, zinc) and waste disposal (arsenic, cadmium, chromium, copper, lead, mercury, zinc) (Ross 1994). Ecological and biological balance in soils is preserved by bioremediation. This process is based on the ability of microorganisms to exploit the metabolic potential of their cells to transform, decompose and immobilize different contaminants, including heavy metals. Therefore metal-containing soils are a potential reservoir for nanoparticle-producing yeast strains with commercial value.

Experimental work with known culture collection strains is always preferable considering the vast possibilities for references with scientific publications regarding the specific strain. Various processes and experiments require isolation of new yeast strains following verified and well-established procedures. The ultimate source of microorganisms used in biotechnological processes is the environment. Yeast strains can be isolated relatively easily from their natural habitats. Isolation is based on creating conditions beneficial for the growth of the desired species, and simultaneously suppressing the development of side micro flora. The process of pure yeast culture isolation from nature includes introducing selective or enrichment media, different temperatures, pH and aerobic/anaerobic conditions.

In nature yeasts commonly exist in the form of microbial associations particularly with bacteria and filamentous fungi. As a general rule the fast growth enables unobstructed yeast isolation from associations with fungus without the necessity of selective inhibitors, although some rapidly growing fungi (e.g., *Rhizopus* sp.), which cover the yeast colonies, present a potential difficulty (Campbell and Duffus 1988).

Selective media for the determination of presence and number of yeast colony-forming units in mixed microbial associations are suggested by Beuchat (1992). Bacterial growth can be successfully controlled by the use of potato dextrose agar or tryptone glucose yeast extract media acidified with organic acids (tartaric, lactic, citric). Yeast cells undergoing stress conditions, for instance those isolated from soils with increased heavy metal content, are more sensitive towards acidified media. Therefore media containing antibacterial antibiotics such as oxytetracycline, chloramphenicol, chlortetracycline, gentamycin, kanamycin, streptomycin or a combination of them in concentration 10–100  $\mu\text{g ml}^{-1}$  are more appropriate for yeast isolation (Campbell and Duffus 1988; Beuchat 1992).

Yeast identification is based on morphological, physiological, biochemical analysis and genetic characteristics. Traditional identification procedures require 60–90 tests and 2–4 weeks processing time which qualify them as obsolete in terms of

rapid and reliable manipulation of numerous samples of isolated strains. Modern identification strategies are based on molecular biology methods including protein electrophoresis, DNA analysis, chromosome karyotype and analysis of cell fatty acids. One of the most precise and modern methods for identification and determination of taxonomic affiliation is based on molecular genetics: DNA reassociation, characteristic of ribosomal RNA (Yamada et al. 1992), DNA (Lachance 1988; Shen and Lachance 1993) and PCR investigations of specific DNA sequences (Fell 1993).

Several identification kits and automated systems combining simple operation, speed and sufficient accuracy (over 80%) are successfully developed. Identification systems such as API (Analytical Profile Index) 20 C and ID32C, Vitek ID32, Uni Yeast Tek, Abbot Quantum II and others are based mostly on carbohydrates assimilation. The results are obtained within 2–3 days of incubation. Some systems require additional tests and/or morphological investigations.

Soil type and mechanical composition together with climate and agricultural–ecological characteristics of the region are of significant importance for the isolation of yeasts from nature and providing the optimal conditions for selective growth of desired microorganisms.

## 9.4 Cultivation Strategies

The cultivation stage is of fundamental importance for the entire biotechnological process, where product's application and characteristics dictate the choice of synthetic pathway. The precise optimization of the cultivation conditions depends on various factors and requires thorough understanding of the whole process.

For bioremediation of heavy metals and formation of biogenic nanoparticles several characteristics are required: a high heavy metal uptake rate, an effective mechanism for metal sequestration–inactivation, an appropriate heavy metal storage and large biomass production. The heavy metal uptake is the most critical point regarding process modification and optimization. All the following processes depend on it. In the case of cadmium uptake the amount of cadmium accumulated in cells is presumably proportional to the amount of CdS nanoparticles formed, a reaction supported by the presence of sulfur (Mendoza-Cozatl et al. 2005). The final CdS nanoparticle yield of a single cultivation is determined by two major factors: the initial glucose concentration in the feeding medium, which determines the final biomass concentration, and the CdS saturation level, which limits the amount of intracellular CdS nanoparticles in every cell (Williams et al. 2002). The present chapter intends to provide solutions for two main challenges, regarding the cultivation conditions, namely the optimized culture feeding profile and the specific scheme for the introduction of precursor for nanoparticles formation (e.g., cadmium ions). These two factors require detailed consideration and more profound studies have been conducted with *S. pombe* and *C. glabrata*, providing good examples and process understanding.

The first step in optimization of the cultivation strategy is to achieve high biomass concentrations. With a given yield the final biomass concentrations depend directly on the amount of sugar provided. However, high initial glucose concentrations lead in most microorganisms to the production of byproducts. Especially in yeasts, high glucose concentrations in the medium lead to the formation of ethanol and other fermentative byproducts by overloading respiration capacity known as Crabtree effect. This lowers the final yield and may have in addition inhibitory effects on growth rates. For industrial yeast production fed-batch strategies are applied, where glucose is constantly fed in amounts that can be used up by the cells immediately. An exponential feeding strategy leads to low constant glucose concentrations and therefore to constant specific growth rates keeping the cells in a defined physiological state. For most yeast strains a specific growth rate below  $0.2 \text{ h}^{-1}$  has been found to prevent ethanol formation.

Although according to some authors (De'Deken 1966; Heslot et al. 1970a; Barford 1985) *S. pombe* are species not exhibiting glucose repression, it has been found that under certain conditions the fission yeasts show high respiratory quotient values and glucose repressed mitochondrial respiration (Heslot et al. 1970b). For *S. pombe* cultivations the microbial biomass concentration is directly proportional to the product yield, therefore an introduction of fed-batch process, where the specific growth rate can be maintained at defined levels, glucose repression minimized, and ethanol synthesis decreased for higher levels of cell density, is required (Besli et al. 1997; Olsson and Nielsen 2000).

The other important CdS-nanoparticle-producing yeast strain, *C. glabrata*, assimilates only glucose and trehalose, and does not exhibit the common, for species assimilating sucrose, melibiose, maltose and lactose, glucose repression (Hazen 1995). *C. glabrata* can utilize glucose and ethanol as substrates and demonstrate diauxie.

The second important issue is to achieve high intracellular CdS concentrations. Analogous to Crabtree effect, high initial cadmium concentration leads to growth inhibition. For an optimized approach, cadmium needs to be provided in amounts which induce particle formation but does not lead to extracellular or intracellular bulk accumulation of the heavy metal. Therefore, the precursor feeding rate has to be adapted to the physiological state of the cells with respect to cadmium uptake and precipitation capacity. The high intracellular nanoparticle concentration depends on the CdS saturation level and is cytologically determined. This factor could be clarified after complex physiological analysis on the effect of cadmium ions concentration which induce CdS nanoparticles formation and the influence of the increased GSH and/or cysteine cell concentrations. GSH and cysteine are components of the chelating layer covering CdS nanoparticles and control their size and specific optic-electronic properties (Dameron et al. 1989a). The control of the intracellular levels of these two components regulates the CdS nanoparticle yield.

Numerous publications describe for the formation of CdS nanoparticles from *S. pombe* media, containing yeast extract, malt extract, peptone and glucose, as most

appropriate (Reese et al. 1988; Mehra and Winge 1991; Williams et al. 1996a, b, 2002; Kowshik et al. 2002b). Experiments have also been conducted with minimal media such as the synthetic Edinburgh minimal medium (EMM), designed especially for *S. pombe* cultivation, but suitable only for molecular and genetic investigations of the fission yeast (Nasim et al. 1989; Moreno et al. 1991). Studies over the past few years demonstrate that *S. pombe* grow relatively poor on media based on nonfermentable carbon sources such as glycerol, ethanol and galactose (Stiefel et al. 2004; Westwood et al. 2004). The most suitable cultivation temperature referred to in most of the scientific sources is 30°C.

Dameron et al. (1989a) reported for the first time that different cultivation conditions determine whether the CdS crystals in *C. glabrata* are covered and stabilized by phytochelatins or oligomer mixture of GSH and  $\gamma$ -Glu-Cys dipeptide. In addition, this is also the first evidence for biologically synthesized GSH–metal complex. The nature of the chelating peptide is determined by the composition of the cultivation medium. *C. glabrata* culture cultivated on minimal synthetic medium (1.25% nitrogenous bases, 2% glucose and mixture of uracil and amino acids) produced mixture of polymerized phytochelatins, covering the nanocrystals. By cultivation on rich culture medium composed of 1% yeast extract, 2% triptone and 2% dextrose, *C. glabrata* covers nanoparticles with a mixture of GSH and  $\gamma$ -glutamylcysteine (Dameron et al. 1989a). This influence of the cultivation medium is not observed for *S. pombe*, synthesizing phytochelatins on both minimal and rich medium (Reese et al. 1988). Additional analyses suggest that this effect is partially due to the yeast extract in the medium, without the full understanding of the regulatory mechanism (Dameron et al. 1989a).

Regarding the above-mentioned characteristics, numerous authors (Mehra et al. 1988, 1994; Dameron et al. 1989a; Barbas et al. 1992) define cultivation on minimal medium, temperature 30°C and good aeration (160 min<sup>-1</sup> shaking flasks conditions and 1 dm<sup>3</sup> air per 1 dm<sup>3</sup> culture medium per minute for bioreactor conditions) as optimal conditions for the synthesis of CdS nanoparticles by *C. glabrata*. The induction of the CdS nanoparticles synthesis is mediated by the addition of 0.5–1 mM cadmium ions in the medium. The choice of cultivation media composition for *C. glabrata* is crucial for the stability of the CdS nanoparticles formed. The synthesis of phytochelatin layer guarantees higher stability and monodispersity of the resultant metal–peptide complexes.

Experiments with *Y. lipolytica*, producing gold nanoparticles, demonstrate the significance of cultivation conditions not only for the synthesis but also for the properties of the product. Varying cell densities and gold salt concentrations can be applied for particle size control (Pimprikar et al. 2009). Intermediate cell concentrations (10<sup>10</sup> ml<sup>-1</sup>) and lower gold salt concentrations result in nanoparticles synthesis. Higher salt concentrations lead to gold deposition on specific sites due to capping agent limitations. Very high cell concentrations (10<sup>11</sup> ml<sup>-1</sup>) lead to uniform gold distribution in the form of spherical nanoparticles. The mean particle size increases with higher concentrations of the gold salt and constant cell concentration. On the other hand, same concentrations of gold salt (1 mM) and increasing cell concentrations lead to a decrease in particle size (Pimprikar et al. 2009). Further



experiments with the same yeast species reveal pH–particle size dependency. Several authors report that acidic pH favors gold crystal formation rather than nanoparticle synthesis (He et al. 2007; Agnihotri et al. 2009). The phenomenon of smaller gold nanoparticles being produced at higher pH is also observed for chemical synthesis (Kundu et al. 2005).

The duration of the cultivation process is important for the high nanoparticle yield. It is determined by the time by which yeasts reach the detoxification capacity of their cells and achieve nanoparticle saturation levels. Studies involving the formation of CdS nanoparticles in yeast suggest different cultivation times (Dameron et al. 1989b; Williams et al. 1996a, 2002) but in all experiments conducted, a tendency is observed – a maximum cadmium concentration in the cells is measured around 24 h after the addition of cadmium to the medium. Ten hours after reaching maximum concentration the intracellular cadmium level decreases (Williams et al. 2002). This is the necessary period for the CdS nanoparticles to reach saturation level. These 10 h are intensive phase of cadmium absorption and its active cell efflux. After this period the level of intracellular cadmium remains stable, as a result of the detoxification capacity of the chelating peptides, converting the toxic ions into metal–peptide complex and terminating the cadmium efflux from the cell (Williams et al. 1996a, 2002).

Selecting the precise time for the extraction and isolation of nanoparticles from the cell is a critical point in the process due to the possibility of biomass lysis. Small delay could induce a “leak” of particles in the culture medium, hindering the subsequent purification stages. In the case of CdS nanocrystals the most stable particles remain longer in the cell, allowing the elongation of the peptides in the chelating layer (Hayashi et al. 1988). Longer phytochelatin are the basis for more stable metal–peptide complexes. Increase in the yield of more stable CdS nanoparticles is achieved by conducting fed-batch yeast cultivations.

CdS nanoparticle formation is a well-studied phenomenon comprising stress protein reaction. It depends on the precise moment of cadmium addition to the medium. Cadmium introduction in the middle to late exponential phase provides maximum CdS nanoparticle production (Dameron et al. 1989b; Williams et al. 1996a). Addition of cadmium in the beginning of the exponential phase negatively influences cell metabolism and eventually leads to heavy metal efflux from the cell in the form of unstable CdS microcrystals. Cadmium introduction during the stationary phase does not induce CdS nanoparticle formation due to the decreased absorption and sulfide formation rates during that stage (Williams et al. 1996a).

According to Williams et al. (1996a) in batch cultivation of *S. pombe* the production of CdS nanocrystals is limited by a saturation factor. Therefore, the nanoparticle yield can be increased only by increasing the final biomass concentration in every cultivation. This is achieved by cultivating *S. pombe* under fed-batch conditions, adapted to principles defining the relation between physiological state and CdS nanoparticle formation.

In accordance with the optimization criteria given above, a two-phase process strategy has been proposed by Krumov et al. (2007). In the first phase, a normal fed-batch has been carried out to achieve high biomass concentrations under

defined specific growth rates. As the extracellular cadmium concentration and the intracellular particle formation would lead to growth rate reduction, cadmium is provided in a fed-batch strategy as well, in the second process phase. In this case, cadmium is provided in several consecutive batches with low amounts thus preventing accumulation over a critical threshold. Recent studies revealed an optimized strategy for cadmium introduction in three steps at equal 6-h intervals resulting in considerably increased amounts of accumulated heavy metal resulting in up to 20 mg cadmium per gram yeast biomass specific uptake (Krumov et al. 2007). This gives the opportunity for a higher CdS nanoparticle yield and broadens the perspectives for industrial scale application of the process.

## 9.5 Downstream Processes: Challenges and Solutions

As described above, most of the yeast species form nanoparticles in their own cells, incorporating different mechanisms and mostly as a result of detoxification activity. The intracellular origin and location of these nanoparticles and the presence of stabilizing peptides (e.g., phytochelatins) require the elaboration of suitable, complex strategy for their recovery from the cell and purification, applying mild conditions to minimize product loss, change of properties and agglomeration.

### 9.5.1 Purification Strategies

#### 9.5.1.1 Cell Disruption

The recovery of intracellular nanoparticles from yeasts is preceded by a cell disruption procedure, specially designed to provide a good base for the following downstream processes. In biotechnology, cell disruption is an important step in the isolation and purification of intracellular products. The choice of appropriate disruption technique is based on a number of factors including sample volume, cell wall rigidity, desired level of disruption efficiency, stability of the isolated molecules or components, further purification steps, etc. Cell wall solidity can turn the disruption of yeast cells into a rather complicated and difficult process. In search of the optimal disruption method, corresponding to all requirements, the techniques elaborated are divided into two major groups – physical (mechanical and nonmechanical) and chemical methods.

The specific nature of the intracellularly formed nanoparticles and the essence of the peptide layer demand disruption strategy, employing relatively mild conditions. The chemical disruption, successfully applied for a number of processes, is not relevant for isolation of intracellular nanoparticles due to the aggressive nature of some of the reagents used (e.g., sodium hypochlorite, trichloromethane, *n*-hexane, hydrogen peroxide) and the risk of destroying the metal–peptide complex (Breddam and Beenfeldt 1991; Bairbakhish et al. 1999).

Cell disintegration by means of enzymes such as zymolase is effective and specific. This enzyme specifically destroys the  $\beta$ -1,3 bonds between glucans and causes cell wall destabilization (Knorr et al. 1979; Schlegel and Zaborosch 1992). One drawback of the method regarding the specific process is that the additional protein introduction, in the form of an enzyme, is a potential hindrance for the subsequent nanoparticle purification steps.

From the group of nonmechanical methods, freeze-thawing guarantees relatively mild and clean conditions. Williams et al. together with other authors (Williams et al. 1996b, 2002; Kowshik et al. 2002b) classify the freeze-thawing disintegration as the most appropriate and successful for isolation of CdS nanoparticles from yeast. This technique is simple, without chemical reagents intervention or additional components introduction, which provides cleaner starting material for further purification (Williams et al. 2002). After cultivation, yeast biomass is frozen under  $-70^{\circ}\text{C}$  (Williams et al. 1996b). Studies conducted by Kowshik et al. (2002a, b) revealed that the release of CdS nanoparticles from the cells is not influenced by the temperature in the range between  $-70^{\circ}\text{C}$  and  $-20^{\circ}\text{C}$ . This suggested disintegration strategy with biomass freezing under  $-20^{\circ}\text{C}$  and thawing under  $4^{\circ}\text{C}$  for 2–4 h (Kowshik et al. 2002a, b).

Techniques not involving the introduction of additional components in the yeast suspension are preferable (Campbell and Duffus 1988). The majority of mechanical methods for disruption of yeast cells utilize specially constructed technical devices. Two major approaches are developed. One is based on forcing cooled or frozen yeast biomass through a narrow opening, resulting in resilience and elongation forces, and the formation or phase changes, disrupting the cells – French press (Campbell and Duffus 1988). The second approach utilizes active stirring of yeast cell suspensions together with abrasive particles or grains – bead milling or bead beater. Disadvantages of the second strategy are necessity of grains removal, the mixture of disrupted and intact cells, and heat generation (Campbell and Duffus 1988). For analytical purposes and smaller sample volumes excellent disruption results are achieved with a method based on bead milling. This approach involves special lysing matrixes for systems for rapid isolation of proteins from yeast cells.

High-pressure homogenization is a simple method appropriate for large volumes of yeast suspensions and is significantly faster than all other methods (Siddiqi et al. 1997). Experiments involving isolation of CdS nanoparticles from yeasts demonstrate that this method guarantees highest percentage disrupted cells (Krumov et al. 2007). High-pressure homogenization is widely used for large-scale operations. Its advantages together with the requirements of the specific product turn this technique into a promising solution for the production of nanoparticles with industrial relevance.

### 9.5.1.2 Isolation and Purification of Nanoparticles from Yeast

The majority of the scientific literature in the field of bioremediation mainly considers the induced synthesis of chelating peptides (phytochelatins, metallothioneins)

and their characterization, and to a lesser extent the microbial formation of nanocrystals. The complex interactions of too many variables and parameters, together with the search for standard, defined process conditions, are the reasons for the lack of adapted clear and precise procedure for the optimized microbiological production of nanoparticles, specifically regarding the purification step (Williams et al. 1996a). The absence of a defined system of technology procedures for isolation and purification of biogenic nanoparticles is partially due to the specificity of the product, the submicron dimensions, and the lack of adequate equipments for precise quantification and characterization in the past. Current analytical technologies give the opportunity by combining analysis of metal concentration, precise fractionation and studies of metal binding peptides by HPLC and post-column quantifications to determine the optimal parameters of biogenic nanoparticle purification process.

Part of the protocols for isolation of metal-peptide nanocomplexes are based on the metallothioneins isolation methods (Rausser 1990). They comprise subjecting cell isolates to a combination of size exclusion chromatography (SEC) using Sephadex G-75 or Sephadex G-50 columns (Casterline and Barnett 1982; Wagner and Trotter 1982; Grill et al. 1985; Obata and Umebayashi 1986), followed by ion-exchange chromatography (IEC) using DEAE anion exchange column (Rausser 1984; Grill et al. 1985).

As an alternative to these isolation and purification methods another scientific group suggests preliminary chromatographic processing on DEAE and QAE anion exchange column, followed by SEC on Sephadex G-75 or Sephadex G-50 columns. The proposed strategy eludes one step of freeze-drying or ultrafiltration concentration of the extract, prior to column injection (Rausser and Curvetto 1980; Murasugi et al. 1981b).

With relative levels of success different purification approaches are also applied. Phytochelatin metal complexes with high purity are obtained after covalent affinity chromatography with thiopropyl Sepharose 6B column and preceding SEC (Jackson et al. 1987).

Deriving knowledge from successful strategies for isolation and purification of cadmium-peptide complexes from plants, a number of authors suggest combination of chromatographic methods for the purification of the same complexes but derived from the yeasts *S. pombe* and *C. glabrata* (Murasugi et al. 1981a; Mehra et al. 1988; Dameron et al. 1989a; Mehra and Mulchandani 1995).

Dameron et al. (1989a) purify CdS-PC complexes from *C. glabrata* by means of combination of IEC using anion exchange column and SEC, while Mehra et al. (1988) utilize for the same purpose combination of SEC with Sephadex G-75 column, IEC with anion exchange column, and again SEC using Sephadex G-50 column. Both approaches result in isolation of different phytochelatin isoforms, respectively, complexes with different composition of the phytochelatin layer, which are further separated by reverse phase HPLC.

For the isolation and purification of CdS-PC complexes from *S. pombe* a slightly different approach is introduced. Murasugi et al. (1981b) successfully separate two different types of CdS-PC complexes from the fission yeast by two consecutive SECs using Sephadex G-50 column.

The common element in all metal–peptide nano-complex purification approaches is SEC. It is the most simple and mild, regarding process conditions, chromatographic method. The low resolution of this technique allows applications as final, completion step not only in one bioproduct purification technology but also in the very beginning of the downstream processes. For the purification of nanoparticles derived from yeasts, fractionation by means of SEC can be introduced for the isolation of one or more components, separation of monomers from aggregates and molecular weight determination. Applied generally for the separation of proteins, recent findings demonstrate the relevance and efficiency of one step SEC for the purification of CdS nanoparticles isolated from *S. pombe* (Krumov et al. 2007). The possibilities that this technique presents for scaling up the operations to industrial level make SEC an attractive and reliable purification tool in the process chain. Metal–peptide complexes isolated in distinct, separate fractions are later more comfortable object for characterization by different methods.

### 9.5.2 Product Characterization

The concluding stage of every industrially significant process chain comprises evaluation of the properties and the quality of the final product. The importance of detailed and correct characterization of nanoparticles and the identification of their properties derive from the correlation between these properties and the practical application of this class of materials.

The problems and the challenges in characterizing biogenic nanoparticles produced by yeasts are similar to those synthesized by physical (top down) or chemical (bottom up) approach. The difficulties in nano-analysis are derived by the specificity of the processes – dynamic analytics close to the atomic size range, unstable and sensitive samples, containing heterogeneous, polydisperse nanoparticles in extremely low concentrations ( $<1 \mu\text{g L}^{-1}$  or  $\mu\text{g kg}^{-1}$ ), and possibility to determine only an “equivalent” size of often not spherical particles. In addition, peculiar for the yeast-derived nanoparticles is the stabilizing peptide layer, which requires additional considerations during characterization.

For process development and subsequent applications, numerous characteristics and properties are of great significance. Amongst them are size and size distribution, structure/crystallinity and shape, composition and concentration, agglomeration state and surface functionality (Hassellöv and Kaegi 2009). Numerous methods and techniques for characterizing nanomaterials are available. That is due to the specificity of the object and the necessity to employ often more than one technique to obtain a relevant result for one and the same parameter. Characterization methods could be systemized in several directions. Several of the most powerful and undisputed techniques are based on the visualization of nanoparticles – including transmission electron microscopy (TEM), scanning electron microscopy (SEM), environmental scanning electron microscopy (ESEM), and atomic force microscopy (AFM). Nanoparticle size is best measured by TEM.

High-resolution TEM (HRTEM) can visualize lattice fringes, leading to crystallographic information about the particle, including its phase and crystal axes (Murphy and Coffey 2002). Particle size and size distribution which are important from commercial point of view are also analyzed by light scattering (static and dynamic), Laser-induced breakdown detection (LIBD), Single particle counting, Small-angle X-ray scattering (SAXS) and X-ray diffraction (XRD). Particle size distribution measurements are sometimes difficult to interpret because of the ambiguous results often obtained. The distortion and controversy of the findings derive from the frequent formation and presence of agglomerates, screening the real diameter of the single nanoparticles. In process development these methods have more referent and supplementary function. Concentration and composition are determined by nephelometric methods, gravimetric methods, atomic absorption spectroscopy (AAS), Inductively coupled plasma optical emission spectrometry or mass spectrometry (ICP OES or ICP MS).

Proteomics methods are adapted for the characterization of basically new and relatively unknown product – the peptide-covered nanoparticles. To study the cell response of *S. pombe* towards heavy metal ions in culture media Bae and Chen (2004) conduct investigations based on mass spectrometric analysis of biomolecules derived from *S. pombe*. Detailed structural information can be obtained by applying mass spectrometers with more than one analyzer – tandem mass spectrometers (Bae and Chen 2004, Downard 2004). They are the structural components in the approaches for analyzing metalloproteins. In studies focused on the mechanism of detoxification, the protein ligand identifications are always used parallel to metal concentration analysis, including ICP OES and ICP MS, which guarantee detection of concentrations in the ppm range (Nies and Silver 2007).

In scientific literature published over the last few years the successful application of combination of Matrix assisted laser desorption ionization (MALDI) and electro spray ionization time-of-flight (ESI TOF) mass spectrometers together with ICP MS is discussed, delivering complementary information about metal-binding proteins (Nies and Silver 2007). The combination between ESI and ICP has supplied complementary data for the characterization of phytochelatins, induced by cadmium ions in some plants (Vacchina et al. 2000). The application of ESI MS in proteomics and specifically in studying the complex formation by metals and phytochelatins/metallothioneins is reported in the scientific works of other authors (McSheehy and Mester 2003). This approach has contributed for the discovery of the molecular microheterogeneity of GSH and phytochelatins (Vacchina et al. 2000).

Analyses of the peptide layer and metal–protein complexes are important but from commercial and application point of view probably more interesting are the core-related properties of the product. A significant number of all the scientific works in the field are directed towards synthesis, characterization and in general better understanding of semiconductor nanoparticles. Structural phenomena, derived from electron transfers and bandgap width, are the basis for the different absorption and emission spectra of these nanoparticles according to their size and element composition (Murphy and Coffey 2002). Dameron and Winge (1990b) successfully characterize peptide covered CdS nanoparticles by means of

photoluminescent analysis. According to these studies, luminescence correlates with particle size – for particles with bigger Stokes radius the emission spectrum is shifted towards higher wavelengths.

## 9.6 Conclusions

Society's constant demand for new technologies and new materials determine the current scientific urge and competition to improve existing strategies for nanoparticle synthesis and to develop new ones. The biotechnological production of inorganic nanoparticles is an interesting and promising alternative to the known and established physical and chemical methods. This new approach, whose full commercial potential is still to be revealed, has fundamentals dating back 570 million years, defining one of the oldest processes on Earth – the biomineralization. The ability of yeast strains (particularly *S. pombe* and *C. glabrata*) to form nanoparticles, under specific stress conditions, is known to science for the last 20 years. During this period the precise molecular mechanisms of this process, its physiological and genetic fundamentals have been profoundly studied and revealed. Despite the knowledge and the significant process clarity, this pathway still undergoes difficulties to exit the world of fundamental theory and to succeed into complete, applied and functioning technology. In the present chapter, we have collected the basic knowledge about this process, combined and enhanced with our own achievements and experience, resulting in the elaboration of innovative complete process chain for the production of nanoparticles by yeasts. The technology developed is a successful tool to transfer the laboratory scale process into an industrially relevant one, giving solutions to production challenges and answering technological questions. The proposed optimized cultivation strategy together with the simplified and yet reliable downstream processing is essential for big scale applications. The presented process chain demonstrates again the advantages and almost unlimited possibilities of biotechnological processes for the synthesis of fine, high-quality, state-of-the-art products, with supreme level of control and technological freedom.

**Acknowledgments** The authors would like to express their gratitude to Prof. Dr. Ursula Obst, Dr. Gerald Brenner-Weiss, Dipl.-Ing. Frank Kirschhöfer from Institute for Functional Interfaces, Dr. Patrick Kölsch and Silvia Andraschko from Institute of Toxicology and Genetics, Karlsruhe Institute of Technology, Germany, for their support, suggestions and immeasurable proficiency in conducting the analytical experiments.

## References

- Agnihotri M, Joshi S, Kumar AR, Zinjarde S, Kulkarni S (2009) Biosynthesis of gold nanoparticles by the tropical marine yeast *Yarrowia lipolytica*. *Mater Lett* 63(15):1231–1234
- Bae W, Chen X (2004) Proteomic study for the cellular responses to Cd<sup>2+</sup> in *Schizosaccharomyces pombe* through amino acid-coded mass tagging and liquid chromatography tandem mass spectrometry. The American Society for Biochemistry and Molecular Biology, Bethesda, MD

- Bae W, Mehra RK (1998) Properties of glutathione- and phytochelatin-capped CdS bionanocrystallites. *J Inorg Biochem* 69(1–2):33–43
- Bae W, Chen W, Mulchandani A, Mehra RK (2000) Enhanced bioaccumulation of heavy metals by bacterial cells displaying synthetic phytochelatin. *Biotechnol Bioeng* 70(5):518–524
- Bairbakhish AN, Bollman J, Sprengel C, Thierstein HR (1999) Disintegration of aggregates and coccospheres in sediment trap samples. *Mar Micropaleontol* 37(2):219–223
- Bankar AV, Kumar AR, Zinjarde SS (2009) Environmental and industrial applications of *Yarrowia lipolytica*. *Appl Microbiol Biotechnol* 84(5):847–865
- Barbas J, Santhanagopalan V, Blaszczyński M, Ellis WRJ, Winge DR (1992) Conversion in the peptides coating cadmium:sulfide crystallites in *Candida glabrata*. *J Inorg Biochem* 48(2):95–105
- Barford JP (1985) Control of fermentation and respiration in *Schizosaccharomyces pombe*. *J Ferment Technol* 63(6):495–558
- Barnett JA, Payne RW, Yarrow D (1990) Yeasts: characteristics and identification, 2nd edn. Cambridge University Press, Cambridge
- Besli N, Gul E, Turker M (1997) Application of fuzzy control to fed-batch yeast fermentation. *Lect Note Comput Sci* 1226:207–216
- Beuchat LR (1992) Media for detecting and enumerating yeasts and moulds. *Int J Food Microbiol* 17(2):145–158
- Braun R, Sarikaya M, Schulten K (2002) Genetically engineered gold-binding polypeptides: structure prediction and molecular dynamics. *J Biomater Sci Polym Ed* 13(7):747–757
- Breddam K, Beenfeldt T (1991) Acceleration of yeast autolysis by chemical methods for production of intracellular enzymes. *Appl Microbiol Biotechnol* 35(3):323–329
- Breierova E, Vajczikova I, Sasinkova V, Stratilova E, Fisera M, Gregor T, Sajbidor J (2002) Biosorption of cadmium ions by different yeast species. *Z Naturforsch C* 57(7–8):634–639
- Brown S, Sarikaya M, Johnson E (2000) A genetic analysis of crystal growth. *J Mol Biol* 299(3):725–735
- Brus L (1986) Electronic wave-functions in semiconductor clusters – experiment and theory. *J Phys Chem* 90(12):2555–2560
- Butt TR, Ecker DJ (1987) Yeast metallothionein and applications in biotechnology. *Microbiol Rev* 51(3):351–364
- Campbell I, Duffus JH (1988) Yeast a practical approach. IRL, Oxford
- Carney CK, Harry SR, Sewell SL, Wright DW (2007) Detoxification biominerals. *Top Curr Chem* 270:155–185
- Casterline JL, Barnett NM (1982) Cadmium-binding components in soybean plants. *Plant Physiol* 69(5):1004–1007
- Cherian G, Chan H (1993) Biological functions of metallothionein – a review. In: Suzuki KT, Imura N, Kimura M (eds) *Metallothionein III, biological roles and medical implications*. Birkhauser, Basel, pp 87–109
- Clemens S, Kim EJ, Neumann D, Schroeder JI (1999) Tolerance to toxic metals by a gene family of phytochelatin synthases from plants and yeast. *Embo J* 18(12):3325–3333
- Cobbett CS (2000) Phytochelatin and their roles in heavy metal detoxification. *Plant Physiol* 123(3):825–832
- Cobbett C, Goldsbrough P (2002) Phytochelatin and metallothioneins: roles in heavy metal detoxification and homeostasis. *Annu Rev Plant Biol* 53:159–182
- Csank C, Hayens K (2000) *Candida glabrata* displays pseudohyphal growth. *FEMS Microbiol Lett* 189(1):115–120
- Dameron CT, Winge DR (1990a) Peptide-mediated formation of quantum semiconductors. *Trends Biotechnol* 8(1):3–6
- Dameron CT, Winge DR (1990b) Characterization of peptide-coated cadmium-sulfide crystallites. *Inorg Chem* 29(7):1343–1348
- Dameron CT, Smith BR, Winge DR (1989a) Glutathione-coated cadmium-sulfide crystallites in *Candida-glabrata*. *J Biol Chem* 264(29):17355–17360



- Dameron CT, Reese RN, Mehra RK, Kortan AR, Carroll PJ, Steigerwald ML, Brus LE, Winge DR (1989b) Biosynthesis of cadmium-sulfide quantum semiconductor crystallites. *Nature* 338 (6216):596–597
- De'Deken RH (1966) The crabtree effect: a regulatory system in yeast. *J Gen Microbiol* 44 (2):157–165
- Downard K (2004) Mass spectrometry: a foundation course. Royal Society of Chemistry, London
- Dujon B et al (2004) Genome evolution in yeasts. *Nature* 430(6995):35–44
- Fell JW (1993) Rapid identification of yeast species using three primers in a polymerase chain reaction. *Mol Mar Biol Biotechnol* 2(3):174–180
- Gericke M, Pinches A (2006) Biological synthesis of metal nanoparticles. *Hydrometallurgy* 83 (1–4):132–140
- Goksungur Y, Uren S, Guvenc U (2005) Biosorption of cadmium and lead ions by ethanol treated waste baker's yeast biomass. *Bioresour Technol* 96(1):103–109
- Grill E, Winnacker EL, Zenk MH (1985) Phytochelatin: the principal heavy-metal complexing peptides of higher plants. *Science* 230(4726):674–676
- Grill E, Winnacker EL, Zenk MH (1986) Synthesis of 7 different homologous phytochelatin in metal-exposed *Schizosaccharomyces pombe* cells. *FEBS Lett* 197(1–2):115–120
- Grill E, Winnacker EL, Zenk MH (1987) Phytochelatin, a class of heavy-metal-binding peptides from plants, are functionally analogous to metallothioneins. *Proc Natl Acad Sci U S A* 84(2): 439–443
- Grill E, Löffler S, Winnacker EL, Zenk MH (1989) Phytochelatin, the heavy-metal-binding peptides of plants, are synthesized from glutathione by a specific gamma-glutamylcysteine dipeptidyl transpeptidase (phytochelatin synthase). *Proc Natl Acad Sci U S A* 86(18): 6838–6842
- Ha SB, Smith AP, Howden R, Dietrich WM, Bugg S, O'Connell MJ, Goldsbrough PB, Cobbett CS (1999) Phytochelatin synthase genes from Arabidopsis and the yeast *Schizosaccharomyces pombe*. *Plant Cell* 11(6):1153–1163
- Hassellöv M, Kaegi R (2009) Analysis and characterization of manufactured nanoparticles in aquatic environments. In: Lead JR, Smith E (eds) *Nanoscience and nanotechnology: environmental and human health implications*. Wiley, New York, pp 211–266
- Hayashi Y, Nakagawa CW, Uyakul D, Imai K, Isobe M, Goto T (1988) The change of cadystin components in Cd-binding peptides from the fission yeast during their induction by cadmium. *Biochem Cell Biol* 66(4):288–295
- Hayashi Y, Nakagawa CW, Mutoh N, Isobe M, Goto T (1991) Two pathways in the biosynthesis of cadystins (GammaEC)NG in the cell-free system of the fission yeast. *Biochem Cell Biol* 69 (2–3):115–121
- Hazen KC (1995) New and emerging yeast pathogens. *Clin Microbiol Rev* 8(4):462–478
- He S, Guo Z, Zhang S, Wang J, Gu N (2007) Bio-synthesis of gold nanoparticles using the bacteria *Rhodospseudomonas capsulata*. *Mater Lett* 61:3984–3987
- He W, Zhou WJ, Wang YJ, Zhang XD, Zhao HS, Li ZM, Yan SP (2009) Biomineralization of iron phosphate nanoparticles in yeast cells. *Mater Sci Eng* 29(4):1348–1350
- Heslot H, Goffeau A, Louis C (1970a) Respiratory metabolism of a petite-negative yeast *Schizosaccharomyces pombe* 972 h<sup>-1</sup>. *J Bacteriol* 104(1):473–481
- Heslot H, Louis C, Goffeau A (1970b) Segregational respiratory-deficient mutants of a petite-negative yeast *Schizosaccharomyces pombe* 972 h<sup>-1</sup>. *J Bacteriol* 104(1):482–491
- Hui YH (2006) *Handbook of food science, technology, and engineering*, vol. 4, CRC Press, Taylor & Francis Group
- Ito H, Inouhe M, Tohoyama H, Joho M (2007) Characteristics of copper tolerance in *Yarrowia lipolytica*. *BioMetals* 20(5):773–780
- Jackson PJ, Unkefer CJ, Doolen JA, Watt K, Robinson NJ (1987) Poly(-y glutamylcysteinyl) glycine: its role in cadmium resistance in plant cells. *Proc Natl Acad Sci U S A* 84(19): 6619–6623

- Jha A, Prasad K, Kulkarni AR (2009) Synthesis of TiO<sub>2</sub> nanoparticles using microorganisms. *Colloids Surf B: Biointerfaces* 71(2):226–229
- Kagi JHR (1993) Evolution, structure, and chemical activity of class I metallothioneins: an overview. In: Suzuki KT, Imura N, Kimura M (eds) *Metallothionein III, biological roles and medical implications*. Birkhäuser, Basel, pp 29–56
- Kagi JHR, Schaffer A (1988) Biochemistry of metallothionein. *Biochemistry* 27(23):8509–8515
- Knorr D, Shetty KJ, Kinsella JE (1979) Enzymatic lysis of yeast cell walls. *Biotechnol Bioeng* 21(11):2011–2021
- Kondo N, Isobe M, Imai K, Goto T, Murasugi A, Hayashi Y (1983) Structure of cadystin, the unit-peptide of cadmium-binding peptides induced in a fission yeast, *Schizosaccharomyces pombe*. *Tetrahedron Lett* 24(9):925–928
- Kowshik M, Vogel W, Urban J, Kulkarni SK, Paknikar KM (2002a) Microbial synthesis of semiconductor PbS nanocrystallites. *Adv Mater* 14(11):815–818
- Kowshik M, Deshmukh N, Vogel W, Urban J, Kulkarni SK, Paknikar KM (2002b) Microbial synthesis of semiconductor CdS nanoparticles, their characterization, and their use in the fabrication of an ideal diode. *Biotechnol Bioeng* 78(5):583–588
- Kowshik M, Ashtaputre S, Kharrazi S, Vogel W, Urban J, Kulkarni SK, Paknikar KM (2003) Extracellular synthesis of silver nanoparticles by a silver-tolerant yeast strain MKY3. *Nanotechnology* 14(1):95–100
- Krumov N, Oder S, Perner-Nochta I, Angelov A, Posten C (2007) Accumulation of CdS nanoparticles by yeasts in a fed-batch bioprocess. *J Biotechnol* 132(4):481–486
- Krumov N, Perner-Nochta I, Oder S, Gotcheva V, Angelov A, Posten C (2009) Production of inorganic nanoparticles by microorganisms. *Chem Eng Technol* 32(7):1026–1035
- Kundu S, Pal A, Ghosh SK, Nath S, Panigrahi S, Praharaj S (2005) Shape-controlled synthesis of gold nanoparticles from gold(III)-chelates of beta-diketones. *J Nanopart Res* 7(6):641–650
- Lachance MA (1988) Restriction mapping of rDNA and taxonomy of *Kluyveromyces van der Walt* emend. van der Walt. *Yeast S(Special Issue)* S379–S383
- Lindner P (1893) *Schizosaccharomyces pombe* n. sp., ein neuer Gärungsreger. *Wochenschrift für Brauerei* 10:1298–1300
- Mandal D, Bolander ME, Mukhopadhyay D, Sarkar G, Mukherjee P (2006) The use of microorganisms for the formation of metal nanoparticles and their application. *Appl Microbiol Biotechnol* 69(5):485–492
- Mann S (1993) Molecular tectonics in biomineralization and biomimetic materials chemistry. *Nature* 365(6446):499–505
- McSheehy S, Mester Z (2003) The speciation of natural tissues by electrospray-mass spectrometry II: bioinduced ligands and environmental contaminants. *Trends Anal Chem* 22:311–326
- Mehra RK, Mulchandani P (1995) Glutathione-mediated transfer of Cu(I) into phytochelatins. *Biochem J* 307:697–705
- Mehra RK, Winge DR (1988) Cu(I) binding to the *Schizosaccharomyces pombe* gamma-glutamyl-transferase peptides varying in chain lengths. *Arch Biochem Biophys* 265(2):381–389
- Mehra RK, Winge DR (1991) Metal-ion resistance in fungi – molecular mechanisms and their regulated expression. *J Cell Biochem* 45(1):30–40
- Mehra RK, Tarbet EB, Gray WR, Winge DR (1988) Metal-specific synthesis of two metallothioneins and  $\gamma$ -glutamyl peptides in *Candida glabrata*. *Proc Natl Acad Sci U S A* 85:8815–8819
- Mehra RK, Mulchandani P, Hunter TC (1994) Role of Cds quantum crystallites in cadmium resistance in *Candida glabrata*. *Biochem Biophys Res Commun* 200(3):1193–1200
- Mendoza-Cozatl D, Loza-Tavera H, Hernandez-Navarro A, Moreno-Sanchez R (2005) Sulfur assimilation and glutathione metabolism under cadmium stress in yeast, protists and plants. *Microbiol Rev* 29(4):653–671
- Moreno S, Klar A, Nurse P (1991) Molecular genetic analysis of the fission yeast *Schizosaccharomyces pombe*. *Methods Enzymol* 194:795–823
- Murasugi A, Wada C, Hayashi Y (1981a) Cadmium-binding peptide induced in fission yeast, *Schizosaccharomyces pombe*. *J Biochem* 90(5):1561–1564

- Murasugi A, Wada C, Hayashi Y (1981b) Purification and unique properties in UV and CD spectra of Cd-binding peptides from *Schizosaccharomyces pombe*. *Biochem Biophys Res Commun* 103(3):1021–1028
- Murasugi A, Wada C, Hayashi Y (1983) Occurrence of acid-labile sulfide in cadmium-binding peptide-1 from fission yeast. *J Biochem* 93(2):661–664
- Murphy CJ, Coffey JL (2002) Quantum dots: a primer. *Appl Spectrosc* 56(1):16–27
- Nasim A, Young P, Johnson BF (1989) *Molecular biology of the fission yeasts*. Academic, New York
- Nies DH, Silver S (2007) *Molecular microbiology of heavy metals*. Springer, Berlin
- Nobel A (1868) Improved explosive compound. US Letters Patent No 78317
- Nozik AJ, Williams F, Nenadovic MT, Rajh T, Micic OI (1985) Size quantization in small semiconductor particles. *J Phys Chem* 89(3):397–399
- Obata H, Umebayashi M (1986) Characterization of cadmium-binding complexes from the roots of cadmium-treated rice plant. *Soil Sci Plant Nutr* 32(3):461–467
- Olsson L, Nielsen J (2000) The role of metabolic engineering in the improvement of *Saccharomyces cerevisiae*: utilisation of industrial media. *Enzyme Microb Technol* 26(9–10):785–792
- Ortiz DF, Ruscitti T, Mccue KF, Ow DW (1995) Transport of metal-binding peptides by Hmt1, a Fission Yeast Abc-Type vacuolar membrane-protein. *J Biol Chem* 270(9):4721–4728
- Perego P, Howell SB (1997) Molecular mechanisms controlling sensitivity to toxic metal ions in yeast. *Toxicol Appl Pharmacol* 147(2):312–318
- Pimprikar PS, Joshi SS, Kumar AR, Zinjarde SS, Kulkarni SK (2009) Influence of biomass and gold salt concentration on nanoparticle synthesis by the tropical marine yeast *Yarrowia lipolytica* NCIM 3589. *Colloids Surf B Biointerfaces* 74(1):309–316
- Rausser WE (1984) Isolation and partial purification of cadmium-binding protein from roots of the grass *agrostis-gigantea*. *Plant Physiol* 74(4):1025–1029
- Rausser WE (1990) Phytochelatins. *Annu Rev Biochem* 59:61–86
- Rausser WE (1995) Phytochelatins and related peptides – structure, biosynthesis, and function. *Plant Physiol* 109(4):1141–1149
- Rausser WE (1999) Structure and function of metal chelators produced by plants – the case for organic acids, amino acids, phytin, and metallothioneins. *Cell Biochem Biophys* 31(1):19–48
- Rausser WE, Curvetto NR (1980) Metallothionein occurs in roots of *Agrostis* tolerant to excess copper. *Nature* 287(5782):563–564
- Reese RN, Mehra RK, Tarbet EB, Winge DR (1988) Studies on the  $\gamma$ -glutamyl Cu-binding peptide from *Schizosaccharomyces pombe*. *J Biol Chem* 263(9):4186–4192
- Ross S (1994) *Toxic metals in soil-plant systems*. Wiley, Chichester, UK
- Rossetti R, Ellison JL, Gibson JM, Brus LE (1984) Size effects in the excited electronic states of small colloidal CdS crystallites. *J Chem Phys* 80(9):4464–4469
- Salt DE, Wagner GJ (1993) Cadmium transport across tonoplast of vesicles from oat roots – evidence for a  $\text{Cd}^{2+}/\text{H}^{+}$  antiport activity. *J Biol Chem* 268(17):12297–12302
- Schlegel HG, Zaborosch C (1992) *Allgemeine Mikrobiologie*. Georg Thieme Verlag, Stuttgart
- Shen R, Lachance MA (1993) Phylogenetic study of ribosomal DNA of cactophilic *Pichia* species by restriction mapping. *Yeast* 9(4):315–330
- Siddiqi SF, Titchener-Hooker NJ, Shamlou PA (1997) High pressure disruption of yeast cells: the use of scale down operations for the prediction of protein release and cell debris size distribution. *Biotechnol Bioeng* 55(4):642–649
- Slocik JM, Knecht MR, Wright DW (2004) Biogenic nanoparticles. In: Nalwa HS (ed) *Encyclopedia of nanoscience and nanotechnology*. American Scientific Publishers, Stevenson Ranch CA, pp 293–308
- Stiefel J, Wang L, Kelly DA, Janoo R, Seitz J, Whitehall SK, Hoffman CS (2004) Suppressors of an adenylate cyclase deletion in the fission yeast *Schizosaccharomyces pombe*. *Eukaryot Cell* 3(3):610–619
- Strouhal M, Kizek R, Vacek J, Trnkova L, Nemeč M (2003) Electrochemical study of heavy metals and metallothionein in yeast *Yarrowia lipolytica*. *Bioelectronics* 60(1–2):29–36

- Vacchina V, Lobinski R, Oven M, Zenk MH (2000) Signal identification in size-exclusion HPLC-ICP-MS chromatograms of plant extracts by electrospray tandem mass spectrometry (ES MS/MS). *J Anal At Spectrom* 15:529–534
- Vatamaniuk OK, Mari S, Lu YP, Rea PA (1999) AtPCS1, a phytochelatin synthase from *Arabidopsis*: isolation and in vitro reconstitution. *Proc Natl Acad Sci U S A* 96(12):7110–7115
- Vatamaniuk OK, Mari S, Lu YP, Rea PA (2000) Mechanism of heavy metal ion activation of phytochelatin (PC) synthase – blocked thiols are sufficient for PCSynthase-catalyzed transpeptidation of glutathione and related thiol peptides. *J Biol Chem* 275(40):31451–31459
- Wagner GJ, Trotter MM (1982) Inducible cadmium binding complexes of cabbage and tobacco. *Plant Physiol* 69(4):804–809
- Westwood PK, Martin IV, Fantes PA (2004) Fission yeast Cdc37 is required for multiple cell cycle functions. *Mol Genet Genomics* 271(1):82–90
- Williams P, Keshavarz-Moore E, Dunnill P (1996a) Production of cadmium sulphide microcrystallites in batch cultivation by *Schizosaccharomyces pombe*. *J Biotechnol* 48(3):259–267
- Williams P, Keshavarz-Moore E, Dunnill P (1996b) Efficient production of microbially synthesized cadmium sulfide quantum semiconductor crystallites. *Enzyme Microb Technol* 19(3):208–213
- Williams P, Keshavarz-Moore E, Dunnill P (2002) *Schizosaccharomyces pombe* fed-batch culture in the presence of cadmium for the production of cadmium sulphide quantum semiconductor dots. *Enzyme Microb Technol* 30(3):354–362
- Wood V et al (2002) The genome sequence of *Schizosaccharomyces pombe*. *Nature* 415:871–880
- Wünschmann J, Beck A, Meyer L, Letzel T, Grill E, Lenzian KJ (2007) Phytochelatin synthase is synthesized by two vacuolar serine carboxypeptidases in *Saccharomyces cerevisiae*. *FEBS Lett* 581(8):1681–1687
- Yamada Y, Maeda K, Nagahama T, Banno I, Lachance MA (1992) The phylogenetic relationships of the genus *Sporopachydermia* Rodriguez de Miranda (*Saccharomycetaceae*) based on the partial sequences of 18 S and 26 S ribosomal RNAs. *J Gen Appl Microbiol* 38:179–183
- Zenk MH (1996) Heavy metal detoxification in higher plants – a review. *Gene* 179(1):21–30

# **Part III**

## **Applications**

# Chapter 10

## Applications of Gold Nanoparticles: Current Trends and Future Prospects

Zygmunt Sadowski and Irena H. Maliszewska

### 10.1 Introduction

Gold nanoparticles are typical in the size range of 1–100 nm. Their physical and chemical properties are different from the same material in bulk form. The main property is a large surface-to-volume ratio. Most of the nanoparticles have the size range of biomolecules and cellular organelles. This gives a possibility of interaction between the gold nanoparticles and the biomolecules and in consequence various medical applications (Azzazy and Mansour 2009).

For biological applications, gold nanoparticles are conjugated with biospecific recognition molecules, such as antibodies, DNA probe molecules, biotin, and enzymes. Most of these applications are based on the unique optical properties of gold. A list of different properties of gold nanoparticles for biological assay and sensor applications contain (1) surface plasmon resonance (SPR), (2) luminescence, (3) surface-enhanced Raman scattering, (4) catalytic effect, and (5) amplification effect (Sow and Wee 2009).

Gold nanoparticles also exhibit unique electronic properties. In the nano-electronic field, one of the most daunting challenges is how to connect individual nanoelectronic components together into the electrical circuits.

Gold nanoparticles are usually connected with ligands. Alkanethiols are the most common ligands used for passivation of gold nanoparticles. The photoelectron emission behavior has arisen from the combination of Au nanoparticles and alkene ligands. For example, gold nanoparticles exhibit size-controlled plasmon exciton. These plasmon absorbance bands are sensitive to the dielectric properties of the stabilizing layers of Au nanoparticles. The coupling of biomolecules to gold might allow the use of the optical properties of gold. This phenomenon called plasmon–plasmon interaction allows the use of gold nanoparticles as labels for colorimetric detection of biomolecules (Huo 2007).

---

Z. Sadowski (✉) and I.H. Maliszewska

Wrocław University of Technology, Chemical Faculty Wybrzeże, Wyspińskiego 27, 50370 Wrocław, Poland

e-mail: zygmunt.sadowski@pwr.wroc.pl; irena.helena.maliszewska@pwr.wroc.pl

**Table 10.1** Summary of gold nanoparticles applications

Application area	Main reference
Fluorescent biological label	Jain et al. (2006)
Drug and gene delivery	Ghosh et al. (2008)
Animal viruses transport with gold templates	Goicochea et al. (2007)
Biodetection of pathogens	Wilson (2008)
Gold nanoparticles in electroanalysis	Welch and Compton (2006)
Probing of DNA structure	Liu et al. (2002)
Antibacterial activity of gold nanoparticles	Beermann et al. (2007)
Tumor destruction via heating (hyperthermia) photothermal therapy	El-Sayed et al. (2006) Jain et al. (2007)
Saccharides sensor and glucose oxidation	Aslan et al. (2004) Ramanaviciene et al. (2009)
Catalysis of oxidation reactions	Thompson (2007)
Low-temperature oxidation of CO	Moroz et al. (2009)
Antibacterial efficacy of antibiotics conjugated to gold nanoparticles	Grace and Pandian (2007)

Gold nanoparticles have been used with a long history as a contrast agent for scanning electron and light microscopy in histopathology study. Gold nanoparticles can be used as electrochemical biosensors. Gold nanoparticles play an important role in improving biosensor performance due to their large effective surface area and excellent biocompatibility.

In this respect, the main application fields of gold nanoparticles are summarized in Table 10.1.

This chapter is aimed at summarizing the unique optical and catalytic properties of gold nanoparticle, and hybrid system has also been discussed. Moreover, the applications such as drug delivery using gold nanoparticles and antibacterial behavior of gold will be considered.

## 10.2 Gold Nanoparticles Synthesis with Biomolecule Protection

Colloidal gold as a nanomaterial has historical roots in Egypt and China. The actual scientific investigations are focused on the biological synthesis of gold and silver nanoparticles using microorganisms and plant extracts (Sadowski 2010).

The most popular method of gold nanoparticle synthesis involves the reduction of tetrachloroauric acid ( $\text{HAuCl}_4$ ) by various reducing agents. However, the high surface energy of gold nanoparticle makes them extremely reactive. To avoid their aggregation or precipitation, a special stabilizer must be used. One of the popular methods for the passivation of gold nanoparticles' surface is biomolecule monolayer. For instance, peptides not only reduced tetrachloroauric acid, but also coated the surface of created gold nanoparticles (Guo and Wang 2007).

The biomolecule–nanoparticle hybrid systems have been obtained using polypeptides, thiolated peptides, lipids, and phospholipids. Thiolated gold nanoparticles

are extremely stable and often used to study nanoparticles formation. The nanoparticles exhibit similar dimension to those of biomolecules, and the interaction of nanoparticles with biomolecules gives novel hybrid nanobiomaterials. These novel materials have been reported as useful for biomedical application. For this application, the interaction of gold nanoparticles with functional biomaterials is very important. Liposome is the useful tool in the drug-delivery system. The location of gold nanoparticles in the lipid bilayer was investigated by Park et al. (2006). Figure 10.1 shows the scheme of gold nanoparticles loaded in the liposome bilayer.

Recently, the homopolymers and block polymers capable of stabilizing gold nanoparticles effectively by steric stabilization have shown much potential in advanced materials (Li et al. 2009). It should be remembered that polymer chains adsorbed on the surface of gold nanoparticles cannot only enhance the stability of gold cores, but also functionalize the gold core, particularly, when the intelligent polymers are used. The intelligent polymers are also known as “environmentally sensitive” polymers. Polyelectrolyte-protected gold nanoparticles have been commonly prepared via a two-step method where gold salt was first mixed with polyelectrolyte, followed by the addition of a reducing agent under rapid stirring (Luo 2007).

A simple method for the preparation of gold nanoparticles using Pluronic P123 [block polymer (poly(ethylene oxide)-poly(propylene oxide)-poly(ethylene oxide))] and halide or ions is gold salt photoreduction (Cha et al. 2009). That novel procedure was simple, gold particles were formed inside the micelles with two-layer structures. By modulating the block copolymer concentration and composition and adding NaF salt, gold nanoparticles with different size and morphology could be obtained (Chen et al. 2007).

Gold nanoparticles were also incorporated into thermoresponsive polymer poly (*N*-isopropylacrylamide) (PNIPAM). These gold nanoparticle–thermoresponsive polymer hybrids may be of interest especially in regard to photothermal cancer therapy (Tang et al. 2008).

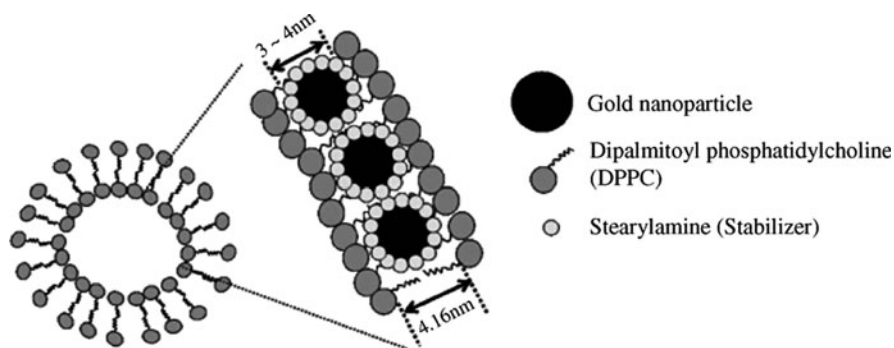


**Fig. 10.1** Scheme of gold nanoparticles located in the liposome bilayer from (Park et al. (2006)



Stable gold nanoparticles were directly prepared by using amphiphilic multi-block copolymer containing multiple functional thiol end groups as stabilizing agents. The gold nanoparticles suspension obtained by using this method can be stable for a wide range of pH up to pH = 9. The optical properties of the gold nanoparticles also depended on the pH value (Du et al. 2008).

### ***10.2.1 Dendrimer-Protected Gold Nanoparticles***

Dendrimers are macromolecular compounds that comprise series branches around an inner core. Applying dendrimers as protecting agents for gold nanoparticles creates new opportunities for nanotechnology due to the following advantages (1) dendrimers yield well-defined nanoparticle replicas, (2) gold nanoparticles are well stabilized, (3) the dendrimer branches can take a contact with small molecules, and (4) the gold nanoparticle protected by dendrimer possess very small size (typical 1–5 nm). Two commercially available dendrimers are poly(amidoamine) PAMAM and poly(propylene amine). An early example of gold nanoparticle dendrimer interaction is a gold nanoparticle coated by PAMAM dendrimer (Hiraiwa et al. 2006).

Dendrimers offer the opportunity to design well-defined nanocarriers for delivery of gold nanoparticles to cells. A new type of metal(Au)–dendrimer hybrid materials may be advantageous in catalysis, biomedical applications, as well as cancer cell labeling and treatment (Shi et al. 2006). In this process, dendrimers act as nanoreactors for the nucleation and growth of nanoparticles allowing control of the particle size and size distribution. The fabrication of multifunctional, dendrimer-stabilized Au nanoparticles for biological and biomedical applications remains challenging.

The initial step for the production of multifunctional, glycodendrimer-stabilized Au nanoparticles with a small particle size and low polydispersity was a metal complex creation with functional groups within the dendrimer scaffold. It was observed that the size of Au–dendrimer hybrid decreases with the increase of the number of dendrimer generation (Pietsch et al. 2009).

A possible mechanism of gold nanoparticle–dendrimer hybrid creation assumes that the segments of dendrimer possess focal points. The focal point is hydroxyl groups, which are capable of gold complexation. The specific gold–dendrimer interactions can be utilized to control the stability of gold nanoparticles. The dendrimer focal point appears to be a site where the gold may nucleate and grow (Jiang et al. 2007).

The formation of self-assembled gold nanoparticle–dendrimer clusters was demonstrated by the wavelength broadening and shifting at 520 nm. The change in cluster size and size distribution results showed that the peak shifts to higher wavelength for the lower generation dendrimer. It is connected with the steric hindrance (Pan et al. 2005). The synthesis of gold nanoparticle-cored dendrimers opens new ways to the preparation of well-defined molecular objects.

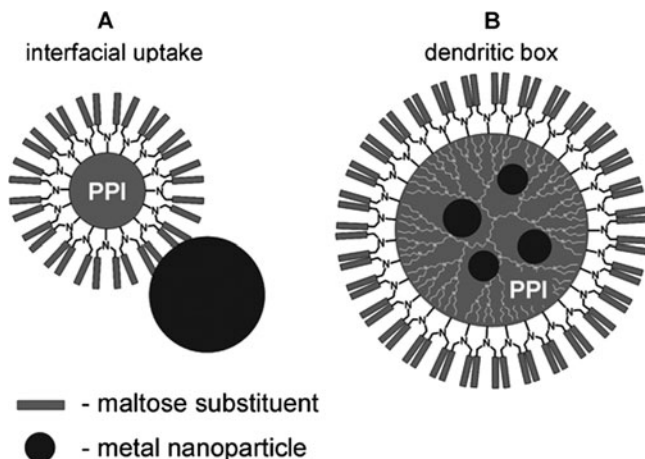


**Fig. 10.2** Schematic structure of gold nanoparticles with maltose-modified PPI dendrimer (*black circle* – gold nanoparticle) Pietsch et al. (2009)

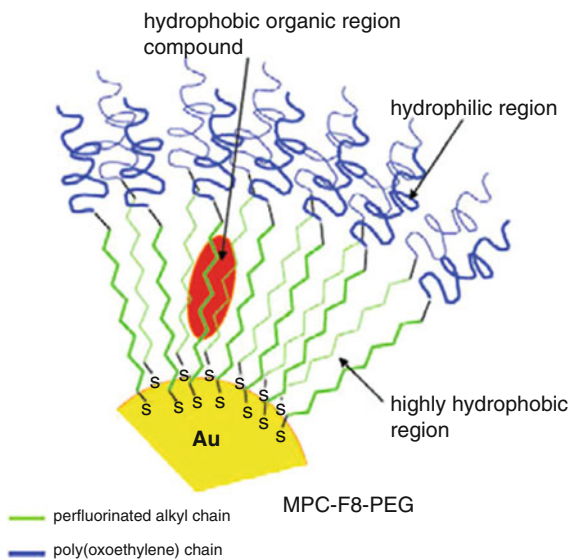
A new family of PPI (poly(propyleneimine)) dendrimers (G2–G5) with a dense maltose shell were used to stabilize gold nanoparticles in water (Pietsch et al. 2009). The initial results suggest that gold nanoparticle–PPI dendrimer hybrid coated with a maltose shell (Fig. 10.2) may be beneficial in biological and medical applications. It is a fact that dendrimer-stabilized gold nanoparticles will provide an interesting alternative to synthetic polymer frequently used in pharmaceuticals and drug delivery.

### 10.2.2 Modification of Gold Nanoparticle Surface

Gold nanoparticles are surrounded by a layer of stabilizing molecules. These molecules can be replaced by other macromolecules. In this way, the surface of gold nanoparticles can be modified either by coating or by grafting a macromolecule whose properties alter nanoparticles' surface characteristics. This adsorption mainly changes nanoparticles' zeta potential and their hydrophobicity. It was deduced that gold nanoparticles may be soluble in water (Agbenyega 2008). Water-soluble gold nanoparticles typically contain terminal carboxylate groups at their periphery. The carboxy groups are used to attach amino groups of biomolecules (Fig. 10.3).

Polymeric-coated particles are of special interest from the pharmaceutical point of view. They are stable in the gastrointestinal tract and can protect gold nanoparticles from gastrointestinal environment. The main criteria dictating polymer eligibility for drug delivery have been bioavailability, biocompatibility, and optimal degradation rate. Recently, encapsulation of gold nanoparticles in core–shell structures has been attempted with various methods (Zhang et al. 2006).

**Fig. 10.3** Schematic of water soluble gold nanoparticles from Agbenyega (2008)



Chitosan is a polysaccharide biopolymer derived by deacetylation of chitin. The stabilization of gold nanoparticles with chitosan has been reported (Du et al. 2007). Chitosan was mixed with enzymes and gold nanoparticles to construct biosensors through simple one-step electrodeposition. An electrochemical deposition method for the preparation of a biocomposite composed of chitosan, gold nanoparticles, and enzyme was proposed (Luo et al. 2004). It was shown that the electrochemically deposited biocomposite is suitable for enzyme immobilization and biosensor construction.

Polymers acting as protecting agents provide a good opportunity for monodisperse gold particles. Additionally, the particle size could be controlled precisely by the molar ration of gold to polymer ligands.

The different polymers and copolymers used to protect the gold nanoparticles have been investigated (des Rieux et al. 2006).

The glucose sensing is based on the aggregation of gold nanoparticles covered by dextran. Dextran-coated gold nanoparticles were aggregated with addition of ConA (concanavalin A) resulting in an increase in absorbance of nanoparticles at 650 nm, where the post addition of glucose caused the dissociation of the aggregates and thus a decrease in the absorbance. Gold nanoparticles aggregation induced by organic reagents has been taken for DNA and antibodies analysis (Aslan et al. 2004).

The formation of hybrid systems comprising gold nanoparticles and biomolecules paves the way for cell markers to biosensing, bioimaging, and targeted drug delivery.

### 10.3 Gold Nanoparticles as a Sensor

Gold nanoparticles are a very attractive material for biosensor, chemisensor, genosensor, and immunosensor production. Additionally, the unique physical and chemical properties of gold nanoparticles provide excellent prospects for the realization of this aim. Gold nanoparticles can be used as passive labels or as active sensors (Sperling et al. 2008).

Gold nanoparticles have been widely used to construct biosensors because of their excellent ability to immobilize biomolecules. Many kinds of biosensors, such as enzyme sensor, immunosensor, and DNA sensor, have been prepared based on the application of gold nanoparticles (Huo 2007).

Developing rapid DNA-detection method is important for life science research. Gold nanoparticle probes heavily functionalized with thiolated oligonucleotides have emerged as an attractive alternative to molecular probes for nucleic acid detection. A two-color-change method for detection and simultaneous validation of single-nucleotide polymorphisms in DNA target using Ag/Au core-shell and pure gold nanoparticle probes was proposed (Cao et al. 2005).

Bioelectronics may be defined as the field emerging from the integration of biomaterials, such as redox proteins, antigens/antibodies, DNA, receptors, field-effect transistors, or piezoelectric crystals (Willner et al. 2002). The electrical DNA detection method using a semi-assembly multilayer gold nanoparticles structure between the nanogap electrodes has been presented (Tsai et al. 2005). In this method, an electrical approach is used to detect DNA hybridization through the establishment of gold nanostructure on the gap surface between two electrodes. The electrical current through multilayer gold nanoparticle structures is much greater than that through monolayered gold nanoparticle structure. DNA can be detected through a significant degradation in electrical resistance.

The microgravimetric quartz crystal microbalance can be used for DNA hybridization detection. The use of DNA-capped gold nanoparticles as an amplifier was shown as a promising means for sensitivity enhancement. The systems of a probe/target/probe-nanoparticles sandwich and a dendritic structure based on DNA-capped gold nanoparticles were developed (Liu et al. 2002). The microgravimetric detection method was further extended to analyze proteins by using gold nanoparticles as “weight labels” and as catalytic sites for enlargement of nanoparticles and the amplified sensing of the proteins.

The development of DNA-labeled gold nanoparticles has opened up a new field of bionanotechnology. The DNA-oligonucleotides employed in this study were 24-mers. The oligonucleotides were coupled to the gold nanoparticles via thiol groups using the linker:  $-\text{O}-(\text{CH}_2)_6-\text{SH}$  (Beermann et al. 2007).

Gold nanoparticle-antibody was applied to the signal enhancement of SPR for immunosensing. Among the types of immunosensors, electrochemical immunosensors achieve excellent detection limits. This limit was  $0.25 \text{ pg ml}^{-1}$ , which is three orders of magnitude lower than that obtained by a conventional immunoassay (Guo and Wang 2007).

The modification of gold nanoparticles with thiol-modified oligonucleotides is a well-known procedure (Steinbruck et al. 2009). Thiol-modified oligonucleotides were attached to the gold nanoparticles surfaces. The resulting nanoparticle network leads to average particle distances below the particles' diameter, resulting in color change of the solution (red to blue) associated with a large red shift of the extinction maximum easily observed by the naked eye. The colorimetric detection of biomolecules was based on this phenomenon.

The mean distance between gold nanoparticles in a typical sol is greater than 1,000 nm. The distance-dependent color changes were detected for gold nanoparticles conjugated with antibodies. At high concentration of cross-linked molecules, the visible color changes from red to blue. The aggregation of gold nanoparticles by cross-linking DNA hybridization may also change the color of the colloidal solution. This phenomenon was adapted to DNA analysis (Wilson 2008).

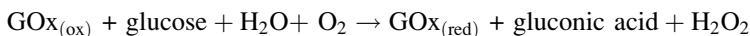
Finally, gold nanoparticles can be used for developing sensitive electrochemical detection methods. These methods are coupled with enzyme detection. If molecules in a narrow gap between electrodes are labeled with gold nanoparticles, there is a decrease in resistance that can be measured. One example is the antibodies immobilized in the gap between two electrodes by capture target molecules give a high electrical resistance. In this case, when the target molecules are sandwiched and antibodies are conjugated to gold nanoparticles the resistance is still high. The catalytic deposition of metallic silver around the gold nanoparticles bridges the gap between electrodes and the resistance is low.

Gold nanoparticles are able to control the electrode microenvironment. There are some advantages to the use of gold nanoparticles for modification of electrodes when compared to a macroelectrode. First at all, there is a high effective surface area and lower cost (Welch and Compton 2006). Colloidal gold can be used to modify the carbon paste electrode. An extremely small amount of gold (0.006% w/w) can produce a huge increase in the electrochemical signal. The addition of albumin to a preparation of gold nanoparticles led to a better dispersion of the gold nanoparticles in the carbon paste, which also increases the sensitivity of the electrode. This electrode can be employed to detect hydrogen peroxide, dopamine, and hydroquinone.

Recently, glucose oxidase–single Au nanoparticle hybrid was synthesized. Glucose oxidase is a typical globular protein. The gold nanoparticles may act as an electron acceptor. Electron transfer properties of gold nanoparticles with glucose oxidase were exploited in a number of amperometric biosensors. Glucose oxidase (GOx) catalyzes the oxidation of  $\beta$ -D-glucose to gluconic lactone. The GOx catalyzes glucose and produces electrons that can be transferred towards an electrode through gold nanoparticles. This system can be used to detect glucose in the blood of diabetic patients (Chen et al. 1998).

Gold nanoparticles can be used as a very efficient redox mediator suitable for biosensor design. Gold nanoparticles were studied as potential redox mediator for glucose oxidase (GOx). Gold nanoparticles wired with glucose oxidase provide a special microenvironment. Glucose oxidase is a homodimer flavoprotein

containing two active sites per molecule. This process has occurred according to the reaction:



Glucose during the oxidation produces electrons that can be transferred towards electrode through gold nanoparticles. This procedure can be used to detect glucose in the blood. This method was based on the spectrophotometric method (Ramanaviciene et al. 2009). As a spectrophotometrical detector, DCPIP dye was used. The oxidized form of DCPIP is blue and it has an optical absorption peak at 600 nm. In the reduced form, DCPIP loses its specific color. This dye behavior gives a possibility for enzymatic reaction control. The obtained data showed that the enzymatic reaction rate of GOx in the presence of gold nanoparticles, which transfer electrons from GOx towards the DCPIP, was 1.48 times higher (Ramanaviciene et al. 2009).

## 10.4 Catalytic Properties of Gold Nanoparticles

The discovery in 1987 by Haruta and coworkers that gold nanoparticles with size of <5 nm supported on the metal oxides manifested a high catalytic activity has opened a new route in catalytic science (Haruta et al. 1997). Gold nanoparticles participated in a series of important processes including hydrocarbon selective oxidation, hydrogenation, and water-gas shift reaction. The new gold catalyst system, consisting of nanoparticulate gold on oxide support, is used for low-temperature CO oxidation. It was shown that catalytical activity of gold nanoparticles in CO oxidation is strongly dependent on the support material. As support materials metal oxide ( $\text{TiO}_2$ ,  $\text{Al}_2\text{O}_3$ ,  $\text{Co}_3\text{O}_4$ ,  $\text{Fe}_2\text{O}_3$  and  $\text{NiO}$ ), hydroxides ( $\text{Be}(\text{OH})_2$  and  $\text{Mg}(\text{OH})_2$ ) and carbon materials were used. From the practical point of view, alumina ( $\text{Al}_2\text{O}_3$ ) would be a preferable support for Au catalyst, because it is cheap and possesses a high and thermally stable surface area.

The various synthesis routes, such as sol–gel technique, deposition–precipitation (DP method), metal organic-chemical vapor deposition (CVD method), impregnation and dip coating, are employed. For instance, the catalysts with a gold loading of 1–2 wt% were prepared via deposition of Au complexes onto different alumina (with  $\gamma$ - and  $\alpha$ - $\text{Al}_2\text{O}_3$  as the support) by using various methods. The gold nanoparticles have size of 3–5 nm. The Au/ $\text{Al}_2\text{O}_3$  catalysts were prepared by DP method (Moroz et al. 2009). Anionic Au hydroxide complexes were adsorbed onto an  $\text{Al}_2\text{O}_3$  support from an alkalized  $\text{HAuCl}_4$  solution. Impregnation was followed by reduction with  $\text{H}_2$ . Using the CVD method, an organogold precursor was deposited on hydrated alumina in a rotating reactor. Generally, the Au/ $\text{Al}_2\text{O}_3$  catalysts prepared by the DP method demonstrated the highest activity in CO oxidation as compared to the catalyst obtained by the CVD method.

Although there are various methods to prepare Au nanoparticles, gold nanoparticles supported on one-dimension nanostructures such as nanowires and nanotubes

have been an attractive composite for heterogeneous catalysis. An Au nanoparticle can be directly deposited on the  $\text{SiO}_x\text{NW}$  (nanowire) surface without any surface pretreatment using only a physical deposition system. It was showed (Table 10.2) that gold nanoparticles deposited on the  $\text{SiO}_x\text{NWs}$  were much finer in size compared to the gold nanoparticles deposited on a flat  $\text{SiO}_2$  substrate.

Extraordinarily high catalytic activity of supported Au nanoparticles for oxidation of CO at room temperature arises from the reaction of CO adsorbed on the step, edge, and corner sites of metallic gold particles. The studies towards CO oxidation reactivity based on the density functional theory (DFT) showed that the periphery of the interface between an Au particle and an oxide support is responsible (Molina and Hammer 2005).

Many of the heterogeneous catalysts used in industry today consist of nanoparticles of a catalytically active material anchored on a support. Modern nanotechnology methods offer the synthesis of heterogeneous catalysts. The surface of heterogeneous catalyst made with gold nanoparticles deposited on the mica surface is illustrated in Fig. 10.4.

Gold has traditionally been known as a catalytically active material. Very active catalysts were produced by Au nanoparticles which are supported on the base metal oxides or carbon. Two-dimensional (2-D) Au islands are initially formed on the support surface. The islands that are only one atom thick have relative large gaps, whereas islands with a thickness of three or more atoms layers exhibit metallic properties. The sensitivity of CO oxidation on  $\text{Au/TiO}_2$  originates from quantum size effects with respect to the thickness of the Au particles. It has been found that Au particles of less than 5 nm diameters were active for low-temperature CO oxidation (Chen and Goodman 2006).

The low-temperature oxidation of CO on supported Au particles showed a marked reaction rate increase as the diameter of the Au particles was reduced below 3.5 nm (Chen and Goodman 2006). A further reduction in the diameter of gold nanoparticles leads to a decrease in the catalytic activity. Also, the apparent activation energy for the oxidation CO reaction between 350 and 450 K varies from 1.7 to 5 kcal/mol as the Au particle size is increased from 2.5 to 6.0 nm.

The CO adsorption study on Au particles ranging in size from 1.8 to 3.1 nm supported on  $\text{TiO}_2$  showed that the heat of adsorption increases sharply with decreasing gold particle size (Fig. 10.5).

**Table 10.2** Average Au particle number density deposited on the  $\text{SiO}_x\text{NWs}$  and flat  $\text{SiO}_2$  substrate from Kim et al. (2009)

Si:O ratio	Deposition thickness (nm)	Particles size (nm)	Particle number density (particles $\text{cm}^{-1}$ )
1:1.7	2	$4.7 \pm 1.2$	$1.28 \times 10^{12}$
1:1.7	3	$5.6 \pm 2.1$	$1.05 \times 10^{12}$
1:1.1	2	$3.6 \pm 0.9$	$2.01 \times 10^{12}$
1:0.8	2	$3.2 \pm 0.7$	$2.54 \times 10^{12}$
–	1	$4.5 \pm 1.1$	$1.12 \times 10^{12}$
–	2	$7.3 \pm 1.6$	$3.10 \times 10^{11}$
–	3	$13.1 \pm 5.0$	$2.18 \times 10^{11}$

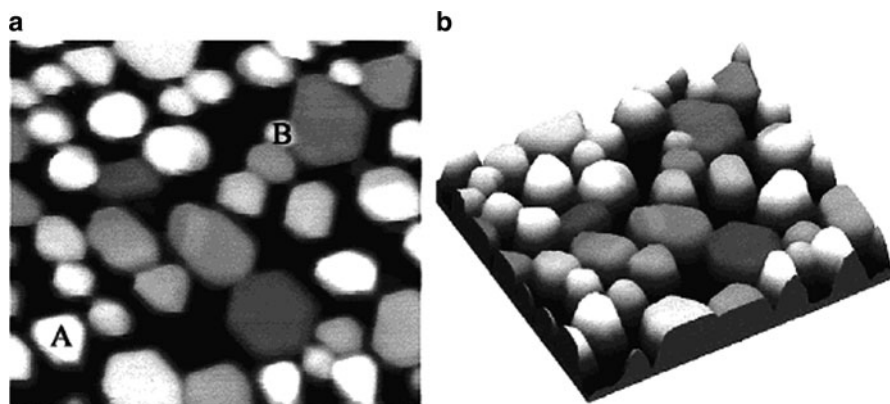


Fig. 10.4 AFM topographic image of gold nanoparticles on mica support, (a) 2D top view image, (b) 3D representation from Ferrero et al. (2001)

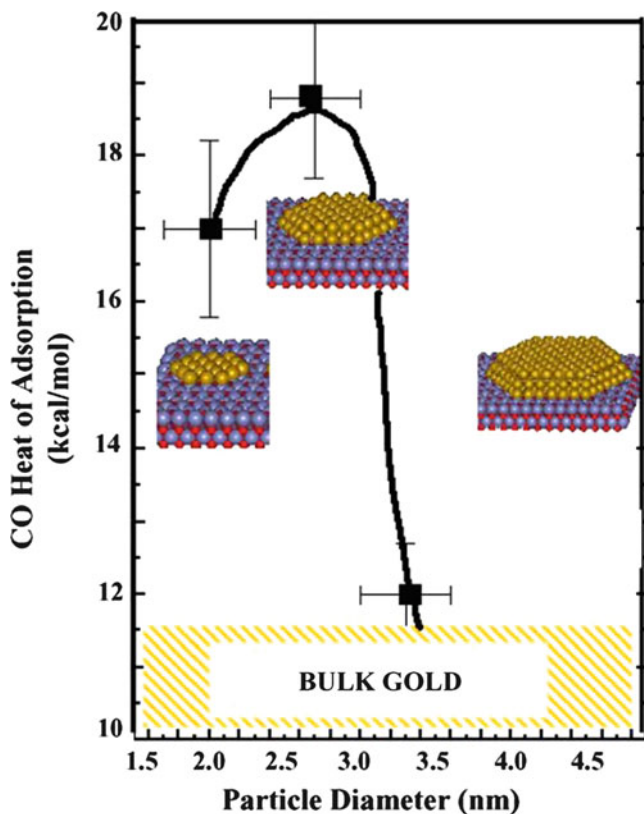
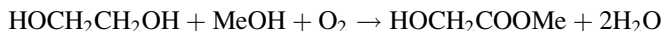


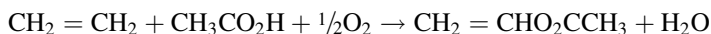
Fig. 10.5 Heats of CO adsorption as a function of gold particle diameter from Chen and Goodman (2006)



The first practical application of Au–Pd catalyst was established for the manufacture of vinyl acetate monomer (VAM) and for production of methyl glycolate. The one-step direct production of methyl glycolate from ethylene glycol and methanol using Au–Pd/Al<sub>2</sub>O<sub>3</sub> catalyst can be described by the following reaction:



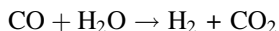
Au nanoparticles play an important role in VAM production using Au–Pd catalysts. Methyl glycolate is used as a solvent for the semiconductor manufacturing process and as a base product for cosmetic. Moreover, VAM can also be manufactured from ethylene, acetic acid, and oxygen using Au–Pd catalysts (Thompson 2007).



It has been shown that the gold particle size and catalyst activity depend on the support material, the synthesis method, and activation procedure. It was discovered that gold nanoparticles supported on Co<sub>3</sub>O<sub>4</sub>, Fe<sub>2</sub>O<sub>3</sub>, and TiO<sub>2</sub> oxides have high activity for many reactions. For this reason, many studies have been carried out to prepare gold nanoparticles on the surface of metal oxides and zeolites for various reactions (Janssens et al. 2006).

A number of nanogold catalysts were prepared by depositing gold on different metal oxides, using the homogeneous deposition precipitation (HDP) technique. These catalysts have showed a high active for oxidation of CO. For instance, gold supported on reducible oxides (TiO<sub>2</sub>, CeO<sub>2</sub>, Fe<sub>2</sub>O<sub>3</sub>, Co<sub>3</sub>O<sub>4</sub>, and MnO<sub>x</sub>) is generally considered to be more active and stable than that supported on nonreducible oxides (SiO<sub>2</sub>, Al<sub>2</sub>O<sub>3</sub>) (Wang et al. 2009).

Nanoparticles of Au adhered onto oxide surface can also be used to catalyze the water–gas shift to produce hydrogen from CO and steam (Thompson 2007). The process goes according to reaction:



Au catalysts have received a lot of attention for CO oxidation in hydrogen systems. This phenomenon can be used for the preparation of gas sensors. Gas sensors based on nanoparticulate Au have therefore been developed for detecting a number of gasses, including CO and NO<sub>x</sub>.

A high catalytic activity of gold nanoparticles can be used in propylene epoxidation (Haruta and Date 2001). Propylene oxide is used for producing polyurethane and polyols. The current industrial process needs two-stage chemical reactions using either Cl<sub>2</sub> or organic peroxides, yielding byproducts. Using Au catalysts, it is possible to produce polypropylene in one stage with byproducts other than H<sub>2</sub>O. However, there are three factors which must be realized for the direct epoxidation of propylene. The first one is the preparation of the catalyst. Only the DP method gives the epoxidation with the process recovery up to 90%. During the catalyst

preparation, strong contact of Au particles with  $\text{TiO}_2$  support gives long distance between gold particles on the support surface. The second condition is the appropriate selection of support materials. It must be  $\text{TiO}_2$  with a crystalline structure of anatase. The third one is the size distribution of gold nanoparticles.

Au/oxide catalysts are useful systems in catalytical hydrogenation of unsaturated hydrocarbon (Haruta and Date 2001). A characteristic feature of gold catalysts is that hydrogenation process runs very selectively. Butadiene was converted to butanes and acetylene was converted to ethylene.

Gluconic acid is useful as a food additive. It is industrially produced by fermentation. However, the enzymatic reaction rate is slow. A new route which can improve the glucose oxidation process is an application of heterogeneous catalysts. Glucose oxidation process using gold catalysts has been investigated by several research teams (Corma and Garcia 2008). Mainly, Au nanoparticles supported on metal oxide like  $\text{Al}_2\text{O}_3$  were used as catalysts. These catalysts showed a high stability. It is supported by the observation that catalytic activity of nanoparticles does not significantly decrease after 18 batches of glucose oxidation.

The catalytic hydrogenation of  $\alpha$ ,  $\beta$ -unsaturated aldehydes gives allylic alcohol. This reaction is an important step in the industrial synthesis of fine chemicals, particularly of pharmaceuticals and cosmetics (Schimpf et al. 2002). The experimental data showed that catalytic activity and selectivity to the desired allyl alcohol are increased with increasing gold particle size. It was explained by electronic and geometrical effects.

Carbon materials have also been used as supports for gold nanoparticles (Okatsu et al. 2009). Carbon materials are electrically conductive and stable in both acidic and basic environments. They are combustible enough to allow the recovery of catalytic gold. Gold catalysts were prepared by using Au precursors with amounts corresponding to a theoretical Au loading of 1.0 wt% with respect to the weight of carbon support. The deposition reduction method was used for gold nanoparticles with diameters below 10 nm deposited on porous carbon support. It was observed that metal time yield (MTY),  $(\text{mol}_{\text{Glucose}}/\text{mol}_{\text{Au}}/\text{s})$  increases sharply as the diameter of gold nanoparticles becomes smaller than 10 nm. However, the reaction orders with respect to glucose were much longer over Au/carbon catalysts than over Au/metal oxide catalysts.

Photocatalytic degradation of organic pollutants using gold nanoparticles has been extensively investigated to solve environmental problems (Tian et al. 2008). Semiconductors such as ZnO and  $\text{TiO}_2$  have been recognized to be preferable support materials. Deposition of noble metal nanoparticles has enhanced the photocatalytic activity. It has been confirmed that the catalytic properties of Au/oxide catalyst depend significantly on the size of Au particles. Gold loaded on  $\text{TiO}_2$  (Au/ $\text{TiO}_2$ ) catalysts was prepared using Au(I)-thiosulfate complex  $\text{Au}(\text{S}_2\text{O}_3)_2^{3-}$  as the gold precursor for the first time. The diameter of Au nanoparticles was from 1.8 to 3.0 nm. The photocatalytic activity of Au/ $\text{TiO}_2$  catalysts was evaluated from the analysis of the photodegradation of methyl orange (Wu and Teng 2006).

## 10.5 Utilization of Gold Nanoparticles in Biomedical Applications

Gold nanoparticles have numerous promising applications in nanomedicine field. These applications include biosensing, bioimaging, bioassay, and targeted drug and gene delivery. The idea of multifunctional nanoparticles for drug delivery is presented in Fig. 10.6.

Gold nanoparticles are used to produce thermal tumor ablation and new therapeutic agents. Also, gold nanoparticle can be used for the detection of an antigen in conjugation with an antibody. Most of these applications use the unique optical properties of gold nanoparticles such as SPR, photoluminescence, surface-enhanced Raman scattering (SERS) effect.

The phenomenon of plasmon resonance can be observed for gold nanoparticles with 3 nm diameter. An enhanced electromagnetic field appears at the surface of gold nanoparticles. As a result of the enhanced electromagnetic field, absorption and scattering properties of gold nanoparticles are changed. For spherical gold nanoparticles of 5 nm diameter, the absorption bend is located at 520 nm. It was shown that the magnitude of light scattering by an 80-nm gold nanoparticle is five orders higher than light emission from strong fluorescing dyes. This is a basis of gold nanoparticles use for biological labeling, detection, and diagnostic (Schultz 2003; Jain et al. 2006).

Gold nanoparticles with a well-controlled size are suitable for a colorimetric indicator because the color can be changed in terms of SPR, which is strongly influenced by the particle size and agglomeration. The specific color of the scattered

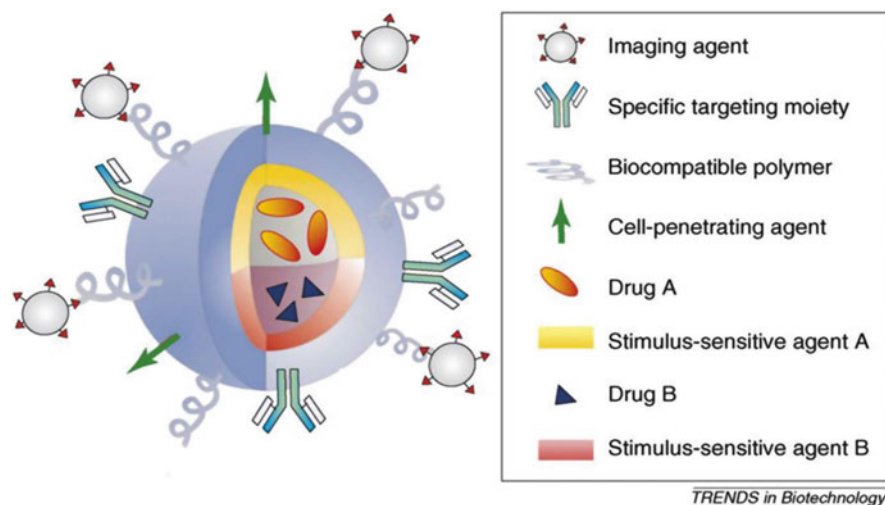


**Fig. 10.6** Diverse application of gold nanoparticles in human therapy from (Ghosh et al. 2008). *GNP* gold nanoparticles

light is also a function of the size, shape, and material properties of the particle. For instance, the agglomeration of gold nanoparticles caused a red shift and a broadening of the surface plasmon absorption peak (Son et al. 2007).

The surface enhancement of the Raman scattering technique is based on the observation of some bands in the Raman spectra of molecules adsorbed on specially prepared gold specimens gives a possibility for the surface complex determination. This increase is nine orders higher than traditionally measured factors. Such an enhancement makes possible the detection of a single molecule (Nie and Emory 1997).

There are three distinct ways of using the light scattering for biological diagnostic application. The detection of trace amounts of biomolecules, critical for early imaging and diagnosis of cancer, will be facilitated by the imaging molecule-dense gold nanoparticles.

For cancer therapy, selective delivery and targeting of nanoparticles to tumors is a key to overcome the problems of toxicity and to increase therapeutic effects. For tumor-selective delivery of gold, nanoparticles–antigens hybrid on tumor cells must be used (Cai et al. 2009). Tumor antigens include growth factors and their receptors, hormones, and glycoconjugates. Antibodies conjugated with gold nanoparticles were fabricated through modifying gold nanoparticles by cysteamine and conjugating the amine-functional group with an antibody. Conjugation of antibody onto gold nanoparticle surface induced the increase in average diameter of nanoparticles.

It is obvious that most biomedical applications of gold nanoparticles and nanorods are based on the gold conjugates. Gold nanoparticle contains hundreds to thousands of surface active gold atoms that are able to connect through the Au–S dative bond oligonucleotides, antibodies, peptides, and carbohydrates. Such nanostructures are called bioconjugates (Khlebtsov et al. 2006; Khlebtsov and Dykman 2010).

A variety of traditional and modern techniques including (1) fluorescence microscopy, (2) photothermal coherence tomography, (3) multiphoton microscopy, (4) X-ray scattering, and (5)  $\gamma$  radiation have been used by photodiagnostic. The photodiagnostic is based on the color changes resulting from the formation of a network (aggregation) of gold nanoparticles. Using these techniques, it is possible to detect RNA, protein and antibodies, as well as molecules and metal ions.

Nowadays, the cancer diagnosis using current optical imaging technologies such as optical coherence tomography (OCT) and reflectance confocal microscopy (RCM) is based on the imaging of microanatomical features of diseased tissue (Jain et al. 2007).

An important application of gold nanoparticles in the biomedical field is for photothermal therapy. Gold nanoparticles are much more efficient photon-thermal energy converters than typical organic dye molecules. The absorption band was four to five orders of magnitude greater than those of photothermal dyes. The irradiation by laser beam of the gold nanoparticles causes the absorption and conversion of photon energy into thermal energy. As a result, the local temperature of gold nanoparticles dramatically increases. The dramatic temperature increase can cause a sudden release of heat to the surrounding environment. It can be used for photothermal destruction of cancer cells.

A thermal therapy causes necrosis of the cells through lysis and rupture of membranes and release of digestive enzymes. Recently, gold-coated silica nano-shells with a tunable absorption in the near infrared region have been used as both imaging and therapy agents (El-Sayed et al. 2006).

To analyze the paths of gold nanoparticles in the breast cancer cell, cells were first grown in dishes and incubated for 30 min with gold nanoparticles. Gold nanoparticles were coated with biopolymers (BSA) and conjugated to Alexo-647 fluorescent dye. The dish with bacteria was placed in a microscope. Gold nanoparticles were localized only in either endosomes or lysosomes (Chithrani et al. 2009).

The TEM image showed that gold nanoparticles were with mean diameters of 14.2 nm. The surface of the gold nanoparticles was modified with BSA to determine the effect of protein coating on their cellular uptake and processing. It was observed that cellular uptake of gold nanoparticles was dependent on both their size and surface coating. Gold nanoparticles with a diameter of 50 nm had the greatest degree of cellular uptake. In addition, uncoated gold nanoparticles showed a higher uptake as compared with gold nanoparticles coated with any of the proteins. The kinetic study showed that the fraction of gold nanoparticles in lysosomes increases with time.

## 10.6 Antibacterial Activity of Drug-Coated Gold Nanoparticles

The antibacterial activities of drugs-capped gold nanoparticles were investigated against strains of Gram-positive and Gram-negative microorganisms. Various strains of Gram-positive and Gram-negative bacteria like *Micrococcus luteus*, *Staphylococcus aureus*, *Pseudomonas aeruginosa*, and *Escherichia coli* were chosen to probe the antibacterial efficacy of antibiotics-coated gold nanoparticles (Grace and Pandian 2007). The predominant antimicrobial activity of gold nanoparticles can be attributed to the strong cytotoxicity to various bacteria cells. Gold nanoparticles interact with the functional groups on the bacteria cell surface and inactivate bacteria.

Gold nanoparticles can be used as a probe for the detection of various aminoglycosidic antibiotics like streptomycin, gentamicin, and neomycin. The antibacterial activity of drugs-capped Au nanoparticles (Au@drugs) was investigated against various strains of Gram-positive and Gram-negative bacteria, such as *S. aureus*, *M. luteus*, *E. coli*, and *P. aeruginosa*.

The antibacterial efficiencies of gold nanoparticles conjugated with ampicillin, streptomycin, and kanamycin were investigated (Saha et al. 2007). Obtained results suggest that antibiotic nonconjugated with gold nanoparticles might be used in therapy for their great efficiency and stability. Consist with this the antibacterial action of gentamicin and mixture of gentamicin and gold nanoparticles on *E. coli* was examined (Burygin et al. 2009). The mechanism of gentamicin action is linked to disruption of ribosomal synthesis of protein. The obtained results showed that the

**Table 10.3** Antibacterial and antifungal activity of 5FU coated gold nanoparticles from Selvaraj and Alagar (2007)

Microorganisms	Nature of bacteria	Levels of zone of inhibition	
		Pure 5FU	Au@5FU
<i>M. luteus</i>	Gram-positive	19	27
<i>S. aureus</i>	Gram-positive	20	31
<i>P. aeruginosa</i>	Gram-negative	23	35
<i>E. coli</i>	Gram-negative	27	43
<i>A. fumigatus</i>		23	32
<i>A. niger</i>		19	29

difference between pure gentamicin and its mixture with gold nanoparticles was not significant. It may suggest that the conjugation between gold nanoparticle and antibiotic was not stable and the amount of antibiotic was unsuitable. Additionally, the mechanism of interaction between gold nanoparticles and the constituents of the outer membrane of bacteria cells is still unanswered. It can be supposed that the gold particles cause structural changes, degradation, and finally cell death.

The anticancer drug 5-fluorouracil (5FU) and colloidal gold complex (Au@5FU) were observed to have appreciable antibacterial and antifungal activity against *M. luteus*, *S. aureus*, *P. aeruginosa*, *E. coli*, *Aspergillus fumigatus*, and *Aspergillus niger* (Selvaraj and Alagar 2007). The growth inhibition effect by both pure anticancer drug and drug-coated gold nanoparticles against both bacteria and fungal organisms is presented in Table 10.3.

The conclusion from the presented data is the combination of gold nanoparticles with drug 5FU results in a strong inhibition effect.

Hyperbranched PAMAM served as both the reductant and stabilizer to prepare the antibacterial gold and silver nanoparticles (Zhang et al. 2008). The nanoparticles size could be controlled by adjusting the molar ratio of N/Au or N/Ag in the feed. The antimicrobial activity of colloid composites was searched against a wide range of Gram-positive and Gram-negative bacteria, and fungi. The high antibacterial activity can be described as a summation of the effect of metallic nanoparticles and an effect of PAMAM.

## 10.7 Gold Nanoparticles as Carriers for Drug and Gene Delivery Application

Gold nanocarriers provided a new group of target-specific deliveries of therapeutic agents. The therapeutic agent could be small drug molecules or large biomolecules, such as DNA, RNA, and proteins. The gold nanoparticles are essentially inert and nontoxic. They are able to penetrate the cell to facilitate cellular internalization and connective tissue permeation, thus enabling the drugs to be delivered efficiently to the targeted cell without clogging capillaries. A second advantage is that gold particles are easy to synthesize.

There are two main categories of drug delivery systems. The first group consists of the capsulation. The capsulation has an ability to contain a relatively large amount of drug within the capsule. The second group of drug delivery systems involves the attachment of the drugs to the carriers. Multifunctional delivery nanosystems are presented in Fig. 10.7.

Targeting of drugs is a central goal of the delivery system. One way to achieve it could be the conjugation of the drug delivery particle with a ligand that specifically recognizes the target (cell). The special protein can be employed as a targeting ligand (Han et al. 2007).

Gold nanoparticles are frequently used as carriers as they are inert and nontoxic. The monodisperse gold nanoparticles with the size range from 1.5 to 15 nm can form the core. It was recognized that the accumulation of gold nanoparticles in various tissues was found to be dependent on particle size. Smaller size, 15 nm gold nanoparticles showed higher distribution in tissues compared to larger particles (Sonavane et al. 2008).

The gold nanoparticle surface has a strong binding affinity towards thiols, disulfides, and amines. The most popular technology is based on using the thiolate intermediate linkers such as  $\text{HS}(\text{CH}_2)_n\text{R}$  ( $\text{R}=\text{COOH}$ ,  $\text{OH}$  or  $\text{SO}_3\text{H}$ ) or directly the thiol-functionalized biomolecules. In particular, the simple gold-thiol group allows

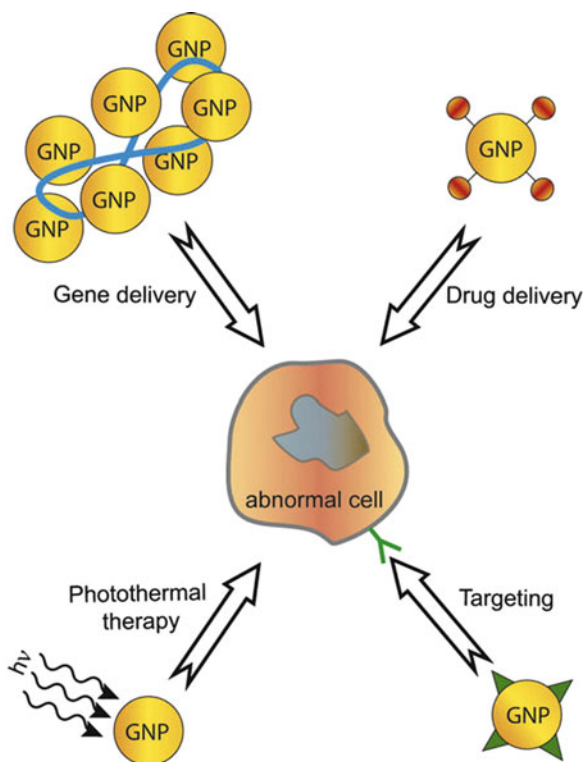


**Fig. 10.7** Multifunctional nanoparticle or nanocapsule for drug delivery from Sanvicens and Marco (2008)

the surface conjugation of various peptides, proteins, and DNA. Oligonucleotides with alkanethiol functional groups as anchors were bound to the surface of 16 nm diameter gold particles and the resulting labels were created. The substitution of thiolate ligands (RS) by functional thiolates (R'SH) can be described by following equation:



Oligonucleotides, peptides, and polyethylene glycol are easily attached to gold nanoparticles (AuNP) in this way.

Thanks to advances in molecular biology and genomic research for numerous diseases, such as sickle-cell anemia, HIV, Parkinson's disease, Huntington's disease, and Alzheimer's disease we have found a genetic identity. In consequence, a responsive gene therapy may be prescribed. In consequence, gene therapy can be used for the treatment or prevention of these diseases.

Gold nanoparticles are attractive candidates for gene delivery. Gene delivery accelerates the results when DNA is transported inside the cell nucleus of the target cell. Gold nanoparticles were synthesized by reduction of tetrachloroauric acid with sodium citrate as described by Turkewich with certain modifications (Ghosh et al. 2008). The results of initial studies showed that the cellular uptake of gold nanoparticles is dependent on the size and surface properties. The size and shape of gold nanoparticles can be tailored to the range between 2 and 10 nm. Gold nanoparticle showed negative zeta potential ( $-22 \pm 1.8$ ;  $-20 \pm 2.1$ ;  $-16 \pm 3.1$  mV). An increase in particle size showed a slight decrease in zeta potential (Chithrani et al. 2009).

The size and charge of DNA is the major limiting factor in its low transfer into the nucleus. DNA is highly negatively charged and for better gene transfer, its charge is neutralized using either cations or cationic polymers. The addition of this reagent causes a collapse of the DNA molecules. It is referred to as "counterion condensed" DNA (Labhasetwar 2005). The condensed DNA is more stable in the body.

In reality, gold nanoparticles functionalized with cationic quaternary ammonium groups bind plasmid DNA through electrostatic interactions and protect DNA from enzymatic digestion. These electrostatic DNA–nanoparticle conjugates provide an effective means of gene delivery in the cell.

It is known that gold combines firmly with biomolecules possessing sulfur (thiol) groups, such as mercapto groups, via Au–S bond. Nucleic acid can be easily modified with thiols group. Upon immersion of a clean gold surface in a solution of thiol-derivatized oligonucleotides, the sulfur adsorbs onto the gold surface forming a single layer of molecules, where the hydrocarbon is now replaced with DNA. Chemisorption of thiolated DNA leads to surface coverage of about  $10^{13}$  molecules/cm<sup>2</sup> (Bashir 2001). Recently, cationic gold nanoparticles modified by 2-aminoethanethiol have been used as a gene delivery system (Kawano et al. 2006). In general, polycationic compounds are used for condensing DNA and transporting it inside the cell.



Gold nanoparticles can also be used as a template for transport of an animal virus, prevented by a protein layer (Goicochea et al. 2007). Preparation of such gold with alphavirus particles require a two-step procedure: first the virus is assembled on gold templates, second the addition of the membrane layer. Plant viruses and bacteriophages have been proposed for diagnostic imaging because of their low toxicity even at high doses.

Magnetic nanoparticles have been attractive materials in biology and biomedicine because they can interact with or bind to biomolecules such as proteins, antibodies, DNA, or RNA (Kinoshita et al. 2007). The immobilization of gold nanoparticles onto the surface of magnetic iron oxide nanoparticles caused such composites to exhibit a magnetic property. Gold nanoparticles combine firmly with biomolecules possessing sulfur groups. Created aggregates enclosing DNA, gold nanoparticle, and magnetic support can be magnetically separated.

## 10.8 Conclusion

Production of gold nanoparticles has opened up novel technological application in various fields. Now, the commercial exploration period has entered the field of gold nanoparticles. The unique size-dependent properties of gold nanoparticles make this material important in many areas of human activity. The main target of gold nanoparticles is for their application in catalysts, medicines, nanosensors, and nanoelectronics.

The unique optical and chemical properties of gold nanoparticles have attracted much attention in the field of intelligent medical technology. Gold nanoparticles were applied to the medical field including tumor imaging, photothermal therapy, and gene and drug delivery. The photothermal effect, whereby absorbed light by gold particles is converted to the heat, is used for photothermal therapy. The heat produced by the photothermal effect can destroy the cellular function of the cell and caused cell death. This finding might be utilized in cancer therapies.

The gold nanoparticles are already appearing in pharmacy as novel tools for drug delivery formulation. Nanomedicines can be dramatically changed both medical treatment and cancer therapies. One limitation of the drug delivery systems is that the volume of drug that can be carried by individual gold nanoparticle is very limited.

Gene therapy has emerged as a potentially powerful therapeutic platform. The results indicate that the E gene leads to the death of tumor cells. Gold nanoparticles provide attractive candidates for gene delivery. A more sophisticated approach is to modify the surface of gold nanoparticles by the addition of either an antibody or ligands with affinity for the desired target. These involve coating the gold nanoparticles with a self-assembled layer of a thiolated PEG (poly-ethyleneglycol) or liposome. Gold nanoparticles offer a new method of tumor targeting. It may raise the potential application of these gold nanoparticles in the relative biomedical and bioengineering areas.

The remarkable catalytic activity of Au nanoparticles has been observed for heterogeneous catalysis. A key issue of this heterogeneous catalysis is the interaction between Au nanoparticles and their support material. The special catalytic properties of supported gold nanoparticles depend upon the particle morphology. Highly dispersed Au/TiO<sub>2</sub> catalysts exhibited high catalytic activity in CO oxidation at low temperature. Defect sites on the oxide support play an important role in the CO oxidation in these conditions. Generally, gold nanocomposites are expected to find potential applications as catalysts and antibacterial agents.

**Acknowledgments** This work was supported by MNiSzW Grant # NN 204 290134.

## References

- Agbenyega J (2008) Water soluble gold: biomaterials. *Mater Today* 11:13
- Aslan K, Zhang J, Lakowicz RJ, Geddes DC (2004) Saccharide sensing using gold and silver nanoparticles: a review. *J Fluorescence* 14:391–400
- Azzazy HME, Mansour MHM (2009) *In vitro* diagnostic properties of nanoparticles. *Clin Chem Acta* 403:1–8
- Bashir R (2001) DNA nanobiostuctures. *Mater Today* 4:30–39
- Beermann B, Carrillo-Nava E, Scheffer A, Buscher B, Jawalekar MA, Seela F, Hinz H-J (2007) Association temperature governs structure and apparent thermodynamics of DNA-gold nanoparticles. *Biophys Chem* 126:124–131
- Burygin LG, Khlebtsov NB, Shantrokha NA, Dykman AL, Bagatyrev AV, Khlebtsov GN (2009) On the enhanced antibacterial activity of antibiotics mixed with gold nanoparticles. *Nanoscale Res Lett* 4:794–801
- Cai H-H, Yang P-H, Cai J (2009) Immunoassay detection using functionalized nanoparticle probes coupled with resonance Rayleigh scattering. *Sens Actuators B: Chem* 135:603–609
- Cao CY, Jin R, Thaxton SC, Mirkin AC (2005) A two-color-change, nanoparticle-based method for DNA determination. *Talanta* 67:449–455
- Cha S-H, Kim K-H, Lee W-K, Lee JC (2009) Preparation of gold microparticles using halide ions in bulk block copolymers phases via photoreduction. *J Solid State Chem* 182:1575–1580
- Chen SM, Goodman WD (2006) Structure-activity relationships in supported Au catalysts. *Catal Today* 111:22–33
- Chen X-Y, Li J-R, Li X-C, Jiang L (1998) A new step to the mechanism of the enhancement effect of gold nanoparticles on glucose oxidase. *Biochem Biophys Res Commun* 245:352–355
- Chen S, Guo C, Liu H-Z, Liang X-F, Wang J, Me J-H, Zheng L (2007) Dissipative particle dynamics simulation of gold nanoparticles stabilization by PEO-PPO-PEO block copolymer micelles. *Colloid Polym Sci* 285:1543–1552
- Chithrani DB, Stewart J, Allen C, Jaffray AD (2009) Intracellular uptake, transport, and processing of nanostructures in cancer cells. *Nanomedicine* 5:118–127
- Corma A, Garcia H (2008) Supported gold nanoparticles as catalysts for organic reactions. *Chem Soc Rev* 37:2096–2126
- des Rieux A, Fievez V, Garinot M, Schneider Y-J, Preat V (2006) Nanoparticles as potential oral delivery systems of proteins and vaccines: a mechanistic approach. *J Control Release* 116:1–27
- Du Y, Luo X-L, Xu J-J, Chen H-Y (2007) A simple method to fabrication a chitosan-gold nanoparticles film and its application in glucose biosensor. *Bioelectrochemistry* 70:432–347
- Du B, Zhao B, Tao P, Yin K, Lei P, Wang Q (2008) Amphiphilic multiblock copolymer stabilized Au nanoparticles. *Colloids Surf A: Physicochem Eng Asp* 317:194–205
- El-Sayed HI, Huang X, El-Sayed AM (2006) Selective laser photo-thermal therapy of epithelial carcinoma using anti-EGFR antibody conjugated gold nanoparticles. *Cancer Lett* 239:129–135

- Ferrero S, Piednoir A, Henry RC (2001) Atomic scale imaging by UHV-AFM of nanosized gold particles on mica. *Nano Lett* 1:227–230
- Ghosh P, Han G, De M, Kim KC, Rotello MV (2008) Gold nanoparticles in delivery applications. *Adv Drug Deliv Rev* 60:1307–1315
- Goicochea LN, De M, Rotello MV, Mukhopadhyay S, Dragnea B (2007) Core-like particles of an enveloped animal virus can self-assemble efficiently on artificial templates. *Nano Lett* 7: 2281–2290
- Grace NG, Pandian K (2007) Antibacterial efficacy of aminoglycosidic antibiotics protected gold nanoparticles – a brief study. *Colloids Surf A: Physicochem Eng Asp* 297:63–70
- Guo S, Wang E (2007) Synthesis and electrochemical application of gold nanoparticles. *Anal Chem Acta* 598:181–192
- Han G, Ghosh P, De M, Rotello MV (2007) Drug and gene delivery using gold nanoparticles. *Nanobiotechnology* 3:40–45
- Haruta M, Date M (2001) Advances in the catalysis of Au nanoparticles. *Appl Catal A* 222: 427–437
- Haruta M, Tanaka K, Ueda A, Torres Sanchez MR (1997) Selective oxidation of CO in hydrogen over gold supported on manganese oxide. *J Catal* 168:125–127
- Hiraiwa D, Yashimura T, Esumi K (2006) Interaction forces between poly(amidoamine) PAMAM dendrimers adsorbed on gold surfaces. *J Colloid Interface Sci* 298:982–986
- Huo Q (2007) A perspective on bioconjugated nanoparticles and quantum dots. *Colloids Surf B: Biointerfaces* 50:1–10
- Jain KP, Lee SK S, El-Sayed HI, El-Sayed AM (2006) Calculated absorption and scattering properties of gold nanoparticles of different size, shape, and composition: applications in biological imaging and biomedicine. *J Phys Chem B* 110:7238–7248
- Jain KP, El-Sayed HI, El-Sayed AM (2007) Au nanoparticles target cancer. *Nanotoday* 2:18–29
- Janssens WVT, Carlsson A, Puig-Molina A, Clause SB (2006) Relation between nanoscale Au particle structure and activity for CO oxidation on supported gold catalysts. *J Catal* 240:108–113
- Jiang G, Wang L, Chen W (2007) Studies on the preparation and characterization of gold nanoparticles protected by dendrons. *Mater Lett* 61:278–283
- Kawano T, Yamagata M, Takahashi H, Niidome Y, Yamada S, Katayama Y, Niidome T (2006) Stabilizing of plasmid DNA in vivo by PEG-Modified cationic gold nanoparticles and the gene expression assisted with electrical pulses. *J Control Release* 111:382–389
- Khlebtsov GN, Dykman AL (2010) Optical properties and biomedical applications of plasmonic nanoparticles. *J Quant Spectrosc Radiact Transf* 111:1–35
- Khlebtsov B, Zharov V, Melnikov A, Tuchin V, Khlebtsov N (2006) Optical amplification of photothermal therapy with gold nanoparticles and nanoclusters. *Nanotechnology* 17: 5167–5179
- Kim JH, An HH, Kim HS, Kim HY, Yoon SC (2009) Direct deposition of size-tunable Au nanoparticles on silicon oxide nanowires. *J Colloid Interface Sci* 337:289–293
- Kinoshita T, Seino S, Mizukoshi Y, Nakagawa T, Yamamoto AT (2007) Functionalization of magnetic gold/iron-oxide composite nanoparticles with oligonucleotides and magnetic separation of specific target. *J Magn Magn Mater* 331:255–258
- Labhasetwar V (2005) Nanotechnology for drug and gene therapy: the importance of understanding molecular mechanisms of delivery. *Curr Opin Biotechnol* 16:674–680
- Li D, He Q, Li J (2009) Smart core/shell nanocomposites: intelligent polymers modified gold nanoparticles. *Adv Colloid Interface Sci* 149:28–38
- Liu T, Tang J, Jiang L (2002) Sensitivity enhancement of DNA sensors by nanogold surface modifications. *Biochem Biophys Res Commun* 295:14–16
- Luo Y (2007) Size-controlled preparation of polyelectrolyte-protected gold nanoparticles by natural sunlight radiation. *Mater Lett* 61:2164–2166
- Luo X-L, Xu J-J, Du Y, Chen H-Y H-Y (2004) A glucose biosensor based on chitosan-glucose oxidase-gold nanoparticles biocomposite formed by one step electrodeposition. *Anal Biochem* 334:284–289

- Molina ML, Hammer B (2005) Some recent theoretical advances in the understanding of the catalytic activity of Au. *Appl Catal A: General* 291:21–31
- Moroz LB, Pyrjaev AP, Zaikovskii IV, Bukhtiyarov IV (2009) Nanodispersed Au/Al<sub>2</sub>O<sub>3</sub> catalysts for low-temperature CO oxidation: Results of research activity at the Borekov Institute of Catalysis. *Catal Today* 144:292–305
- Nie S, Emory RS (1997) Probing single molecules and single nanoparticles by surface-enhanced Raman scattering. *Science* 275:1102–1108
- Okatsu H, Kinoshita N, Akita IT, Haruta M (2009) Deposition of gold nanoparticles on carbons for aerobic glucose oxidation. *Appl Catal A: General* 369:8–14
- Pan B, Gao F, Ao L, Tian H, He R, Cui D (2005) Controlled self-assembly of thiol-terminated poly (amidoamine) dendrimer and gold nanoparticles. *Colloids Surf A: Physicochem Eng Asp* 259: 89–94
- Park H-S, Oh G-S, Mun Y-J, Han S-S (2006) Loading of gold nanoparticles inside the DPPC bilayers of liposome and their effects on membrane fluidities. *Colloids Surf B: Biointerface* 48:112–118
- Pietsch T, Appelhans D, Gindy N, Voit B, Fahmi A (2009) Oligosaccharide-modified dendrimers for templating gold nanoparticles: Tailoring the particle size as a function of dendrimer generation and – molecular structure. *Colloids Surf A Physicochem Eng Asp* 341:93–102
- Ramanaviciene A, Nastajute G, Snitka V, Kausaite A, German N, Barauskas-Memenas D (2009) Spectrophotometric evaluation of gold nanoparticles as red-ox mediator for glucose oxidase. *Sensors Actuators B* 137:483–489
- Sadowski Z (2010) Biosynthesis and application of silver and gold nanoparticles. In: David Pozo Perez (ed) *Silver nanoparticles*. INTECH Education and Publishing KG, Vienna, pp 334–354
- Saha B, Bhattacharya J, Mukherjee A, Santra GAK, RC DKA, Karmakar P (2007) In vitro structural and functional evaluation of gold nanoparticles conjugated antibiotics. *Nanoscale Res Lett* 2:614–622
- Sanvicens N, Marco PM (2008) Multifunctional nanoparticles – properties and prospects for their use in human medicine. *Trends Biotechnol* 26:425–433
- Schimpf S, Lucas M, Mohr C, Rodemerck U, Bruckner A, Radnik J, Hofmeister H, Claus P (2002) Supported gold nanoparticles: in-depth catalyst characterization and application in hydrogenation and oxidation reactions. *Catal Today* 72:63–78
- Schultz AD (2003) Plasmon resonant particles for biological detection. *Curr Opin Biotechnol* 14:13–22
- Selvaraj V, Alagar M (2007) Analytical detection and biological assay of antileukemic drug 5-fluorouracil using gold nanoparticles as probe. *Int J Pharmaceutics* 337:275–281
- Shi X, Ganser RT, Sun K, Balogh PL (2006) Characterization of crystalline dendrimer-stabilized gold nanoparticles. *Nanotechnology* 17:1072–1078
- Son JS, Bai X, Lee BS (2007) Inorganic hollow nanoparticles in nanomedicine. Part 2: Imaging, diagnostic, and therapeutic applications. *Drug Discov Today* 12:657–663
- Sonavane G, Tomoda K, Makino K (2008) Biodistribution of colloidal gold nanoparticles after intravenous administration: Effect of particle size. *Colloids Surf B: Biointerfaces* 66:274–280
- Sow CH, Wee STA (2009) Chemically Linked AuNP-Alkane network for enhanced photoemission and field emission. *ACS Nano* 3:2722–2730
- Sperling AR, Gil RP, Zhang F, Zanella M, Parak JW (2008) Biological application of gold nanoparticles. *Chem Soc Rev* 37:1896–1908
- Steinbruck A, Csaki A, Ritter K, Leich M, Kohler JM, Fritzsche W (2009) Gold and gold-silver core-shell nanoparticle constructions with defined size based on DAN hybridization. *J Nanopart Res* 11:623–633
- Tang T, Krysmann JM, Hamley WI (2008) In situ formation of gold nanoparticles with a thermoresponsive block copolymer corona. *Colloids Surf A: Physicochem Eng Asp* 317: 764–767
- Thompson TD (2007) Using gold nanoparticles for catalysis. *Nano Today* 2:40–43

- Tian B, Zhang J, Tong T, Chen F (2008) Precipitation of Au/Ag catalysts from Au(I)-thiosulfate complex and study of their photocatalytic activity for the degradation of methyl orange. *Appl Catal B: Environmental* 79:394–401
- Tsai C-Y, Chang L-T, Chen C-C, Ko F-H, Chen P-H (2005) An ultra sensitive DNA detection by using gold nanoparticles multilayer in nano-gap electrodes. *Microelectronic Eng* 78–79: 546–555
- Wang L-C, Liu O, Huang X-S, Liu Y-M, Cao Y, Fan K-N (2009) Gold nanoparticles supported on manganese oxides for low-temperature CO oxidation. *Appl Catal B: Environmental* 88: 204–212
- Welch MC, Compton GR (2006) The use of nanoparticles in electroanalysis: a review. *Anal Bioanal Chem* 384:601–619
- Willner I, Willner B, Katz E (2002) Functional biosensor systems via surface-nanoengineering of electronic elements. *Rev Mol Biotechnol* 82:325–355
- Wilson R (2008) The used of gold nanoparticles in diagnostics and detection. *Chem Soc Rev* 37:2028–2045
- Wu J-J, Teng C-H (2006) Photocatalytic properties of nc-Au/ZnO nanorod composites. *Appl Catal B: Environmental* 66:51–57
- Zhang Z, Wang F, Chen F, Shi G (2006) Preparation of polythiophene coated gold nanoparticles. *Mater Lett* 60:1039–1042
- Zhang Y, Peng H, Huang W, Zhou Y, Yan D (2008) Facile preparation and characterization of highly antimicrobial colloid Ag or Au nanoparticles. *J Colloid Interface Sci* 325:371–376

# Chapter 11

## Biogenic Silver Nanoparticles: Application in Medicines and Textiles and Their Health Implications

Priscyla D. Marcato and Nelson Durán

### 11.1 Introduction

In today's nanobiotechnology one of the most exciting research topics is the formation of nanoparticles by biological systems. Fungi, bacteria, yeasts, actinomycetes and plants have inherent capacity to reduce metals through their specific metabolic pathways (Ahmad et al. 2003; Kowshik et al. 2003; Durán et al. 2005; Ankanwar et al. 2005; Harris and Bali 2008; Sintubin et al. 2009).

Different types of nanomaterials like copper, zinc, titanium, magnesium, gold and silver have arising as antimicrobial materials, especially silver nanoparticles that are more efficient. These materials exhibit antimicrobial activity against bacteria, viruses and other eukaryotic microorganisms (Rai et al. 2009).

The actual mechanism of formation, for instance, of silver nanoparticles, in all of these microorganisms and plants, is still an open question, even though much research has been attempted to find different ways to investigate the possible mechanisms (Durán et al. 2005; Rai et al. 2009; Durán et al. 2009, 2010a). Similar aspects occurred with the antibacterial activity of silver nanoparticles. One such aspect proven for silver nanoparticles is that for antibacterial activity, size, morphology and concentrations are all important. For example, small particles have larger surface areas to be in contact with the bacterial cells, showing a larger activity (Baker et al. 2005). The antimicrobial efficacy of the nanoparticles also

---

P.D. Marcato

Chemistry Institute, Biological Chemistry Laboratory, Universidade Estadual de Campinas, C.P. 6154, CEP 13083-970 Campinas, São Paulo, Brazil  
e-mail: pmarcato@gmail.com

N. Durán (✉)

Chemistry Institute, Biological Chemistry Laboratory, Universidade Estadual de Campinas, C.P. 6154, CEP 13083-970 Campinas, São Paulo, Brazil

and

Natural Science and Humanity Center, Universidade Federal de ABC, Santo Andre CEP 09.210-170, São Paulo, Brazil  
e-mail: duran@iqm.unicamp.br

**Table 11.1** Antibacterial activities of silver nanoparticles biological and chemically synthesized

Bacteria strain	MIC (Ag–fungal) ( $\mu\text{g/mL}$ )	MIC (Ag–Chemical) ( $\mu\text{g/mL}$ )
<i>S. aureus</i> ATCC 05923	1.9	15.0
<i>S. epidermitis</i> ATCC 12228	0.9	7.5
<i>B. subtilis</i> ATCC 6633	1.9	30.0
<i>E. coli</i> ATCC 25923	1.8	30.0

depends on the shape or morphology of the nanoparticles. This can be confirmed by studying the inhibition of bacterial growth by differently shaped nanoparticles (Rai et al. 2009). Furthermore, very recently, a difference in the antimicrobial activity between biologically and chemically synthesized silver nanoparticles has been clearly demonstrated (Table 11.1) (Brocchi et al. 2010).

Due to the antimicrobial activity of silver nanoparticles, these particles have been applied to fabrics to produce sterile materials. Ilic et al. (2009) verified that cotton with 10  $\mu\text{g/mL}$  and 50  $\mu\text{g/mL}$  of silver nanoparticles exhibited antimicrobial activity against *Staphylococcus aureus*, *Escherichia coli* and *Candida albicans*. However, after 5 wash cycles the fabrics with 10  $\mu\text{g/mL}$  had released their silver nanoparticles while the fabrics with 50  $\mu\text{g/mL}$  had released 98.4% of the nanoparticles. To increase the adhesion of silver nanoparticles in the fabrics several strategies have been studied. These results showed that the amount of silver nanoparticles impregnated in the fabrics influenced its laundering durability.

Perelshtein et al. (2008) used ultrasound irradiation to synthesize and to deposit silver nanoparticles on different types of fabrics (nylon, cotton and polyester). This method increased particle adhesion and the particles were stable in the fabrics for at least 20 washing cycles.

Another possibility to enhance adhesion is fabric surface modification. Dastjerdi et al. (2009) modified a polyester surface with crosslinkable polysiloxane. In this study it was observed that the polysiloxane treatment decreased silver nanoparticle release and increased long-term microbiological properties.

Khalil-Abad et al. (2009) produced cationized cottons and thereafter impregnated these fabrics with silver nanoparticles. The silver content, analyzed by ICP, in these fabrics was much larger than in normal cotton due to the positive charge on cationized surface cotton. Furthermore, the antibacterial activity was enhanced due to the increased content of silver nanoparticles in these cationized fabrics.

A further possibility was applied using biogenic silver nanoparticles to treat fabrics. Due to the protein around the biogenic particles, these particles have stronger affinity and adhesion in fabric fibers (Marcato et al. 2010; Durán et al. 2010a, b). Other applications of silver nanoparticles are in association with antibiotics to improve their effects (Gade et al. 2008; Brocchi et al. 2010) and in wound healing (Tian et al. 2007; Maneerung et al. 2008).

In the next item different aspects related to the biogenesis of silver nanoparticles produced by fungi, and multiple applications of biogenic metal nanoparticles, synergistic antibiotic effects, their applications on textile fabrics and their potential importance in some neglected diseases will be discussed.

## 11.2 Multiple Applications of Metal Nanoparticles

There are excellent reviews, which have been published related to the biological synthesis of metallic nanoparticles and their implication in several areas (Mandal et al. 2006; Gericke and Pinches 2006; Chen and Schluesener 2008; Singh et al. 2008; Bhattacharya and Mukherjee 2008; Mohanpuria et al. 2008; Durán et al. 2008; Marcato and Durán 2008; Rai et al. 2009; Sharma et al. 2009; Kumar and Yadav 2009; Durán et al. 2009, 2010b; Thakkar et al. 2009)

Metal nanoparticles have many physicochemical and optoelectronic properties (Chandrasekharan and Kamat 2000; Krolikowska et al. 2003). Due to their diverse properties, metal nanoparticles have multiple applications in various fields like electronics, agriculture and medicine. Some of the nanoparticles that can be produced by fungi may be of particular relevance to new and emerging technologies. The use of silver coatings in solar absorption systems has already been mentioned. Other applications in such areas include the use of gold nanoparticles as precursors to coatings for electronic applications and for drug carriers (Mukherjee et al. 2001; Sugunan et al. 2007; Han et al. 2007) and platinum nanoparticles in the production of fuel cells (Riddin et al. 2006).

### 11.2.1 Antibiotic Effect of Biogenically Produced Silver Nanoparticles

Applications in the field of medicine include the formulations of many potential antimicrobial agents, which are effective against many human pathogens including multidrug-resistant bacteria (Ingle et al. 2008). Rai et al. (2009) suggested that the silver nanoparticles produced by fungi are novel and new generation of antimicrobial materials. An important aspect in this area is the synergistic effect of silver nanoparticles and antibiotics (Marcato and Durán 2008) with important application in some neglected diseases (Durán et al. 2009).

A study was carried out with clindamycin and silver nanoparticles produced chemically or biogenically (Durán et al. 2005; Marcato et al. 2005) (Fig. 11.1). After

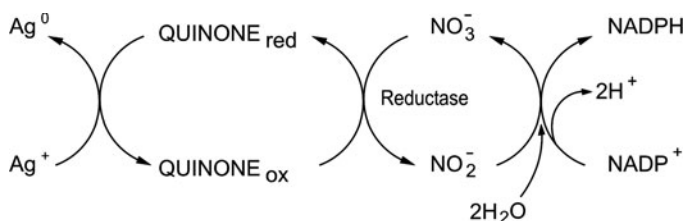


**Fig. 11.1** Diagram of the silver nanoparticles formation by fungi (Modified from Durán et al. 2005)



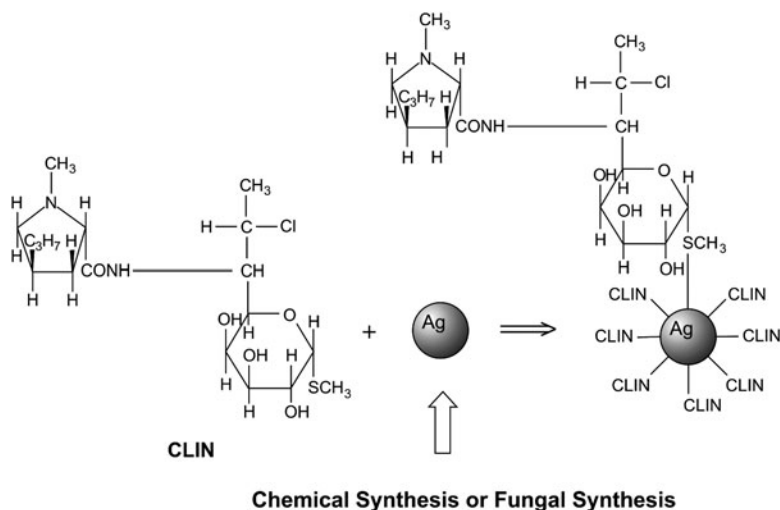


**Fig. 11.2** Structures and diagram of the complex between clindamycin and silver nanoparticles produced by chemical and biological methods (Modified from Brocchi et al. 2010)

both particle syntheses, the silver nanoparticles were chemically associated with clindamycin and purified before being used as an antibacterial compound (Fig. 11.2). Preliminary antibacterial activity experiments with two new formulations against several bacteria, such as *S. aureus* Methicillin-resistant strains (Rib1, BEC 9393) and *Staphylococcus epidermidis* strain (Ap1E) showed a significant effect. Both nanoparticles (chemical and biological) exhibited antimicrobial activity, but a slightly lower MIC values were observed with the biosynthetic nanoparticles. Furthermore, this activity depended upon the bacterial strain analyzed and also the size of the nanoparticles (Brocchi et al. 2010). This was also true for the clindamycin-associated silver nanoparticles. In addition, the biosynthetically obtained nanoparticles were more stable than the chemical ones (Durán et al. 2008; Durán et al. 2010b).

Ingle et al. (2008) have evaluated the antibacterial activity of biosynthesized silver nanoparticles produced by *Fusarium acuminatum* on different human pathogens. These authors reported efficient antibacterial activity of silver nanoparticles against multidrug resistant and highly pathogenic bacteria, such as, *S. aureus*, *S. epidermidis*, *Salmonella typhi* and *E. coli*. Silver nanoparticles showed remarkable antimicrobial effects than silver ions (1.4–1.9 folds). The maximum antibacterial activity of silver nanoparticles was against *S. aureus*, followed by *S. epidermidis*, *S. typhi* and the minimum was for *E. coli*. This result demonstrated that specific efficiency of silver nanoparticles can be related with differences due to the strain, which can be related to the bacterial membrane structure. However, it warrants further investigation.

Sadowski et al. (2008) and Maliszewska and Sadowski (2009) have studied the kinetics of extracellular synthesis of silver nanoparticles using a cell-free filtrate of

two *Penicillium* strains. The nanoparticles were evaluated for their antimicrobial activity against gram-positive and gram-negative bacteria. As results, *Bacillus cereus*, *S. aureus*, *E. coli* and *Pseudomonas aeruginosa* were effectively inhibited.

Shahverdi et al. (2007) reported the synthesis of silver nanoparticles using *Klebsiella pneumoniae*. Afterwards, these nanoparticles were associated with several antibiotics and the antimicrobial activity was evaluated against *S. aureus* and *E. coli*. The antibacterial activities of penicillin G, amoxicillin, erythromycin, clindamycin, and vancomycin were increased in the presence of silver nanoparticles against both test strains. The highest enhancing effects were observed for vancomycin, amoxicillin and penicillin G against *S. aureus*.

Thirumurugan et al. (2009) synthesized silver nanoparticles using potato pathogenic fungus *Phytophthora infestans*, evaluated its antibacterial activity by the disc diffusion method and through minimum inhibition concentrations (MIC). The silver nanoparticles exhibited discrete antibacterial activity against seven clinically isolated pathogenic bacteria (*E. coli*, *S. typhi*, *K. pneumoniae*, *Proteus vulgaris*, *Bacillus subtilis*, and *S. aureus*) at a concentration of 5 µg/ml.

Polydispersed silver nanoparticles of 5–40 nm were produced by *Trichoderma viride* and the antimicrobial activities of these particles associated with various antibiotics were evaluated against gram-positive and gram-negative bacteria (Fayaz et al. 2009). The antibacterial effects of ampicillin, kanamycin, erythromycin and chloramphenicol were increased in the presence of silver nanoparticles, and the highest enhancing effect was shown by ampicillin. This research provided helpful insight into the development of new antimicrobial agents by proposing a mechanism to explain this phenomenon (Fayaz et al. 2009). In this work the biogenic silver nanoparticles showed higher effects on growth of gram-negative and gram-positive bacteria. This is related to the cell-wall composition of both types of bacteria. The first has a layer of lipopolysaccharides at the exterior, with negative charges that interact easily with the small positive charges of silver nanoparticles while the negatively charged silver nanoparticles can attack the gram-negative bacteria by metal depletion. The cell-wall in gram-positive bacteria is principally composed of a thick layer of peptidoglycan that makes it difficult for silver nanoparticles to penetrate. The antibacterial activity of several antibiotics increased in the presence of silver nanoparticles against test strains possibly through silver nanoparticle chelation. The percentage increase in ampicillin with silver nanoparticles against gram positive and gram negative bacteria was almost the same. The ampicillin action is through cell-wall lysis and this effect, enhanced by complexation with silver nanoparticles, increased the silver nanoparticle penetration into the bacterium. The silver nanoparticles–ampicillin complex reacts with DNA and prevents DNA unwinding, producing large damage to bacterial cells. Previously it was demonstrated that the covalent or charged complex exerted an important synergistic effect between the metallic nanoparticles and the antibiotics in these cases (Gu et al. 2003; Wei et al. 2007; Grace and Pandian 2007; Durán et al. 2008, 2010a, b; Marcato et al. 2008; Patil et al. 2009).

The silver nanoparticles produced from *Aspergillus niger* showed remarkable antibacterial activity against gram-positive (*S. aureus*) and gram-negative (*E. coli*)

bacteria. The reduction of the silver ions might have occurred by a nitrate-dependent reductase enzyme and a shuttle quinone extracellular process. The antibacterial activity of silver nanoparticles showed a maximum growth inhibition with *S. aureus* more than with *E. coli*. The growth inhibitions against bacteria were similar to that of gentamycin (Gade et al. 2008).

Silver nanoparticles from *S. aureus* were evaluated for their antimicrobial activities against different pathogenic organisms, showing a very sensitive activity against methicillin-resistant *S. aureus* followed by methicillin-resistant *S. epidermidis* and *Streptococcus pyogenes* and activity against *S. typhi* and *K. pneumoniae* (Nanda and Saravanan 2009).

### 11.2.2 Application of Biogenic Silver Nanoparticles in Fabrics

With respect to the application of silver nanoparticles is the production of sterile materials, most studies in the literature about producing sterile fabrics with silver use silver ions or silver nanoparticles produced by chemical methods. However, some studies have applied biogenic silver nanoparticles in fabrics. Durán et al. (2007) studied the impregnation of biogenic silver nanoparticles in cotton and polyester fabrics. The particles were produced by *Fusarium oxysporum* and 2% silver nanoparticles impregnated in the fabrics were obtained. These fabrics exhibited high antibacterial effects against *S. aureus* (99.9% bacterial reduction). The fabrics, after the antibacterial assay, were analyzed by SEM-EDS showing the presence of the silver peak and the absence of the contamination with bacteria (Figs. 11.3 and 11.4). However, bacterial contamination on top of the fabric was

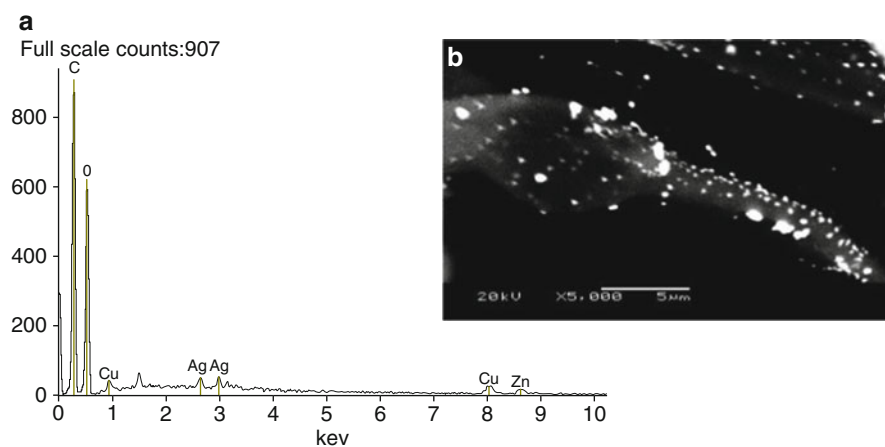


**Fig. 11.3** EDS spectrum of the cotton fabrics containing silver nanoparticles. The inset shows the SEM micrograph of the cotton fibers

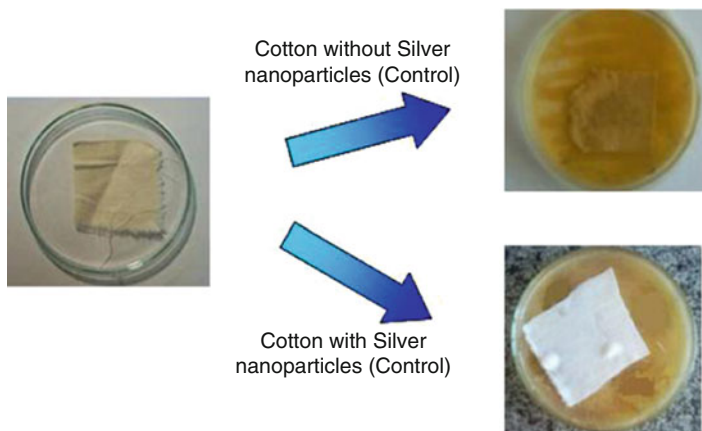


**Fig. 11.4** Cotton fabrics with and without silver nanoparticles evaluated for antibacterial activity (*S. aureus*)

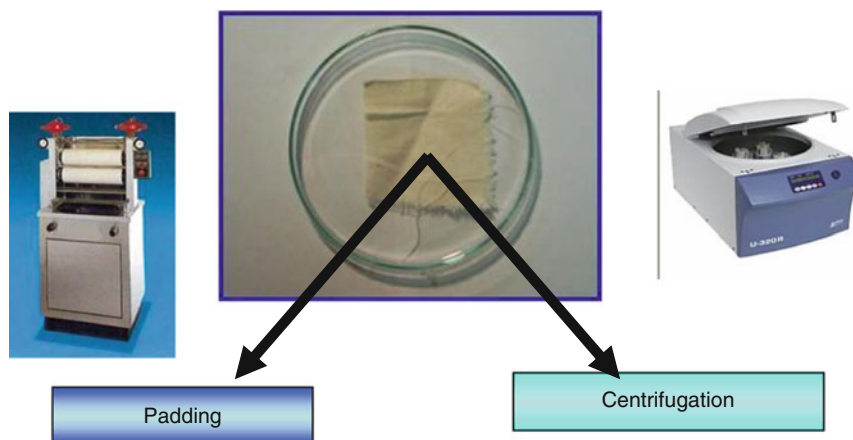


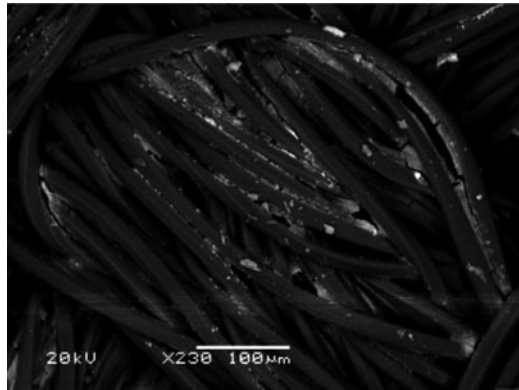
**Fig. 11.5** Tissue impregnation by silver nanoparticles

observed in the samples without silver nanoparticles as shown in Fig. 11.4. These results demonstrated that silver nanoparticles can be used to produce sterile fabrics. This silver nanoparticle dispersion will be reinvestigated for impregnation of other fabrics, for example, working in a closed circuit to cause less damage to the environment. In another study, the impregnation of cotton and polyester fabrics with biogenic silver nanoparticles from *F. oxysporum* was carried out by two different methods: padding and centrifugation. The results showed different homogeneity in the silver nanoparticle distributions in the fabrics, both methods being adequate for impregnation (Fig. 11.5). Figures 11.6 and 11.7 show the backscattering image of cotton and polyester fabrics impregnated with silver nanoparticles by

**Fig. 11.6** Backscattering images of cotton fabric impregnated with silver nanoparticles by centrifugation method



**Fig. 11.7** Backscattering images of polyester fabric impregnated with silver nanoparticles by centrifugation method



the centrifugation method, respectively. Agglomerated silver nanoparticles (white regions) were observed in both cases. However, the padding method appeared to yield more homogeneous impregnations than the centrifugation process (not shown) (Huber et al. 2009; Marcato et al. 2010). These methods were shown to be extremely efficient for the absorption of the silver nanoparticles in the textile. Furthermore, antibacterial activity was observed at least for three washes (Fig. 11.8) demonstrating the large adhesion of these particles in the fabric fibers. This efficient adhesion can be due to fungal protein around the silver nanoparticles. The fabrics impregnated with these particles maintained their antibacterial activity at least 20 wash cycles, as demonstrated by Marcato et al. (2010). Thus, this study showed the possibility to produce sterile materials without fabric surface modification with great laundering durability. The literature reports a lot of fabric materials having silver nanoparticles, mainly chemically synthesized ones. However, in the first washing, the most of the silver was released to the environment. However, the high adhesion of biogenic silver nanoparticles in fabrics decreases the environmental impact of particle release in the washing processes. However, the study of

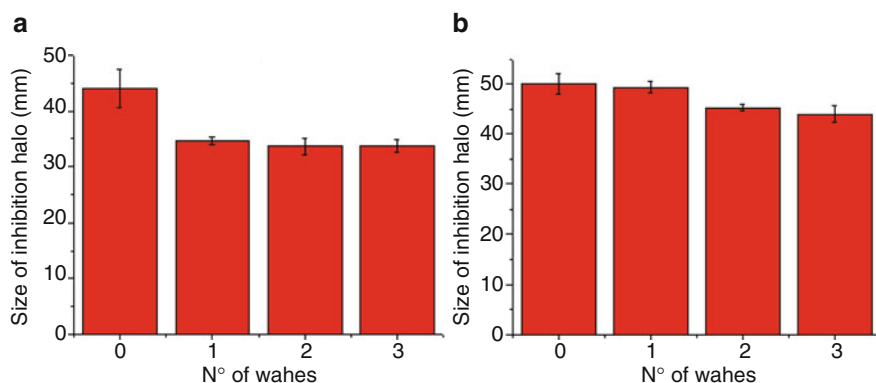


**Fig. 11.8** Antimicrobial activities against *S. aureus* of cotton and polyesters fabrics impregnated with silver nanoparticles before and after several washes

treatment of these released particles is very important. Durán et al. (2010c) studied the bioremediation process of biogenic silver nanoparticles released from fabrics in the washing process. This treatment was based on biosorption, which was very efficient for the elimination of silver nanoparticles remaining in the wash water. The process also allowed the recovery of silver material that was leached into the effluent for reutilization, avoiding any effect to the eco-environment. This is the first bioremediation process related to production of fabrics and the subsequent washing process.

### 11.3 Health Implications

The great benefits of silver nanoparticles were discussed above. However, studies of toxicity and cytotoxicity of these particles are very important before their application. The following are the health implications.

#### 11.3.1 Cytotoxicity and Toxicity of Silver Nanoparticles

A continuous debate on the advantages and disadvantages of the use of silver products in health care and medicine has been discussed (Bhattacharya and Mukherjee 2008). The results in the literature are not comparable because different cell cultures, animals, concentration, nanoparticle morphologies and sizes have been used. However, some indication about the effect of silver nanoparticles appears in the literature. There are several ways that nanoparticles can access the human body such as by inhalation (Oberdorster 2001), oral ingestion (Jani et al. 1990)

and contact with the skin (Kreilgaard 2002). After uptake, these particles can disseminate to different body tissues (Oberdorster et al. 2002, 2004; Borm and Kreyling 2004). Despite this, few toxicology studies are at present available.

### 11.3.1.1 Cytotoxicity

There are no reports on the cytotoxicity of biogenic silver nanoparticles but there are several about chemically or physically synthesized nanoparticles. These are discussed in the next paragraph.

Hussain et al. (2005) evaluated the acute cytotoxicity of silver nanoparticles with different sizes (15 or 100 nm) in a rat liver derived cell line (BRL 3A). In this study, it was observed that cytotoxicity was dose-dependent. The mitochondrial function decreased significantly in cells exposed to the nanoparticles and cells treated with higher doses (25–50  $\mu\text{g/mL}$ ) of particles exhibited cellular shrinkage and irregular shape.

Braydich-Stolle et al. (2005) studied the cytotoxicity of silver nanoparticles in C18-4 cells of a mouse cell line with spermatogonial stem cell characteristics. Silver nanoparticles with sizes of 15 nm exhibited morphologic alteration in cells at a concentration of 10  $\mu\text{g/mL}$ .

The cytotoxic effect of chemically synthesized silver nanoparticles with various sizes in macrophage cells was studied. There was no significant effect on cell proliferation at a concentration of 1  $\mu\text{g/mL}$ . However, the cell population was dramatically decreased and the cell size increased when the cells were treated with 10  $\mu\text{g/mL}$  of silver nanoparticles. Furthermore, by TEM analysis it was observed that silver nanoparticles are trapped in the cytoplasm (Yen et al. 2009).

Hep G2 has been used for assessment of in vitro cytotoxicity of many toxic agents as well as nanoparticles (Ponti et al. 2008). Considering these facts, Hep G2 cells were selected for evaluation of in vitro toxicity of silver nanoparticles (Jain et al. 2009). The toxicity of chemically synthesized silver nanoparticles in the presence of plant extract (capped protein silver nanoparticles) (Paknikar 2009) was evaluated on these cells with a specific mitochondrial marker (XTT assay). Results obtained showed a decrease of mitochondrial function in cells exposed to silver nanoparticles (12.5–400  $\mu\text{g/mL}$ ) in a dose-dependent manner. The  $\text{IC}_{50}$  value of silver nanoparticles was found to be 251  $\mu\text{g/mL}$  (Jain et al. 2009).

A cytotoxicity assay of chemically synthesized silver nanoparticles with sizes of 7–20 nm in primary cells lines from fibroblasts and liver cells was carried out. The results obtained by XTT assays showed a dose-dependent decrease in viability for both cell types. When the cells were treated with silver nanoparticles in the concentration range of 6.25–50  $\mu\text{g/mL}$ , the cell morphology was dramatically changed. The  $\text{IC}_{50}$  values were 10.6  $\mu\text{g/mL}$  and 11.6  $\mu\text{g/mL}$  for primary fibroblasts and primary liver cells, respectively. Furthermore, when the cells were treated with silver nanoparticles at concentrations of 5%  $\text{IC}_{50}$ , cellular antioxidant mechanism protecting the cells from possible oxidative damage was verified. Thus, in this case,

the *in vitro* results indicated that the safe concentration of silver nanoparticles is 1.56–6.25 µg/mL (Arora et al. 2009).

Safaepour et al. (2009) studied the cytotoxicity of silver nanoparticles at different concentrations (1, 2, 3, 4, 5 µg/mL) in fibrosarcoma-Wehi 164 cells. The particles were prepared with geraniol oil in the presence of polyethylene glycol 4000 and a silver nitrate solution in a microwave oven. Cytotoxicity analyses of the samples showed a direct dose–response relationship, increasing at higher concentrations. The IC<sub>50</sub> of silver nanoparticles was 2.6 µg/mL.

Starch-coated chemically synthesized silver nanoparticles were shown to be cytotoxic, genotoxic and antiproliferic on human lung fibroblast cells (IMR-90) and human glioblastoma cells (U251) at 25 µg/mL (Asharani et al. 2009).

Silver nanoparticles were prepared chemically and capped with albumin, probably similar to those synthesized biogenically by organisms. The toxicity of the nanoparticle preparations against MT-2 cells was determined using the Trypan Blue exclusion assay. The EC<sub>50</sub> with uncapped silver nanoparticles and the capped ones were 5 µg/mL and 15 µg/mL, respectively. In other words the toxicity to these cells was decreased 2.4-fold with protein capped silver nanoparticles (Elechiguerra et al. 2005).

Silver nanoparticles chemically synthesized in the presence of cellulose gum (average value of 735 nm by PCS) were used to perform a transcutaneous passage assay using human skin. The results showed that Ag nanoparticles are not able to penetrate human skin, thus implying that they function only as a preservative. The concentration that showed antimicrobial activity (50 ppm) did not show cytotoxicity against HaCaT keratinocytes and did not affect UVB-induced cell death. These results suggest that Ag nanoparticles of these sizes may have potential for use as a preservative in cosmetics (Kokura et al. 2010).

### 11.3.1.2 Toxicity

Takenaka et al. (2001) studied systemic pulmonary distribution of inhaled ultrafine silver particles (4–10 nm) in rats. The authors verified low concentrations of silver in the liver, kidney, spleen, brain and heart. The level of silver in the liver, lungs and blood decreased rapidly with time. Nasal cavities and lung-associated lymph nodes showed relatively high concentrations. The fast clearance of ultrafine silver nanoparticles can be due to rapid solubilization of these particles in the lung and silver nanoparticles enter the blood capillaries by diffusion.

A similar study was made by Sung et al. (2008, 2009). Rats were exposed to silver nanoparticles (18 nm) for 90 days to evaluate the *in vivo* effect of particle inhalation. Chronic alveolar inflammation, including thickened alveolar walls and small granulomatous lesions was observed after silver nanoparticle exposition, indicating lung function changes.

Rahman et al. (2009) evaluated the effects of silver nanoparticles of 25 nm size on gene expression in different regions of the mouse brain. Adult male C57BL/6N mice were administered (*i.p.*) 100 mg/kg, 500 mg/kg or 1,000 mg/kg silver



nanoparticles and sacrificed after 24 h. Considering the blood volume in mice of 1.8 mL/30 g of weight (Golde et al. 2005), the silver nanoparticles concentration applied in the mice was  $\sim 1,700 \mu\text{g/mL}$ , at the lowest concentration. This particle concentration was extremely high and it is not usually applied in any biological studies. After 24 h, significant alterations in genes expression in the caudate, frontal cortex and hippocampus of mice were observed. Not surprisingly, the data suggest that these nanoparticles may produce apoptosis and neurotoxicity by generating free radical-induced oxidative stress (Rahman et al. 2009).

A study tested the oral toxicity of chemically synthesized (unfunctionalized) silver nanoparticles (60 nm) over a period of 28 days in Sprague-Dawley rats following Organization for Economic Cooperation and Development (OECD) test guideline 407 with Good Laboratory Practice (GLP) application. Males (283 g) and females (192 g) were divided into four groups: vehicle control, low-dose group (30 mg/kg),  $\sim 50 \mu\text{g/mL}$  (Golde et al. 2005) for males, middle-dose group (300 mg/kg) and high-dose group (1,000 mg/kg). After 28 days of exposure, the blood biochemistry and hematology were normal. However, some significant dose-dependent changes were found in the alkaline phosphatase and cholesterol values in both sexes, seeming to indicate that exposure to more than 300 mg of silver nanoparticles may result in slight liver damage. The present results suggest that silver nanoparticles do not induce genetic toxicity in male and female rat bone marrow in vivo after oral administration (Kim et al. 2008). This probably was due to a high size of the nanoparticles.

Toxicity and biocompatibility of silver nanoparticles were evaluated in vivo using zebrafish embryos (Lee et al. 2007). The embryos were treated with spherical silver nanoparticles with sizes of  $11.6 \pm 3.5 \text{ nm}$ . It was observed that a single silver nanoparticle was transported into and out of embryos through chorion pore canals. Furthermore, the biocompatibility and toxicity of silver nanoparticles and types of abnormalities observed in zebrafish are highly dependent on the dose of particles, with a critical concentration of  $0.19 \text{ nmol/L}$ .

Starch and bovine serum albumin (BSA) as capping agents on chemically synthesized silver nanoparticles showed deleterious effects and distribution patterns in zebrafish embryos (*Danio rerio*). Toxicological endpoints like mortality, hatching, pericardial edema and heart rate were recorded and these effects were only observed at concentration over  $25 \mu\text{g/mL}$  of silver nanoparticles (Asharani et al. 2008).

### **11.3.2 Biogenic Silver Nanoparticles Applied to Health**

Besides the application of biogenic silver nanoparticles, as discussed before, silver nanoparticles can also be applied to improve health. For example, these particles can be used as antibacterial material to avoid bacterial infections. Biogenic silver nanoparticles exhibit great antibacterial activity in low concentration. Gade et al. (2008) verified that biogenic silver nanoparticles produced by *Aspergillus niger*

(10 µg/mL) showed remarkable antibacterial activity against gram-positive (*S. aureus*) and gram-negative (*E. coli*) bacteria. Fayaz et al. (2009) reported that the MIC (minimal inhibition concentration) of silver nanoparticles synthesized by *T. viridi* was 30 µg/mL with *E. coli*. Silver nanoparticles produced by *Aspergillus clavatus* showed a MIC values within 6–10 µg/mL for *C. albicans*, *P. fluorescence* and *E. coli* (Verma et al. 2010).

Raffi et al. (2008) reported that silver nanoparticles synthesized by the inert gas condensation (IGC) method were an effective bactericide against *E. coli* at concentration of 60 µg/ml.

Panacek et al. (2006) described the synthesis of silver nanoparticles of different sizes using four kinds of saccharides as substrates. The antimicrobial properties of these nanoparticles against many Gram-positive and Gram-negative bacteria including multidrug-resistant strains were found to be size dependent. Nanoparticles with size >25 nm exhibited MIC of 6.75–54 µg/mL, whereas 25-nm-sized particles showed MIC in the range of 1.69–13.5 µg/mL. This is an important result, particularly when antibiotic resistance among bacterial species is increasing at an alarming rate and very few alternative options are available to address the issue.

Cho et al. (2005) reported that poly-(*N*-vinyl-2-pyrrolidone) (PVP)-stabilized silver nanoparticles showed MIC of 5 µg/ml against *S. aureus* and 10 µg/ml against *E. coli*. *S. aureus* and *E. coli* were completely inhibited at 50 and 100 µg/ml silver.

An interesting observation on variation in antimicrobial activity of silver nanoparticles due to strain specificity has been discussed by Ruparelia et al. (2008). They showed that among the tested strains of *E. coli* (four strains), *B. subtilis* and *S. aureus* (three strains), *E. coli* strains showed maximum variation in silver nanoparticle-induced antimicrobial activity. The results of Jain et al. (2009) have corroborated these findings of strain-dependent variation in antimicrobial response to silver nanoparticles activity. In another study the MIC and MBC of Acticoat™ with *S. aureus*, *S. epidermidis*, *E. coli*, *K. aerogenes* and *P. aeruginosa* was reported to be 5–12.5 µg/ml (Burrel et al. 1995; Yin et al. 1999), but the concentration of silver released from Acticoat™ is normally in the range of 60–80 µg/ml (Wright et al. 1998), which is extremely high and probably toxic.

Slow release Acticoat dressing having silver nanoparticles was used in a post-cardiac surgery mediastinitis in patients with persistently positive microbiological cultures despite vacuum-assisted closure (VAC) therapy. Negative cultures were obtained within 72 h and patients were discharged within a maximum of 20 days (Totaro and Rambaldini 2009).

Another application of biogenic silver nanoparticles in health is its application in a neglected disease, leishmaniasis. Nanobiotechnology can be a promising technology to cure this parasitic disease (Marcato et al. 2008; Durán et al. 2009; Bergman-Rossi et al. 2010). A study of BALB/c mice infected with  $2 \times 10^6$  promastigotes of *Leishmania amazonensis* GFP in the ear showed that after 10 days of treatment (twice a week for four weeks) the wound in the control (mice treated with PBS solution) was large, while the wound of the mice treated with amphotericin B (positive control) exhibited low size of lesion (Fig. 11.9). The same result as with amphotericin B was observed when biogenic silver nanoparticles

**Fig. 11.9** Mice ears infected with *L. amazonensis* GFP: (a) no treatment (PBS), (b) Chemical nano-Ag, (c) Biogenic nano-Ag, (d) Amphotericin B

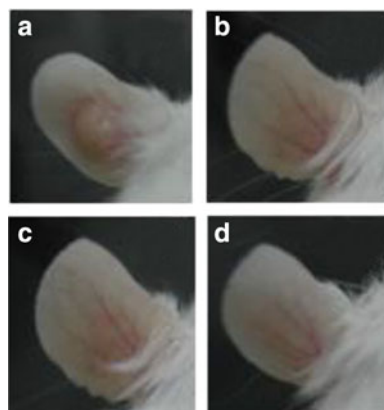


**Table 11.2** Efficiency of silver nanoparticles in the murine cutaneous leishmaniasis via Intraleisional treatment after 40 days of infection

Components	Concentration (µg/kg)	Lesions (mm × 10 <sup>-2</sup> )	FU (fluorescence units)
Control (PBS)	0.0	100	13,500
Amphotericin B	2,000.0	30	4,000
Silver nanoparticles Biol.	6.5	30	5,000
Silver nanoparticles Chem.	21.6	50	11,000

were used but with a 300-fold lower concentration, demonstrating to be a good option for leishmaniasis treatment. Chemically synthesized silver nanoparticles also decreased the wound when applied in 100-fold less concentration than amphotericin B. Parasitemia by specific fluorescence units 42 days after the infection showed the same results (Table 11.2).

## 11.4 Final Remarks

Different aspects related to the biogenesis of silver nanoparticles by fungi and the synergistic effect with antibiotics is the most relevant and with great potential to produce a final product, especially on neglected diseases, have been discussed in this chapter. Other products with immediate application are in sterile textile fabrics against contamination in hospitals (white coats, sheets, surgical coats, medical scrubs, etc.). This chapter also showed the relevance of cytotoxicity and toxicity effects of these particles before their use. Silver nanoparticles produced by biosynthetic or chemical methods exhibit cytotoxic and toxic potential that is dose-dependent. Thus, these studies indicate that it is possible to prepare a safe product with great benefits in different areas. It is important that the Governmental Foundations select the conditions to use in practice for final products such as pharmaceutical, food or environmental applications.

**Acknowledgements** Support from FAPESP, CNPq, MCT, the Brazilian Network of Nanocosmetics, the Brazilian Network of Nanobiotechnology (CNPq/MCT) and the Indo/Brazil Program (DST/CNPq) is acknowledged.

## References

- Ahmad A, Senapati S, Khan MI, Kumar R, Sastry M (2003) Extracellular biosynthesis of monodisperse gold nanoparticles by a novel extremophilic actinomycete, *Thermomonospora* sp. *Langmuir* 19:3550–3553
- Ankamwar B, Damle C, Absar A, Murali S (2005) Biosynthesis of gold and silver nanoparticles using *Embllica officinalis* fruit extract, their phase transfer and transmetallation in an organic solution. *J Nanosci Nanotechnol* 5:1665–1671
- Arora S, Jain J, Rajwade JM, Paknikar KM (2009) Interactions of silver nanoparticles with primary mouse fibroblasts and liver cells. *Toxicol Appl Pharmacol* 236:310–318
- AshaRani PV, LianWu Y, Gong Z, Valiyaveettil S (2008) Toxicity of silver nanoparticles in zebra fish models. *Nanotechnology* 19:255102
- AshaRani PV, Hande MP, Valiyaveettil S (2009) Anti-proliferative activity of silver nanoparticles. *BMC Cell Biol* 10:65. doi:10.1186/1471-2121-10-65
- Baker C, Pradhan A, Pakstis L, Pochan DJ, Shah SI (2005) Synthesis and antibacterial properties of silver nanoparticles. *J Nanosci Nanotechnol* 5:244–249
- Bergman-Rossi B, Marcato PD, De Conti R, Durán N (2010) Efficiency of biogenic and chemical silver nanoparticles in the murine cutaneous leishmaniasis via intralesional treatment. *J Biomed Nanotechnol* (in press)
- Bhattacharya R, Mukherjee P (2008) Biological properties of “naked” metal nanoparticles. *Adv Drug Deliv Rev* 60:1289–1306
- Borm PJ, Kreyling W (2004) Toxicological hazards of inhaled nanoparticles-potential implications for drug delivery. *J Nanosci Nanotechnol* 4:521–531
- Braydich-Stolle L, Hussain S, Schlager JJ, Hofmann MC (2005) In vitro cytotoxicity of nanoparticles in mammalian germline stem cells. *Toxicol Sci* 88:412–419
- Brocchi M, Marcato PD, De Conti R, Gonzaga AC, Ditondo-Micas AF, Nakasato G, Alves OL and Durán N (2010) A comparison of silver nanoparticles produced chemically and by fungal biosynthesis conjugated to clindamycin acting on several bacteria. *J Nanosci Nanotechnol*, (in press)
- Burrell RE, McIntosh CL, Morris IR (1995) Process of activating antimicrobials materials. US Patent 5(455):886
- Chandrasekharan N, Kamat PV (2000) Improving the photoelectrochemical performance of nanostructured TiO<sub>2</sub> films by adsorption of gold nanoparticles. *J Phys Chem B* 104: 10851–10857
- Chen X, Schluesener HJ (2008) Nanosilver: a nanoproduct in medical application. *Toxicol Lett* 176:1–12
- Cho KH, Park JE, Osaka T, Park SG (2005) The study of antimicrobial activity and preservative effects of nanosilver ingredient. *Electrochim Acta* 51:956–960
- Dastjerdi R, Montazera M, Shahsavan S (2009) A new method to stabilize nanoparticles on textile surfaces. *Colloids Surf A Physicochem Eng Asp* 345:202–210
- Durán N, Marcato PD, Alves OL, De Souza GIH, Espósito E (2005) Mechanistic aspects of biosynthesis of silver nanoparticles by several *Fusarium oxysporum* strains. *J Nanobiotechnol* 3:8. doi:10.1186/1477-3155-3-8
- Durán N, Marcato PD, De Souza GIH, Alves OL, Espósito E (2007) Antibacterial effect of silver nanoparticles produced by fungal process on textile fabrics and their effluent treatment. *J Biomed Nanotechnol* 3:203–208

- Durán N, Marcato PD, De Conti R, Alves OL, Brocchi M (2008) Silver nanoparticles: control of pathogens, toxicity and cytotoxicity. *Nanotoxicology* 2:S32
- Durán N, Marcato PD, Teixeira Z, Duran M, Costa FTM, Brocchi M (2009) State of the art of nanobiotechnology applications in neglected diseases. *Curr Nanosci* 5:396–408
- Durán N, Marcato PD, De Conti R, Alves OL, Costa FTM, Brocchi M (2010a) Potential use of silver nanoparticles on pathogenic bacteria, their toxicity and possible mechanisms of action. *J Braz Chem Soc* 21:949–959
- Durán N, Marcato PD, Ingle A, Gade A, Rai M (2010b) Fungi-mediated synthesis of silver nanoparticles: characterization processes and applications, Chap. 16. In: Rai M, Kövics G (eds) *Progress in mycology: biosynthesis of nanoparticles by microbes and plants*. Scientific Publishers, Rajasthan, India, pp 425–449. ISBN 978-81-7233-636-3
- Durán N, Marcato PD, Alves OL, Da Silva JPS, De Souza GIH, Rodrigues FA, Espósito E (2010c) Ecosystem protection by effluent bioremediation: Silver nanoparticles impregnation in a textile fabrics process. *J Nanopart Res* 12:285–292
- Elechiguerra JL, Burt JL, Morones JR, Camacho-Bragado A, Gao X, Lara HH, Yacaman MJ (2005) Interaction of silver nanoparticles with HIV-1. *J Nanobiotechnol* 3: doi:10.1186/1477-3155-3-6
- Fayaz AM, Balaji K, Girilal M, Yadav R, Kalaichelvan PT, Venketesan R (2009) Biogenic synthesis of silver nanoparticles and their synergistic effect with antibiotics: a study against gram-positive and gram-negative bacteria. *Nanomedicine:NBM* 2009;xx:1–7, doi:10.1016/j.nano.2009.04.006.
- Gade AK, Bonde P, Ingle AP, Marcato PD, Durán N, Rai MK (2008) Exploitation of *Aspergillus niger* for synthesis of silver nanoparticles. *J Biobased Matter Bioenergy* 2:243–245
- Gericke M, Pinches A (2006) Biological synthesis of metal nanoparticles. *Hydrometallurgy* 83:132–140
- Golde WT, Gollobin P, Rodriguez LL (2005) A rapid, simple, and humane method for submandibular bleeding of mice using a lancet. *Lab Anim* 34:39–43
- Grace AN, Pandian K (2007) Antibacterial efficacy of aminoglycosidic antibiotics protected gold nanoparticles – a brief study. *Colloids Surf A Physicochem Eng Aspects* 297:63–70
- Gu H, Ho PL, Tong E, Wang L, Xu B (2003) Presenting vancomycin on nanoparticles to enhance antimicrobial activities. *Nano Lett* 3:1261–1263
- Han G, Ghosh P, Rotello VM (2007) Functionalized gold nanoparticles for drug delivery. *Nanomedicine* 2:113–123
- Harris AT, Bali R (2008) On the formation and extent of uptake of silver nanoparticles by live plants. *J Nanopart Res* 10:691–695
- Huber SC, Marcato PD, Nakazato G, Martin D, Durán N (2009) Textile fabrics loading biosynthetic silver nanoparticles: bactericidal activity against gram-positive and gram-negative bacteria. In: CIFARP-2009, 7th. Int. Congress of Pharm. Sci. 6–9 September, Riberão Preto, SP, Abstr. FQ 012
- Hussain SM, Hess KL, Gearhart JM, Geiss KT, Schlager JJ (2005) In vitro toxicity of nanoparticles in BRL 3A rat liver cells. *Toxicol In Vitro* 19:975–983
- Ilic V, Saponjic Z, Vodnik V, Potkonjak B, Jovancic P, Nedeljkovic J, Radetic M (2009) The influence of silver content on antimicrobial activity and color of cotton fabrics functionalized with Ag nanoparticles. *Carbohydr Polym* 78:564–569
- Ingle A, Gade A, Pierrat S, Sönnichsen C, Rai M (2008) Mycosynthesis of silver nanoparticles using the fungus *Fusarium acuminatum* and its activity against some human pathogenic bacteria. *Curr Nanosci* 4:141–144
- Jain J, Arora S, Rajwade JM, Orray P, Khandelwal S, Paknikar MK (2009) Silver nanoparticles in therapeutics: development of an antimicrobial gel formulation for topical use. *Mol Pharm* 6:1388–1401
- Jani P, Halbert GW, Langridge J, Florence AT (1990) Nanoparticle uptake by the rat gastrointestinal mucosa: quantitation and particle size dependency. *J Pharm Pharmacol* 42:821–826

- Khalil-Abad MS, Yazdanshenas ME, Nateghi MR (2009) Effect of cationization on adsorption of silver nanoparticles on cotton surfaces and its antibacterial activity. *Cellulose* 16:1147–1157
- Kim YS, Kim JS, Cho HS, Rha DS, Kim JM, Park JD, Choi BS, Lim R, Chang HK, Chung YH, Kwon IH, Jeong J, Han BS, Yu IJ (2008) Twenty-eight-day oral toxicity, genotoxicity, and gender-related tissue distribution of silver nanoparticles in Sprague-Dawley rats. *Inhal Toxicol* 20:575–583
- Kokura S, Handa O, Takagi T, Ishikawa T, Naito Y, Yoshikawa T (2010) Silver nanoparticles as a safe preservative for use in cosmetics. *Nanomedicine: NBM* 2010;xx:1–5, doi:[10.1016/j.nano.2009.12.002](https://doi.org/10.1016/j.nano.2009.12.002)
- Kowshik M, Ashtaputre S, Kharrazi S, Vogel W, Urban J, Kulkarani SK, Paknikar KM (2003) Extracellular synthesis of silver nanoparticles by a silver-tolerant yeast strain MKY3. *Nanotechnology* 14:95–100
- Kreilgaard M (2002) Influence of microemulsions on cutaneous drug delivery. *Adv Drug Deliv Rev* 54(1 Suppl):S77–S98
- Krolkowska A, Kudelski A, Michota A, Bukowska J (2003) SERS studies on the structure of thioglycolic acid monolayers on silver and gold. *Surf Sci* 532:227–232
- Kumar V, Yadav SK (2009) Plant-mediated synthesis of silver and gold nanoparticles and their applications. *J Chem Technol Biotechnol* 84:151–157
- Lee KJ, Nallathambi PD, Browning LM, Osgood CJ, Xu HN (2007) In vivo imaging of transport and biocompatibility of single silver nanoparticles in early development of zebrafish embryos. *ACS Nano* 1:133–143
- Maliszewska I, Sadowski Z (2009) Synthesis and antibacterial activity of silver nanoparticles. *J Phys Conf Ser* 146:1–6
- Mandal D, Bolander ME, Mukhopadhyay D, Sarkar G, Mukherjee P (2006) The use of microorganisms for the formation of metal nanoparticles and their application. *Appl Microbiol Biotechnol* 69:485–492
- Maneering T, Tokura S, Rujiravanit R (2008) Impregnation of silver nanoparticles into bacterial cellulose for antimicrobial wound dressing. *Carbohydr Polym* 72:43–51
- Marcato PD, Durán N (2008) New aspects of nanopharmaceutical delivery systems. *J Nanosci Nanotechnol* 8:2216–2229
- Marcato PD, De Souza GIH, Alves OL, Espósito E, Duran N (2005) Antibacterial activity of silver nanoparticles synthesized by *Fusarium oxysporum* strain. In: *Proceedings of 2nd Mercosur Congr. on Chem. Eng., 4th Mercosur Congr. on Process Sys. Eng.*, pp. 1–5
- Marcato PD, De Conti R, Bergmann BR, Duran N (2008) Silver nanoparticles/Clindamycin: Antileishmanial activity. In: *Proceedings of 7th Bras. MRS, Met. (SBPMAT) 7: H583*
- Marcato PD, Huber SC and Durán N (2010). Biogenic silver nanoparticles in textile sterilization: Cotton and polyester fabrics. *J Nanopart Res* (Submitted)
- Mohanpuria P, Rana NK, Yadav SK (2008) Biosynthesis of nanoparticles: technological concepts and future applications. *J Nanopart Res* 10:507–517
- Mukherjee P, Ahmad A, Mandal D, Senapati S, Sainkar SR, Khan M (2001) Bioreduction of AuCl<sub>3</sub> by the fungus, *Verticillium* species and surface trapping of the gold nanoparticles formed. *Angew Chem Int Ed* 40:3585–3583
- Nanda A, Saravanan M (2009) Biosynthesis of silver nanoparticles from *Staphylococcus aureus* and its antimicrobial activity against MRSA and MRSE. *Nanomedicine NBM* 5:452–456
- Oberdorster G (2001) Pulmonary effects of inhaled ultrafine particles. *Inter Arch Occupat Environ Health*. 74:1–8
- Oberdorster G, Sharp Z, Atudorei V, Elder A, Gelein R, Lunts A, Kreyling W, Cox C (2002) Extrapulmonary translocation of ultrafine carbon particles following whole-body inhalation exposure of rats. *J Toxicol Environ Health A* 65:1531–1543
- Paknikar KM (2009) Stabilizing solutions for submicronic particles, methods for making the same and method of stabilizing submicronic particles. *US Patent* 7(514):600

- Panacek A, Kvitek L, Pucek R, Kolar M, Vecerova R, Pizurova N, Sharma VK, Nevecna T, Zboril R (2006) Silver colloid nanoparticles: synthesis, characterization, and their antibacterial activity. *J Phys Chem B* 110:16248–16253
- Patil SS, Dhupal RS, Varghese MV, Paradkar AR, Khanna PK (2009) Synthesis and antibacterial studies of chloramphenicol loaded nano-silver against *Salmonella typhi*. *Synth React Inorg Met Org Nano Met Chem* 39:65–72
- Perelshstein I, Applerot G, Perkas N, Guibert G, Mikhailov S, Gedanken A (2008) Sonochemical coating of silver nanoparticles on textile fabrics (nylon, polyester and cotton) and their antibacterial activity. *Nanotechnology* 19:1–6
- Ponti J, Colognato R, Franchini F, Gioria S, Simonelli F, Abbas K, Rossi F (2008) Uptake and cytotoxicity of gold nanoparticles in MDCK and HepG2 cell lines can be found under [http://www.riskcenter.jp/nanorisk.symposium/index\\_e.html2008](http://www.riskcenter.jp/nanorisk.symposium/index_e.html2008). . [http://www.aist-riss.jp/projects/nedo-nanorisk/nanorisk\\_symposium2008/pdf/03\\_122\\_en\\_ROSSI.pdf](http://www.aist-riss.jp/projects/nedo-nanorisk/nanorisk_symposium2008/pdf/03_122_en_ROSSI.pdf)
- Raffi M, Hussain F, Bhatti TM, Akhter JI, Hameed A, Hasan MM (2008) Antibacterial characterization of silver nanoparticles against *E. coli* ATCC-15224. *J Mater Sci Technol* 24:192–196
- Rahman MF, Wang J, Patterson TA, Saini UT, Robinson BL, Newport GD, Murdock RC, Schlager JJ, Hussain SM, Ali SF (2009) Expression of genes related to oxidative stress in the mouse brain after exposure to silver-25 nanoparticles. *Toxicol Lett* 187:15–21
- Rai M, Yadav A, Gade A (2009) Silver nanoparticles as a new generation of antimicrobials. *Biotechnol Adv* 27:76–83
- Riddin TL, Gericke M, Whiteley CG (2006) Analysis of the inter- and extracellular formation of platinum nanoparticles by *Fusarium oxysporum* f. sp. *lycopersici* using response surface methodology. *Nanotechnology* 17:3482–3489
- Ruparelia JP, Chatterjee AK, Duttagupta SP, Mukherji S (2008) Strain specificity in antimicrobial activity of silver and copper nanoparticles. *Acta Biomater* 4:707–716
- Sadowski Z, Maliszewska IH, Grochowalska B, Polowczyk I, Koźlecki T (2008) Synthesis of silver nanoparticles using microorganisms. *Mat Sci Pol* 26:419–424
- Safaepour M, Ar S, Shahverdi HR, Khorramizadeh MR, Gohari AR (2009) Green synthesis of small silver nanoparticles using geraniol and its cytotoxicity against fibrosarcoma-Wehi 164. *Avicenna J Med Biotech* 1:111–115
- Shahverdi AR, Fakhimi A, Shahverdi HR, Minaian S (2007) Synthesis and effect of silver nanoparticles on the antibacterial activity of different antibiotics against *Staphylococcus aureus* and *Escherichia coli*. *Nanomedicine NBM* 3:168–171
- Sharma VK, Yngard RA, Lin Y (2009) Silver nanoparticles: green synthesis and their antimicrobial activities. *Adv Colloid Interf Sci* 145:83–96
- Singh M, Singh S, Prasad S, Gambhir IS (2008) Nanotechnology in medicine and antibacterial effect of silver nanoparticles. *Dig J Nanomater Biostruct* 3:115–122
- Sintubin L, De Windt W, Dick K, Mast J, Van der Ha Verstraete D, Boon N (2009) Lactic acid bacteria as reducing and capping agent for the fast and efficient production of silver nanoparticles. *Appl Microbiol Biotechnol* 84:741–749
- Sugunan A, Melin P, Schnürer J, Hilborn JG, Dutta J (2007) Nutrition-driven assembly of colloidal nanoparticles: growing fungi assemble gold nanoparticles as microwires. *Adv Mater* 19:77–81
- Sung JH, Ji JH, Yoon JU, Kim DS, Song MY, Jeong J, Han BS, Han JH, Chung YH, Kim J, Kim TS, Chang HK, Lee EJ, Lee JH, Yu IJ (2008) Lung function changes in Sprague-Dawley rats after prolonged inhalation exposure to silver nanoparticles. *Inhal Toxicol* 20:567–574
- Sung JH, Ji JH, Park JD, Yoon JU, Kim DS, Jeon KS, Song MY, Jeong J, Han BS, Han JH, Chung YH, Chang HK, Lee JH, Cho MH, Kelman BJ, Yu IJ (2009) Subchronic inhalation toxicity of silver nanoparticles. *Toxicol Sci* 108:452–461
- Takenaka S, Karg E, Roth C, Schulz H, Ziesenis A, Heinzmann U, Schramel P, Heyder J (2001) Pulmonary systemic distribution of inhaled ultrafine silver particles in rats. *Environ Health Perspect* 109:547–551
- Thakkar KN, Mhatre SS, Parikh RY (2009) Biological synthesis of metallic nanoparticles. *Nanomedicine: NBM* 2009;xx:1–6, doi:[10.1016/j.nano.2009.07.002](https://doi.org/10.1016/j.nano.2009.07.002).

- Thirumurugan G, Shaheedha SM, Dhanaraju MD (2009) In vitro evaluation of antibacterial activity of silver nanoparticles synthesised by using *Phytophthora infestans*. *Int J Chem Tech Res* 1:714–716
- Tian J, Wong KKL, Ho CM, Lok CN, Yu WY, Che CM, Chiu JF, Tam PKH (2007) Topical delivery of silver nanoparticles promotes wound healing. *ChemMedChem* 2:129–236
- Totaro P, Rambaldini M (2009) Efficacy of antimicrobial activity of slow release silver. Nanoparticles dressing in post-cardiac surgery mediastinitis. *Interact CardioVasc Thor Surg* 8:153–154
- Verma VC, Kharwar RN, Gange AC (2010) Biosynthesis of antimicrobial silver nanoparticles by the endophytic fungus *Aspergillus clavatus*. *Nanomedicine* 5:33–40
- Wei QS, Ji J, Fu JH, Shen JC (2007) Norvancomycin-capped silver nanoparticles: synthesis and antibacterial activities against *E. coli*. *Sci China B Chem* 50:418–424
- Wright JB, Hansen DL, Burrell RE (1998) The comparative efficacy of two antimicrobial barrier dressings. *Wounds* 10:179–188
- Yen HJ, Hsu SH, Tsai CL (2009) Cytotoxicity and immunological response of gold and silver nanoparticles of different sizes. *Small*. doi:[10.1002/sml.200900126](https://doi.org/10.1002/sml.200900126)
- Yin HQ, Langford R, Burrell RE (1999) Comparative evaluation of the antimicrobial activity of Acticoat™ antimicrobial barrier dressing. *J Bum Care Rehabil* 20:195–200



# Chapter 12

## Nanobiosensors and Their Applications

A. Reshetilov, P. Iliasov, T. Reshetilova, and Mahendra Rai

### 12.1 Introduction

Recently, the words “nanotechnology” and “nanobiotechnology” are rather often used by world scientific community and also in everyday life, which is far from studying the problems of man. Such use bears a particular meaning? for a certain range of people; for others, it only means a notion about novel technology that promises solution of many problems, but it is rarely explained or not clarified at all. Trying to define, one may say that a section of science and technology, in which processes occurring in structures within a corresponding size are considered, is called nanotechnology. The latter is defined as a science destined to create materials, devices, and systems with preset functions that are made of nanosized elements (Evdokimov et al. 2006). Definition is a starting point of development of any area of research, and this is why it is helpful to give some general definition about what nanobiotechnology is. Further, the definition proposed by the US Nanoscale Science, Engineering and Technology Subcommittee (NSETS) in the report of the year 2003 is taken as basic. Authors pay attention to the fact that actually nanobiotechnology is a sphere, where coupling between nanotechnology and biology and medicine is observed. In its turn, nanotechnology is regarded as an area of study aimed at understanding and control of processes that take place in structures within 1–100 nanometers (nm) by size, where their properties differ by principle from those of individual atoms and molecules, which incorporate common macro-subjects that surround man (Vogel and Baird 2003).

---

A. Reshetilov (✉), P. Iliasov, and T. Reshetilova  
G.K. Skryabin Institute of Biochemistry and Physiology of Microorganisms, RAS, 142290,  
Pushchino, Nauki Av., 5, Russia  
e-mail: anatol@ibpm.pushchino.ru

M. Rai  
Biotechnology Department, SGB Amravati University, Amravati 444 602, Maharashtra, India

Nanotechnology is an interdisciplinary area, and as it is based on using the approaches of other sciences, this science is meant to apply nanosized materials for the development of devices and systems, in which unusual known or earlier unknown nanoeffects are employed with new aims. As a substantial part of biology is based on the events that take place in nanoscale (membranes, cell fragments, enzymes, nucleic acids, etc.), they decided not to change the name of already known areas and describe phenomena by introduction of the notion “nanotechnology”. According to the essence of the process, novel studies were to be classified as nanobiotechnological only in the cases if they (a) use nanotechnology tools and concepts to study biology or develop medical interventions, (b) propose to engineer biological molecules toward functions very different from those they have in nature, (c) manipulate biosystems using nanotechnology tools rather than synthetic chemical or biochemical approaches.

It is marked in the mentioned NSETS reports that now nanotechnology is at the development stage that does not permit long-term forecasts about the respective technologies; at the same time, there are lots of short-time/“hot” projects, which are in the score of attention and supported financially. The following aspects under study may be regarded as examples:

- Use of fluorescence in semiconductive nanocrystals (quantum dots) for the development of dynamic angiography of capillaries located at a distance of hundred microns from the skin (animal’s models)
- Development of nanoelectromechanical sensors that allow detection of single molecules of chemical weapon – a significant advance in the area of sensor construction
- Formulation of rocket/jet fuels and explosives, which have the energetic yield twice exceeding the known ones
- Creation of the prototypes of memory devices by orders exceeding the existing ones by volume, etc.

Nanobiotechnology is a component of nanotechnology. The area of nanobiotechnology that refers to solution of medical problems is defined by the term “nanomedicine”, which speaks about certain order of the structure of studies, namely, its improvement by division into more definite sections. Some problems of this area can be designated as follows:

- Could a method be elaborated and the analytical system constructed, which could detect the appearance of the single cell that potentially leads to a cancer disease?
- Could a broken cell or its part be substituted by a miniature biological device?
- Could a molecular-scale pump be inserted close to a target cell for drug delivery, if necessary, etc.

Naturally, the research that gives an answer to the above questions, starts beyond the boundaries of medicine and is based on using novel physical and chemical approaches.

## 12.2 Nanobiotechnology and Biosensors

The aim of this chapter is partly to discover the essence of inter-penetration of nanobiotechnology and biosensors, biosensors and nanobiosensors, elucidation of the interrelationship between them, the attempt to understand, if common tasks exist, and what methods are used to solve them.

The simplest comparison of biosensors and nanobiosensors could be made by analyzing the definitions of investigated areas. In accordance with the definition given in the journal *Biosensors and Bioelectronics* a biosensor is an analytical device that contains biological material (tissues, cells of microorganisms, organelles, cell receptors, enzymes, immune and active components, nucleic acids, etc.) which is in immediate contact with a physicochemical transducer or a transducing system. The latter can be presented by optical, electro-chemical, thermometric, piezoelectric, and magnetic devices. Normally, the transducer gives periodic or constant analog/digit signals proportional to the concentration of a single compound or a group of analyzed compounds.

By this definition, the biosensor is set structurally (biological material and a transducer) and functionally (the measurement of the concentration of a compound). It corresponds to the essence and designation of the biosensor – in the end, the biosensor is the analytical instrument. The definition does not implicate the restrictions related to the sizes of the device itself or its components as well as the ways of its construction. It immediately follows from the definition that a general function of the biosensor is the use of biomaterial for realization of novel analytical functions.

Many principles and problems in the biosensor area are close to nanobiotechnological and nanobiosensor tasks in their essence. Let us give some formulations:

- There is a tendency to miniaturize the biosensor recognition site (Turner et al. 1987).
- The possibilities of creation of multi-component molecular structures with new functions are considered (Plekhanova et al. 2003; Hasunuma et al. 2004).
- Electrochemical and optical methods for constructing systems of extra-sensitive detection based on the use of artificial molecular complexes are employed (Lioubashevski et al. 2004).
- A search for novel schemes and solutions that might improve the quality of receptor elements is undertaken – detection of novel compounds based on using new enzymes, biomaterials, and principles of construction of receptor site (Reshetilov et al. 1998).
- The approaches of microelectronic technology and nanotechnology, which originate from the class of the earlier known ones and allow creation of analytical nanobiosensors, are used.
- The question as to the possibility of detection of single molecules was first put up in the area of biosensor technology (Haustein and Schwille 2004; Ros et al. 2004; Olejnikov et al. 2007); now such questions are regarded as pertinent to the nanobiosensor area.

- As a working instrument, the scanning probe microscopes have been examined; combined systems that couple optical technologies (surface plasmon resonance) with electrochemical ones are being created.
- The techniques related to self-assembling structures are used – the application of Langmuir–Blodgett films, the self-assembling and immobilization of protein containing layers on carrying surfaces for creation of analytical systems (Narváez et al. 2000), etc.
- The development of biomaterial coupling to elements of solid-state microelectronics, nanobiotransistors in particular, is envisaged (Stern et al. 2007).
- Microchips are being created – coupling of protein and nucleic molecules to analytical systems and the recording elements of electrochemistry and optics (Zasedatelev et al. 2006).
- The structures of the type “polyelectrolyte-antibody-antigen-protein label” are constructed, in which the principles of assembling aimed at obtaining the structures with analytical properties are used (Plekhanova et al. 2003; Evtushenko et al. 2007).

Some of the mentioned tasks were originally associated with studies devoted to classical macroscopic biosensors. Alongside the development of nanotechnologies, they were also inherited by nanobiosensors. In connection with this, one may conclude that there are intersections as to the aims of study, methods of realization/construction, which, on the whole, are rather close. As an example, it may be indicated that as the history of development goes, many tasks – initially typical of classical biosensor technology – entered the basis of nanomedicine and biosensors at further development – for instance, DNA chips.

Many novel themes in the list of sections of the world congress on biosensors “Biosensors-2010” also testify to essential shift of interests in the field of nanobiosensors. Thus, the work is planned in the following trends: nanobiosensors, nanomaterials, and analytical systems; the examination of Lab-on-a chip (LoC) systems is being suggested, whose creation is based on use of nanotechnologies; nanomaterials are often used in the development of novel enzyme-based biosensors; the creation of the “electronic nose” type structures is frequently based on using nanotechnology; micro-fluidics also suggest use of nanosystem technology.

Taking into account the above, let us consider the tasks as well as certain peculiarities acquired by biosensors at shift from macro- to nano-sizes.

### 12.3 Application of Nanomethods in Biosensor Development

High emphasis has been placed recently on silicon-based transducers in the field of bio-analytical applications due to their favorable characteristics, which include sensitivity, speed, miniaturization, and low cost. This interest is presented in many works that have monitored biological events such as nucleic acid hybridization, protein–protein interactions, antigen–antibody binding, and enzyme–substrate

reactions using these transducers. Ion-sensitive field-effect transistor (ISFET) is one of the popular electrochemical biosensors, and has been introduced as the first miniaturized silicon-based chemical sensor. In the recent years, great progress has been made in applying FET-type biosensors for highly sensitive biological detection. Among them, the ISFET is one of the intriguing approaches in electrochemical biosensing technology. Lee et al. (2009) considered some of the main advances in this field over the past few years, explore their application prospects, and discuss the main issues, approaches, and challenges with the purpose of extending their applications for reliable and sensitive analysis of various biomaterials such as DNA, proteins, enzymes, and cells.

The recent works have shown the development of nanosensors and application of nanomaterials in combination with field-effect transistors. One distinct advantage of the semiconductor-based biosensors such as ISFETs, as opposed to optical systems, is their suitability for miniaturized measurement systems, thereby allowing their easy integration into the carry-on electronics. In this aspect, ISFET is considered as an instrument of small size and weight, which can be successfully used for development of a portable monitoring system, i.e., a hand-held drug monitoring system. When it comes to biosensor sensitivity and specificity, both fabrication of a nano-scale device and elimination of nonspecific molecular adsorption would contribute to improvement in the limit of detection and selectivity of the biosensor (Schöning and Poghossian 2006).

A variety of metallic nanoparticles (NPs), semiconductor quantum dots, and functionalized redox molecules applied as optically or electrochemically active labels have been developed.

Qu et al. (2009) demonstrated a direct and simple method of formation of a composite film consisting of polypyrrole and gold NPs. The composite facilitated the deposition of different polymers including proteins (Qu et al. 2009). Based on this method, an ISFET-type micro-potentiometric Hb/HbA1c immunosensor was developed, and hemoglobin (Hb) and hemoglobin-A1c (HbA1c) were detected in whole blood with improved sensitivity.

A series of methods have been developed for stable immobilization of enzymes on the gate surface of ISFETs. For example, Vijayalakshmi et al. (2008) developed a technique where lipase was immobilized onto magnetic nickelferrite NPs, and then the resulting enzyme-modified NPs could be retained at the gate surface, because the magnet continued to run from the bottom of the ISFET gate. The advantages of the proposed method underlie (1) improved mass transfer, (2) possibility to be applicable for a multiple detection system based on FET device, and (3) increased amount of bound enzyme on the surface.

Although the ISFET-based enzyme sensors demonstrate high stability and activity, their measurement range could be restricted using the solution parameters such as pH or buffer capacity, because the ISFETs operation is highly influenced by the buffer conditions. To overcome this problem, several approaches such as application of additional charged polymeric membranes and buffer solutions with low capacities have been attempted. Recently, for the improvement of the functioning of ISFETs, another type of ISFET, the so-called region ISFET (RISFET)

has been proposed by Risveden et al. (2007). The developed RISFET has an extraordinary feature: its performance depends on the strength of electrical field generated by the ion molecule reaction occurring in a unique region flanked by the sensing electrodes. The authors have suggested that the developed RISFET device is a model of a promising nanobiosensor, because it allows for dielectrophoretic trapping of a single enzyme, thereby allowing the analysis of small volumes of fluid containing the low amount of analytes.

In future, ISFET biosensors may have advanced performance and special properties resulting from their coupling with nanomaterials such as NPs, nanotubes, and nanowires. The integration of ISFET in microsystems such as micro-total-analysis-system ( $\mu$ -TAS) or LoC may also provide small packaged sensor systems with ultrahigh sensitivity. These ISFET biosensors could be useful for biomedicine, clinical diagnosis, environmental monitoring, and point-of-care-testing system (Abramova and Bratov 2009; Lee et al. 2009).

The important problem concerning the particular case of using nanobiosensors, namely, detection of pathogenic microorganisms, has been analyzed in the work (Sanvicens et al. 2009). The review considers different types of nanobiosensors and their applications with optical, electrochemical, and magnetic transducers. The authors put a high emphasis on the development of novel NP-based technology that allows sensitive detection of bacteria in unprocessed and complex samples. It should be noted that selective and sensitive detection of pathogenic bacteria is extremely important for the fields such as clinical diagnostics, environmental monitoring, and food safety. Standard approaches are based on polymerase chain reaction (PCR), culture and colony counting, and immunological methods. Unfortunately, the reliability of these techniques cannot be considered as satisfactory especially with respect to the necessary detectability and specificity towards the target. In this context, biosensors offer several advantages over the existing techniques (e.g., limited hands-on time, high-throughput screening, improved detectability, real-time analysis, and label-free detection methods and devices) (Skottrup et al. 2008). At the same time, most of the modern biosensor systems cannot detect bacteria at concentrations below ten colony-forming units per milliliter (CFU/mL) without bacteria pre-enrichment of the sample. This is a crucial factor, since even a single cell may lead to serious health risk, so the research into bacterial biosensing aims to achieve ultrasensitive detection of infectious agents in complex biological matrices. Introduction of nanotechnology approaches into biosensors holds great promise for addressing the analytical needs of medical diagnostic systems (Sanvicens et al. 2009). In this context, NPs have raised great expectations with respect to generating enhanced signal-to-noise ratios, reducing response times, and using them in multiplexed systems.

Considerable quantity of NP-based biosensors has been developed for the specific detection of biologically relevant molecules (e.g., nucleic acids, proteins, and enzymes) and sometimes for the detection of infectious agents. It is known that the optical biosensors based on surface plasmon resonance (SPR) are highly sensitive. Nevertheless, the sensitivity of SPR biosensors is sometimes limited by the inability to measure small changes in refractive index. In this context, gold NPs

(AuNPs) have demonstrated their potential to amplify SPR detection. Thus, Joung et al. (2008) employed AuNPs in a signal-amplification method for high-sensitivity detection of *Escherichia coli* 16s rRNA using peptide nucleic acid probes with an SPR biosensor system. The promising approach in the SPR technique is the variant of replacement of conductive metal surface of an SPR sensor by noble-metal NPs. In this case, light interacts with the particles possessing much smaller dimensions than the incident wavelength that leads to a plasmon oscillating locally around the NP with a frequency resonant to the incident photon frequency. The phenomenon is known as the localized SPR (LSPR). The LSPR spectrum of metal NPs is characterized by the presence of intense adsorption and scattering peaks, which greatly improve the sensitivity of the sensors (McFarland and Van Duyne 2003).

Magnetic particles were traditionally used for concentration, separation, purification, and identification of molecules and specific cells. In the recent years, the magnetic properties of some NPs have also been used as labels in biosensing. In the work by Koets et al. (2009), a magneto-resistant sensor with super paramagnetic particles used as detection labels was applied for the determination of *E. coli* and *Salmonella*. The detection of magnetic particles by a magneto-resistance sensor was shown to be very powerful, since the magnetic particles speed up the assay by reducing diffusion limitations. Moreover, the absence of magnetic materials in biological samples means that background signals of the sensor are low.

Recently, electrochemical biosensors have been extensively used with different types of NPs. Such combination makes it possible to use the positive electric properties of NPs and their electrocatalytic activity for improvement of measurement rate, selectivity, and sensitivity. The applications of NPs can be found in two categories related to electrochemical biosensors (Sanvicens et al. 2009):

- Novel electrochemical transducers that show enhanced immobilization capacities, low background current, and improved electrochemistry
- Labels for signal amplification of biorecognition events

*E. coli* was determined with a level of detection of 10 CFU/mL using a tyrosinase biosensor to determine phenol, by employing Fe<sub>3</sub>O<sub>4</sub> magnetic NP-coated carbon nanotubes (CNTs). The detection principle was based on the determination of phenol produced by an enzymatic reaction in the bacteria-containing solution (Cheng et al. 2008). Using horseradish peroxidase-labeled antibodies against *S. aureus* enterotoxin B immobilized onto nanogold/chitosan-multi-walled CNTs, *S. aureus* enterotoxin B was detected with a conductometric immunobiosensor in the linear range 0.5–83.5 ng/mL (Chen 2007). Field-effect transistors fabricated using semiconducting single-walled CNTs could monitor a direct charge-transfer reaction between the analyte and the CNT. The CNT structure allowed increasing the sensitivity to the point where single-molecule detection was possible (Gruner 2006). An example of the application of FETs in bacteria detection is the work of Villamizar et al. (2008), who reported the development of CNT-FET for the detection of *Salmonella infantis* at 100 CFU/mL in 1 h. Similarly, *E. coli* has been detected using an aptamer-functionalized CNT-FET (So et al. 2008).

## 12.4 Cell-Based Biosensors and Nanotechnology

As appears from the above-mentioned, nanobiosensors represent intensively developing area of focus in biosensorics. The list of the nanobiosensors developed to date includes significant number of enzyme, nucleic acid, receptor, and immune-based bioanalytical devices. A completely different type of situation takes place in the field of cell-based biosensors. It is well known that the bacterial and yeast cells as well as the cells of macroorganisms are characterized by micrometer-scale sizes that cast serious doubt on the acceptability of the term “nanobiosensor” towards the cell-based sensors even if it is referred to the device based on a single cell. The only exclusion is represented by nanobacteria whose size may be as small as 200 nm but they have not been utilized in biosensors so far.

Thus, the outline of prospects of the cell-based biosensors in this sense allows speaking not about cell-based nanobiosensors but only about the coupling of cell-based biosensors with nanotechnological advances. This coupling may be realized at least by means of two ways:

- The utilization of nanomaterials and nanoscale structures in biosensors
- Application of cell-based biosensors for the determination of specific nanomaterials (for example, metal NPs)

Nanomaterials (CNT, NP-based composites, nanostructured polymers, metal NPs, etc.) have widely been used in enzyme, DNA- and immunosensors for immobilization of biomaterials or alteration of transducer characteristics but quite rarely have been utilized in cell-based sensors. Thus, CNT were used in *Pseudomonas* cell-based biosensor for modification of carbon paste electrode; the effect of CNT content as well as conventional parameters of the sensor has been investigated (Timur et al. 2007). In addition, CNT-modified chitosan matrix was used for immobilization of *Pseudomonas* cells in a sensor's bioreceptor in parallel with the non-modified one; so, the nanoparticle effect on the efficiency of biosensor performances was tested (Odaci et al. 2008).

A new type of bacterial cell detector based on polyaniline nanofibrils has been designed and tested against bacteria *Klebsiella pneumoniae*, *P. aeruginosa*, *E. coli*, and *Enterococcus faecalis*. The cells attaching conducting nanofibrils modify locally the electrical conductivity that ensured the entrapment of cells and made the detection of  $10^5$ – $10^6$  CFU/ml possible (Langer et al. 2009). Although the work is related not to microbial biosensors but to the detection of bacteria, the technique described could be used for immobilization of the microbial cells in a sensor's bioreceptor.

The nanofabricated polyelectrolyte films based on poly (acrylic acid) and poly (allylamine hydrochloride) and other weak polyions were developed by Mendelsohn (2002). The chemical and structural properties of the films could be controlled with nanoscale precision by adjusting the pH of the polymer solutions. The efficiency of films as carriers for immobilization of mammalian fibroblasts was demonstrated. The possibility of the films' utilization in biosensor devices was proposed.



The nanostructured transducer represented by an array of nano-volume chambers on a silicon chip was used for the monitoring of bioprocesses in bacterial cells integrated within the chambers. Each chamber represented an electrochemical cell with three electrodes and could be monitored in parallel with other chambers. The device could be applied as a microphysiometer allowing tracking various reactions of the bacterial cells or as a microbial sensor ensuring the detection of target compounds (Popovtzer et al. 2005; Popovtzer et al. 2006).

The electrochemical approach for the investigation of metabolism of single cell using Kelvin nanoprobe described by Cheran et al. (2008) also deserves attention in the sense of development of microbial sensors. The authors have developed the vibrational methods which were capable of examining populations of neurons, smooth muscle, and human red blood cells on a substrate in a label-free fashion. The Kelvin nanoprobe possessed sub-micron resolution and has been successfully employed in the characterization of the cells.

Vertically aligned carbon nanofiber arrays were utilized as the interface between the electrode and neurons immobilized on a polypyrrole film (Nguyen-Vu et al. 2005). The same technique seems to be promising for the development of mediator-less microbial and enzyme sensors.

The determination of nanomaterials using the cell-based sensors is possible if the NPs are used by the cells as a source of carbon and/or energy or if they alter the cell metabolism (for example, possess toxicity or ability to induce enzyme expression). To date, a number of microbial sensors for the detection of metal ions have been described. Ramanathan et al. (1997) made a survey of bacterial biosensors for the detection of heavy metals. The approach is based on genetic modification of bacteria by DNA fusion bearing the regulatory region of the metal-resistance operon and reporter genes, e.g., the bioluminescent sensor which is based on recombinant *E. coli* strains for the measurement of toxicity of arsenic compounds (Cai and DuBow 1997).

The optical bacterial biosensor for zinc and copper detection in soil samples was based on the consortium containing the reporter bioluminescent *Rhizobium leguminosarum* biovar *trifolii* and *E. coli* strains. Bacterial suspension was used for registration. It was shown that EC<sub>25</sub> (concentration that lowered the sensor signal by 25%) for zinc ions in the samples under study was 0.3 mg/l (Chaudri et al. 2000).

In the recombinant strain constructed for bioavailable mercury detection in soil samples, the activity of the *luxCDABE* operon was regulated due to the promoter-operator system of the *mer*-operon providing cell resistance to mercury. The lower detection limit of such biosensor was around 20 ng of mercury per gram of soil (Rasmussen et al. 2000).

Thus, the construction of microbial bioluminescent and catalytic sensors for the detection of metal ions is a rather widespread approach in biosensor analysis; there is a significant probability that the sensors would also be able to detect the equivalent nanosized metals (maybe, with decreased sensitivity). It is very likely that a number of such publications will appear in years to come, and at least one work has already been described (Kasemets et al. 2009). In the work, the toxic effect of nanosized ZnO, CuO, and TiO<sub>2</sub> to *Saccharomyces cerevisiae* was

evaluated using biosensor approach. The effect of metal oxide nanoparticles, their bulk forms, and respective ionic forms were compared.

## 12.5 State-of-Art in Russian Research into Nanobiotechnology and Nanobiosensors

The research carried out at the Engelgardt Institute of Molecular Biology RAS pursues creation of structured materials based on DNA molecules. Different strategies of obtaining molecular structures by the method of “step-by-step” and “all at once” construction have been developed: such structures can be used as “carriers” of genetic material or biologically active compounds. Nanoconstructions with controllable physicochemical properties can also be used as a basis of biosensors detecting biologically active compounds, e.g., as optical filters (Evdokimov et al. 2006). At the same Institute, gel structures with DNA and protein molecules are developed for use in diagnostic chips for the detection of biological weapon agents, tuberculosis, AIDS, human genome fragments, etc. (Zasedatelev et al. 2006; V.A. Engelgardt Institute of Molecular Biology Russian Academy of Sciences 2010).

The joint studies of Shemyakin and Ovchinnikov Institute of Bioorganic Chemistry and University of Rheims pursue development of a technology for the synthesis of the biomarkers of new generation for different fields of clinical diagnostics, including cancerous and inflammatory diseases, and for the creation of new types of liquid- and solid-phase nanosensors for concurrent registration of many parameters. The review material presents advances in the methods of synthesis of fluorescent nanocrystals (quantum dots, QDs). QDs are detected as individual objects by fluorescent microscopes allowing visualization of the processes on the level of single molecules. The advantage of QDs over organic fluorophores is their high brightness, uniquely high photostability, and narrow emission peak. The fluorescence wavelength of QDs strictly depends on their size; at the same time, only one emission source is sufficient for excitation of QDs of all colors. Due to such unique properties, QDs are ideal fluorophores for supersensitive multicolor detection of biological objects and medical diagnostics requiring simultaneous registration of many parameters (Olejnikov et al. 2007).

The raster mapping of metabolic activity of a single cell, organelle, or microorganism using raster phase microscopy has been developed. The images of mitochondria, HCT 116 cells, yeasts, and thyroid cells showed the areas of such activity of less than 100 nm, which significantly exceeds the classical resolution limit in optics. The nature and possible character of interpretation of local metabolic processes are discussed (Ivanov et al. 2007).

The microfluid chip has been developed for immobilization and fluorescence intensity analysis of green fluorescent protein (GFP) from single immobilized cells of *Helicobacter pylori* strains. The possibility of culturing *H. pylori* cells inside microfluid channels during several hours without the loss of their viability has been

demonstrated. Variability of the patterns of expression of GFP from single cells has been assessed (Momyaliev et al. 2007). A method of purification of recombinant proteins using nickel NPs has been proposed. The method speeds up the purification of target preparation and reduces its cost. Recombinant proteins are bound directly in the crude cell lysate and the particles are separated from unbound proteins by the magnetic separation procedure eliminating the necessity for the expensive chromatographic methods. The method can be used in structural proteomics, in the X-ray structure analysis of proteins with unknown functions, antigen mapping of proteins, and development of vaccines based on recombinant proteins (Lazarev et al. 2007). Hydrocolloid compositions (alleviation of skin irritation, adhesive supinators, wound, ulcer, and burn dressings, and the means of delivery of medicines through skin) comprised liquid–crystal hydroxypropylcellulose and layered aluminosilicates, so that it was possible to suggest the application of nanocomposite carriers in real products (Kulichihin et al. 2006).

As a result of the nanobiotechnological study carried out at Moscow State University, the combinations of light- and temperature-sensitive materials with urease have been examined and the possibility of controlling the enzyme activity through exposure of artificial structures to heat and light has been shown. The study has demonstrated that an “enzyme–polymer” system is not only characterized by the mere sum of properties of individual components but also can acquire new properties. The developed system can also be used as a basis of a biosensor (Eremeev and Kazanskaya 1999).

Protein–protein interaction has been studied by the example of an “antibody–antigen–enzyme” system for creating a complex with possible modulation of enzyme activity during the interaction of coupled proteins. The authors have created an enzyme complex, which enhanced the catalytic activity of immobilized cholinesterase during the binding of antibody to antigen. This property improves the quality of biosensor analysis; however, in the first place, the attention is drawn to the authors’ approach to solution of one of the basic problems of nanobiotechnology: creation of molecular structures with the novel properties (Medyantseva et al. 1999). The development and characteristics of electrochemical biosensors based on the electrodes modified by carbon nanotubes for direct detection of DNA are presented (Abdullin et al. 2007); this research trend relates to biosensor studies and to nanobiotechnology. The novelty of this work is that the author has surveyed the alteration of electrode characteristics during the replacement of carbon electrodes by the electrodes modified with nanotubes; such changeover made it possible to propose the method of direct detection of DNA. The new approach in surface exploration extending the field of application of atomic force microscopy by obtaining multiparameter information on an object is presented in Molchanov et al. (2004); multiple applications of this approach have been illustrated and, in particular, the results of surface modification with polyaniline have been studied. The methods of enzyme immunodetection and scanning force microscopy (SFM) have been used to study the peculiarities of antibodies behavior on graphite surface modified by polyelectrolytes. The methods of obtaining stable films for solid-phase analysis have been developed in the format of counting single interactions by the

SFM method (Evtushenko et al. 2007). The method for manufacturing highly resistant tyrosinase biosensors based on the nanostructured films of polyelectrolytes has been developed. The dependence of activity of tyrosinase electrodes on enzyme concentration in the solution, from which the enzyme had been adsorbed on the surface of biosensors, was investigated (Dubacheva et al. 2007). Concluding the comparison, let us note that the more complete analysis of biosensor research in Russia can be found in the review offering other examples of the studies that couple the problems of biosensors and nanotechnology (Reshetilov 2007).

The new principles of biosensor development are intensively searched at the science and production association “Nanostructured Glass Technology” (Saratov). The product of development represents the new generation of miniature, completely integrated biosensors based on nanostructural materials for highly efficient systems of analysis of biomaterials and biological liquids. The goal of these works is to obtain precise information on the concentrations and molecular compositions of tested substances. The directions and fields of possible applications of proposed biosensors are rather diverse: laboratories of biochemical analysis, medical clinical diagnostics, pharmacology, process monitoring, raw stuff and product quality control in pharmaceutical, biotechnological and food industries, environmental monitoring, certification and expertise of goods, scientific and educational laboratories. The construction of an optical nanostructural biosensor for detection of ultra-low concentrations of biological substances is being developed (LLC SPE “Nanostructured Glass Technology” 2010).

## 12.6 Conclusions

In conclusion, we would like to mention what nanotechnology and nanosensors can afford. It is well known that the small dimensions of nanoparticles lead to considerable increase in the surface-to-volume ratio that results in the predomination of the surface phenomena over the chemistry and physics in the bulk. This fact explains most of the advantages of nanosensors over the traditional ones observed in a number of publications – the increase in sensitivity, better limits of detection, decrease in volume of the sample being analyzed, the possibility of direct (label-free) detection and elimination of some reagents and pretreatment steps, etc. So, the science of nanomaterials deals with the new phenomena and the nanosensor devices being built which takes advantage of these phenomena.

Nevertheless, one cannot deny the powerful analytical basis represented by macro-sized, i.e., traditional, biosensors. From the chronological point of view, biosensor technology can be considered as a basis, on which the analytical biotechnology and nanobiotechnology started to develop. At present, the analytical nanobiotechnology is an area of extensive goals and objectives. The common point of contact providing undoubted benefit is application of biological material in the macro- and nano-format for construction of analytical devices.

**Acknowledgments** The work was partially supported by the grant for research work in the scope of Federal target program “Scientific and research-pedagogic personnel of innovative Russia” for 2009–2013 (GK NK-no. 37(4)).

## References

- Abdullin TI, Nikitina II, Ishmukhametova DG, Budnikov GK, Konovalova OA, Salakhov MK (2007) Carbon nanotube-modified electrodes for electrochemical DNA-sensors. *J Anal Chem Russ* 62:599–603
- Abramova N, Bratov A (2009) Photocurable polymers for ion selective field effect transistors. 20 years of applications. *Sensors* 9:7097–7110
- Cai J, DuBow MS (1997) Use of a luminescent bacterial biosensor for biomonitoring and characterization of arsenic toxicity of chromated copper arsenate (CCA). *Biodegradation* 8:105–111
- Chaudri AM, Lawlor K, Preston S, Paton GI, Killham K, McGrath SP (2000) Response of a Rhizobium-based luminescence biosensor to Zn and Cu in soil solutions from sewage sludge treated soils. *Soil Biol Biochem* 32:383–388
- Chen Z-G (2007) Conductometric immunosensors for the detection of staphylococcal enterotoxin B based bio-electrocatalytic reaction on micro-comb electrodes. *Bioprocess Biosyst Eng* 31:345–350
- Cheng Y, Liu Y, Huang J, Li K, Xian Y, Zhang W, Jin L (2008) Amperometric tyrosinase biosensor based on Fe<sub>3</sub>O<sub>4</sub> nanoparticles-coated carbon nanotubes nanocomposite for rapid detection of coliforms. *Electrochim Acta* 54:2588–2594
- Cheran L-E, Cheung S, Wang X, Thompson M (2008) Probing the bioelectrochemistry of living cells. *Electrochim Acta* 53:6690–6697
- Dubacheva GV, Porus MV, Sokolovskaya LG, Sigolaeva LV, Pergushev DV, Yaroslavov AA, Eremenko AV, Kurochkin IN, Varfolomeev SD (2007) Nanostructural polyelectrolyte films for highly sensitive tyrosinase biosensors constructing. *Nanotechnol Rus* 2:154–159
- Eremeev NL, Kazanskaya NF (1999) Linked enzyme reactions producing responses in stimulus-sensitive polymer systems. *Sensornye Sist* 13:239–245
- Evdokimov YM, Zakharov MA, Skuridin SG (2006) Nanotechnology based on nucleic acids. *Her Russ Acad Sci* 1:5–11
- Evtushenko EG, Kurochkin IN, Doncova EA, Budashov IA, Eremenko AV, Golovachenko VA, Polynceev DG, Tur DR, Pergushov DV, Papkov IS, Zezin AB, Varfolomeev SD (2007) Antibody nanofilms based on polyelectrolytes for extremely sensitive immunoassays. *Nanotechnol Rus* 2:145–153
- Gruner G (2006) Carbon nanotube transistors for biosensing applications. *Anal Bioanal Chem* 384:322–335
- Hasunuma T, Kuwabata S, Fukusaki E, Kobayashi A (2004) Real-time quantification of methanol in plants using a hybrid alcohol oxidase-peroxidase biosensor. *Anal Chem* 76:1500–1506
- Haustein E, Schwille P (2004) Single-molecule spectroscopic methods. *Curr Opin Struct Biol* 14:531–540
- Ivanov AB, Kretushev AV, Ignat'ev PS, Vyshenskaya TV, Tychinskii VP (2007) Raster method of localization of nanosized areas of metabolic activity in phase images of cells. *Nanotechnol Rus* 2:120–125
- Joung HA, Lee NR, Lee SK, Ahn J, Shin YB, Choi HS, Lee CS, Kim S, Kim MG (2008) High sensitivity detection of 16s rRNA using peptide nucleic acid probes and a surface plasmon resonance biosensor. *Anal Chim Acta* 630:168–173
- Kasemets K, Ivask A, Dubourguier HC, Kahru A (2009) Toxicity of nanoparticles of ZnO, CuO and TiO<sub>2</sub> to yeast *Saccharomyces cerevisiae*. *Toxicol In Vitro* 23:1116–1122

- Koets M, van der Wijk T, van Eemeren JT, van Amerongen A, Prins MW (2009) Rapid DNA multi-analyte immunoassay on a magneto-resistance biosensor. *Biosens Bioelectron* 24:1893–1898
- Kulichihin VG, Antonov SV, Makarova VV, Semakov AV, Singh P (2006) Hydrocolloid adhesives for biomedical application based on nanocomposite concept. *Nanotechnol Rus* 1:170–182
- Langer JJ, Langer K, Barczyński P, Warchol J, Bartkowiak KH (2009) New “ON-OFF”-type nanobiosensor. *Biosens Bioelectron* 24:2947–2949
- Lazarev VN, Filatova EV, Levickii SA, Nikolaev EN, Leipunskii IO, Jigach AN, Kuskov ML, Govorun VM (2007) Development of method for purification of recombinant proteins using nickel nanoparticles. *Nanotechnol Rus* 2:133–140
- Lee C-S, Kim SK, Kim M (2009) Ion-sensitive field-effect transistor for biological sensing. *Sensors* 9:7111–7131
- Lioubashevski O, Chegel VI, Patolsky F, Katz E, Willner I (2004) Enzyme-catalyzed bio-pumping of electrons into Au-nanoparticles: a surface plasmon resonance and electrochemical study. *J Am Chem Soc* 126:7133–7143
- LLC SPE “Nanostructured Glass Technology” (2010) Biochips/Products/Main page/LLC SPE “Nanostructured Glass Technology” (LLC SPE “NGT”). <http://ngt2005.narod.ru/catalog/Biochip/>. Cited 2 Jan 2010
- McFarland AD, Van Duyne RP (2003) Single silver nanoparticles as real-time optical sensors with zeptomole sensitivity. *Nano Lett* 3:1057–1062
- Medyantseva EP, Kutyreva MP, Khaldeeva EV, Glushko NI, Budnikov GK (1999) Determination of the *Phytophthora infestans* antigen with the use of an immunoenzyme amperometric sensor. *J Anal Chem Russ* 54:1147–1151
- Mendelsohn JD (2002) Polyelectrolyte multilayers: nanofabricated architectures for bio-interface materials. Massachusetts Institute of Technology, Department of Materials Science and Engineering, Ph.D. thesis: 135 p.
- Molchanov SP, Chernova-Kharaeva IA, Abdullaeva SH and Alekperov SD (2004) Electrochemical modification of polyaniline surface using SPM. Proceedings of I International Scientific Seminar “Light in Nanosize Solids”, Baku
- Momynaliev KT, Lazarev VN, Kostryukova ES, Chelysheva VV, Selezneva OV, Kravchenko EV, Govorun VM (2007) Microfluid technologies for detection of intracellular processes in bacterial cell. *Nanotechnol Rus* 2:126–132
- Narváez A, Suárez G, Popescu IC, Katakis I, Domínguez E (2000) Reagentless biosensors based on self-deposited redox polyelectrolyte-oxidoreductases architectures. *Biosens Bioelectron* 15:43–52
- Nguyen-Vu TDB, Chen H, Cassell AM, Andrews R, Meyyappan M, Li J (2005) Vertically aligned carbon nanofiber arrays: an advance toward electrical-neural interfaces. *Small* 2:89–94
- Odaci D, Timur S, Telefoncu A (2008) Bacterial sensors based on chitosan matrices. *Sens Actuators B Chem* 134:89–94
- Olejnikov VA, Sukhanova AV, Nabiev IR (2007) Fluorescent semiconductor nanocrystals for biology and medicine. *Nanotechnol Rus* 2:160–173
- Plekhanova YV, Reshetilov AN, Yazynina EV, Zherdev AV, Dzantiev BB (2003) A new assay format for electrochemical immunosensors: polyelectrolyte-based separation on membrane carriers combined with detection of peroxidase activity by pH-sensitive field-effect transistor. *Biosens Bioelectron* 19:109–114
- Popovtzer R, Neufeld T, Biran D, Ron EZ, Rishpon J, Shacham-Diamand Y (2005) Novel integrated electrochemical nano-biochip for toxicity detection in water. *Nano Lett* 5:1023–1027
- Popovtzer R, Neufeld T, Ron EZ, Rishpon J, Shacham-Diamand Y (2006) Electrochemical detection of biological reactions using a novel nano-bio-chip array. *Sens Actuators B Chem* 119:664–672

- Qu L, Xia S, Bian C, Sun J, Han J (2009) A micro-potentiometric hemoglobin immunosensor based on electropolymerized polypyrrole-gold nanoparticles composite. *Biosens Bioelectron* 24:3419–3424
- Ramanathan S, Ensor M, Daunert S (1997) Bacterial biosensors for monitoring toxic metals. *Trends Biotechnol* 15:500–506
- Rasmussen LD, Sorensen SJ, Turner RR, Barkay T (2000) Application of a mer-lux biosensor for estimating bioavailable mercury in soil. *Soil Biol Biochem* 32:639–646
- Reshetilov AN (2007) Biosensor development in Russia. *Biotechnol J* 2:849–862
- Reshetilov AN, Efremov DA, Iliasov PV, Boronin AM, Kukushkin NI, Greene RV, Leathers TD (1998) Effects of high oxygen concentrations on microbial biosensor signals. Hyperoxygenation by means of perfluorodecalin. *Biosens Bioelectron* 13:795–799
- Risveden K, Ponten JF, Calander N, Willander M, Danielsson B (2007) The region ion sensitive field effect transistor, a novel bioelectronic nanosensor. *Biosens Bioelectron* 22:3105–3112
- Ros R, Eckel R, Bartels F, Sischka A, Baumgarth B, Wilking SD, Puhler A, Sewald N, Becker A, Anselmetti D (2004) Single molecule force spectroscopy on ligand-DNA complexes: from molecular binding mechanisms to biosensor applications. *J Biotechnol* 112:5–12
- Sanvicens N, Pastells C, Pascual N, Marco M-P (2009) Nanoparticle-based biosensors for detection of pathogenic bacteria. *Trends Anal Chem* 28:1243–1252
- Schöning MJ, Poghossian A (2006) Bio FEDs (field-effect devices): state-of-the-art and new directions. *Electroanalysis* 18:1893–1900
- Skottrup PD, Nicolaisen M, Justesen AF (2008) Towards on-site pathogen detection using antibody-based sensors. *Biosens Bioelectron* 24:339–348
- So HM, Park DW, Jeon EK, Kim YH, Kim BS, Lee CK, Choi SY, Kim SC, Chang H, Lee JO (2008) Detection and titer estimation of *Escherichia coli* using aptamer-functionalized single-walled carbon-nanotube field-effect transistors. *Small* 4:197–201
- Stern E, Klemic JF, Routenberg DA, Wyrembak PN, Turner-Evans DB, Hamilton AD, LaVan DA, Fahmy TM, Reed MA (2007) Label-free immunodetection with CMOS-compatible semiconducting nanowires. *Nature* 445:519–522
- Timur S, Anik U, Odaci D, Gorton L (2007) Development of a microbial biosensor based on carbon nanotube (CNT) modified electrodes. *Electrochem Commun* 9:1810–1815
- Turner APF, Karube I, Wilson GS (eds) (1987) *Biosensors: fundamentals and applications*. Oxford University Press, New York
- V.A. Engelgardt Institute of Molecular Biology Russian Academy of Sciences (2010) Laboratory of biological microchips. <http://www.biochip.ru/en/index.html>. Cited 2 Jan 2010
- Vijayalakshmi A, Tarunashree Y, Baruwati B, Manorama SV, Narayana BL, Johnson RE, Rao NM (2008) Enzyme field effect transistor (ENFET) for estimation of triglycerides using magnetic nanoparticles. *Biosens Bioelectron* 23:1708–1714
- Villamizar RA, Maroto A, Rius FX, Inza I, Figueras MJ (2008) Fast detection of *Salmonella* *Infantis* with carbon nanotube field effect transistors. *Biosens Bioelectron* 24:279–283
- Vogel V, Baird B (2003) Nanobiotechnology. In: National Nanotechnology Initiative Workshop. October 9–11, Arlington, VA, USA: pp 1–106
- Zasedatelev A, Nasedkina T, Rubina A, Gryadunov D (2006) In: Proceedings of NATO advanced research workshop “commercial and pre-commercial cell detection technologies for defense against bioterror – technology, market and society”, Brno, Czech Republic

# Chapter 13

## Metallic Nanoparticles: Biological Perspective

Sunil K. Singh, Siddhartha Shrivastava, and Debabrata Dash

### 13.1 Introduction

In recent years research involving NPs has generated a great deal of interest from scientists and engineers of nearly all disciplines. Among different nanomaterials employed for biomedical research, metallic NPs have been proved to be the most convenient and suitable. Based on their unique optical, electrical, magnetic properties, specific heats, melting points, and surface reactivities, metallic NPs have found significant applications in a wide spectrum of biomedical utilities like imaging, sensing, drug delivery, and gene targeting. As all the properties of metallic NPs are size and shape dependent, methods for their preparation are one of the primary thrust areas of researchers.

Nanostructured metal colloids have been obtained by “top-down” and “bottom-up” approaches. A typical “top-down” also called as physical method involving the mechanical grinding of bulk metals and subsequent stabilization of the resulting nanosized metal particles by the addition of colloidal protecting agents (Gaffet et al. 1996; Amulyavichus et al. 1998). The “bottom-up” i.e., chemical methods of wet chemical nanoparticle preparation rely on the chemical reduction of metal salts, electrochemical pathways, or the controlled decomposition of metastable organo-metallic compounds. A large variety of stabilizers, e.g., donor ligands, polymers, and surfactants, are used to control the growth of the primarily formed nanoclusters and to prevent them from agglomerating.

The present chapter is concerned about biomedical or biological applications of metallic NPs; we do not have scope to describe all the existing methods for preparation of metallic NPs. This section will be restricted to synthesis of biocompatible metallic NPs, which can be easily administered under *in vivo* conditions. In this context, some major advances have been made by employing methods based on chemical reactions in solution (often termed “wet chemistry”). A wet chemical

---

S.K. Singh, S. Shrivastava, and D. Dash (✉)

Department of Biochemistry, Institute of Medical Sciences, Banaras Hindu University, Varanasi 221005, India

e-mail: ddass@satyam.net.in



procedure involves growing NPs in a liquid medium containing various reactants, in particular reducing agents, e.g., sodium borohydride (Kim et al. 2007) or potassium bitartrate (Tan et al. 2003) or methoxypolyethylene glycol (Mallick et al. 2004) or hydrazine (Li et al. 1999). Generally, in these methods glucose or some biocompatible reagent are used as reducing agents in place of strong chemical reductants. Stabilizing agents, e.g., donor ligands, polymers, and surfactants are often employed to prevent NPs from agglomeration and are such that they are easily miscible under cellular conditions. A surfactant is a molecule that is dynamically adsorbed to the surface of the NPs under the reaction conditions. It must be mobile enough to provide access for the addition of monomer units, while stable enough to prevent the aggregation of NPs. The choice of surfactant varies from case to case: a molecule that binds too strongly to the surface of the NPs is not suitable, as it would not allow the NPs to grow. On the other hand, a weakly coordinating molecule would yield large particles, or aggregates (Peng et al. 1998). Some examples of a suitable surfactant or stabilizing agent include, for instance, alkyl thiols, phosphines, phosphine oxides, phosphates, amides or amines, carboxylic acids, sodium dodecyl benzyl sulfate, or polyvinyl pyrrolidone (Li et al. 1999; Zameer et al. 2008; Ghosh and Kolay 2008; Redd et al. 2009; Akbarzadeh et al. 2009). As most of the surfactants used are not compatible to cells and tissues, bovine serum albumin is a popular choice to use as stabilizing agent. Scientists have endeavored to make use of microorganisms as possible eco-friendly nanofactories for the synthesis of metallic NPs (Bolander et al. 2006) such as cadmium sulfide (Ahmad et al. 2002), gold (Mukherjee et al. 2002), and silver (Basavaraja et al. 2008). We shall discuss in detail about this biogenic synthesis of various metallic nanomaterials in their respective sections. In recent years, metallic NPs and their alloys have been studied extensively in various fields like sensor technology (Han et al. 2001), optical devices (Kamat 2002), catalysis (Kim et al. 2003b), biological labeling (Nicewarner-Pena et al. 2001), drug delivery system (Mann and Ozin 1996), and treatment of some cancers (O'Neal et al. 2004). Metallic NPs are quite suitable as a marker for the optical detection of biomolecules in applications such as antimicrobial, antiplatelet, stabilization of proteins, drug delivery, or in photothermal therapeutic applications, due to their excellent SPR properties. These are the extremely promising prospects in the field of health and medicine. This article provides the researchers a comprehensive present status of the field and points them to other appropriate opportunities where these metallic nanomaterials can be employed to cater unmet biomedical goals. In this report we discuss various types of metallic NPs (Table 13.1) which are belonging to different groups of periodic table and their

**Table 13.1** Metals that exist in the form of nanopowders and nanostructured metal colloids from different Groups of Periodic table

Cr	Mn	Fe	Co	Ni	Cu
Mo	–	Ru	Rh	Pd	Ag
–	Re	Os	Ir	Pt	Au

Adapted from Bonnemann et al. (1996).

applications in biomedical fields. This table gives the overview of some metals that exist in the form of nanopowder and their colloidal state.

## 13.2 Application Potential of Silver Nanoparticles in Biological Sciences

Silver NPs are generally smaller than 100 nm and contain 20–15,000 silver atoms. Silver NPs have been receiving considerable attention as a result of their unique physical, chemical, biological properties, and their important applications in optics, electronics, and biomedicine. Hence, there is a growing need to develop environmentally benign metallic NPs synthesis process that does not use toxic chemicals and involves environmentally friendly procedures for the synthesis and assembly of metallic NPs. Silver NPs are synthesized through both physical and chemical methods. But mostly the silver NPs are synthesized through chemical method because of their simplicity and cost effectiveness that involves chemical reduction of silver ions in aqueous solutions with or without stabilizing agents, thermal decomposition in organic solvents. In this context, some major advances have been made by employing methods based on chemical reactions in which citric acid, glucose, or some biocompatible reagents are used as reducing agents in place of strong chemical reductants. Stabilizing agents, e.g., donor ligands, polymers, and surfactants are often employed to prevent silver NPs from agglomeration. In our earlier reports we have successfully synthesized biocompatible silver NPs with enhanced stabilization having antibacterial property by using glucose as reducing agent (Shrivastava et al. 2007) and bovine serum albumin as stabilizing agent (Singh et al. 2009). As mentioned above biogenic process involving microorganisms is another approach for biosynthesis of biocompatible silver NPs. Several attempts have been made in this direction. Klaus et al. (1999) have shown that bacterium *Pseudomonas stutzeri* AG259, isolated from silver mine, played a major role in the reduction of the  $\text{Ag}^+$  ions and the formation of silver NPs when placed in a concentrated aqueous solution of silver nitrate. Silver NPs of well-defined size and distinct topography are formed within the periplasmic space of the bacteria. Basavaraja et al. (2008) and Nanda and Saravanan (2009) have synthesized the silver NPs by using fungus *Fusarium semitectum* and *Staphylococcus aureus*, respectively. Recently, another group has successfully synthesized silver NPs having synergistic effect against gram positive and gram negative bacteria (Fayaz et al. 2010).

Metallic NPs of silver have aptly been investigated for their antibacterial property. Commendable efforts have been made to explore this property using electron microscopy, which has revealed size-dependent interaction of silver NPs with bacteria (Morones et al. 2005). Metallic NPs of silver have thus been studied as a medium for antibiotic delivery (Li et al. 2005), and to synthesize composites for use as disinfecting filters (Jain and Pradeep 2005) and coating materials

(Li et al. 2006). However, the bactericidal property of these metallic NPs depends on their stability in the growth medium, since this imparts greater retention time for bacterium–nanoparticle interaction. There lies a strong challenge in preparing metallic NPs of silver stable enough to significantly restrict bacterial growth. In our earlier report we showed the synthesis of highly stable metallic NPs of silver endowed with significant antibacterial properties. Efforts have been made to understand the underlying molecular mechanism of such antimicrobial actions (Shrivastava et al. 2007; Durán et al. 2007; Rai et al. 2009). In this report we have for the first time shown that silver NPs can bring about changes in tyrosine phosphoproteome of bacteria, thus impacting bacterial cell signaling. Besides their innate antibacterial property, silver NPs could have many other applications in areas such as non-linear optics, spectrally selective coating for solar energy absorption, and intercalation materials for electrical batteries, effectively used for improving the conductivity of electronically conductive adhesives (ECAs), as optical receptors and biolabeling (Kowshik et al. 2003). In biomedical applications, it was reported by Elechiguerra et al. (2005) that silver NPs in a size range 1–10 nM bind to HIV-1 in a size-dependent fashion. The authors have shown that silver NPs inhibit HIV-1 infection in CD4+MT-2 cells and cMAGI HIV-1 reporter cells. At present use of silver is reemerging as a viable treatment for infections encountered in burns (Moyer 1965; Klasen 2000). More recently, silver has also been used as a biocide to prevent infection in burns, traumatic wounds, and diabetic ulcers (Silver et al. 2006). Other uses include improved surface coating for indwelling catheters and other medical devices implanted on/within the body (Darouiche 1999; Stevens et al. 2009; Chen and Schluesener 2008).

Recently, we have for the first time showed that silver NPs have innate anti-platelet property and can effectively prevent integrin-mediated platelet responses, both *in vivo* and *in vitro*, in a concentration-dependent manner (Shrivastava et al. 2009). Our findings further suggest that these metallic NPs do not confer any lytic effect on platelets and thus hold potential to be promoted as antiplatelet/antithrombotic agent after careful evaluation of toxic effects. Thus, use of silver NPs is becoming more and more widespread in medicine and related applications and due to increasing exposure toxicological and environmental issues need to be raised. There has been a continuous debate on the advantages and disadvantages of the use of silver products in health care and medicine (Silver et al. 2006). Probably, one of the most reported side effects of silver products is argyria. Argyria occurs when sub-dermal silver deposits in skin microvessels resulting in an irreversible gray to black coloration of the skin (Kakurai et al. 2003). This permanent discoloration is not physically harmful but remains an inherent serious cosmetic problem (Silver et al. 2006). There are also some reports of kidney toxicity and cytotoxicity (Chaby et al. 2005). Liver toxicity has also been observed following acute silver toxicity due to nanocrystalline silver (Trop 2006). Therefore, understanding the kinetics and toxicity of silver NPs *in vivo* is very important in the context of the underlying medical debate regarding the safety of silver NPs and nanomaterials coated with silver. There are several reports that clearly demonstrate that silver, in minute concentrations, is non-toxic to human cells. The epidemiological history of

silver has established non-toxicity in normal use (Silver 2003; Silver et al. 2006). Thus, it is our opinion that these are questions that need to be imperatively answered before people rush to indulge into the silver NPs boom.

### 13.3 Gold Nanoparticles as Important Biomedical Tool

In past decades, gold NPs have attracted a continuous interest and have been explored as a model platform for biomedical research because of their unusual but unique physical and chemical properties (Katz and Willner 2004; Alivisatos 2004; Ghadiali and Stevens 2008; Stewart et al. 2008; Murphy et al. 2008). Gold NPs are inert, which makes them relatively more biocompatible. The synthesis of gold NPs with diameters ranging from a few to several hundreds of nanometres is well established in aqueous solution as well as in organic solvents. Like silver NPs, gold NPs are also synthesized through chemical reduction method. In typical syntheses, gold salts such as  $\text{HAuCl}_4$  are reduced by the addition of a reducing agent which leads to the nucleation of Au ions to NPs. Turkevich et al. (1951) for the first time synthesized the colloidal gold  $\text{Au}^0$  from  $\text{Au}^{\text{III}}$  by using citric acid as reducing agent, a method that is still used now-a-days to subsequently replace the citrate ligand of these gold NPs by appropriate ligands of biological interest (Daniel and Astruc 2004). Recent modifications of the Turkevitch method have allowed better size distribution and size control within the 9–120 nm range (Kimling et al. 2006). In addition, stabilizing agents are also required which are either adsorbed or chemically bound to the surface of the gold NPs. These stabilizing agents (often also called a surfactant) are typically charged, so that the equally charged NPs repel each other so that they are colloidally stable. Gold NPs can be stabilized by a large variety of stabilizers (ligands, surfactants, polymers, dendrimers, biomolecules, etc.) (Daniel and Astruc 2004). The most robust gold NPs were disclosed by Giersig and Mulvaney (1993) that can be stabilized by thiolates using the strong Au–S bond between the soft acid Au and the soft thiolate base. Along this line, by far the most popular synthetic method using such sulfur coordination for gold NPs stabilization is the Shiffrin–Brust biphasic synthesis using  $\text{HAuCl}_4$ , a thiol, tetraoctylammonium bromide, and  $\text{NaBH}_4$  in water–toluene yielding thiolate-gold NPs (Brust et al. 1994). Functional thiolates can also be introduced using this method or upon subsequent bimolecular substitution of a thiolate ligand by such a functional thiol (Templeton et al. 2001). Oligonucleotides, peptides, and poly-ethylene glycol are easily attached to gold NPs in this way. Since the solubility of these gold NPs is controlled by the solubilizing properties of the terminal group of the thiolate ligands, gold NPs can be transferred from an aqueous phase to an organic phase or vice versa by appropriate ligand exchange. Water-soluble gold NPs typically contain terminal carboxylate groups at their periphery. The carboxy group is used to attach the amino groups of biomolecules using 1-ethyl-3-(3-dimethylaminopropyl)-carbodiimide-HCl (EDC) (Sperling et al. 2008). With related strategies almost all kinds of biological molecules can be attached to the particle surface. Though such

protocols are relatively well established, bioconjugation of gold NPs still is not trivial and characterization of synthesized conjugates is necessary, in particular to rule out aggregation effects or unspecific binding during the conjugation reaction. In particular, in many conjugation protocols the number of attached molecules per gold NPs is only a rather rough estimate, as no standard method for determining the surface coverage of particles modified with molecules has yet been established (Demers et al. 2000; Pellegrino et al. 2007).

Very interestingly, not only spherical gold NPs but also NPs bearing various shapes and geometries such as rod or hollow shells can also be synthesized by using appropriate techniques. Gold NPs have been primarily used for labeling applications. In this regard, the particles are directed and enriched at the region of interest and they provide contrast for the observation and visualization of this region. Gold NPs strongly absorb and scatter visible light. Upon light absorption the light energy excites the free electrons in the gold NPs to a collective oscillation, the so-called surface plasmon. Generally, the optical properties of small metallic NPs are dominated by collective oscillation of electrons at surfaces (known as Surface Plasmon Resonance or SPR) that are in resonance with the incident electromagnetic radiation (El-Sayed 2001; Liz-Marzán 2004; Daniel and Astruc 2004). For gold, it happens that the resonance frequency of this oscillation, governed by its bulk dielectric constant, lies in the visible region of the electromagnetic spectrum (El-Sayed 2001). Because metallic NPs have a high surface area to volume ratio, the plasmon frequency is exquisitely sensitive to the dielectric (refractive index) nature of its interface with the local medium. Any change to the environment of these particles (surface modification, aggregation, medium refractive index, etc.) leads to colorimetric changes of the dispersions (Murphy 2002; Kelly et al. 2003; Daniel and Astruc 2004; Rosi and Mirkin 2005; Burda et al. 2005; Niemeyer and Simon 2005). Due to coupling of the plasmons, aggregation of gold NPs is often accompanied by a distinct color change from red (disperse) to blue (aggregated).

As the gold NPs provide excellent contrast for TEM imaging with high lateral resolution (Faulk and Taylor 1971) and are more stable (do not suffer from photo-bleaching), which is a major limitation for fluorescence based methods, they are widely used in immunostaining and single particle tracking for visualizing structures within single cells. Gold NPs have also been used for a long time for delivery of molecules into cells. For this purpose the molecules are adsorbed on the surface of the gold NPs and the whole conjugate is introduced into the cells. Introduction into cells can either be forced as in the case of gene guns or achieved naturally by particle ingestion. Inside cells the molecules will eventually detach themselves from the gold NPs. This particle uptake-mediated delivery of molecules into cells is used mainly for two applications. First, in gene therapy DNA is introduced into cells, which subsequently causes the expression of the corresponding proteins (Salem et al. 2003; Rosi et al. 2006). Second, in drug targeting anticancer drugs are delivered specifically to cancer tissue (Rojo et al. 2004; Jain et al. 2007). Delivery applications using gold NPs have been reviewed recently (Ghosh et al. 2008). Besides imaging, gold NPs also act as a heat source because the free electrons in the gold NPs are excited upon absorption of light. Excitation at the plasmon

resonance frequency causes a collective oscillation of the free electrons. Upon interaction between the electrons and the crystal lattice of the gold NPs, the electrons relax and the thermal energy is transferred to the lattice. Subsequently, the heat from the gold NPs is dissipated into the surrounding environment (Govorov et al. 2006). Controlled heating of gold NPs can be used in several ways for manipulating the surrounding tissues (Pissuwan et al. 2006). Due to the heat released by the gold NPs to the surrounding tissue, cancerous tissues can be destroyed locally (Hyperthermia) (Huff et al. 2007; Lowery et al. 2006) without exposing the entire organism to elevated temperatures.

Based upon bioconjugation ability, surface plasmon, fluorescence quenching, surface enhanced Raman scattering, and electron transfer characteristics, gold NPs have highly been explored in the field of sensor. Although gold NPs are composed of an inert material and have extraordinary properties, biocompatibility issues have to be well addressed. Several groups have examined the cellular uptake and cellular toxicity of gold NPs. Cells exposed to gold NPs will incorporate the particles (similar to NPs of other materials) and store inside the cells in perinuclear compartments, vesicular structures close to the cell nucleus (Chithrani et al. 2006; Patra et al. 2007). Due to particle internalization, cells or tissues in contact with gold NPs will be exposed to the particles for extended periods of time. Inflammatory effects in tissues caused by gold NPs have been demonstrated. However, in cell culture experiments gold NPs are regarded as biocompatible and acute cytotoxicity has not been observed so far (Connor et al. 2005). In particular, no release of toxic ions as in the case of cadmium NPs (Kirchner et al. 2005) has been reported. On the other hand, there are few examples of toxic effects related to the nature of gold, which might depend on the cell line (Shukla et al. 2005; Patra et al. 2007). For example, 33 nm citrate-capped gold nanospheres were found to be non-toxic to baby hamster kidney and human hepatocellular liver carcinoma cells, but were cytotoxic to a human carcinoma lung cell line as reported by Patra et al. (2007). Gold cytotoxicity also depend on surface chemistry (Goodman et al. 2004), and on the particle size (Pan et al. 2007). The toxicity of the gold NPs is related to their interactions with the cell membrane, a feature initially mediated by their strong electrostatic attraction to the negatively charged bilayer. However, to determine and understand the toxic effects of gold NPs, strategies and interpretation of the data must be done correctly and assumptions must be taken into consideration to ameliorate the observed toxicity.

### 13.4 Other Biomedically Important Nanoparticles

Metallic NPs are among the most widely used types of engineered nanomaterials. Apart from the above discussed biomedical applications of silver and gold NPs, metallic NPs are also used in integration with magnetic NPs. They together form heterodimer structures that offer two distinct surfaces and properties to allow different kinds of functional molecules to attach onto the specific parts of the

heterodimers, which may bind to multiple receptors or act as agents for multimodality imaging (Gao et al. 2009). Magnetic NPs are well-established nanomaterials that provide many exciting opportunities in biomedical applications. They not only deliver controllable sizes ranging from a few up to tens of nanometers, but they can also be manipulated by external magnetic force along with enhancement of contrast in magnetic resonance imaging (MRI). As a result, these NPs have been found promising in several applications in biology and medicine, including protein purification, drug delivery, imaging, tagging, sensing, and separation in recent years (Qiang et al. 2006; Majewski and Thierry 2007). Biomedical applications of magnetic NPs can be classified according to their application inside or outside the body. In vivo applications could further be separated into therapeutic (hyperthermia and drug-targeting) and diagnostic (nuclear magnetic resonance (NMR) imaging) applications. As far as in vitro applications are concerned, their main uses lie in diagnostics (separation/selection and bioassays). Iron and their oxides such as magnetite ( $\text{Fe}_3\text{O}_4$ ) or maghemite ( $\gamma\text{-Fe}_2\text{O}_3$ ) are by far the most commonly employed for biomedical applications (Qiang et al. 2006; Majewski and Thierry 2007). They are also used in conjugation with compounds such as dextran or starch as a coating material to increase their further biocompatibility (Hatch and Stelter 2001; Zhao et al. 2002; Fritzsche and Taton 2003; Kim et al. 2003a; Tada et al. 2003).

Other magnetic nanomaterials such as cobalt and nickel NPs are also used in biomedical field but are of little interest because of their toxicity, susceptible to oxidation (Majewski and Thierry 2007). Magnetic NPs, like silver or gold particles, have been frequently synthesized by the reduction of metal salts using reducing agents in the presence of surfactant molecule (Frey et al. 2009). Recently, techniques and procedures for producing monodispersed and size-controllable magnetic NPs (e.g., FePt,  $\text{Fe}_3\text{O}_4$ , and  $\gamma\text{-Fe}_2\text{O}_3$ ) have advanced considerably (Sun 2006; Park et al. 2007), which leads to very active explorations of the applications of magnetic NPs, in the field of biomedicine. One of the simplest and most efficient methods of developing integrated metallic and magnetic NPs is the sequential growth of metallic components (e.g., Ag or Au) onto a “colloidosome” (i.e., the self-assembly of NPs at a liquid–liquid interface) of magnetic NPs (Gu et al. 2005). The metallic nucleation takes place on the exposed surface of the magnetic NPs and produces the heterodimers of two distinct nanospheres. Yu et al. (2005) reported another way to fabricate  $\text{Fe}_3\text{O}_4$ -Au heterodimers in a homogeneous organic solvent, where the thermal decomposition of  $\text{Fe}(\text{CO})_5$  onto the surface of the gold NPs and the following oxidation of intermediate result in uniform  $\text{Fe}_3\text{O}_4$ -Au heterodimers. The heterodimer structure offers particles with two distinct surfaces. Different kinds of functional molecules can covalently bind to the specific parts of the heterodimers. For instance,  $\text{Fe}_3\text{O}_4$  can support a specific biomolecule for targeting using dopamine as a robust anchor (Xu et al. 2004; Lee et al. 2007). For the Ag or Au component, one can use the well-developed gold-thiol chemistry for the attachment of thiol-terminated biomolecules (Cao et al. 2002; Love et al. 2005). Together with own distinct functionalities, these multifunctional heterodimers can respond to

magnetic forces, show enhanced resonance absorption and scattering, and bind with specific receptors. Using epidermal growth factor receptor isoform A (EGFRA)-conjugated  $\text{Fe}_3\text{O}_4$ -Au heterodimer NPs, Xu et al. (2008) have demonstrated their dual-functional imaging property for cell tracking. This type of heterodimer nanoparticle may have great potential in multimodal biomedical applications (Jiang et al. 2008), especially for molecular imaging, but a substantive amount of work need to be done to achieve these promising applications.

### 13.5 Future Directions and Conclusion

NPs, whether they originate from semiconductors or from metals, are generally associated with the appearance of novel properties. As all the properties of metallic NPs are size and shape dependent, methods for their preparation are one of the primary thrust areas of researchers. Even the most difficult step in all synthetic procedures, the achievement of monodispersity of the particles can be controlled satisfactorily. Because of the long history of metal NPs, there has been plenty of time to develop perfect syntheses. One decisive finding opened up completely novel strategies for metal NPs synthesis: the use of protecting ligand shells, usually consisting of organic molecules. Amines, phosphines, phosphine oxides, thiols, and numerous other classes of compounds have been used. Such coordinating molecules not only support the synthesis of monodisperse NPs by their kinetic and size-limiting functions, but also make the particles soluble in solvents depending on the chemical nature of the ligand molecules. Metallic NPs are quite suitable as markers for the optical detection of biomolecules as well as in antimicrobial, antiplatelet, protein stabilization, drug delivery, and photothermal applications, due to their excellent SPR properties. In biosciences, NPs are replacing organic dyes in the applications that require high photostability as well as high multiplexing capabilities. There are some developments in directing and remotely controlling the functions of nanoprobe, for example driving magnetic NPs to the tumor and then making them either release the drug load or just heat them (hyperthermal therapy) in order to destroy the tumor. The major trend in further development of nanomaterials is to make them multifunctional and controllable by external signals or by local environment, thus essentially turning them into nanodevices with extremely promising prospects in the field of health and medicine. The toxic effects of metallic NPs must be taken into consideration before making assumptions regarding their potential therapeutic applications. Combining distinctive novel properties of NPs provides unique opportunity for physicists, chemists, biologists, and material scientists to mold the new area of nanobiotechnology.

**Acknowledgements** The authors are thankful to the Department of Biotechnology, Government of India, Indian Council of Medical Research, and the DST-UNANST, Banaras Hindu University, for the grants.



## References

- Ahmad A, Mukherjee P, Mandal D, Senapati S, Islam Khan M, Kumar R, Sastry M (2002) Enzyme mediated extracellular synthesis of CdS nanoparticles by the fungus *Fusarium oxysporum*. *J Am Chem Soc* 124:12108–12109
- Akbarzadeh A, Zare D, Farhangi A, Mehrabi MR, Norouzian D, Tangestaninejad S, Moghadam M, Bararpour N (2009) Synthesis and characterization of gold nanoparticles by tryptophane. *Am J Appl Sci* 6:691–695
- Alivisatos AP (2004) The use of nanocrystals in biological detection. *Nat Biotechnol* 22:47–51
- Amulyavichus A, Daugvila A, Davidonis R, Sipavichus C (1998) Study of chemical composition of nanostructural materials prepared by laser cutting of metals. *Fizika Metallov I Metallove-denie* 85:111–117
- Basavaraja S, Balaji SD, Lagashetty A, Rajasab AH, Venketaraman A (2008) Extracellular biosynthesis of silver nanoparticles using the fungus *Fusarium semitectum*. *Mater Res Bull* 43:1164–1170
- Bolander ME, Mukhopadhyay D, Sarkar G, Mukherjee P (2006) The use of microorganisms for the formation of metal nanoparticles and their application. *Appl Microbiol Biotechnol* 69:485–492
- Bonnemann H, Braun G, Brijoux W (1996) Nanoscale colloidal metals and alloys stabilized by solvents and surfactants. Preparation use as catalyst precursors. *J Organomet Chem* 520:143–162
- Brust M, Walker M, Bethell D, Schiffrin DJ, Whyman RJ (1994) Synthesis of thiol-derivatized gold nanoparticles in a 2-phase liquid–liquid system. *J Chem Soc, Chem Commun*: 801–802
- Burda C, Chen X, Narayanan R, El-Sayed MA (2005) Chemistry and properties of nanocrystals of different shapes. *Chem Rev* 105:1025–1102
- Cao YWC, Jin RC, Mirkin CA (2002) Nanoparticles with Raman spectroscopic fingerprints for DNA and RNA detection. *Science* 297:1536–1540
- Chaby G, Viseux V, Poulain JF, De Cagny B, Denoeux JP, Lok C (2005) Topical silversulfadiazine-induced acute renal failure. *Ann Dermatol Vénéréol* 132:891–893
- Chen X, Schluesener HJ (2008) Nanosilver: a nanoproduct in medical application. *Toxicol Lett* 176:1–12
- Chithrani BD, Ghazan AA, Chan CW (2006) Determining the size and shape dependence of gold nanoparticle uptake into mammalian cells. *Nano Lett* 6:662–668
- Connor EE, Mwamuka J, Gole A, Murphy CJ, Wyatt MD (2005) Gold nanoparticles are taken up by human cells but do not cause acute cytotoxicity. *Small* 1:325–327
- Daniel MC, Astruc D (2004) Gold nanoparticles: assembly, supramolecular chemistry, quantum-sized-related properties, and applications towards biology, catalysis and nanotechnology. *Chem Rev* 104:293–346
- Darouiche RO (1999) Anti-infective efficacy of silver-coated medical prostheses. *Clin Infect Dis* 29:1371–1377
- Demers LM, Mirkin CA, Mucic RC, Robert A, Reynolds I, Letsinger RL, Elghanian R, Viswanadham G (2000) A fluorescence-based method for determining the surface coverage and hybridization efficiency of thiol-capped oligonucleotides bound to gold thin films and nanoparticles. *Anal Chem* 72:5535–5541
- Durán N, Marcato PD, De Souza GIH, Alves OL, Esposito E (2007) Antibacterial effect of silver nanoparticles produced by fungal process on textile fabrics and their effluent treatment. *J Biomed Nanotechnol* 3:203–208
- Elechiguerra JL, Burt JL, Morones JR, Camacho-Bragado A, Gao X, Lara HH, Yacaman MJ (2005) Interaction of silver nanoparticles with HIV-1. *J Nanobiotechnol* 3:6
- El-Sayed MA (2001) Some interesting properties of metals confined in time and nanometer space of different shapes. *Acc Chem Res* 34:257–264
- Faulk WP, Taylor GM (1971) An immunocolloid method for the electron microscope. *Immunochimistry* 8:1081–1083

- Fayaz AM, Balaji K, Girilal M, Yadav R, Kalaichelvan PT, Venketesan R (2010) Biogenic synthesis of silver nanoparticles and their synergistic effect with antibiotics: a study against gram-positive and gram-negative bacteria. *Nanomedicine* 6:103–109
- Frey NA, Peng S, Cheng K, Sun S (2009) Magnetic nanoparticles: synthesis, functionalization, and applications in bioimaging and magnetic energy storage. *Chem Soc Rev* 38:2532–2542
- Fritzsche W, Taton TA (2003) Metal nanoparticles as labels for heterogeneous, chip-based DNA detection. *Nanotechnology* 14:R63–R73
- Gaffet E, Tachikart M, El Kedim O, Rahouadj R (1996) Nanostructural materials formation by mechanical alloying: morphologic analysis based on transmission and scanning electron microscopic observations. *Mater Charact* 36:185–190
- Gao J, Gu H, Xu B (2009) Multifunctional magnetic nanoparticles: design, synthesis, and biomedical applications. *Acc Chem Res* 42:1097–1107
- Ghadiali JE, Stevens MM (2008) Enzyme-responsive nanoparticle systems. *Adv Mater* 20:4359–4363
- Ghosh KK, Kolay S (2008) Preparation of Ag nanoparticles in surfactant solution. *J Dispersion Sci Technol* 29:676–681
- Ghosh P, Han G, De M, Kim CK, Rotello VM (2008) Gold nanoparticles in delivery applications. *Adv Drug Deliv Rev* 60:1307–1315
- Giersig M, Mulvaney P (1993) Preparation of ordered colloid monolayers by electrophoretic deposition. *Langmuir* 9:3408–3413
- Goodman CM, McCusker CD, Yilmaz T, Rotello VM (2004) Toxicity of gold nanoparticles functionalized with cationic and anionic side chains. *Bioconjug Chem* 15:897–900
- Govorov AO, Zhang W, Skeini T, Richardson H, Lee J, Kotov NA (2006) Gold nanoparticle ensembles as heaters and actuators: melting and collective plasmon resonances. *Nanoscale Res Lett* 1:84–90
- Gu HW, Yang ZM, Gao JH, Chang CK, Xu B (2005) Heterodimers of nanoparticles: formation at a liquid–liquid interface and particle-specific surface modification by functional molecules. *J Am Chem Soc* 127:34–35
- Han M, Gao X, Su JZ, Nie S (2001) Quantum-dot-tagged microbeads for multiplexed optical coding biomolecules. *Nat Biotechnol* 19:631–635
- Hatch GP, Stelter RE (2001) Magnetic design considerations for devices and particles used for biological high gradient magnetic separation systems. *J Magn Magn Mater* 225:262–276
- Huff TB, Tong L, Zhao Y, Hansen MN, Cheng JX, Wei A (2007) Hyperthermic effects of gold nanorods on tumor cells. *Nanomedicine* 2:125–132
- Jain P, Pradeep T (2005) Potential of silver nanoparticle-coated polyurethane foam as an anti-bacterial water filter. *Biotechnol Bioeng* 90:59–63
- Jain PK, El-Sayed IH, El-Sayed MA (2007) *Nano Today* 2:18–29
- Jiang J, Gu HW, Shao HL, Devlin E, Papaefthymiou GC, Ying JY (2008) Bifunctional Fe<sub>3</sub>O<sub>4</sub>-Ag heterodimer nanoparticles for two-photon fluorescence imaging and magnetic manipulation. *Adv Mater* 20:4403–4407
- Kakurai M, Demitsu T, Umemoto N, Ohtsuki M, Nakagawa H (2003) Activation of mast cells by silver particles in a patient with localized argyria due to implantation of acupuncture needles. *Br J Dermatol* 148:822
- Kamat PV (2002) Photophysical, photochemical and photocatalytic aspects of metal nanoparticles. *J Phys Chem B* 106:7729–7744
- Katz E, Willner I (2004) Integrated nanoparticle-biomolecule hybrid systems: synthesis, properties, and applications. *Angew Chem Int Ed* 43:6042–6108
- Kelly KL, Coronado E, Zhao LL, Schatz GC (2003) The optical properties of metal nanoparticles: the influence of size, shape, and dielectric environment. *J Phys Chem B* 107:668–677
- Kim DK, Mikhaylova M, Zhang Y, Muhammed M (2003a) Protective coating of superparamagnetic iron oxide nanoparticles. *Chem Mater* 15:1617–1627
- Kim YC, Park NC, Shin JS, Lee SR, Lee YJ, Moon DJ (2003b) Partial oxidation of ethylene to ethylene oxide over nanosized Ag/ $\alpha$ -Al<sub>2</sub>O<sub>3</sub> catalysts. *Catal Today* 87:153–162

- Kim JS, Kuk E, Yu KN, Kim JH, Park SJ, Lee HJ (2007) Antimicrobial effects of silver nanoparticles. *Nanomedicine* **NBM** 3:95–101
- Kimling J, Maier M, Okenve B, Kotaidis V, Ballot H, Plech A (2006) Turkevich method for gold nanoparticle synthesis revisited. *J Phys Chem B* **110**:15700–15707
- Kirchner C, Liedl T, Kudera S, Pellegrino T, Javier AM, Gaub HE, Stölzle S, Fertig N, Parak WJ (2005) Cytotoxicity of colloidal CdSe and CdSe/ZnS nanoparticles. *Nano Lett* **5**:331–338
- Klasen HJ (2000) A historical review of the use of silver in the treatment of burns. II Renewed interest silver. *Burns* **26**:131–138
- Klaus T, Joerger R, Olsson E, Granqvist CG (1999) Silver-based crystalline nanoparticles, microbially fabricated. *Proc Natl Acad Sci USA* **96**:13611–13614
- Kowshik M, Ashtaputre SH, Kharazi SH (2003) Extracellular synthesis of silver nanoparticles by a silver-tolerant yeast strain MKY3. *Nanotechnology* **14**:95–100
- Lee H, Dellatore SM, Miller WM, Messersmith PB (2007) Mussel-inspired surface chemistry for multifunctional coatings. *Science* **318**:426–430
- Li Y, Duan X, Qian Y, Li Y, Liao H (1999) Nanocrystalline silver particles: synthesis, agglomeration, and sputtering induced by electron beam. *J Colloid Interface Sci* **209**:347–349
- Li P, Li J, Wu C, Wu Q, Li J (2005) Synergistic antibacterial effects of  $\beta$ -lactam antibiotic combined with silver nanoparticles. *Nanotechnology* **16**:1912–1917
- Li Y, Leung P, Yao L, Song QW, Newton E (2006) Antimicrobial effect of surgical masks coated with nanoparticles. *J Hosp Infect* **62**:58–63
- Liz-Marzán LM (2004) Nanomaterials: formation and color. *Mater Today* **7**:26–31
- Love JC, Estroff LA, Kriebel JK, Nuzzo RG, Whitesides GM (2005) Self assembled monolayers of thiolates on metals as a form of nanotechnology. *Chem Rev* **105**:1103–1169
- Lowery AR, Gobin AM, Day ES, Halas NJ, West JL (2006) Immunonanoshells for targeted photothermal ablation of tumor cells. *Int J Nanomed* **1**:149–154
- Majewski P, Thierry B (2007) Functionalized magnetite nanoparticles – synthesis, properties, and bio-applications. *Crit Rev Solid State Mater Sci* **32**:203–215
- Mallick K, Witcomb MJ, Scurell MS (2004) Polymer stabilized silver nanoparticles: a photochemical synthesis route. *J Mater Sci* **39**:4459–4463
- Mann S, Ozin GA (1996) Synthesis of inorganic materials with complex form. *Nature* **382**:313–318
- Morones JR, Elechiguerra JL, Camacho A, Holt K, Kouri JB, Ramirez JT, Yacaman MJ (2005) The bactericidal effect of silver nanoparticles. *Nanotechnology* **16**:2346–2353
- Moyer CA (1965) A treatment of burns. *Trans Stud Coll Physicians Phila* **33**:53–103
- Mukherjee P, Senapati S, Mandal D, Ahmad A, Khan MI, Kumar R (2002) Extracellular synthesis of gold nanoparticles by the fungus *Fusarium oxysporum*. *Chem Biochem* **3**:461–463
- Murphy CJ (2002) Nanocubes and nanoboxes. *Science* **298**:2139–2141
- Murphy CJ, Gole AM, Stone JW, Sisco PN, Alkiany AM, Goldsmith EC, Baxter SC (2008) Gold nanoparticles in biology: beyond toxicity to cellular imaging. *Acc Chem Res* **41**:1721–1730
- Nanda A, Saravanan M (2009) Biosynthesis of silver nanoparticles from *Staphylococcus aureus* and its antimicrobial activity against MRSA and MRSE. *Nanomed Nanotechnol Biol Med* **5**:452–456
- Nicewarner-Pena SR, Freeman RG, Reiss BD, He L, Pena DJ, Walton ID, Cromer R, Keating CD, Natan MJ (2001) Submicrometer metallic barcodes. *Science* **294**:137–141
- Niemeyer CM, Simon U (2005) DNA-based assembly of metal nanoparticles. *Eur J Inorg Chem* **18**:3641–3655
- O'Neal DP, Hirsch LR, Halas NJ, Payne JD, West JL (2004) Photo-thermal tumor ablation in mice using near infrared-absorbing nanoparticles. *Cancer Lett* **209**:171
- Pan Y, Neuss S, Leifert A, Fischler M, Wen F, Simon U, Schmid G, Brandau W, Jahnke-Dechent W (2007) Size-dependent cytotoxicity of gold nanoparticles. *Small* **3**:1941–1949
- Park J, Joo J, Kwon SG, Jang Y, Hyeon T (2007) Synthesis of monodisperse spherical nanocrystals. *Angew Chem Int Ed* **46**:4630–4660

- Patra HK, Banerjee S, Chaudhuri U, Lahiri P, Dasgupta AK (2007) Cell selective response to gold nanoparticles. *Nanomedicine* 3:111–119
- Pellegrino T, Sperling RA, Alivisatos AP, Parak WJ (2007) Gel electrophoresis of gold-DNA nanoconjugates. *J Biomed Biotechnol* 2007:26796–26804
- Peng X, Wickham J, Alivisatos AP (1998) Kinetics of II-VI and III-V colloidal semiconductor nanocrystal growth: “focusing” of size distributions. *J Am Chem Soc* 120:5343–5344
- Pissuwan D, Valenzuela SM, Cortie MB (2006) Therapeutic possibilities of plasmonically heated gold nanoparticles. *Trends Biotechnol* 24:62–67
- Qiang Y, Antony J, Sharma A, Nutting J, Sikes D, Meyer D (2006) Iron/iron oxide core-shell nanoclusters for biomedical applications. *J Nanopart Res* 8:489–496
- Rai M, Yadav A, Gade A (2009) Silver nanoparticles as a new generation of antimicrobials. *Biotechnol Adv* 27:76–83
- Redd AS, Chen CY, Baker SC, Chen CC, Jean JS, Fan CW, Chen HR, Wang JC (2009) Synthesis of silver nanoparticles using surfactin: a biosurfactant as stabilizing agent. *Mater Lett* 63:1227–1230
- Rojo J, Diaz V, de la Fuente JM, Segura I, Barrientos AG, Riese HH, Bernad A, Penades S (2004) Gold glyconanoparticles as new tools in antiadhesive therapy. *ChemBiochem* 5:291–297
- Rosi NL, Mirkin CA (2005) Nanostructures in biodiagnostics. *Chem Rev* 105:1547–1562
- Rosi NL, Giljohann DA, Thaxton CS, Lytton-Jean AKR, Han MS, Mirkin CA (2006) Oligonucleotide-modified gold nanoparticles for intracellular gene regulation. *Science* 312:1027–1030
- Salem AK, Searson PC, Leong KW (2003) Multifunctional nanorods for gene delivery. *Nat Mater* 2:668–671
- Shrivastava S, Bera T, Roy A, Singh G, Ramachandrarao P, Dash D (2007) Characterization of enhanced antibacterial effects of novel silver nanoparticles. *Nanotechnology* 18:225103–225111
- Shrivastava S, Bera T, Singh SK, Singh G, Ramachandrarao P, Dash D (2009) Characterization of antiplatelet properties of silver nanoparticles. *ACS Nano* 3:1357–1364
- Shukla R, Bansal V, Chaudhary M, Basu A, Bhonde RR, Sastry M (2005) Biocompatibility of gold nanoparticles and their endocytotic fate inside the cellular compartment: a microscopic overview. *Langmuir* 21:10644–10654
- Silver S (2003) Bacterial silver resistance: molecular biology and uses and misuses of silver compounds. *FEMS Microbiol Rev* 27:341–353
- Silver S, Phung LT, Silver G (2006) Silver as biocides in burn and wound dressings and bacterial resistance to silver compounds. *J Ind Microbiol Biotechnol* 33:627–634
- Singh SK, Shrivastava S, Nayak M, Sinha ASK, Jagannadham MV, Dash D (2009) Stabilization of protein by biocompatible nanoparticles of silver. *J Bionanosci* 3:1–9
- Sperling RA, Rivera Gil P, Zhang F, Zanella M, Parak WJ (2008) Biological applications of gold nanoparticles. *Chem Soc Rev* 37:1896–1908
- Stevens KNJ, Crespo-Biel O, van den Bosch EEM, Dias AA, Knetsch Menno LW, Aldenhoff Yvette BJ, van der Veen FH, Maessen JG, Stobberingh EE, Koole LH (2009) The relationship between the antimicrobial effect of catheter coatings containing silver nanoparticles and the coagulation of contacting blood. *Biomaterials* 30:3682–3690
- Stewart ME, Anderton CR, Thompson LB, Maria J, Gray SK, Rogers JA, Nuzzo RG (2008) Nanostructured plasmonic sensors. *Chem Rev* 108:494–521
- Sun SH (2006) Recent advances in chemical synthesis, self-assembly, and applications of FePt nanoparticles. *Adv Mater* 18:393–403
- Tada MS, Hatanaka H, Sanbonsugi N, Matsushita AM (2003) Method for synthesizing ferrite nanoparticles 30 nm in diameter on neutral pH condition for biomedical applications. *J Appl Phys* 93:7566–7568
- Tan Y, Dai Y, Li Y, Zhua D (2003) Preparation of gold, platinum, palladium and silver nanoparticles by the reduction of their salts with a weak reductant-potassium bitartrate. *J Mater Chem* 13:1069–1075
- Templeton AC, Wuelfing WP, Murray RW (2001) Monolayer protected cluster molecules. *Acc Chem Res* 33:27–36

- Trop M (2006) Silver-coated dressing acticoat caused raised liver enzymes and argyria like symptoms in burn patient. *J Trauma* 61:1024
- Turkevich J, Stevenson PC, Hillier J (1951) A study of the nucleation and growth processes in the synthesis of colloidal gold, *Discuss. Faraday Soc*: 55–75
- Xu CJ, Xu KM, Gu HW, Zheng RK, Liu H, Zhang XX, Guo ZH, Xu B (2004) Dopamine as a robust anchor to immobilize functional molecules on the iron oxide shell of magnetic nanoparticles. *J Am Chem Soc* 126:9938–9939
- Xu CJ, Xie J, Ho D, Wang C, Kohler N, Walsh EG, Morgan JR, Chin YE, Sun SH (2008) Au–Fe<sub>3</sub>O<sub>4</sub> dumbbell nanoparticles as dual-functional probes. *Angew Chem Int Ed* 47:173–176
- Yu H, Chen M, Rice PM, Wang SX, White RL, Sun SH (2005) Dumbbell-like bifunctional Au–Fe<sub>3</sub>O<sub>4</sub> nanoparticles. *Nano Lett* 5:379–382
- Zameer S, Yutaka I, Masahiro S, Hajime K, Yukiya H, Toshiro Y, Takako N, Hironobu KA, Kenji A (2008) Morphol size controlled synthesis silver nanoparticles aqueous surfactant polymer solutions. *Colloid Polym Sci* 286:403–410
- Zhao M, Kircher MF, Josephson L, Weissleder R (2002) Differential conjugation of Tat peptide to superparamagnetic nanoparticles and its effect on cellular uptake. *Bioconjug Chem* 13:840–844

# Index

## A

Acanthile, 155–156  
Acid-fast staining, 184  
Actinomycetate, 160  
Agarose gel, 188  
Agglomeration, 164, 168, 286, 287  
Alloy, 153, 154, 157, 166, 169  
Antibacterial, 287, 288  
    activity, 226, 240–241  
Antibiotics, 250–254, 261, 262  
Antimicrobial, 249–254, 257, 259, 261  
Apoptosis, 22, 23  
*Aspergillus clavatus*, 261  
*Aspergillus niger*, 253–254, 260–261  
AuNP. *See* Gold nanoparticles  
Au–Pd catalyst, 236  
Auxenic culture, 180–181

## B

*Bacillus cereus*, 253  
*Bacillus subtilis*, 253, 261  
Bacteria, 249–255, 260, 261  
Bactericidal activity, 164  
Basic local alignment search tool (BLAST), 185, 189  
Bi-functionality of silver ions, 23, 28  
Bimetallic gold-palladium nanoparticles, 68  
Bioconjugation, 289–291  
Biogenic nanoparticles, 1–10  
Bioimaging, 66, 145–146  
Biological agents, 2–5, 9  
Biologically-controlled mineralization, 79  
Biologically-induced mineralization, 79  
Biological method, 3–5  
Biomarker, 94  
Biomass production, 207  
Biomimetic, 142–143

Biom mineralization, 203–205, 216  
    of bacteria magnetosome, 75, 79, 84, 87, 88, 94  
Biomolecules, 135–148  
Bio-nanomaterials, 193  
Biorecognition, 135, 146–147  
Biorecovery of gold, 39, 40, 61  
Bioreduction, 155–157, 160, 162, 168, 169  
    cytoplasmic hydrogenase, 120, 123–124, 128  
    periplasmic hydrogenase, 116, 119–123  
    two step mechanism, 120, 123–124, 128  
Bioremediation, 198, 199, 206, 207, 212  
Biosensor, 226, 230–232  
Biosorption *Patrz.*, 156  
Biosynthesis, 197, 198, 202, 203  
    of gold nanoparticles, 37–70  
    of silver nanoparticles  
        *Bacillus licheniformis*, 19, 20, 22  
        defense mechanism, 21, 23  
        immobilization of nitrate reductase, 27  
        mechanism of synthesis, 21–25  
        problems with biosynthesis, 18  
        scaling-up, 28–30  
        size control, 24–27  
Biosynthetic methods, 178  
BLAST. *See* Basic local alignment search tool (BLAST)  
Bottom-up processes, 177–178  
By magnetotactic cocci bacteria, 64

## C

Cadmium introduction, 210, 211  
Cadmium sulfide (CdS), 199–201, 204, 205, 207–216  
*Candida albicans*, 250, 261  
*Candida glabrata*, 200–202, 204, 205, 207–209, 213, 216

- Carbon nanotubes (CNTs), 275, 276, 279  
 Catalase test, 184–185  
 Catalytic process, 233–237  
 CdS. *See* Cadmium sulfide  
 Cell based biosensors, 276–278  
 Cell disruption, 211–212  
 Characterization, 198, 213–216  
 Chemical method, 1, 2, 4, 5, 9  
 Chemolithotrophy, 197  
 CNTs. *See* Carbon nanotubes  
 Colorimetric, 290  
 Concluding comments  
   two different enzymes, 128  
 Crabtree effect, 208  
 Cultivation, 198, 207–212, 216  
   conditions, 207, 209  
   medium, 209  
 Cyanobacteria, 38–44, 53–55, 61–65, 69  
 Cyanobacterium, 160, 161  
 Cysteine, 160, 161  
 Cytochromes, 163  
 Cytoplasmic membrane, 164–165  
 Cytoskeletal filaments, 89  
 Cytotoxicity, 257–260, 262, 288, 291
- D**
- Dendrimers, 67, 228–229  
 Density functional theory (DFT), 234  
 Deposition-precipitation (DP) method,  
   233, 236  
 Desulfhydrase, 161  
 Detection  
   biologically-relevant molecules, 274  
   infectious agents, 274  
   single molecules, 270, 271, 275  
 Determination of specific nanomaterials,  
   276, 277  
 Detoxification, 197, 200–203, 210, 211, 215  
 DFT. *See* Density functional theory  
 Diatoms, 154  
 DLS. *See* Dynamic light scattering (DLS)  
 Downstream processes, 211–216  
 DP method. *See* Deposition-precipitation (DP)  
   method  
 Drug delivery, 142–145  
   particle, 242  
 Dynamic light scattering (DLS), 190, 192
- E**
- EDS. *See* Energy dispersive spectroscopy  
   (EDS)  
 Electron cryotomography, 87  
 Electron holography, 84  
 Electrophoresis, 185, 187–189  
 Electro spray ionization time-of-flight  
   (ESI TOF), 215  
 Electrostatic interaction, 164, 169  
 Endophytic fungus, 168  
 Energy dispersive spectroscopy (EDS),  
   190, 193  
 Enzymes, 154–157, 159–162, 164–169  
   hydrogenases, 110–113, 116, 120  
 Enzyme synthesis  
   nitrate reductase, 116–117  
*Escherichia coli*, 250, 252–254, 260–261  
 ESI TOF. *See* Electro spray ionization time-  
   of-flight  
 Ethidium bromide, 187–188  
 Eukaryote synthesis of platinum nanoparticles  
   *Fusarium*, 115–117, 125–128  
 Extracellular formation, 60, 69  
 Extracellular nanoparticles, 199
- F**
- Fabrics, 250, 254–257, 262  
 Fed-batch, 208, 210–211  
 Fourier transform infrared spectroscopy  
   (FTIR), 190, 191  
 FTIR. *See* Fourier transform infrared  
   spectroscopy (FTIR)  
 Fungi, 163–170, 249–251, 262  
*Fusarium acuminatum*, 252  
*Fusarium oxysporum*, 254, 255
- G**
- Glucose oxidase (GOx), 232–233  
 Glutathione (GSH), 199, 201–205, 208,  
   209, 215  
 Gold, 37–70  
 Gold biosorption, 39, 40, 60–62, 65  
 Gold(III)-chloride complex, 39, 44–62,  
   64–65, 69  
 Gold nanoparticles (AuNP), 37–70, 158–160,  
   164–166, 168, 289–292  
   applications, 226  
   biomedical applications, 238–240  
   biomolecule protection, 226–230  
   description, 225  
   drug and gene delivery application,  
     241–244  
   as sensor, 231–233  
 Gold precipitation, 40, 41, 44, 60–65, 69  
 Gold sulfide, 44, 63–65, 69  
 Gold(I)-thiosulfate complex, 39–44, 62–64, 69  
 GOx. *See* Glucose oxidase  
 Gram stain, 182, 184

- Greigite, 76–84, 86, 87, 94, 154  
  crystal morphology, 80–83  
GSH. *See* Glutathione
- H**  
Heterodimers, 291–293  
Homogeneous deposition precipitation (HDP)  
  technique, 236  
Homogenization, 212  
Hydrogenlyase reactions, 162  
Hyperthermia, 291, 292
- I**  
ICP MS. *See* Inductively coupled plasma mass  
  spectrometry  
ICP OES. *See* Inductively coupled plasma  
  optical emission spectrometry  
Identification, 206–207, 214, 215  
IEC. *See* Ion-Exchange Chromatography  
Inductively coupled plasma mass spectrometry  
  (ICP MS), 215  
Inductively coupled plasma optical emission  
  spectrometry (ICP OES), 215  
Interaction, 135–148  
Intracellular nanoparticles, 199, 208, 211  
Intracellular synthesis, 69  
Ion-exchange chromatography (IEC), 213  
Ion-sensitive field-effect transistor (ISFET),  
  272–274  
ISFET. *See* Ion-sensitive field-effect transistor  
Isolation, 198, 206–207, 210–214
- K**  
*Klebsiella pneumoniae*, 253, 254
- L**  
*Leishmania amazonensis*, 261, 262  
Lipids, 135, 139, 140  
Lipopolysaccharide, 63
- M**  
Mackinawite, 79, 84  
Maghemite, 163  
Magnetic force microscopy, 84, 93  
Magnetic nanoparticles (NPs), 291–293  
Magnetite, 76, 78–84, 87–90, 92–94, 154,  
  163, 167  
  crystal defects, 83, 84  
  crystal morphology, 81–83, 88  
Magneto-aerotaxis, 85, 86  
  axial, 85  
  polar, 85, 86  
Magnetofossils, 93–94  
Magnetosomes, 75–94  
  applications, 92–93  
  arrangement in cell, 84  
  chain, synthesis of, 86–87, 89  
  composition, 79–81  
  gene island, 91–92  
  gene organization and regulation, 90–91  
  membrane, 87–88, 90, 94  
  membrane proteins, 88–91, 93  
  morphology, 88, 94  
  size, 81, 88  
  transport of iron, 86–87, 90  
  vesicle, 86–90  
*Magnetospirillum*, 78, 80–84, 87, 89, 91, 92  
Magnetotactic bacteria, 153, 154, 163  
  autotrophy, 78  
  diversity, 76–77, 91–92  
  ecology, 77–78  
  phylogeny, 77, 84  
  physiology, 78–79  
  thermophilic, 79  
Magnetotaxis, 75, 81, 84–86  
MALDI. *See* Matrix assisted laser desorption  
  ionization  
Matrix assisted laser desorption ionization  
  (MALDI), 215  
Mechanism for platinum reduction  
  Pt (II) and Pt (IV), 120, 123, 124  
Mechanisms, 5–7, 9, 197, 199–205, 207, 209,  
  211, 215, 216  
Metallic nanoparticles (NPs), 273, 285–293  
Metallothioneins, 200–203, 212–213, 215  
Metal-triggered biotransformation, 204  
Metal uptake rate, 207  
Meteorite ALH84001, 93  
Microaerophiles, 78, 85  
Microbial screening, 178–180  
Microelectronics, 271, 272  
Microgravimetric detection method, 231
- N**  
Nanobiosensors, 269–280  
Nanobiotechnology, 249, 261  
Nanomaterials, 272–274, 276, 277, 280  
Nanoparticles, 135–148, 197–216, 249–262  
  applications, 105, 108  
  properties, 105–108, 110  
  safety, 107  
  synthesis, 103–128  
Nanotechnology, 1, 7, 9, 269–272, 274,  
  276–278, 280  
  hydrogenase/reductase, 110–118, 128  
Nitrate-dependent reductase, 157, 166–168



- Nitrate reductase, 21–24, 26–31, 157, 166–169  
 Nitroreductase, 156–157  
 Noble metal nanoparticles, 199  
 Nucleic acid, 135–137
- O**  
 OCT. *See* Optical coherence tomography  
 Octahedral gold, 41, 43, 44, 61, 63, 64  
 Oligonucleotides, 136–137, 147, 231, 232, 239, 243  
 Optical coherence tomography (OCT), 239  
 Organogold, 66  
 Oxidase test, 185
- P**  
 Palladium nanoparticles, 162  
 PCR. *See* Polymerase chain reaction (PCR)  
 Periplasmic hydrogenase, 158, 162  
 Periplasmic proteins, 63, 64  
 Photoluminescent analysis, 215–216  
 Photoreduction, 156–157  
 Photothermal therapy, 226, 239, 244  
 Physical method, 1, 3–5, 9  
 Phytochelatins, 163, 167, 201–205, 209–213, 215  
*Phytophthora infestans*, 253  
 Piperitone, 156  
 Plants, 249, 258  
 Platinum nanoparticles, 161, 162  
 PNIPAM. *See* Poly (N-isopropylacrylamide)  
 Pollution control, 68  
 Poly (N-isopropylacrylamide) (PNIPAM), 227  
 Poly(propyleneimine) (PPI), 229  
 Polymerase chain reaction (PCR), 185–189  
 Powder X-ray diffraction (XRD), 190, 193  
 PPI. *See* Poly(propyleneimine)  
 Precursor feeding rate, 208  
 Prokaryote synthesis of platinum nanoparticles sulfate reducing bacteria (SRB), 119–124  
 Prokaryotic fossils, 94  
 Protein, 135, 137–139, 146, 147  
 Proteomics, 215  
*Proteus vulgaris*, 253  
*Pseudomonas aeruginosa*, 253, 261  
 Purification, 198, 210–214  
 Pyrite, 79  
 Pyrrhotite, 79
- Q**  
 Qualitative analysis  
   energy dispersive x-ray (EDAX), 119, 127  
   transmission electron microscopy, 118
- Quantitative analysis  
   UV/vis, 118  
 Quantum dots, 160, 163, 167
- S**  
*Salmonella typhi*, 252–254  
 Scanning electron microscope, 191–192  
*Schizosaccharomyces pombe*, 200–205, 207–210, 213–216  
 SEC. *See* Size exclusion chromatography  
 Selective media, 206  
 Self-assembling structures, 272  
 Semiconductor nanocrystals, 200  
 Serial dilution, 179  
 SERS. *See* Surface-enhanced Raman scattering  
 Silica, 153, 154, 167  
 Silver, 249–262  
 Silver nanoparticles (NPs), 156, 157, 163–169, 287–289  
 Size distribution, 199, 200, 214–215  
 Size exclusion chromatography (SEC), 213–214  
 Spore stain, 184  
 SPR. *See* Surface plasmon resonance  
 16s rDNA method, 185–189  
 Stabilizing agents, 286, 287, 289  
*Staphylococcus aureus*, 250, 252–255, 257, 261  
*Staphylococcus epidermidis*, 252, 254, 261  
 State-of-art in Russian research, 278–280  
 Streak plate method, 181  
*Streptococcus pyogenes*, 254  
 Sulfate-reducing bacteria, 40–43, 159, 160  
 Surface-enhanced Raman scattering (SERS), 225, 238  
 Surface plasmon resonance (SPR), 225, 231, 238, 290, 293  
 Surfactants, 285–287, 289  
 Synthesis  
   biological, 110–119, 127  
   chemical, 108–109, 119  
   eukaryote, 103–128  
   ion exchange, 108  
   micelles/pyrolysis, 109  
   passive, 110, 111, 125, 128  
   prokaryote, 103–128  
   pyrolysis, 109  
   sol process, 109

**T**

TAE buffer. *See* Tris-acetate EDTA (TAE) buffer  
TEM. *See* Transmission electron microscopy  
Titanium, 167  
Top-down methods, 177–178  
Toxicity, 201, 202  
Transmission electron microscopy (TEM), 191, 192, 214–215  
*Trichoderma viride*, 253  
Tris-acetate EDTA (TAE) buffer, 188

**U**

UO<sub>2</sub> nanoparticles, 162, 163  
Upstream processes, 206–207  
UV-visible spectrometry, 190, 191

**V**

Vacuoles, 199, 203, 205  
VAM. *See* Vinyl acetate monomer  
Vinyl acetate monomer (VAM), 236

**W**

Water purification, 68  
Water-soluble gold nanoparticles, 229, 230

**Y**

Yeasts, 155, 163, 164, 169, 198–216, 249

**Z**

Zebrafish, 260  
Zinc phosphate, 14  
Zirconia, 267